frontiers | Research Topics

Aquaculture environment regulation and system engineering

Edited by
Ce Shi, Zhangying Ye and Dibo Liu

Published in
Frontiers in Marine Science

ISSN 1664-8714
ISBN 978-2-8325-2977-5
DOI 10.3389/978-2-8325-2977-5

About Frontiers

Frontiers is more than just an open access publisher of scholarly articles: it is a pioneering approach to the world of academia, radically improving the way scholarly research is managed. The grand vision of Frontiers is a world where all people have an equal opportunity to seek, share and generate knowledge. Frontiers provides immediate and permanent online open access to all its publications, but this alone is not enough to realize our grand goals.

Frontiers journal series

The Frontiers journal series is a multi-tier and interdisciplinary set of open-access, online journals, promising a paradigm shift from the current review, selection and dissemination processes in academic publishing. All Frontiers journals are driven by researchers for researchers; therefore, they constitute a service to the scholarly community. At the same time, the *Frontiers journal series* operates on a revolutionary invention, the tiered publishing system, initially addressing specific communities of scholars, and gradually climbing up to broader public understanding, thus serving the interests of the lay society, too.

Dedication to quality

Each Frontiers article is a landmark of the highest quality, thanks to genuinely collaborative interactions between authors and review editors, who include some of the world's best academicians. Research must be certified by peers before entering a stream of knowledge that may eventually reach the public - and shape society; therefore, Frontiers only applies the most rigorous and unbiased reviews. Frontiers revolutionizes research publishing by freely delivering the most outstanding research, evaluated with no bias from both the academic and social point of view. By applying the most advanced information technologies, Frontiers is catapulting scholarly publishing into a new generation.

What are Frontiers Research Topics?

Frontiers Research Topics are very popular trademarks of the *Frontiers journals series*: they are collections of at least ten articles, all centered on a particular subject. With their unique mix of varied contributions from Original Research to Review Articles, Frontiers Research Topics unify the most influential researchers, the latest key findings and historical advances in a hot research area.

Find out more on how to host your own Frontiers Research Topic or contribute to one as an author by contacting the Frontiers editorial office: frontiersin.org/about/contact

Aquaculture environment regulation and system engineering

Topic editors

Ce Shi — Ningbo University, China

Zhangying Ye — Zhejiang University, China

Dibo Liu — Leibniz-Institute of Freshwater Ecology and Inland Fisheries (IGB), Germany

Citation

Shi, C., Ye, Z., Liu, D., eds. (2023). *Aquaculture environment regulation and system engineering*. Lausanne: Frontiers Media SA. doi: 10.3389/978-2-8325-2977-5

Table of contents

frontiers | Frontiers in Marine Science

TYPE Editorial
PUBLISHED 27 June 2023
DOI 10.3389/fmars.2023.1236868

OPEN ACCESS

EDITED AND REVIEWED BY
Yngvar Olsen,
Norwegian University of Science and Technology, Norway

*CORRESPONDENCE
Ce Shi
shice3210@126.com

RECEIVED 08 June 2023
ACCEPTED 15 June 2023
PUBLISHED 27 June 2023

CITATION
Shi C (2023) Editorial: Aquaculture environment regulation and system engineering.
Front. Mar. Sci. 10:1236868.
doi: 10.3389/fmars.2023.1236868

Editorial: Aquaculture environment regulation and system engineering

Ce Shi[1,2,3,4,5]*

[1]Marine Economic Research Center, Donghai Academy, Ningbo University, Ningbo, China, [2]College of Biosystems Engineering and Food Science (BEFS), Zhejiang University, Hangzhou, China, [3]Key Laboratory of Green Mariculture (Co-Construction by Ministry and Province), Ministry of Agriculture and Rural, Ningbo, China, [4]Key Laboratory of Aquacultural Biotechnology, Ningbo University, Chinese Ministry of Education, Ningbo, China, [5]Collaborative Innovation Center for Zhejiang Marine High-Efficiency and Healthy Aquaculture, Ningbo University, Ningbo, China

KEYWORDS

aquaculture, recirculating aquaculture system, environment regulation, intelligent equipment, behavior

Editorial on the Research Topic
Aquaculture environment regulation and system engineering

Aquatic products are a major source of high-quality foods for humans, and as the population grows, global fisheries and aquaculture production is expanding. Since the 1990s, capture production of fisheries has reached a bottleneck and tended to stabilize at around 90 million tons (FAO, 2022). In contrast, aquaculture production has entered a rapidly developing period, and aquaculture has now become one of the fastest-growing areas of food production. In 2020, aquaculture provided 88 million tonnes of aquatic products worldwide (FAO, 2022), significantly contributing to global food and nutrition security. Furthermore, aquaculture will play an increasing role in global aquatic product supply to fill the gap between declining capture production and increasing human demand (Zhang et al., 2022a).

To keep up with the continuous expansion of the aquaculture industry, the intensive and efficient aquaculture mode represented by indoor factory recirculating aquaculture system (RAS) is emerging and developing and gradually replacing the traditional pond culture (Campanati et al., 2022; Chen and Gao, 2023). The indoor factory RAS maximizes aquaculture efficiency by regulating various environmental factors to the optimum level (Xiao et al., 2019; Li et al., 2023). Various environmental factors can affect the growth, reproduction, and health of aquatic organisms, such as light (Ruchin, 2021; Xu et al., 2022a; Xu et al., 2022b; Xu et al., 2022c; Zhang et al., 2022b; Zhao et al., 2023a), temperature (Liu et al., 2022a; Liu et al., 2022b), salinity (Boeuf and Payan, 2001; Deane and Woo, 2009), dissolved oxygen (Waldrop et al., 2020), flow velocity (Gao et al., 2017; Zhao et al., 2023b), tank color (Shi et al., 2019; Wang et al., 2019; Ma et al., 2021; McLean, 2021), tank size (Yu et al., 2022), tank substrate (Tierney et al., 2020), etc. Many studies have demonstrated promoting aquatic organism growth by manipulating environmental factors (Li et al., 2020; Chen et al., 2021; Chen et al., 2022; Chen et al., 2023; Yu et al., 2023). Therefore, understanding the environmental demand of aquatic animals is the premise of designing an intensive aquaculture system. In this Research Topic, it has collected several research

papers on the light and temperature requirements of fish involving *Oncorhynchus mykiss* (Xu H. et al.; Xu H. et al.; Ma S. et al.; Ma Z. et al.), *Salmo salar* (Dempsey et al.), and *Takifugu rubripes* (Liu S. et al.), which provide theoretical references for the environmental settings of intensive aquaculture system.

After clarifying the environmental demands, establishing an intensive aquaculture system has become a new challenge. The establishment of an optimum system needs interdisciplinary knowledge such as hydromechanics and computer-based intelligent control technology (Hu et al., 2021; Yang et al., 2021). This Research Topic contains cutting-edge research on the engineering & design of aquaculture facilities and artificial intelligence in aquaculture, including the design of a new type of inlet pipe to improve the self-purification capacity of aquaculture tanks (Zhang et al.); the inlet layout on solid waste removal from aquaculture tanks (Hu et al.); the ability of ultrafiltration membranes to remove viruses and bacteria from aquaculture waters (Mota et al.); and commercial-scale wetland system to treat aquaculture wastewater (Li et al.). In addition, a computer vision-based study of fish appetite grading (Wei et al.) and a study of fish swimming behavior (Xiang et al.) were also collected on this Research Topic. The above studies provide a research basis for developing intensive & intelligent aquaculture facilities.

On the other hand, intensive aquaculture systems are often capital & technology-intensive. For a lot of developing countries, the extensive aquaculture system is also prevalent. Reservoirs are an important artificial water body, and aquaculture production in reservoirs is one of the important ways of inland aquaculture. This Research Topic included related studies on fish distribution in reservoirs based on hydroacoustic surveys (Mei et al.; Luo et al.), which provided an ecological theoretical basis for conducting reservoir aquaculture. In addition, microorganisms in cultured water are increasingly of interest because of their close relationship with the growth and health of the animals. Microbial composition in shrimp-crab polyculture systems (Liu H. et al.) and in offshore shellfish farming waters (Gao et al.) are also included in this Research Topic to provide new insights into the microecological environment of aquaculture systems.

In conclusion, the basic knowledge of bioengineering interfaces in aquaculture is important in designing and developing effective aquaculture systems. This Research Topic, which combines the latest research on the environmental demands of aquatic organisms, the development of aquacultural facilities & equipment and the knowledge of extensive aquaculture system, expands the horizons on aquaculture environment regulation and system engineering.

Author contributions

The author confirms being the sole contributor of this work and has approved it for publication.

Funding

This Editorial was sponsored by the National Natural Science Foundation of China (Grant Nos. 31972783 and 32172994), Key Scientific and Technological Grant of Zhejiang for Breeding New Agricultural Varieties (2021C02069-6), the Province Key Research and Development Program of Zhejiang (2021C02047), the China Agriculture Research System of MOF and MARA (China Agriculture Research System of Ministry of Finance and Ministry of Agriculture and Rural Affairs), the K. C. Wong Magna Fund of Ningbo University and the Scientific Research Foundation of the Graduate School of Ningbo University (IF2022152).

Acknowledgments

Thank Prof. Zhangying Ye and Dr. Dibo Liu for their contribution to this topic. Thank Dr. Hanying Xu for his help in preparing this editorial.

Conflict of interest

The author declares that the research was conducted in the absence of any commercial or financial relationships that could be construed as a potential conflict of interest.

Publisher's note

References

Boeuf, G., and Payan, P. (2001). How should salinity influence fish growth? *Comp. Biochem. Physiol. C-Toxicology Pharmacol.* 130 (4), 411–423. doi: 10.1016/S1532-0456(01)00268-X

Campanati, C., Willer, D., Schubert, J., and Aldridge, D. C. (2022). Sustainable intensification of aquaculture through nutrient recycling and circular economies: more fish, less waste, blue growth *Rev. Fish. Sci. Aquac* 30 (2), 143–169. doi: 10.1080/23308249.2021.1897520

Chen, W. J., and Gao, S. Y. (2023). Current status of industrialized aquaculture in China: a review. *Environ. Sci. pollut. Res.* 30 (12), 32278–32287. doi: 10.1007/s11356-023-25601-9

Chen, S. J., Liu, J. H., Shi, C., Migaud, H., Ye, Y. F., Song, C. B., et al. (2023). Effect of photoperiod on growth, survival, and lipid metabolism of mud crab *Scylla paramamosain* juveniles. *Aquaculture* 567, 739279. doi: 10.1016/j.aquaculture.2023.739279

Chen, S. J., Migaud, H., Shi, C., Song, C. B., Wang, C. L., Ye, Y. F., et al. (2021). Light intensity impacts on growth, molting and oxidative stress of juvenile mud crab *Scylla paramamosain*. *Aquaculture* 545, 737159. doi: 10.1016/j.aquaculture.2021.737159

Chen, S. J., Shi, C., Migaud, H., Song, C. B., Mu, C. K., Ye, Y. F., et al. (2022). Light spectrum impacts on growth, molting, and oxidative stress response of the mud crab *Scylla paramamosain*. *Front. Mar. Sci.* 9. doi: 10.3389/fmars.2022.840353

Deane, E. E., and Woo, N. Y. S. (2009). Modulation of fish growth hormone levels by salinity, temperature, pollutants and aquaculture related stress: a review. *Rev. Fish Biol. Fisheries* 19 (1), 97–120. doi: 10.1007/s11160-008-9091-0

FAO (2022). *The state of world fisheries and aquaculture 2022. towards blue transformation* (Rome: FAO). doi: 10.4060/cc0461en

Gao, X. L., Li, X. A., Zhang, M., Wu, F. C., Shi, C., and Liu, Y. (2017). Effects of flow velocity on growth, food intake, body composition, and related gene expression of *Haliotis discus hannai* ino. *Aquaculture* 481, 48–57. doi: 10.1016/j.aquaculture.2017.08.023

Hu, X. L., Liu, Y., Zhao, Z. X., Liu, J. T., Yang, X. T., Sun, C. H., et al. (2021). Real-time detection of uneaten feed pellets in underwater images for aquaculture using an improved YOLO-V4 network. *Comput. Electron. Agric.* 185, 106135. doi: 10.1016/j.compag.2021.106135

Li, H., Cui, Z. G., Cui, H. W., Bai, Y., Yin, Z. D., and Qu, K. M. (2023). Hazardous substances and their removal in recirculating aquaculture systems: a review. *Aquaculture* 569, 739399. doi: 10.1016/j.aquaculture.2023.739399

Li, N., Zhou, J. M., Wang, H., Wang, C. L., Mu, C. K., Shi, C., et al. (2020). Effects of light intensity on growth performance, biochemical composition, fatty acid composition and energy metabolism of *Scylla paramamosain* during indoor overwintering. *Aquaculture Rep.* 18, 100443. doi: 10.1016/j.aqrep.2020.100443

Liu, J. H., Chen, S. J., Ren, Z. M., Ye, Y. F., Wang, C. L., Mu, C. K., et al. (2022b). Effects of diurnal temperature fluctuations on growth performance, energy metabolism, stress response, and gut microbes of juvenile mud crab *Scylla paramamosain*. *Front. Mar. Sci.* 9. doi: 10.3389/fmars.2022.1076929

Liu, J. H., Shi, C., Ye, Y. F., Ma, Z., Mu, C. K., Ren, Z. M., et al. (2022a). Effects of temperature on growth, molting, feed intake, and energy metabolism of individually cultured juvenile mud crab Scylla paramamosain in the recirculating aquaculture system. *Water* 14 (19), 2988. doi: 10.3390/w14192988

Ma, X. C., Zhang, G. L., Gao, G. C., Wang, C. L., Mu, C. K., Ye, Y. F., et al. (2021). Effects of tank color on growth, stress and carapace color of juvenile mud crab *Scylla paramamosain*. *J. Ningbo Univ. (NSEE)* 34 (6), 43–49.

McLean, E. (2021). Fish tank color: an overview. *Aquaculture* 530, 735750. doi: 10.1016/j.aquaculture.2020.735750

Ruchin, A. B. (2021). Effect of illumination on fish and amphibian: development, growth, physiological and biochemical processes. *Rev. Aquaculture* 13 (1), 567–600. doi: 10.1111/raq.12487

Shi, C., Wang, J. C., Peng, K. W., Mu, C. K., Ye, Y. F., and Wang, C. L. (2019). The effect of tank colour on background preference, survival and development of larval swimming crab *Portunus trituberculatus*. *Aquaculture* 504, 454–461. doi: 10.1016/j.aquaculture.2019.01.032

Tierney, T. W., Fleckenstein, L. J., and Ray, A. J. (2020). The effects of density and artificial substrate on intensive shrimp *Litopenaeus vannamei* nursery production. *Aquacultural Eng.* 89, 102063. doi: 10.1016/j.aquaeng.2020.102063

Waldrop, T., Summerfelt, S., Mazik, P., Kenney, P. B., and Good, C. (2020). The effects of swimming exercise and dissolved oxygen on growth performance, fin condition and survival of rainbow trout *Oncorhynchus mykiss*. *Aquaculture Res.* 51 (6), 2582–2589. doi: 10.1111/are.14600

Wang, J. C., Peng, K. W., Lu, H. D., Li, R. H., Song, W. W., Liu, L., et al. (2019). The effect of tank colour on growth performance, stress response and carapace colour of juvenile swimming crab *Portunus trituberculatus*. *Aquaculture Res.* 50 (9), 2735–2742. doi: 10.1111/are.14224

Xiao, R. C., Wei, Y. G., An, D., Li, D. L., Ta, X. X., Wu, Y. H., et al. (2019). A review on the research status and development trend of equipment in water treatment processes of recirculating aquaculture systems. *Rev. Aquaculture* 11 (3), 863–895. doi: 10.1111/raq.12270

Xu, H. Y., Dou, J., Wu, Q. Y., Ye, Y. F., Song, C. B., Mu, C. K., et al. (2022b). Investigation of the light intensity effect on growth, molting, hemolymph lipid, and antioxidant capacity of juvenile swimming crab *Portunus trituberculatus*. *Front. Mar. Sci.* 9. doi: 10.3389/fmars.2022.922021

Xu, H. Y., Dou, J., Wu, Q. Y., Ye, Y. F., Wang, C. L., Song, C. B., et al. (2022a). Photoperiod affects the survival rate but not the development of larval swimming crab *Portunus trituberculatus*. *Aquaculture Int.* 30 (4), 1769–1778. doi: 10.1007/s10499-022-00875-x

Xu, H. Y., Shi, C., Ye, Y. F., Song, C. B., Mu, C. K., and Wang, C. L. (2022c). Time-restricted feeding could not reduce rainbow trout lipid deposition induced by artificial night light. *Metabolites* 12, 904. doi: 10.3390/metabo12100904

Yang, X. T., Zhang, S., Liu, J. T., Gao, Q. F., Dong, S. L., and Zhou, C. (2021). Deep learning for smart fish farming: applications, opportunities and challenges. *Rev. Aquaculture* 13 (1), 66–90. doi: 10.1111/raq.12464

Yu, K. J., Shi, C., Liu, X. Z., Ye, Y. F., Wang, C. L., Mu, C. K., et al. (2022). Tank bottom area influences the growth, molting, stress response, and antioxidant capacity of juvenile mud crab *Scylla paramamosain*. *Aquaculture* 548, 737705. doi: 10.1016/j.aquaculture.2021.737705

Yu, K. J., Shi, C., Ye, Y. F., Li, R. H., Mu, C. K., Ren, Z. M., et al. (2023). The effects of overwintering temperature on the survival of female adult mud crab, *Scylla paramamosain*, under recirculating aquaculture systems as examined by histological analysis of the hepatopancreas and expression of apoptosis-related genes. *Aquaculture* 565, 739080. doi: 10.1016/j.aquaculture.2022.739080

Zhang, W. B., Belton, B., Edwards, P., Henriksson, P. J. G., Little, D. C., Newton, R., et al. (2022a). Aquaculture will continue to depend more on land than sea. *Nature* 603 (7900), E2–E4. doi: 10.1038/s41586-021-04331-3

Zhang, F. F., Zhang, S., Ren, Z. M., Song, C. B., Ye, Y. F., Mu, C. K., et al. (2022b). Light spectrum impacts on development respiratory metabolism and antioxidant capacity of larval swimming crab *Portunus trituberculatus*. *Front. Mar. Sci.* 9. doi: 10.3389/fmars.2022.1071469

Zhao, Z. J., Ding, A. X., Ren, Z. M., Shi, C., Mu, C. K., Wang, C. L., et al. (2023b). Effects of flow velocity on growth, stress and glucose metabolism of mud crab *Scylla paramamosain*. *J. Ningbo Univ. (NSEE)* 36 (2), 9–14.

Zhao, Y., Dou, J., Xu, H. Y., Ma, Z., Ye, Y. F., Mu, C. K., et al. (2023a). Light intensity and photoperiod interaction affects the survival, development, molting and apoptosis-related genes of swimming crab *Portunus trituberculatus* larvae. *Fishes* 8, 221. doi: 10.3390/fishes8050221

frontiers | Frontiers in Marine Science

TYPE Original Research
PUBLISHED 24 August 2022
DOI 10.3389/fmars.2022.997817

OPEN ACCESS

EDITED BY
Ce Shi,
Ningbo University, China

REVIEWED BY
Meng Li,
Department of Environmental Biotechnology, (HZ), Germany
Wansheng Jiang,
Jishou University, China
Donghong Niu,
Shanghai Ocean University, China

*CORRESPONDENCE
Lingling Wang
wanglingling@dlou.edu.cn
Linsheng Song
lshsong@dlou.edu.cn

SPECIALTY SECTION
This article was submitted to Marine Fisheries, Aquaculture and Living Resources, a section of the journal Frontiers in Marine Science

RECEIVED 19 July 2022
ACCEPTED 03 August 2022
PUBLISHED 24 August 2022

CITATION
Gao L, Yu Z, Liu C, Kong N, Wang L and Song L (2022) Characteristics and particularities of bacterial community variation in the offshore shellfish farming waters of the North Yellow Sea.
Front. Mar. Sci. 9:997817.
doi: 10.3389/fmars.2022.997817

Characteristics and particularities of bacterial community variation in the offshore shellfish farming waters of the North Yellow Sea

Lei Gao[1,2], Zichao Yu[1,2], Chao Liu[1,2], Ning Kong[1,2], Lingling Wang[1,2,3,4]* and Linsheng Song[1,2,3,4]*

[1]Liaoning Key Laboratory of Marine Animal Immunology and Disease Control, Dalian Ocean University, Dalian, China, [2]Liaoning Key Laboratory of Marine Animal Immunology, Dalian Ocean University, Dalian, China, [3]Laboratory of Marine Fisheries Science and Food Production Process, Qingdao National Laboratory for Marine Science and Technology, Qingdao, China, [4]Dalian Key Laboratory of Aquatic Animal Disease Prevention and Control, Dalian Ocean University, Dalian, China

Bacteria in coastal waters drive global biogeochemical cycling and are strongly related to coastal environmental safety. The bacterial community in offshore shellfish farming waters of North China has its own characteristics and particularities, while the knowledge is limited. In this study, the bacterial community characteristics, the particularities of bacterial community in the waters with surface cold patches (SCPs) and the variation of pathogenic bacteria were investigated in the offshore shellfish farming waters in the North Yellow Sea (NYS) from 2017 to 2019. For all studied samples, Desulfobacterales acted as the keystone species taxon in microbial co-occurrence networks, and the proportional abundance of Actinobacteriota was found to be as low as 1.3%. The abundance of *Marinobacter* and *Synechococcus* was remarkably prominent in 13 genera with nitrogen-transforming function. The top two different bacterial functions in the spatial analysis (between the waters with SCPs and the ambient waters) were xenobiotics biodegradation and metabolism and metabolism of cofactors and vitamins, which were same with that in the seasonal analysis (between spring and summer). The abundance differences of most pathogenic bacteria analyzed in this study (11 out of 12 genera) also had the same variation dynamics between the spatial analysis and the seasonal analysis. An ANN predictive model for *Vibrio* abundance was constructed for *Vibrio* forecasting, with acceptable predictive accuracy. According to the above results, the bacterial community in the shellfish aquaculture waters in this study was characterized by the enhancing ability of nitrogen removal. Temperature was concluded as the predominant environmental factor to drive the variation of bacterial community function and pathogenic bacteria patterns in the offshore shellfish farming waters with SCPs. The results of this study will further our understanding of the bacterial community characteristics in offshore shellfish

farming waters, and help for *Vibrio* forecasting and coastal environmental safety in aquaculture seawater.

KEYWORDS

shellfish aquaculture, bacterial community, *Vibrio*, surface cold patches, predictive model

Introduction

Bacteria are important components in the marine ecosystem, driving global biogeochemical cycling (Falkowski et al., 2008). They play important roles in maintenance and sustainability of microbial food webs and contribute to the rapid adjustment towards marine environmental changes and deterioration (Dash et al., 2013). The marine planktonic bacteria, especially those distributed near the coast, are of importance in people's life due to their close relationships to human and animal's health, industry and tourism, as about 60% of the world's population residing within 100 km of the coast (Vitousek et al., 1997).

Shellfish have been considered as "keystone species" and "ecosystem engineers" in coastal environment (Gutiérrez et al., 2003; Newell, 2004). The shellfish aquaculture industry, which is always located near the coast, has greatly developed in recent years to meet the growing global demand for protein (eg. 17.7 million tons in 2018) and contribute to world economic development (FAO, 2020). Shellfish are known to modify microbial assemblages by filtering water and transferring nutrients in the water system. On one hand, shellfish aquaculture can reduce water turbidity and improve nutrient recycling in anthropogenic impacted coastal environment, thus acting as an excellent nutrient bioextraction system in eutrophic areas. On the other hand, the suspension filtering and deposition through shellfish aquaculture are always involved in nutrient flux regulation and plankton speciation, which sometimes stimulates the growth of red tide species of plankton (Dumbauld et al., 2009; He et al., 2017). The increasing farming areas and stocking density have raised considerable concern, due to their influence on the marine environment (Yuan et al., 2010; Han et al., 2013). Even though there were some reports about the microbiome in the coastal environment, the bacterial community dynamics concluded from different studies are not always in strong agreement, because of different biogeographic and environmental features (Hartwick et al., 2019). The effect of shellfish aquaculture on the microbial community is quite complex, and the understanding of bacterial community characteristics in offshore shellfish farming waters is very limited.

The North Yellow Sea (NYS) is closed to a continental margin of major economic importance in China and Korea with unique oceanographic characteristics. Shellfish aquaculture is an important industry in the NYS and plays critical roles in the development of the marine economy. It is located near the coastal areas, especially around the islands off the coast, rearing Yesso scallop (*Patinopecten yessoensis*), Pacific oyster (*Crassostrea gigas*) and bay scallop (*Argopecten irradians irradians*), etc. In recent years, aquaculture and industrial wastes run-off and atmospheric deposition also affected the nutrient concentrations in the NYS, further leading to the change of microbial community and dynamics and even hypoxic dead zones (Lin et al., 2005; Tang, 2009). The NYS is always considered as one of the most complicated continental sea areas in the world, due to the seasonal variation of strong currents, wind stress and nutrient-enriched freshwater outflows in the shallow sea area (Hur et al., 1999). The Yellow Sea is also well known because of the Yellow Sea Cold Water Mass, which is a basin-scale water mass of relatively low temperature lying under the seasonal thermocline. Surface cold patches (SCPs) could be observed scattering around the Yellow Sea Cold Water Mass in boreal summer, in contrast to the ambient waters with relative higher sea surface temperature (Xia and Guo, 1983; Zou et al., 2001). The environmental particularity of SCPs was speculated to result in different bacterial communities in shellfish farming waters, while the principal environmental parameter involved in this was not clear. The dynamics of bacterial community variation in the NYS or even in its offshore shellfish farming waters are attracting increasing interest in recent years.

Pathogenic bacteria in coastal waters are strongly related to the health of human and animals. The environmental problems caused by microbiome change and the infections caused by pathogenic bacteria have been reported frequently in shellfish farming waters (Azandégbé et al., 2012; He et al., 2017). Among various potential pathogenic bacteria, the prevalence patterns of *Vibrio* spp. in marine environment are attracting widespread concern, since they include some pathogenic species that could infect to human and other organisms, such as *V. parahaemolyticus* and *V. vulnificus*. Pathogenic species of *Vibrio* spp. in seawater can cause seafood-borne illnesses

through consumption of contaminated seafood and cause wound infections by exposure of an open wound to seawater, probably resulting in diarrhea, septicemia and even death (Hsieh et al., 2008). The forecasting of *Vibrio* abundance and breakout would help to prevent human illness by identifying and reporting the forecasting information and making it publicly available (Froelich et al., 2013; Izumiya et al., 2017).

In short, investigating the characteristics and dynamics of bacterial community variation and potentially pathogenic bacteria in the offshore shellfish farming waters in the NYS would contribute to coastal environmental safety. To achieve this, in the present study, seawater samples were collected from two offshore shellfish farming areas (the waters with SCPs and the ambient waters) in the NYS from every March to August in 2017-2019 with the aims to (1) illuminate the characteristics of bacterial community in the offshore shellfish farming waters and its seasonal dynamics; (2) reveal the particularities of bacterial community in the waters with SCPs; (3) analyze the variation patterns of pathogenic bacteria abundance and develop a predictive model for *Vibrio* abundance level.

Material and methods

Sample collection

Two sampling regions (location X and location Z) were set for the offshore Yesso scallop farming waters in the NYS (Figure S1). The geographic coordinates of location X and Z are N39°17'44"–E122°40'38" and N39°1'7"–E122°42'2", respectively. According to Lü et al. (2010), the location X could be considered as within SCPs and the location Z was among the ambient region with relative higher sea surface temperature, because our three-year data also showed that the surface water temperature in summer in location X was generally 2-3°C lower than that in location Z. There were three sampling sites included in each region as three parallels. The sampling experiments were carried out from March to August in 2017-2019, as March to August was the main period of scallop farming. In this study, spring was defined from March to May, and summer from June to August. Seawater samples were collected at 3 m of depth where scallops were suspension-cultured and were then stored at 4°C within 1 h before further processing as previous description (Yu et al., 2019a; Yu et al., 2019b).

Determination of water parameters

Water temperature (T), salinity (Sal), pH and dissolved oxygen (DO) were monitored using an YSI Professional Plus meter (YSI, Yellow Springs, Ohio, USA) *in situ*. According to the procedures of the National Specification for Marine Monitoring (SOA of China, 2007), the concentration of TAN, NO_2–N, NO_3–N, PO_4-P and SiO_4-Si of the water were analyzed using indophenol blue spectrophotometric method, N-(1-naphthyl)-ethylenediamine dihydrochloride spectrophotometric method, Zn-Cd reduction method, Phosphomolybdenum blue spectrophotometric method and Silicon molybdenum yellow Spectrophotometry method, respectively. The concentration of Chl-*a* was measured with spectrophotometry after extraction with acetone (Lorenzen, 1967).

DNA extraction and high–throughput sequencing

One liter of seawater was filtered using 0.22 μm pore size membranes (Sagon, Shanghai, China) to enrich the microbial cells for each sample, which was then used for genomic DNA extraction using the Water DNA Kit (Omega, GA, USA) following the manufacturer's instruction. DNA quality and quantity were analyzed by 1% agarose gel electrophoresis and NanoDrop spectrophotometer (Thermo Fisher Scientific, DE, USA). The high-throughput sequencing of the V3–V4 hypervariable region of 16S rDNA genes was performed using the Illumina HiSeq platform by Novogene (Beijing, China) with low-quality reads filtered.

Amplicon sequence analysis

The raw reads of the 16S rDNA sequence were processed using Quantitative Insights into Microbial Ecology (QIIME 2) pipeline (Bolyen et al., 2019). Paired-end reads were imported, then trimmed and denoised using DADA2 to remove chimeras and obtain amplicon sequence variants (ASVs). The abundance of nitrogen-transforming bacteria was calculated as log10 (relative abundance proportion * 10000 + 1). Taxonomy was assigned at the single nucleotide level to the ASVs using a feature classifier against a trained SILVA 138 SSU database. Alpha diversity and beta diversity were evaluated using the Shannon diversity index and unweighted UniFrac distances, respectively.

Statistical analysis

MicrobiomeAnalyst (http://www.microbiomeanalyst.ca) was used to compare the abundance and diversity of the bacterial community and to generate visual exploration, with ASV data and the metadata files (Chong et al., 2020). The functional profiles and metabolic pathways of the bacterial communities were predicted using Phylogenetic Investigation of Communities by Reconstruction of Unobserved States

(PICRUSt) 2 software (Douglas et al., 2020). KEGG database was used for the annotation of predicted genes. STAMP software was used for differential analysis of functional profiles (Parks et al., 2014). The co-occurrence ecological network was analyzed using the online Molecular Ecological Network Analysis (MENA) pipeline (http://ieg2.ou.edu/MENA) (Deng et al., 2012), and the network construction was performed using Cytoscape software (Shannon et al., 2003). Redundancy analysis (RDA) was conducted to reveal the effect of environmental factors on the abundance and diversity of bacterial communities using CANOCO software (version 5) (Šmilauer and Lepš, 2014). Correlations between the *Vibrio* abundance and environmental factors were investigated through Spearman's correlation analysis and Pearson's correlation analysis using SPSS 26 (SPSS Inc. Chicago, IL) statistical software package. P-value<0.05 was considered statistically significant. P-value<0.01 was considered extremely significant.

Construction of the predictive model

A predictive model was constructed for the level of *Vibrio* abundance in this study. First, the co-occurrence relationships between the *Vibrio* abundance and the bacterial abundance at order level were investigated using MENA pipeline to get the order taxa (VAO) that were directly associated with the *Vibrio* variation. Second, all tested environmental factors and the VAO abundance were analyzed for their correlation with the *Vibrio* abundance in the next month using Spearman's correlation analysis and Pearson's correlation analysis, to get the factors (VAF, including environmental factors and order taxa) that had significant associations with *Vibrio* variation in the next month in both results of correlation analysis. Third, three levels of *Vibrio* relative abundance were set as High Level (proportional abundance ≥ 2%), Moderate Level (2% > proportional abundance ≥ 0.5%), and Low Level (proportional abundance< 0.5%). The multi-layer feed-forward artificial neural network (ANN) modeling was used to construct and test the neural networking by SPSS 26, using the VAFs as input variables and the *Vibrio* level in the next month as output variable. The feasible ANN model was constructed by trial and error. The ANN was classified into three layers, including input, hidden and output layers. The three layers processed signals and searches to obtain the best linear and nonlinear relationships between the input and output data. In this model, about 70% of the input data was used for training, with the remaining 30% used for testing. Levenberg–Marquardt algorithm was applied for modeling and calculating the weights among the input, hidden and output layers through modifying the learning rate and the number of hidden layers and neurons.

Results

Composition, function and co-occurrence of bacterial community

High-throughput sequencing of 16S rDNA was performed to obtain 12,988,676 sequences, which were clustered into 16,747 ASVs. A total of 415 orders across 56 phyla in all samples were detected through direct taxonomical classification and annotation. Proteobacteria (58.6%), Bacteroidetes (18.6%), Cyanobacteria (12.3%), Firmicutes (3.4%) and Verrucomicrobiota (2.0%) were dominant phyla in seawater accounting for 95.0% of the total abundance (Figure 1A). The average proportional abundance of Actinobacteriota was 1.3%. The abundance of nitrogen-transforming bacteria was investigated, and 13 genera were found in our samples (Figure 2). Among them, *Marinobacter* and *Synechococcus* were consistently present in all samples, and their abundance was markedly higher than that of the other nitrogen-transforming bacteria.

The KEGG pathways that the bacterial community involved were predicted to explore the potential biosynthetic and ecological functions. By searching against the KEGG database using PICRUSt2, a total of 188 third-level pathways were identified, including Valine, leucine and isoleucine biosynthesis, C5-Branched dibasic acid metabolism and Biosynthesis of ansamycins, etc. After grouping into second-level pathways, 36 pathways were determined, including carbohydrate metabolism, infectious disease and replication and repair, etc. For the further grouped first-level pathways, six types were identified (Figure 1A). The co-occurrence analysis was performed to investigate the interaction relationships among specific taxa and to construct the microbial co-occurrence networks. A total of 114 orders (belong to 22 phyla) were included in the network construction (Figure 1B). In general, complex co-occurrence relationships were showed for the whole bacterial community in this result. Among all orders listed in this work, the orders in Proteobacteria processed dominate positions in co-occurrence relationship, which occupied 48.1% of the co-occurrence degree in the whole microbiota. Desulfobacterales was suggested to be the keystone species taxon, as it was most directly associated among all orders in this network.

For the composition variation of bacterial community between spring and summer, some apparent patterns could be observed among different years, indicating that bacterial compositions differed in interannual patterns (Figure 3A). In the PCA analysis of bacterial beta diversity, the bacterial community differed obviously between spring and summer (Figure 3B). This difference could be investigated more clearly in the analysis among different months. Progressive changes could be outlined in bacterial community patterns from March

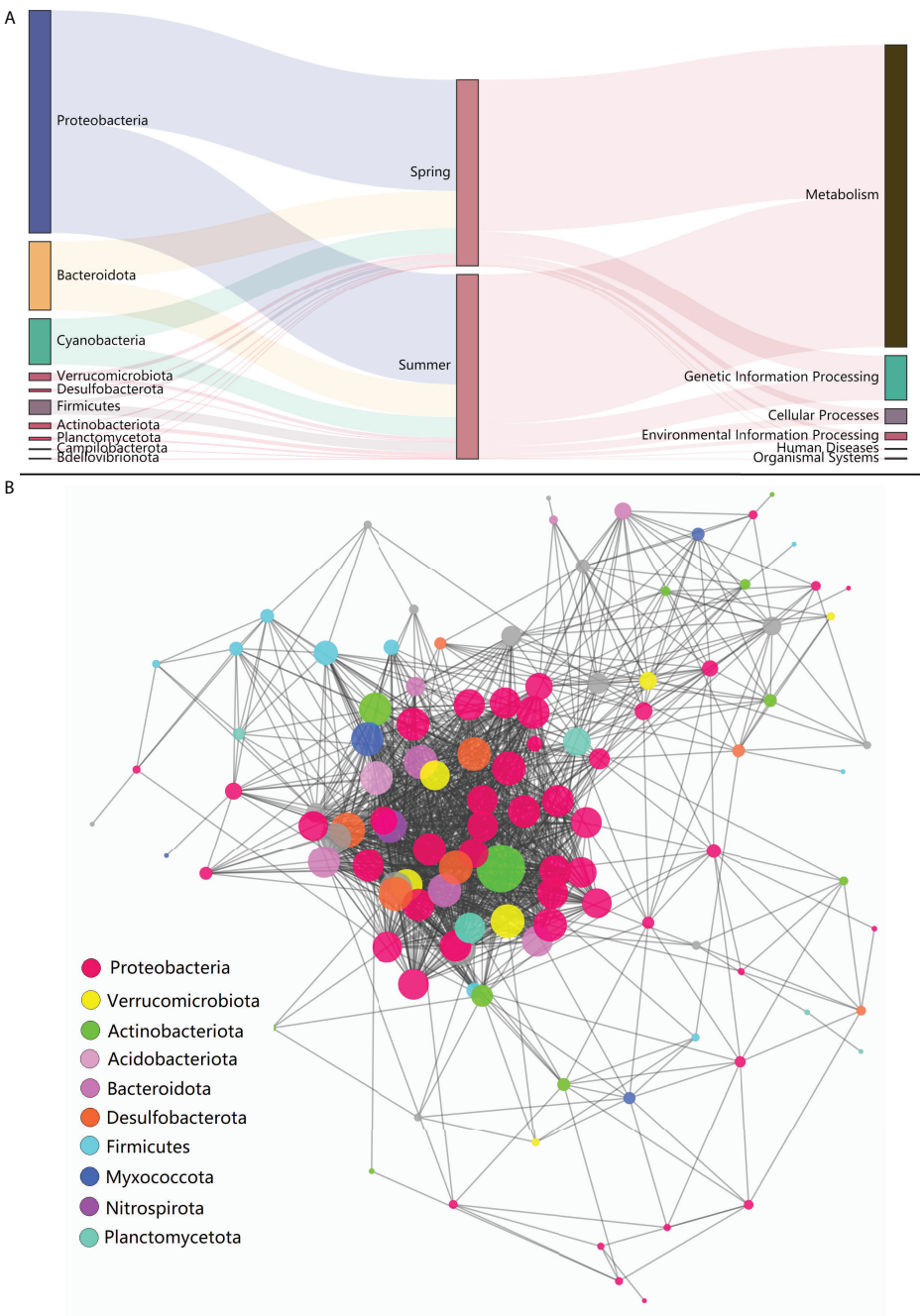

FIGURE 1
Composition, function and co-occurrence of bacterial community. **(A)** Distribution profiles of phylum taxa and functional pathways of the bacterial community; **(B)** Microbial co-occurrence networks at phylum-order level.

to August (Figure 3B). Microbiota comparisons were conducted between spring and summer by LEfSe analysis. Firmicutes and Bacteroidota were identified as discriminative features at phylum level (Figure 3C). Seven genus taxa were identified as discriminative features at genus level, in which *Vibrio* genus was found to be significantly abundant in summer (Figure 3C). The variation of bacterial functional patterns was pronounced at seasonal scales, and the seasonal variation could be discriminated from PCA analysis (Figure 3D). The differently predicted pathways between spring and summer were mainly related to metabolism and cell functional pathways, in which the top two different pathways were xenobiotics biodegradation and

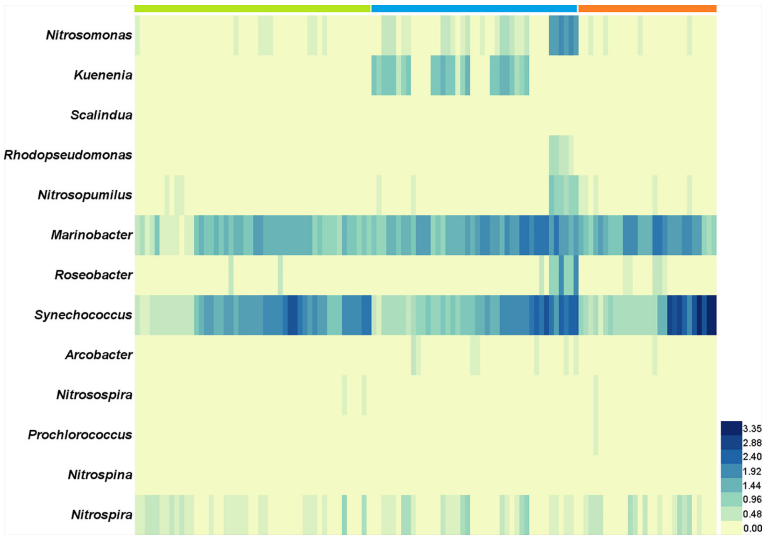

FIGURE 2
The abundance variation of 13 genera of nitrogen-transforming bacteria in the offshore shellfish farming waters. The x-axis is samples in chronological order. Green: 2017; blue: 2018; orange: 2019.

metabolism and metabolism of cofactors and vitamins (Figure 3E). The pathways related to infectious disease were also found to be differently enriched between spring and summer.

The composition and function characteristics of bacterial community in the waters with SCPs

The difference in alpha diversity was non-significant between the two locations (Figure 4A). Differences could be found in some of the most dominant phyla between locations, that the samples from location X had a higher relative abundance of Bacteroidota and Actinobacteriota, and lower relative abundance of Firmicutes (Figure 4B). The differences became even more pronounced in specific seasons or months. For instance, in summer, the variation of six phyla, such as Actinobacteriota, Planctomycetota and Patescibacteria, etc., had significantly different patterns between the two locations (Figure 4C). When further focused on the situation of August, Actinobacteriota was identified as the only discriminative feature at phylum level between the two locations by LEfSe analysis. The functional patterns of the bacterial community did

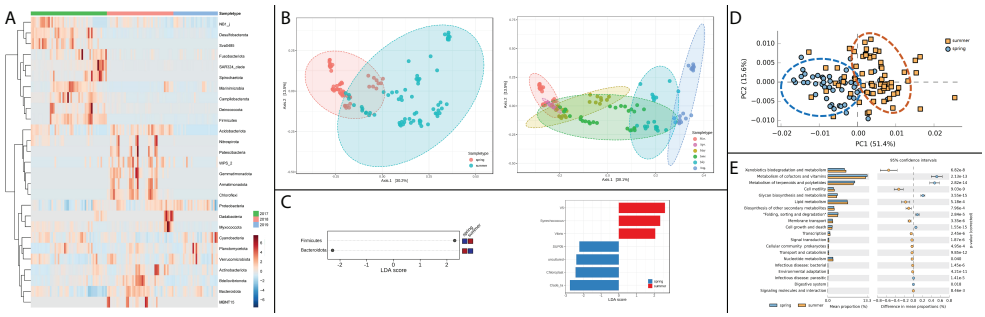

FIGURE 3
Temporal variation of bacterial community and function in shellfish farming areas. **(A)** Annual abundance heatmap at phylum level; **(B)** Seasonal (left) and monthly (right) variation of alpha diversity; **(C)** Discriminative features of bacterial community at phylum level (left) and genus level (right); **(D)** Principal components analysis (PCA) of bacterial functional characterization; **(E)** The functional pathways in significantly temporal variation patterns.

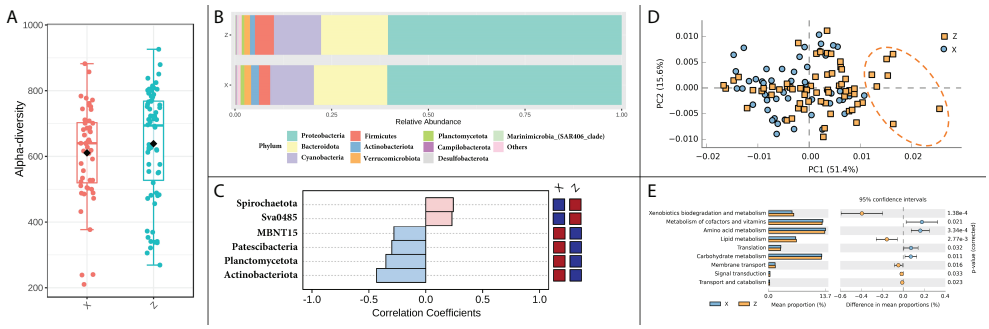

FIGURE 4
Spatial variation of bacterial community and function in shellfish farming areas. **(A)** Bacterial alpha diversity; **(B)** Bacterial relative abundance in phylum level; **(C)** The phyla in significantly spatial variation patterns. **(D)** Principal components analysis (PCA) of bacterial functional characterization; **(E)** The functional pathways in significantly spatial variation patterns.

not differ markedly between locations, but still showing a few differences that could be observed in PCA analysis on PC1 axis, which explained 51.4% of the total variation (Figure 4D). The differently predicted pathways between locations were mainly enriched in metabolism pathways, in which the top two different pathways were xenobiotics biodegradation and metabolism and metabolism of cofactors and vitamins (Figure 4E).

Variation patterns of pathogenic bacteria abundance

During the sampling period of different months, the *Vibrio* abundance generally increased with warming temperature (Figure 5). In order to fully investigate the seasonal variation of potential pathogenic bacteria, the abundance of 12 genera of

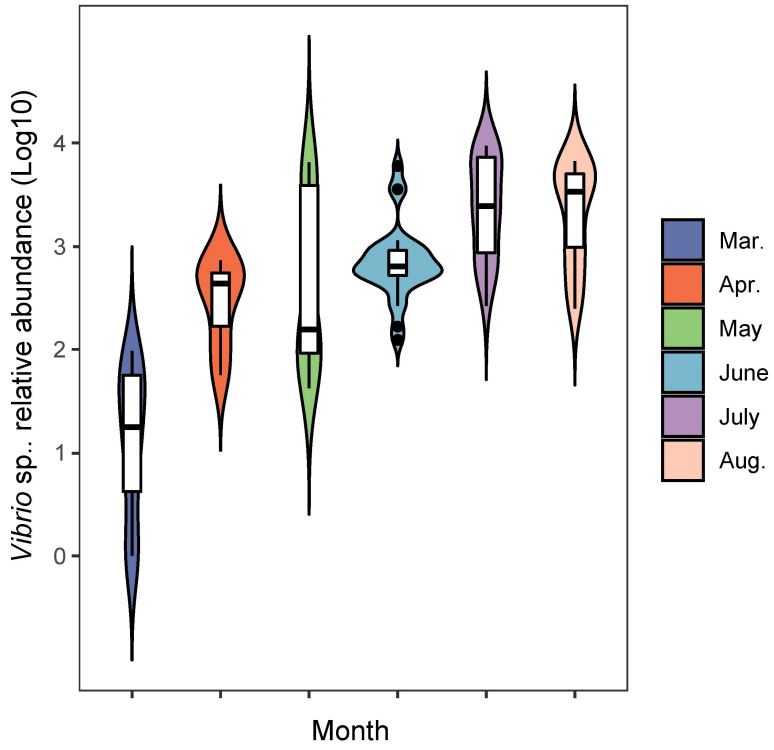

FIGURE 5
The monthly variation of *Vibrio* abundance in shellfish farming areas.

common pathogenic bacteria were analyzed (Figure 6). For the comparison between spring and summer, the average abundance of five genera were higher in spring than in summer (fold of (log10 abundance): 1.02-2.70), including *Shewanella*, *Pseudomonas*, *Streptococcus*, *Campylobacter* and *Escherichia*. The average abundance of the other seven genera were lower in spring than in summer (fold of (log10 abundance): 0.34-0.97), including *Vibrio*, *Aeromonas*, *Photobacterium*, *Francisella*, *Staphylococcus*, *Clostridium* and *Legionella*. For the comparison between the two locations, the average abundance of four genera were higher in location X than in location Z (fold of (log10 abundance): 1.02-1.41), including *Shewanella*, *Streptococcus*, *Campylobacter* and *Escherichia*. The average abundance of eight genera were lower in location X than in

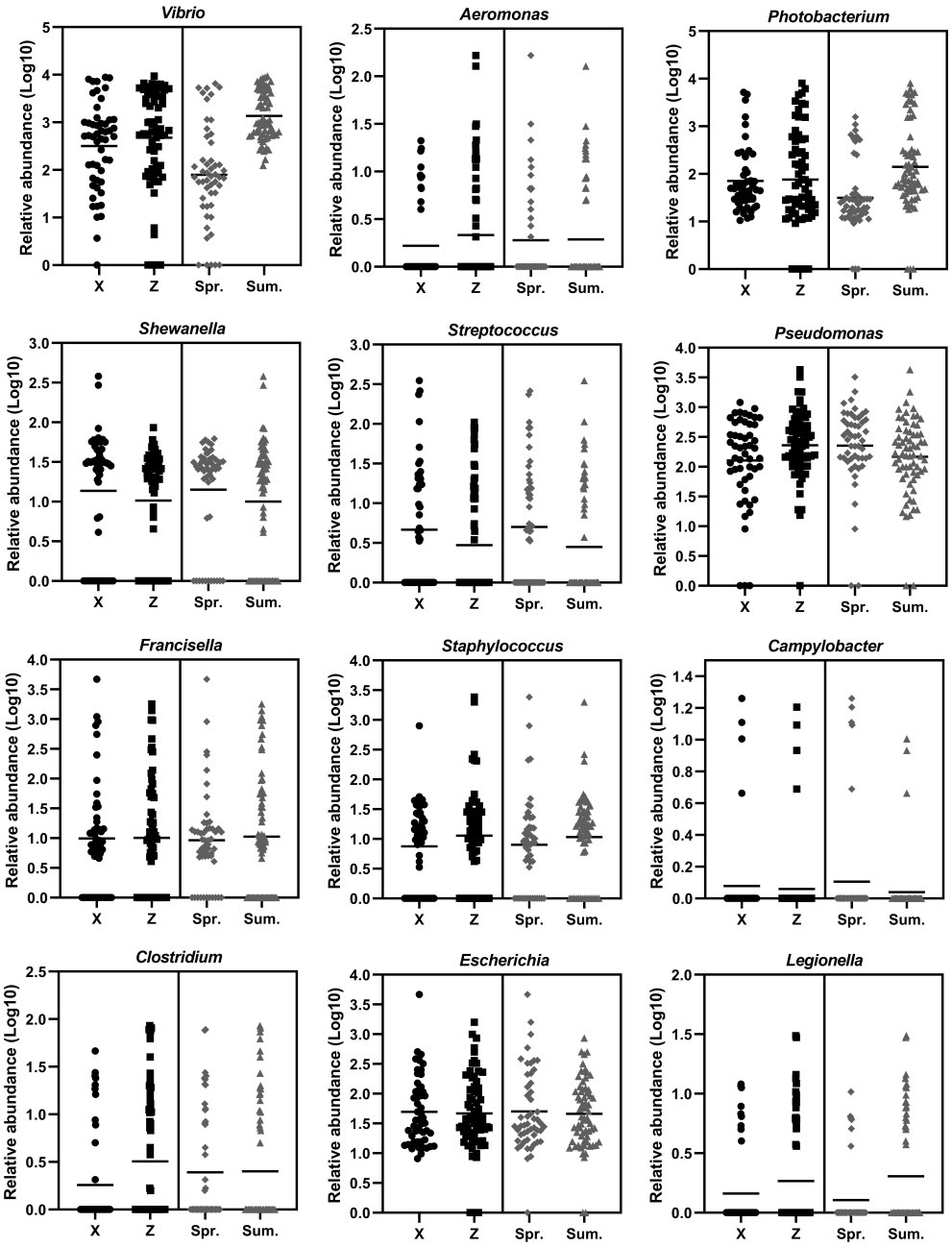

FIGURE 6
The temporal and spatial variation of the abundance of 12 genera of potential pathogenic bacteria. X indicates location X. Z indicates location Z. Spr. indicates spring. Sum. indicates summer.

location Z (fold of (log10 abundance): 0.51-0.99), including *Vibrio*, *Pseudomonas*, *Aeromonas*, *Photobacterium*, *Francisella*, *Staphylococcus*, *Clostridium* and *Legionella*.

Relationships between environmental factors and bacterial community

The relationships between the environmental factors and bacterial community were analyzed and were presented in the RDA biplot (Figure 7A). The first and second RDA axes explained 45.88% and 12.14% of the total variation, respectively. The top three significant environmental factors that constrained the bacterial community were DO, T and Chl-*a*, with the explaining rate of 33.6%, 33.4% and 28.3%, respectively. T and Chl-*a* had a strong negative influence on the abundance of most phyla taxa located in the upper right quadrant and the lower right quadrant, while DO had a strong positive influence instead. WPS-2 generally had an opposite relationship with environmental factors compared to some other phyla that had a positive relationship with DO and a negative relationship with T and Chl-*a*. T and DO almost had no influence on the abundance of SAR324. For specific pairs of environmental factors, T and DO had opposite influences on the bacterial community, while Chl-*a* and SiO_4 had similar influences on the bacterial community. Through Spearman's correlation analysis and Pearson's correlation analysis, the environmental factors that were significantly associated with the *Vibrio* abundance in both analyses were identified, including T, DO, Chl-*a*, SiO_4, PO_4 and Si/N (Figure 7B). The environmental factors that had correlation coefficients above 0.5 in both analyses were T and SiO_4.

Prediction for *Vibrio* abundance level

Before the construction of ANN model, 41 VAOs were found to be directly associated with the *Vibrio* abundance. After the correlation analysis, 32 VAFs were found to be significantly associated with the *Vibrio* abundance in the next month. One hidden layer and 8 neurons in the hidden layer were finally used for the ANN model training, with structure exhibition in Figure 8A. The predictive accuracy was shown in Table S1. The mean predictive accuracy for training samples was 95.8%, with each sub-accuracy above 85%. The mean predictive accuracy for testing samples was 96.4%, with each sub-accuracy above 85%. The prediction probability can also be seen in Figure 8B, which showed acceptable performance of the ANN model for the *Vibrio* abundance level prediction.

Discussion

Characteristics of bacterial community in the offshore shellfish farming waters and its seasonal dynamics

The bacterial phyla dominant in our samples were investigated and were generally consistent with previous studies, in which Proteobacteria, Bacteroidetes, Cyanobacteria and Actinobacteriota, etc. were characterized as the top ubiquitous phyla in the Yellow Sea or other adjacent sea areas (Yu et al., 2018; Kim et al., 2019). However, the proportional abundance of Proteobacteria in this study (58.63%) is relatively higher than that in some other studies (generally below 50%) (He et al., 2017; Yu et al., 2018). The higher abundance of

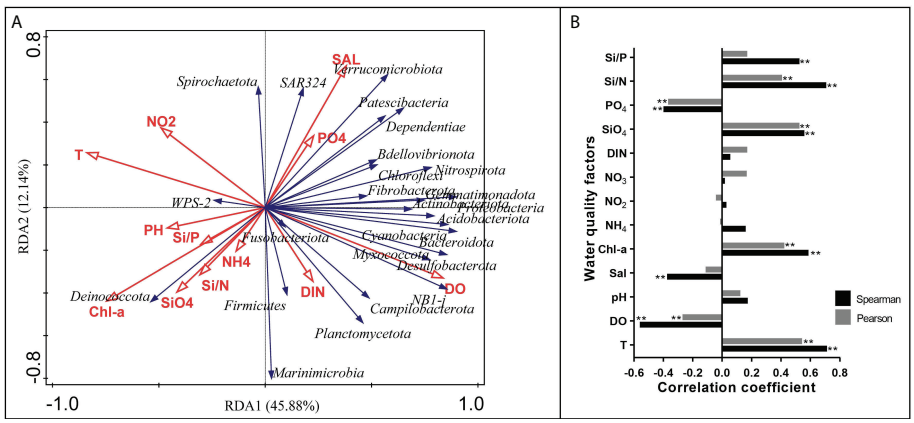

FIGURE 7
Relationships between environmental factors and bacterial community. **(A)** RDA ordination plot for the first two principal dimensions of the relationships between the phylum taxa abundance and environmental factors in shellfish farming areas. **(B)** The correlation between *Vibrio* abundance and environmental factors using Spearman's correlation analysis and Pearson's correlation analysis. "**" represent an extremely significant difference ($P<0.01$).

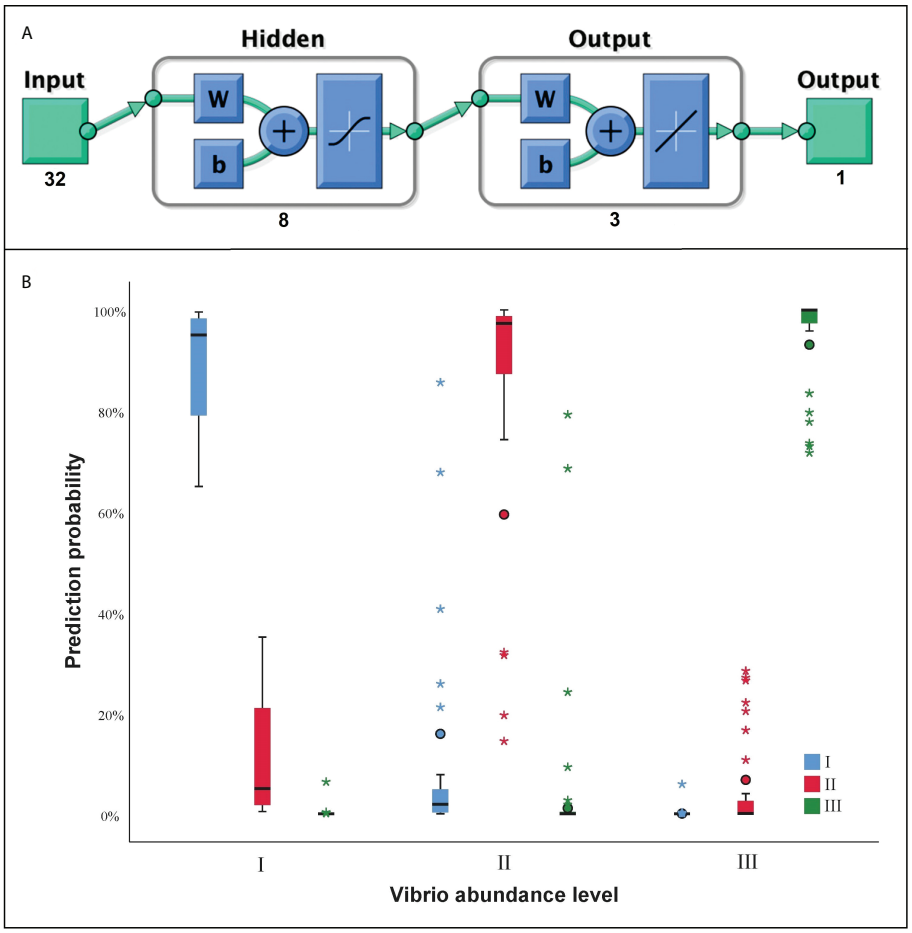

FIGURE 8
The artificial neural network (ANN) for *Vibrio* abundance prediction. **(A)** The structure of ANN layer; **(B)** The prediction probability of ANN model at three abundance level of *Vibrio*. "I, II, III" indicate the three levels of prediction.

Proteobacteria is in agreement with their dominant positions in co-occurrence relationships of microbiota in this study. Proteobacteria is always the dominant bacterial taxon in seawater, and its further increase may preempt the space of other bacteria and reduce microbiota diversification.

The seasonal and monthly variation of the bacterial community was more pronounced than inter-annual variation, mainly due to the intra-annual environmental changes. This followed common sense and was in agreement with other reports. Kim et al. (2019) found that bacterial abundance closely fitted a chronological seasonal pattern in the bays of the Yellow Sea, and temporal patterns of microbial communities were also observed in the New Jersey coast and the Pearl River Estuary area (Nelson et al., 2008; Xie et al., 2018). The monthly progressive changes of bacterial community patterns were probably caused by one factor that was in continuously unidirectional changes, which was most likely the water temperature. Water temperature was always considered as the most important environmental factors that drove the bacterial community (Kim et al., 2019). We can also have this inference according to the results of RDA analysis. The relative high T and low DO in summer may play important roles in constraining and shaping the bacterial community. Except for T and DO, in the present study, Chl-*a* was another important environmental factor that was associated with bacterial community variation. Previous studies also reported that the Chl-*a* was the key predictor of microbiota, and some bacterial taxa were clearly correlated with Chl-*a* (Kim et al., 2019). It should be noted that shellfish aquaculture always has a great influence on the phytoplankton abundance and community, as phytoplankton is the main food source of shellfish. Thus, the bacterial community in the offshore shellfish farming waters would have specific structure patterns, resulted from the phytoplankton variation.

In the present study, Desulfobacterales acted as the keystone species taxon in co-occurrence relationships of microbiota and

may function in nitrogen metabolism with further effect on other bacterial communities through nitrogen cycling. Desulfobacterales plays important roles in nitrogen cycling and removal, and could contribute about 12% of the genes in nitrogen pathways (Nie et al., 2021). Recently, dominant sulfate reducing microorganisms (SRM) within Desulfobacterales were also reported in the sediments of coastal oyster aquaculture ecosystems (Mara et al., 2021). The proportional abundance of Actinobacteriota (1.3%) in this study was obviously lower than that in other studies, in which it was reported up to 5%-20% (He et al., 2017; Yu et al., 2018). The abundance of Actinobacteriota has been proved to be strongly correlated with nitrogen cycling, and it can thrive under oligotrophic conditions and be suppressed with high organic matter and inorganic nutrient availability (Kulaš et al., 2021; Wang et al., 2021). The impact of shellfish farming on nitrogen cycling has been investigated in previous reports by analyses of water/sediment quality parameters (Erler et al., 2017; Jiang et al., 2020; Pan et al., 2021). The understanding of the bacterial community characteristics involved in nitrogen cycling in shellfish farming water is very limited. In order to further explore the details of nitrogen-transforming function of bacterial community, the commonly reported nitrogen-transforming bacteria (Kuypers et al., 2018) were investigated in our study. The presence of *Marinobacter* and *Synechococcus* was remarkably prominent in all 13 genera with nitrogen-transforming function. *Marinobacter* and *Synechococcus* were mainly responsible for the process and remove of organic nitrogen and NH_4^+ in seawater. The bacterial community characteristics involved in nitrogen cycling were rarely reported in the Yellow Sea (Bai et al., 2012; Yu et al., 2018; Jing et al., 2019; Yang et al., 2022). Together, the above results indicated that the bacterial community in the shellfish aquaculture waters in this study was characterized by the enhancing ability of nitrogen removal.

The particularities of bacterial community in the waters with SCPs

The bacterial community between the two locations had less variation compared to the seasonal variation. Greater temporal variation and less spatial variation of the bacterial community were also found in the Yellow Sea area and some aquaculture sea areas (He et al., 2017; Kim et al., 2019). Spatial differentiation may superficially mask the environmental effects only when the physicochemical factors are closely related to the spatial conditions. Otherwise, persistent environmental heterogeneity would cover the geographic difference and shape the microbial diversity directly at intermediate spatial scales (Crossland et al., 2005; Wang et al., 2015).

SCP is an important geographic feature of the Yellow Sea and some other seas. Its formation results from the upwelling, which carries the cold deep water up to the sea surface. The more water exchange in vertical direction may change the water environment and bring more nutrients and attachments from the bottom water layer to surface water layer (Lü et al., 2010; Huang et al., 2018; Lin et al., 2019). In our study, the bacterial community variation between the two locations had more significant differences in summer than that in spring. It was suggested that different geographic conditions may lead to the variation of the bacterial community, mainly through the environmental factor variation. Environmental factors always play key roles in the spatial variation of the bacterial community. For instance, the different concentration levels of Chl-*a* were reported to be in charge of the bacterial community diversity between two stations of the Yellow Sea (Kim et al., 2019).

Interestingly, consistency was found in two points between the spatial analysis (location X *vs* location Z) and the seasonal analysis (spring *vs* summer). First, the top two differently predicted pathways of microbial function in both spatial analysis and seasonal analysis were same, and they were xenobiotics biodegradation and metabolism and metabolism of cofactors and vitamins, which may indicate the occurrence of environmental stresses and resultant activation of stress responses (Huo et al., 2019; Ye et al., 2021). Second, 11 of the 12 common genera of pathogenic bacteria (except for *Pseudomonas*) had the same dynamic patterns in the spatial and seasonal analyses, in other words, if the abundance of one pathogenic bacterial genus was higher (or lower) in the waters with SCP than that in ambient waters, it was most likely that the abundance of the pathogenic bacterial genus was also higher (or lower) in spring than that in summer. Temperature was the predominant environmental factor that drove the seasonal dynamic of bacterial community variation between spring and summer. Temperature was also the most critical feature that distinguished the waters with SCP from ambient waters. As there are highly similar dynamic patterns of bacterial community variation between the seasonal and spatial analyses, it is reasonable to speculate that temperature is the predominant environmental factor to drive the variation of bacterial community function and pathogenic bacteria patterns in the offshore shellfish farming waters with SCPs.

Vibrio abundance variation and the predictive model construction

The *Vibrio* abundance generally increased with the elevated water temperature and showed clear seasonal patterns, consistent with some other reports (Hsieh et al., 2008; Vezzulli et al., 2009; Oberbeckmann et al., 2012; Froelich et al., 2015). The enrichment of the pathways related to infectious disease in summer suggested that the risk from pathogenic bacteria increased in summer and need more attention. Shellfish aquaculture was found to play important roles in shaping *Vibrio* characteristics (Joye and Anderson, 2008; Feinman et al., 2018), probably through disturbing the structure of

phytoplankton and zooplankton, both of which served as determinants of *Vibrio* presence and abundance (Johnson, 2015). There were many reports about the *Vibrio* variation in water environment, in which the key environmental factors that affect *Vibrio* community were identified and the variation tendency of *Vibrio* was speculated based on environmental factors (Hsieh et al., 2008; Oberbeckmann et al., 2012; Johnson, 2015). In the present study, except for T, SiO_4-Si was also found to be significantly associated with the *Vibrio* abundance. We speculate that: On one hand, SiO_4-Si exists in the sea-water column as a sol state, which could provide attachment for the growth of *Vibrio*. On the other hand, phytoplankton and Chl-*a* are key drivers of the bacterial community. SiO_4-Si is an important component of some phytoplankton taxa such as diatom (DeLuca et al., 2020) and could thus influence the *Vibrio* abundance. However, as shown in Figure 6, the *Vibrio* abundance in the same month of the different years differed apparently based on the three-year data, suggesting that it is infeasible to estimate the *Vibrio* abundance only according to environmental factors or historical values of *Vibrio* abundance.

In recent years, some studies of model establishment and *Vibrio* prediction have been reported. Hidemasa Izumiya et al. conducted a multi-coastal study to examine relationships between environmental factors and *Vibrio* and build a linear regression model for *Vibrio* prediction (Izumiya et al., 2017). Brett Froelich et al. conducted a five-parameter mechanistic model to predict *Vibrio* abundance in the river based on environmental processes (Froelich et al., 2013). According to the previous reports, the construction of *Vibrio* predictive model is better to be improved in two points. First, environmental factors were always included in the predictive model construction as the only type of input variables in most of the previous studies. Aside from the environmental factors, *Vibrio* are also likely to respond to, or be associated with, many other aquatic bacterial species (Johnson, 2015) in some ways, such as quorum sensing. The interactions between *Vibrio* and other bacterial communities should also be included in the studies of *Vibrio* forecasting. Second, among the environmental factors, one factor usually has weak or strong dependence on others. The exclusive effect of one environmental factor on *Vibrio* abundance is hard to assess. The relationship between *Vibrio* and input variables of the predictive model is not a direct correlation but rather the relation to which many variables contribute. Multiple regression analysis is not good at the modelling with too many input variables in the construction of *Vibrio* predictive model. Therefore, an integrated model that has environmental factors and bacterial species as input variables should be established to better understand the variation of *Vibrio* abundance.

Our study improved the *Vibrio* predictive modelling by (1) including the environmental factors as well as bacterial species as input variables for more accurate prediction of *Vibrio* abundance; (2) using ANN to solve the complex mapping relationships between dozens of input variables and *Vibrio* abundance and to construct the predictive model. The accuracy was acceptable, with 95.8% of accuracy for training samples and 96.4% for testing samples. The spatial scope of model application and the accuracy will be further improved in our future studies through the inclusion of more data for model training, as the *Vibrio* prediction is better to be processed according to regional differences, rather than using a "one-size-fits-all" approach. The results of this study will contribute to the monitoring and modelling efforts of *Vibrio* abundance in the NYS for area-specific *Vibrio* forecasting and public health risk prediction.

Conclusions

The main conclusions drawn from this study are as following (Figure S2):

- The bacterial community in the shellfish aquaculture waters in this study was characterized by the enhancing ability of nitrogen removal.
- Temperature was the predominant environmental factor to drive the variation of bacterial community function and pathogenic bacteria patterns in the offshore shellfish farming waters with SCPs.
- An ANN predictive model for *Vibrio* abundance was constructed in this study for *Vibrio* forecasting, with acceptable predictive accuracy.

Data availability statement

The data presented in the study are deposited in the GenBank repository, accession number PRJNA861897.

Author contributions

LG: Methodology, Formal analysis, Writing original draft; ZY: Investigation, Sample collection; CL and NK: Sample collection; LW and LS: Writing Review & Editing, Supervision, Funding acquisition. All authors contributed to the article and approved the submitted version.

Funding

This research was supported by a grant (41961124009) from National Science Foundation of China, National key R&D Program of China (2018YFD0900501), China Agriculture Research System of MOF and MARA, the Fund for Outstanding Talents and Innovative Team of Agricultural Scientific Research in MARA, the Research Foundation for Climbing Scholar in Liaoning, and Distinguished Professor in Liaoning (XLYC1902012), Key R&D Program of Liaoning Province (2017203001, 2017203004), the Scientific Research

Project of Liaoning Province Department of Education (No. QL201902), the Research Foundation for Talented Scholars in Dalian Ocean University (to LW), and the Science and Technology Innovation Fund of Dalian (2021JJ13SN73).

Conflict of interest

The authors declare that the research was conducted in the absence of any commercial or financial relationships that could be construed as a potential conflict of interest.

Publisher's note

All claims expressed in this article are solely those of the authors and do not necessarily represent those of their affiliated organizations, or those of the publisher, the editors and the reviewers. Any product that may be evaluated in this article, or claim that may be made by its manufacturer, is not guaranteed or endorsed by the publisher.

Supplementary material

The Supplementary Material for this article can be found online at: https://www.frontiersin.org/articles/10.3389/fmars.2022.997817/full#supplementary-material

SUPPLEMENTARY FIGURE 1
Location X and location Z were set as the two sampling regions for the offshore Yesso scallop farming waters in the NYS. Horizontal distribution of mean sea surface temperature in August of 2004–2008 was showed. This figure is cited from (Lü et al., 2010).

SUPPLEMENTARY FIGURE 2
Graphical abstract of this study.

SUPPLEMENTARY TABLE 1
The prediction accuracy of ANN model for *Vibrio* abundance for both training samples and testing samples.

References

Azandégbé, A., Poly, F., Andrieux Loyer, F., Kérouel, R., Philippon, X., and Nicolas, J. L. (2012). Influence of oyster culture on biogeochemistry and bacterial community structure at the sediment–water interface. *FEMS Microbiol. Ecol.* 82 (1), 102–117. doi: 10.1111/j.1574-6941.2012.01410.x

Bai, X., Wang, M., Liang, Y., Zhang, Z., Wang, F., and Jiang, X. (2012). Distribution of microbial populations and their relationship with environmental variables in the North Yellow Sea, china. J. *Ocean U. China* 11 (1), 75–85. doi: 10.1007/s11802-012-1799-8

Bolyen, E., Rideout, J. R., Dillon, M. R., Bokulich, N. A., Abnet, C. C., Al Ghalith, G. A., et al. (2019). Reproducible, interactive, scalable and extensible microbiome data science using QIIME 2. *Nat. Biotechnol.* 37 (8), 852–857. doi: 10.1038/s41587-019-0209-9

Chong, J., Liu, P., Zhou, G., and Xia, J. (2020). Using MicrobiomeAnalyst for comprehensive statistical, functional, and meta-analysis of microbiome data. *Nat. Protoc.* 15 (3), 799–821. doi: 10.1038/s41596-019-0264-1

Crossland, C. J., Kremer, H. H., Lindeboom, H., Crossland, J. I. M., and Le Tissier, M. D. (2005). *Coastal fluxes in the anthropocene: the land-ocean interactions in the coastal zone project of the international geosphere-biosphere programme* (Berlin: Springer Science & Business Media).

Dash, H. R., Mangwani, N., Chakraborty, J., Kumari, S., and Das, S. (2013). Marine bacteria: potential candidates for enhanced bioremediation. *Appl. Microbiol. Biot.* 97 (2), 561–571. doi: 10.1007/s00253-012-4584-0

DeLuca, N. M., Zaitchik, B. F., Guikema, S. D., Jacobs, J. M., Davis, B. J., and Curriero, F. C. (2020). Evaluation of remotely sensed prediction and forecast models for vibrio parahaemolyticus in the Chesapeake bay. *Remote Sens. Environ.* 250, 112016. doi: 10.1016/j.rse.2020.112016

Deng, Y., Jiang, Y. H., Yang, Y., He, Z., Luo, F., and Zhou, J. (2012). Molecular ecological network analyses. *BMC Bioinform.* 13 (1), 1–20. doi: 10.1186/1471-2105-13-113

Douglas, G. M., Maffei, V. J., Zaneveld, J. R., Yurgel, S. N., Brown, J. R., Taylor, C. M., et al. (2020). PICRUSt2 for prediction of metagenome functions. *Nat. Biotechnol.* 38 (6), 685–688. doi: 10.1038/s41587-020-0548-6

Dumbauld, B. R., Ruesink, J. L., and Rumrill, S. S. (2009). The ecological role of bivalve shellfish aquaculture in the estuarine environment: A review with application to oyster and clam culture in West Coast (USA) estuaries. *Aquaculture* 290 (3-4), 196–223. doi: 10.1016/j.aquaculture.2009.02.033

Erler, D. V., Welsh, D. T., Bennet, W. W., Meziane, T., Hubas, C., Nizzoli, D., et al. (2017). The impact of suspended oyster farming on nitrogen cycling and nitrous oxide production in a sub-tropical Australian estuary. *Estuar. Coast. Shelf Sci.* 192, 117–127. doi: 10.1016/j.ecss.2017.05.007

Falkowski, P. G., Fenchel, T., and Delong, E. F. (2008). The microbial engines that drive earth's biogeochemical cycles. *Science* 320 (5879), 1034–1039. doi: 10.1126/science.1153213

FAO (2020). *The state of world fisheries and aquaculture 2020, sustainability in action* (Rome: Food and Agriculture Organization of the United Nations).

Feinman, S. G., Farah, Y. R., Bauer, J. M., and Bowen, J. L. (2018). The influence of oyster farming on sediment bacterial communities. *Estuaries Coast.* 41 (3), 800–814. doi: 10.1007/s12237-017-0301-7

Froelich, B., Ayrapetyan, M., Fowler, P., Oliver, J., and Noble, R. (2015). Development of a matrix tool for the prediction of vibrio species in oysters harvested from North Carolina. *Appl. Environ. Microb.* 81 (3), 1111–1119. doi: 10.1128/AEM.03206-14

Froelich, B., Bowen, J., Gonzalez, R., Snedeker, A., and Noble, R. (2013). Mechanistic and statistical models of total vibrio abundance in the neuse river estuary. *Water Res.* 47 (15), 5783–5793. doi: 10.1016/j.watres.2013.06.050

Gutiérrez, J. L., Jones, C. G., Strayer, D. L., and Iribarne, O. O. (2003). Mollusks as ecosystem engineers: The role of shell production in aquatic habitats. *Oikos* 101 (1), 79–90. doi: 10.1034/j.1600-0706.2003.12322.x

Han, Q., Wang, Y., Zhang, Y., Keesing, J., and Liu, D. (2013). Effects of intensive scallop mariculture on macrobenthic assemblages in Sishili Bay, the Northern Yellow Sea of China. *Hydrobiologia* 718 (1), 1–15. doi: 10.1007/s10750-013-1590-x

Hartwick, M. A., Urquhart, E. A., Whistler, C. A., Cooper, V. S., Naumova, E. N., and Jones, S. H. (2019). Forecasting seasonal vibrio parahaemolyticus concentrations in New England shellfish. *Int. J. Environ. Res. Public Health* 16 (22), 4341. doi: 10.3390/ijerph16224341

He, Y., Sen, B., Shang, J., He, Y., Xie, N., Zhang, Y., et al. (2017). Seasonal influence of scallop culture on nutrient flux, bacterial pathogens and bacterioplankton diversity across estuaries off the bohai Sea coast of Northern China. *Mar. pollut. Bull.* 124 (1), 411–420. doi: 10.1016/j.marpolbul.2017.07.062

Hsieh, J. L., Fries, J. S., and Noble, R. T. (2008). Dynamics and predictive modelling of vibrio spp. in the neuse river estuary, north Carolina, USA. *Environ. Microbiol.* 10 (1), 57–64. doi: 10.1111/j.1462-2920.2007.01429.x

Huang, M., Liang, X. S., Wu, H., and Wang, Y. (2018). Different generating mechanisms for the summer surface cold patches in the Yellow Sea. *Atmos. Ocean* 56 (4), 199–211. doi: 10.1080/07055900.2017.1371580

Huo, D., Sun, L., Zhang, L., Ru, X., Liu, S., and Yang, H. (2019). Metabolome responses of the sea cucumber apostichopus japonicus to multiple environmental stresses: Heat and hypoxia. *Mar. Pollut. Bull.* 138, 407–420. doi: 10.1016/j.marpolbul.2018.11.063

Hur, H., Jacobs, G., and Teague, W. (1999). Monthly variations of water masses in the Yellow and East China seas, November 6, 1998. *J. Oceanogr.* 55 (2), 171–184. doi: 10.1023/A:1007885828278

Izumiya, H., Furukawa, M., Ogata, K., Isobe, J., Watanabe, S., Sasaki, M., et al. (2017). A double-quadratic model for predicting vibrio species in water environments of Japan. *Arch. Microbiol.* 199 (9), 1293–1302. doi: 10.1007/s00203-017-1402-1

Jiang, H., Lan, W., Li, T., Xu, Z., Liu, W., and Pan, K. (2020). Isotopic composition reveals the impact of oyster aquaculture on pelagic nitrogen cycling in a subtropical estuary. *Water Res.* 187, 116431. doi: 10.1016/j.watres.2020.116431

Jing, X., Gou, H., Gong, Y., Ji, Y., Su, X., Zhang, J., et al. (2019). Seasonal dynamics of the coastal bacterioplankton at intensive fish-farming areas of the yellow Sea, China revealed by high-throughput sequencing. *Mar. Pollut. Bull.* 139, 366–375. doi: 10.1016/j.marpolbul.2018.12.052

Johnson, C. N. (2015). Influence of environmental factors on vibrio spp. in coastal ecosystems. *Microbiol. Spectr.* 3 (3), VE–0008-2014. doi: 10.1128/microbiolspec.VE-0008-2014

Joye, S. B., and Anderson, I. C. (2008). *Nitrogen in the marine environment* (Burlington, MA: Academic Press).

Kim, J. G., Gwak, J. H., Jung, M. Y., An, S. U., Hyun, J. H., Kang, S., et al. (2019). Distinct temporal dynamics of planktonic archaeal and bacterial assemblages in the bays of the yellow Sea. *PloS One* 14 (8), e0221408. doi: 10.1371/journal.pone.0221408

Kulaš, A., Marković, T., Žutinić, P., Kajan, K., Karlović, I., Orlić, S., et al. (2021). Succession of microbial community in a small water body within the alluvial aquifer of a large river. *Water* 13 (2), 115. doi: 10.3390/w13020115

Kuypers, M. M., Marchant, H. K., and Kartal, B. (2018). The microbial nitrogen-cycling network. *Nat. Rev. Microbiol.* 16 (5), 263–276. doi: 10.1038/nrmicro.2018.9

Lin, L., Liu, D., Luo, C., and Xie, L. (2019). Double fronts in the yellow Sea in summertime identified using sea surface temperature data of multi-scale ultra-high resolution analysis. *Cont. Shelf Res.* 175, 76–86. doi: 10.1016/j.csr.2019.02.004

Lin, C., Ning, X., Su, J., Lin, Y., and Xu, B. (2005). Environmental changes and the responses of the ecosystems of the Yellow Sea during 1976–2000. *J. Mar. Syst.* 55 (3-4), 223–234. doi: 10.1016/j.jmarsys.2004.08.001

Lorenzen, C. J. (1967). Determination of chlorophyll and pheo-pigments: spectrophotometric equations 1. *Limnol. Oceanogr.* 12 (2), 343–346. doi: 10.4319/lo.1967.12.2.0343

Lü, X., Qiao, F., Xia, C., Wang, G., and Yuan, Y. (2010). Upwelling and surface cold patches in the Yellow Sea in summer: Effects of tidal mixing on the vertical circulation. *Cont. Shelf Res.* 30 (6), 620–632. doi: 10.1016/j.csr.2009.09.002

Mara, P., Edgcomb, V. P., Sehein, T. R., Beaudoin, D., Martinsen, C., Lovely, C., et al. (2021). Comparison of oyster aquaculture methods and their potential to enhance microbial nitrogen removal from coastal ecosystems. *Front. Mar. Sci.* 8, 174. doi: 10.3389/fmars.2021.633314

Nelson, J. D., Boehme, S. E., Reimers, C. E., Sherrell, R. M., and Kerkhof, L. J. (2008). Temporal patterns of microbial community structure in the mid-Atlantic bight. *FEMS Microbiol. Ecol.* 65 (3), 484–493. doi: 10.1111/j.1574-6941.2008.00553.x

Newell, R. I. (2004). Ecosystem influences of natural and cultivated populations of suspension-feeding bivalve molluscs: A review. *J. Shellfish Res.* 23 (1), 51–62.

Nie, S., Zhang, Z., Mo, S., Li, J., He, S., Kashif, M., et al. (2021). Desulfobacterales stimulates nitrate reduction in the mangrove ecosystem of a subtropical gulf. *Sci. Total Environ.* 769, 144562. doi: 10.1016/j.scitotenv.2020.144562

Oberbeckmann, S., Fuchs, B. M., Meiners, M., Wichels, A., Wiltshire, K. H., and Gerdts, G. (2012). Seasonal dynamics and modeling of a vibrio community in coastal waters of the north Sea. *Microb. Ecol.* 63 (3), 543–551. doi: 10.1007/s00248-011-9990-9

Pan, K., Lan, W., Li, T., Hong, M., Peng, X., Xu, Z., et al. (2021). Control of phytoplankton by oysters and the consequent impact on nitrogen cycling in a subtropical bay. *Sci. Total Environ.* 796, 149007. doi: 10.1016/j.scitotenv.2021.149007

Parks, D. H., Tyson, G. W., Hugenholtz, P., and Beiko, R. G. (2014). STAMP: statistical analysis of taxonomic and functional profiles. *Bioinformatics* 30 (21), 3123–3124. doi: 10.1093/bioinformatics/btu494

Shannon, P., Markiel, A., Ozier, O., Baliga, N. S., Wang, J. T., Ramage, D., et al. (2003). Cytoscape: A software environment for integrated models of biomolecular interaction networks. *Genome Res.* 13 (11), 2498–2504. doi: 10.1101/gr.1239303

Šmilauer, P., and Lepš, J. (2014). *Multivariate analysis of ecological data using CANOCO 5* (Cambridge: Cambridge University Press).

SOA of China (2007). *Specification for marine monitoring* (China: Standards Press of China, Beijing, China).

Tang, Q. (2009). *Changing states of the yellow Sea Large marine ecosystem: anthropogenic forcing and climate impacts. sustaining the world's large marine ecosystems* (Amsterdam: Elsevier Science Press).

Vezzulli, L., Pezzati, E., Moreno, M., Fabiano, M., Pane, L., Pruzzo, C., et al. (2009). Benthic ecology of vibrio spp. and pathogenic vibrio species in a coastal Mediterranean environment (La spezia gulf, Italy). *Microb. Ecol.* 58 (4), 808–818. doi: 10.1007/s00248-009-9542-8

Vitousek, P. M., Mooney, H. A., Lubchenco, J., and Melillo, J. M. (1997). Human domination of earth's ecosystems. *Science* 277 (5325), 494–499. doi: 10.1126/science.277.5325.494

Wang, S., Li, X., Zhang, M., Jiang, H., Wang, R., Qian, Y., et al. (2021). Ammonia stress disrupts intestinal microbial community and amino acid metabolism of juvenile yellow catfish (Pelteobagrus fulvidraco). *Ecotox. Environ. Safe* 227, 112932. doi: 10.1016/j.ecoenv.2021.112932

Wang, K., Ye, X., Chen, H., Zhao, Q., Hu, C., He, J., et al. (2015). Bacterial biogeography in the coastal waters of northern zhejiang, East China Sea is highly controlled by spatially structured environmental gradients. *Environ. Microbiol.* 17 (10), 3898–3913. doi: 10.1111/1462-2920.12884

Xia, Z., and Guo, B. (1983). The cold water and upwelling in the tip areas of Shandong peninsula and liaodong peninsula. *J. Oceanography Huanghai Bohai Seas* 1 (1), 13–19.

Xie, W., Luo, H., Murugapiran, S. K., Dodsworth, J. A., Chen, S., Sun, Y., et al. (2018). Localized high abundance of marine group II archaea in the subtropical pearl river estuary: Implications for their niche adaptation. *Environ. Microbiol.* 20 (2), 734–754. doi: 10.1111/1462-2920.14004

Yang, B., Gao, X., Zhao, J., Xie, L., Liu, Y., Lv, X., et al. (2022). The impacts of intensive scallop farming on dissolved organic matter in the coastal waters adjacent to the yangma island, Northern Yellow Sea. *Sci. Total Environ.* 807, 150989. doi: 10.1016/j.scitotenv.2021.150989

Ye, G., Zhang, X., Yan, C., Lin, Y., and Huang, Q. (2021). Polystyrene microplastics induce microbial dysbiosis and dysfunction in surrounding seawater. *Environ. Int.* 156, 106724. doi: 10.1016/j.envint.2021.106724

Yuan, X., Zhang, M., Liang, Y., Liu, D., and Guan, D. (2010). Self-pollutant loading from a suspension aquaculture system of Japanese scallop (Patinopecten yessoensis) in the changhai sea area, Northern Yellow Sea of China. *Aquaculture* 304 (1-4), 79–87. doi: 10.1016/j.aquaculture.2010.03.026

Yu, Z., Liu, C., Fu, Q., Lu, G., Han, S., Wang, L., et al. (2019a). The differences of bacterial communities in the tissues between healthy and diseased yesso scallop (Patinopecten yessoensis). *AMB Express* 9 (1), 1–13. doi: 10.1186/s13568-019-0870-x

Yu, Z., Liu, C., Wang, F., Xue, Z., Zhang, A., Lu, G., et al. (2019b). Diversity and annual variation of phytoplankton community in yesso scallop (Patinopecten yessoensis) farming waters of Northern Yellow Sea of China. *Aquaculture* 511, 734266. doi: 10.1016/j.aquaculture.2019.734266

Yu, S., Pang, Y., Wang, Y., Li, J., and Qin, S. (2018). Distribution of bacterial communities along the spatial and environmental gradients from bohai Sea to Northern Yellow Sea. *PeerJ* 6, e4272. doi: 10.7717/peerj.4272

Zou, E., Guo, B., Tang, Y., Lee, J., and Lie, H. (2001). An analysis of summer hydrographic features and circulation in the Southern Yellow Sea and the northern East China Sea. *Oceanologia Limnologia Sin.* 32 (3), 348–348.

frontiers | Frontiers in Marine Science

TYPE Brief Research Report
PUBLISHED 13 September 2022
DOI 10.3389/fmars.2022.1000703

OPEN ACCESS

EDITED BY
Ce Shi,
Ningbo University, China

REVIEWED BY
Jiamin Sun,
Shanghai Ocean University, China
Kai Zhang,
Pearl River Fisheries Research Institute (CAFS), China
Xiaona Ma,
Jiangsu Ocean University, China

*CORRESPONDENCE
Jian Zhu
zhuj@ffrc.cn

SPECIALTY SECTION
This article was submitted to Marine Fisheries, Aquaculture and Living Resources, a section of the journal Frontiers in Marine Science

RECEIVED 22 July 2022
ACCEPTED 26 August 2022
PUBLISHED 13 September 2022

CITATION
Li B, Jia R, Hou Y and Zhu J (2022) Treating performance of a commercial-scale constructed wetland system for aquaculture effluents from intensive inland *Micropterus salmoides* farm. *Front. Mar. Sci.* 9:1000703. doi: 10.3389/fmars.2022.1000703

Treating performance of a commercial-scale constructed wetland system for aquaculture effluents from intensive inland *Micropterus salmoides* farm

Bing Li, Rui Jia, Yiran Hou and Jian Zhu*

Key Laboratory of Integrated Rice-Fish Farming Ecology, Ministry of Agriculture and Rural Affairs, Freshwater Fisheries Research Center, Chinese Academy of Fishery Sciences, Wuxi, China

In intensive inland fish farming, discharge of untreated effluents adversely affects adjacent water bodies and causes water pollution. Thus, it is highly necessary to treat the effluents from inland fish farm. In this study, we built a commercial-scale integrated constructed wetland (CW) system with vertical subsurface flow, and monitored the purifying effect. During fish farming and discharge of effluents periods, the water samples were collected to detected the total nitrogen (TN), total phosphorus (TP), ammonia nitrogen (NH_4^+-N), nitrate nitrogen (NO_3^--N), nitrite nitrogen (NO_2^--N) and chemical oxygen demand (COD_{Mn}). Results showed that the system was stable and significantly improved water quality from fish pond. During the fish farming period, the removal efficiency for TN, TP, NH_4^+-N, NO_3^--N, NO_2^--N, and COD was 24.93–43.72%, 61.92–72.18%, 56.29–68.63%, 56.66–64.81%, 56.42–64.19% and 28.37–42.79%, respectively. Similarly, these parameters were also markedly decreased by the integrated CW system during sewage discharge period, and the average total removal rate for TN, TP, NH_4^+-N, NO_3^--N, NO_2^--N, and COD was 50.24%, 64.48%, 61.36%, 62.65%, 56.16% and 37.32%, respectively. It was worth noting that three key parameters for effluents detection TN, TP and COD values were below the threshold values of water quality of Class II in freshwater sewage discharge standard of China (SCT9101-2007). In conclusion, this study evidently demonstrated that application of CW system was an environmental sustainable sewage treatment strategy in intensive inland fish farming.

KEYWORDS

constructed wetland, removal efficiency, total nitrogen, aquaculture effluents, recirculation aquaculture system

Introduction

Aquaculture products are key protein source in the global food production, which are increasing constantly in recent decades (FAO, 2020). They are mainly from marine water culture, inland freshwater culture and capture fisheries. In China, inland freshwater culture is the most important farming model, with a total area of 5,116.32 thousands ha and production of 30.14 million tons in 2019 (Yu et al., 2020). In the intensive inland freshwater farming, high-quality freshwater inflow was required. In turn, discharge of effluents can contaminate adjacent water bodies, which causes many environmental issues.

Like livestock farming and husbandry, large amounts of waste in aquaculture are generated, such as uneaten feed, feces, and dissolved material, which may be released into surface water and cause water pollution (Sindilariu et al., 2009). The pollution problem has aroused widespread concern as it exerts an adverse effect to aquatic ecological integrity (Turcios and Papenbrock, 2014). Excessive input nitrogen (N) and phosphorus (P) in aquatic ecosystems can promote the growth of algae and other phytoplankton, and subsequently cause dissolved oxygen (DO) depletion, water quality deterioration, and even death of aquatic animals (Bhateria and Jain, 2016; Wang et al., 2021). In China, the discharge standard of aquaculture effluents has been issued to prevent the harmful environmental effect (SCT9101-2007) (Ministry of Agriculture and Rural Affairs, 2007). However, existing methods for the treatment of aquaculture effluents, such as bio-filter and physical filter, require high investment and increase the cost of farming, which is beyond the reach of most of small producers. Therefore, it is highly necessary to seek effective method with a relatively low cost to address sustainability issues of inland fish farming.

Constructed wetland (CW) is one of the most promising methods for dealing with aquaculture effluents as it possesses some advantages, such as low cost, ecological benefit and ease of operation and maintenance (Tepe, 2018; Hang Pham et al., 2021). When integrated with special matrix and aquatic plants, CW can effectively remove many types of contaminants from wastewater, including organic matter, N, P, suspended solids, heavy metals and pathogenic microorganism through the coordinated action of biological, physical and chemical processes (Almuktar et al., 2018; Wang et al., 2021). Meanwhile, substrate microorganisms (e.g. nitrifying bacteria and denitrifying bacteria) play a pivotal role in conversion of nutrients, especially N, in wastewater (Liang et al., 2003; Li et al., 2018).

In aquaculture, CW has been applied to treat the discharged effluents from farms (Schulz et al., 2003; Sindilariu et al., 2007), or as a water filter unit to connect with recirculating aquaculture system (Zhang et al., 2010; Shi et al., 2011). According to surface area, the CW is classified into lab-scale CW (< 10 m^2) (Saeed and Sun, 2013; Jesus et al., 2017), pilot-scale CW (10-100m^2) (Papaevangelou et al., 2016; Uggetti et al., 2016) and commercial-scale CW (> 100 m^2) (Tilley et al., 2002; Shi et al., 2011) in research or farming practice regarding aquaculture. Early study reported that a hybrid free water surface-horizontal subsurface flow CW (surface area of 5 m^2) could remove 95% of total inorganic N and 32-71% of P in effluents from milkfish (*Chanos chanos*) pond (Lin et al., 2002). Horizontal subsurface flow CW (28 m^2) effectively reduced the total suspended solids (TSS), chemical oxygen demand (COD), total nitrogen (TN) and total phosphorus (TP) concentrations in effluents form the flow-through trout fish farm (Chazarenc et al., 2007). Vertical flow CW (80 m^2) for treatment of aquaculture ponds water proved to be very effective and the reduction amounted to 61.5% of ammonia nitrogen (NH_4^+-N), 68% of nitrate nitrogen (NO_3^--N) and 20% of P (Li et al., 2007). Shi et al. (2011) built a combination CW (221.0 m^2) to purify brackish effluent from commercial recirculating and super-intensive shrimp farming systems, and it exhibited good removal of TN (67%), TAN (71%) and TSS (66%). It is apparent that the most of these studies were conducted at lab-scale and pilot-scale systems. However, there was relatively little published research regarding practical application of a commercial-scale CW in aquaculture of China, and thus, its treatment performance needs to be further evaluated.

Based on the issues addressed above, we built a commercial-scale integrated CW system (2,400 m^2) with vertical subsurface flow, which connected with fish ponds with a total surface area of 19,200 m^2 to form a recirculating pond system. The objective of this study was to evaluate the performance of the CW system to manage the pond water quality with no water exchange during the farming period. Further, we examine whether the system improved the quality of effluents to comply with the discharge standard at the end of farming.

Materials and methods

Aquaculture system and constructed wetland design

The experiment was conducted in Wujiang modern agriculture industrial park (Suzhou, China), where we built an integrated CW system with a vertical subsurface flow. The CW system was connected with 7 fish ponds with a total surface area of 19,200 m^2 to form a recirculating pond system (Figure S1).

The CW system (total surface area 2,400 m^2) was consisted of sedimentation pond (250 m^2), aeration pond (250 m^2), constructed wetland (1,800 m^2) and stabilize water pond (100 m^2) (Figure S1). The wetland was filled with three layers of media. The bottom was filled with 30 cm of cobblestone

(diameter 8-10 cm), the middle layer was filled with 25 cm of pelelith (diameter 4-6 cm) and the top was filled 25 cm of pelelith (diameter 2-4 cm). Three types of macrophytes *Thalia dealbata*, *Iris* germanica and *Canna indica* were selected to plant into the wetland due to stronger uptake capacity of N, P and metal. The planning density was one plant/m^2. The mean hydraulic loading rate (HLR) was 0.6 m^3/m^2 d and hydraulic retention time (HRT) was 0.83 d. The water in CW-fish pond recirculating system was not renewed during the experiment. The system ran from early Jun to late November 2020.

Fish culture

The largemouth bass (*Micropterus salmoides*) were provided by Suzhou Tongli Modern Agriculture Development Co. LTD (Suzhou, China). The stocking density was 30,000 fish/hm^2 with an average initial weight of 20 ± 2 g/fish. The fish were fed on a commercial pellet diet containing 47% crude protein, 5% crude lipids, 18.0% crude ash and 3.0% crude fiber (Changzhou Haida Biological Feed Co., Ltd, Changzhou, China). During the farming period, the fish were fed 3–4 times daily and feeding amount was approximately 2–4% of the fish weight. The management of fish farming was operated according to the method reported by Sun (Sun, 2020). The use of fish was approved by the Freshwater Fisheries Research Centre (FFRC) of the Chinese Academy of Fishery Sciences, Wuxi, China.

Water sampling and parameters detection

During the fish farming period, water samples were collected from the fish pond, sedimentation pond, aeration pond (inlet of wetland) and outlet of wetland once per 24-25 days from July 10 to October 20, 2020. During the sewage discharge period, water samples were collected from the fish pond, sedimentation pond, aeration pond (inlet of wetland) and outlet of wetland once per 9 days from November 1 to November 21, 2020. In each sampling site, we randomly collected the water samples *via* the five-point sampling method (Jiang et al., 2017).

The temperature and DO were detected using an YSI-DO 200 (YSI Inc., Ohio, USA), and the pH was measured using PHS-3CT acidometer (Shanghai Huyueming Scientific Instrument Co., LTD, China).The water quality parameters including COD_{Mn}, TN, NO_3^--N, NO_2^--N, NH_4^+-N and TP were measured using standard methods (Wei, 2002). The COD content was measured using potassium permanganate as an oxidant. The TN concentration was detected according to alkaline potassium persulfate digestion method. The TP concentration was determined by ammonium molybdate spectrophotometric method. The NO_3^--N concentration was tested with UV spectrophotometry method. The NO_2^--N was examined using N-(1-naphthalene) –ethylenediamine as a chromogenic agent. The NH_4^+-N concentration was analyzed by nesslers reagent spectrophotometry method. Removal efficiency (%) of the CW for each water quality parameter was calculated using following equation.

$$\text{Removal efficiency} \quad (\%) = (C_0 - C_1)/C_0 \times 100$$

Where C_0 and C_1 is the concentration of the target parameter in outflow and inflow of wetland, respectively.

Statistical analysis

Data are analyzed using SPSS 24.0 and values are expressed as the mean ± standard error of the mean (SEM). Normal distribution was assessed by Kolmogorov–Smirnov test, and homogeneity of variance was examined by Levene teste. Difference among different groups were analyzed by One-way analysis of variance (ANOVA) with LSD *post hoc* test. *P* value less than 0.05 were considered to be statistically significant.

Results

Running parameters of the integrated CW system

During the experiment period, there was a similar change of temperature in fish pond, sedimentation pond, aeration pond, and CW outlet, ranging from 20.7°C to 32.2°C. Average pH value was 7.31 ± 0.15, 7.29 ± 0.19, 7.17 ± 0.34 and 7. 09 ± 0.28 in fish pond, sedimentation pond, aeration pond and CW outlet, respectively. The average DO value was 5.82 ± 0.51 mg/L, 5.07 ± 0.37 mg/L, 6.38 ± 0.58 mg/L and 2.07 ± 0.29 mg/L in fish pond, sedimentation pond, aeration pond and CW outlet, respectively. The DO reduction showed an oxygen depletion in the CW, which may be related to the aerobic respiration of heterotrophic microorganisms (Hang Pham et al., 2021). During the experiment period, the integrated CW system operated stably.

Changes of water quality parameters during fish farming period

During the fish farming period, the TN concentration successively decreased when the water flowed through sedimentation pond, aeration pond and CW, and significant difference was observed between CW inlet and CW outlet ($p < 0.05$; Figure 1A). The average TN concentration was 8.65 mg/L, 8.25 mg/L, 7.82 mg/L and 5.33 mg/L in fish pond, sedimentation pond, aeration pond (CW inlet) and CW outlet, respectively. Total TN removal rate of the integrated CW system ranged from 24.93 to 43.73% during the monitoring period (Figure 1B).

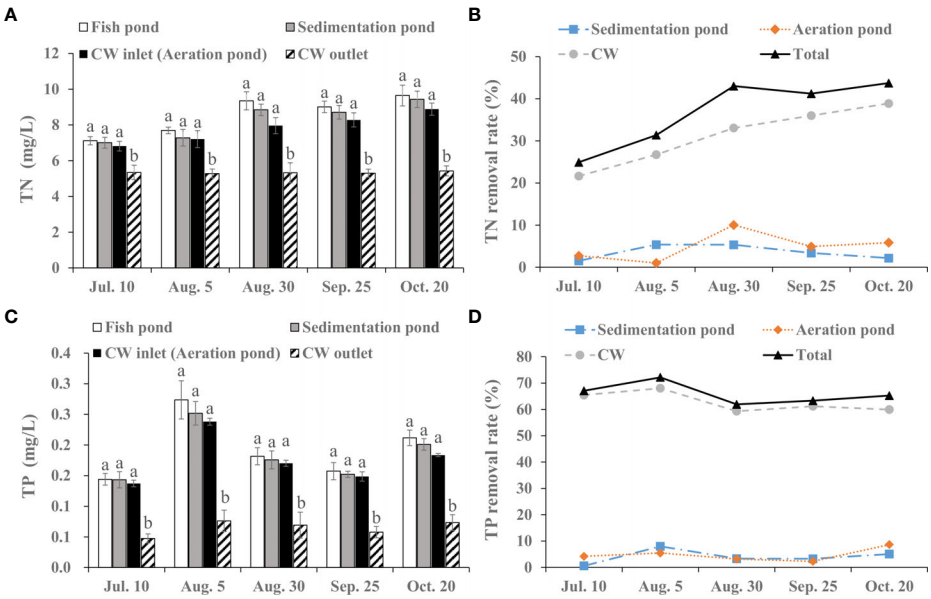

FIGURE 1
Removal efficiency of integrated CW system on TN and TP during the fish farming period. **(A)** TN value in the fish pond, sedimentation pond, CW inlet (aeration pond) and CW outlet. **(B)** TN removal rate of the sedimentation pond, aeration pond and CW. **(C)** TP value in the fish pond, sedimentation pond, CW inlet (aeration pond) and CW outlet. **(D)** TP removal rate of the sedimentation pond, aeration pond and CW. The value is expressed as mean ± SE (n = 5). Different small letters in bar graph indicate significant difference ($p < 0.05$) among fish pond, sedimentation pond, CW inlet (aeration pond) and CW outlet.

The integrated CW system significantly removed TP concentration in effluents from fish pond, and TP value at the CW inlet was clearly higher than that at the CW outlet ($p < 0.05$; Figure 1C). Meanwhile, there was a stable total removal rate on TP ranging from 61.92 to 72.19%. Average removal rate was 4.02%, 4.76% and 62.79% in sedimentation pond, aeration pond and CW, respectively (Figure 1D).

As shown in Figure 2A, average NH_4^+-N concentration in water generally decreased from fish pond to CW outlet, and the decrease exhibited significant difference between the CW inlet and CW outlet during fish farming period ($p < 0.05$). Average reduction rate of NH_4^+-N was 2.75%, 2.82% and 60.81% in the sedimentation pond, aeration pond and CW, respectively (Figure 2B).

The variation of NO_2^--N level followed a similar trend to NH_4^+-N, decreasing from 0.04 mg/L (mean) at the fish pond to 0.016 mg/L (mean) at the CW outlet when the water flowed through sedimentation pond, aeration pond and CW (Figure 2C). Specifically, NO_2^--N level was obviously reduced at the CW outlet compared with the CW inlet during the July 10–October 20 ($p < 0.05$), and average total reduction rate of NO_2^--N was 60.54% (Figure 2D).

The integrated CW system showed a high removal effect for NO_3^--N, with an average total removal rate of 59.66% (Figure 2F). In addition, average NO_3^--N concentration was 0.135 mg/L, 0.127 mg/L, 0.117 mg/L and 0.055 mg/L in fish pond, sedimentation pond, aeration pond (CW inlet) and CW outlet, respectively, and there was a significant difference between the CW inlet and CW outlet ($p < 0.05$; Figure 2E).

The COD_{Mn} is frequently used to evaluate COD content in aquaculture effluents. Concentration of COD_{Mn} displayed a nonlinear decrease in different sampling time when the water flowed through sedimentation pond, aeration pond and CW (Figure 2G). Notably, COD_{Mn} value at CW inlet was higher than that at CW outlet ($p < 0.05$). Meanwhile, this system showed a stable removal efficiency for COD_{Mn} with 30.51–42.79% removal rate (Figure 2H).

Changes of water quality parameters during the effluents discharge period

During the effluents discharge period, average TN concentration decreased from 9.89 mg/L to 4.92 mg/L when the water from fish pond flowed through the CW system (Figure 3A). Compared with CW inlet, TN value was clearly reduced at CW outlet ($p < 0.05$), with an average reduction rate of 43.17% (Figure 3B).

Similarly, The TP concentration was effectively reduced by the CW system. The TP concentration was prominently lowered from 0.25 mg/L at fish pond to 0.09 mg/L at CW outlet, with a relatively stable average removal rate of 64.48% ($p < 0.05$; Figure 3C). The removal rate was 2.18–8.49% in sedimentation

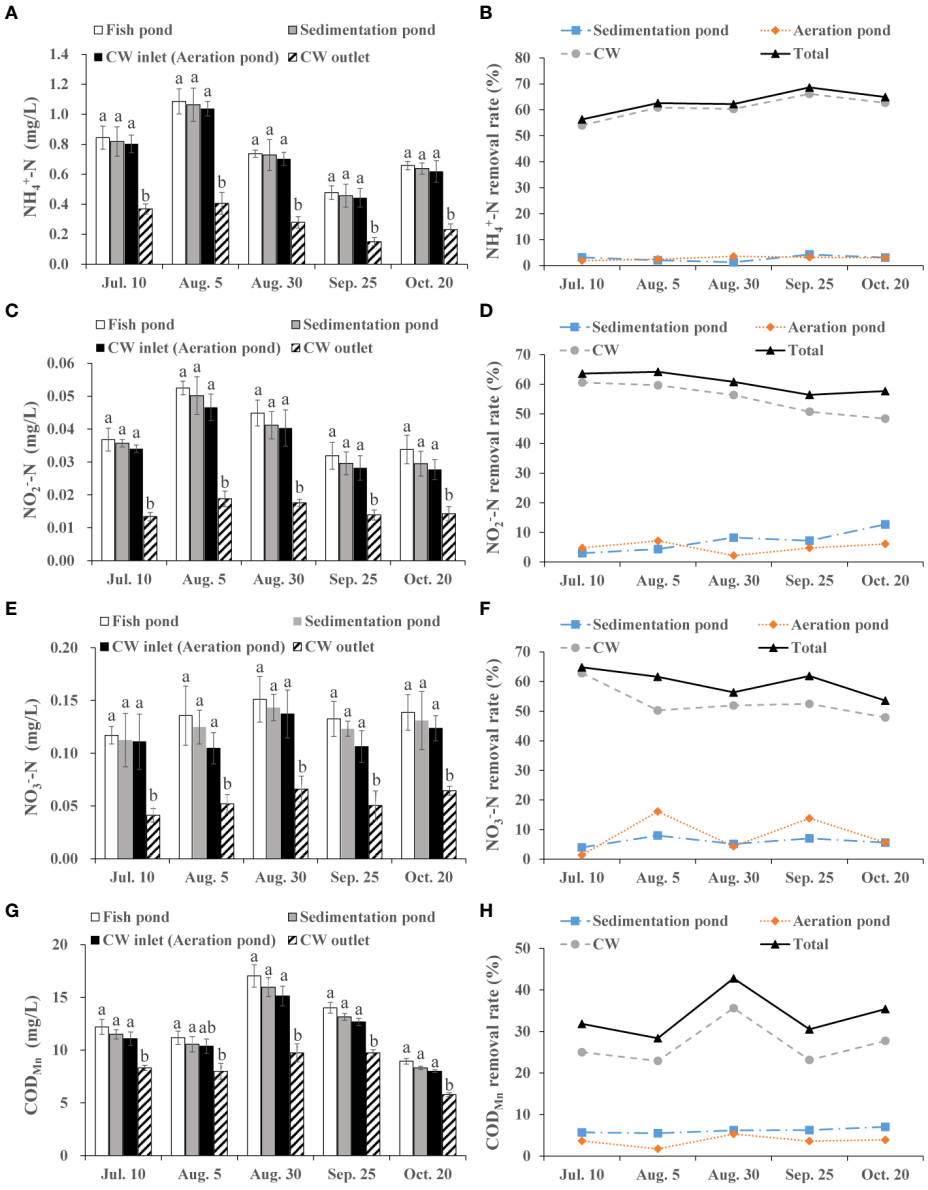

FIGURE 2
Removal efficiency of integrated CW system on NH_4^+-N, NO_3^--N, NO_2^--N and COD_{Mn} during the fish farming period. **(A)** NH_4^+-N value in the fish pond, sedimentation pond, CW inlet (aeration pond) and CW outlet. **(B)** NH_4^+-N removal rate of the sedimentation pond, aeration pond and CW. **(C)** NO_2^--N value in the fish pond, sedimentation pond, CW inlet (aeration pond) and CW outlet. **(D)** NO_2^--N removal rate of the sedimentation pond, aeration pond and CW. **(E)** NO_3^--N value in the fish pond, sedimentation pond, CW inlet (aeration pond) and CW outlet. **(F)** NO_3^--N removal rate of the sedimentation pond, aeration pond and CW. **(G)** COD_{Mn} value in the fish pond, sedimentation pond, CW inlet (aeration pond) and CW outlet. **(H)** COD_{Mn} removal rate of the sedimentation pond, aeration pond and CW. The value is expressed as mean ± SE (n = 5). Different small letters in bar graph indicate significant difference ($p < 0.05$) among fish pond, sedimentation pond, CW inlet (aeration pond) and CW outlet.

pond, 7.16–10.10% in aeration pond and 55.37–62.89% in CW (Figure 3D).

As shown in Figure 4A, The NH_4^+-N concentration showed a decreasing tendency in water from fish pond to CW outlet, and there was a significant difference between the CW inlet and CW outlet ($p < 0.05$). The average removal rate was 5.73%, 9.81% and 54.57% in the sedimentation pond, aeration pond and CW, respectively (Figure 4B).

The NO_2^--N concentration was successively decreased in fish pond, sedimentation pond, aeration pond (CW inlet) and CW outlet, and the decrease showed significant difference between the CW inlet and CW outlet ($p < 0.05$; Figure 4C). The integrated

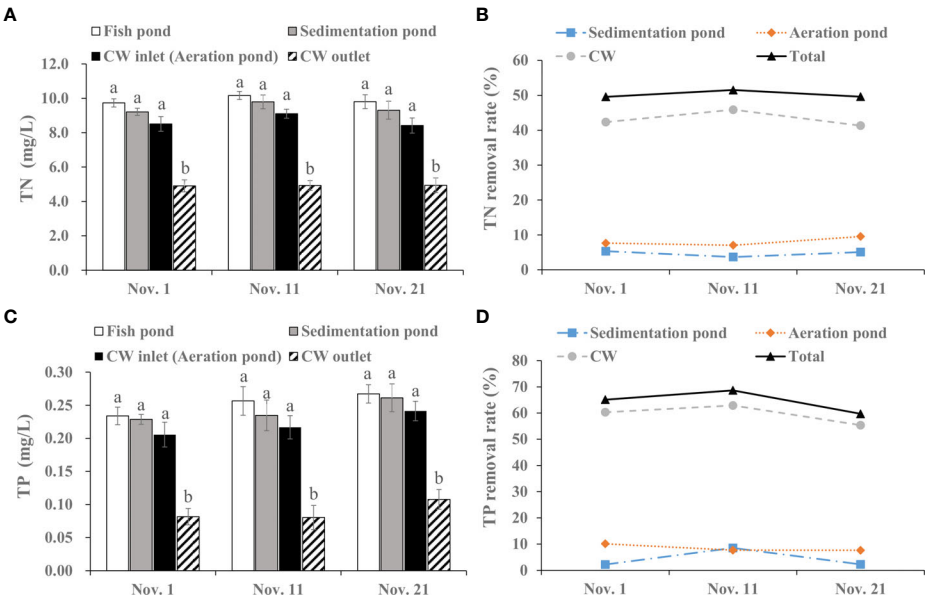

FIGURE 3
Removal efficiency of integrated CW system on TN and TP during the effluents discharge period. **(A)** TN value in the fish pond, sedimentation pond, CW inlet (aeration pond) and CW outlet. **(B)** TN removal rate of the sedimentation pond, aeration pond and CW. **(C)** TP value in the fish pond, sedimentation pond, CW inlet (aeration pond) and CW outlet. **(D)** TP removal rate of the sedimentation pond, aeration pond and CW. The value is expressed as mean ± SE (n = 5). Different small letters in bar graph indicate significant difference ($p< 0.05$) among the fish pond, sedimentation pond, CW inlet (aeration pond) and CW outlet.

CW system has a stable removal rate ranging 54.27% to 58.55% during the effluents discharge period (Figure 4D).

Variation of the NO_3^--N level followed a similar trend to NO_2^--N. The average NO_3^--N level was 0.126 mg/L, 0.115 mg/L, 0.107 mg/L and 0.047 mg/L in the fish pond, sedimentation pond, aeration pond (CW inlet) and CW outlet, respectively (Figure 4E). The integrated CW system strongly reduced NO_2^--N level in the aquaculture effluents with a total average removal rate 62.65% (Figure 4F).

During the effluents discharge period, the average COD_{Mn} concentration was 11.03 mg/L, 10.30 mg/L, 9.95 mg/L and 6.84 mg/L in the fish pond, sedimentation pond, aeration pond and CW outlet, respectively (Figure 4G), and the value at CW outlet was apparently lower than that at other sampling sites ($p< 0.05$). Meanwhile, the integrated CW system has a distinct impact on COD_{Mn} reduction, and removal rate ranged from 32.33% to 43.04% (Figure 4H).

Discussion

In aquaculture effluents, inorganic N is a key pollutant, primarily generated from residual feeds and feces (Piedrahita, 2003). Overloading N can cause eutrophication, algal blooms and water anoxia, which may further lead to abnormal changes in physiology and behavior of aquatic animals (Banerjee et al., 2021). Thus TN level is a common parameter used to assess water quality in aquaculture. A CW (9.5 m^2) was used to treat effluents from a recirculating aquaculture system farmed *Oreochromis niloticus*, and there was a 95.5% removal rate for TN (Behrends et al., 1999). Similarly, Lin et al. (2002) built a hybrid CW (5 m^2) to treat effluents of *Chanos chanos* farming, and TN concentration was significantly removed by the CW system. Zhang et al. (2010) used a farm-scale CW (320 m^2) to improve water quality in *Ictalurus punctatus* farming, and the TN removal rate was 48%. In addition, TN removal rate was related to types of CW systems, such as, 12.4% in floating-bed CW, 64.7% in horizontal subsurface flow CW, and 23.0% in surface flow CW (Bai et al., 2020). In the present study, the TN removal rate was 36.85% during the fish farming period and 50.24% during the effluents discharge period, indicating the integrated CW system has a high removal rate for inorganic N. In addition, the average TN value was 4.92 mg/L at CW outlet during the effluents discharge period, which met the water quality of Class II in the freshwater sewage discharge standard of China (SCT9101-2007).

In aquaculture practice, NH_4^+-N, NO_2^--N and NO_3^--N are ubiquitous pollutants, and have received the most attention due to high toxicity on aquatic animals (Molayemraftar et al., 2022). High levels of NH_4^+-N and NO_2^--N have been reported to inhibit growth performance, induce tissue damage or even death in aquatic animals (Ip and Chew, 2010; Kroupova et al., 2018).

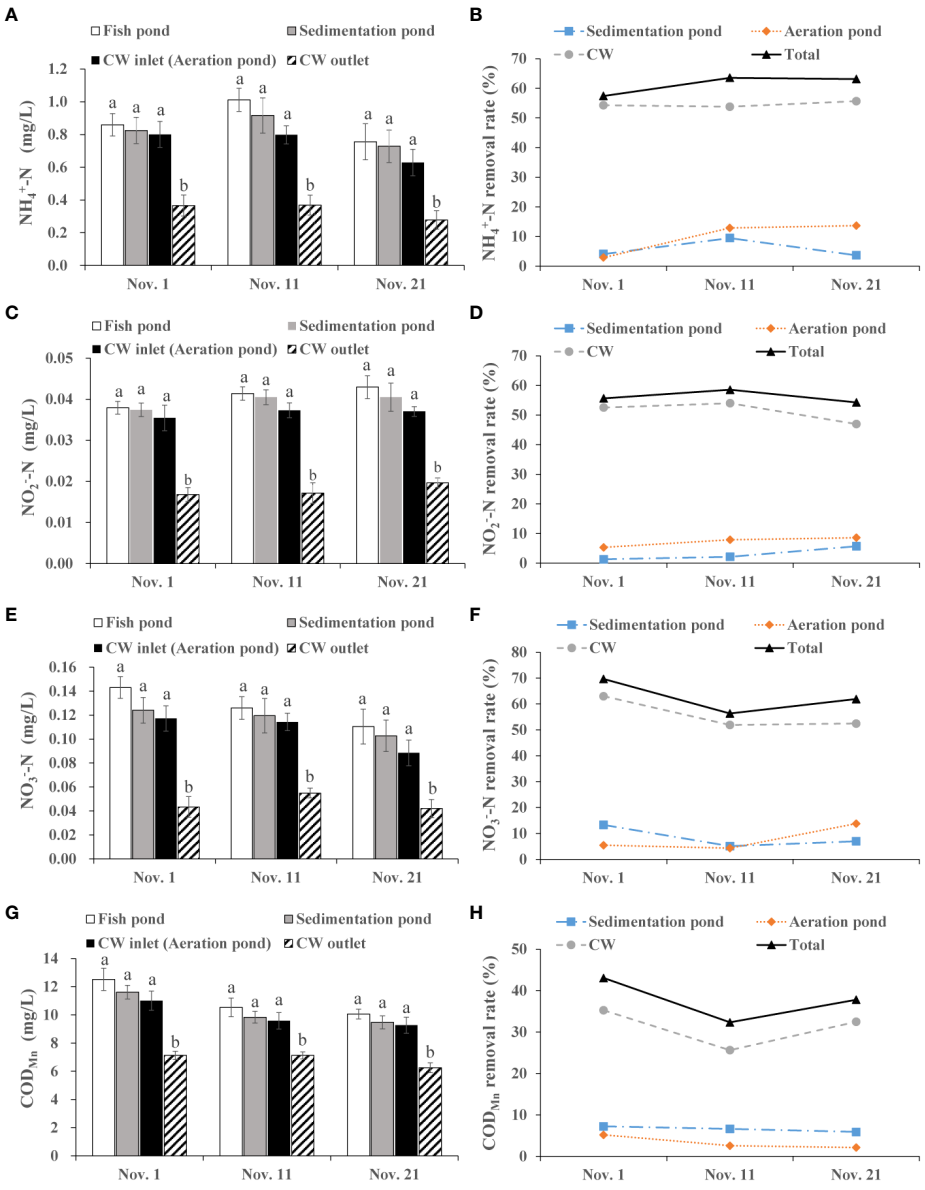

FIGURE 4
Removal efficiency of integrated CW system on NH_4^+-N, NO_3^-N, NO_2^--N and COD_{Mn} during the effluents discharge period. **(A)** NH_4^+-N value in the fish pond, sedimentation pond, CW inlet (aeration pond) and CW outlet. **(B)** NH_4^+-N removal rate of the sedimentation pond, aeration pond and CW. **(C)** NO_2^--N value in the fish pond, sedimentation pond, CW inlet (aeration pond) and CW outlet. **(D)** NO_2^--N removal rate of the sedimentation pond, aeration pond and CW. **(E)** NO_3^--N value in the fish pond, sedimentation pond, CW inlet (aeration pond) and CW outlet. **(F)** NO_3^--N removal rate of the sedimentation pond, aeration pond and CW. **(G)** COD_{Mn} value in the fish pond, sedimentation pond, CW inlet (aeration pond) and CW out. **(H)** COD_{Mn} removal rate of the sedimentation pond, aeration pond and CW. The value is expressed as mean ± SE (n = 5). Different small letters in bar graph indicate significant difference ($p < 0.05$) among fish pond, sedimentation pond, CW inlet (aeration pond) and CW outlet.

Chronic NO_3^--N exposure reduces growth, increases susceptibility to hypoxia, disrupts endocrine system and affects the health status in fish (Monsees et al., 2017; Kellock et al., 2018; Isaza et al., 2021). It has been reported that CW was an efficient and cost-effective management practice to maintain reasonable concentrations of NH_4^+-N, NO_2^--N and NO_3^--N (Lin et al., 2010). Mahmood et al. (2016) structured a CW-commercial ponds of *Macrobrachium rosenbergii* system, and found that the 43.8% NO_3^--N, 25.7% NH_4^+-N and 14.3% NO_2^--N were removed. In a lab-scale closed recirculation aquaculture system, horizontal subsurface flow CW removed 99% NO_2^--N and 82–99% NO_3^--N, but had lower removal rate for NH_4^+-N (10%) (Hang Pham

et al., 2021). In this work, the The CW system exhibited a high and stable removal rate for NH_4^+-N (62.93%), NO_3^--N (59.66%) and NO_2^--N (60.54%), and improved substantially water quality form the fish pond during the fish farming period. It is worth noting that the average NH_4^+-N concentration at CW outlet was below 0.5 mg/L during the effluents discharge period, meeting environmental quality standard of Class II for surface water in China (GB3838-2002). The data also indicated that the integrated CW system had a high removal efficiency for inorganic N in aquaculture effluents, which reduced aquaculture-included environmental contamination.

In CW system, N removal is a complex process, which may be related to sedimentation, uptake of aquatic plant, adsorption of media and biodegradation (Liu et al., 2019; Lu et al., 2020). N as an essential nutrient can be absorbed by aquatic plants, thus some aquatic plants are planted in CW to remove N. CW planted *Thalia dealbata* and *Pontederia cordata* displayed 66.44% and 68.56% TN reduction rate and 54.09% and 77.39% NH_4^+-N reduction rate (Liu, 2011). In a CW planted *Canna indica*, the removal rate for NH_4^+-N was 45.3-84.5% (Zhu et al., 2004). In this study, the *Thalia dealbata*, *Iris germanica* and *Canna indica* were planted into the CW to clean the effluents from fish pond, which reflected that the inorganic N removal was related to uptake of the aquatic plants. However, some researchers suggested that CW removed N primarily through ammonification, nitrification and denitrification, but not aquatic plants uptake (Uusheimo et al., 2018; Liu et al., 2019; Lu et al., 2020). In addition, the substrates of CW, such as pebbles and pelelith, have been reported to have strong adsorption on N (Wang et al., 2018). Previous study suggested that, in commercial-scale CW system, TN removal rate was often around 40%, of which limiting factors were organic carbon concentration and low DO level (Xie et al., 2018; Lu et al., 2020). In this study, we speculated the major limiting factor for N removal was the DO level (2.07 ± 0.29 mg/L in CW outlet), because heterotrophic microorganisms played an important role in N removal process (Friedland, 2004).

Apart from N, P level is another important parameter evaluating water quality. P can promote algal growth and has a significant impact on microcystins production by *Microcystis aeruginosa* in aquatic environment (Dai et al., 2016). High concentration of P deteriorated not only water quality (Smith et al., 1999), but caused microcystins accumulation though enhancing *Microcystis* biomass (Wang et al., 2010). CW has the potential to treat P in aquaculture effluents. For example, CW as a recirculation filter in large-scale shrimp aquaculture was effective in removal of TP (65%) (Tilley et al., 2002); a laboratory-scale CW markedly removed the TP (average reduction rate 31%) from *Litopenaeus vannamei* farming water (Hang Pham et al., 2021). In line with previous studies, our data showed that the integrated CW system effectively removed TP with an average removal rate of 65.95% during the fish farming period. Interestingly, our data also displayed that the average TP concentration was 0.09 mg/L at CW outlet, which lower than the threshold value (0.5 mg/L) in the freshwater effluents discharge standard Class II of China (SCT9101-2007). P removal in CW is a manifold process including physical, chemical and biological forces (Sindilariu et al., 2007). It also depends on the ecological situations, type of CW and planted macrophytes (Kumar and Dutta, 2019). P as an essential mineral can be absorbed by macrophytes in CW system. Various macrophytes possesses different uptake capacity of P, such as 48.1% for *Canna indica* and 76% for *Thalia dealbata* (BU et al., 2010; Yang et al., 2021). In addition, the P removal was related to adherence capability of a range of filter media in CW (Vohla et al., 2011; Wu et al., 2015).

Like TN and TP, COD concentration is a key monitoring parameter during aquaculture effluents discharge period. It is also used to evaluate organic pollutant in aquatic environment. Numerous studies suggested that CW had a strongly positive impact on the removal of organic matter with 59.7–89.0% COD reduction rate (Tuszyńska and Obarska-Pempkowiak, 2008). In the current study, the COD concentration was also clearly reduced by CW system, with 28.37–42.79% reduction rate. Meanwhile, the average COD concentration was 6.84 mg/L, below the threshold value (15 mg/L) in freshwater effluents discharge standard of China (SCT9101-2007). In CW, the COD can be removed by sedimentation and filtration suspended solids (Hang Pham et al., 2021). However, our data showed that the COD removal rate of sedimentation was 5.88-7.33% which was much lower than that of CW, reflecting the COD may be removed mainly *via* filtration of CW media. On the other hand, biodegradation by aerobic and anaerobic microorganisms was also an important removal mechanism of organic matter (Kumar and Dutta, 2019). In the aerobic biodegradation process, oxygen transfer may be a limiting factor for COD removal. Thus, the low COD reduction in this study may be related to DO level (2.07 ± 0.29 mg/L at CW outlet).

Conclusion

In the study, we built a commercial-scale vertical subsurface flow CW connected with fish ponds, which run stably during the fish farming and effluents discharge periods. During the fish farming period, the integrated CW system had high and stable removal efficiency for TN of 24.93–43.72%, TP of 61.92–72.18%, NH_4^+-N of 56.29–68.63%, NO_3^--N of 56.66–64.81% and NO_2^--N of 56.42–64.19%. During the effluents discharge period, average value of TN, TP and COD, three key parameters for effluents detection, was 4.92 mg/L, 0.09 mg/L and 6.84 mg/L, respectively, which met the water quality of Class II in freshwater effluents discharge standard of China (SCT9101-2007). Finally, this study evidently demonstrated that application of CW was an environmental sustainable sewage treatment strategy in intensive fish culture system.

Data availability statement

The original contributions presented in the study are included in the article/Supplementary Material. Further inquiries can be directed to the corresponding author.

Author contributions

BL: Conceptualization, writing—original draft preparation, software; RJ: methodology, investigation validation, formal analysis, resources, YH: data cu-ration, writing—review and editing; JZ: visualization, supervision, project administration, funding acquisition. All authors read and approved the final version of the manuscript.

Funding

This study was supported by Central Public-interest Scientific Institution Basal Re-search Fund, CAFS (2020TD60), earmarked fund for CARS (CARS-45-20), and National Key R&D Program of China (2019YFD0900305).

Conflict of interest

The authors declare that the research was conducted in the absence of any commercial or financial relationships that could be construed as a potential conflict of interest.

Publisher's note

All claims expressed in this article are solely those of the authors and do not necessarily represent those of their affiliated organizations, or those of the publisher, the editors and the reviewers. Any product that may be evaluated in this article, or claim that may be made by its manufacturer, is not guaranteed or endorsed by the publisher.

Supplementary material

The Supplementary Material for this article can be found online at: https://www.frontiersin.org/articles/10.3389/fmars.2022.1000703/full#supplementary-material

References

Almuktar, S. A., Abed, S. N., and Scholz, M. (2018). Wetlands for wastewater treatment and subsequent recycling of treated effluent: A review. *Environ. Sci. pollut. Res.* 25, 23595–23623. doi: 10.1007/s11356-018-2629-3

Bai, X., Zhu, X., Jiang, H., Wang, Z., He, C. , Sheng, L., et al. (2020). Purification effect of sequential constructed wetland for the polluted water in urban river. *Water* 12, 1054. doi: 10.3390/w12041054

Banerjee, S., Maity, S., Guchhait, R., Chatterjee, A., Biswas, C., Adhikari, M., et al. (2021). Toxic effects of cyanotoxins in teleost fish: A comprehensive review. *Aquat. Toxicol.* 240, 105971. doi: 10.1016/j.aquatox.2021.105971

Behrends, L. L., Houke, L., Bailey, E., and Brown, D. (1999). "Reciprocating subsurface flow constructed wetlands for treating high-strength aquaculture wastewater," in *Wetlands and Remediation Conference*, Salt Lake City, Utah. 16–17.

Bhateria, R., and Jain, D. (2016). Water quality assessment of lake water: A review. *Sustain. Water Resour. Manage.* 2, 161–173. doi: 10.1007/s40899-015-0014-7

BU, F., Luo, G., Xu, X., Cao, J., and Shu, W. (2010). Canna indica and acorus calamus ecological floating beds for purification of micro-polluted source water. *China Water Wastewater* 26, 14–17. doi: 10.19853/j.zgjsps.1000-4602.2010.03.006

Chazarenc, F., Brisson, J., and Comeau, Y. (2007). Slag columns for upgrading phosphorus removal from constructed wetland effluents. *Water Sci. Technol.* 56, 109–115. doi: 10.2166/wst.2007.499

Dai, R. H., Wang, P. F., Jia, P. L., Zhang, Y., Chu, X. C., and Wang, Y. F. (2016). A review on factors affecting microcystins production by algae in aquatic environments. *World J. Microbiol. Biotechnol.* 32, 51. doi: 10.1007/s11274-015-2003-2

FAO. (2020). The State of World Fisheries and Aquaculture 2020. *Sustainability in action* (Rome). doi: 10.4060/ca9229e

Friedland, J. M. (2004). *Effectiveness of treatment and diversity of microbial populations within a constructed wetland treating wastewater* (Morgantown, West Virginia: West Virginia University).

Hang Pham, T. T., Cochevelou, V., Khoa Dinh, H. D., Breider, F., and Rossi, P. (2021). Implementation of a constructed wetland for the sustainable treatment of inland shrimp farming water. *J. Environ. Manage.* 279, 111782. doi: 10.1016/j.jenvman.2020.111782

Ip, Y. K., and Chew, S. F. (2010). Ammonia production, excretion, toxicity, and defense in fish: A review. *Front. Physiol.* 1, 134. doi: 10.3389/fphys.2010.00134

Isaza, D. F. G., Cramp, R. L., and Franklin, C. E. (2021). Exposure to nitrate increases susceptibility to hypoxia in fish. *Physiol. Biochem. Zool.* 94, 124–142. doi: 10.1086/713252

Jesus, J. M., Cassoni, A. C., Danko, A. S., Fiúza, A., and Borges, M.-T. (2017). Role of three different plants on simultaneous salt and nutrient reduction from saline synthetic wastewater in lab-scale constructed wetlands. *Sci. Total Environ.* 579, 447–455. doi: 10.1016/j.scitotenv.2016.11.074

Jiang, J., Song, Z., Yang, X., Mao, Z., Nie, X., Guo, H., et al. (2017). Microbial community analysis of apple rhizosphere around bohai gulf. *Sci. Rep.* 7, 1–9. doi: 10.1038/s41598-017-08398-9

Kellock, K. A., Moore, A. P., and Bringolf, R. B. (2018). Chronic nitrate exposure alters reproductive physiology in fathead minnows. *Environ. pollut.* 232, 322–328. doi: 10.1016/j.envpol.2017.08.004

Kroupova, H. K., Valentova, O., Svobodova, Z., Sauer, P., and Machova, J. (2018). Toxic effects of nitrite on freshwater organisms: a review. *Rev. Aquac.* 10, 525–542. doi: 10.1111/raq.12184

Kumar, S., and Dutta, V. (2019). Constructed wetland microcosms as sustainable technology for domestic wastewater treatment: An overview. *Environ. Sci. pollut. Res.* 26, 11662–11673. doi: 10.1007/s11356-019-04816-9

Liang, W., Wu, Z.-b., Cheng, S.-p., Zhou, Q.-h., and Hu, H.-y. (2003). Roles of substrate microorganisms and urease activities in wastewater purification in a constructed wetland system. *Ecol. Eng.* 21, 191–195. doi: 10.1016/j.ecoleng.2003.11.002

Lin, Y. F., Jing, S. R., Lee, D. Y., Chang, Y. F., and Sui, H. Y. (2010). Constructed wetlands for water pollution management of aquaculture farms conducting earthen pond culture. *Water Environ. Res.* 82, 759–768. doi: 10.2175/106143010X12609736966685

Lin, Y.-F., Jing, S.-R., Lee, D.-Y., and Wang, T.-W. (2002). Nutrient removal from aquaculture wastewater using a constructed wetlands system. *Aquaculture* 209, 169–184. doi: 10.1016/S0044-8486(01)00801-8

Liu, Y. (2011). *The ecological evaluation of to nitrogen and phosphorus removals of domestic sewage for constructed wetland plants* (Nanchang China: Nanchang University).

Liu, F.-f., Fan, J., Du, J., Shi, X., Zhang, J., and Shen, Y. (2019). Intensified nitrogen transformation in intermittently aerated constructed wetlands: Removal

pathways and microbial response mechanism. *Sci. Total Environ.* 650, 2880–2887. doi: 10.1016/j.scitotenv.2018.10.037

Li, G., Wu, Z., Cheng, S., Liang, W., He, F., Fu, G., et al. (2007). Application of constructed wetlands on wastewater treatment for aquaculture ponds. *Wuhan Univ. J. Natural Sci.* 12, 1131–1135. doi: 10.1007/s11859-007-0116-7

Li, B., Yang, Y., Chen, J., Wu, Z., Liu, Y., and Xie, S. (2018). Nitrifying activity and ammonia-oxidizing microorganisms in a constructed wetland treating polluted surface water. *Sci. Total Environ.* 628, 310–318. doi: 10.1016/j.scitotenv.2018.02.041

Lu, J., Guo, Z., Kang, Y., Fan, J., and Zhang, J. (2020). Recent advances in the enhanced nitrogen removal by oxygen-increasing technology in constructed wetlands. *Ecotoxicol. Environ. Saf.* 205, 111330. doi: 10.1016/j.ecoenv.2020.111330

Mahmood, T., Zhang, J., and Zhang, G. (2016). Assessment of constructed wetland in nutrient reduction, in the commercial scale experiment ponds of freshwater prawn macrobrachium rosenbergii. *Bull. Environ. Contam. Toxicol.* 96, 361–368. doi: 10.1007/s00128-015-1713-3

Ministry of Agriculture and Rural Affairs, C. (2007). Requirement for water discharge from freshwater aquaculture pond. (Beijing: Standards Press of China) pp. 1–4.

Molayemraftar, T., Peyghan, R., Jalali, M. R., and Shahriari, A. (2022). Single and combined effects of ammonia and nitrite on common carp, cyprinus carpio: Toxicity, hematological parameters, antioxidant defenses, acetylcholinesterase, and acid phosphatase activities. *Aquaculture* 548, 737676. doi: 10.1016/j.aquaculture.2021.737676

Monsees, H., Klatt, L., Kloas, W., and Wuertz, S. (2017). Chronic exposure to nitrate significantly reduces growth and affects the health status of juvenile Nile tilapia (Oreochromis niloticus l.) in recirculating aquaculture systems. *Aquac. Res.* 48, 3482–3492. doi: 10.1111/are.13174

Papaevangelou, V. A., Gikas, G. D., Tsihrintzis, V. A., Antonopoulou, M., and Konstantinou, I. K. (2016). Removal of endocrine disrupting chemicals in HSF and VF pilot-scale constructed wetlands. *Chem. Eng. J.* 294, 146–156. doi: 10.1016/j.cej.2016.02.103

Piedrahita, R. H. (2003). Reducing the potential environmental impact of tank aquaculture effluents through intensification and recirculation. *Aquaculture* 226, 35–44. doi: 10.1016/S0044-8486(03)00465-4

Saeed, T., and Sun, G. (2013). A lab-scale study of constructed wetlands with sugarcane bagasse and sand media for the treatment of textile wastewater. *Bioresource Technol.* 128, 438–447. doi: 10.1016/j.biortech.2012.10.052

Schulz, C., Gelbrecht, J., and Rennert, B. (2003). Treatment of rainbow trout farm effluents in constructed wetland with emergent plants and subsurface horizontal water flow. *Aquaculture* 217, 207–221. doi: 10.1016/S0044-8486(02)00204-1

Shi, Y., Zhang, G., Liu, J., Zhu, Y., and Xu, J. (2011). Performance of a constructed wetland in treating brackish wastewater from commercial recirculating and super-intensive shrimp growout systems. *Bioresource Technol.* 102, 9416–9424. doi: 10.1016/j.biortech.2011.07.058

Sindilariu, P.-D., Brinker, A., and Reiter, R. (2009). Factors influencing the efficiency of constructed wetlands used for the treatment of intensive trout farm effluent. *Ecol. Eng.* 35, 711–722. doi: 10.1016/j.ecoleng.2008.11.007

Sindilariu, P.-D., Schulz, C., and Reiter, R. (2007). Treatment of flow-through trout aquaculture effluents in a constructed wetland. *Aquaculture* 270, 92–104. doi: 10.1016/j.aquaculture.2007.03.006

Smith, V. H., Tilman, G. D., and Nekola, J. C. (1999). Eutrophication: impacts of excess nutrient inputs on freshwater, marine, and terrestrial ecosystems. *Environ. pollut.* 100, 179–196. doi: 10.1016/S0269-7491(99)00091-3

Sun, L. (2020). Technical points of largemouth bass pond culture. *Sci. Fish Farming* 10, 39–40. doi: 10.3969/j.issn.1004-843X.2020.10.020

Tepe, Y. (2018). "Treatment of effluents from fish and shrimp aquaculture in constructed wetlands," in *Constructed wetlands for industrial wastewater treatment* (Chichester, UK: John Wiley & Sons, Ltd), 105–125.

Tilley, D. R., Badrinarayanan, H., Rosati, R., and Son, J. (2002). Constructed wetlands as recirculation filters in large-scale shrimp aquaculture. *Aquac. Eng.* 26, 81–109. doi: 10.1016/S0144-8609(02)00010-9

Turcios, A., and Papenbrock, J. (2014). Sustainable treatment of aquaculture effluents–what can we learn from the past for the future? *Sustainability* 6, 836–856. doi: 10.3390/su6020836

Tuszyńska, A., and Obarska-Pempkowiak, H. (2008). Dependence between quality and removal effectiveness of organic matter in hybrid constructed wetlands. *Bioresource Technol.* 99, 6010–6016. doi: 10.1016/j.biortech.2007.12.018

Uggetti, E., Hughes-Riley, T., Morris, R. H., Newton, M. I., Trabi, C. L., Hawes, P., et al. (2016). Intermittent aeration to improve wastewater treatment efficiency in pilot-scale constructed wetland. *Sci. Total Environ.* 559, 212–217. doi: 10.1016/j.scitotenv.2016.03.195

Uusheimo, S., Huotari, J., Tulonen, T., Aalto, S., Rissanen, A., and Arvola, L. (2018). High nitrogen removal in a constructed wetland receiving treated wastewater in a cold climate. *Environ. Sci. Technol.* 52, 13343–13350. doi: 10.1021/acs.est.8b03032

Vohla, C., Kõiv, M., Bavor, H. J., Chazarenc, F., and Mander, Ü. (2011). Filter materials for phosphorus removal from wastewater in treatment wetlands–a review. *Ecol. Eng.* 37, 70–89. doi: 10.1016/j.ecoleng.2009.08.003

Wang, Q., Niu, Y., Xie, P., Chen, J., Ma, Z., Tao, M., et al. (2010). Factors affecting temporal and spatial variations of microcystins in gonghu bay of lake taihu, with potential risk of microcystin contamination to human health. *Sci. World J.* 10, 1795–1809. doi: 10.1100/tsw.2010.172

Wang, J., Wang, W., Xiong, J., Li, L., Zhao, B., Sohail, I., et al. (2021). A constructed wetland system with aquatic macrophytes for cleaning contaminated runoff/storm water from urban area in Florida. *J. Environ. Manage.* 280, 111794. doi: 10.1016/j.jenvman.2020.111794

Wang, H. X., Xu, J. L., Sheng, L. X., and Liu, X. J. (2018). A review of research on substrate materials for constructed wetlands. *Mater. Sci. Forum* 913, 917–929. doi: 10.4028/www.scientific.net/MSF.913.917

Wei, F. (2002). *Monitor and AnalysisMethod of water and wastewater (The fourth edition)* (Beijing: Chinese Environmental Science Publication House).

Wu, H., Zhang, J., Ngo, H. H., Guo, W., Hu, Z., Liang, S., et al. (2015). A review on the sustainability of constructed wetlands for wastewater treatment: Design and operation. *Bioresource Technol.* 175, 594–601. doi: 10.1016/j.biortech.2014.10.068

Xie, A., Chen, H., and You, S. (2018). Advance of nitrogen removal in constructed wetland. *IOP Conf. Ser.: Mater. Sci. Eng.* 301, 012120. doi: 10.1088/1757-899X/301/1/012120

Yang, X., Li, Y., Wang, H., Zhou, J., and Lv, D. (2021). Purification effects of aquatic plants on nitrogen and phosphorus in eutrophic water bodies. *J. Dali Univ.* 6, 65–67. doi: 10.3969/j.issn.2096-2266.2021.12.013

Yu, X., Xu, L., and Wu, F. (2020). *China Fishery statistical yearbook* (Beijing: China Agriculture Press).

Zhang, S.-y., Zhou, Q.-h., Xu, D., He, F., Cheng, S.-p., Liang, W., et al. (2010). Vertical-flow constructed wetlands applied in a recirculating aquaculture system for channel catfish culture: effects on water quality and zooplankton. *Pol. J. Environ. Stud.* 19, 1063–1070.

Zhu, X., Cui, L., Liu, W., and Liu, Y. (2004). Removal efficiencies of septic tank effluent by simulating vertical - flow constructed canna indica Linn wetlands. *J. Agro-environment Sci.* 24, 761–765. doi: 1672-2043(2004)04-0761-05

frontiers | Frontiers in Marine Science

TYPE Brief Research Report
PUBLISHED 15 September 2022
DOI 10.3389/fmars.2022.1012893

OPEN ACCESS

EDITED BY
Ce Shi,
Ningbo University, China

REVIEWED BY
Chengyue Liu,
South China Sea Institute of Oceanology, (CAS), China
Zhe Pan,
Hebei Agricultural University, China

*CORRESPONDENCE
Jie He
he_0902@126.com

†These authors have contributed equally to this work and share first authorship

SPECIALTY SECTION
This article was submitted to Marine Fisheries, Aquaculture and Living Resources, a section of the journal Frontiers in Marine Science

RECEIVED 06 August 2022
ACCEPTED 29 August 2022
PUBLISHED 15 September 2022

CITATION
Liu H, Chai X, Zhang D, Xu W and He J (2022) Effect of *Sinonovacula constricta* on sediment microbial numbers and easily degradable organics in shrimp-crab polyculture systems. *Front. Mar. Sci.* 9:1012893. doi: 10.3389/fmars.2022.1012893

Effect of *Sinonovacula constricta* on sediment microbial numbers and easily degradable organics in shrimp-crab polyculture systems

Huiling Liu[1,2†], Xinru Chai[1,2†], Dongxu Zhang[2], Wenjun Xu[2] and Jie He[2*]

[1]School of Fishery, Zhejiang Ocean University, Zhoushan, China, [2]Zhejiang Province Key Laboratory of Mariculture and Enhancement, Zhejiang Marine Fisheries Research Institute, Zhoushan, China

To explore the influence of different densities of *Sinonovacula constricta* on the composition of easily degradable organic matter and related functional bacteria, four experimental ecosystems were established: three polyculture systems (PMB_1, PMB_2, and PMB_3) of *Portunus trituberculatus* and *Marsupenaeus japonicus* with different stocking densities of *S. constricta* (11.6, 23.1, and 34.7×10^4 ind./hm^2, respectively) and a polyculture system with only *P. trituberculatus* and *M. japonicus* (PM). Among the easily degradable organic components in all aquaculture systems, protein content was the highest (0.74%~0.86%), followed by carbohydrates (0.16%~0.21%) and lipids (0.06%~0.13%). In the high-density (34.7×10^4 ind./hm^2) *S. constricta* mixed culture system, the contents of carbohydrates, lipids, and proteins in the sediment were significantly lower than those of the other polyculture systems. The number of cellulose-decomposing bacteria in PMB_3 was 3.79×10^6 cfu/g, which was significantly higher than that in the other systems. The number of starch-degrading bacteria and glutin-degrading bacteria was the lowest in PMB_3, 1.26×10^4 cfu/g, and 160.00 cfu/g, respectively. The number of lipid-degrading bacteria in PMB_3 was 0.77×10^4 cfu/g, which was significantly lower than that in the other systems. The easily degradable organics content in sediment was significantly positively correlated with the corresponding functional bacteria. The results showed that mixed culture of *S. constricta* could reduce the content of easily degradable organics in the sediment of mariculture ponds and change the number of functional bacteria in the sediment and the availability of degradable organic sediments may determine the abundance of corresponding degradable bacteria.

KEYWORDS

***Sinonovacula constricta*, easily degradable organics, functional bacteria, different densities, sediment**

Introduction

In aquatic ecosystems, sediments are not only the repository of nutrients and organic particles in water but also the nutrient source of the overlying water and are an important part of the aquatic environment (Søndergaard et al., 1999). Simple organic compounds such as carbohydrates, starches, and proteins in sediments are quickly decomposed by functional bacteria, but lignin and resin are resistant to microbial decomposition and are not easily oxidized (Zaki et al., 2015; Wang et al., 2019). Easily degradable organics are decomposed into small molecular organic matter or inorganic matter through a series of microbial catabolic activities, which participate in the biogeochemical cycle of the polyculture ecosystem, thereby affecting the entire aquaculture environment (Behera et al., 2022). Studies have shown that the degradable components in surface sediments can affect the dynamics and metabolism of bottom fauna (Grant and Hargrave, 1987; Dell'Anno et al., 2000), and the content of degradable parts in organic matter can also be used to evaluate the nutritional status of ecosystems (Dell'Anno et al., 2002; Pusceddu et al., 2003).

Sediment is the habitat of many farmed animals and is very important to the success of farming (Boyd, 1995). During the farming period, residual baits and feces are continuously accumulated in the sediment, which increases the organic matter content of the sediment (Liu et al., 2022). It was reported that approximately 40.44% of sedimentary organic matter in shellfish aquaculture ecosystems can be assimilated by benthic bait animals, but 59.56% of sedimentary organic matter still needs microbial transformation (Ji et al., 1998). The degradation of easily degradable organics in sediments involves various types of functional bacteria, such as proteolytic bacteria, cellulose-decomposing bacteria, and starch-decomposing bacteria (Prijambada et al., 2009; Artha et al., 2019). These functional bacteria can produce proteases, dehydrogenases, lipases, amylases, oxidases, decarboxylases, and other extracellular enzymes acting on organic matter. Through anaerobic or aerobic processes, a series of biochemical reactions occur to degrade organic matter gradually and ultimately convert it into inorganic elements that can be absorbed and utilized by phytoplankton and aquaculture animals (Pisarek and Grata, 2013; Gawas et al., 2019). For example, the amylase secreted by starch-degrading bacteria can decompose the insoluble starch in the sediment into soluble monosaccharides, which are further decomposed into CO_2 and participate in the carbon cycle at the water-air interface (Prijambada et al., 2009; Artha et al., 2019). Different types of functional bacteria secrete different extracellular enzymes to promote the degradation of easily degradable organic matter in sediment, which plays an important role in the circulation of biogenic elements in the aquaculture system.

Benthic shellfish change the physical properties of the sediment, such as its spatial heterogeneity, surface composition, particle size distribution, and porosity, by digging holes and *via* ventilation, excretion, and other biological disturbances (Thayer, 1979) and then affect the easily degradable organics in sediment and its related decomposing bacteria. In addition, benthic shellfish can also transfer particulate organic matter (POM) from water into the sediment in the form of feces or pseudofeces through the filtering effect (Newell, 2004). *Sinonovacula constricta* is a common zoobenthos species in coastal areas of China. It has a filter-feeding habit and is one of the important cultured shellfish in coastal areas of China (Chang, 2007). Studies have shown that the water transparency was greatly improved during the rapid growth of razor clam from June to October (Ren and Li, 2016), and the sediment organic matter content in the polyculture pond was significantly lower than that in the monoculture pond (He and Li, 2013). This is because *S. constricta* absorbs suspended organic substances from the upper water surface through its water pipe, improves water transparency, and reduces organic matter content in sediments (Tsuchiya and Kurihara, 1979; Lukwambe et al., 2018). When its distribution density is high, the ability of the population to remove organic matter in sediments is significantly strengthened (Tsuchiya and Kurihara, 1979; Lukwambe et al., 2018). However, there is a lack of research on the effect of filter-feeding shellfish in polyculture ecosystems on easily degradable organics, which thus needs further study. Based on the above understanding, four experimental ecosystems were established in this study: *S. constricta* was mixed into a *Portunus trituberculatus–Marsupenaeus japonicus* polyculture ecosystem at different densities to clarify the effects on the distribution and proportion of easily degradable organics in sediment and the changes in the number of easily degradable organics-degrading bacteria in different marine aquaculture ponds.

Materials and methods

Sampling ponds

The culture ponds were located on Changbai Island, Zhoushan city, Zhejiang Province (30°10′ N, 122°02′ E), and the size of the ponds was 1.33×10^4 m^2. Three ponds were stocked with *P. trituberculatus*, *M. japonicus*, and *S. constricta*, which were termed PMB_1, PMB_2, and PMB_3 according to the stocking density of *S. constricta* from low to high. The fourth pond was stocked with *P. trituberculatus* and *M. japonicus* only and was termed PM. The stocking time of *S. constricta* was early April, the stocking time of *P. trituberculatus* was early June, and the stocking time of *M. japonicus* was early July. The stocking densities of *P. trituberculatus* and *M. japonicus* in all ponds were 31.2×10^4 and 22.5×10^4 ind./hm^2, respectively. The stocking densities of *S. constricta* in PMB_1, PMB_2, and PMB_3 were 11.6×10^4, 23.1×10^4, and 34.7×10^4 ind./hm^2. The stocking

densities of *P. trituberculatus* and *M. japonicus* were according to practical experience as well as the low stocking density of *S. constricta* in PMB_1, and the middle and high density of *S. constricta* were set based on the above practical stocking density. The initial average individual weights of *P. trituberculatus*, *M. japonicus*, and *S. constricta* were 0.0240, 0.0087, and 0.3240 g, respectively. During the farming period, frozen trash fish were fed as the main feed once a day in the morning and evening. The protein, lipid, and carbohydrate contents of frozen trash fish were 15.4%, 3.3%, and 0.3%, respectively. Water exchange was carried out through the inlet and outlet of the pond, and the water exchange capacity of the different breeding ponds was consistent.

Sample collection and processing

The sediment samples from each pond were collected from April to December 2020. The initial sampling time was early April, and the sediment samples at the end of each month were collected in the middle ten days. Three sampling points were selected along the diagonal line in each pond, and four sediment samples were collected at each sampling point using a sediment column sampler (diameter: 10 cm), mixed evenly and placed in an incubator. According to Chai et al. (2022), the sediment temperature ranged from 7.47 to 30.13°C during the farming season in all the aquaculture systems, with an average of (21.36 ± 6.76)°C. The mean sediment pH values of PM, PMB_1, PMB_2, and PMB_3 were 7.55 ± 0.10, 7.58 ± 0.10, 7.56 ± 0.11, and 7.65 ± 0.07, respectively. The mean sediment redox potential (ORP) of PM, PMB_1, PMB_2, and PMB_3 were (-153.85 ± 26.87) mV, (-147.15 ± 28.56) mV, (-141.11 ± 23.00) mV and (-141.19 ± 18.90) mV, respectively.

Determination of the organic matter content

After the mud samples were mixed evenly, 40 g of each sample was freeze-dried with a freeze-drying machine. The mud samples were ground into powder by a bowl mill and passed through a 100-mesh standard test sieve. The filtered fine powder was collected and ignited at 450°C for 5 hours. The weight difference before and after ignition was calculated. The ratio of lost mass to dry sample mass was the organic matter content (OM, $mg{\cdot}g^{-1}$).

Determination of easily degradable organics

In the analysis of easily degraded organic matter in the sediment, the phenol–sulfuric acid method was used for the determination of carbohydrates (Masuko et al., 2005). According to the Editorial Board of the Water and Wastewater Monitoring and Analysis Methods of the State Environmental Protection Administration (2002), the Lowry method was used for the determination of proteins, and the methanol-chloroform method was used for the determination of lipids (Bligh and Dyer, 1959).

Statistics of functional bacteria

The bacterial counts of different groups in sediment samples were performed by the maximum possible count (MPN) and plate count (CFU) methods (Xu and Zheng, 1986). The MPN method was used for starch-degrading bacteria and glutin-degrading bacteria, and the CFU method was used for cellulose-degrading bacteria and lipid-degrading bacteria. In the MPN counting method, the mud samples were serially diluted 10 times to the final dilution, and when bacterial growth was not observed after inoculation, this was considered the critical stage. Then, 1 mL of each of the last five diluents in the series was placed into the corresponding liquid medium, and three parallel dilutions were performed; this MPN counting method is also called the three-tube method. The plate counting method (CFU) also used sample serial dilution, with three parallel dilutions performed, and 0.1 mL diluents were added to each plate for uniform coating. The culture temperature of all biological samples was 30°C, and the culture time was the same as the previous corresponding index.

Statistical analysis

In the statistical analysis, the mean values of four parallel samples were taken as the measured values of each sampling point. SPSS 22.0 and SigmaPlot 14.0 were used for data analysis. Repeated-measures analysis of variance was used to analyze the differences in the number of microorganisms in the sediment of the different breeding systems and the differences in the number of easily biodegradable organic substances in the sediment of the different breeding systems.

Results

Changes in easily degradable organics in the sediment

During the farming period, the carbohydrate content of the sediment in the different breeding systems generally showed a trend of first increasing and then decreasing (Figure 1A). The carbohydrate content ranges in the sediments of PM, PMB_1, PMB_2 and PMB_3 were 0.04~0.40%, 0.05~0.35%, 0.04~0.43% and 0.04~0.33%, respectively, and the average values were (0.20 ± 0.12) %, (0.21 ± 0.09) %, (0.21 ± 0.12) %, and (0.16 ± 0.11) %,

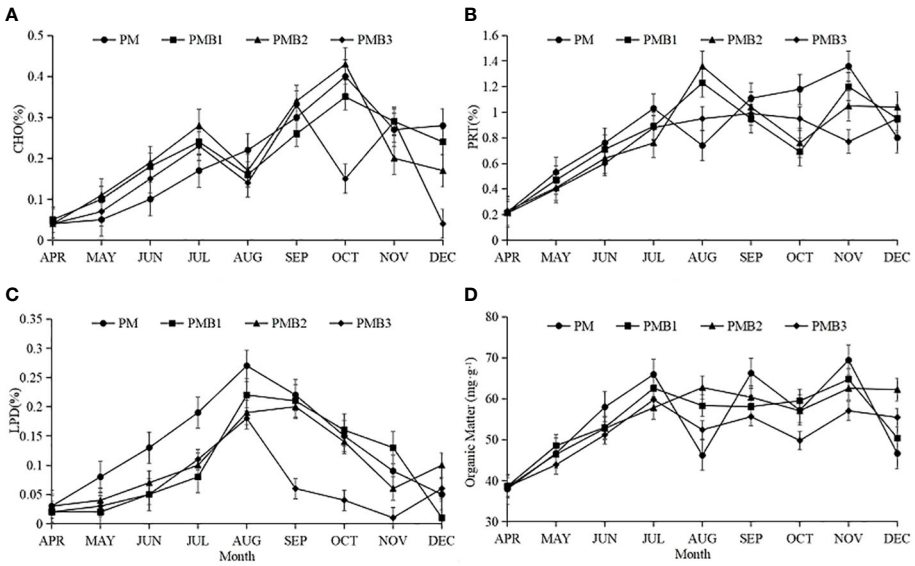

FIGURE 1
Changes in sediment easily degradable organics during the farming period. The data are shown as the means±SDs. **(A)**, change of CHO; **(B)**, change of PRT; **(C)**, change of LPD; **(D)**, change of Orgnic matters. CHO, carbohydrate in the sediment; PRT, protein in the sediment; LPD, lipid in the sediment.

respectively. The results of the difference analysis showed that the carbohydrate content in the sediment of the PMB_3 system was the lowest, which was significantly lower than that of the other polyculture ecosystems ($P < 0.05$), and there was no significant difference among PM, PMB_1, and PMB_2 ($P > 0.05$).

As shown in Figure 1B, during the farming period, the protein content ranges in the sediments of PM, PMB_1, PMB_2 and PMB_3 were 0.22~1.36%, 0.21~1.23%, 0.23~1.36% and 0.21~0.99%, respectively, and the average values were (0.86 ± 0.35) %, (0.81 ± 0.33) %, (0.81 ± 0.35) % and (0.74 ± 0.28) %, respectively. The results of the difference analysis showed that the sediment protein content of the PMB_3 system was the lowest, which was significantly lower than that of the other polyculture ecosystems ($P < 0.05$). The protein content in the sediment of the PM system was the highest, followed by PMB_1 and PMB_2, and there was no significant difference between PMB_1 and PMB_2 ($P > 0.05$).

During the farming period, the trend of lipid content in the four breeding systems increased first and then decreased, with the highest content found in August (Figure 1C). The lipid content ranges in the sediments of PM, PMB_1, PMB_2, and PMB_3 were 0.03~0.27%, 0.01~0.22%, 0.03~0.19%, and 0.01~0.18%, respectively, and the average values were (0.13 ± 0.08) %, (0.10 ± 0.08) %, (0.10 ± 0.06) %, and (0.06 ± 0.05) %, respectively. The results of the difference analysis showed that the lipid content in the sediment of PMB_3 was the lowest, which was significantly lower than that of the other polyculture ecosystems ($P < 0.05$). The lipid content of the sediment in the PM system was the highest, followed by PMB_1 and PMB_2, and there was no significant difference between PMB_1 and PMB_2 ($P > 0.05$).

As shown in Figure 1D, during the farming period, the organic matter contents in PM, PMB_1, PMB_2, and PMB_3 sediments ranged from 37.91 to 69.41 $mg{\cdot}g^{-1}$, from 38.62 to 64.72 $mg{\cdot}g^{-1}$, from 38.45 to 62.72 $mg{\cdot}g^{-1}$ and from 38.47 to 59.78 $mg{\cdot}g^{-1}$, with average values of (54.91 ± 11.05) $mg{\cdot}g^{-1}$, (54.86 ± 8.12) $mg{\cdot}g^{-1}$, (55.59 ± 8.36) $mg{\cdot}g^{-1}$ and (51.51 ± 6.74) $mg{\cdot}g^{-1}$, respectively. The difference analysis showed that the organic matter content of the PMB_3 sediment was significantly lower than that of the other treatment groups ($P < 0.05$) and that there was no significant difference among PM, PMB_1, and PMB_2 ($P > 0.05$).

Changes in the number of functional bacteria in the sediment

The number of starch-degrading bacteria in the PM and PMB_1 sediments increased first and then decreased but remained low (Figure 2A). The number of starch-degrading bacteria in PMB_2 and PMB_3 decreased continuously from the beginning of the culture (Figure 2A). The number of starch-degrading bacteria in the PM, PMB_1, PMB_2, and PMB_3 sediments ranged from 4.5×10^2 to 2.5×10^4 cfu/g, 4.5×10^2 to 2.5×10^4 cfu/g, 1.5×10^4 to 9.8×10^4 cfu/g and 9×10^2 to 4.5×10^4 cfu/g, respectively. The average values were (2.47 ± 1.03) $\times10^4$ cfu/g, (1.82 ± 0.86) $\times10^4$ cfu/g, (1.87 ± 0.97) $\times10^4$ cfu/g and (1.26 ± 0.90) $\times10^4$ cfu/g, respectively. The number of starch-degrading bacteria in the PMB_3 sediment was the lowest, which was significantly lower than that in the other treatment groups ($P < 0.05$). Systems PM and PMB_1 were significantly higher than PMB_3

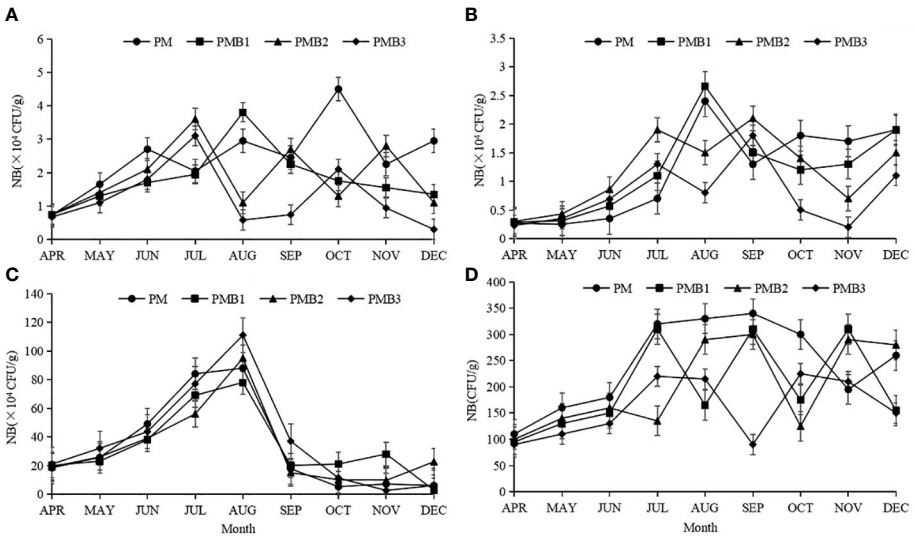

FIGURE 2
Changes in the number of functional bacteria in sediment during the farming period. The data are shown as the means ± SDs. **(A)**, the number of starch-degrading bacteria; **(B)**, the number of lipid-degrading bacteria; **(C)**, the number of cellulose-decomposing bacteria; **(D)**, the number of glutin-degrading bacteria.

($P < 0.05$), and there was no significant difference between PMB_1 and PMB_2 ($P > 0.05$), PM was the highest ($P < 0.05$).

The number of lipid-degrading bacteria in the PM and PMB_1 sediments showed a trend of first increasing and then decreasing (Figure 2B). The number of bacteria in the PMB_2 and PMB_3 polyculture ecosystems showed the same trend, showing a trend of first increasing and then decreasing and then increasing and then decreasing (Figure 2B). The number of lipid-degrading bacteria in PM, PMB_1, PMB_2, and PMB_3 ranged from 2.5×10^3 to 2.4×10^4 cfu/g, 2.9×10^3 to 2.7×10^4 cfu/g, 3.0×10^3 to 2.1×10^4 cfu/g and 2×10^3 to 1.8×10^4 cfu/g, with average values of $(1.19 \pm 0.81) \times10^4$ cfu/g, $(1.20 \pm 0.77) \times10^4$ cfu/g, $(1.19 \pm 0.64) \times10^4$ cfu/g and $(0.77 \pm 0.54) \times10^4$ cfu/g, respectively. The number of lipid-degrading bacteria in the PMB_3 sediment was the lowest, which was significantly lower than that in the other systems ($P < 0.05$). There was no significant difference among the other systems ($P > 0.05$).

The number of cellulose-decomposing bacteria in the sediment of the four polyculture ecosystems first increased and then decreased, reaching a maximum in August, but the number in PMB_2 and PMB_3 increased sharply in August, and the growth rate was faster than that of PM and PMB_1 (Figure 2C). The number of cellulose-degrading bacteria in the PM, PMB_1, PMB_2, and PMB_3 sediments varied from 5.2×10^4 to 8.8×10^5 cfu/g, 2.8×10^4 g to 8.3×10^5 cfu/g, 9.57×10^4 to 9.5×10^5 cfu/g, and 2.6×10^4 to 1.11×10^6 cfu/g, with averages of $(3.34 \pm 3.27) \times10^5$ cfu/g, $(3.33 \pm 2.47) \times10^5$ cfu/g, $(3.25 \pm 2.78) \times10^6$ cfu/g and $(3.79 \pm 3.57) \times10^6$ cfu/g, respectively. In PMB_3 and PMB_1, the number of cellulose-degrading bacteria in the sediment was the highest, which was significantly higher than that in the other treatment groups ($P < 0.05$). The numbers in the PM and PMB_2 systems were the lowest, and there was no significant difference between the two groups ($P > 0.05$).

The number of glutin-degrading bacteria in the PM sediment increased first and then showed a relatively stable trend, while the number in the other systems increased first and then showed a fluctuating trend and remained low (Figure 2D). The number of gelatinolytic bacteria in the PM, PMB_2, PMB_1, and PMB_3 sediments varied from 110 to 340 cfu/g, 95 to 310 cfu/g, 100 to 300 cfu/g and 90 to 225 cfu/g, with average values of (243.89 ± 84.62) cfu/g, (200.00 ± 85.59) cfu/g, (202.22 ± 84.86) cfu/g, and (160.00 ± 57.72) cfu/g, respectively. The number of glutin-degrading bacteria in the PMB_3 sediment was the lowest ($P < 0.05$) and that in PM was the highest ($P < 0.05$). The numbers in PMB_1 and PMB_2 were significantly higher than that in PMB_3, and there was no significant difference between the former two groups ($P > 0.05$).

Correlation between the number of different groups of bacteria and easily degradable organics in sediment

Correlation analysis showed that the carbohydrate content in sediment was positively correlated with the number of starch-degrading bacteria ($P < 0.05$) and negatively correlated with the number of cellulose-decomposing bacteria ($P < 0.05$) (Table 1). The protein content was positively correlated with the number of gelatin-decomposing bacteria ($P < 0.01$). The lipid content was negatively correlated with the number of lipid-decomposing

TABLE 1 Correlation between organic matter in sediment and the number of bacteria.

	CHO	PRT	LPD
Starch-degrading bacteria	0.829*	-0.494	0.070
Glutin-degrading bacteria	-0.824*	0.761	0.481
Lipid-degrading bacteria	-0.601	0.906**	0.511
Cellulose-degrading bacteria	-0.114	-0.374	-0.830*

CHO, carbohydrate in the sediment; PRT, protein in the sediment; LPD, lipid in the sediment. The values are represented as the means ± SDs. *correlation is significant at the 0.05 level; **correlation is significant at the 0.01 level.

bacteria ($P < 0.05$). There was no significant correlation between the number of functional bacteria and the content of easily degradable organics in the sediment.

Discussion

The results showed that protein was the main easily degradable organics in the sediment of the polyculture system, with an average content of 0.8%, followed by carbohydrates (0.2%) and lipids (0.1%). In the Chaohu Lake ecosystem, the composition of easily degradable organics in surface sediments is mainly carbohydrates, followed by proteins and lipids (He et al., 2016). There are significant differences between polyculture ecosystems and lakes, which may be related to sediment sources. In lake ecosystems, degradable organic compounds such as carbohydrates, proteins, and lipids mainly come from higher-plant residues, zooplankton, plant excreta, and corpses (Baldi et al., 2010; Zhang et al., 2017). Feeding feed is an important difference between polyculture ecosystems and other aquatic ecosystems. Feed is rich in protein, and feed residue settles into the bottom mud, increasing the content of protein in sediment. Therefore, the protein content of easily degraded organic matter is the highest in the polyculture system. In addition, the contents of various substances in sediments in the algae-type lake area of the Taihu Lake were higher than those in the pond aquaculture ecosystem, and their compositions were lipids (0.77%), carbohydrates (0.45%), and proteins (0.08%) (Qi et al., 2019). This may be related to the influence of breeding management measures in the artificial breeding system. Lake ecosystems usually have existed for several decades. A large amount of organic matter is deposited in the sediment environment, while mariculture ponds are dried and dredged every year. This management method leads to the exposure of a large amount of organic matter to the air and to oxidation, which results in the degradation of sediments.

Previous studies have shown that cultured shellfish can accelerate the sedimentation of various organic substances in water (Hatcher et al., 1994). At the same time, shellfish exert the filter-feeding effect of continuous organic matter assimilation, significantly reducing sediment organic matter accumulation. In this study, the order of organic matter content in sediments of all aquaculture systems was PM > PMB_1 > PMB_2 > PMB_3, showing that the organic matter content in the sediment of PMB_3, which had the highest *S. constricta* density, was the lowest, and was significantly lower than that in the other polyculture ecosystems. This shows that mixed culture of *S. constricta*, especially a high-density mixed culture, will affect the content of organic matter in the sediment. In the pond polyculture ecosystem, suspended particles such as residual bait, excrement of cultured animals, and plankton in water are the main sources of sediment organic matter. The higher the density of *S. constricta* is, the stronger the sediment purification effect of this filter-feeding shellfish on the environment will be, and thus the stronger the feeding ability of filter-feeding benthic animals on bacteria, particulate organic matter and attached animals and plants in water will be, resulting in a lower content of sediment organic matter in the high-density *S. constricta* mixed pond than that in the shrimp and crab mixed pond. In this study, the content of easily degraded organic matter was also affected by the mixed culture of *S. constricta*. The results showed that the content of carbohydrates, lipids, and proteins in the PMB_3 sediment was the lowest, which was significantly lower than that in the other polyculture ecosystems. This may be related to the content of organic matter in the sediment. The higher the density of *S. constricta* is, the stronger the sediment purification effect of this filter-feeding shellfish on the environment and the lower the organic matter content in the sediment will be, thus reducing the total content of carbohydrates, lipids, and proteins in sediment. In addition, the nutrients required for the survival of filter-feeding shellfish are mainly proteins, lipids, and carbohydrates. Therefore, the higher the density of *S. constricta* in mixed polyculture, the greater the demand for nutrients and sediment protein.

Bacterial communities in sediments could affect the transformation processes of organic matter, and the changes in organic matter composition in sediments could also in turn change the abundance and composition of bacterial communities (Judd et al., 2006). The results of the correlation analysis showed that different types of easily degradable organics were significantly positively correlated with their corresponding functional bacteria (Table 1). Previous studies also found that the total number of bacteria in the sediment ecosystem was closely related to the concentration of organic matter, and the number was positively correlated with the change in organic matter content (Albertelli et al., 1999; Hjelm et al., 2004), which is consistent with the conclusion of this study. In the aquaculture ecosystem, with the extension of breeding time, organic matter is enriched at the bottom of the pond, creating a good living environment for bacteria and promoting their mass reproduction. Therefore, the availability of readily biodegradable organic sediments may determine the abundance of corresponding decomposing bacteria.

According to previous studies, the change in bacterial number in sediment was controlled by temperature (Garland and Mills, 1991), organic matter content in sediment (Classen et al., 2003; Xu et al., 2020), redox conditions in sediment (Muyzer et al., 1993), and feeding effects of small and large benthic animals (Sherysheva, 2021). In this study, the numbers of starch-degrading bacteria, glutin-degrading bacteria, and lipid-degrading bacteria were the smallest in PMB_3, followed by PMB_2 and PMB_1, indicating that the mixed culture of different densities of *S.constricta* in the breeding system had an effect on the number of functional bacteria in the sediment. With the increase in breeding density, the number of starch-decomposing bacteria, gelatin-decomposing bacteria, and lipid-decomposing bacteria in the sediment decreased. The higher density of *S. constricta* can reduce the accumulation of residual bait in the sediment through the filter-feeding effect so that the organic matter content in the sediment is reduced, thus reducing the energy supply of functional bacteria. In addition, the number of cellulose-degrading bacteria was the largest in all breeding systems, which may be related to the environment of the breeding ponds. During the farming period, *Suaeda salsa* and other cellulose-rich plants grew in the pond dam and the surrounding shallow water area. Their dead bodies were deposited on the surface of the sediment, which may have promoted the growth and reproduction of cellulose-decomposing bacteria. The number of cellulose-decomposing bacteria in sediment was the highest in the polyculture ecosystem, which may be related to the higher biomass of *S. salsa* in the shallow water around PMB_3.

Based on the data on the physical and chemical factors of sediment from Chai et al. (2022), it was found that temperature had no significant effect on the change in organic matter content in sediment, while Ladd et al. (1981) found that increasing temperature would accelerate the decomposition rate of soil organic matter, which is inconsistent with the conclusions of this study. This may be because the increase in sediment temperature affects the appetite of benthic organisms, making the residual bait accumulate, and the sedimentation rate of sediment is much larger than the decomposition rate of organic matter, resulting in the non-significant effect of temperature on the change in organic matter content. In addition, based on the sediment physical and chemical factor data of Chai et al. (2022), it was found that the pH value and redox potential of sediment were negatively correlated with the content of easily degraded organic matter in sediment and the number of starch-degrading bacteria, glutin-degrading bacteria, and lipid-degrading bacteria (see Table 2). The reason for this result may be that the accumulation of easily degradable organics in sediment leads to an increase in the number of corresponding functional bacteria, thus accelerating the decomposition rate of organic matter. During the decomposition process, oxidized inorganic substances act as electron acceptors and are continuously reduced, resulting in a decrease in the redox potential in the sediment (Lv et al., 2018), while the decomposition of organic matter also releases HCO_3^- and CO_2, resulting in a decrease in pH in the sediment (Shakir et al., 2016). Previous studies have found that the oxidation–reduction potential (ORP) value can be affected by the number or activity of bacteria (Senga et al., 2010; Bollag and Stotzky, 2021).

TABLE 2 Correlation analysis between environmental factors and sediment easily degradable organics and functional bacteria.

Environmental factors	ST	$pH_{sediment}$	$ORP_{sediment}$
OM	0.300	-0.782**	-0.574**
CHO	0.310	-0.689**	-0.473**
PRT	0.283	-0.715**	-0.765**
LPD	0.675**	-0.638**	-0.766**
Starch-degrading bacteria	0.322	-0.545**	-0.412*
Glutin-degrading bacteria	0.288	-0.541**	-0.718**
Lipid-degrading bacteria	0.248	-0.694**	-0.618**
Cellulose-degrading bacteria	0.572**	-0.213	-0.233

ST, sediment temperature; $ORP_{sediment}$, sediment redox potential; $pH_{sediment}$, sediment pH; OM, organic matter in the sediment; CHO, carbohydrate in the sediment; PRT, protein in the sediment; LPD, lipid in the sediment. The values are represented as the means ± SDs. *correlation is significant at the 0.05 level; **correlation is significant at the 0.01 level.

Conclusion

In this study, through the analysis and comparison of easily degradable organics and related functional bacteria in the sediments of different polyculture ecosystems, it was found that the composition of easily degradable organics in the sediments was different from that in other aquatic ecosystems. Protein was the dominant factor, followed by carbohydrates and lipids. Affected by the biological disturbance of *Sinonovacula constricta*, the content of organic matter and the number of bacteria in the sediment changed, thereby affecting pH and ORP in the sediment. The pH and ORP are important factors that reflect the changes in the number of easily degradable organics and related functional bacteria in the sediment. During the farming period, the contents of carbohydrates, lipids, and proteins in the sediment of polyculture system PMB_3 were the lowest, and the easily degradable organics in the sediment were significantly correlated with its corresponding functional bacteria. High-density *S. constricta* coculture could significantly reduce the contents of carbohydrates, lipids, and proteins in sediment and the number of starch-degrading bacteria, glutin-degrading bacteria, and lipid-degrading bacteria. This study confirmed that the mixed culture of *S. constricta* can affect the content and proportion of easily degradable organics in the sediment and provide a basis for understanding the influence of *S. constricta* mixed culture on the sediment environment of marine aquaculture ponds.

Data availability statement

The original contributions presented in the study are included in the article/supplementary material. Further inquiries can be directed to the corresponding author.

Author contributions

HL and XC: Investigation, Formal analysis, Writing-original draft. DZ: Conceptualization, Data curation, Formal analysis. WX: Visualization, Writing-reviewing, and editing. JH: Supervision, Funding acquisition, Writing-reviewing, and editing. All authors contributed to manuscript revision, read, and approved the submitted version.

Funding

This work was supported by the National Science Foundation of China (Grant No. 32002395, 32172993); the Basic public welfare program of Zhejiang Province (Grant No. LGN22C190005); the Major Agricultural Technology Cooperation Plan of Zhejiang Province (Grant No. 2020XTTGSC03); the science and technology project of Zhoushan City and Putuo District (Grant No. 2018C31078, 2020JH131); the planned project of Zhejiang Marine Fisheries Research Institute (HYS-CZ-202105, HYS-CZ-202209).

Conflict of interest

The authors declare that the research was conducted in the absence of any commercial or financial relationships that could be construed as a potential conflict of interest.

Publisher's note

All claims expressed in this article are solely those of the authors and do not necessarily represent those of their affiliated organizations, or those of the publisher, the editors and the reviewers. Any product that may be evaluated in this article, or claim that may be made by its manufacturer, is not guaranteed or endorsed by the publisher.

References

Albertelli, G., Covazzi-Harriague, A., Danovaro, R., Fabiano, M., Fraschetti, S., and Pusceddu, A. (1999). Differential responses of bacteria, meiofauna and macrofauna in a shelf area (Ligurian Sea, NW mediterranean): role of food availability. *J. Sea Res.* 42 (1), 11–26. doi: 10.1016/S1385-1101(99)00012-X

Artha, O. A., Pramono, H., and Sari, L. A. (2019). Identification of extracellular enzyme-producing bacteria (proteolytic, cellulolytic, and amylolytic) in the sediment of extensive ponds in Tanggulrejo, Gresik, *IOP Conf. Ser.: Earth Environ. Sci.* 236 (1), 012003. doi: 10.1088/1755-1315/236/1/012003

Baldi, F., Marchetto, D., Pini, F., Fani, R., Michaud, L., Giudice, A. L., et al. (2010). Biochemical and microbial features of shallow marine sediments along the Terra Nova bay (Ross Sea, Antarctica). *Cont. Shelf Res.* 30 (15), 1614–1625. doi: 10.1016/j.csr.2010.06.009

Behera, P. K., Das, S. K., Ghosh, D., Mani, D., Kalpana, M. S., Ikehara, M., et al. (2022). Organic biogeochemical study of deeper southeastern Bengal basin sediments in West Bengal, India. *Org. Geochem.* 170, 104451. doi: 10.1016/j.orggeochem.2022.104451

Bligh, E. G., and Dyer, W. J. (1959). A rapid method of total lipid extraction and purification. *Can. J. Biochem. Physiol.* 37 (8), 911–917. doi: 10.1139/o59-099

Bollag, J. M., and Stotzky, G. (2021). *Soil biochemistry* Volume 7. (US: CRC Press).

Boyd, C. E. (1995). *Bottom soils, sediment, and pond aquaculture*. (US: Springer).

Chai, X. R., Xu, W. J., Zhang, D. X., He, J., and Liu, H. L. (2022). Effects of sinonovacula constricta polyculture on sedimentary environment in the integrated culture system of portunus trituberculatus and marsupenaeus japonicus. *Oceanol. Limnol. Sin* 53 (3), 718–25. doi: 10.11693/hyhz20211100276

Chang, Y. Q. (2007). *Mulluscs culture and enhancement* (China: China Agriculture Press).

Classen, A. T., Boyle, S. I., Haskins, K. E., Overby, S. T., and Hart, S. C. (2003). Community-level physiological profiles of bacteria and fungi: plate type and incubation temperature influences on contrasting soils. *FEMS Microbiol. Ecol.* 44 (3), 319–328. doi: 10.1016/s0168-6496(03)00068-0

Dell'Anno, A., Mei, M. L., Pusceddu, A., and Danovaro, R. (2002). Assessing the trophic state and eutrophication of coastal marine systems: a new approach based on the biochemical composition of sediment organic matter. *Mar. Pollut. Bull.* 44 (7), 611–622. doi: 10.1016/S0025-326X(01)00302-2

Dell'Anno, A., Fabiano, M., Mei, M. L., and Danovaro, R. (2000). Enzymatically hydrolyzed protein and carbohydrate pools in deep-sea sediments: Estimates of the potentially bioavailable fraction and methodological considerations. *Mar. Ecol.: Prog. Ser.* 196, 15–23. doi: 10.3354/meps196015

Editorial board of the Water and Wastewater Monitoring and Analysis Methods of the State Environmental Protection Administration (2002). *Water and wastewater monitoring and analysis methods. 4th ed.* (China: China Environmental Science Press).

Garland, J. L., and Mills, A. L. (1991). Classification and characterization of heterotrophic microbial communities on the basis of patterns of community-level sole-carbon-source utilization. *Appl. Environ. Microbiol.* 57 (8), 2351–2359. doi: 10.1002/bit.260380413

Gawas, V. S., Shivaramu, M. S., Damare, S. R., Pujitha, D., Meena, R. M., and Shenoy, B. D. (2019). Diversity and extracellular enzyme activities of heterotrophic bacteria from sediments of the central Indian ocean basin. *Sci. Rep.* 9 (1), 1–9. doi: 10.1038/s41598-019-45792-x

Grant, J., and Hargrave, B. T. (1987). Benthic metabolism and the quality of sediment organic carbon. *Biol. Oceanogr.* 4 (3), 243–264. doi: 10.1080/01965581.1987.10749493

Hatcher, A. J. G. B., Grant, J., and Schofield, B. (1994). Effects of suspended mussel culture (Mytilus spp.) on sedimentation, benthic respiration and sediment nutrient dynamics in a coastal bay. *Mar. Ecol. Prog. Ser.* 115, 219–219. doi: 10.3354/meps115219

He, Y. Z., Ke, F., Feng, M. H., Li, W. C., Chen, X. C., and Zhou, F. (2016). Characteristics and distribution of biodegradable compounds of surface sediments in lake chaohu. *J. Lake Sci.* 28 (1), 40–49. doi: 10.18307/2016.0105

He, L. H., and Li, J. S. (2013). The sediment oxygen demand in the integrated prawn and solenidae ponds. *Chin. Agric. Sci. Bull.* 29 (35), 80–83. doi: 10.11924/j.issn.1000-6850.2013-2275

Hjelm, M., Riaza, A., Formoso, F., Melchiorsen, J., and Gram, L. (2004). Seasonal incidence of autochthonous antagonistic roseobacter spp. and vibrionaceae strains in a turbot larva (Scophthalmus maximus) rearing system. *Appl. Environ. Microbiol.* 70 (12), 7288–7294. doi: 10.1128/AEM.70.12.7288-7294.2004

Ji, R. B., Mao, X. H., and Zhu, M. Y. (1998). Impacts of coastal shellfish aquaculture on bay ecosystem. *Adv. Mar. Sci.* 16 (1), 21–27. https://kns.cnki.net/kcms/detail/detail.aspx?dbcode=CJFD&dbname=CJFD9899&filename=

HBHH801.003&uniplatform=NZKPT&v=8UL9Zv6kaz3UTYWMwxf22XelzdVeMqAdoAlJRutddk4chkqN8RsYS5UN33OONsSl

Judd, K. E., Crump, B. C., and Kling, G. W. (2006). Variation in dissolved organic matter controls bacterial production and community composition. *Ecology* 87 (8), 2068–2079. doi: 10.1890/0012-9658(2006)87[2068:VIDOMC]2.0.CO;2

Ladd, J. N., Oades, J. M., and Amato, M. (1981). Microbial biomass formed from 14C, 15N-labelled plant material decomposing in soils in the field. *Soil Biol. Biochem.* 13 (2), 119–126. doi: 10.1016/0038-0717(81)90007-9

Liu, Q., Li, J., Shan, H., Xie, Y., and Zhang, D. (2022). Specific patterns and drivers of the bacterial communities in the sediment of two typical integrated multitrophic aquaculture systems. *Aquacult. Int.* 30 (3), 1–20. doi: 10.1007/S10499-022-00862-2

Lukwambe, B., Yang, W., Zheng, Y., Nicholaus, R., Zhu, J., and Zheng, Z. (2018). Bioturbation by the razor clam (Sinonovacula constricta) on the microbial community and enzymatic activities in the sediment of an ecological aquaculture wastewater treatment system. *Sci. Total Environ.* 643, 1098–1107. doi: 10.1016/j.scitotenv.2018.06.251

Lv, X., Yu, P., Mao, W., and Li, Y. (2018). Vertical variations in bacterial community composition and environmental factors in the culture pond sediment of sea cucumber apostichopus japonicus. *J. Coast. Res.* 84 (10084), 69–76. doi: 10.2112/SI84-010.1

Masuko, T., Minami, A., Iwasaki, N., Majima, T., Nishimura, S. I., and Lee, Y. C. (2005). Carbohydrate analysis by a phenol–sulfuric acid method in microplate format. *Anal. Biochem.* 339 (1), 69–72. doi: 10.1016/j.ab.2004.12.001

Muyzer, G., De Waal, E. C., and Uitterlinden, A. (1993). Profiling of complex microbial populations by denaturing gradient gel electrophoresis analysis of polymerase chain reaction-amplified genes coding for 16S rRNA. *Appl. Environ. Microbiol.* 59 (3), 695–700. doi: 10.1080/15389588.2015.1013535

Newell, R. I. (2004). Ecosystem influences of natural and cultivated populations of suspension-feeding bivalve molluscs: a review. *J. Shellfish Res.* 23 (1), 51–62. https://schlr.cnki.net/Detail/index/GARJ0010_1/NSTL0A423DF5658765D12D60CD88A385A9C5

Pisarek, I., and Grata, K. (2013). The influence of the organic matter of sewage sediments on biological activity of microorganisms which carry out the transformations of carbon and nitrogen compounds. *Pol. J. Microbiol.* 62 (4), 445. doi: 10.1016/B978-0-12-417029-2.00007-8

Prijambada, I. D., Widada, J., Kabirun, S., and Widianto, D. (2009). Secretion of organic acids by phosphate solubilizing bacteria isolated from oxisols. *J. Trop. Soils* 14 (3), 245–251. doi: 10.5400/JTS.2009.V14I3.%P

Pusceddu, A., Dell'Anno, A., Danovaro, R., Manini, E., Sara, G., and Fabiano, M. (2003). Enzymatically hydrolyzable protein and carbohydrate sedimentary pools as indicators of the trophic state of detritus sink systems: a case study in a Mediterranean coastal lagoon. *Estuaries* 26 (3), 641–650. doi: 10.1007/bf02711976

Qi, C., Fang, J. q., Zhang, L. m., Lei, B., Tang, X. c., and Wang, g. x. (2019). Composition and distribution of biodegradable compounds in phytoplankton-dominated zone of lake taihu. *J. Lake Sci.* 31 (4), 941–949. doi: 10.18307/2019.0423

Ren, Y. J., and Li, Y. R. (2016). Pond farming experiment of sinonvacula constricta in tianjin. *Tianjin Agric. Sci.* 22 (9), 67–70. doi: 10.3969/j.issn.1006-6500.2016.09.016

Søndergaard, M., Jensen, J. P., and Jeppesen, E. (1999). Internal phosphorus loading in shallow Danish lakes. *Hydrobiologia* 408-409, 145–152. doi: 10.1023/A:1017063431437

Senga, Y., Okumura, M., and Seike, Y. (2010). Seasonal and spatial variation in the denitrifying activity in estuarine and lagoonal sediments. *J. Oceanogr.* 66 (1), 155–160. doi: 10.1007/s10872-010-0013-0

Shakir, E. M. A. N., Al-Mashhady, A. A., Al-Janabi, Z. Z., and Al-Obaidy, A. H. M. (2016). Geochemical and geo-statistical assessment of heavy metals concentration in sediment of shatt Al-basrah, Iraq. *J. Basic Appl. Res. Int.* 18 (4), 233–239. doi: 10.1016/j.ecss.2009.12.019

Sherysheva, N. G. (2021). Ecological trends of spatial distribution and of size-morphological structure of bacteriobenthos in the kuibyshev reservoir, the Volga river, Russia. *IOP Conf. Ser.: Earth Environ. Sci* 818 (1), 012049. doi: 10.1088/1755-1315/818/1/012049

Thayer, C. W. (1979). Biological bulldozers and the evolution of marine benthic communities. *Science* 203 (4379), 458–461. doi: 10.1126/science.203.4379.458

Tsuchiya, M., and Kurihara, Y. (1979). The feeding habits and food sources of the deposit-feeding polychaete, neanthes japonica (Izuka). *J. Exp. Mar. Biol. Ecol.* 36 (1), 79–89. doi: 10.1016/0022-0981(79)90101-1

Wang, S., Xu, J., Zhang, X., Wang, Y., Fan, J., Liu, L., et al. (2019). Structural characteristics of humic-like acid from microbial utilization of lignin involving different mineral types. *Environ. Sci. Pollut. Res.* 26 (23), 23923–23936. doi: 10.1007/s11356-019-05664-3

Xu, J., Roley, S. S., Tfaily, M. M., Chu, R. K., and Tiedje, J. M. (2020). Organic amendments change soil organic c structure and microbial community but not total organic matter on sub-decadal scales. *Soil Biol. Biochem.* 150, 107986. doi: 10.1016/j.soilbio.2020.107986

Xu, G. H., and Zheng, H. Y. (1986). *Manual of soil microbial analysis methods* (China: China Agriculture Press).

Zaki, M. S., Authman, M. M., and Abbas, H. H. (2015). Bioremediation of petroleum contaminants in aquatic environments. *Life Sci. J.* 12 (5), 127–139. doi: 10.1007/978-94-017-2986-4_15

Zhang, Y., Su, Y., Liu, Z., Yu, J., and Jin, M. (2017). Lipid biomarker evidence for determining the origin and distribution of organic matter in surface sediments of lake taihu, Eastern China. *Ecol. Indic.* 77, 397–408. doi: 10.1016/j.ecolind.2017.02.031

frontiers | Frontiers in Marine Science

TYPE Original Research
PUBLISHED 18 October 2022
DOI 10.3389/fmars.2022.1040225

OPEN ACCESS

EDITED BY
Ce Shi,
Ningbo University, China

REVIEWED BY
Fang Wang,
Ocean University of China, China
Zhen Ma,
Dalian Ocean University, China

*CORRESPONDENCE
Ming Duan
duanming@ihb.ac.cn
Jianghui Bao
baojianghui@ihb.ac.cn

†These authors share first authorship

SPECIALTY SECTION
This article was submitted to Marine Fisheries, Aquaculture and Living Resources, a section of the journal Frontiers in Marine Science

RECEIVED 09 September 2022
ACCEPTED 28 September 2022
PUBLISHED 18 October 2022

CITATION
Xiang L, Mi X, Dang Y, Zeng Y, Jiang W, Du H, Twardek WM, Cooke SJ, Bao J and Duan M (2022) Shyer fish are superior swimmers in Siberian sturgeon (*Acipenser baerii*). *Front. Mar. Sci.* 9:1040225. doi: 10.3389/fmars.2022.1040225

Shyer fish are superior swimmers in Siberian sturgeon (*Acipenser baerii*)

Lingli Xiang[1,2†], Xiangyuan Mi[1,3†], Yingchao Dang[4,5], Yu Zeng[2], Wei Jiang[4,5], Hao Du[6], William M. Twardek[7], Steven J. Cooke[7], Jianghui Bao[1*] and Ming Duan[1*]

[1]State Key Laboratory of Freshwater Ecology and Biotechnology, Institute of Hydrobiology, Chinese Academy of Sciences, Wuhan, China, [2]College of Life Sciences, China West Normal University, National Freshwater Fisheries Engineering Technology Research Center (Wuhan) Southwest Branch, Nanchong, China, [3]College of Advanced Agricultural Sciences, University of Chinese Academy of Sciences, Beijing, China, [4]Chinese Sturgeon Research Institute, China Three Gorges Corporation, Yichang, China, [5]Hubei Key Laboratory of the Three Gorges Project for Conservation of Fishes, Yichang, China, [6]Key Laboratory of Freshwater Biodiversity Conservation and Utilization, Ministry of Agriculture/Yangtze River Fisheries Research Institute, Chinese Academy of Fisheries Science, Wuhan, China, [7]Fish Ecology and Conservation Physiology Laboratory, Department of Biology and Institute of Environmental and Interdisciplinary Science, Carleton University, Ottawa, ON, Canada

Differences in individual personality are common amongst animals, which can play an ecological and evolutionary role given links to fitness. Personality affects animal life processes and outputs (e.g., behavior, life history, growth, survival, reproduction), and has become a common theme in animal behavioral ecology research. In the present study, we used Siberian Sturgeon to explore how personality traits of boldness and shyness are related to swimming performance, post exercise recovery and phenotypic morphology. Firstly, our results indicated that the Siberian sturgeon juveniles of shyness were better swimmers, validating evolutionary biology trade-off theory. The critical swimming speed (U_{crit}) of the shy groups was higher than that of the bold groups. Secondly, the shy groups were more resilient after exercise fatigue. The swimming fatigue recovery ability, the glucose and lactic acid concentration recovery ability of shy groups were greater than that of bold groups. Thirdly, the shy groups were more streamlined. Compared with bold groups, shy groups had smaller caudate stalk lengths, caudate stalk heights, superior caudal lobes, and inferior caudal lobes. In general, we demonstrated that shy Siberian sturgeon had better swimming performance from physiology and morphology. These research results further enrich the theoretical viewpoints of fish behavior biology, more importantly, which provided a good example for studying the relationship between sturgeon's "personality" and swimming performance.

KEYWORDS

individual differences, Siberian sturgeon (*Acipenser baerii*), swimming performance trade-off, morphology, physiology

Introduction

Animal personality has been broadly defined as interindividual differences in behavior that remain consistent over time and contexts (Slater, 1981; Smith, 1982; Caro and Bateson, 1986; Clark and Ehlinger, 1987; Réale et al., 2007; Roche et al., 2016). Research on animal personality has covered diverse taxa including mammals, birds, reptiles, amphibians, fish, arthropods and mollusks (Gosling, 2001). Personality affects animal life processes and fitness, and has become the basis for much research in behavioral ecology (Réale et al., 2007). One of the most commonly focused dimensions of personality is the shyness-boldness continuum. The terms shy and bold refer to the propensity of an individual to take risks, especially in novel environments (Brown et al., 2007). Shy individuals react to novelty by retreating, reducing activity levels, and becoming more vigilant. In contrast, bold individuals are more likely to approach novel objects and increase activity levels and exploratory behavior (Brown et al., 2007). In the case of fish, personality influences various behaviors (including feeding, reproduction, migration, etc.) and is related to physiological processes (e.g., metabolism, immunity), cognitive abilities, morphology, and thus to growth and survival (Zhang and Wang, 2021).

The study of swimming performance in fish species has a long history, classified as steady or unsteady swimming (Webb, 1984; Langerhans, 2009b; Domenici, 2010). The trade-off between the two primary swimming modes, steady and unsteady swimming, is presumed to exist in fish species employing relatively coupled locomotor systems (i.e. the same morphological structures are used for propulsion during both steady and unsteady swimming) (Webb, 1978; Webb, 1984). The trade-off is thought to be of general evolutionary importance in fish (Lighthill, 1969; Webb, 1982; Lighthill, 2006; Langerhans, 2007; Langerhans, 2008). From an ecological and evolutionary perspective, the trade-off can occur when an increase in fitness due to a change in one trait is opposed by a decrease in fitness due to a concomitant change in another characteristic (Stephens and Krebs, 1986; Roff, 1992; Reznick et al., 2000). For example, the northern pike (*Esox lucius*) has much higher swimming velocities during acceleration tests but is a poor endurance swimmer (Harper and Blake, 1990). Fitness trade-off is an ecological mechanism that produces and maintains individual behavioral differences within a population (Kern et al., 2016). Personality may be one of the reasons for differences in individual swimming performance within a population. Shy zebrafish (*Danio rerio*) often avoid predators ('flight') and exhibit higher steady-swimming performance and, thus, greater energetic efficiency during routine activities. In contrast, bold zebrafish usually adopt a defensive strategy against predators ('fight'), showing higher fast-start swimming performance, achieving greater access to food resources and higher foraging efficiency; meanwhile, the risk of predation is higher (Kern et al., 2016). The cost-benefit trade-offs associated with energy expenditure and personality differences may be one of the most critical ecological mechanisms for the generation and coexistence of different swimming performances in fish (Stamps, 2007).

Significant variations in swimming performance exist among fishes, and morphology is considered the primary determinant of this diversity of swimming performance (Webb, 1984). Morphological characteristics associated with swimming can affect the performance of critical activities such as foraging, predator evasion and migration (Bruckerhoff and Magoulick, 2017). Morphology differences in body and fin shape are thought to be strong selective pressures acting upon swimming phenotypes (Webb, 1984; Blake, 2010). For instance, Australian smelt (*Retropinna semoni*) from river populations tended to have dorso-ventrally deeper bodies and larger heads compared to reservoir conspecifics, with a narrower, fusiform body shape and smaller head (Svozil et al., 2020). Morphological variation associated with different personality types may also be an essential manifestation of variation in fish swimming performance. Studies on zebrafish across numerous generations have found that bold, exploratory, and risk-taking individuals tend to have a more slender body and more significant caudal regions, with high fast-start swimming performance and low, stable swimming performance, which can improve survival rates in predatory encounters (Walker et al., 2005; Langerhans, 2009a). In some cases, certain personalities only enhance swimming performance when combined with a specific morphological characteristic (Roff and Fairbairn, 2012). The association between the morphology and swimming performance of fish with different personality traits requires further research.

Physiological variation associated with different personality types may also be an essential manifestation of variation in fish swimming performance (Careau et al., 2008; Biro and Stamps, 2010; Reale et al., 2010). Physiological specialization is considered one of the main determinants of diversity in locomotor capacities (Reidy et al., 2000). The metabolic rate of risk-taking carp (*Cyprinus carpio*) is significantly higher than that of risk-avoiding individuals (Huntingford et al., 2010). Moreover, cortisol receptor gene expression, plasma glucose and lactate levels are considerably lower in risk-taking carp than in risk-avoiding conspecifics (Huntingford et al., 2010). Bold mulloway (*Argyosomus japonicus*) exhibits lower cortisol levels than shy individuals (Raoult et al., 2012). During uniformly accelerated swimming to fatigue of White bream (*Parabramis pekinensis*), plasma glucose concentration decreased while lactic acid concentration increased (Wang, 2015). Yet, these studies focus on a single relationship between personality and physiology or swimming performance. Research on how fitness regulates the relationship between physiological performance and swimming performance of fish with different personalities is notably lacking.

Siberian sturgeon (*Acipenser baerii*), belonging to the class Osteichthyes, Actinopterygii, Chondrostei, Acipenseriformes, is the earliest specific trans-estuarine fish group. The species achieves a large body size, has a long life span, and has extremely important scientific value in studying evolutionary biology (Birstein et al., 1997). Here, we tested some theoretical concepts in evolutionary biology, 1) Are there personality differences between individuals of Siberian sturgeon? 2) What are the effects of personality differences on swimming performance? 3) What are the effects of personality differences on morphology and physiological performance, which correlates with swimming performance? Findings from this work will further enrich the theoretical knowledge pertaining to sturgeon evolutionary biology and may help inform conservation efforts for endangered sturgeon species in artificial propagation programs.

Materials and methods

Source of fish and rearing condition

One hundred juvenile Siberian sturgeon (mean total length ± SD =15.48 ± 1.80 cm and mean body weight ± SD = 13.13 ± 3.82 g) were collected from Wanming Fishery hatchery farm in Jingmen City, Hubei Province, China. Sturgeons are transported and housed in a recirculating aquaculture system (the following abbreviation is RAS; Yuya Technology (Shanghai) Co., LTD) at the laboratory of Institute of Hydrobiology, Chinese Academy of Sciences. Water temperature was maintained at 23.0 ± 0.5°C; dissolved oxygen was greater than 6 mg/L; pH was maintained at 7~8; And 12 h:12 h light: dark regime were based on natural lighting (lights on at 0700 hours). The Siberian sturgeons were fed on 3% of body weight commercial food twice at 8:00 am and 6:00 pm per day. Healthy fish were randomly selected for experimentation with food withheld for 48h before each experiment.

Experimental overview

To control for acclimatization effects, experiments started a month after laboratory housing. We started with the personality test and subjected fish to a classic "boldness" assay (Kern et al., 2016). We then assigned individuals to the boldness and shyness group and returned them to the RAS. After 2 rest days, we conducted the swimming performance test. A total of 30 bold individuals and 30 shy individuals were tested. Once the swimming performance test was completed, the individual was anaesthetized with MS-222 (0.033 g/L), and blood was sampled for physiological status analysis. Body weight was measured, and pictures of the body were taken (Nikon D810) for morphology analysis. To control the potential circadian rhythm affect, all the tests were conducted from 8:00 am to 12:00 am.

Personality test

A dark/light maze that was divided by a baffle into one shaded ("dark") arm (50 × cm) with a lid on top and one exposed ("light") arm (50 × cm) was used to assess "boldness" (Figure 1). The black cloth around the maze minimized external visual disturbance. The behavior of the test fish was recorded with a web camera (BASLER, acA1920-155uc, made in Germany, 25 frames/s) placed about 1.5 m above the maze. For each personality experiment, fish were selected randomly and transferred into a black container (10L) positioned adjacent to the test device. The container was filled with water with the same properties as the RAS. Fish were gently transferred into the shaded arms with the baffle "closed". After a two-minute acclimation period, the baffle was removed, and the exploratory behavior of the tested fish was recorded with cameras. A total of eight minutes were recorded, after which individuals were returned to a separate glass holding tank for further experiments.

Time spent in the dark arms was an indication of "boldness". Bold individuals were defined as individuals that spent more than four minutes in the exposed arms as per (Brown et al., 2005; Maximino et al., 2010), and vice versa. However, if the fish still had not emerged after eight minutes, the trial was terminated, and the individual was allocated a ceiling value of 480 s (Brown et al., 2005; Maximino et al., 2010). In addition, the animal behavior analysis system (Noldus, Ethovision XT10.0, The Netherlands) was also used to analyze the cumulative exploration time of experimental fish in the exposed arms. The water within the maze was replaced completely between individuals for each experiment. Each individual was tested no more than three times, with each retest occurring three days apart to assess short-term repeatability. The fish with the same results in two continuous tests was defined as the bold individual or shy individual. Otherwise, the experimental fish will be discarded, and the selection will be made again.

Swimming performance test

We conducted the swimming performance test following the personality test. A self-manufactured swimming tunnel combined with a web camera (fixed 1.5 m above the swimming device; BASLER, acA1920-155uc, made in Germany, 25 frames/s) was used to assess swimming performance (Figure 2). The LS300-type portable flow rate measuring instrument was used to calibrate the flow rate, and a linear relationship was established between the flow rate (Y) and the adjustment frequency (X): Y= 0.2517X + 0.6231, R=0.9975 (Figure 3).

Stepped velocity tests were carried out to measure the critical swimming speed of each fish (U_{crit}) (Hammer, 1995). The test fish was measured for body length and introduced to the tunnel to acclimate at 0.5 BL/s for 2 h. Then the water velocity was

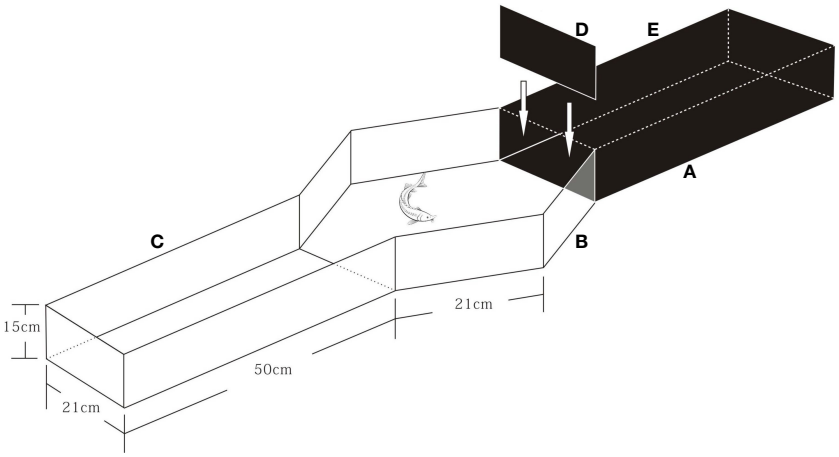

FIGURE 1
Experimental apparatus for testing fish personality. The device was divided into 3 parts: **(A)** is a cuboid dark area (length×width×height = 50cm×21cm×15cm), equipped with a black opaque lid **(E)** and an opaque baffle **(D)**; **(B)** is a hexagon lit area (side length = 21cm); **(C)** is a lit area with the same shape as A.

increased by 1 BL/s every 20 min until the fish became fatigued (Shi et al., 2012; Downie and Kieffer, 2017). Fatigue was defined as the point at which the fish could no longer swim away from the steel wire mesh positioned downstream of the swimming area (> 20 s) (Lee et al., 2003). The water velocity and swimming fatigue time (Endurance: defined as the time it took for the fish to stop swimming and fall back to the downstream wire mesh) were recorded. The flow speed was then decreased to 0.5 BL/s for a 60 min recovery test, and the recovery time was defined as the time the fish removed itself from the steel mesh and began swimming once again. Then a second stepped velocity test was undertaken (the test method was the same as the first time). In each trial, the water in the tunnel was the same as that of the RAS described above. The water was kept aerated when no fish were tested. Videos were playback by Quick Time Player at 0.5 times the speed for the tail beat frequency analysis.

U_{crit} were calculated according to equation (1) (Brett, 1964):

$$U_{crit} = U + \Delta U \times t/\Delta t \quad (1)$$

where U (cm/s) is the highest velocity at which fish swam for the full-time interval ΔU, m/s) is the speed step, t (min) is the time to fatigue during the last velocity step, and Δt (min) is the time step (20 min). The body cross-sectional area of the test fish in this study did not exceed 10% of the cross-sectional area of the swimming area, minimizing the need for a U_{crit} correction (Jain, 2003; Wang, 2009).

The recovery ratio (R) of Ucrit (cm/s) was a measure of a fish's ability to recover from fatigue. A lower R-value indicates

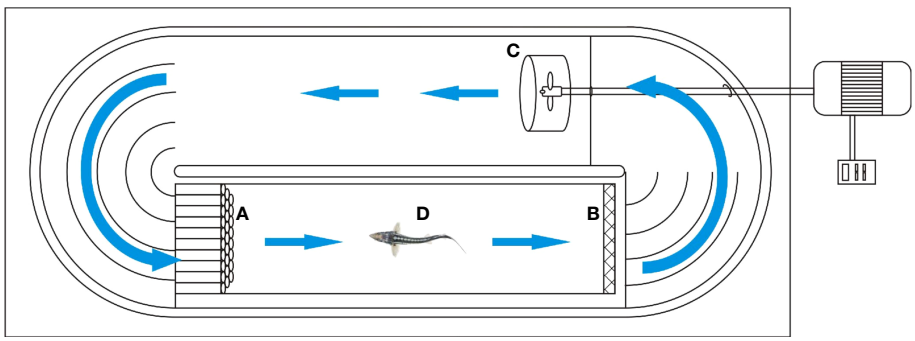

FIGURE 2
Experimental apparatus for testing swimming performance. **(A)** is the rectifier; **(B)** is the wire mesh; **(C)** is the propeller; **(D)** is the swimming test area (50cm×10cm×10cm); The frequency converter controls the motor, and the motor controls the three-blade propeller to create water flow, and the water circulates in the oval swimming tank, and the direction of the blue arrow is the direction of the water flow.

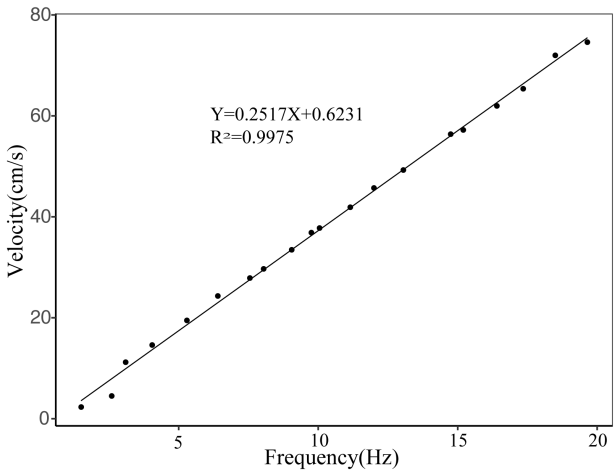

FIGURE 3
The relationship between frequency and velocity. Control the speed of water flow by adjusting the frequency of the inverter of the device of swimming performance test.

incomplete recovery and a larger effect of fatigue on subsequent swimming performance. The value of R was calculated using equation (2) (Farrell et al., 1998):

$$R = U_{crit2}/U_{crit1} \times 100\,\% \quad (2)$$

where U_{crit1} and U_{crit2} indicated the U_{crit} of the first stepped velocity test and second stepped velocity test, respectively.

One minute per five minutes videos was selected for swimming states analysis, and the average value for each flow velocity gradient in the test was calculated. The swimming states of fish were classified into four types according to swimming speed: countercurrent forward: V=M+N, countercurrent stationery: V=M, Float downstream: V=M-N, and countercurrent backward: V=N-M. The proportion of each swimming state (P) was also calculated (Iwata, 1995). The value of P (%) was calculated using equation (3):

$$P = t_1/T \quad (3)$$

Where V is the actual swimming speed, M is the flow velocity, and N is the instantaneous swimming speed of the experimental fish measured by the Ethovision XT10.0. t_1 is the duration of a specific swimming state (s), and T is the total observation time (s).

The tail beat frequency (TBF) is the complete tail-beating process of the experimental fish while swimming (Ohlberger et al., 2007). Every five minutes, a 20 s period of the video was selected from the whole video to calculate TBF. For each velocity, the value of TBF (times/s) was calculated using equation (4):

$$TBF = TBT/t \quad (4)$$

TBT is the total number of tail beats of each fish during the period of observation, and t is the total time of observation.

Physiological status test

After the swimming performance test was completed, the fish was anaesthetized with MS-222 (33 mg/L), and blood was sampled. Body weight was measured, and pictures of the body were taken (Nikon D810) for morphology analysis. Then returned, the fish to a holding tank (70×50×20 cm) for recovery. Blood was sampled three times at 0 h, 3 h and 24 h, respectively, to understand the recovery pattern of these blood physiology parameters following swimming. In addition, the blood of eight untreated fishes was sampled and analyzed to rule out the effect of MS-222. The blood samples were stored in a refrigerator (4°C) for 2 hours prior to centrifugation (4000 r/min, 20 min), while the centrifugal supernatant was stored separately at -20°C. The supernatant sample was bathed in 4°C water to prevent sample distortion before being tested. Physiological indicators were measured using kits developed by the Nanjing Jiancheng Institute of Biological Engineering and a 721 UV spectrophotometer (Svalheim et al., 2017; Yuan et al., 2018). Glucose, lactic acid and total protein were analyzed to characterize energy consumption in this study, which was determined by the glucose oxidase, colorimetric and biuret methods. All tests were carried out in strict accordance with the kit's instructions (http://www.njjcbio.com).

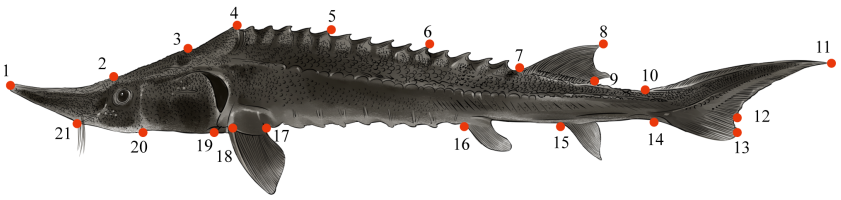

FIGURE 4
The 21 landmarks used for examination of lateral body shape (boldness depicted). 1. Snout tip; 2. Upper snout end; 3. Upper head end; 4. Dorsal origin; 5-6. Dorsal rhomboid primitive spikes; 7. Origin of dorsal fin base; 8. Highest point of dorsal fin; 9. Base end of dorsal fin; 10. Dorsal origin of caudal fin; 11. Upper lobe terminal of caudal fin; 12. Deepest part of the caudal fin; 13. Lower lobe terminal caudal fin; 14. Ventral origin of caudal fin; 15. Origin of anal fin; 16. Origin of pelvic fin; 17. End of pectoral fin; 18. Origin of pectoral fin; 19. Lower head end; 20. Base of operculum; 21. Lower snout end.

Morphological characteristics measurement

Morphological characteristics were analyzed by TPS series software (http://life.bio.sunysb.edu/morph). Twenty-one landmark points were selected to obtain the corresponding x, y coordinate values (2D) for geometric morphometry by tpsDig2 (Figure 4) (Bookstein, 1997). The validity of the landmark points was tested by tpsSmall. Procrustes analysis was used to superimpose the landmark points of all samples by tpsRelw, and the landmark points of each sample were translated, centered, rotated and zoomed. The centroid distance and mean shape were calculated, and the partial warp and relative warp principal component analyses (RWA) were performed. Lastly, the relative warp scores (RW) were used for subsequent analysis (Rohlf, 1990; Rohlf, 1993). The relative warp (RW) was mapped on the thin plate spline to visualize the results (Bookstein, 1989), while a grid deformation map of all samples was constructed using tpsRegr to analyze and compare morphological differences.

Data analysis

T-tests were used to compare the initial differences in body length and weight between bold and shy groups. Two-way repeated measures ANOVA in a general linear model (GLM) was used to assess for differences in swimming performance an physiological indicators between different personality types (shy and bold) over time. The subject's internal factors included personality (two levels: "bold" and "shy") and test (two levels of test: the first and the second stepped velocity test, which formed 4 treatment groups; physiological test at three levels: 0 h, 3 h, 24 h, a total of 6 treatment groups). The dependent variables were swimming performance which included critical swimming speed, fatigue time, fatigue recovery time, and physiological index. For each treatment group, all response variables were evaluated for normality and equal variance using the Shapiro-Wilkins normality test as well as density plots. If the data was not normally distributed, it was converted logarithmically. Before assessing whether there was an interaction between personality and testing time, it was necessary to evaluate whether the interaction conforms to Mauchly's Test of Sphericity. When the conditions of the spherical hypothesis were violated ($p< 0.05$), an epsilon(ϵ) correction was required, and for epsilon(ϵ)< 0.75, the Greenhouse-Geisser method was used for correction, while for epsilon(ϵ) > 0.75, the Huynh-Feldt method was used. When the condition of the spherical hypothesis was satisfied, the covariance matrix of the dependent variable for interaction term personality*time was equal ($p > 0.05$). Then, we analyzed whether the effect of the interaction on the dependent variables was statistically significant. If the interactions were significant, differences in the swimming performance and physiological index concentrations between the bold and shy groups were compared at different time levels to test the separate effects of the treatment group and to examine the impact of time alone by comparing differences in time factors between the two personality groups. When only two groups were compared, there was no need to test the spherical hypothesis. Otherwise, the main effects of personality and time were analyzed. If the main effect of a factor with more than two intra-level groups was significant, a pairwise comparison was required. In addition, a one-way analysis of variance (ANOVA) was used to compare differences in the physiological index concentrations at different time levels between the bold and shy groups and the control group. Differences in the time ratio of swimming state and the tail beat frequency across personality groups were tested by t-test. Hotelling T^2 method of multivariate analysis of variance (MANOVA) in a general linear model (GLM) was used to examine and compare differences in relative distortion scores of fish with either personality group. All data analysis and plots were performed in R Studio Version 1.3.1, and significance was considered at an α level of 0.05.

Results

Personality identification

Consistent interindividual variation in fish's tendency to explore the exposed arms was founded. According to the proportion of the cumulative time spent exploring the bright area, 60 individuals could be clearly identified as a personality group, which included 30 bold individuals and 30 shy individuals.

Swimming performance of different personalities of the Siberian sturgeon

There were no differences in body length and weight between the bold and shy groups. For the swimming performance experiment, the interaction of personality and time significantly affected U_{crit} ($F_{1,23} = 9.16$, $p< 0.001$). The single effects of personality indicated that the U_{crit} of shy groups was significantly higher than that of bold groups ($F_{1,23} = 18.51$, $p< 0.05$). The U_{crit} of the shy groups increased in the second time test ($F_{1,23} = 1.12$, $p > 0.05$), while that of the bold groups decreased significantly ($F_{1,32} = 8.87$, $p< 0.05$) (Table 1; Figures 5A, B). In addition, the recovery rate of the shy groups (R=104%) was higher than ($p > 0.05$) for the bold groups (R=95%). The interaction between personality and time had no significant effect on the fatigue recovery time of test fish ($F_{1,22} = 1.59$, $p > 0.05$), and the main effects of personality and time had no significant impact on the fatigue recovery time of test fish ($p > 0.05$) (Table 1; Figure 5C).

The proportion of time of swimming states and tail beat frequency of fish under different flow velocities indicated that bold groups stay in a state of countercurrent forward swimming for a longer period than shy groups ($p< 0.05$) but spend less time in countercurrent stationery and float downstream swimming states than shy groups ($p< 0.05$) (Table 2; Figure 6A). Moreover, the tail beat frequency of fish in the shy group was significantly higher than that of fish in the bold group as the flow velocity increased ($p< 0.05$) (Table 2; Figure 6B).

Physiological characteristics of different personalities of the Siberian sturgeon

The personality and time interaction had a statistically significant effect on plasma glucose and lactate concentration ($p< 0.05$). The separate effect of personality at each time level showed that the glucose and lactate concentrations of shy groups were higher than that of bold groups ($p< 0.05$). The separate effect of time showed that the plasma glucose and lactate acid concentrations in the bold and shy groups changed significantly over time ($p< 0.05$). The results of the one-way analysis of variance revealed that at the 24th hour of recovery, the plasma glucose concentration of the shy groups was significantly higher than that of the control group ($F_{1,\ 24} = {}_{14.38,}$ $p< 0.05$), indicating that the plasma glucose concentration of the shy groups rose faster than that of the bold groups. At the beginning of the recovery (i.e., at0 h), the plasma lactate concentration of fish in the shy group was significantly higher than the control groups ($F_{1,\ 24} = {}_{11.05,}$ $p< 0.05$); at 24 h, there was no significant difference compared to the control group, indicating that the plasma lactate recovery ability of shy groups was greater than that of bold groups (Table 3; Figures 7A, B).

For total protein concentrations in plasma, the interaction between personality and time was not statistically significant ($F_{1.19,\ 10.68} = 1.390$, $p > 0.05$). The main effect of personality on total protein concentration was statistically significant, with the mean total protein concentration in the shy group being higher than that of the bold group ($F_{1,\ 9} = 6.38$, $p< 0.05$). For the main effect of time, the influence of time on total protein concentration was statistically significant ($F_{2,\ 18} = 61.86$, $p< 0.001$). The results of the one-way analysis of variance showed that at 0 h, the total protein concentration of the bold group and the shy group was significantly higher than that of the control group ($p< 0.05$); at 24 h, there was no significant difference between the total protein concentration of the two groups and the control group. Overall, the total protein concentration of fish declined over time after the swimming performance test, and it was always higher in the shy group than that of the bold group (Table 3; Figure 7C).

TABLE 1 Summary statistics for swimming performance parameters and the results of general linear models (GLM) examining variation in swimming performance parameters between bold and shy Siberian sturgeon.

Test	Personality	Fatigue time (min)	Recovery time (min)	U_{crit} (cm/s)
First	Bold sturgeon	44.52 ± 2.99	64.36 ± 18.56	31.93 ± 2.12
	Shy sturgeon	53.54 ± 2.09	53.80 ± 11.74	43.58 ± 1.92
Second	Bold sturgeon	37.31 ± 3.54	57.56 ± 21.39	28.45 ± 2.39
	Shy sturgeon	57.43 ± 2.44	75.52 ± 21.90	45.17 ± 2.21
Time	F, *p*	0.03, 0.87	0.004, 0.95	1.19, 0.29
Personality	F, *p*	17.42, **0.001**	0.33, 0.57	20.99, **0.001**
Time*personality	F, *p*	14.21, **0.001**	1.59, 0.22	9.16, **0.006**

Statistically significant outcomes are shown in bold.
This symbol of "*" represents the interaction between personality and test time.

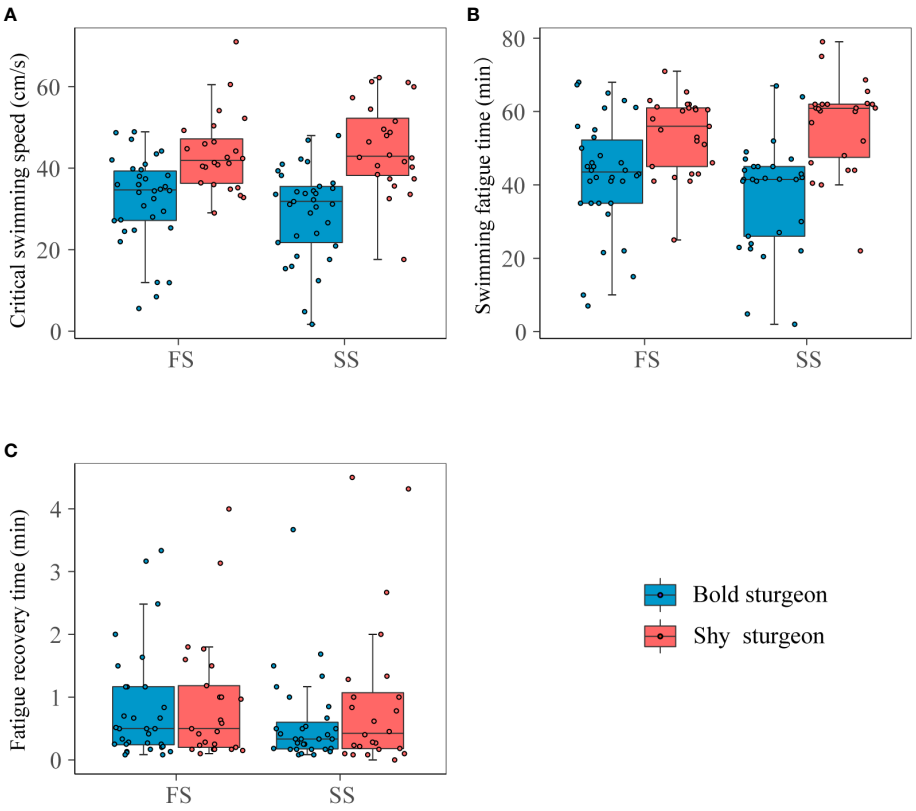

FIGURE 5
Swimming performance of different personalities. Blue and red represented bold sturgeon and shy sturgeon respectively; FS and SS represented the first and second swimming performance test respectively. **(A)** was the critical swimming speed, **(B)** was the swimming fatigue time (endurance), and **(C)** was the fatigue recovery time.

The effect of personality on morphological characteristics of the Siberian sturgeon

In the geometric analysis based on landmark points, the regression coefficients were all greater than 0.99, emphasizing the validity of the landmark points selected. The relative warp principal component analysis extracted a total of 24 principal components, of which the eigenvalues of the first three principal components were 0.331, 0.123, and 0.108, and the total contribution rate was 66.89%, 9.22%, and 7.20%. A total of 83.31% of the intraspecific morphological differences were

TABLE 2 Changes in the proportion of time spent in swimming state with individual differences and the tail beat frequency.

Personality	Water velocity	Countercurrent Forward (%)	Countercurrent Stationary (%)	Float downstream (%)	Countercurrent Backward (%)	Tail beat frequency (times/s)
Bold sturgeon	1BL/s	0.54 ± 0.19	0.24 ± 0.21	0.04 ± 0.06	0.17 ± 0.14	3.69 ± 0.83
	2BL/s	0.49 ± 0.18	0.21 ± 0.12	0.01 ± 0.02	0.17 ± 0.11	4.15 ± 1.98
	3BL/s	0.19 ± 0.31	0.11 ± 0.27	0.00 ± 0.01	0.08 ± 0.16	0.84 ± 1.75
Shy sturgeon	1BL/s	0.26 ± 0.15	0.47 ± 0.22	0.07 ± 0.05	0.18 ± 0.09	3.11 ± 1.35
	2BL/s	0.29 ± 0.15	0.51 ± 0.16	0.06 ± 0.05	0.13 ± 0.05	4.64 ± 1.04
	3BL/s	0.23 ± 0.19	0.44 ± 0.29	0.04 ± 0.05	0.13 ± 0.10	4.31 ± 2.18
df		61.12	78.96	78.04	61.86	2.76
p		**0.009**	**0.001**	**0.001**	0.76	0.39

Statistically significant outcomes are shown in bold.

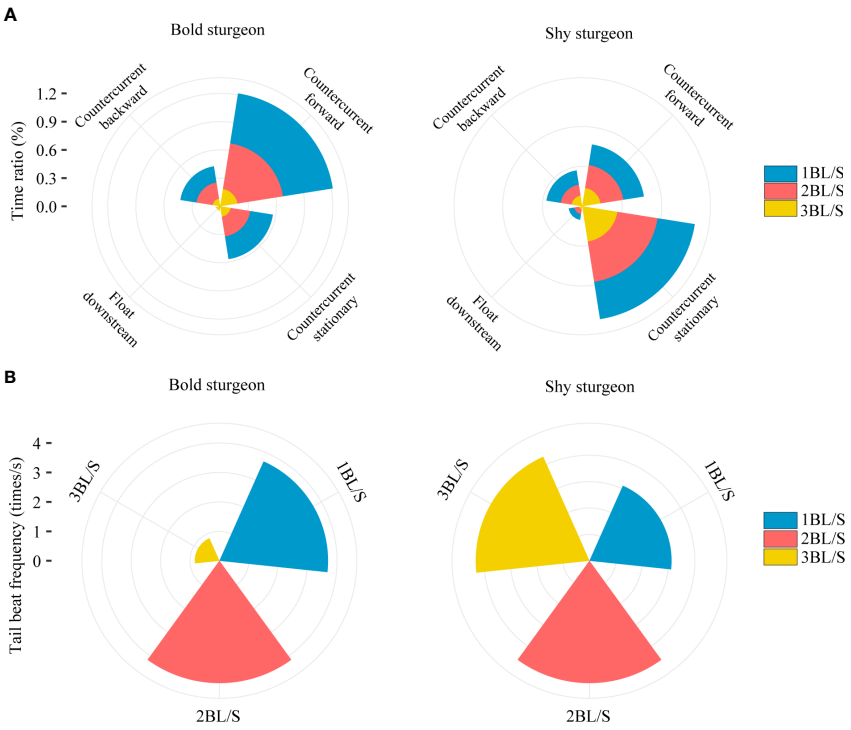

FIGURE 6
Changes in the proportion of time spent in swimming state and the tail beat frequency with different personalities. Blue, red and yellow represented 1BL/s flow rate, 2BL/s flow rate and 3BL/s flow rate, respectively. **(A)** showed the time proportion of swimming state of sturgeon with two personalities at different flow velocity. **(B)** showed the tail beat frequency of two personalities at different flow velocity.

explained (Table 4). The contribution rate of 21 landmark points in the relative distortion principal component analysis showed that landmark points 12 (deepest part of the caudal fin) and 13 (lower lobe terminal caudal fin) have the largest contribution rate, followed by landmark points 9 (base end of the dorsal fin), 10 (dorsal origin of caudal fin), 14 (ventral origin of caudal fin), 18 (origin of pectoral fin), and 19 (lower head end). The total contribution rate of these seven traits was 86.12%. There were

TABLE 3 Blood of plasma glucose, lactic acid and total protein levels (Mean±SD) in individual differences test fish at each test stage, and the results of general linear models (GLM) examining variation in different physiological indicators between bold and shy test Siberian sturgeon.

Test	Test time	Plasma Glucose (mmol /L)	Lactic acid (mmol/L)	Total Protein (g/L)
Bold sturgeon	0h	3.29 ± 0.18	6.19 ± 0.51	29.52 ± 1.26
	3h	3.40 ± 0.12	4.59 ± 0.28	25.50 ± 0.69
	24h	3.88 ± 0.20	2.69 ± 0.32	20.12 ± 1.37
Shy sturgeon	0h	3.47 ± 0.15	8.04 ± 0.32	34.59 ± 1.47
	3h	4.16 ± 0.23	5.28 ± 0.27	29.94 ± 1.44
	24h	5.06 ± 0.28	2.80 ± 0.31	22.23 ± 2.17
Normal	0h	4.38 ± 1.07	2.50 ± 0.88	17.79 ± 9.04
	3h	4.17 ± 1.19	2.08 ± 1.12	17.57 ± 6.33
	24h	3.84 ± 1.68	2.61 ± 0.76	19.52 ± 4.26
Time	F, *p*	15.36, **0.001**	73.82, **0.001**	61.86, **0.001**
Personality	F, *p*	17.08, **0.001**	11.60, **0.002**	6.38, **0.03**
Time*personality	F, *p*	3.27, **0.04**	4.47, **0.02**	1.39, 0.27

Statistically significant outcomes are shown in bold.
This symbol of "*" represents the interaction between personality and test time.

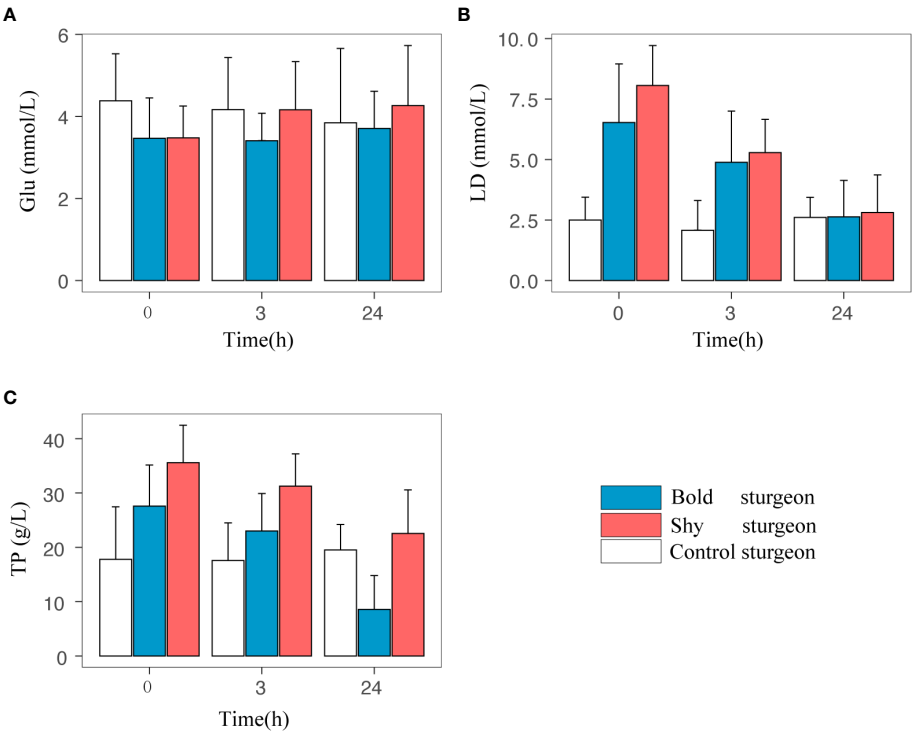

FIGURE 7
Physiological changes in different personalities. 0h, 3h and 24h are the fatigue recovery time of the test Siberian sturgeon; Glu, LD, TP are the concentration of glucose, lactic acid and total protein in the blood respectively.

significant differences in the caudal fin, caudal stalk, pectoral fin, and head of fishes with different personalities. The Hotelling T^2 test showed that the bold and shy groups had significant differences in the former three relative distortions ($F_{3,21}$ = 0.914, $p< 0.05$) and that the two personalities of sturgeons had significant differences in RW1 ($p< 0.05$). When the first relative warp was mapped on the thin plate spline, we could visualize its shape (Figure 8). The caudate stalk length, upper caudal lobe and the lower caudal lobe of the bold groups were significantly larger than those of the shy groups, while the head height, snout thickness, snout length, body height, and body length of the bold groups were significantly smaller than those of the shy groups.

Discussion

Our research showed that there were indeed individuals with different personalities in the Siberian sturgeon population. Individuals with different personalities have evolved not only a series of behavioral differences but also divergences in physiological performance and morphology. First, we found that shy groups had a significantly higher U_{crit} than bold groups. Other studies have shown that personality can affect the swimming performance of fish. For instance, in Trinidadian killifish (*Rivulus hartii*), individuals from high-predation sites were faster sprinters but had reduced U_{crit} (Oufiero et al., 2011). Shy wild-type zebrafish (*Danio rerio*) were slower in movement

TABLE 4 Eigenvalues and contribution rates of the first 5 principal components of relative warps scores of different morphological features of the test Siberian sturgeon.

Principal component	Eigen values	Contribution rate	Cumulative contribution rate
1	0.33145	66.89%	66.89%
2	0.12304	9.22%	76.11%
3	0.10874	7.20%	83.31%
4	0.06880	2.88%	86.19%
5	0.06127	2.29%	88.48%

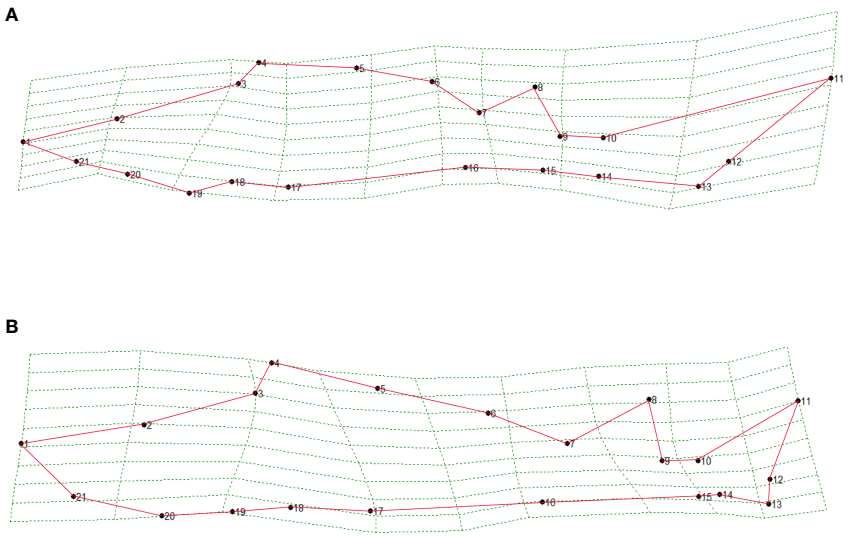

FIGURE 8
Grid deformation and variation visualization of morphological features of bold **(A)** and shy **(B)** test Siberian sturgeon.

and exhibited higher stable swimming performance, while bold fish were more agile and exhibited higher quick-start swimming performance (Kern et al., 2016). Fish with different personalities have evolved different swimming strategies depending on their prey and habitat, often at the expense of another form of locomotion (Webb, 1978; Webb, 1984). This phenomenon is manifested as a trade-off between stable swimming performance (aerobic swimming) and unstable swimming performance (anaerobic swimming), and its ecological mechanism reflects a trade-off between energy gain and cost (Webb, 1984; Langerhans, 2007; Langerhans, 2008). In addition, we also found that the proportion of time that bold groups swam countercurrent forward during the experiment was higher than that of shy groups, while the proportion of time that they were countercurrent stationery and 'float downstream' was lower than that of shy groups. This may be related to the fact that bold animals are highly exploratory and aggressive, tend to engage in active avoidance, or cope with stressful stimuli through a "fight or flight" response. Conversely, shy animals typically undertake a passive "freeze and hide" response (Benhaïm et al., 2016). The higher tail beat frequency of the shy group with higher flow rates may be related to swimming fatigue in the bold group before reaching the U_{crit} of the shy group.

Our research revealed that the morphology of fish differed based on their personality type (shy *vs.* bold). Shy groups had smaller caudate stalk lengths, caudate stalk heights, superior caudal lobes, and inferior caudal lobes compared with bold groups, while the head height, body height, snout thickness, snout length, and body length were larger in bold fish. Other studies have shown that strong selective pressure affects the morphology of fish with different personalities and that morphology further affects swimming performance. Western mosquito fish (*Gambusia affinis*) from high predation risk areas have smaller heads and larger tails and have a stronger ability to start swimming quickly compared to those from low predation risk areas that have larger heads, smaller tails, and more streamlined, stable swimming (Langerhans, 2009). It has long been suggested that the divergences in swimming performance occurred, at least partially, *via* morphological change, as morphology has a significant impact on swimming transport costs (Peres-Neto and Magnan, 2004; Langerhans, 2008; Langerhans, 2009a). Changes in body shape would affect fish hydrodynamics and, ultimately drag coefficients and U_{crit} (Ostenfeld, 1998; Lee et al., 2003). Morphological variations that are poorly suited to produce maximum thrust and minimum drag in GH-transgenic *C. carpio* may be responsible for their lower swimming performance compared with non-transgenic controls (Li et al., 2009). The morphology of the fins of juvenile Atlantic salmon (*Salmon salar*) living in slow- and fast-flowing environments differs significantly (Pa´ez et al., 2008). In this study, we believe that the larger head and smaller caudal of shy groups made the overall body shape more streamlined, which may minimize recoil energy loss and enhance stable swimming performance (Webb, 1984).

In addition to morphological performance, we also found that the physiological performance of fish with different personalities was different. The ability to recover following swimming fatigue was greater in shy *vs.* bold groups following the two swimming performance tests. With respect to

physiology, the blood glucose concentration of shy fish increased faster than that of bold groups, and the ability to recover from elevated blood lactate levels scavenging was greater in shy fish. Further, their total protein concentrations were consistently higher than that of bold fish. These findings suggest that personality affects the physiological performance of fish, which in turn affects the swimming performance of fish. Prolonged exercise training on the swimming performance of juvenile common carp (*Cyprinus carpio*) revealed that trained fish exhibited higher lactate clearance and significantly increased aerobic swimming performance (He et al., 2013). Studies have shown that strenuous exercise led to accumulations of total protein in blood serum, and the increased levels of total protein resulted primarily from lactate accumulation due to anaerobic metabolism in white muscle tissue (Genz et al., 2013). Previous studies have shown that physiological traits represent different adaptive strategies to respond to environmental challenges (Kristiansen and Fern, 2007). Various degrees of physiological resilience may be influenced mainly by genetics, environment, and the interaction between genetic and environmental factors (Julia et al., 2011; Careau and Garland, 2012). In this study, individual differences were measured in the absence of social interaction and with equal and predominantly constant environmental conditions, suggesting that the stronger physiological resilience of shy individuals may be influenced primarily by a genetic basis. In addition, we believe that due to the sufficient energy accumulation caused by the passive "freeze and hide" response of shy groups, high-level energy reserves could be prioritized for physiological recovery (Magnhagen and Borcherding, 2008). Previous studies have shown that individual differences in personality type and energy utilization efficiency affect individual fitness (Biro and Stamps, 2008; Biro and Dingemanse, 2009). For instance, it is possible that bolder katydid spend more time gathering information about all the available options but owing to the limited time and attention, this leads to lower biomass consumed (i.e. lower foraging efficiency) when compared to shy katydids (Tan et al., 2018). We speculate that the bold groups in this study may have spent more time gathering information about potential food choices within the environment and resulting in less time for food (Tan et al., 2018). This condition allowed shy groups to benefit by having a higher food intake, maximizing their growth (Tan et al., 2018). In addition, because proactive individuals are usually aggressive, dominant, and bold, they are more likely to engage in energetically costly behavior, which leads to higher daily energy expenditure (DEE) and resting standard metabolism (Stamps, 2007). Therefore, it was possible that because the metabolic intensity of bold groups was higher than that of shy groups, the physiological indicators of bold groups were always lower than those of shy groups in the process of fatigue recovery (Huntingford et al., 2010).

Conclusion

In the present study, different personality types affected the swimming performance of Siberian sturgeon. In general, we demonstrated that shy Siberian sturgeon had better swimming performance from physiology and morphology. Morphology and physiology also differed across personality types, which may have contributed to the observed differences in swimming performance. Our research results further validate the theoretical viewpoints pertaining to the energetic trade-offs associated with an animal's life-history strategy. A lower U_{crit} and slower physiological recovery rate may place bold groups at a disadvantage when competing with shy wild-type groups in their natural habitat, though further research is needed to assess this hypothesis. Our results also provide further knowledge on the links between personality and swimming performance in sturgeon and theoretical support for improving the conservation of sturgeon. For example, sturgeon could be selectively cultivated with different risk coping styles so that they evolve not only a range of behavioral differences but also differences in morphological performance and physiological performance, and selectively release sturgeon with different personality traits for the actual conditions of the natural environment. Future research could investigate other aspects of personality and how these relate to physiology, morphology, and swimming performance in sturgeon.

Data availability statement

The original contributions presented in the study are included in the article/Supplementary Material. Further inquiries can be directed to the corresponding authors.

Ethics statement

This study was reviewed and approved by Research Ethics Committee of Institute of Hydrology, CAS.

Author contributions

LX (Co-first authors): Conceptualization, Methodology, Software, Investigation, Formal Analysis, Writing-Original Draft. XM(Co-first authors): Conceptualization, Methodology, Software, Investigation, Writing-Original Draft. YD: Resources, Supervision. YZ: Writing-Review and Editing. WJ: Resources, Supervision. HD: Resources. WT: Writing-Review. SC: Writing-Review. JB (Co-corresponding authors): Conceptualization, Writing-Review and Editing. MD (Co-corresponding authors): Conceptualization, Funding Acquisition, Writing-Review and Editing. All authors contributed to the article and approved the submitted version.

Funding

This work was financially supported by the National Natural Science Foundation of China (grant number 32172955), the Hubei Key Laboratory of Three Gorges Project for Conservation of Fishes (grant number 201902), the National Natural Science Foundation of China (grant number 32202914), the Open Innovation Fund of Changjiang Survey Planning Design and ResearchCo., Ltd (grant number CX2021K03), the National Key R & D Program of China (grant number 2018YFD 0900605), the Natural Science Foundation of Hubei Province (grant number 2020CFB832), and the Scientific Instrument Developing Project of the Chinese Academy of Sciences (grant number YJKYYQ20190055). The funders were not involved in the study design, collection, analysis, interpretation of data, the writing of this article, or the decision to submit it for publication.

Conflict of interest

Authors YD and WJ were employed by the Chinese Sturgeon Research Institute, China Three Gorges Corporation.

The remaining authors declare that the research was conducted in the absence of any commercial or financial relationships that could be construed as a potential conflict of interest.

Publisher's note

All claims expressed in this article are solely those of the authors and do not necessarily represent those of their affiliated organizations, or those of the publisher, the editors and the reviewers. Any product that may be evaluated in this article, or claim that may be made by its manufacturer, is not guaranteed or endorsed by the publisher.

Supplementary material

The Supplementary Material for this article can be found online at: https://www.frontiersin.org/articles/10.3389/fmars.2022.1040225/full#supplementary-material

References

Benhaïm, M. D., Ferrari, S., Chatain, B., and Bégout, M. (2016). The shy prefer familiar congeners. *Behav. Processes*. 126, 113–120. doi: 10.1016/j.beproc.2016.03.008

Biro, P. A., and Dingemanse, N. J. (2009). Sampling bias resulting from animal personality. *Trends Ecol. Evol.* 24 (2), 66–67. doi: 10.1016/j.tree.2008.11.001

Biro, P. A., and Stamps, J. A. (2008). Are animal personality traits linked to life-history. productivity? *Trends Ecol. Evol.* 23 (7), 361–368. doi: 10.1016/j.tree.2008.04.003

Biro, P. A., and Stamps, J. A. (2010). Do consistent individual differences in metabolic rate. promote consistent individual differences in behavior? *Trends Ecol. Evol.* 25 (11), 653–659. doi: 10.1016/j.tree.2010.08.003

Birstein, V. J., Bemis, W. E., and Waldman, J. R. (1997). The threatened status of acipenseriform. species: a summary. *Environ. Biol. Fishes*. 48, 427–435. doi: 10.1007/0-306-46854-9_33

Blake, R. W. (2010). Fish functional design and swimming performance. *J. Fish Biol.* 65 (5), 1193–1222. doi: 10.1111/j.0022-1112.2004.00568.x

Bookstein, F. L. (1989). *Principal Warps: thin-plate splines and the decomposition of deformation*. IEEE Transactions on Pattern Analysis and Machine Intelligence, 6 (11), 567–585. doi: 10.1109/34.24792

Bookstein, F. (1997). Landmark methods for forms without landmarks: morphometrics of group differences in outline shape. *Med. Image Anal.* 1, 225–243. doi: 10.1109/MMBIA.1996.534080

Brett, J. R. (1964). The respiratory metabolism and swimming performance of young. sockeye salmon. *J.Fish.Res.Bd.Can* 21 (5), 1183–1226. doi: 10.1139/f64-103

Brown, C., Jones, F., and Braithwaite, V. (2005). In situ examination of boldness–shyness traits in the tropical poeciliid, brachyraphis episcopi. *Anim. Behav.* 70 (Pt5), 1003–1009. doi: 10.1016/j.anbehav.2004.12.022

Brown, C., Jones, F., and Braithwaite, V. A. (2007). Correlation between boldness and body mass in natural populations of the poeciliid brachyrhaphis episcopi. *J. Fish Biol.* 71 (6), 1590–1601. doi: 10.1111/j.1095-8649.2007.01627.x

Bruckerhoff, L. A., and Magoulick, D. D. (2017). Hydrologic regimes as potential drivers of morphologic divergence in fish. *Evol. Ecol.* 31 (4), 517–531. doi: 10.1007/s10682-017-9897-0

Careau, V., and Garland, T. (2012). Performance, personality, and energetics: correlation, causation, and mechanism. *Physiol. Biochem. Zool* 85 (6), 543–571. doi: 10.1086/666970

Careau, V., Thomas, D., Humphries, M. M., and D Réale, (2008). Energy metabolism and. animal personality. *Oikos* 117 (5), 641–653. doi: 10.1111/j.0030-1299.2008.16513.x

Caro, T. M., and Bateson, P. (1986). Organization and ontogeny of alternative tactics. *Anim. Behav.* 34 (5), 1483–1499. doi: 10.1016/S0003-3472(86)80219-6

Clark, A. B., and Ehlinger, T. J. (1987). Pattern and adaptation in individual behavioral differences. *Perspect. Ethology*, 7, 1–47. doi: 10.1007/978-1-4613-1815-6_1

Domenici, P. (2010). "Escape responses in fish: kinematics, performance and behavior," in *Fish locomotion: an eco-ethological perspective*. Eds. P. Domenici and B. G. Kapoor. Florida, US. 123–170.

Downie, A. T., and Kieffer, J. D. (2017). Swimming performance in juvenile shortnose sturgeon (Acipenser brevirostrum): the influence of time interval and velocity increments on critical swimming tests. *Conserv. Physiol.* 5 (1), 1–12. doi: 10.1093/conphys/cox038

Farrell, A. P., Gamperl, A. K., and Birtwell, I. K. (1998). Prolonged swimming, recovery and repeat swimming performance of mature sockeye salmon oncorhynchus nerka exposed to moderate hypoxia and pentachlorophenol. *J. Exp. Biol.* 201 (Pt14), 2183–2193. doi: 10.1242/jeb.201.14.2183

Genz, J., Jyde, M. B., Svendsen, J. C., Steffensen, J. F., and Ramlov, H. (2013). Excess post-hypoxic oxygen consumption is independent from lactate accumulation in two cyprinid fishes. *Comp. Biochem. Phys. A* 165 (1), 54–60. doi: 10.1016/j.cbpa.2013.02.002

Gosling, S. D. (2001). From mice to men: what can we learn about personality from animal research? *Psychol. Bull.* 127 (1), 45–86. doi: 10.1037/0033-2909.127.1.45

Hammer, C. (1995). Fatigue and exercise tests with fish. *Comp. Biochem. Physiol. A-Mol. Integr. Physiol.* 112 (1), 1–20. doi: 10.1016/0300-9629(95)00060-K

Harper, D. G., and Blake, R. W. (1990). Fast-start performance of rainow trout salmo gairdneri and northern pike esox lucius. *J. Exp. Biol.* 150, 321–342.

He, W., Xia, W., Cao, Z. D., and Fu, S. J. (2013). The effect of prolonged exercise training on swimming performance and the underlying biochemical mechanisms in juvenile common carp (Cyprinus carpio). *Comp. Biochem. Physiol. Part A Mol. Integr. Physiol.* 166 (2), 308–315. doi: 10.1016/j.cbpa.2013.07.003

Huntingford, F. A., Andrew, G., Mackenzie, S., Morera, D., Coyle, S. M., Pilarczyk, M., et al. (2010). Coping strategies in a strongly schooling fish, the. common carp cyprinus carpio. *J. Fish Biol.* 76 (7), 1576–1591. doi: 10.1111/j.1095-8649.2010.02582.x

Iwata, M. (1995). Downstream migratory behavior of salmonids and its relationship with cortisol and thyroid hormones: A review. *Aquaculture* 135 (1-3), 131–139. doi: 10.1016/0044-8486(95)01000-9

Jain, K. E. (2003). Influence of seasonal temperature on the repeat swimming performance of rainbow trout oncorhynchus mykiss. *J. Exp. Biol.* 206 (20), 3569–3579. doi: 10.1242/jeb.00588

Mas-Munoz, J., Komen, H., Schneider, O., Visch, S. W., and Schrama, J. W. (2011). Feeding behaviour, swimming activity and boldness explain variation in feed intake and growth of sole (*Solea solea*) reared in captivity. *PloS One* 6 (6), e21393. doi: 10.1371/journal.pone.0021393

Kern, E., Robinson, D., Gass, E., Godwin, J., and Langerhans, R. B. (2016). Correlated evolution of personality, morphology and performance. *Anim. Behav.* 117, 79–86. doi: 10.1016/j.anbehav.2016.04.007

Kristiansen, T. S., and Fern, A. (2007). Individual behaviour and growth of halibut (hippoglossus l.) fed sinking and floating feed: Evidence of different coping styles. *Appl. Anim. Behav. Sci.* 104 (3-4), 236–250. doi: 10.1016/j.applanim.2006.09.007

Langerhans, R. B. (2009). Trade-off between steady and unsteady swimming underlies predator-driven divergence in gambusia affinis. *J. Evol. Biol.*(2009) 22 (5), 1057–1075. doi: 10.1111/j.1420-9101.2009.01716.x

Langerhans, R. B. (2007). Evolutionary consequences of predation: avoidance, escape, reproduction, and diversification. *Springer Berlin Heidelberg*, 177–220. doi: 10.1007/978-3-540-46046-6_10

Langerhans, R. B. (2008). Predictability of phenotypic differentiation across flow regimes in fishes. *Integr. Comp. Biol.* 48, 750–768. doi: 10.1093/icb/icn092

Langerhans, R. B. (2009a). Morphology, performance, fitness: functional insight into a. post-pleistocene radiation of mosquitofish. *Biol. Lett.* 5 (4), 488–491. doi: 10.1098/rsbl.2009.0179

Langerhans, R. B. (2009b). Trade-off between steady and unsteady swimming underlies predator-driven divergence in gambusia affinis. *J. Evolutionary Biol.* 22 (5), 1057–1075. doi: 10.1111/j.1420-9101.2009.01716.x

Lee, C. G., Devlin, R. H., and Farrell, A. P. (2003). Swimming performance, oxygen consumption and excess post-exercise oxygen consumption in adult transgenic and ocean-ranched coho salmon. *J. Fish Biol.* 62, 753–766. doi: 10.1046/j.1095-8649.2003.00057.x

Lee, C. G., Farrell, A. P., Lotto, A., Hinch, S. G., and Healey, M. C. (2003). Excess post-exercise oxygen consumption. in adult sockeye(Oncorhynchus nerka)and coho(O.kisutch)salmon following critical speed swimming. *J. Exp. Biol.* 206, 3253–3260. doi: 10.1242/jeb.00548

Lighthill, M. J. (1969). Hydromechanics of aquatic animal propulsion. *Annu. Rev. Fluid Mech.* 1 (1), 413–446. doi: 10.1146/annurev.fl.01.010169.002213

Lighthill, M. J. (2006). Aquatic animal propulsion of high hydromechanical efficiency. *J. Fluid Mech.* 44 (02), 265–301. doi: 10.1017/S0022112070001830

Li, D., Hu, W., Wang, Y., Zhu, Z., and Fu, C. (2009). Reduced swimming abilities in fast-growing transgenic common carp cyprinus carpio associated with their morphological variations. *J. Fish Biol.* 74 (1), 186–197. doi: 10.1111/j.1095-8649.2008.02128.x

Magnhagen, C., and Borcherding, J. (2008). Risk-taking behaviour in foraging perch: does predation pressure influence age-specific boldness? *Anim. Behav.* 75 (2), 509–517. doi: 10.1016/j.anbehav.2007.06.007

Maximino, C., Thiago, M., Dias, C., Gouveia, A., and Morato, S. (2010). Scototaxis as anxiety-like behavior in fish. *Nat. Protoc.* 5 (2), 209. doi: 10.1038/nprot.2009.225

Ohlberger, J., Staaks, G., and Hlker, F. (2007). Estimating the active metabolic rate (AMR) in fish based on tail beat frequency (TBF) and body mass. *J. Exp. Zool. Part A.* 307 (5), 296–300. doi: 10.1002/jez.384

Ostenfeld, T. (1998). Transgenesis changes body and head shape in pacific salmon. *J. Fish Biol.* 52, 850–854. doi: 10.1111/j.1095-8649.1998.tb00825.x

Oufiero, C. E., Walsh, M. R., Reznick, D. N., and Garland, T. (2011). Swimming performancetrade-offsfs across a gradient in community composition in trinidadian killifish (Rivulus hartii). *Ecology* 92, 170–179. doi: 10.1890/09-1912.1

Pa´ez, D. J., Hedger, R., Bernatchez, L., and Dodson, J. J. (2008). The morphological plastic. response to water current velocity varies with age and sexual state in juvenile Atlantic salmon, salmo salar. *Freshw. Biol.* . 53, 1544–1554. doi: 10.1111/j.1365-2427.2008.01989.x

Peres-Neto, P. R., and Magnan, P. (2004). The influence of swimming demand on phenotypic plasticity and morphological integration: a comparison of two polymorphic charr species. *Oecologia* 140, 36–45. doi: 10.1007/s00442-004-1562-y

Raoult, V., Brown, C., Zuberi, A., and Williamson, J. E. (2012). Blood cortisol concentrations predict boldness in juvenile mulloway (Argyosomus japonicus). *J. Ethol.* 30 (2), 225–232. doi: 10.1007/s10164-011-0314-9

Reale, D., Garant, D., Humphries, M. M., Bergeron, P., Careau, V., and Montiglio, P. O. (2010). Personality and the emergence of the pace-of-life syndrome concept at the population level. *Philos. Trans. R. Soc Lond. Ser. A-Math. Phys. Eng. Sci.* 365 (1560), 4051–4063. doi: 10.1098/rstb.2010.0208

Réale, D., Reader, S. M., Sol, D., McDougall, P. T., and Dingemanse, N. J. (2007). Integrating animal temperament within ecology and evolution. *Biol. Rev.* 82, 291–318. doi: 10.1111/j.1469-185X.2007.00010.x

Reidy, S. P., Kerr, S. R., and Nelson, J. A. (2000). Aerobic and anaerobic swimming performance of individual Atlantic cod. *J. Exp. Biol.* 203 (Pt 2), 347–357. doi: 10.1242/jeb.203.2.347

Reznick, D., Nunney, L., and Tessier, A. (2000). Big houses, big cars, superfleas and the costs of reproduction. *Trends Ecol. Evol.* 15, 421–425. doi: 10.1016/S0169-5347(00)01941-8

Roche, D. G., Careau, V., and Binning, S. A. (2016). Demystifying animal 'personality' (or not): why individual variation matters to experimental biologists. *J. Exp. Biol.* 219, 3832–3843. doi: 10.1242/jeb.146712

Roff, D. A. (1992). *The evolution of life histories : theory and analysis* (New York: Chapman and Hall). doi: 10.1002/9781444304312.ch2

Roff, D. A., and Fairbairn, D. J. (2012). A test of the hypothesis that correlational selection generates genetic correlations. *Evolution* 66 (9), 2953–2960. doi: 10.1111/j.1558-5646.2012.01656.x

Rohlf, F. J. (1990). *Fitting curves to outlines* (The University of Michigan Museum of Zoology: Michigan Morphometrics Workshop).

Rohlf, F. J. (1993). Relative warp analysis and an example of its application to mosquito wings. *Contribution to Morphometrics.* 8, 131–159.

Shi, X. T., Chen, Q. W., Liu, D. F., Huang, Y, Zhuang, P, Chen, Z. Q, et al. (2012). Critical swimming speed of juvenile mullet. *J. Hydrobiology.* 36 (01), 133–136. doi: 10.3724/SP.J.1035.2012.00133

Slater, P. (1981). Individual differences in animal behavior. *SpringerPlus*, 35–39. doi: 10.1007/978-1-4615-7575-7_2

Smith, J. M. (1982). Evolution and the theory of games: Frontmatter. Cambridge, UK: Cambridge University Press, 1–4 doi: 10.1017/CBO9780511806292

Stamps, J. A. (2007). Growth-mortalittrade-offsfs and "personality traits" in animals. *Ecol. Lett.* 10 (5), 355–363. doi: 10.1111/j.1461-0248.2007.01034.x

Stephens, D. W., and Krebs, J. R. (1986). Foraging theory. *J. Ecol.* 49 (5), 247. doi: 10.2307/1381654

Svalheim, R. A., Karlsson-Drangsholt, A., Olsen, S. H., Johnsen, H. K., and Aas-Hansen, O. (2017). Effects of exhaustive swimming and subsequent recuperation on flesh quality in unstressed Atlantic cod (Gadus morhua). *Fish Res.* 193, 158–163. doi: 10.1016/j.fishres.2017.04.008

Svozil, D. P., Baumgartner, L. J., Fulton, C. J., Kopf, R. K., and Watts, R. J. (2020). Morphological predictors of swimming speed performance in river and reservoir populations of Australian smelt retropinna semoni. *J. Fish Biol.* 97, 1632–1643. doi: 10.1111/jfb.14494

Tan, M. K., Chang, C. C., and Hugh, T. W. (2018). Shy herbivores forage more. efficiently than bold ones regardless of information-processing overload. *Behav. Processes.* 149 (1), 52–58. doi: 10.1016/j.beproc.2018.02.003

Walker, J. A., Ghalambor, C. K., Griset, O. L., et al. (2005). Do faster starts increase the probability of evading predators? *Funct. Ecol.* 19 (5), 808–815. doi: 10.1111/j.1365-2435.2005.01033.x

Wang, P. Y. X. (2009). Effect of temperature on swimming performance in juvenile southern catfish (*Silurus meridionalis*). *Comp. Biochem. Phys. A* 153 (2), 125–130. doi: 10.1016/j.cbpa.2009.01.013

Wang, J. W. (2015). Effects of hypoxia on critical swimming and uniform accelerated swimming ability of juvenile parabramis bream and its biochemical mechanism. Chongqing Normal University. 11-15.

Webb, P. W. (1978). Sprint performance and body form in seven species of teleost. *J. Exp. Biol.* 74, 211–226. doi: 10.1242/jeb.74.1.211

Webb, P. W. (1982). Locomotor patterns in the evolution of actinopterygian fishes. *Am. Zool.* 22 (2), 329–342. doi: 10.1093/icb/22.2.329

Webb, P. W. (1984). Body form, locomotion and foraging in aquatic vertebrates. *Am. Zool.* 24, 107–120. doi: 10.1093/icb/24.1.107

Yuan, X., Huang, Y. P., Cai, L., Johnson, D., Tu, Z. Y., and Zhou, Y. H. (2018). Physiological responses to swimming fatigue in juvenile largemouth bronze gudgeon coreius guichenoti. *J. Fish Biol.* 92(4), 1192–1197. doi: 10.1007/s10750-019-04049-4

Zhang, D., and Wang, L. P. (2021). Knowing fish, knowing fish, managing fish: starting from personality research. *China Fisheries Science.* 28 (10), 13. doi: 10.12264/JFSC2021-0406

frontiers | Frontiers in Marine Science

TYPE Original Research
PUBLISHED 20 October 2022
DOI 10.3389/fmars.2022.1029483

OPEN ACCESS

EDITED BY
Jinghui Fang,
Yellow Sea Fisheries Research Institute (CAFS), China

REVIEWED BY
Yiran Hou,
Freshwater Fisheries Research Center (CAFS), China
Lingling Wang,
Dalian Ocean University, China

*CORRESPONDENCE
Ce Shi
shice3210@126.com
Chunlin Wang
wangchunlin@nbu.edu.cn

SPECIALTY SECTION
This article was submitted to Marine Fisheries, Aquaculture and Living Resources, a section of the journal Frontiers in Marine Science

RECEIVED 27 August 2022
ACCEPTED 06 October 2022
PUBLISHED 20 October 2022

CITATION
Xu H, Shi C, Ye Y, Mu C and Wang C (2022) Photoperiod-independent diurnal feeding improved the growth and feed utilization of juvenile rainbow trout (*Oncorhynchus mykiss*) by inducing food anticipatory activity. *Front. Mar. Sci.* 9:1029483. doi: 10.3389/fmars.2022.1029483

Photoperiod-independent diurnal feeding improved the growth and feed utilization of juvenile rainbow trout (*Oncorhynchus mykiss*) by inducing food anticipatory activity

Hanying Xu[1,2], Ce Shi[1,2,3]*, Yangfang Ye[1,3], Changkao Mu[1,3] and Chunlin Wang[1,3]*

[1]Key Laboratory of Aquacultural Biotechnology Ministry of Education, Ningbo University, Ningbo, China, [2]Marine Economic Research Center, Dong Hai Strategic Research Institute, Ningbo University, Ningbo, China, [3]Collaborative Innovation Center for Zhejiang Marine High-efficiency and Healthy Aquaculture, Ningbo, China

A three-month culture experiment was designed to assess the effects of photoperiod and feeding regime on growth, feed utilization, and food anticipatory activity (FAA) of juvenile rainbow trout. The experiment included two photoperiods: 24L:0D (LL) and 12L:12D (LD); three feeding regimes: random feeding (R), mid-dark stage feeding (D), and mid-light stage feeding (L). A total of six treatment groups (R-LL, D-LL, L-LL, R-LD, D-LD, L-LD) were defined. The experimental results showed that the growth and feed utilization of the scheduled feeding groups (D and L groups) were significantly higher than those of the R group under both photoperiods, and there was no statistical difference between the D and L groups. A typical FAA was observed in the L group, independent of the photoperiod. Also, the digestive enzyme activity of the L group was synchronized by the feeding time under both photoperiods. There were rhythms in serum levels of glucose (GLU), triglyceride (TG), and total-cholesterol (T-CHO) in the D and L groups. Serum GLU also had a rhythm in the R group, but the peaks occurred at the feeding point (LL group) or after the feeding point (LD group), reflecting a possible passive rise in GLU after feeding. Serum cortisol was higher in the R group than in the scheduled feeding group, indicating that random feeding caused stress to juvenile rainbow trout. Serum insulin levels were found to increase before feeding in all three feeding regimes, probably reflecting the anticipation of food induced by the last meal. Serum melatonin levels were suppressed by the LL group. Serum 5-HT levels were synchronized by meal time in the R and L groups. Finally, rhythms of appetite-related genes were observed under all three feeding regimes, and more genes were rhythmic under LL, suggesting that food can strongly synchronize the feeding rhythm of juvenile rainbow trout when lacking light

zeitgeber. In summary, this study concluded that diurnal feeding (L group) independent of photoperiod induced typical FAA in juvenile rainbow trout and that the LD (12L:12D) photoperiod and L (mid-light phase) feeding were recommended in the juvenile rainbow trout aquaculture.

KEYWORDS

photoperiod, feeding regime, food anticipatory activity, rainbow trout oncorhynchus mykiss, digestive enzyme

Introduction

Light (main characteristics include: spectrum, light intensity, and photoperiod) is an important abiotic factor that plays a vital role in the entire life cycle of fish, from embryonic development to gonadal maturation (Villamizar et al., 2011; Imsland et al., 2020). Photoperiod is the most primary zeitgeber of the fish biological clock system, affecting its growth (Wei et al., 2019; Singh and Zutshi, 2020), reproduction (Foss et al., 2020; Imsland et al., 2020), locomotion (Almazán-Rueda et al., 2004), metabolism (Paredes et al., 2014; Wei et al., 2019), and immunity (Leonardi and Klempau, 2003; Esteban et al., 2006). Aquaculture has widely used photoperiod manipulation to improve productivity (Imsland et al., 2020; Ruchin, 2021). It has been observed in most intensively farmed fish that extended light periods promote somatic growth (Boeuf and Le Bail, 1999; Aride et al., 2021; Li et al., 2022), while extended darkness periods promote gonadal development and maturation (Hermelink et al., 2017; Lundova et al., 2019). Constant light (LL) has been implemented in commercial production in freshwater recirculation aquaculture systems (RAS) of Atlantic salmon smolts (Lorgen-Ritchie et al., 2022; Ytrestøyl et al., 2022). Several studies have shown that LL does not negatively affect behavior (Hamilton et al., 2022), survival (Nemova et al., 2020), flesh quality (Imsland et al., 2019), and immune gene expression (Ytrestøyl et al., 2022) in salmonids. However, LL exposure is considered a stressor in some fish, such as black sea turbot (*Psetta maeotica*) (Turker, 2005), Atlantic cod (*Gadus morhua*) (Giannetto et al., 2014), and largemouth bass (*Micropterus salmoides*) (Malinovskyi et al., 2022), etc. More importantly, light, as the most important zeitgeber, plays a crucial role in the regulation of biological circadian rhythms, and the absence of photoperiod can cause metabolic disorders and further develop into metabolic diseases (Bass, 2012; Coomans et al., 2015; Kopp et al., 2016; Hillyer et al., 2021).

Like photoperiod, feeding is another crucial zeitgeber, providing the organism with a temporal cue to its environment (Stephan, 2002; López-Olmeda, 2017). Moreover, feeding appears to be preferential to photoperiod in regulating biological clock oscillations in peripheral tissues such as the liver and intestine (Stephan, 2002; Heyde and Oster, 2019). Feeding has been shown to reset the peripheral biological clock and affect metabolic processes (Bass, 2012). For fish, it is difficult to obtain food continuously in the natural environment, thus exhibiting different feeding rhythms such as diurnal and nocturnal predators (López-Olmeda and Sánchez-Vázquez, 2010; Kousoulaki et al., 2015). Further, feeding time preference was influenced by the season in some fishes, e.g., European sea bass (*Dicentrarchus labrax* L.) showed diurnal feeding in spring, summer, and autumn nocturnal feeding in winter (Sánchez-Vázquez et al., 1998). Matching feeding times to feeding rhythms can significantly improve growth and feed utilization in many fish species (López-Olmeda and Sánchez-Vázquez, 2010), such as channel catfish (*Ictalurus punctatus*) (Noeske-Hallin et al., 1985), rainbow trout (*Oncorhynchus mykiss*) (Boujard et al., 1995), European sea bass (Azzaydi et al., 2000), African catfish (*Clarias gariepinus*) (Hossain et al., 2001), and Senegalese sole (*Solea senegalensis*) (Marinho et al., 2014). Conversely, misaligned feeding (e.g., feeding during the resting phase) can lead to the decoupling of the central and peripheral biological clock oscillations of the organism, resulting in metabolic disturbances (Opperhuizen et al., 2016; Oishi and Hashimoto, 2018; Challet, 2019).

The positive effects of scheduled feeding were mainly based on food anticipatory activity (FAA), a behavior present in almost all fish (López-Olmeda, 2017), manifested by an increase in locomotion from a few minutes or hours before mealtime, as well as an increase in feeding-related endocrine and digestive and metabolic enzyme activity (Stephan, 2002; Vera et al., 2007). In addition, FAA could persist for several days when deprived of the food zeitgeber, suggesting the presence of endogenous oscillators guiding the FAA, known as food entrainment oscillators (FEOs, Davidson, 2006; López-Olmeda and Sánchez-Vázquez, 2010; Patton and Mistlberger, 2013). Despite numerous studies in model animals such as mice, the exact organization or localization of FEOs remains unknown, and many findings support that FEOs can work independently of the traditional biological clock system (feedback loops) (Davidson, 2006; Page et al., 2020). In fish, the understanding and working pathways of FEOs are still very vague and

fragmented, and some hormones are thought to play an important role, such as ghrelin (Nisembaum et al., 2014a) and orexin (Hoskins and Volkoff, 2012; Nisembaum et al., 2014b).

The effects of light and food on fish circadian rhythms have been studied in several species. In zebrafish (*Danio rerio*) (Paredes et al., 2015) and gilthead sea bream (*Sparus aurata*) (Paredes et al., 2014), the rhythm of lipid metabolism genes in the liver was found to be pulled by the photoperiod independent of feeding time. In contrast, in rainbow trout (Hernández-Pérez et al., 2015), food was found to affect the rhythm of hepatic glucose and lipid metabolism gene expression more than light. Vera et al. (2013) also observed liver biological clock gene expression rhythms in the gilthead sea bream entrained by food independent of light. In addition, the expression of different biological clock genes in rainbow trout liver (Hernández-Pérez et al., 2017) and goldfish (*Carassius auratus*) gut (Nisembaum et al., 2012) was pulled by light and food, respectively, suggesting an interaction between these two zeitgebers. In zebrafish, neither regular feeding (diurnal feeding) nor altered feeding (nocturnal feeding) affected the expression rhythm of gut biological clock genes, but altered feeding shifted the expression rhythm of gut melatonin synthase genes, indicating that gut biological clock genes are entrained by photoperiod and melatonin synthesis is synchronized by feeding time (Mondal et al., 2022). On the other hand, food and light also impacted the locomotor activity and FAA of the fish. In zebrafish (Blanco-Vives and Sánchez-Vázquez, 2009), feeding was found to be synchronized with locomotor activity and independent of photoperiod. It was also observed in goldfish that scheduled feeding under LL synchronized the rhythm of biological clock genes in the optic tectum and hypothalamus and elicited FAA, while rhythmic expression of biological clock genes in the liver was also observed in the random feeding group, suggesting that the biological clock in the liver is synchronized by the last meal time, and FAA independent of the liver biological clock system (Feliciano et al., 2011). However, in tambaqui (*Colossoma macropomum*), mid-dark phase feeding caused FAA, while mid-light phase feeding was futile (Fortes-Silva et al., 2018). Notably, as a strictly nocturnal species, tench (*Tinca tinca*) elicited FAA in the light phase feeding under a constant dark but not LD (12L:12D) environment (Herrero et al., 2005). Whether scheduled feeding can induce FAA in fish seems closely related to feeding time and photoperiod.

Rainbow trout is a high-value economically farmed fish widely farmed worldwide (especially in European countries) (Öz, 2018). Global aquaculture production reached 848,051 tons, with a value of $3.88 billion in 2018 (FAO, 2020). Rainbow trout is famous among consumers as a high-grade aquatic product in China due to its bright color, delicious taste, and rich nutrition. However, there is still a vast gap between production and market demand due to the lack of cold-freshwater resources. Previous studies found that rainbow trout farming in seawater can achieve faster growth rates (Landless, 1976; Shepherd et al., 2005), higher feed conversion efficiencies (Landless, 1976), and stronger immunity (Yada et al., 2001). Based on this discovery, in recent years, some researchers have attempted to aquaculture rainbow trout using offshore fish cages (such as "Shenlan 1") in the cold-water masses of the Yellow Sea in China (Dong, 2019; Chu et al., 2020). Nowadays, rainbow trout has emerged as a promising candidate fish for deep-sea aquaculture (Dong, 2019; Huang et al., 2021).

Currently, the "mountain-sea transfer" culturing method has been used to culture rainbow trout in seawater (Dong, 2019). In brief, rainbow trout larvae are hatched in low-temperature freshwater nurseries. The fry (about 5 g) is transferred to mountainous areas with abundant cold-freshwater resources for large-size juvenile culture. After growing to approximately 150 g, the juveniles are transported to seawater domestication systems for one week and finally transferred to the offshore fish cage for culture to commercial fish (weight above 4 kg). During this process, cultivating fish from fry to juveniles is a crucial step, which directly affects the later mariculture success rate. Whether light and food can be manipulated to promote rainbow trout growth during the freshwater culture is vital to the success of the "mountain-sea transfer" culturing method. Therefore, the objectives of this study were 1) to investigate whether the photoperiod/feeding regimes can induce FAA and promote growth in juvenile rainbow trout and 2) the effects of different photoperiod/feeding regimes on behavioral, digestive, metabolic, endocrine, and appetite rhythms in juvenile rainbow trout.

Materials and methods

Ethical issues

This study was approved by the Animal Care and Use Committee of Ningbo University.

Fish

This research was conducted in the Intelligent Aquaculture Laboratory, School of Marine Sciences, Ningbo University. The juvenile rainbow trout were obtained from a commercial nursery (Shandong, China) and cultured in a recirculating aquaculture system (RAS) (HISHING, Qingdao, China) from July to November 2020. All fish were acclimatized in the RAS for one month before the culture experiment. During the acclimation period, the fish were randomly fed a commercial diet (Tech-Bank, Ningbo, China, Supplementary Table 1) at about 2% of body weight, with a photoperiod of 12L:12D (lights-on at 6:00, the light intensity on the water surface is 100-200 lx), water temperature controlled at 15.5-17.5°C, dissolved oxygen was kept saturated, and ammonia nitrogen < 0.05mg/L.

Experiment design

A total of 840 healthy rainbow trout were weighed and randomly distributed to 42 tanks (1.0m× H 0.8m, Supplementary Figure 1), with 20 fish per tank. The experiment included two photoperiods: 24L:0D (LL, the light intensity on the water surface is 100-200 lx) and 12L:12D (LD, lights-on at 6:00, light-off at 18:00, the light intensity on the water surface is 100-200 lx); three feeding regimes: random feeding (R), mid-dark stage feeding (D), and mid-light stage feeding (L). Briefly, a random feeding schedule for the R group was obtained using a random number generator software according to the method described by Nisembaum et al. (2012); In group D, we fed at 24:00 daily; in group L, we fed at 12:00 daily. A total of six experimental treatments were combined: R-LL, D-LL, L-LL, R-LD, D-LD, and L-LD, and each treatment included seven tanks. The growth experiment lasted three months, and the cultural management and environmental conditions were consistent with the acclimation.

Fish locomotion observation

In this experiment, an underwater infrared camera (SLD-EX300Q, Hengdun Shunli Da electronic technology Co., Ltd.,

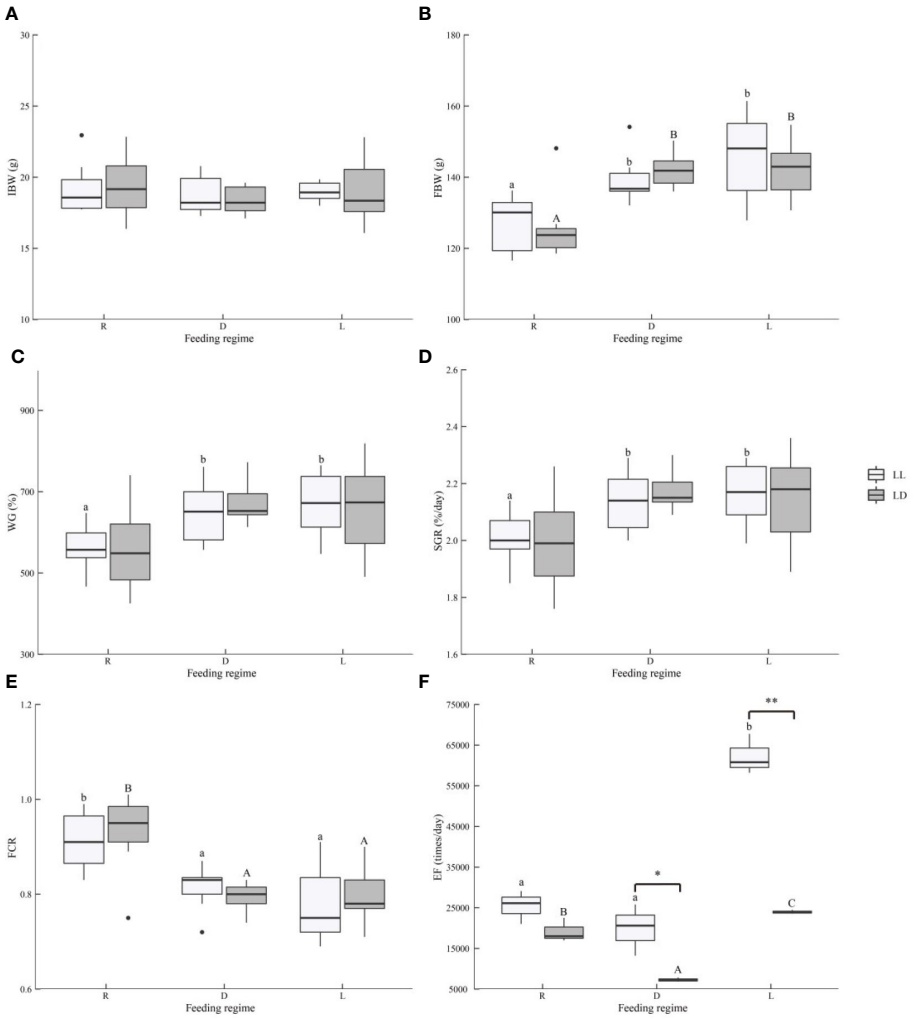

FIGURE 1
Growth performance, feed utilization, and locomotion of juvenile *Oncorhynchus mykiss* under different experimental treatment. **(A)**. IBW, Initial body weight, **(B)**. FBW, Final body weight, **(C)**. WG, Weight gain (%) = 100 × (final weight − initial weight)/initial weight, **(D)**. SGR, Specific growth rate (%/day) = 100 × (ln final weight − ln initial weight)/94 days, **(E)**. FCR, Feed conversion ratio = dry feed consumed/wet weight gain, **(F)**. EF, Exercise frequency. Different lowercase letters and capital letters indicate significant difference among different feeding strategy at the LL (constant light) and LD (12L: 12D, lights-on at 6:00), respectively ($P < 0.05$). Asterisks denote significant differences between photoperiods at the same feeding regime (*, $P < 0.05$; **, $P < 0.01$).

Jinan, China) was used to observe the exercise frequency (EF) of juvenile rainbow trout. The number of times the fish swam through the observation area was recorded as EF. Fish locomotion data were collected from October 2nd to 4th, 2020 (2 months after the growth experiment was conducted) for 72 hours. As Mistlberger (1994) described, a typical FAA is usually defined as a rapid increase in activity from minutes to hours before the feeding point, reaching more than twice the basal activity and lasting at least 30 minutes.

Sample collection

Following the 3-month growth experiment, all fish were starved for 24 hours, while samples were taken afterward. The 24th hour after food deprivation was ZT0 (feeding point), and samples were taken every 4 hours for 24 hours, for a total of 7 sampling points (ZT0, ZT4, ZT8, ZT12, ZT16, ZT20, ZT24), corresponding to 7 tanks in each treatment, to avoid the stimulation of fish by sampling. Each sampling point was operated as follows: first, the fish in the tank were anesthetized using MS-222 (50mg/L, Shanghai Macklin Biochemical Co., Ltd., Shanghai, China), and then 12 fish were randomly taken from the tank for weight and body length measurement (to calculate the condition factor (CF)); the blood was immediately collected from each fish by the tail vein method and stored overnight at 4°C; then, the fish were dissected immediately after blood collection, the brain, liver (weighing to calculate the hepatosomatic index (HSI)), and digestive tract (scraping off intestinal fat to calculate the intraperitoneal fat ratio (IPF)) were isolated, quick frozen in liquid nitrogen and stored at -80°C.

Digestive enzymes

First, the digestive tract was homogenized in saline (0.9% NaCl, 4°C) in a ratio of 1:9 (W: V). The homogenate was centrifuged at 3000 rpm for 10 min at 4°C to obtain the supernatant. Amylase (C016-1-1), lipase (A054-2-1), pepsin (A080-1-1), and chymotrypsin (A080-3-1) activity in the digestive tract were assayed using commercial kits (Nanjing Jiancheng Bioengineering Institute, Nanjing, China) according to the instructions.

Serum metabolites and hormones

Fish blood was left overnight at 4°C and then centrifuged at 4°C for 10 minutes at 2500 rpm, and the supernatant was taken as serum. Serum glucose (Glu, A154-2-1), triglyceride (TG, A110-1-1), and total-cholesterol (T-CHO, A111-1-1) were measured by commercial kits (Nanjing Jiancheng Bioengineering Institute, Nanjing, China) according to the instructions. Serum cortisol, insulin, melatonin, and serotonin (5-HT) levels were measured using commercial enzyme linked immunosorbent assay (ELISA) kits (Shanghai Qiaodu Biotechnology Co., Ltd., Shanghai, China) according to the instructions.

Gene expression

The total RNA of the brain and digestive tract was extracted with a commercial kit RNA isolator (R401-01, Vazyme, Nanjing, China). The quality of total RNA was checked by ultramicro-spectrophotometer (Nanodrop 2000, Thermo Scientific, Waltham, USA) and 1% gel electrophoresis. The RNA was reverse transcribed into cDNA using a HiFiScript cDNA synthesis kit (CW2569M, CWBIO, Beijing, China).

The real-time PCR was used to analyze the relative expression of appetite-related genes in the brain (agouti-related peptide (*agrp*), cocaine- and amphetamine-related transcript (*cart*), neuropeptide Y (*npy*), *orexin*, pro-opio melanocortin (*pomc*)) and digestive tract (Ghrelin/Obestatin prepropeptide (*ghrl*) and *leptin*). The total reaction volume includes 10 µl of 2 × MagicSYBR Mixture (CW3008H, CWBIO, Beijing, China), 2 µl of cDNA, 0.4 µl of each primer (10 µM), and 7.2 µl of ddH_2O. A Real-Time PCR System (QuantStudio^{TM} 6 Flex, Life Technologies, Carlsbad, USA) was used with the program as follows: 95°C for 30 s; 45 cycles at 95°C for 5 s, 60°C for 30 s; and 95°C for 15 s. The specific primers used in this study are shown in Supplementary Table 2 and synthesized by a commercial company (Youkang Biological Technology Co., Ltd, Hangzhou, China). The relative expression level of target genes is normalized by *β-actin* and elongation factor-1α (*ef1α*) and calculated by the comparative CT method ($2^{-\Delta\Delta CT}$ method) (Livak and Schmittgen, 2001).

Statistical analysis

All statistical analyses were performed on SPSS 22.0 and R 4.1.2 software. First, all data were checked for homogeneity and normal distribution through Levene's test and Kolmogorov-Smirnov test, respectively. Then a two-way ANOVA was performed with photoperiod and feeding regime. Meanwhile, t-tests were performed for photoperiod, and one-way ANOVA followed by Duncan's multiple range test was performed for the feeding regime to check the effect on IBW, FBW, WG, SGR, FCR, EF, HSI, IPF, and CF. $P < 0.05$ and $P < 0.01$ were considered significant differences and extremely significant differences, respectively. In addition, cosinor analysis [performed using the circacompare R package (Parsons et al., 2020)] was performed to detect the circadian rhythms in digestive enzyme activity, serum metabolite and hormone levels, and appetite-related gene expression. $P < 0.05$ indicates the presence of circadian rhythms.

Results

Growth performance, feed utilization, and morphology

In the present study, photoperiod did not affect the growth and feed utilization of juvenile rainbow trout (Figures 1A–E and Supplementary Table 3). Scheduled feeding (D and L groups) significantly increased the final body weight (FBW) and decreased the feed conversion ratio (FCR) of juvenile rainbow trout ($P<0.05$). The scheduled feeding (D and L groups) significantly increased specific growth rate (SGR) under LL ($P<0.05$), although there was no statistical difference, and higher weight gain (WG) and SGR were also observed with scheduled feeding (D and L groups) under LD ($P>0.05$). There was no interaction between photoperiod and feeding regime on growth and feed utilization of juvenile rainbow trout (Supplementary Table 3). Feeding time (D or L groups) did not affect the growth and feed utilization of juvenile rainbow trout (Figures 1A–E). Morphological parameters (HSI, IPF, and CF) were not affected by the experimental treatment (Supplementary Table 3 and Supplementary Figure 2, $P>0.05$).

Locomotion

The EF of juvenile rainbow trout was significantly influenced by photoperiod and feeding regime (Figures 1F, 2, and

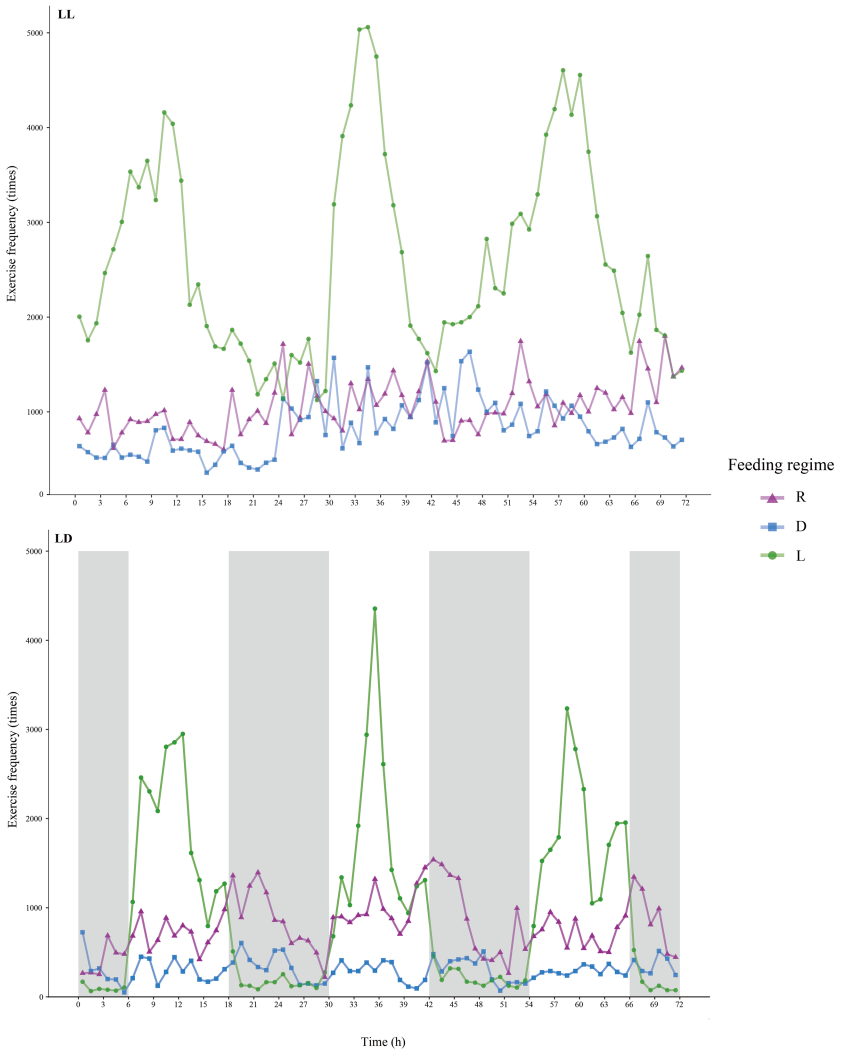

FIGURE 2
Exercise frequency of juvenile *Oncorhynchus mykiss* under different experimental treatment. The bright bars indicate the light period and the dark bars indicate the dark period.

Supplementary Table 3). The EF of juvenile rainbow trout in the LL group was higher than that of the LD group ($P<0.05$); the EF of juvenile rainbow trout in the L group was significantly higher than that of the other groups under both photoperiods ($P<0.05$). There was an interaction between photoperiod and feeding regime on the locomotion of juvenile rainbow trout (Supplementary Table 3). Under LL, the EF of the L group was significantly higher than that of the R and D groups; under LD, EF showed L>R>D.

Under both photoperiods, the EF of juvenile rainbow trout in the L group was significantly higher before feeding and then decreased, a typical FAA (Figure 2). However, no typical FAA was observed in both R and D groups under both photoperiods (Figure 2).

Digestive enzyme

In this study, amylase activity showed a significant rhythm under LL for all three feeding regimes, while no rhythm was observed under LD (Figures 3A, 6). Under LL, the amylase activity of the L and D groups increased before feeding and peaked at ZT2 and ZT4, respectively. In comparison, the amylase activity of the R group peaked before feeding (ZT18).

Lipase activity showed significant rhythms in R and L groups under both photoperiods (Figures 3B, 6). In the L group, lipase activity increased before the feeding point, peaked at the feeding point (ZT0), and then decreased. However, lipase activity in the R group increased after feeding and then decreased.

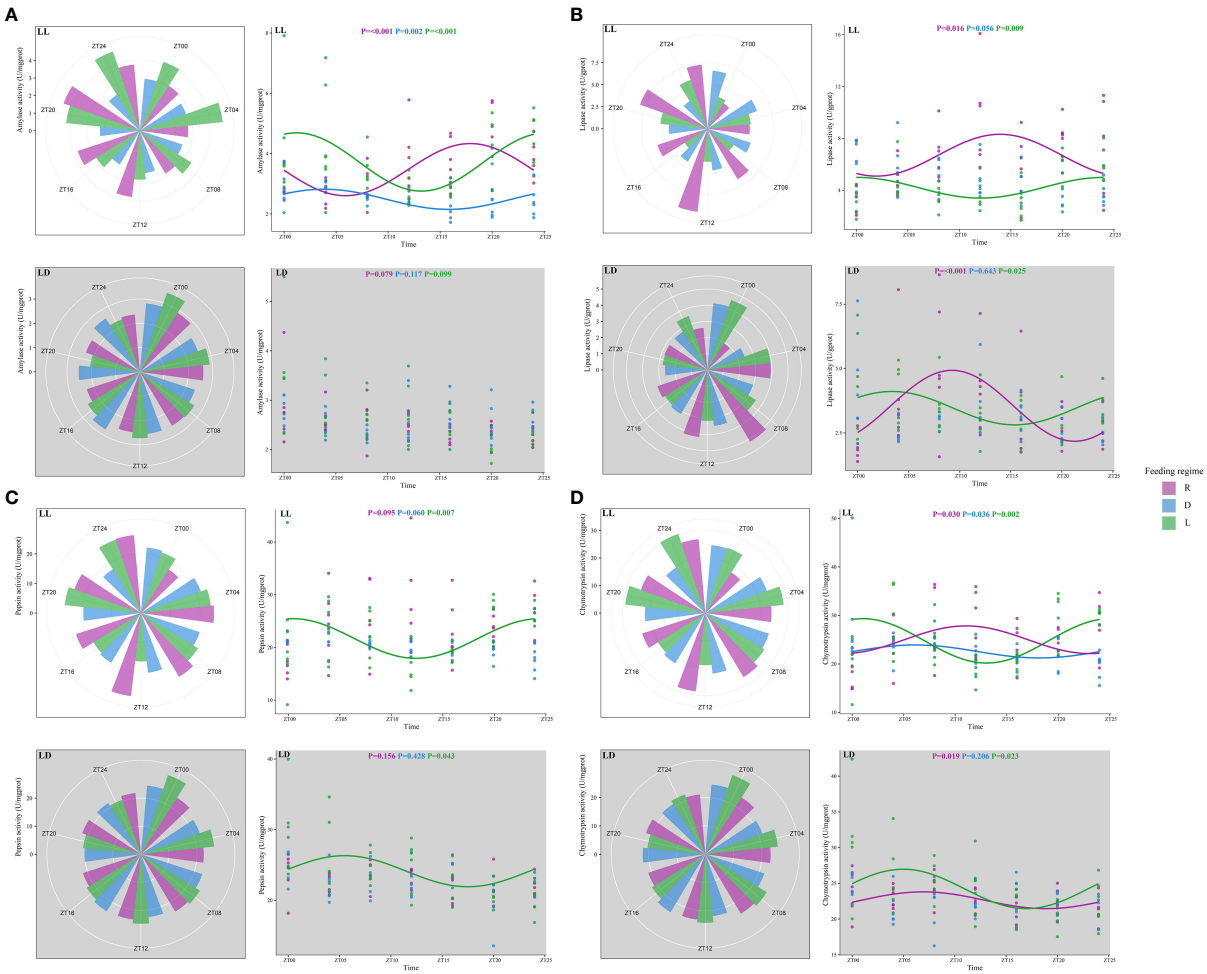

FIGURE 3
Digestive enzyme activity of juvenile *Oncorhynchus mykiss* under different experimental treatment. **(A)**. Amylase, **(B)**. Lipase, **(C)**. Pepsin, **(D)** Chymotrypsin. The cosine curve denotes the presence of rhythmic oscillations ($P < 0.05$).

There was a significant rhythm of pepsin activity in the L group under both photoperiods (Figures 3C, 6). Pepsin activity increased before feeding, peaked at the feeding point (ZT0), and then decreased.

The chymotrypsin activity was significantly rhythmic under LL for all three feeding regimes (Figures 3D, Figure 6). The L and D groups showed increased chymotrypsin activity before feeding, peaking at the feeding point (ZT0) and then decreasing. Chymotrypsin activity in the R group increased after feeding. Under LD, chymotrypsin activity of L and R groups increased before feeding, peaked after feeding (ZT7), and then decreased.

Serum metabolites and hormones

In the present study, the experimental treatments affected serum levels of metabolites and hormones (Figures 4, 6). Serum GLU levels increased before feeding and decreased after feeding in the D (peaked at ZT20 under LD) and L (peaked at ZT0 under LL, peaked at ZT23 under LD) groups. In the R group, serum GLU levels peaked at the ZT0 (LL) and ZT3 (LD), respectively (Figures 4A, 6). Serum TG levels were significantly higher in the scheduled feeding group (D and L groups) than in the R group and were found to peak after feeding (ZT4) under all three feeding regimes (Figures 4A, 6). Serum T-CHO levels in the scheduled feeding group also increased and peaked after feeding (Figures 4A, 6).

Serum cortisol levels were not affected by photoperiod, but random feeding caused a significant increase in serum cortisol levels (Figure 4B). Serum insulin levels were significantly higher in the R and D groups than in the L group, and peaked before feeding (ZT20-ZT23) under all three feeding regimes (Figures 4B, 6). Serum melatonin levels were significantly lower in the LL group than in the LD group. There was no circadian rhythm observed in serum melatonin levels under LD. Serum melatonin levels showed R>D>L under both photoperiods (Figure 4B). Serum serotonin levels were significantly higher in the LL group than in the LD group. Serum serotonin levels peaked before feeding (ZT23-ZT0) in both the R and L groups and then decreased (Figures 4B, 6).

Appetite-related gene expression

Overall, more appetite-related genes showed circadian rhythms under LL compared to LD. And all appetite-related genes showed significant circadian rhythms under different feeding regimes (Figure 5).

Under LL, all appetite-related genes showed circadian rhythms in the R group, and the peaks were mostly concentrated around ZT15-ZT18 (except *leptin* and *npy*); in the L group, all genes except *orexin* showed significant circadian rhythms with peaks around ZT10-ZT13; in the D group, only *leptin* and *orexin* genes showed circadian rhythms with peaks around ZT11 and ZT14, respectively (Figures 5, 6).

Under LD, significant circadian rhythms were observed only in the *cart*, *ghrl*, *leptin*, and *npy* genes. In the R group, circadian rhythms were observed in *ghrl* (peak at ZT23) and *leptin* (peak at ZT5) genes; in the L group, circadian rhythms were observed in *cart* (peak at ZT0), *ghrl* (peak at ZT14), and *leptin* (peak at ZT13) genes; in the D group, circadian rhythms were observed in *cart* (peak at ZT22), *ghrl* (peak at ZT15), *leptin* (peak at ZT1), and *npy* (peak at ZT3) genes (Figures 5, 6).

Discussion

Growth performance and food anticipatory activity

Rainbow trout mortality was not observed in this study, indicating that our aquaculture environment was suitable for the survival of juvenile rainbow trout. In the present study, photoperiod did not affect growth performance (FBW, WG, SGR) and feed utilization (FCR) of juvenile rainbow trout. Similar results have been reported in other fish species, such as lenok (*Brachymystax lenok*) (Liu et al., 2015), pacamã catfish (*Lophiosilurus alexandri*) (Kitagawa et al., 2015), Amazonian ornamental (*Heros severus*) (Veras et al., 2016), zebrafish (Abdollahpour et al., 2020), and largemouth bass (Malinovskyi et al., 2022). However, in some fish, compared to LD, LL promoted somatic growth and feed utilization, e.g., Caspian roach (*Rutilus rutilus caspicus*) (Shahkar et al., 2015), gibel carp (*Carassius auratus*) (Wei et al., 2019), winter flounder (*Pseudopleuronectes americanus*) (Casey et al., 2020), Nile tilapia (*Oreochromis niloticus*) (Martínez-Chávez et al., 2021). LL promotes somatic growth in fish mainly attributed to the suppression of gonadal development (Doyle et al., 2021), increased feed intake (Wei et al., 2019; Martínez-Chávez et al., 2021), enhanced digestive enzyme activity (Shan et al., 2008; Ramzanzadeh et al., 2016), and upregulation of gene expression of growth-related hormones (growth hormone (GH) and insulin-like growth factor (IGF-1)) (Li et al., 2022). Conversely, some studies have found that compared to LD, LL inhibited the growth of some fish, such as anemonefish (*Amphiprion melanopus*) (Arvedlund et al., 2000), wild carp (*Cyprinus carpio*) (Ghomi et al., 2011), and European sea bass (Li et al., 2021). Li et al. (2021) found that feed intake and digestion were elevated in European sea bass under LL exposure. However, antioxidant enzyme activity was elevated and accompanied by more frequent locomotion leading to an increase in non-growth energy consumption, which ultimately inhibited fish growth (Li et al., 2021). Similarly, Valenzuela et al. (2022) found that LL exposure caused stress in rainbow trout and impacted immune system function. In this study, the growth performance and feed utilization of juvenile rainbow trout did

10.3389/fmars.2022.1029483

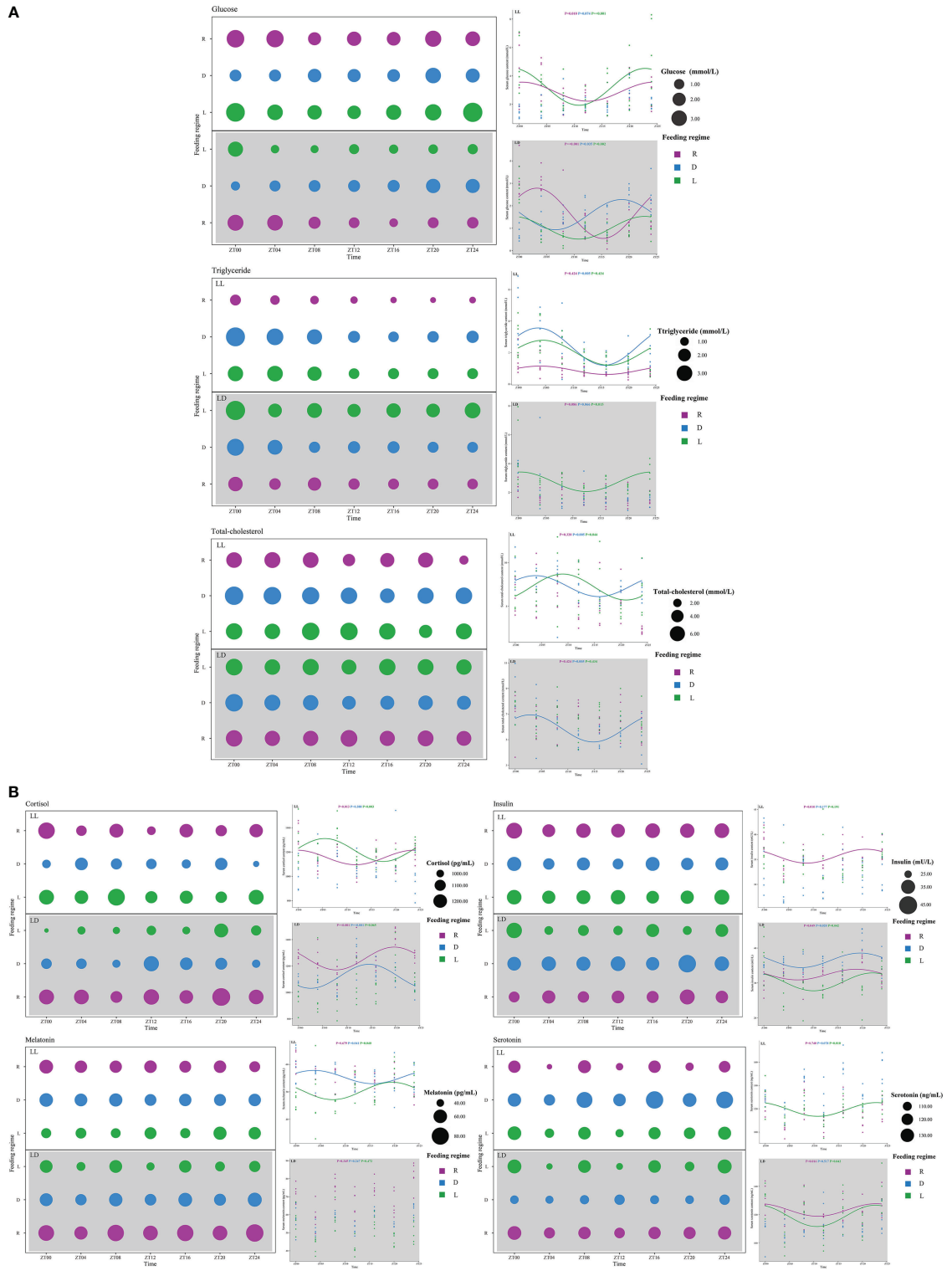

FIGURE 4
Serum metabolites **(A)** and hormones **(B)** of juvenile *Oncorhynchus mykiss* under different experimental treatment. The cosine curve denotes the presence of rhythmic oscillations ($P < 0.05$).

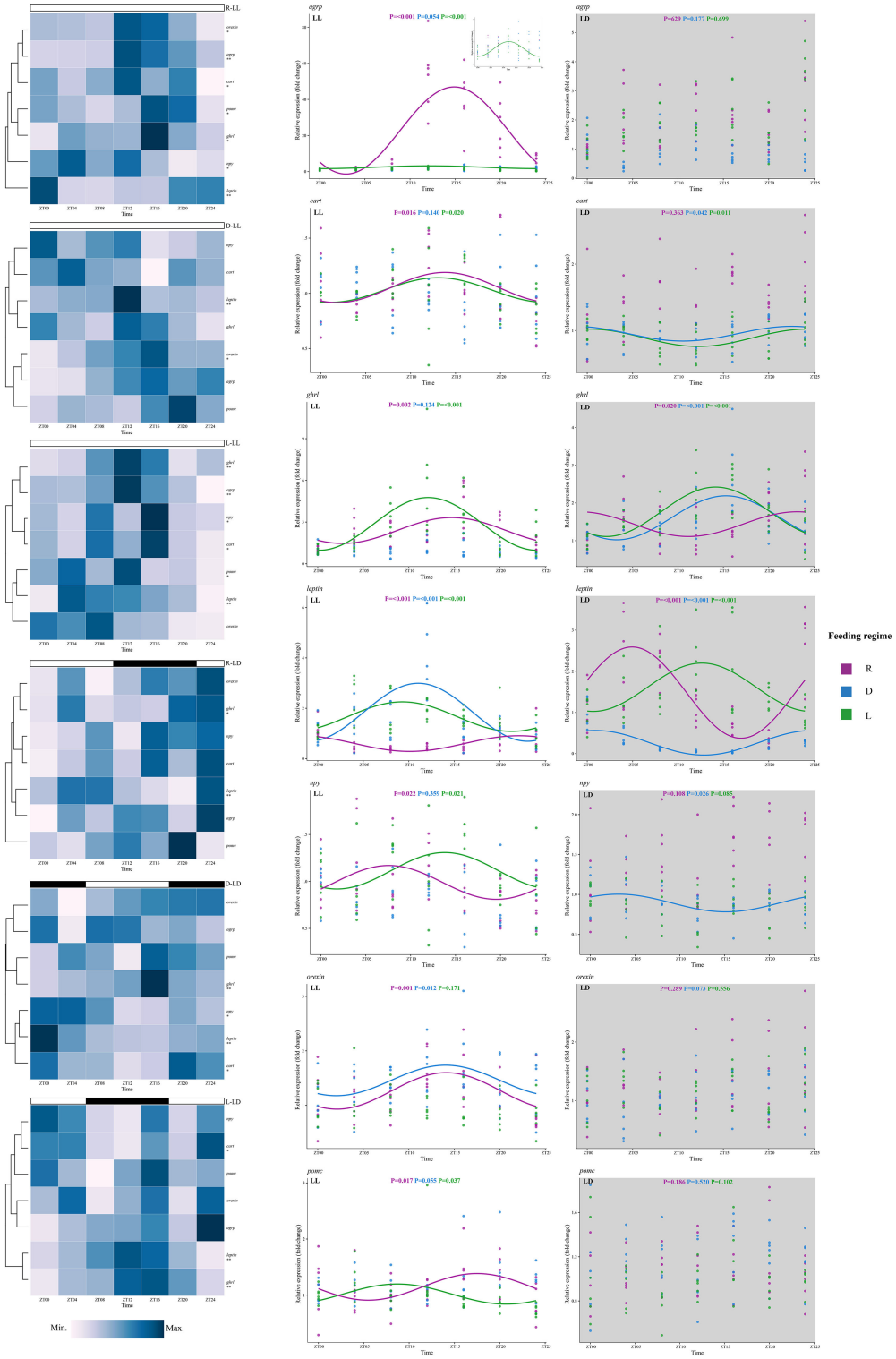

FIGURE 5
Expression of feeding-related genes of juvenile *Oncorhynchus mykiss* under different experimental treatment. Asterisks denote the presence of diurnal oscillations (*, $P < 0.05$; **, $P < 0.01$). The cosine curve denotes the presence of rhythmic oscillations ($P < 0.05$).

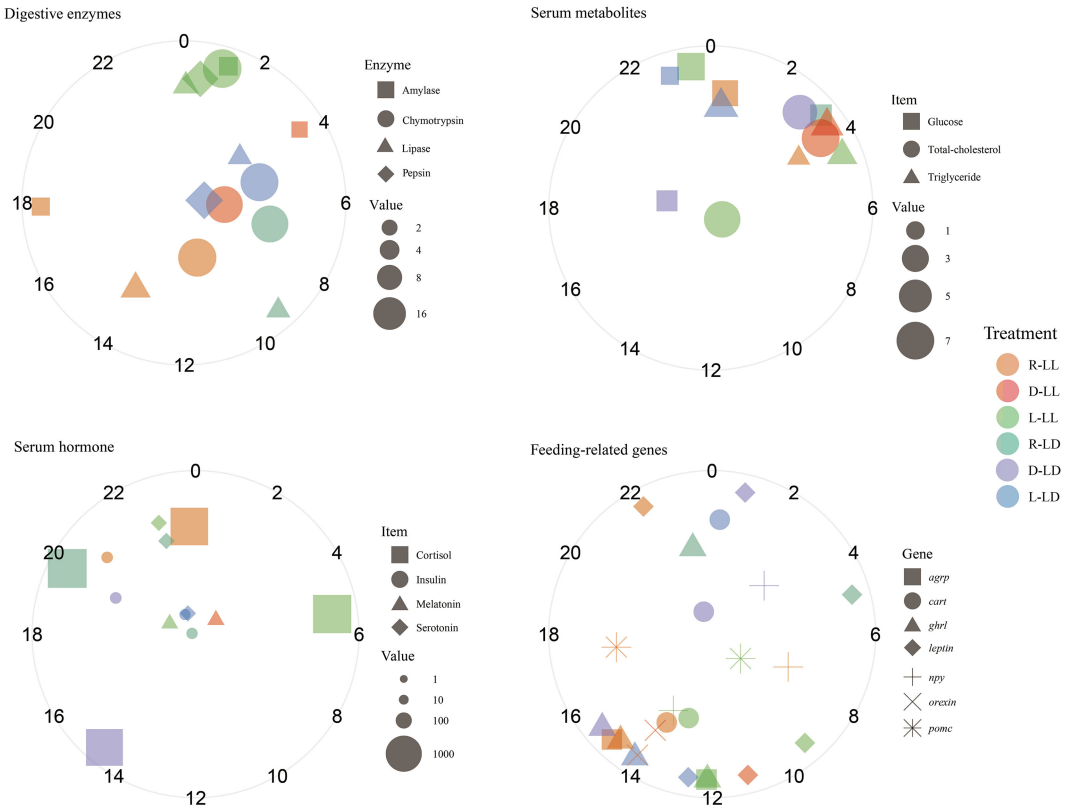

FIGURE 6
The peak time of the indicator with diurnal oscillation in this study. The distance from the center of the clock indicates significance, with closer to the edge of the clock indicating stronger rhythmic oscillations (smaller *P* values).

not show statistical differences between LL and LD groups. This result may be attributed to several reasons: 1) fixed feeding rates in both groups; 2) only amylase and lipase activity was increased in the LL group; 3) more frequent activity in the LL group; 4) no significant stress was observed in the LL group. In this study, fish feeding was fixed at about 2% of body weight for the different treatments. In addition, only significantly elevated amylase and lipase activities were observed in the LL group, while pepsin and chymotrypsin activities were not affected by photoperiod. On the other hand, the EF of rainbow trout in the LL group was significantly higher than that in the LD group. Also, although the serum GLU levels were significantly higher in the LL group than in the LD group, there was no significant difference in serum cortisol levels between the photoperiods. In summary, it is hypothesized that digestion and absorption of feeds were improved in rainbow trout under LL. However, it may not have caused significant stress, the more frequent locomotion also increased energy expenditure under LL, so LL did not promote growth and feed utilization in juvenile rainbow trout. It is also noteworthy that compared to LD, LL significantly increased the WG of largemouth bass for the first 8 weeks; however, after 12 weeks, the WG difference disappeared between these two groups (Malinovskyi et al., 2022). The culture period in this study was 3 months, so further studies are needed to determine whether short-term LL exposure would promote the growth of juvenile rainbow trout.

Scheduled feeding (D and L groups) significantly improved juvenile rainbow trout's growth and feed utilization independent of photoperiod. Scheduled feeding induced FAA within almost all fish species (López-Olmeda, 2017). Similarly, this study observed the typical FAA behavior in the L group and was independent of photoperiod. Under both photoperiods, the locomotion of rainbow trout in the L group increased rapidly before the feeding point and decreased after feeding. Surprisingly, the D group did not exhibit FAA under both photoperiods, and rainbow trout are typically diurnal fish (Iigo and Tabata, 1997; Sánchez-Vázquez and Tabata, 1998; Bolliet et al., 2001), suggesting that shift feeding does not induce FAA in the rainbow trout. Similar results were reported in tambaqui, as nocturnal fish (Fortes-Silva et al., 2016), where typical FAA was found in the mid-dark feeding group rather than the mid-light feeding group under an LD environment (Fortes-Silva et al., 2018). Fortes-Silva et al. (2018) concluded that daytime feeding generally does not alter the locomotion of nocturnal fish. Another study in tench (*Tinca tinca*) (strictly nocturnal species)

also found that daytime feeding failed to elicit FAA under an LD environment (Herrero et al., 2005). However, daytime feeding elicited FAA in a constant dark environment (Herrero et al., 2005). Herrero et al. (2005) concluded that mealtime became the dominant zeitgeber for synchronous locomotion in the absence of photoperiod. Similarly, an earlier study found that the demand-feeding rhythm of rainbow trout under LL was synchronized by dark period feeding (Bolliet et al., 2001). Unexpectedly, in this study, under LL, the typical FAA was still not present in the D group, although there was a higher EF at the feeding point. This result may be related to the different observation methods, as Bolliet et al. (2001) directly recorded the baiting behavior of fish through electronic self-feeders connected to a computer, whereas in the present study, the locomotion of fish was recorded through a video camera. In fish, the exact location and mechanism of FEOs that cause FAA are still poorly understood (Nisembaum et al., 2014a), and the present study also cannot explain why the D group did not cause typical FAA. However, the results of this study showed that rainbow trout have strong diurnal behavior, which could not be altered by shift feeding. The nocturnal feeding also inhibited the locomotion of rainbow trout, which reduced energy consumption and may partially explain the improved growth performance of the D group.

Digestive enzyme rhythms

FAA is not only an increase in locomotion before feeding but also accompanies the preparation of the digestive and endocrine systems for the upcoming meal (Stephan, 2002; Vera et al., 2007). First, in the L group, all four digestive enzymes showed significant rhythms under both photoperiods (except for amylase in the L-LD group), and in the L-LL group, the peak of all four digestive enzyme activities was concentrated around the feeding point (ZT0), while in the L-LD group, the peak of the three digestive enzymes was moved to around ZT4. This result indicated that scheduled diurnal feeding under LL could fully synchronize the rhythm of digestive enzyme activity; however, under LD, photoperiod affected the rhythm of digestive enzyme activity (Lazado et al., 2017), delaying the peak of digestive enzyme activity. In the D group, although only rhythms in amylase and chymotrypsin activities were observed under LL, the trend for both was consistent with the L group, with both rising before the feeding point and peaking at ZT4. This result suggested that scheduled nocturnal feeding can partially synchronize the rhythm of digestive enzyme activity in rainbow trout in the absence of a photoperiod.

Noteworthy, significant rhythms were also observed for amylase, lipase, and chymotrypsin in the R group. However, these peaks in enzyme activity were not clustered but rather scattered at different points in the day. In permit (*Trachinotus falcatus*), Lazado et al. (2017) also found a rhythm in digestive enzyme activity and diversity of peaks between different digestive enzymes. This result indicated that there is a rhythm of digestive enzyme activity in the digestive tract of rainbow trout, but random feeding could not synchronize the rhythm of digestive enzymes. In other words, rainbow trout could not anticipate the feeding point under random feeding and failed to increase the digestive enzyme activity before the feeding point to improve the digestion and utilization of feed. Similar results have been widely reported in different fish species. Regardless of the photoperiod, scheduled feeding induced a significant increase in digestive enzyme activity before the feeding point, but this phenomenon disappeared under random feeding (Vera et al., 2007; Montoya et al., 2010; Lazado et al., 2017).

Serum metabolites and hormone rhythms

Further analysis of serum metabolite levels revealed significant rhythms in serum GLU, TG, and T-CHO in the scheduled feeding groups (D and L groups). First, the L group serum GLU showed a rapid increase and peak before the feeding point and a decrease after feeding under both photoperiods, a trend consistent with locomotion. GLU is a substrate for energy metabolism (Haman et al., 1997), which showed that an elevated energy requirement accompanies FAA before the feeding point. The D group observed a similar serum GLU rhythm under LD, but the peak was advanced. In the R group, significant rhythms in GLU were also present, but the peaks occurred at the feeding point (LL group) and after feeding (LD group), respectively, which may reflect a passive rise in GLU caused by feeding rather than anticipation of food.

Wagner and Congleton (2004) suggested that serum TG and T-CHO levels in salmonids represent lipid metabolism and nutritional status, respectively. Overall, TG and T-CHO levels were significantly lower in the R group than in the scheduled feeding groups (D and L groups), reflecting a poor metabolic and nutritional status. On the other hand, under LL, a TG peak was observed around ZT4 for all three feeding strategies, which is consistent with an increase in lipid metabolism levels after feeding, and the same rhythmic trend was observed in the R group, implying that the last meal also induced a rhythm in lipid metabolism. Similarly, Feliciano et al. (2011) found in goldfish that the biological clock gene expression rhythm of the liver, a central metabolic organ, was synchronized by the last meal. Daily metabolic oscillations were also driven by the last meal in the randomly fed rat (Escobar et al., 2007). As a nutritional indicator, the rhythm of serum T-CHO was only found in the scheduled feeding group. The serum T-CHO levels peaked at ZT4 (D group) and ZT8 (L group). This result revealed the differential effect of feeding time on the rhythm of lipid metabolism in rainbow trout.

Insulin is a peptide hormone that widely exists in vertebrates and plays a fundamental role in growth, development, and metabolic regulation (Hernández-Sánchez et al., 2006). The best-known function of insulin is to regulate blood GLU levels

(Caruso and Sheridan, 2011). In general, serum insulin levels rise after a meal to suppress the rise in blood glucose and then quickly return to normal levels. Carnivorous fish are considered non-insulin-dependent diabetes mellitus (Salgado et al., 2004), and insulin and blood glucose levels take longer to recover after meals (Navarro et al., 1993). In the present study, serum insulin levels were significantly higher in the R and D groups compared to the L group, reflecting the increased insulin resistance in rainbow trout. Further analysis of insulin rhythms showed that serum insulin levels increased and peaked before feeding and decreased after feeding for all three feeding regimes. The rainbow trout were starved for 24 h before sampling. They were also starved during the sampling period, so the rise in serum insulin levels in this study was not a passive rise caused by feeding. The results of this study may suggest that rainbow trout can release insulin into serum earlier to maintain blood GLU homeostasis based on the timing of the last meal.

In fish, cortisol can increase the rate of energy metabolism in response to the high energy demands of stress (Mommsen et al., 1999). In the present study, high cortisol levels were detected in the serum of the R group. Random feeding as a stressor has been found to cause increased serum cortisol levels in other teleosts, such as gilthead seabream (Sánchez et al., 2009) and goldfish (Saiz et al., 2021). A recent study found that long-term treatment with high cortisol resulted in atrophy of the digestive tissues of rainbow trout, hindering nutrient assimilation and energy absorption while increasing routine energy expenditure, ultimately impeding growth (Pfalzgraff et al., 2021). Therefore, the significantly poor growth performance and feed utilization of the R group in this study were strongly associated with high cortisol levels. On the other hand, LL appears to be an acceptable light environment for rainbow trout and does not cause serum cortisol rises. Similar results have been reported in juvenile red sea bream (Biswas et al., 2006). Consistent with the results of this study, Saiz et al. (2021) found that random feeding resulted in higher cortisol levels compared to the absence of photoperiod in goldfish, suggesting that food is a more critical zeitgeber for fish welfare.

Melatonin is an important mediator for organisms to receive environmental time cues (Mondal et al., 2022). In fish, the pineal gland receives external light signals and converts time cues into biological signals *via* melatonin, which regulates endogenous biological clock rhythms (Yasmin et al., 2021). In the present study, melatonin levels were significantly lower in the LL group than in the LD group. The inhibition of melatonin synthesis and secretion by light has been widely reported in fish (Masuda et al., 2003; Ziv et al., 2007). The feeding regime also affected serum melatonin levels. In the present study, serum melatonin levels were found to show R>D>L. Studies in recent years have found that many peripheral tissues are also critical sources of serum melatonin, such as the intestine (Mukherjee and Maitra, 2015). Moreover, melatonin production was found to be regulated by feeding independent of photoperiod in the intestine of rainbow trout (Lepage et al., 2005), carp (*Catla catla*) (Mukherjee et al., 2014a; Mukherjee et al., 2014b), and zebrafish (Mondal et al., 2022). Surprisingly, no circadian rhythm of serum melatonin levels was observed under LD in the present study, and it is speculated that serum melatonin comes from different tissues, including the pineal gland and intestine, regulated by light and food, respectively, so that these two zeitgebers may mask the rhythm of serum melatonin. In addition, no serum melatonin rhythms were also observed in the R-LL group, and similar results have been reported in Atlantic salmon (*Salmo salar*), where Huang et al. (2010) suggested that LL treatment may mask serum melatonin fluctuations.

Serotonin, also known as 5-hydroxytryptamine (5-HT), is an essential neurotransmitter and a precursor of melatonin distributed in the nervous system and many other peripheral tissues (Lillesaar, 2011). Many physiological functions and behaviors of animals are affected by 5-HT, including locomotion, sleep, appetite, and reproduction (Lucki, 1998). In zebrafish, 5-HT levels in the brainstem and spinal cord correlate with locomotion, and 5-HT increased swimming in early juvenile stages (Brustein et al., 2003). Similarly, the present study observed higher locomotion and serum 5-HT levels under LL. In vertebrates, tryptophan is synthesized into serotonin by tryptophan hydroxylase-1 (Tph1) and decarboxylation (Borjigin et al., 1999; Mondal et al., 2022). In zebrafish, *tph1* gene expression was guided by the feeding time, independent of photoperiod, with the highest expression at the point of feeding (Mondal et al., 2022). An increase in intestinal 5-HT levels after feeding was also found in Atlantic salmon (Mardones et al., 2022). 5-HT promotes intestinal peristalsis and secretion and thus regulates the digestive process (Kindt and Tack, 2007; Hasler, 2009). In the present study, serum 5-HT levels in the L group increased rapidly and peaked before feeding, suggesting that rainbow trout in the L group were able to prepare for the upcoming meal to improve digestibility. Similar rhythms were also found in the R-LD group, suggesting that the last meal can also synchronize the rhythm of serum 5-HT. Surprisingly, no rhythm of serum 5-HT was observed in the D group, implying that scheduled nocturnal feeding could not synchronize the serum 5-HT rhythm of rainbow trout.

Appetite rhythms

The circadian system plays an important role in the temporal regulation of metabolic processes and food intake to ensure energy efficiency (Page et al., 2020). Many areas of the brain are involved in the regulation of food intake, with the hypothalamus being the central area (Page et al., 2020). The arcuate nucleus (ARC) in the hypothalamus contains two distinct opposing populations of nuclei (Delgado et al., 2017; Page et al., 2020): neuropeptide Y (NPY) and agouti-related peptide (AgRP) (Broberger et al., 1998) neurones are orexigenic

with their activation increasing food intake, while the pro-opio melanocortin (POMC) (Joseph et al., 1985) and cocaine- and amphetamine-related transcript (CART) (Kristensen et al., 1998) neurones are considered anorexigenic with their activation reducing food intake. NPY/AgRP can be stimulated by ghrelin (ghrl) and inhibited by leptin (Hahn et al., 1998). In contrast, POMC/CART can be stimulated by leptin and inhibited by ghrl (Broberger, 2005). Therefore, we further analyzed the effects of light and food on appetite-related gene expression rhythms.

The rhythmic expression of *ghrl* and *leptin* genes was observed in the L group under both photoperiods. The *ghrl* gene expression peaked about 2 h later than *leptin*, and LD delayed the peak expression of both genes by about 2 h, suggesting that photoperiod affected the rhythm of appetite-related hormones. Further, in the L-LL group, the expression of both *pomc* and *cart* genes rose after feeding and reached a trough around the next feeding point, consistent with the observation of FAA. Similarly, previous studies have also observed an increase in rainbow trout *pomc* gene expression after feeding (Gong and Björnsson, 2014; Naderi et al., 2018). A significant increase in *cart* gene expression was also observed in Siberian sturgeon (*Acipenser baerii*) after 3 h of feeding (Zhang et al., 2018). In the present study, significant rhythms were observed in the expression of both *npy* and *agrp* genes in L-LL, and the trends were consistent with *pomc* and *cart* genes. Further, *npy* gene expression in the L-LL group peaked at ZT14 (10 h before feeding) and reached a trough at ZT2 (2 h after feeding). Similarly, a previous study on rainbow trout found that the *npy* gene peaked at ZT16 (8 h before feeding) and reached a trough at ZT4 (4 h after feeding) (Naderi et al., 2018). However, the *cart* gene expression rhythm showed an opposite trend under L-LD, peaking at the feeding point (ZT0). The same results were reported in rainbow trout under LD photoperiod (Naderi et al., 2018), and Mercer et al. (2003) also found that this gene expression was regulated by photoperiod.

Although no typical FAA was observed in the D group under both photoperiods in this study, some appetite-related genes showed significant rhythms. Under LL, *leptin* and *orexin* gene expression was observed to be rhythmic. The expression trend of the *leptin* gene was similar to that of the L group, which may indicate that *leptin* gene expression was synchronized by scheduled feeding when lacking a photoperiod. Interestingly, in the D group, the rhythms of *leptin* gene expression were reversed between the LD and LL photoperiods, reflecting the complex effect of shifting feeding on fish feeding rhythms, and further studies are needed to explain this phenomenon. Significant *cart*, *ghrl*, and *npy* gene expression rhythms were also observed under LD. The gene expression trend of the *ghrl* gene was similar to that of the L group, while the peak of *cart* and *npy* gene expression was before and after feeding, respectively. As mentioned above, CART suppresses appetite, and NPY enhances appetite in fish (Delgado et al., 2017), and the disruption of the peak expression of both genes may suggest that shifting feeding disrupts the normal feeding rhythm of rainbow trout.

In addition, rhythms in the expression of some appetite-related genes were also observed in the R group. All genes measured under LL exhibited significant rhythms, indicating that feeding rhythms in rainbow trout can be elicited by just one meal when lacking light zeitgeber. Similarly, last meal induced metabolic rhythms has been reported in other species (Escobar et al., 2007; Feliciano et al., 2011).

Orexin is also a feeding regulatory neuropeptide secreted by the hypothalamus (Matsuda et al., 2012) but is not involved in the integrative core described above (Delgado et al., 2017). Some studies in mice have speculated that orexin could be involved in regulating FAA (Page et al., 2020). However, different results have been reported in some studies, Kaur et al. (2008) and Clark et al. (2009) observed a decrease in FAA in orexin-deficient mice; in contrast, Gunapala et al. (2011) found no change in FAA in orexin knockout mice. In the present study, the rhythm of orexin gene expression was observed only in R-LL and D-LL groups. Therefore, the results of this study suggest that the expression of the *orexin* gene in rainbow trout does not seem to be directly associated with FAA.

Conclusion

In this study, growth and feed utilization of juvenile rainbow trout were enhanced by scheduled feeding (D and L groups) and were independent of photoperiod. Typically FAA was observed in the L group, where locomotion rose before the feeding point, accompanied by rhythmic synchronization of digestive enzyme activity, serum metabolites and hormones, and appetite-related gene expression. Although typical FAA behavior was not observed in the D group, an increase in digestive enzyme activity and serum GLU levels before feeding was detected, suggesting the presence of food anticipation. Notably, although FAA was not present in the R group, rhythms were observed in digestive enzyme activity, serum metabolite and hormone levels, and appetite-related gene expression. Overall, this study found that only mid-light stage feeding induced typical FAA in rainbow trout independent of photoperiod.

Data availability statement

The raw data supporting the conclusions of this article will be made available by the authors, without undue reservation.

Ethics statement

The animal study was reviewed and approved by Animal Care and Use Committee of Ningbo University.

Author contributions

Conceptualization, CS and HX; methodology, HX; formal analysis, HX; resources, CS; investigation, HX; writing—original draft preparation, HX; writing—review and editing, HX, CS, YY, CM and CW; supervision, CS and CW; project administration, CW; funding acquisition, CS All authors have read and agreed to the published version of the manuscript.

Funding

This study was supported by the National Key Research and Development Program of China (Project No. 2019YFD0901000), The Province Key Research and Development Program of Zhejiang (Project No. 2021C02047), and K.C. Wong Magna Fund from Ningbo University.

Acknowledgments

The authors also thank Professor Herve Migaud for his constructive comments on this research.

Conflict of interest

The authors declare that the research was conducted in the absence of any commercial or financial relationships that could be construed as a potential conflict of interest.

Publisher's note

Supplementary material

The Supplementary Material for this article can be found online at: https://www.frontiersin.org/articles/10.3389/fmars.2022.1029483/full#supplementary-material

References

Abdollahpour, H., Falahatkar, B., and Lawrence, C. (2020). The effect of photoperiod on growth and spawning performance of zebrafish, danio rerio. *Aquaculture. Rep.* 17, 100295. doi: 10.1016/j.aqrep.2020.100295

Almazán-Rueda, P., Schrama, J. W., and Verreth, J. A. J. (2004). Behavioural responses under different feeding methods and light regimes of the African catfish (*Clarias gariepinus*) juveniles. *Aquaculture* 231 (1-4), 347–359. doi: 10.1016/j.aquaculture.2003.11.016

Aride, P. H. R., Gomes, M. F. S., Azevedo, D. G., Sangali, G. R., Silva, A. C. F., Lavander, H. D., et al. (2021). Dusky grouper *Epinephelus marginatus* growth and survival when exposed to different photoperiods. *Fishes* 6 (3), 31. doi: 10.3390/fishes6030031

Arvedlund, M., McCormick, M. I., and Ainsworth, T. (2000). *Effects of photoperiod on growth of larvae and juveniles of the anemonefish amphiprion melanopus* Vol. 23 (Australia: Naga, the ICLARM Quarterly), 18–23. Available at: http://hdl.handle.net/1834/25680.

Azzaydi, M., Martinez, F. J., Zamora, S., Sánchez-Vázquez, F. J., and Madrid, J. A. (2000). The influence of nocturnal vs. diurnal feeding under winter conditions on growth and feed conversion of European sea bass (*Dicentrarchus labrax* l.). *Aquaculture* 182 (3-4), 329–338. doi: 10.1016/S0044-8486(99)00276-8

Bass, J. (2012). Circadian topology of metabolism. *Nature* 491 (7424), 348–356. doi: 10.1038/nature11704

Biswas, A. K., Seoka, M., Tanaka, Y., Takii, K., and Kumai, H. (2006). Effect of photoperiod manipulation on the growth performance and stress response of juvenile red sea bream (*Pagrus major*). *Aquaculture* 258 (1-4), 350–356. doi: 10.1016/j.aquaculture.2006.03.048

Blanco, A. M., Velasco, C., Bertucci, J. I., Soengas, J. L., and Unniappan, S. (2018). Nesfatin-1 regulates feeding, glucosensing and lipid metabolism in rainbow trout. *Front. Endocrinol.* 9. doi: 10.3389/fendo.2018.00484

Boeuf, G., and Le Bail, P. Y. (1999). Does light have an influence on fish growth? *Aquaculture* 177 (1-4), 129–152. doi: 10.1016/S0044-8486(99)00074-5

Bolliet, V., Aranda, A., and Boujard, T. (2001). Demand-feeding rhythm in rainbow trout and European catfish: Synchronisation by photoperiod and food availability. *Physiol. Behav.* 73 (4), 625–633. doi: 10.1016/S0031-9384(01)00505-4

Borjigin, J., Li, X. D., and Snyder, S. H. (1999). The pineal gland and melatonin: Molecular and pharmacologic regulation. *Annu. Rev. Pharmacol. Toxicol.* 39, 53–65. doi: 10.1146/annurev.pharmtox.39.1.53

Boujard, T., Gélineau, A., and Corraze, G. (1995). Time of a single daily meal influences growth performance in rainbow trout (*Oncorhynchus mykiss*). *Aquaculture. Res.* 26 (5), 341–349. doi: 10.1111/j.1365-2109.1995.tb00922.x

Broberger, C. (2005). Brain regulation of food intake and appetite: molecules and networks. *J. Internal Med.* 258 (4), 301–327. doi: 10.1111/j.1365-2796.2005.01553.x

Broberger, C., Johansen, J., Johansson, C., Schalling, M., and Hokfelt, T. (1998). The neuropeptide y agouti gene-related protein (AGRP) brain circuitry in normal, anorectic, and monosodium glutamate-treated mice. *Proc. Natl. Acad. Sci. United. States America* 95 (25), 15043–15048. doi: 10.1073/pnas.95.25.15043

Brustein, E., Chong, M., Holmqvist, B., and Drapeau, P. (2003). Serotonin patterns locomotor network activity in the developing zebrafish by modulating quiescent periods. *J. Neurobiol.* 57 (3), 303–322. doi: 10.1002/neu.10292

Caruso, M. A., and Sheridan, M. A. (2011). New insights into the signaling system and function of insulin in fish. *Gen. Comp. Endocrinol.* 173 (2), 227–247. doi: 10.1016/j.ygcen.2011.06.014

Casey, P., Butts, I. A. E., Zadmajid, V., Sorensen, S. R., and Litvak, M. K. (2020). Prolonged photoperiod improves the growth performance for a hatchery reared right-eyed flatfish. *Aquacultural. Eng.* 90, 102089. doi: 10.1016/j.aquaeng.2020.102089

Challet, E. (2019). The circadian regulation of food intake. *Nat. Rev. Endocrinol.* 15 (7), 393–405. doi: 10.1038/s41574-019-0210-x

Chu, Y. I., Wang, C. M., Parka, J. C., and Lader, P. F. (2020). Review of cage and containment tank designs for offshore fish farming. *Aquaculture* 519, 734928. doi: 10.1016/j.aquaculture.2020.734928

Clark, E. L., Baumann, C. R., Cano, G., Scammell, T. E., and Mochizuki, T. (2009). Feeding-elicited cataplexy in orexin knockout mice. *Neuroscience* 161 (4), 970–977. doi: 10.1016/j.neuroscience.2009.04.007

Coomans, C. P., Lucassen, E. A., Kooijman, S., Fifel, K., Deboer, T., Rensen, P. C. N., et al. (2015). Plasticity of circadian clocks and consequences for metabolism. *Diabetes Obes. Metab.* 17 (1), 65–75. doi: 10.1111/dom.12513

Davidson, A. J. (2006). Search for the feeding-entrainable circadian oscillator: a complex proposition. *Am. J. Physiol.-Regul. Integr. Comp. Physiol.* 290 (6), R1524–R1526. doi: 10.1152/ajpregu.00073.2006

Delgado, M. J., Cerdá-Reverter, J. M., and Soengas, J. L. (2017). Hypothalamic integration of metabolic, endocrine, and circadian signals in fish: involvement in the control of food intake. *Front. Neurosci.* 11. doi: 10.3389/fnins.2017.00354

Dong, S. L. (2019). Researching progresses and prospects in large salmonidae farming in cold water mass of yellow Sea. *Periodical. Ocean. Univ. China* 49 (03), 1–6. doi: 10.16441/j.cnki.hdxb.20180303

Doyle, A., Cowan, M. E., Migaud, H., Wright, P. J., and Davie, A. (2021). Neuroendocrine regulation of reproduction in Atlantic cod (*Gadus morhua*): Evidence of *Eya3* as an integrator of photoperiodic cues and nutritional regulation to initiate sexual maturation. *Comp. Biochem. Physiol. A-Molecular. Integr. Physiol.* 260, 111000. doi: 10.1016/j.cbpa.2021.111000

Escobar, C., Martinez-Merlos, M. T., Angeles-Castellanos, M., Minana, M. D., and Buijs, R. M. (2007). Unpredictable feeding schedules unmask a system for daily resetting of behavioural and metabolic food entrainment. *Eur. J. Neurosci.* 26 (10), 2804–2814. doi: 10.1111/j.1460-9568.2007.05893.x

Esteban, M.Á., Cuesta, A., Rodríguez, A., and Meseguer, J. (2006). Effect of photoperiod on the fish innate immune system: a link between fish pineal gland and the immune system. *J. Pineal. Res.* 41, 261–266. doi: 10.1111/j.1600-079X.2006.00362.x

FAO (2020). FAO yearbook. *Fishery and Aquaculture Statistics 2018* (Rome) Food and Agriculture Organization of the United Nations. doi: 10.4060/cb1213t

Feliciano, A., Vivas, Y., de Pedro, N., Delgado, M. J., Velarde, E., and Isorna, E. (2011). Feeding time synchronizes clock gene rhythmic expression in brain and liver of goldfish (*Carassius auratus*). *J. Biol. Rhythms.* 26 (1), 24–33. doi: 10.1177/0748730410388600

Fortes-Silva, R., Do Valle, S. V., and Lopez-Olmeda, J. F. (2018). Daily rhythms of swimming activity, synchronization to different feeding times and effects on anesthesia practice in an Amazon fish species (*Colossoma macropomum*). *Chronobiology. Int.* 35 (12), 1713–1722. doi: 10.1080/07420528.2018.1509078

Fortes-Silva, R., Oliveira, I. E., Vieira, V. P., Winkaler, E. U., Guerra-Santos, B., and Cerqueira, R. B. (2016). Daily rhythms of locomotor activity and the influence of a light and dark cycle on gut microbiota species in tambaqui (*Colossoma macropomum*). *Biol. Rhythm. Res.* 47 (2), 183–190. doi: 10.1080/09291016.2015.1094972

Foss, A., Siikavuopio, S. I., and Imsland, A. K. D. (2020). Effects of altered photoperiod regimes during winter on growth and gonadosomatic index in Arctic charr (*Salvelinus alpinus*) reared in freshwater. *Aquaculture Res.* 51 (4), 1365–1371. doi: 10.1111/are.14481

Ghomi, M. R., Zarei, M., and Sohrabnejad, M. (2011). Effect of photoperiod on growth and feed conversion of juvenile wild carp, *Cyprinus carpio*. *Acta Biologica. Hungarica.* 62 (2), 215–218. doi: 10.1556/ABiol.62.2011.2.12

Giannetto, A., Fernandes, J. M. O., Nagasawa, K., Mauceri, A., Maisano, M., De Domenico, E., et al. (2014). Influence of continuous light treatment on expression of stress biomarkers in Atlantic cod. *Dev. Comp. Immunol.* 44 (1), 30–34. doi: 10.1016/j.dci.2013.11.011

Gong, N. P., and Björnsson, B. T. (2014). Leptin signaling in the rainbow trout central nervous system is modulated by a truncated leptin receptor isoform. *Endocrinology* 155 (7), 2445–2455. doi: 10.1210/en.2013-2131

Gunapala, K. M., Gallardo, C. M., Hsu, C. T., and Steele, A. D. (2011). Single gene deletions of orexin, leptin, neuropeptide y, and ghrelin do not appreciably alter food anticipatory activity in mice. *PloS One* 6 (3), e18377. doi: 10.1371/journal.pone.0018377

Hahn, T. M., Breininger, J. F., Baskin, D. G., and Schwartz, M. W. (1998). Coexpression of agrp and NPY in fasting-activated hypothalamic neurons. *Nat. Neurosci.* 1 (4), 271–272. doi: 10.1038/1082

Haman, F., Powell, M., and Weber, J. M. (1997). Reliability of continuous tracer infusion for measuring glucose turnover rate in rainbow trout. *J. Exp. Biol.* 200 (19), 2557–2563. doi: 10.1242/jeb.200.19.2557

Hamilton, T. J., Szaszkiewicz, J., Krook, J., Richards, J. G., Stiller, K., and Brauner, C. J. (2022). Continuous light (relative to a 12:12 photoperiod) has no effect on anxiety-like behaviour, boldness, and locomotion in coho salmon (*Oncorhynchus kisutch*) post-smolts in recirculating aquaculture systems at a salinity of either 2.5 or 10 ppt. *Comp. Biochem. Physiol. A-Molecular. Integr. Physiol.* 263, 111070. doi: 10.1016/j.cbpa.2021.111070

Hasler, W. L. (2009). Serotonin and the GI tract. *Curr. Gastroenterol. Rep.* 11, 383–391. doi: 10.1007/s11894-009-0058-7

Hermelink, B., Kleiner, W., Schulz, C., Kloas, W., and Wuertz, S. (2017). Photothermal manipulation for the reproductive management of pikeperch *Sander lucioperca*. *Aquaculture. Int.* 25, 1–20. doi: 10.1007/s10499-016-0009-x

Hernández-Pérez, J., Míguez, J. M., Librán-Pérez, M., Otero-Rodiño, C., Naderi, F., Soengas, J. L., et al. (2015). Daily rhythms in activity and mRNA abundance of enzymes involved in glucose and lipid metabolism in liver of rainbow trout, *Oncorhynchus mykiss*. influence of light and food availability. *Chronobiology. Int.* 32 (10), 1391–1408. doi: 10.3109/07420528.2015.1100633

Hernández-Pérez, J., Míguez, J. M., Naderi, F., Soengas, J. L., and López-Patiño, M. A. (2017). Influence of light and food on the circadian clock in liver of rainbow trout, *Oncorhynchus mykiss*. *Chronobiology. Int.* 34 (9), 1259–1272. doi: 10.1080/07420528.2017.1361435

Hernández-Sánchez, C., Mansilla, A., de la Rosa, E. J., and de Pablo, F. (2006). Proinsulin in development: new roles for an ancient prohormone. *Diabetologia* 49 (6), 1142–1150. doi: 10.1007/s00125-006-0232-5

Herrero, M. J., Pascual, M., Madrid, J. A., and Sánchez-Vázquez, F. J. (2005). Demand-feeding rhythms and feeding-entrainment of locomotor activity rhythms in tench (*Tinca tinca*). *Physiol. Behav.* 84 (4), 595–605. doi: 10.1016/j.physbeh.2005.02.015

Heyde, I., and Oster, H. (2019). Differentiating external zeitgeber impact on peripheral circadian clock resetting. *Sci. Rep.* 9, 20114. doi: 10.1038/s41598-019-56323-z

Hillyer, K. E., Beale, D. J., and Shima, J. S. (2021). Artificial light at night interacts with predatory threat to alter reef fish metabolite profiles. *Sci. Total. Environ.* 769, 144482. doi: 10.1016/j.scitotenv.2020.144482

Hoskins, L. J., and Volkoff, H. (2012). Daily patterns of mRNA expression of two core circadian regulatory proteins, Clock2 and Per1, and two appetite-regulating peptides, OX and NPY, in goldfish (*Carassius auratus*). *Comp. Biochem. Physiol. A-Molecular. Integr. Physiol.* 163 (1), 127–136. doi: 10.1016/j.cbpa.2012.05.197

Hossain, M. A. R., Haylor, G. S., and Beveridge, M. C. M. (2001). Effect of feeding time and frequency on the growth and feed utilization of African catfish *Clarias gariepinus* (Burchell 1822) fingerlings. *Aquaculture. Res.* 32, 999–1004. doi: 10.1046/j.1365-2109.2001.00635.x

Huang, T. S., Ruoff, P., and Fjelldal, P. G. (2010). Effect of continuous light on daily levels of plasma melatonin and cortisol and expression of clock genes in pineal gland, brain, and liver in Atlantic salmon postsmolts. *Chronobiology. Int.* 27 (9-10), 1715–1734. doi: 10.3109/07420528.2010.521272

Huang, M., Yang, X. G., Zhou, Y. G., Ge, J., Davis, D. A., Dong, Y. W., et al. (2021). Growth, serum biochemical parameters, salinity tolerance and antioxidant enzyme activity of rainbow trout (*Oncorhynchus mykiss*) in response to dietary taurine levels. *Mar. Life Sci. Technol.* 3 (4), 449–462. doi: 10.1007/s42995-020-00088-2

Iigo, M., and Tabata, M. (1997). Circadian rhythms of locomotor activity in the rainbow trout *Oncorhynchus mykiss*. *Fisheries. Sci.* 63 (1), 77–80. doi: 10.2331/fishsci.63.77

Imsland, A. K. D., Gunnarsson, S., and Thorarensen, H. (2020). Impact of environmental factors on the growth and maturation of farmed Arctic charr. *Rev. Aquaculture.* 12 (3), 1689–1707. doi: 10.1111/raq.12404

Imsland, A. K. D., Roth, B., Doskeland, I., Fjelldal, P. G., Stefansson, S. O., Handeland, S., et al. (2019). Flesh quality of Atlantic salmon smolts reared at different temperatures and photoperiods. *Aquaculture. Res.* 50 (7), 1795–1801. doi: 10.1111/are.14058

Joseph, S. A., Pilcher, W. H., and Knigge, K. M. (1985). Anatomy of the corticotropin-releasing factor and opiomelanocortin systems of the brain. *Fed. Proc.* 44, 100–107.

Kaur, S., Thankachan, S., Begum, S., Blanco-Centurion, C., Sakurai, T., Yanagisawa, M., et al. (2008). Entrainment of temperature and activity rhythms to restricted feeding in orexin knock out mice. *Brain Res.* 1205, 47–54. doi: 10.1016/j.brainres.2008.02.026

Kindt, S., and Tack, J. (2007). Mechanisms of serotonergic agents for treatment of gastrointestinal motility and functional bowel disorders. *Neurogastroenterol. Motil.* 19 (2), 32–39. doi: 10.1111/j.1365-2982.2007.00966.x

Kitagawa, A. T., Costa, L. S., Paulino, R. R., Luz, R. K., Rosa, P. V., Guerra-Santos, B., et al. (2015). Feeding behavior and the effect of photoperiod on the performance and hematological parameters of the pacamã catfish (*Lophiosilurus alexandri*). *Appl. Anim. Behav. Sci.* 171, 211–218. doi: 10.1016/j.applanim.2015.08.025

Kopp, R., Billecke, N., Legradi, J., den Broeder, M., Parekh, S. H., and Legler, J. (2016). Bringing obesity to light: Rev-erb alpha, a central player in light-induced adipogenesis in the zebrafish? *Int. J. Obes.* 40 (5), 824–832. doi: 10.1038/ijo.2015.240

Kousoulaki, K., Saether, B. S., Albrektsen, S., and Noble, C. (2015). Review on European sea bass (*Dicentrarchus labrax*, Linnaeus 1758) nutrition and feed management: a practical guide for optimizing feed formulation and farming protocols. *Aquaculture. Nutr.* 21, 129–151. doi: 10.1111/anu.12233

Kristensen, P., Judge, M. E., Thim, L., Ribel, U., Christjansen, K. N., Wulff, B. S., et al. (1998). Hypothalamic CART is a new anorectic peptide regulated by leptin. *Nature* 393 (6680), 72–76. doi: 10.1038/29993

Landless, P. J. (1976). Acclimation of rainbow trout to sea water. *Aquaculture* 7 (2), 173–179. doi: 10.1016/0044-8486(76)90006-5

Lazado, C. C., Pedersen, P. B., Nguyen, H. Q., and Lund, I. (2017). Rhythmicity and plasticity of digestive physiology in a euryhaline teleost fish, permit (*Trachinotus falcatus*). *Comp. Biochem. Physiol. A-Molecular. Integr. Physiol.* 212, 107–116. doi: 10.1016/j.cbpa.2017.07.016

Leonardi, M. O., and Klempau, A. E. (2003). Artificial photoperiod influence on the immune system of juvenile rainbow trout (*Oncorhynchus mykiss*) in the southern hemisphere. *Aquaculture* 221, 581–591. doi: 10.1016/S0044-8486(03)00032-2

Lepage, O., Larson, E. T., Mayer, I., and Winberg, S. (2005). Tryptophan affects both gastrointestinal melatonin production and interrenal activity in stressed and nonstressed rainbow trout. *J. Pineal. Res.* 38 (4), 264–271. doi: 10.1111/j.1600-079X.2004.00201.x

Lillesaar, C. (2011). The serotonergic system in fish. *J. Chem. Neuroanat.* 41 (4), 294–308. doi: 10.1016/j.jchemneu.2011.05.009

Liu, Y., Li, X., Xu, G. F., Bai, S. Y., Zhang, Y. Q., Gu, W., et al. (2015). Effect of photoperiod manipulation on the growth performance of juvenile lenok, *Brachymystax lenok* (Pallas 1773). *J. Appl. Ichthyology.* 31 (1), 120–124. doi: 10.1111/jai.12632

Livak, K. J., and Schmittgen, T. D. (2001). Analysis of relative gene expression data using real-time quantitative PCR and the $2^{-\Delta\Delta CT}$ method. *Methods* 25 (4), 402–408. doi: 10.1006/meth.2001.1262

Li, X., Wei, P. P., Liu, S. T., Tian, Y., Ma, H., and Liu, Y. (2021). Photoperiods affect growth, food intake and physiological metabolism of juvenile European Sea bass (*Dicentrachus labrax* l.). *Aquaculture. Rep.* 20, 100656. doi: 10.1016/j.aqrep.2021.100656

Li, Y., Zhu, Q. F., Huang, Y., Xu, Q., Dai, X. L., and Ju, C. X. (2022). Cloning and characterization of two types of growth hormone receptors in tomato clownfish (*Amphiprion frenatus*), and their expression under different light spectra and photoperiods. *Aquaculture. Int.* 30 (1), 483–500. doi: 10.1007/s10499-021-00814-2

López-Olmeda, J. F. (2017). Nonphotic entrainment in fish. *Comp. Biochem. Physiol.* 203, 133–143. doi: 10.1016/j.cbpa.2016.09.006

López-Olmeda, J. F., and Sánchez-Vázquez, F. J. (2010). "Feeding rhythms in fish: From behavioural to molecular approach," in *Biological clock in fish*. Eds. E. Kulczykowska, W. Popek and B. G. Kapoor (Enfield, USA: Science Publishers), 155–184.

Lorgen-Ritchie, M., Clarkson, M., Chalmers, L., Taylor, J. F., Migaud, H., and Martin, S. A. M. (2022). Temporal changes in skin and gill microbiomes of Atlantic salmon in a recirculating aquaculture system - why do they matter? *Aquaculture* 558, 738352. doi: 10.1016/j.aquaculture.2022.738352

Lucki, I. (1998). The spectrum of behaviors influenced by serotonin. *Biol. Psychiatry* 44 (3), 151–162. doi: 10.1016/S0006-3223(98)00139-5

Lundova, K., Matousek, J., Prokesova, M., Sebesta, R., Policar, T., and Stejskal, V. (2019). The effect of timing of extended photoperiod on growth and maturity of brook trout (*Salvelinus fontinalis*). *Aquaculture. Res.* 50, 1697–1704. doi: 10.1111/are.14053

Malinovskyi, O., Rahimnejad, S., Stejskal, V., Bonko, D., Stara, A., Velisek, J., et al. (2022). Effects of different photoperiods on growth performance and health status of largemouth bass (*Micropterus salmoides*) juveniles. *Aquaculture* 548, 737631. doi: 10.1016/j.aquaculture.2021.737631

Mardones, O., Oyarzún-Salazar, R., Labbé, B. S., Miguez, J. M., Vargas-Chacoff, L., and Muñoz, J. L. P. (2022). Intestinal variation of serotonin, melatonin, and digestive enzymes activities along food passage time through GIT in *Salmo salar* fed with supplemented diets with tryptophan and melatonin. *Comp. Biochem. Physiol. A-Molecular. Integr. Physiol.* 266, 111159. doi: 10.1016/j.cbpa.2022.111159

Marinho, G., Peres, H., and Carvalho, A. P. (2014). Effect of feeding time on dietary protein utilization and growth of juvenile Senegalese sole (*Solea senegalensis*). *Aquaculture. Res.* 45, 828–833. doi: 10.1111/are.12024

Martínez-Chávez, C. C., Navarrete-Ramírez, P., Parke, D. V., and Migaud, H. (2021). Effects of continuous light and light intensity on the growth performance and gonadal development of Nile tilapia. *Rev. Bras. Zootecnia-Brazilian. J. Anim. Sci.* 50, e20180275. doi: 10.37496/rbz5020180275

Masuda, T., Iigo, M., Mizusawa, K., Naruse, M., Oishi, T., Aida, K., et al. (2003). Variations in plasma melatonin levels of the rainbow trout (*Oncorhynchus mykiss*) under various light and temperature conditions. *Zoological. Sci.* 20 (8), 1011–1016. doi: 10.2108/zsj.20.1011

Matsuda, K., Azuma, M., and Kang, K. S. (2012). Orexin system in teleost fish. *Vitamins. Hormones.* 89, 341–361. doi: 10.1016/B978-0-12-394623-2.00018-4

Mercer, J. G., Ellis, C., Moar, K. M., Logie, T. J., Morgan, P. J., and Adam, C. L. (2003). Early regulation of hypothalamic arcuate nucleus CART gene expression by short photoperiod in the Siberian hamster. *Regul. Peptides.* 111 (1-3), 129–136. doi: 10.1016/S0167-0115(02)00263-X

Mistlberger, R. E. (1994). Circadian food-anticipatory activity: Formal models and physiological mechanisms. *Neurosci. Biobehav. Rev.* 18 (2), 171–195. doi: 10.1016/0149-7634(94)90023-X

Mommsen, T. P., Vijayan, M. M., and Moon, T. W. (1999). Cortisol in teleosts: dynamics, mechanisms of action, and metabolic regulation. *Rev. Fish. Biol. Fisheries.* 9 (3), 211–268. doi: 10.1023/A:1008924418720

Mondal, G., Devi, S. D., Khan, Z. A., Yumnamcha, T., Rajiv, C., Devi, H. S., et al. (2022). The influence of feeding on the daily rhythm of mRNA expression on melatonin bio-synthesizing enzyme genes and clock associated genes in the zebrafish (*Danio rerio*) gut. *Biol. Rhythm. Res.* 53 (7), 1073–1090. doi: 10.1080/09291016.2021.1905989

Montoya, A., López-Olmeda, J. F., Yúfera, M., Sánchez-Muros, M. J., and Sánchez-Vázquez, F. J. (2010). Feeding time synchronises daily rhythms of behaviour and digestive physiology in gilthead seabream (*Sparus aurata*). *Aquaculture* 306, 315–321. doi: 10.1016/j.aquaculture.2010.06.023

Mukherjee, S., and Maitra, S. K. (2015). Gut melatonin in vertebrates: chronobiology and physiology. *Front. Endocrinol.* 6. doi: 10.3389/fendo.2015.00112

Mukherjee, S., Moniruzzaman, M., and Maitra, S. K. (2014a). Impact of artificial lighting conditions on the diurnal profiles of gut melatonin in a surface dwelling carp (*Catla catla*). *Biol. Rhythm. Res.* 45 (6), 831–848. doi: 10.1080/09291016.2014.923618

Mukherjee, S., Moniruzzaman, M., and Maitra, S. K. (2014b). Daily and seasonal profiles of gut melatonin and their temporal relationship with pineal and serum melatonin in carp *Catla catla* under natural photo-thermal conditions. *Biol. Rhythm. Res.* 45 (2), 301–315. doi: 10.1080/09291016.2013.817139

Naderi, F., Hernández-Pérez, J., Chivite, M., Soengas, J. L., Míguez, J. M., and López-Patiño, M. A. (2018). Involvement of cortisol and sirtuin1 during the response to stress of hypothalamic circadian system and food intake-related peptides in rainbow trout, *Oncorhynchus mykiss*. *Chronobiology. Int.* 35 (8), 1122–1141. doi: 10.1080/07420528.2018.1461110

Navarro, I., Carneiro, M. N., Párrizas, M., Maestro, J. L., Planas, J., and Gutiérrez, J. (1993). Post-feeding levels of insulin and glucagon in trout (*Salmo trutta fario*). *Comp. Biochem. Physiol. Part A.: Physiol.* 104 (2), 389–393. doi: 10.1016/0300-9629(93)90335-2

Nemova, N. N., Nefedova, Z. A., Pekkoeva, S. N., Voronin, V. P., Shulgina, N. S., Churova, M. V., et al. (2020). The effect of the photoperiod on the fatty acid profile and weight in hatchery-reared underyearlings and yearlings of Atlantic salmon *Salmo salar* l. *Biomolecules* 10 (6), 845. doi: 10.3390/biom10060845

Nisembaum, L. G., de Pedro, N., Delgado, M. J., and Isorna, E. (2014a). Crosstalking between the "gut-brain" hormone ghrelin and the circadian system in the goldfish. effects on clock gene expression and food anticipatory activity. *Gen. Comp. Endocrinol.* 205, 287–295. doi: 10.1016/j.ygcen.2014.03.016

Nisembaum, L. G., de Pedro, N., Delgado, M. J., Sanchez-Bretano, A., and Isorna, E. (2014b). Orexin as an input of circadian system in goldfish: Effects on clock gene expression and locomotor activity rhythms. *Peptides* 52, 29–37. doi: 10.1016/j.peptides.2013.11.014

Nisembaum, L. G., Velarde, E., Tinoco, A. B., Azpeleta, C., de Pedro, N., Alonso-Gomez, A. L., et al. (2012). Light-dark cycle and feeding time differentially entrains the gut molecular clock of the goldfish (*Carassius auratus*). *Chronobiology. Int.* 29 (6), 665–673. doi: 10.3109/07420528.2012.686947

Noeske-Hallin, T. A., Spieler, R. E., Parker, N. C., and Suttle, M. A. (1985). Feeding time differentially affects fattening and growth of channel catfish. *J. Nutr.* 115 (9), 1228–1232. doi: 10.1093/jn/115.9.1228

Oishi, K., and Hashimoto, C. (2018). Short-term time-restricted feeding during the resting phase is sufficient to induce leptin resistance that contributes to development of obesity and metabolic disorders in mice. *Chronobiology. Int.* 35 (11), 1576–1594. doi: 10.1080/07420528.2018.1496927

Opperhuizen, A. L., Wang, D. W., Foppen, E., Jansen, R., Boudzovitch-Surovtseva, O., de Vries, J., et al. (2016). Feeding during the resting phase causes profound changes in physiology and desynchronization between liver and muscle rhythms of rats. *Eur. J. Neurosci.* 44 (10), 2795–2806. doi: 10.1111/ejn.13377

Öz, M. (2018). Effects of garlic (*Allium sativum*) supplemented fish diet on sensory, chemical and microbiological properties of rainbow trout during storage at -18 °C. *LWT. - Food Sci. Technol.* 92, 155–160. doi: 10.1016/j.lwt.2018.02.030

Page, A. J., Christie, S., Symonds, E., and Li, H. (2020). Circadian regulation of appetite and time restricted feeding. *Physiol. Behav.* 220, 112873. doi: 10.1016/j.physbeh.2020.112873

Paredes, J. F., López-Olmeda, J. F., Martínez, F. J., and Sánchez-Vázquez, F. J. (2015). Daily rhythms of lipid metabolic gene expression in zebra fish liver: response to light/dark and feeding cycles. *Chronobiology. Int.* 32 (10), 1438–1448. doi: 10.3109/07420528.2015.1104327

Paredes, J. F., Vera, L. M., Martinez-Lopez, F. J., Navarro, I., and Vázquez, F. J. S. (2014). Circadian rhythms of gene expression of lipid metabolism in gilthead sea bream liver: synchronisation to light and feeding time. *Chronobiology. Int.* 31 (5), 613–626. doi: 10.3109/07420528.2014.881837

Parsons, R., Parsons, R., Garner, N., Oster, H., and Rawashdeh, O. (2020). CircaCompare: a method to estimate and statistically support differences in mesor,

amplitude and phase, between circadian rhythms. *Bioinformatics* 36 (4), 1208–1212. doi: 10.1093/bioinformatics/btz730

Patton, D. F., and Mistlberger, R. E. (2013). Circadian adaptations to meal timing: neuroendocrine mechanisms. *Front. Neurosci.* 7. doi: 10.3389/fnins.2013.00185

Pfalzgraff, T., Lund, I., and Skov, P. V. (2021). Cortisol affects feed utilization, digestion and performance in juvenile rainbow trout (*Oncorhynchus mykiss*). *Aquaculture* 536, 736472. doi: 10.1016/j.aquaculture.2021.736472

Ramzanzadeh, F., Yeganeh, S., JaniKhalili, K., and Babaei, S. S. (2016). Effects of different photoperiods on digestive enzyme activities in rainbow trout (*Oncorhynchus mykiss*) alevin and fry. *Can. J. Zoology.* 94 (6), 435–442. doi: 10.1139/cjz-2015-0180

Ruchin, A. B. (2021). Effect of illumination on fish and amphibian: development, growth, physiological and biochemical processes. *Rev. Aquaculture.* 13 (1), 567–600. doi: 10.1111/raq.12487

Saiz, N., Gomez-Boronat, M., De Pedro, N., Delgado, M. J., and Isorna, E. (2021). The lack of light-dark and feeding-fasting cycles alters temporal events in the goldfish (*Carassius auratus*) stress axis. *Animals* 11 (3), 669. doi: 10.3390/ani11030669

Salgado, M. C., Metón, I., Egea, M., and Baanante, I. V. (2004). Transcriptional regulation of glucose-6-phosphatase catalytic subunit promoter by insulin and glucose in the carnivorous fish, *Sparus aurata*. *J. Mol. Endocrinol.* 33 (3), 783–795. doi: 10.1677/jme.1.01552

Sánchez, J. A., López-Olmeda, J. F., Blanco-Vives, B., and Sánchez-Vázquez, F. J. (2009). Effects of feeding schedule on locomotor activity rhythms and stress response in sea bream. *Physiol. Behav.* 98 (1-2), 125–129. doi: 10.1016/j.physbeh.2009.04.020

Sánchez-Vázquez, F. J., Azzaydi, M., Martinez, F. J., Zamora, S., and Madrid, J. A. (1998). Annual rhythms of demand-feeding activity in seabass: evidence of a seasonal phase inversion of the diel feeding pattern. *Chronobiology. Int.* 15, 607–622. doi: 10.3109/07420529808993197

Sánchez-Vázquez, F. J., and Tabata, M. (1998). Circadian rhythms of demand-feeding and locomotor activity in rainbow trout. *J. Fish. Biol.* 52 (2), 255–267. doi: 10.1111/j.1095-8649.1998.tb00797.x

Shahkar, E., Kim, D., Mohseni, M., and Khara, H. (2015). Effects of photoperiod manipulation on growth performance and hematological responses of juvenile Caspian roach *Rutilus rutilus caspicus*. *Fisheries. Aquat. Sci.* 18 (1), 51–56. doi: 10.5657/FAS.2015.0051

Shan, X. J., Xiao, Z. Z., Huang, W., and Dou, S. Z. (2008). Effects of photoperiod on growth, mortality and digestive enzymes in miiuy croaker larvae and juveniles. *Aquaculture* 281 (1-4), 70–76. doi: 10.1016/j.aquaculture.2008.05.034

Shepherd, B. S., Drennon, K., Johnson, J., Nichols, J. W., Playle, R. C., Singer, T. D., et al. (2005). Salinity acclimation affects the somatotropic axis in rainbow trout. *Am. J. Physiology-Regulatory. Integr. Comp. Physiol.* 288, R1385–R1395. doi: 10.1152/ajpregu.00443.2004

Singh, A., and Zutshi, B. (2020). Photoperiodic effects on somatic growth and gonadal maturation in mickey mouse platy, *Xiphophorus maculatus* (Gunther 1866). *Fish. Physiol. Biochem.* 46 (4), 1483–1495. doi: 10.1007/s10695-020-00806-8

Stephan, F. K. (2002). The "other" circadian system: food as zeitgeber. *J. Biol. Rhythms.* 17 (4), 284–292. doi: 10.1177/074873002129002591

Turker, A. (2005). Effects of photoperiod on growth and feed utilization of juvenile black Sea turbot (*Psetta maeotica*). *Israeli. J. Aquaculture-Bamidgeh.* 57 (3), 156–163. doi: 10.46989/001c.20413

Valenzuela, A., Rodriguez, I., Schulz, B., Cortes, R., Acosta, J., Campos, V., et al. (2022). Effects of continuous light (LD24:0) modulate the expression of lysozyme, mucin and peripheral blood cells in rainbow trout. *Fishes* 7 (1), 28. doi: 10.3390/fishes7010028

Vera, L. M., De Pedro, N., Gomez-Milán, E., Delgado, M. J., Sánchez-Muros, M. J., Madrid, J. A., et al. (2007). Feeding entrainment of locomotor activity rhythms, digestive enzymes and neuroendocrine factors in goldfish. *Physiol. Behav.* 90 (2-3), 518–524. doi: 10.1016/j.physbeh.2006.10.017

Vera, L. M., Negrini, P., Zagatti, C., Frigato, E., Sanchez-Vazquez, F. J., and Bertolucci, C. (2013). Light and feeding entrainment of the molecular circadian clock in a marine teleost (*Sparus aurata*). *Chronobiology. Int.* 30 (5), 649–661. doi: 10.3109/07420528.2013.775143

Veras, G. C., Paixão, D. J. D. R., Brabo, M. F., Soares, L. M. O., and Sales, A. D. (2016). Influence of photoperiod on growth, uniformity, and survival of larvae of the Amazonian ornamental *Heros severus* (Heckel 1840). *Rev. Bras. Zootecnia-Brazilian. J. Anim. Sci.* 45 (7), 422–426. doi: 10.1590/S1806-92902016000700010

Villamizar, N., Blanco-Vives, B., Migaud, H., Davie, A., Carboni, S., and Sánchez-Vázquez, F. J. (2011). Effects of light during early larval development of some aquacultured teleosts: A review. *Aquaculture* 315 (1-2), 86–94. doi: 10.1016/j.aquaculture.2010.10.036

Wagner, T., and Congleton, J. L. (2004). Blood chemistry correlates of nutritional condition, tissue damage, and stress in migrating juvenile chinook salmon (*Oncorhynchus tshawytscha*). *Can. J. Fisheries. Aquat. Sci.* 61 (7), 1066–1074. doi: 10.1139/F04-050

Wei, H., Cai, W. J., Liu, H. K., Han, D., Zhu, X. M., Yang, Y. X., et al. (2019). Effects of photoperiod on growth, lipid metabolism and oxidative stress of juvenile gibel carp (*Carassius auratus*). *J. Photochem. Photobiol. B-Biology.* 198, 111552. doi: 10.1016/j.jphotobiol.2019.111552

Yada, T., Azuma, T., and Takagi, Y. (2001). Stimulation of non-specific immune functions in seawater-acclimated rainbow trout, *Oncorhynchus mykiss*, with reference to the role of growth hormone. *Comp. Biochem. Physiol. Part B.: Biochem. Mol. Biol.* 129, 695–701. doi: 10.1016/S1096-4959(01)00370-0

Yasmin, F., Sutradhar, S., Das, P., and Mukherjee, S. (2021). Gut melatonin: A potent candidate in the diversified journey of melatonin research. *Gen. Comp. Endocrinol.* 303, 113693. doi: 10.1016/j.ygcen.2020.113693

Ytrestøyl, T., Hjelle, E., Kolarevic, J., Takle, H., Rebl, A., Afanasyev, S., et al. (2022). Photoperiod in recirculation aquaculture systems and timing of seawater transfer affect seawater growth performance of Atlantic salmon (*Salmo salar*). *J. World Aquaculture. Soc.* doi: 10.1111/jwas.12880

Zhang, X., Gao, Y. D., Tang, N., Qi, J. W., Wu, Y. B., Hao, J., et al. (2018). One evidence of cocaine- and amphetamine-regulated transcript (CART) has the bidirectional effects on appetite in Siberian sturgeon (*Acipenser baerii*). *Fish. Physiol. Biochem.* 44 (1), 411–422. doi: 10.1007/s10695-017-0444-2

Ziv, L., Tovin, A., Strasser, D., and Gothilf, Y. (2007). Spectral sensitivity of melatonin suppression in the zebrafish pineal Gland. *Exp. Eye. Res.* 84 (1), 92–99. doi: 10.1016/j.exer.2006.09.004

frontiers | Frontiers in Marine Science

TYPE Original Research
PUBLISHED 24 October 2022
DOI 10.3389/fmars.2022.1008068

OPEN ACCESS

EDITED BY
Ce Shi,
Ningbo University, China

REVIEWED BY
Guancang Dong,
Shandong Freshwater Fisheries Research Institute, China
Biao Guo,
Tianjin Bohai Fisheries Research Institute, China

*CORRESPONDENCE
He Ma
mahe@dlou.edu.cn

SPECIALTY SECTION
This article was submitted to Marine Fisheries, Aquaculture and Living Resources, a section of the journal Frontiers in Marine Science

RECEIVED 31 July 2022
ACCEPTED 11 October 2022
PUBLISHED 24 October 2022

CITATION
Liu S, Fang Y, Liu Y, Li X, Sun F, Wu Y, Ma Z and Ma H (2022) Effects of different LED spectra on growth and expression of GH/IGF-I axis and apoptosis related genes in juvenile *Takifugu rubripes*. *Front. Mar. Sci.* 9:1008068. doi: 10.3389/fmars.2022.1008068

Effects of different LED spectra on growth and expression of GH/IGF-I axis and apoptosis related genes in juvenile *Takifugu rubripes*

Songtao Liu[1,2], Yingying Fang[1,2], Ying Liu[1,3], Xin Li[1,2], Fei Sun[1,2], Yanling Wu[1,2], Zhen Ma[1,2] and He Ma[1,2]*

[1]Key Laboratory of Environment Controlled Aquaculture (Dalian Ocean University) Ministry of Education, Dalian, China, [2]College of Marine Technology and Environment, Dalian Ocean University, Dalian, China, [3]College of Biosystems Engineering and Food Science, Zhejiang University, Hangzhou, China

Light has long been known to have a profound influence on the growth and development of fish. The previous studies showed that different spectra had different effects on the growth of juvenile *Takifugu rubripes*. Among them, green light can promote the growth of *Takifugu rubripes*, but the influence mechanism is unknown. In this study, how different LED spectrums affect fish growth from the perspective of GH/IGF-I axis-related genes and apoptosis genes were deeply explored. In the experiment, juvenile *Takifugu rubripes* with an initial body length of (9.01 ± 0.70) cm and an initial body weight of (18.05 ± 3.17) g were selected as the research objects. 525 *Takifugu rubripes* juveniles were selected, cultured and monitored in five different LED spectrum treatment groups: white light (WL, λ 400-780nm), red light (RL, λ 625-630nm), yellow light (YL, λ 590-595nm), green light (GL, λ 525-530nm) and blue light (BL, λ 450-455nm). The photoperiod was 12L:12D, and the light intensity was set to 250 mW/m^2. The effects of light spectrum on growth, melatonin synthesis, GH/IGF-I axis and relative expressions of apoptosis-related genes in juvenile *Takifugu rubripes* were studied, including arylalkylamine N-acetyltransferase (*AANAT2*), growth hormone (*GH*), growth hormone receptor type 1 (*GHR1*), growth hormone releasing hormone (*GHRH*), insulin-like growth factor type I (*IGF-I*), insulin-like growth factor type II (*IGF-II*), insulin-like growth factor binding protein (*IGFBP*), *Bcl-2* protein family (*Bcl-2*), tumor suppressor *(p53*) and cysteine protease family *(caspase 3, caspase 8, caspase 10*) genes. The results showed that the final weight was the highest in the GL group (29.36 ± 3.78 g) and the lowest in the YL group (21.28 ± 2.56 g). The GL indeed promote the growth of *Takifugu rubripes*. The *GHR1*, *IGF-I*, *IGF-II* and *IGFBP* of juvenile *Takifugu rubripes* cultured under GL were significantly higher than those of WL (control group), BL and YL groups. The relative expression levels of *GH* and *GHRH* genes had no difference from those in the WL control group, and the relative expression levels of apoptosis genes in the GL group were significantly lower than those in the BL and YL groups.

Under RL, the relative expression levels of all growth genes on the GH/IGF-I growth axis were relatively high. But at the same time, the relative expression of *caspase 10* gene in juvenile *Takifugu rubripes* was high, and the growth state was inhibited. It is speculated that RL might disturb the endocrine system of the juvenile *Takifugu rubripes*, thus impeded its growth and development. Therefore, different LED spectra can affect the growth of juvenile *Takifugu rubripes* by affecting the expressions of GH/IGF-I growth axis and apoptosis-related genes: GL significantly promotes the growth of *Takifugu rubripes*, which may be due to that GL promoted the expressions of growth factors genes such as *GHR1*, *IGF-I*, and *IGF-II*, and decreased the expression of apoptosis-related genes, while the situation in the YL, BL and WL groups was on the contrary. RL significantly inhibited the growth of juvenile *Takifugu Rubripes*, which may be due to the fact that juvenile *Takifugu Rubripes* under RL were in a stressful state and the high expression of growth axis-related genes was not sufficient to offset the negative effects of the stress response, resulting in the inhibition of growth performance.

KEYWORDS

***Takifugu rubripes*, LED spectrum, growth, GH/IGF-I axis genes, apoptosis genes**

1 Introduction

As an important and complex ecological environment factor, light generally includes three elements, namely illuminance, spectral composition and photoperiod. It can directly or indirectly influence fish's feeding, growth and development and physiological activities. When light travels underwater, the spectral components of the incident light will change to varying degrees, and the wavelengths will rapidly decay as the depth increases. The short wavelengths of the visible spectrum or blue wavelengths dominate in deep water, while RL can only penetrate shallow water. Therefore, fishes living in different water layers also have great differences in their sensitivity to light. It has been shown that different spectral environments can affect the stress response, physiological state, and behavior of fish, thus affecting growth performance, and have significant species specificity (Karakatsouli et al., 2010). For example, BL is not benefit to the growth of juvenile rainbow trout (*Oncorhynchus mykiss*) and RL is conducive to the growth of juvenile sea bream (*Sparus aurata*) (Wang et al., 2013). When reared under WL, the total length of juvenile European sea bass (*Dicentrarchus labrax*) increased significantly (Villamizar et al., 2009). However, the spectrum has no effect on the growth of juvenile Atlantic salmon (*Salmo salar*) and haddock (*Melanogrammus aeglefinus*) (Stefansson and Hansen, 1989; Downing, 2002).

The pineal gland of most fish has direct photosensitivity, and the effect of light on fish will also affect a series of physiological activities by affecting the secretion of melatonin (Mohamed et al., 2007; Migaud et al., 2012). Melatonin (N-acetyl-5-methoxytryptamine) is synthesized by tryptophan taken up by pineal cells. Aralkylamine N-acetyltransferase (AANAT) is one of the major synthases of melatonin, and its secretion level is consistent with the level of melatonin. The light-induced reduction of *AANAT2* activity and melatonin secretion was a dose-dependent process. Because this is the process of inhibiting neurotransmitter release and depends on the spectral composition (Migaud et al., 2006). The light environment and melatonin will control the neuroendocrine axis, and the melatonin in the pineal gland will target the pituitary gland and surrounding tissues. It regulates the release of growth hormone (GH) and the possibility of affecting other pituitary hormones has not been ruled out (Sánchez-Vázquez et al., 2019). One study found that the expression level of *GH* mRNA was significantly higher after melatonin injection than in the control group and that melatonin played a role in regulating the growth of *Amphiprion clarkii* (Shin et al., 2012). It was also found that melatonin directly promoted the secretion of pituitary growth hormone (GH) in *Oncorhynchus mykiss* (Falcón et al., 2003). Prolonged darkness induces melatonin secretion in *Paralichthys olivaceus*, which increases *GH* mRNA expression and thus promotes weight gain in this species (Kim et al., 2019). Therefore, an increase in melatonin within a certain range can promote fish growth.

Animal growth is mainly regulated by the animal neuroendocrine system, and the growth axis (GH/IGF-I axis)

is at the core of this system (Ayson and Takemura, 2006). Current studies have shown that the endocrine regulation pattern of teleost growth is similar to that of higher vertebrates and is mainly regulated by the growth hormone/insulin-like growth factor axis (GH/IGF-I axis) regulation. Studies have shown that the relative expression levels of *GH* and *IGF-I* in *Megalobrama amblycephala* increase with the increase of lighting time (Tian et al., 2019). And the relative expression of *GH* in the larvae and juveniles of *Takifugu rubripes* under GL is the highest, which is conducive to their growth and development (Wei et al., 2019). Another study found that the expression level of *GH* mRNA in yellowtail clownfish (*Amphiprion clarkii*) was higher in GL and BL conditions than in RL conditions, inducing faster growth (Shin et al., 2012). It was also found that the growth of juvenile turbot (*Scophthalmus maximus*) after metamorphosis was promoted by BL and the juvenile turbot exposed to BL had higher body weight and *IGF-I* mRNA levels (Wu et al., 2020). And the expression level of *GH* gene in the brain tissue of *Takifugu rubripes* under different photoperiods was also significantly different (Wei et al., 2020). However, scientific research on the effect of spectrum on the expressions of GH/IGF-I axis-related genes in juvenile *Takifugu rubripes* is not comprehensive enough, and the mechanism is unclear.

Apoptosis is a normal physiological process used to remove excess, damaged, necrotic or potentially dangerous cells (Xian et al., 2013). Apoptosis is regulated by a series of signal cascades and is affected by environmental factors (Guo et al., 2017). Studies have shown that different environmental temperatures can cause different expression changes of *Bcl-2* in the liver of zebrafish (*Danio rerio*) (Ji et al., 2013). And the expression of apoptosis-related genes in *Penaeus vannamei* may be up-regulated under WL and RL, but they are not affected under BL and GL (Fei et al., 2020a). It was also found that GL effectively reduced oxidative stress and apoptosis in olive flounder (*Paralichthys olivaceus*) induced by temperature, while RL increased oxidative stress and apoptosis (Kim et al., 2016a). And BL environment alleviated cold shock-induced oxidative stress and apoptosis in zebrafish (*Danio rerio*), significantly inhibited *caspase 3*, *caspase 8* and *caspase 9* activity levels (Peng et al., 2022). Thus, the spectrum would have a regulatory effect on the expression of apoptotic genes. So far, there have been few reports on the effects of spectrum composition on cell apoptosis of juvenile *Takifugu rubripes*, and the mechanism of spectrum on cell apoptosis is still unclear. Therefore, it is necessary to study the changes in the expression levels of apoptosis-related genes in juvenile *Takifugu rubripes*, such as the Bcl-2 protein family (Bcl-2), tumor suppressor (p53) and cysteine protease family (caspase 3, caspase 8, caspase 10) genes.

Takifugu rubripes belongs to *Tetraodontiformers*, *Tetraodontoidei*, *Tetraodontidae*, and *Takifugu*. They live near the seabed and are warm-temperate, wide-salt, carnivorous benthic migratory fish, inhabiting reef areas, sandy mud bottoms, estuaries, and offshore coasts. They are mainly distributed along the coasts of China, the Korean Peninsula and the east and west coasts of Japan (Ma et al., 2021). *Takifugu rubripes* has delicious meat and high nutritional value, and it is one of the important economic fish species in northern China, especially in the northern sea area. There has been a saying in China since ancient times that people would die to eat puffer fish. This fish is very popular among Chinese, even Japanese and Korean people. The total production of puffer fish mariculture in 2019 is 17,473t (Zhu et al., 2022). At present, the scale of indoor closed breeding of puffer fish in China is increasing, which requires the use of artificial light source for production, but the corresponding light regulation technology is relatively blank, and relevant research is also urgently needed. (Ma et al., 2014). Studies on the effect of LED light on *Takifugu rubripes* have also been partially carried out. Studies have shown that different light environments affect many physiological characteristics of *Takifugu rubripes* due to the light distribution in the water column and the characteristics of the fish habitat. For example, the effect of spectrum (white, blue and yellow light) and photoperiod on the growth of *Takifugu rubripes* was studied. The results showed that at 80 DPH, the growth performance of WL and YL treatment was better than that of BL with the photoperiod of 12L:12D (Wu et al., 2022). And the digestive enzyme activities of juvenile *Takifugu rubripes* under GL were all higher than other spectral treatment groups (Liu et al., 2021). It was also found that light intensity environment of 250-500 mW/m^2 could protect cell structure and function of juvenile *Takifugu rubripes* from oxidative stress (Li et al., 2022). And photoperiodic environments of 8L:16D and 24L:0D at 30 DPH may cause stress to *Takifugu rubripes*, resulting in elevated alkaline phosphatase (Ma et al., 2021). Other studies have shown that light conditions may affect the expression of *GHRH* and lead to upregulation of *GH* gene in juvenile *Takifugu rubripes* (Liu et al., 2019).

Preliminary studies have proved that different LED spectra could affect the growth of somatic cells in the juvenile *Takifugu rubripes* (Kim et al., 2016b; Liu et al., 2021). The results showed that GL can promote the growth and development of juvenile *Takifugu rubripes*. Compared with RL, the juvenile *Takifugu rubripes* raised under GL has a higher survival rate, better feeding performance and growth status. Current studies on the effects of light environment on *Takifugu rubripes* mainly involve morphological traits, growth and feeding, digestion and metabolism, antioxidant and immunity, as well as the expression of *GH* and *IGF-I* genes. However, the GH/IGF-I growth axis contains multiple genes, and it is uncertain whether GL promotes fish growth through the GH/IGF-I growth axis and apoptosis. Therefore, the effects of different LED spectra (GL, BL, YL, RL and WL) on GH/IGF-I axis related genes and apoptosis related genes of juvenile *Takifugu rubripes* were

investigated, in order to reveal the reasons for the effects of different LED spectra on the growth and development of juvenile *Takifugu rubripes*.

2 Material and methods

2.1 Fish breeding

The juvenile *Takifugu rubripes* used in the experiment originated from Dalian Tianzheng Industrial Co., Ltd. After the juveniles are transported to the laboratory, they are cultured in aquarium barrels (diameter: 80 cm, inner height: 60 cm, effective water volume: 250 L), and domesticated for a week. During the domestication period, commercial buoyant feeds were used for feeding, and they were fed twice a day at 08:30 in the morning and 15:30 in the afternoon. One week later, 525 well-balanced and healthy juvenile *Takifugu rubripes* were selected for the experiment.

2.2 Experimental design

The light sources used in this experiment are LED lamps (model: GK5A; designed by the Institute of Semiconductors, Chinese Academy of Sciences, produced by Shenzhen Overclocking Technology Co., Ltd.). There were 5 LED lights in different colors, including GL (λ525~530 nm), BL (λ450~455 nm), YL (λ590~595 nm), RL (λ625~630 nm) and WL (λ400~780 nm). The light source is installed 1 m directly above the water surface.

The experiments were carried out in a shaded compartment with shading cloth to cover the different treatment groups to avoid cross-contamination of the light source among the treatment groups. Five spectral treatment groups were set up in this experiment, which were green light (GL), blue light (BL), yellow light (YL), red light (RL) and white light (WL) treatment groups. There were 3 repetitions in each treatment group. The breeding barrels are cylindrical barrels made of off-white PE material with a diameter of 80 cm and an inner height of 60 cm. At the beginning of the experiment, 35 domesticated *Takifugu rubripes* juveniles were placed in each breeding bucket, with body length of (9.01 ± 0.70) cm and body weight of (18.05 ± 3.17) g. The experiment period was 30 days. During the experiment, each breeding bucket was continuously aerated with an aeration pump. The experimental light intensity was set at (250 ± 20) mW/m^2. The light intensity of four points was averaged and calibrated at 1 cm above the water surface of each barrel using an SRI 2000 UV spectral illuminance meter (Shangze Co., Ltd.) at 8:30 am daily. The photoperiod was set to 12L:12D controlled by an electronic timer. The fish were feed twice a day at 08:30 am and 15:30 pm. The daily feed weight was calculated based on 2% of the total mass of the fish in each breeding barrel. The remaining bait collected 30 min after feeding, dry it and weigh it. Replace 50% of the volume of water every 2 days.

2.3 Sample collection

2.3.1 Growth experiment

Before the start of the experiment, 3 juvenile fish were randomly taken from each breeding bucket for the initial juvenile fish length and weight measurements. During the experiment, fish body length and fish weight measurement work was performed once every 10 d. At the end of the experiment, 3 fish were randomly selected from each culture bucket, and a total of 9 fish (whole fish) were selected from each treatment for the determination of fish length and fish weight at the end of the experiment.

2.3.1 Collection of visceral tissue samples

The fish were stopped feeding 24 hours at the end of the experiment. Then 3 juveniles were randomly selected from each repeated treatment group and anesthetized with anesthetic (MS-222). The fish were placed on an ice tray, dissected, and their liver, intestine, and brain tissues were taken out. After the tissue was rapidly rinsed with precooled normal saline, the water was sucked dry with absorbent paper and put into the refrigeration tube. Later the tissues were first frozen in liquid nitrogen and then stored in - 80 °C refrigerator for later determination of related gene expressions.

2.4Measurement and analysis of samples

2.4.1 Growth performance measurement

The body length specific growth rate (SGR_L) and body weight specific growth rate (SGR_W) were calculated according to the formula listed below.

$$SGR_L = 100 \times (1nL_2 - 1nL_1)/(T_2 - T_1) \quad ;$$

$$SGR_w = 100 \times (1nW_2 - 1nW_1)/(T_2 - T_1) \quad ;$$

In the formula, L_1 and W_1 are the fish body length (cm) and fish weight (g) at the beginning of the experiment; L_2 and W_2 are fish body length (cm) and fish weight (g) at the end of the experiment; T_1 is the start time of the experiment (d); T_2 is the end time of the experiment (d).

2.4.2 Total RNA extraction and cDNA reverse

Animal tissue total RNA extraction kit (*SteadyPure* Universal RNA Extraction Kit), reverse transcription kit (*Evo M-MLV* RT

Kit), qPCR kit (SYBR Green Premix *Pro Taq* HS qPCR Kit), GL DNA Marker 2000 were purchased from Hunan Accurate Biological Engineering Co., Ltd; 6×DNA Loading Buffer was purchased from G-CLONE (Beijing) Biotechnology Co., Ltd.; GoldView I type nucleic acid stain was purchased from Beijing Solarbio Technology Co., Ltd.; fluorescent quantitative PCR primers were synthesized by Sangon Biotech (Shanghai) Co., Ltd.

According to the instructions of the Total RNA Extraction Kit from Animal Tissues of Hunan Accurate Bioengineering Co., Ltd., the total RNA was extracted from the tissues of juvenile *Takifugu rubripes* under different LED spectrum treatments. The integrity of RNA was detected by taking 3 μL for 1.0% (W/V) agarose gel electrophoresis; 1 μL was taken for micro spectrophotometer (Shanghai Spectrometer Co., Ltd. 754) to determine the concentration. OD_{260}/OD_{280} ratio RNA within the range of 1.9~2.1 can done reverse transcription reaction. According to the instructions of the *Evo M-MLV* RT Kit (Hunan Accurate Bioengineering Co., Ltd.), the first strand of cDNA was synthesized by reverse transcription reaction of 1 μg total RNA with a 20 μL system, and the conditions were 37°C, 15 mins, and 85°C, 5 s. After the reaction, the cDNA was aliquoted and stored at −20°C.

2.4 Real-time quantitative PCR

Real-time quantitative PCR experiments were performed using LightCycler® 96 (BBI, Roche, Germany) instrument and SYBR Green Premix Pro Taq HS qPCR Kit (Hunan Eco Bioengineering Co., Ltd.). According to GenBank's existing redfin puffer *GH*, *GHR1*, *GHRH*, *IGF-I*, *IGF-II*, *IGFBP*, *Bcl-2*, *p53*, *caspase 3*, *caspase 8*, *caspase 10* and β-actin gene sequence, the primer sequences were designed by Primer 5 software, and the primers are shown in Table 1. After multiple determinations, the expression of β-actin was relatively stable, so it was selected as an internal reference gene. The PCR reaction conditions were set as follows: 95°C pre-denaturation for 3 mins, 95°C denaturation for 3s, 60 °C annealing/extension for 30 s, a total of 45 cycles. At the end of the experiment, the melting curves were analyzed. In all PCR processes, there were 3 biological samples in parallel, and each RNA sample had 3 replicates. By using β-actin as the internal reference, the Ct values of each sample were normalized, and the gene expression level of the WL group was used as the benchmark, and the relative gene expressions were calculated by RT-PCR ($2^{-\Delta\Delta Ct}$) relative fluorescence quantification method.

2.5 Data analysis

All statistical analyses were performed in SPSS 22.0 (SPSS Inc., Chicago, IL, USA). In summary, data were expressed as means ± standard deviations (SD) of the mean, with differences

TABLE 1 The sequences of primers for real-time PCR.

Genes	Sequence (5'~3')	GenBank accession No.
AANAT2	F:CTGCAGTACCTGCGCTGTAT R:GGGCCTCTCTCTTTGAAGCC	XM_011604114.2
GH	F:CTCATCAAGGCCAGTCAGGAT R:CTCCACCTTGTGCATGTCCT	XM_003968318
GHR1	F:TTGGGTCAACACGGACTTCT R:CTTCAGGATCTTTTGCCTTCTT	XM_011615550.1
GHRH	F:ACAGCGTCATCTGCTCACCT R:CTGCGTGTCTTTCCGTTCTT	DQ65933
IGF-I	F:GGCAAACAGCGTGAATGAG R:TCAACACGGAAGCCAGGA	AB465576.1
IGF-II	F:GACCGTGAAGCATTCCAAAT R:GCTTTGATCTTCTCCGCTTG	XM_003967358.3
IGFBP	F:TCCAGAGAGCGTTAGACCGA R:ATGTGGAAGTCGCCGTTCTT	NM_001146062.1
Bcl-2	F:GAGGTTCGCGGAGGTGATAG R:CAGCTGTTCAGGGACCCATT	XM_029830403.1
p53	F:ACGATCCCAACAACGAGCTT R:TCTCCTGGGTAATCGGTGGT	XM_003966884.3
caspase 3	F:GAGGCATTGAAACCGACAGC R:CGCGTCAAGATGTGCTGAAG	NM_001032699.1
caspase 8	F:TTCTACCGGGTGCAAACCTC R:AGACCACCAAGGCATCTTCG	XM_011616711.2
caspase 10	F:TCACGCGCTGAAAACAACAG R:TCGCTGCGGTCATGAGATAC	XM_011609433.2
β-actin	F:AGAGGGAAATCGTGCGTGAC R:GAGGAAGGAAGGCTGGAAAAG	XM_003964421.2

10.3389/fmars.2022.1008068

TABLE 2 Growth indexes of juvenile *Takifugu rubripes* under different spectral conditions (Liu et al., 2021) *n*=9; ±SD.

Growth index	Light spectrum treatment groups				
	GL	BL	YL	RL	WL
body length/cm *L*	10.63 ± 0.46^{a}	9.88 ± 0.57^{ab}	9.43 ± 0.15^{b}	9.32 ± 0.17^{b}	10.27 ± 0.80^{a}
body weight/g *W*	29.36 ± 3.78^{a}	25.42 ± 4.09^{b}	21.28 ± 2.56^{c}	22.33 ± 3.61^{bc}	24.79 ± 3.05^{bc}
body length specific growth rate/% SGR_L	0.55 ± 0.14^{a}	0.30 ± 0.19^{ab}	0.15 ± 0.05^{b}	0.12 ± 0.06^{b}	0.43 ± 0.26^{a}
body weight specific growth rate/% SGR_W	1.60 ± 0.41^{a}	1.10 ± 0.52^{b}	0.53 ± 0.39^{c}	0.67 ± 0.56^{bc}	1.04 ± 0.40^{b}

In the same row, values with same small letter superscripts or no letter superscripts mean no significant differences (P>0.05), different small letter superscripts mean significant differences (P<0.05).

among treatments tested using one-way analysis of variance (ANOVA). Data with difference level at P< 0.05 were considered statistically significant. Origin 2017 (Hampton, MA, USA) was used to generate charts.

3 Results

3.1 Growth performance of juvenile *Takifugu rubripes* under different LED spectra

The growth-related indexes of juvenile *Takifugu rubripes* under five LED spectrum conditions are shown in Table 2. The juvenile *Takifugu rubripes* in the GL group was the longest, which was (10.63 ± 0.46) cm. The body length of the juvenile puffer fish in the RL group was the shortest, which was (9.32 ± 0.17) cm. The specific growth rates of body length in the YL group and RL group were significantly lower than those in GL group and WL group (*P*< 0.05). The body weight of juvenile *Takifugu rubripes* in the GL group was the largest, which was (29.36 ± 3.78) g, while that in the YL group was the smallest, which was (21.28 ± 2.56) g. The specific growth rate of body weight in YL group was significantly lower than those in other groups except RL group (*P*< 0.05), while that in the GL group was significantly higher than those in other groups (*P*< 0.05).

3.2 Expression of GH/IGF-I axis-related genes and *AANAT2* in juvenile *Takifugu rubripes* under different LED spectra

The expression levels of GH/IGF-I axis-related genes in the brain tissue of *Takifugu rubripes* juvenile under five LED spectrum conditions are shown in Figures 1, 2. From Figure 1A, it can be seen that different spectra have a significant impact on the relative expression of *GH* gene. Under RL, the relative expression of *GH* gene was significantly higher than those of the other groups (*P*<0.05). There was no significant difference among the expressions of the GL, BL, YL and WL groups (Figure 1A). For the *GHRH* gene, the relative expression of *GHRH* gene in RL group was the highest and significantly higher than those in other groups (*P*<0.05), but there was no significant difference in the expression level among the GL and WL group, BL and RL groups. The relative expressions of *GHRH* genes in the GL and the WL groups were significantly higher than those in BL and RL groups (*P*<0.05) (Figure 1B).

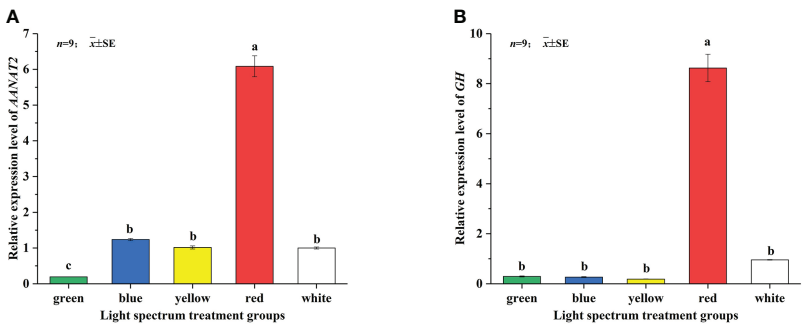

FIGURE 1
Effects of different LED spectra on relative expression of *GH* **(A)** and *GHRH* **(B)** genes in juvenile *Takifugu rubripes*. In the same column diagram, values with same small letter superscripts mean no significant differences (*P*>0.05), different small letter superscripts mean significant sdifferences (*P*<0.05).

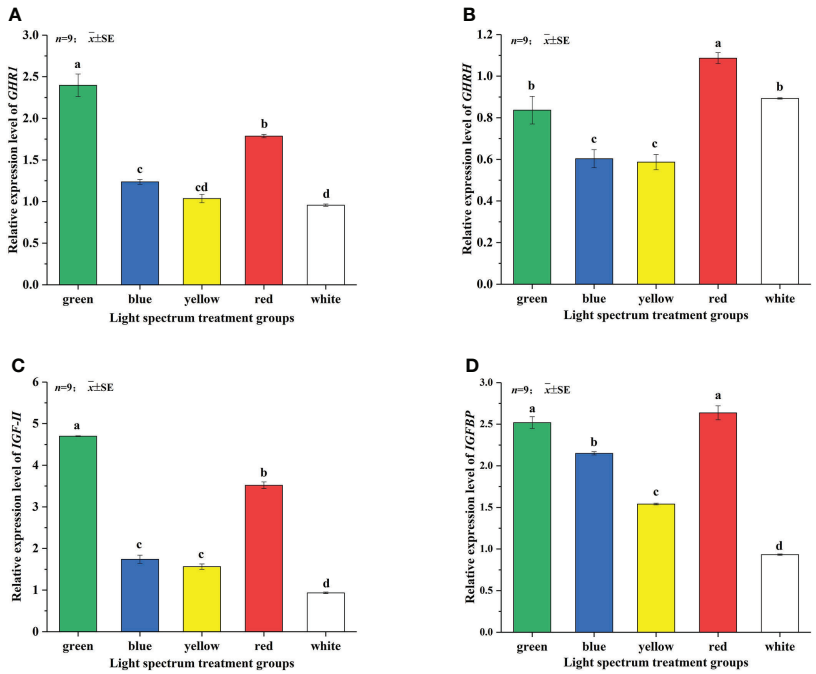

FIGURE 2
Effects of different LED spectra on relative expression of *GHR1* **(A)**, *IGF-I* **(B)**, *IGF-II* **(C)** and *IGFBP* **(D)** genes in juvenile *Takifugu rubripes*. In the same column diagram, values with same small letter superscripts mean no significant differences ($P>0.05$), different small letter superscripts mean significant differences ($P<0.05$).

Figure 2A showed that the different spectra have a greater impact on the relative expression of the *GHR1* gene. The relative expression of *GHR1* gene in the GL group was the highest, which was significantly higher than those of the other treatment groups ($P<0.05$). The relative expression of *GHR1* gene in the WL group was the lowest, which was not significantly different from that in the YL group. But it was significantly lower than those in the GL, BL and RL groups ($P<0.05$). As shown in Figure 2B, the relative expression of *IGF-I* gene of juvenile *Takifugu rubripes* was not significantly different under the GL and RL groups but was significantly higher than under the other treatment groups ($P<0.05$). The relative expression of *IGF-I* gene in the YL group was the lowest and significantly lower than that in the other treatment groups ($P<0.05$). As shown in Figure 2C, the relative expression of *IGF-II* gene in the RL group was significantly lower than that in the GL group ($P<0.05$), and was significantly higher than those in the BL, YL and WL groups ($P<0.05$). There was no significant difference in the relative expression of *IGF-II* gene between the BL and YL groups. It can be seen from Figure 2D that the relative expression of *IGFBP* gene under different light treatments is in the order of RL >GL >BL >YL >WL. There was no significant difference in the expression levels of the GL and RL groups. The expression levels of *IGFBP* gene in BL and YL groups were significantly higher than that in WL group ($P<0.05$).

The expression levels of melatonin-related *AANAT2* gene in the brain of juvenile *Takifugu rubripes* under five LED spectrum conditions are shown in Figure 3. The result showed that different spectra have significant effects on the relative expression of *AANAT2* gene. Under RL, the relative expression of *AANAT2* gene was the highest and significantly higher than those under other groups ($P<0.05$). There was no significant difference in the expressions of the BL, YL and WL groups. The relative gene expression of *AANAT2* in GL group was the lowest and significantly lower than that in the other groups ($P<0.05$).

3.3 Expression of apoptosis-related genes in juvenile *Takifugu rubripes* under different LED spectra

The relative expression levels of apoptosis-related genes in the liver tissue of juvenile *Takifugu rubripes* under the five LED spectrum conditions are shown in Figures 4A–E. There are significant differences in the relative expression of *Bcl-2* gene in the liver of juvenile *Takifugu rubripes* under different spectral

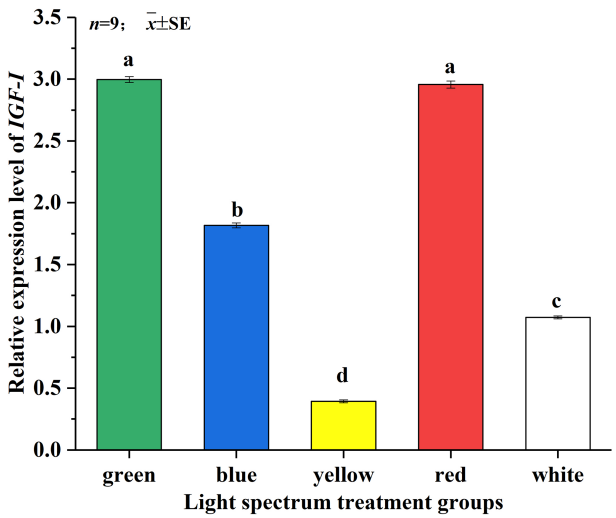

FIGURE 3
Effects of different LED spectra on relative expression of *AANAT2* genes in juvenile *Takifugu rubripes*. In the same column diagram, values with same small letter superscripts mean no significant differences ($P>0.05$), different small letter superscripts mean significant differences ($P<0.05$).

conditions (as shown in Figure 4A). Under the RL group, the relative expression of *Bcl-2* gene was the lowest, which was not significantly different from that under the GL group and significantly lower than those under the BL and WL groups ($P<0.05$). The relative expression of *Bcl-2* gene in the YL group was the highest and was significantly higher than those in the other treatment groups ($P<0.05$). As shown in Figure 4B, the relative expression of *p53* gene between the RL and YL groups have a little difference but no significant difference. The relative expression level of *p53* gene in juvenile *Takifugu rubripes* in the BL group was the highest. And it was significantly higher than the other treatment groups ($P<0.05$). The relative expression of *p53* gene in juvenile *Takifugu rubripes* in the WL group was the lowest and significantly lower than the other treatment groups ($P<0.05$). The relative expression of *caspase 3* gene in the liver tissue of juvenile *Takifugu rubripes* also has significant differences under different spectral conditions (Figure 4C). Among them, under the BL irradiation, the relative expression of *caspase 3* gene was the highest and significantly higher than those under other light groups ($P<0.05$). There was no significant difference in the relative expressions of *caspase 3* gene among the GL, RL and WL groups. The relative expression of *caspase 3* gene in the WL group was the lowest and significantly lower than those in other treatment groups ($P<0.05$). Figure 4D showed that the relative expression of *caspase 8* gene of *Takifugu rubripes* in the BL group was significantly higher than those in the other treatment groups. Moreover, the relative expression of *caspase 8* gene among the three treatment groups of the GL, YL and WL were relatively small, and there was no significant difference. The relative expression of *caspase 8* gene in the RL group was not significantly different from the WL group and significantly higher than those in the GL and YL groups ($P<0.05$). The influence of different LED spectra on the relative expression of *caspase 10* gene is shown in Figure 4E, in the order of YL >RL >BL >GL >WL. There were significant differences between each light groups ($P<0.05$). The relative expression of *caspase 10* gene of *Takifugu rubripes* in the YL group was the highest and significantly higher than those in the other treatment groups ($P<0.05$). The relative expression of *caspase 10* gene in the WL group was the lowest and significantly lower than those in the other treatment groups ($P<0.05$).

4 Discussion

4.1 Effects of different LED spectra on growth, *AANAT2* and GH/IGF-I axis-related genes in juvenile *Takifugu rubripes*

The effect of spectra on the growth and development of fish varies depending on the spectral composition and fish species. For example, GL was found to have a stimulatory effect on somatic cell growth in striped starry flounder (*Verasper moseri*), while RL had an inhibitory effect (Ji et al., 2013); Senegalese sole (*Solea senegalensis*) juveniles have better growth status under BL conditions (Fei et al., 2020a); The juveniles of *Dicentrarchus labrax* grew best in the RL group and worst in the BL group (Liu et al., 2021). The results of our previous study showed that

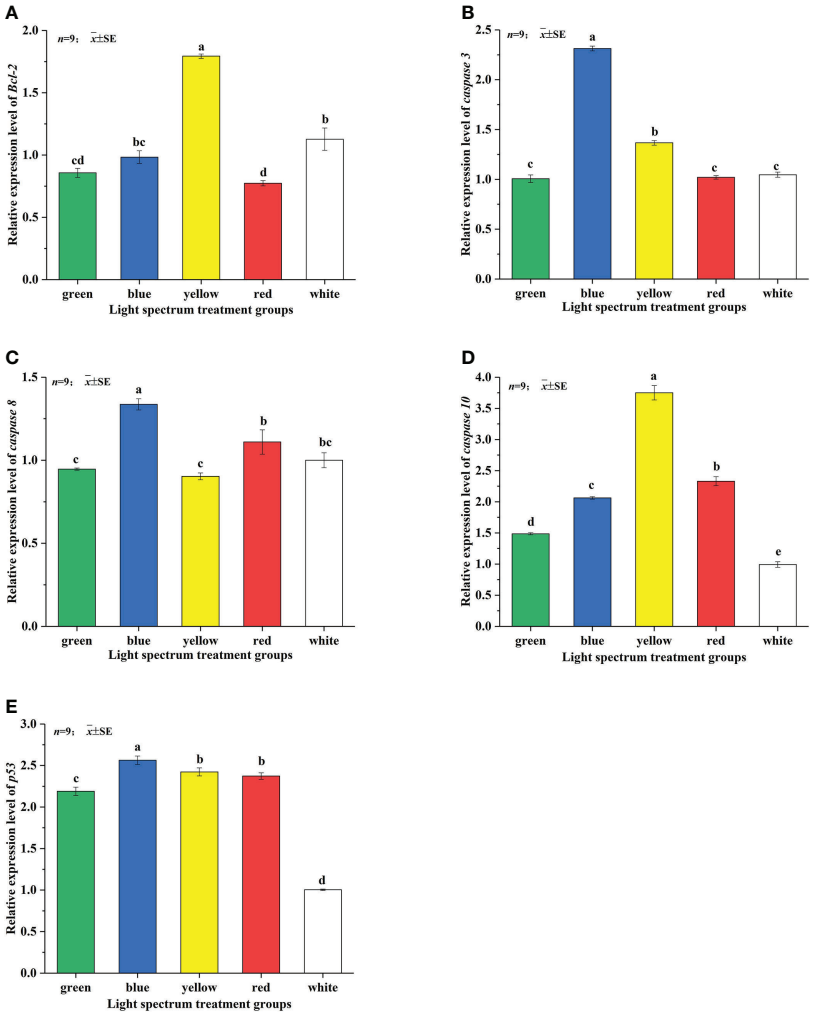

FIGURE 4
Effects of different LED spectra on the relative expression of *Bcl-2* **(A)**, *p53* **(B)**, *caspase 3* **(C)**, *caspase 8* **(D)** and *caspase 10* **(E)** genes in juvenile *Takifugu rubripes*. In the same column diagram, values with same small letter superscripts mean no significant differences ($P>0.05$), different small letter superscripts mean significant differences ($P<0.05$).

different LED spectra had different degrees of influence on the growth and development of juvenile *Takifugu rubripes*. The body weight and SGR_w of the fish under GL were the highest and significantly higher than all other treatment groups, followed by BL, YL and WL, while the mean values of various growth indicators of juvenile *Takifugu rubripes* under RL were the lowest. This result is in general agreement with the finding of Kim et al. (2016b) that the *Takifugu rubripes* grew well under GL and slowly under RL. It has been shown that the reactive oxygen species induced by the red spectrum can oxidatively damage the cellular components of fish target organs such as muscles. For example, RL can induce oxidative stress in the tissues of *Amphiprion clarkii*, which in turn causes oxidative damage to the tissues and leads to the inhibition of growth performance (Shin et al., 2011). Therefore, the juvenile *Takifugu rubripes* did not grow well under the RL environment, which may also be caused by the stress response of the fish under the RL.

The effect of light on fish also affects a range of physiological activities by influencing the secretion of melatonin. Melatonin has many physiological functions, including scavenging free radicals, improving immunity, and inhibiting the oxidation of biomolecules (Wu and Swaab, 2005). Melatonin can be converted into many antioxidant compounds during the oxidation process (Reiter et al., 1997). Therefore, melatonin is considered a broad-spectrum antioxidant and is more effective than other antioxidants in protecting cell membranes. Moreover,

arylalkylamine N-acetyltransferase 2 (AANAT2), a precursor of melatonin, is the rate-limiting enzyme for melatonin synthesis, and its secretion level is consistent with the level of melatonin (Shin et al., 2011). In this study, the increase of AANAT2 gene expression indicates the increase of melatonin secretion was believed. The relative gene expression of *AANAT2* in the GL group was significantly lower than that in the other treatment groups ($P<0.05$); there was no significant difference in the relative gene expression of *AANAT2* between the BL, YL and WL groups, and all of them were significantly lower than that in the RL group ($P<0.05$); the relative gene expression of *AANAT2* in the RL group was significantly higher than those in the other treatment groups ($P<0.05$) (Figure 3 and Table 3). This is similar to the findings of Shin et al. (2011) that red LED spectroscopy produced a stress response in *Amphiprion clarkii*, with more melatonin production and significantly higher *AANAT2* mRNA expression than other spectra treatment groups. Therefore, the higher expression of *AANAT2* in the RL group in this experiment may be due to the RL environment induced stress response in juvenile *Takifugu rubripes*, which led to the elevated expression of *AANAT2* gene and then promoted the synthesis of melatonin in response to oxidative stress. Further studies are needed to confirm the exact cause.

The growth of fish is mainly regulated by the GH/IGF-I growth axis (Li and Lin, 2010). The main factors in this axis include: GH, GHRH, GHR1, IGF-I, IGF-II, IGFBP. It has been shown that the light environment and melatonin affect the neuroendocrine axis and that melatonin in the pineal gland will act on the hypothalamus, pituitary and surrounding tissues to regulate the synthesis and release of growth hormone-releasing hormone (GHRH) and growth hormone (GH), either directly or indirectly (Max and Menaker, 1992). The hypothalamus produces the neuroendocrine factor GHRH that stimulates the synthesis and release of GH from the pituitary gland (Sánchez-Vázquez et al., 2019). Thus, melatonin has an important regulatory role for GHRH and GH. In the present study, as shown in Table 3, the relative expression of *GHRH* genes was significantly higher in the RL group than in the other treatment groups ($P<0.05$), followed by the BL, YL, and WL groups, and significantly lower in the GL group than in the other treatment groups ($P<0.05$). Also, the relative expression of pituitary *GH* gene was significantly higher in the RL group than in the other light groups ($P<0.05$), and there was no significant difference in the expression of *GH* among the remaining four groups. This is similar to the findings of Zhang et al. (2016) that melatonin plays a key role in the GL environment to enhance GH secretion in chicks by increasing *GHRH* expression in the hypothalamus. It has also been shown that the pituitary gland of *in vitro* cultured rainbow trout releases increasing amounts of *GH* when stimulated by certain physiological concentrations of melatonin (Falcón et al., 2003). And carp (*Cyprinus carpio*) GHRH stimulates the pituitary to synthesize and release GH in a dose-dependent manner (McRory et al., 1995). It was also found that the growth hormone releasing hormone (fGHRH-28) of *Paralichthys olivaceus* can induce the expression of *GH* mRNA in the embryonic cell line HINAE (Nam et al., 2011). Therefore, each treatment group may promote the expression of *GHRH* and *GH* in the hypothalamus and pituitary by promoting the release of melatonin.

After GH combines with GHR1 on the liver surface, it stimulates liver cells to synthesize and secrete IGFs. Therefore,

TABLE 3 mRNA level of genes associated with GH/IGF-I axis and apoptosis in juvenile *Takifugu rubripes* exposed to different light spectra in comparison with WL.

Genes	Light spectrum treatment groups				
	GL	BL	YL	RL	WL
AANAT2	↓↓(c)	↑(b)	↑(b)	↑↑(a)	-(b)
GH	↓(b)	↓(b)	↓(b)	↑↑(a)	-(b)
GHRH	↓(b)	↓↓(c)	↓↓(c)	↑↑(a)	-(b)
GHR1	↑↑(a)	↑↑(c)	↑(cd)	↑↑(b)	-(d)
IGF-I	↑↑(a)	↑↑(b)	↓↓(d)	↑↑(a)	-(c)
IGF-II	↑↑(a)	↑↑(c)	↑↑(c)	↑↑(b)	-(d)
IGFBP	↑↑(a)	↑↑(b)	↑↑(c)	↑↑(a)	-(d)
Bcl-2	↓↓(cd)	↓(bc)	↑↑(a)	↓↓(d)	-(b)
p53	↑↑(c)	↑↑(a)	↑↑(b)	↑↑(b)	-(d)
caspase 3	↓(c)	↑↑(a)	↑↑(b)	↓(c)	-(c)
caspase 8	↓(c)	↑↑(a)	↓(c)	↑(b)	-(bc)
caspase 10	↑↑(d)	↑↑(c)	↑↑(a)	↑↑(b)	-(e)

The symbol: "-": control group. "↓": lower but not significant. "↓↓": significantly lower. "↑": higher but not significant. "↑↑": significantly higher. "a", "b", "c", "d", "e": signif. codes.

GH has an important regulatory effect on IGFs, and its expression level can reflect the growth status of animals to some extent (Reinecke, 2010). IGF binds to IGFBP in the liver and reaches the target cells *via* the endocrine pathway, and the adducts act on the IGFR (insulin-like growth factor receptor) on the surface of the target cells to promote the proliferation and growth of the target cells, thereby promoting the growth of the organism (Li et al., 2017). Studies have shown that IGFBPs not only have an IGF-dependent effect but can also act as a carrier of IGF or a regulator of the effectiveness and activity of IGF. During the embryonic and gonadal development of carp (*Cyprinus carpio*), IGFBP may play an important role in their growth and development by regulating the role of IGF in reproduction and embryonic growth (Chen et al., 2009). In the present study, it can be seen from Table 3 that the relative expression of *GHR1* and *IGF-II* genes was significantly higher in the GL group than in the other treatment groups ($P<0.05$), and the relative expression of *IGF-I* and *IGFBP* genes was significantly higher in the GL and RL groups than in the other treatment groups ($P<0.05$). Meanwhile, the relative expression of *GHR1*, *IGF-I* and *IGF-II* genes in the RL group was significantly higher than those in the BL, YL and WL groups ($P<0.05$). This is similar to the findings of Chen et al. (2022) that the relative expression of *GHR*, *IGF-I* and *IGFBP* genes was significantly higher in *Oncorhynchus mykiss* than in each of the remaining treatment groups under light conditions that mimic the light color changes in the natural underwater environment. It has been shown that GH promotes growth through the synergistic action of hepatic GHR, IGF-I and IGFBP, which play a central link in the GH/IGF-I axis (Zou et al., 2022). Therefore, we speculate that the GL group may promote the synthesis and secretion of *IGF* in the liver by promoting the binding of GH and GHR1 in the liver, and promote cell mitosis and differentiation by promoting the binding of IGF and IGFBP in the liver, thus promoting the growth of juvenile *Takifug rubripes*.

Interestingly, the growth status of fish under normal environmental conditions is usually positively correlated with the expression levels of GH/IGF-I axis-related genes *in vivo*, and GH/IGF-I axis-related genes can directly affect growth of fish by stimulating cell differentiation. It has been shown that the expressions of *GHR1* mRNA, *GHR2* mRNA and *IGF* mRNA in the liver of juvenile ocellaris clownfish (*Amphiprion ocellaris*) treated with different light photoperiods are similar to their average body length and weight gains (Li et al., 2017). However, the growth status of fish under certain stress conditions may also be negatively correlated with plasma GH levels or *GH* gene expression levels. For example, the body weight and specific growth rate of Mozambique tilapia (*Oreochromis mossambicus*) after 4 weeks of fasting were significantly reduced, but the plasma GH level and pituitary *GH* mRNA were significantly increased (Fox et al., 2006); Monocrotophos pesticide exposure to Nile tilapia (*Oreochromis niloticus*) for 3 weeks significantly inhibited their growth. However, its GH level was significantly increased, this is probably due to the negative feedback regulation mechanism of liver IGF-I (Cheng et al., 2002). In the present study, the relative expressions of *GHRH* and *GH* genes were at low levels in the GL group, whereas the relative expressions of *IGF-I* and *IGF-II* genes were at high levels. Meanwhile, previous studies have shown that overexpression of *IGF-I* gene can suppress *GH* gene expression in tilapia (Cheng et al., 2002). It has also been shown that *GH* gene can promote the expression of *IGF-I* and *IGF-II* genes, and that there is a negative feedback regulation mechanism among GH, GHRH and IGF-I (Chen et al., 2016). Therefore, we hypothesized that the low expression of *GHRH* and *GH* genes in the GL group was due to the activation of the negative feedback regulatory mechanism of the GH/IGF-I axis by the overexpression of *IGF-I* genes in the liver. In contrast, the relative expression of each growth gene in the RL group was at a high level, but this was not consistent with the trend of growth performance of juvenile *Takifugu rubripes* in the RL group. We speculate that this may be due to the fact that juvenile *Takifugu rubripes* under RL are in a stressful state and the high expression of growth axis-related genes is not sufficient to counteract the negative effects of the stress response, which in turn affects their normal growth. The above is just a speculation, and the true reason needs to be confirmed by more research.

4.2 Effects of different LED spectra on apoptosis-related genes in juvenile *Takifugu rubripes*

Vertebrate cell apoptosis is the programmed cell death controlled by a variety of genes. It is necessary to maintain the body's homeostasis, immune defense, and growth and development. The Bcl-2 protein family is an important regulator of cell apoptosis. The *Bcl-2* gene is a gene that inhibits cell apoptosis and is located in the endoplasmic reticulum. Its expression directly or indirectly affects the release of Ca^{2+} from the endoplasmic reticulum and inhibits apoptosis, thereby protecting cells from apoptosis (Borghetti et al., 2015). In this study, the relative expression of the *Bcl-2* gene in the BL, YL and WL groups was significantly higher than those in the GL and RL groups, and the relative gene expression of *Bcl-2* in the RL group was the lowest (Figure 4 and Table 3). Studies have shown that different environmental temperatures can cause different transcriptional changes of *Bcl-2* in the liver of zebrafish (*Danio rerio*) (Ji et al., 2013); the expression level of *Bcl-2* in the hepatopancreas of *Litopenaeus vannamei* in the full spectrum + UVB (310 nm) group was significantly lower than those in other spectral treatment groups, and the level of

apoptosis inhibition was weaker, resulting in poorer growth performance of shrimp in this spectral treatment group (Fei et al., 2020b). Therefore, the level of apoptosis inhibition was weakest in the RL group, resulting in the highest level of apoptosis in juvenile fish in this group, which in turn led to the inhibition of their growth and development.

p53 is a tumor suppressor, and its product has a regulatory effect on a variety of downstream genes (Yuan et al., 2017). It acts as a transcription factor in regulating the complex DNA damage system. DNA damage will cause an increase in the expression of *p53*, and its product will activate the downstream inhibition of cyclin-dependent kinase activity, thereby inhibiting the progress of the cell cycle (Huang et al., 2020). In this study, it can be seen from Table 3 that when the juvenile *Takifugu rubripes* is exposed to BL, YL and RL, the transcription of the *p53* gene in the liver is upregulated. The expression level of *p53* in the GL group was significantly lower than the BL group, YL group and RL group ($P<0.05$). The study showed that the transcript levels of *p53* in the hepatopancreas of *Litopenaeus vannamei* in the dark group were higher than those in the other treatment groups, and the growth performance of shrimp in this group was poorer (Fei et al., 2020b); When *Penaeus vannamei* were exposed to WL and RL, the *p53* gene transcription was upregulated in the hepatopancreas, while the expression level of *p53* was lower in the GL group than in the other groups. Shrimp in the GL group grew well (Fei et al., 2020b). Therefore, the expression of *p53* is influenced by spectral composition and may trigger apoptosis of hepatocytes in juvenile *Takifugu rubripes*, resulting in impaired liver tissue function and reduced ability to cope with stress responses in juvenile fish, which in turn inhibits their growth and development.

Caspase is a cysteine protease involved in cell apoptosis. Its family members directly or indirectly cause the appearance of the structural features of cell apoptosis and are at the core of the apoptosis pathway. It plays a key role in the entire process of cell apoptosis by initiating the exogenous apoptosis pathway and indirectly initiating the endogenous apoptosis pathway (Sakata et al., 2007). The exogenous apoptosis pathway is regulated by extracellular signals, and extracellular signals can recruit caspase 8 and caspase 10 related proteins. Among them, caspase 3 is an apoptotic protease that is frequently activated and catalyzes the specific cleavage of many key cellular proteins. The activation of caspase 8 and caspase 10 may directly or indirectly activate caspase 3. It was shown that under low temperature stress, the liver of *Epinephelus coioides* activated its apoptotic pathway and induced changes in the expression of the caspase family, Bcl-2, bax and other apoptotic genes, which in turn inhibited the growth and development of *Epinephelus coioides* (Sun et al., 2019); expression of *caspase 3* and *caspase 8* in the hepatopancreas of *Penaeus vannamei* was higher in the full-spectrum and RL groups and lower in the BL and GL groups, and growth performance of *Penaeus vannamei* was inhibited in the full-spectrum and RL groups (Fei et al., 2020a). Therefore, the BL, YL and RL groups may put juvenile *Takifugu rubripes* in an unfavorable environment, inducing upregulation of caspase family-related gene expression, exacerbating apoptosis, and thus inhibiting their growth. In contrast, juvenile *Takifugu rubripes* in the GL group were in a favorable environment with down-regulated expression of caspase family-related genes, which alleviated apoptosis and thus promoted the growth and development of juvenile fish.

Therefore, unfavorable light environmental conditions may increase the expression of apoptotic genes, intensify apoptosis and cause liver tissue damage, thus inhibiting the growth of juvenile *Takifugu rubripes*. The relative expressions of the five apoptotic genes were lower in the GL environment, indicating that a favorable light environment can reduce the expression of apoptotic genes and slow down the apoptotic process, which is beneficial to the growth of juvenile *Takifugu rubripes*.

5 Conclusion

In summary, under an environment with a photoperiod of 12L:12D and an illuminance of (250 ± 20) mW/m^2, five different LED spectra have a certain degree of influence on growth and the expressions of GH/IGF-I growth axis and apoptosis-related genes in the juvenile stage of *Takifugu rubripes*. The better growth performance of juvenile *Takifugu rubripes* cultured under GL was related to the GH/IGF-I growth axis and apoptosis genes. GL significantly promotes the growth of *Takifugu rubripes*, which may be due to that GL promoted the expressions of growth factors such as *GHR1*, *IGF-I*, and *IGF-II*, and decreased the expressions of apoptosis-related genes, while the situation in the YL, BL and WL groups was on the contrary. The RL group significantly inhibited the growth of juvenile *Takifugu rubripes*, which may be due to the fact that juvenile *Takifugu rubripes* under RL environment were in a stressful state and the high expression of growth axis-related genes was not sufficient to offset the negative effects of stress response, resulting in the inhibition of growth performance. Further studies are needed to confirm.

Data availability statement

The original contributions presented in the study are included in the article/Supplementary Material. Further inquiries can be directed to the corresponding author/s.

Ethics statement

This study was reviewed and approved by Animal Care and Use Committee of the Chinese Academy of Fishery Sciences.

Author contributions

SL conducted the sample collection, data curation and draft writing. YF performed the histological analysis. YL conducted the writing-review and editing. XL performed the molecular work. FS conducted the statistical analysis. YW performed the data visualization. ZM and HM contributed to the concept and design of the study. All authors contributed to the article and approved the submitted version.

Funding

This research was supported by Key Program of the National Natural Science Foundation of China (Grant No. 42030408), the Science & Technology Program of Liaoning Province (2021JH2/10200011 and 2019JH2/10200007), Open project of Key Laboratory of Environment Controlled Aquaculture (Dalian Ocean University) Ministry of Education (202202), Science and Technology Innovation Foundation of Dalian (2021JJ13SN72)and Scientific research project of Liaoning Provincial Department of oceans and Fisheries (201728).

Acknowledgments

We would like to thank Changbin Song engineer for his assistance with light source design in our experiments.

Conflict of interest

The authors declare that the research was conducted in the absence of any commercial or financial relationships that could be construed as a potential conflict of interest.

Publisher's note

References

Ayson, F. G., and Takemura, A. (2006). Daily expression patterns for mRNAs of *GH*, *PRL*, *SL*, *IGF-i* and *IGF-II* in juvenile rabbitfish, *Siganus guttatus*, during 24-h light and dark cycles. *Gen. Comp. Endocrinol.* 149, 261–268. doi: 10.1016/j.ygcen.2006.06.006

Borghetti, G., Yamaguchi, A. A., Aikawa, J., Yamazaki, R. K., de Brito, G. A. P., and Fernandes, L. C. (2015). Fish oil administration mediates apoptosis of walker 256 tumor cells by modulation of p53, bcl-2, caspase-7 and caspase-3 protein expression. *Lipids Health Dis.* 14, 1–5. doi: 10.1186/s12944-015-0098-y

Cheng, R., Chang, K. M., and Wu, J. L. (2002). Different temporal expressions of tilapia (*Oreochromis mossambicus*) insulin-like growth factor-I and IGF binding protein-3 after growth hormone induction. *Mar. Biotechnol.*, 4, 218–225. doi: 10.1007/s10126-002-0014-0

Chen, W., Li, W., and Lin, H. (2009). Common carp (*Cyprinus carpio*) insulin-like growth factor binding protein-2 (IGFBP-2): Molecular cloning, expression profiles, and hormonal regulation in hepatocytes. *Gen. Comp. Endocrinol.* 161, 390–399. doi: 10.1016/j.ygcen.2009.02.004

Chen, D., Wang, W., and Ru, S. (2016). Effects of dietary genistein on GH/IGF-I axis of Nile tilapia *Oreochromis niloticus*. *Chin. J. Oceanology Limnology* 34, 1004–1012. doi: 10.1007/s00343-016-4386-9

Chen, X., Zhou, Y., Huang, J., An, D., Li, L., Dong, Y., et al. (2022). The effects of blue and red light color combinations on the growth and immune performance of juvenile steelhead trout, *Oncorhynchus mykiss*. *Aquac Rep.* 24, 1–8. doi: 10.1016/j.aqrep.2022.101156

Downing, G. (2002). Impact of spectral composition on larval haddock, *Melanogrammus aeglefinus l.*, growth and survival. *Aquac Res.* 33, 251–259. doi: 10.1046/j.1355-557x.2002.00668.x

Falcón, J., Besseau, L., Fazzari, D., Attia, J., Gaildrat, P., Beauchaud, M., et al. (2003). Melatonin modulates secretion of growth hormone and prolactin by trout pituitary glands and cells in culture. *Endocrinology*. 144, 4648–4658 doi: 10.1210/en.2003-0707

Fei, F., Gao, X., Wang, X., Liu, Y., Bin, H., and Liu, B. (2020a). Effect of spectral composition on growth, oxidative stress responses, and apoptosis-related gene expression of the shrimp, *Penaeus vannamei*. *Aquac Rep.* 16, 100267. doi: 10.1016/j.aqrep.2019.100267

Fei, F., Liu, B., Gao, X., Wang, X., Liu, Y., and Bin, H. (2020b). Effects of supplemental ultraviolet light on growth, oxidative stress responses, and apoptosis-related gene expression of the shrimp *Litopenaeus vannamei*. *Aquaculture* 520, 735013. doi: 10.1016/j.aquaculture.2020.735013

Fox, B. K., Riley, L. G., Hirano, T., and Grau, E. G. (2006). Effects of fasting on growth hormone, growth hormone receptor, and insulin-like growth factor-I axis in seawater-acclimated tilapia, *Oreochromis mossambicus*. *Gen. Comp. Endocrinol.* 148, 340–347. doi: 10.1016/j.ygcen.2006.04.007

Guo, H., Li, K., Wang, W., Wang, C., and Shen, Y. (2017). Effects of copper on hemocyte apoptosis, ROS production, and gene expression in white shrimp *Litopenaeus vannamei*. *Biol. Trace Elem Res.* 179, 318–326. doi: 10.1007/s12011-017-0974-6

Huang, Z., Liu, X., Ma, A., Wang, X., Guo, X., Zhao, T., et al. (2020). Molecular cloning, characterization and expression analysis of p53 from turbot *Scophthalmus maximus* and its response to thermal stress. *J. Therm Biol.* 90, 102560. doi: 10.1016/j.jtherbio.2020.102560

Ji, W., Liang, H., Zhou, W., and Zhang, X. (2013). Apoptotic responses of zebrafish (*Danio rerio*) after exposure with microcystin-LR under different ambient temperatures. *J. Appl. Toxicol.* 33, 799–806. doi: 10.1002/jat.2735

Karakatsouli, N., Papoutsoglou, E. S., Sotiropoulos, N., Mourtikas, D., Stigen-Martinsen, T., and Papoutsoglou, S. E. (2010). Effects of light spectrum, rearing density and light intensity on growth performance of scaled and mirror common carp *Cyprinus carpio* reared under recirculating system conditions. *Aquac Eng.* 42, 121–127. doi: 10.1016/j.aquaeng.2010.01.001

Kim, B.-H., Hur, S.-P., Hur, S.-W., Lee, C.-H., and Lee, Y.-D. (2016b). Relevance of light spectra to growth of the rearing tiger puffer *Takifugu rubripes*. *Dev. Reprod.* 20, 23 doi: 10.12717/dr.2016.20.1.023

Kim, B. S., Jung, S. J., Choi, Y. J., Kim, N. N., Choi, C. Y., and Kim, J. W. (2016a). Effects of different light wavelengths from LEDs on oxidative stress and apoptosis in olive flounder (*Paralichthys olivaceus*) at high water temperatures. *Fish Shellfish Immunol.* 55, 460–468. doi: 10.1016/j.fsi.2016.06.021

Kim, B.-H., Lee, C.-H., Choi, S.-H., and Lee, Y.-D. (2019). Changes in body growth and growth-related genes under different photoperiods in olive flounder, *Paralichthys olivaceus*. *Dev. Reprod.* 23, 149–160. doi: 10.12717/DR.2019.23.2.149

Li, Z., Li, Y., Cai, S., and Ju, C. (2017). The effects of environmental factors on growth and growth-related genes' expressions of *Amphiprion ocellaris*. *Journal of Shanghai Ocean University*. 26, 321–329. doi: 10.12024/jsou.20160301699

Li, W. S., and Lin, H. R. (2010). The endocrine regulation network of growth hormone synthesis and secretion in fish: Emphasis on the signal integration in somatotropes. *Sci. China Life Sci.* 53, 462–470. doi: 10.1007/s11427-010-0084-6

Li, X., Liu, S., Fan, K., Zhang, J., Wei, P., Liu, Y., et al. (2022). Effects of illumination intensities on growth, digestive and metabolic enzyme activities and antioxidant capacities of juvenile *Takifugu rubripes*. *Aquaculture* 548, 737594. doi: 10.1016/J.AQUACULTURE.2021.737594

Liu, S., Li, Y., Li, X., Wei, P., Ma, H., Liu, Y., et al. (2021). Effects of LED spectra on growth, feeding, and digestive enzyme activities of juvenile *Takifugu rubripes*. *J. Fishery Sci. China* 28, 1011–1019. doi: 10.12264/JFSC2020-0581

Liu, Q., Yan, H., Hu, P., Liu, W., Shen, X., Cui, X., et al. (2019). Growth and survival of *Takifugu rubripes* larvae cultured under different light conditions. *Fish Physiol. Biochem.* 45, 1533–1549. doi: 10.1007/s10695-019-00639-0

Ma, A., Li, W., Wang, X., Yue, L., Zhuang, Z., Meng, X., et al. (2014). Reasearch progress and outlook of *Takifugu rubripes* culture techniques. *Mar. Sci.* 38, 116–121. doi: 10.11759/hykx20121130001

Ma, H., Wei, P., Li, X., Liu, S., Tian, Y., Zhang, Q., et al. (2021). Effects of photoperiod on growth, digestive, metabolic and non-special immunity enzymes of *Takifugu rubripes* larvae. *Aquaculture* 542, 736840. doi: 10.1016/j.aquaculture.2021.736840

Max, M., and Menaker, M. (1992). Regulation of melatonin production by light, darkness, and temperature in the trout pineal. *J. Comp. Physiol. A* 170, 479–489. doi: 10.1007/BF00191463

McRory, J. E., Parker, D. B., Ngamvongchon, S., and Sherwood, N. M. (1995). Sequence and expression of cDNA for pituitary adenylate cyclase activating polypeptide (PACAP) and growth hormone-releasing hormone (GHRH)-like peptide in catfish. *Mol. Cell Endocrinol.* 108, 169–177. doi: 10.1016/0303-7207(94)03467-8

Migaud, H., Ismail, R., Cowan, M., and Davie, A. (2012). Kisspeptin and seasonal control of reproduction in male European sea bass (*Dicentrarchus labrax*). *Gen. Comp. Endocrinol.* 179, 384–399. doi: 10.1016/j.ygcen.2012.07.033

Migaud, H., Taylor, J. F., Taranger, G. L., Davie, A., Cerdá-Reverter, J. M., Carrillo, M., et al. (2006). A comparative ex vivo and *in vivo* study of day and night perception in teleosts species using the melatonin rhythm. *J. Pineal Res.* 41, 42–52. doi: 10.1111/j.1600-079X.2006.00330.x

Mohamed, J. S., Benninghoff, A. D., Holt, G. J., and Khan, I. A. (2007). Developmental expression of the G protein-couple receptor 54 and three *GnRH* mRNAs in the teleost fish cobia. *J. Mol. Endocrinol.* 38, 235–244. doi: 10.1677/jme.1.02182

Nam, B. H., Moon, J. Y., Kim, Y. O., Kong, H. J., Kim, W. J., Kim, K. K., et al. (2011). Molecular and functional analyses of growth hormone-releasing hormone (GHRH) from olive flounder (*Paralichthys olivaceus*). *Comp. Biochem. Physiol. - B Biochem. Mol. Biol.* 159, 84–91. doi: 10.1016/j.cbpb.2011.02.006

Peng, L.b., Wang, D., Han, T., Wen, Z., Cheng, X., Zhu, Q. L., et al. (2022). Histological, antioxidant, apoptotic and transcriptomic responses under cold stress and the mitigation of blue wavelength light of zebrafish eyes. *Aquac Rep.* 26, 101291. doi: 10.1016/J.AQREP.2022.101291

Reinecke, M. (2010). Influences of the environment on the endocrine and paracrine fish growth hormone-insulin-like growth factor-I system. *J. Fish Biol.* 76, 1233–1254. doi: 10.1111/j.1095-8649.2010.02605.x

Reiter, R. J., Carneiro, R. C., and Oh, C. S. (1997). Melatonin in relation to cellular antioxidative defense mechanisms. *Hormone Metab. Res. Hormone Metab. Res.* 29, 363–372 doi: 10.1055/s-2007-979057

Sakata, S.i., Yan, Y. L., Satou, Y., Momoi, A., Ngo-Hazelett, P., Nozaki, M., et al. (2007). Conserved function of caspase-8 in apoptosis during bony fish evolution. *Gene* 396, 134–148. doi: 10.1016/j.gene.2007.03.010

Sánchez-Vázquez, F. J., López-Olmeda, J. F., Vera, L. M., Migaud, H., López-Patiño, M. A., and Míguez, J. M. (2019). Environmental cycles, melatonin, and circadian control of stress response in fish. *Front. Endocrinol. (Lausanne)* 10. doi: 10.3389/fendo.2019.00279

Shin, H. S., Lee, J., and Choi, C. Y. (2011). Effects of LED light spectra on oxidative stress and the protective role of melatonin inrelation to the daily rhythm of the yellowtail clownfish, *Amphiprion clarkii*. *Comp. Biochem. Physiol. - A Mol. Integr. Physiol.* 160, 221–228. doi: 10.1016/j.cbpa.2011.06.002

Shin, H. S., Lee, J., and Choi, C. Y. (2012). Effects of LED light spectra on the growth of the yellowtail clownfish *Amphiprion clarkii*. *Fisheries Science*. 78, 549–556. doi: 10.1007/s12562-012-0482-8

Stefansson, S. O., and Hansen, T. J. (1989). The effect of spectral composition on growth and smolting in Atlantic salmon (*Salmo salar*) and subsequent growth in sea cages. *Aquaculture* 82, 155–162. doi: 10.1016/0044-8486(89)90404-3

Sun, Z., Tan, X., Liu, Q., Ye, H., Zou, C., Xu, M., et al. (2019). Physiological, immune responses and liver lipid metabolism of orange-spotted grouper (*Epinephelus coioides*) under cold stress. *Aquaculture* 498, 545–555. doi: 10.1016/j.aquaculture.2018.08.051

Tian, H., Zhang, D., Li, X., Jiang, G., and Liu, W. (2019). Photoperiod affects blunt snout bream (*Megalobrama amblycephala*) growth, diel rhythm of cortisol, activities of antioxidant enzymes and mRNA expression of GH/IGF-I. *Comp. Biochem. Physiol. B Biochem. Mol. Biol.* 233, 4–10. doi: 10.1016/j.cbpb.2019.03.007

Villamizar, N., García-Alcazar, A., and Sánchez-Vázquez, F. J. (2009). Effect of light spectrum and photoperiod on the growth, development and survival of European sea bass (*Dicentrarchus labrax*) larvae. *Aquaculture* 292, 80–86. doi: 10.1016/j.aquaculture.2009.03.045

Wang, T., Cheng, Y., Liu, Z., Yan, S., and Long, X. (2013). Effects of light intensity on growth, immune response, plasma cortisol and fatty acid composition of juvenile *Epinephelus coioides* reared in artificial seawater. *Aquaculture* 414–415, 135–139. doi: 10.1016/j.aquaculture.2013.08.004

Wei, P., Li, X., Fei, F., Ma, H., Gao, D., Song, C., et al. (2019). Effects of light spectrum on growth and related gene expression of larval and juvenile tiger puffer *Takifugu rubripes*. *J. Dalian Ocean Univ.* 34, 668–673. doi: 10.16535/j.cnki.dlhyxb.2018-230

Wei, P., Li, X., Liu, Y., Li, X., Song, C., Chen, T., et al. (2020). Effects of photoperiod on expression level and daily expression pattern of *GH* and *SS* genes in brain of tiger puffer *Takifugu rubripes*. *J. Dalian Ocean Univ.* 35, 108–113. doi: 10.16535/j.cnki.dlhyxb.2019-160

Wu, Y. H., and Swaab, D. F. (2005). The human pineal gland and melatonin in aging and alzheimer's disease. *J. Pineal Res.* 38, 145–152. doi: 10.1111/j.1600-079X.2004.00196.x

Wu, L., Wang, Y., Han, M., Song, Z., Song, C., Xu, S., et al. (2020). Growth, stress and non-specific immune responses of turbot (*Scophthalmus maximus*) larvae exposed to different light spectra. *Aquaculture*. 520, 734950. doi: 10.1016/j.aquaculture.2020.734950

Wu, Y., Yan, H., Shen, X., Jiang, J., Yuan, Z., Liu, Q., et al. (2022). Effects of different light conditions on growth, muscle nutrients content, and clock gene circadian expression of *Takifugu rubripes*. *Aquac Rep.* 26, 101294. doi: 10.1016/J.AQREP.2022.101294

Xian, J. A., Miao, Y. T., Li, B., Guo, H., and Wang, A. L. (2013). Apoptosis of tiger shrimp (*Penaeus monodon*) haemocytes induced by escherichia coli lipopolysaccharide. *Comp. Biochem. Physiol. - A Mol. Integr. Physiol.* 164, 301–306. doi: 10.1016/j.cbpa.2012.10.008

Yuan, L., Lv, B., Zha, J., and Wang, Z. (2017). Benzo[a]pyrene induced p53-mediated cell cycle arrest, DNA repair, and apoptosis pathways in Chinese rare minnow (*Gobiocypris rarus*). *Environ. Toxicol.* 32, 979–988. doi: 10.1002/tox.22298

Zhang, L., Cao, J., Wang, Z., Dong, Y., and Chen, Y. (2016). Melatonin modulates monochromatic light-induced *GHRH* expression in the hypothalamus and GH secretion in chicks. *Acta Histochem.* 118, 286–292 doi: 10.1016/j.acthis.2016.02.005

Zhu, Y., Chen, X., Pan, N., Liu, S., Su, Y., Xiao, M., et al. (2022). The effects of five different drying methods on the quality of semi-dried *Takifugu obscurus* fillets. *LWT* 161, 113340. doi: 10.1016/j.lwt.2022.113340

Zou, Y., Peng, Z., Wang, W., Liang, S., Song, C., Wang, L., et al. (2022). The stimulation effects of green light on the growth, testicular development and stress of olive flounder *Paralichthys olivaceus*. *Aquaculture*. 546, 737275 doi: 10.1016/j.aquaculture.2021.737275

frontiers | Frontiers in Marine Science

TYPE Original Research
PUBLISHED 07 November 2022
DOI 10.3389/fmars.2022.1035794

OPEN ACCESS

EDITED BY
Ce Shi,
Ningbo University, China

REVIEWED BY
Zhao Yunpeng,
Dalian University of Technology, China
Chunwei Bi,
Ocean University of China, China

*CORRESPONDENCE
Xiaoyu Qu
quxiaoyu@zjou.edu.cn
Dejun Feng
fengdj@zjou.edu.cn

SPECIALTY SECTION
This article was submitted to Marine Fisheries, Aquaculture and Living Resources, a section of the journal Frontiers in Marine Science

RECEIVED 03 September 2022
ACCEPTED 19 October 2022
PUBLISHED 07 November 2022

CITATION
Hu J, Zhang H, Wu L, Zhu F, Zhang X, Gui F, Qu X and Feng D (2022) Investigation of the inlet layout effect on the solid waste removal in an octagonal aquaculture tank. *Front. Mar. Sci.* 9:1035794. doi: 10.3389/fmars.2022.1035794

Investigation of the inlet layout effect on the solid waste removal in an octagonal aquaculture tank

Jiajun Hu[1], Hanwen Zhang[1], Lianhui Wu[2], Fang Zhu[3], Xuefen Zhang[1], Fukun Gui[1], Xiaoyu Qu[4]* and Dejun Feng[1]*

[1]National Engineering Research Center for Marine Aquaculture, Zhejiang Ocean University, Zhoushan, China, [2]Department of Marine Resources and Energy, Tokyo University of Marine Science and Technology, Tokyo, Japan, [3]School of Naval Architecture and Maritime, Zhejiang Ocean University, Zhoushan, China, [4]School of Fisheries, Zhejiang Ocean University, Zhoushan, China

The optimization of the inlet layout in aquaculture systems is essential to ensure minimal solid waste discharge into the environment and improve fish production efficiency. In the present study, laboratory experiments were carried out to investigate the effects of the jetting position d/a (where d is the distance from the pipe axis to the tank side and a is the side length of the tank wall) and the jetting angle θ (the acute angle between the jetting direction and the nearest tank wall) on the solid waste removal efficiency in single-inlet and dual-inlet octagonal Recirculating Aquaculture System (RAS) tanks. To this end, three jetting positions (d/a) of 1/50, 1/8, and 1/4 and ten jetting angles (θ) of 0° to 80° were considered in the experiments. The Particle Image Velocimetry (PIV) technique was applied to measure the flow characteristics in the tank and analyze the solid waste removal under different working conditions. Residual mass of the solid waste, time of complete removal of solid waste, average velocity (v_{avg}), and uniformity coefficient of velocity distribution (DU_{50}) were analyzed to evaluate the solid waste removal efficiency. The obtained results indicate that adjustments of the inlet layout significantly affect the solid waste removal efficiency. It was found that a single-inlet tank with a d/a of 1/8 and θ in the range 10° to 40° has a good solid wastes removal performance, and the optimal efficiency occurs at a jetting angle of 30°. Moreover, the optimal solid waste removal efficiency in a dual-inlet tank can be achieved with a d/a ratio of 1/8 and a θ of 20°. The performed analyses reveal that from the aspect of solid waste removal efficiency, a tank with a d/a ratio of 1/8 outperforms a tank with a d/a ratio of 1/4 or 1/50. The results of this article offer novel insights in the layout of octagonal RAS tanks and provide a guideline to improve self-cleaning features of aquaculture tanks.

KEYWORDS

RAS, inlet layout, solid waste removal efficiency, flow field, octagonal aquaculture tank

1 Introduction

Studies show that China's aquaculture industry has increased steadily in the past few decades. In 2021, China's aquatic and aquaculture products exceeded 67 million and 54 million, respectively (Fisheries and Fishery Administration Bureau of the Ministry of Agriculture and Rural Zones et al., 2022). Despite these promising data, the traditional aquaculture development model is a challenge for the stringent environmental requirements, the safety of aquatic food, and the development of aquaculture (Zhang et al., 2017). Recently, Recirculating Aquaculture System (RAS) has been proposed as an advanced aquaculture method with remarkable advantages to optimize the water consumption in the aquaculture industry and improve the efficiency of aquaculture and land utilization. Studies show that RAS has made great progress in water disinfection, water purification, and the physiological and biochemical metrics in the aquaculture industry (Timmons et al., 1998). The performed analyses revealed that rapid solid waste flushing out of RAS tanks is an essential prerequisite to achieve an appropriate hydrodynamic performance and fish welfare (Gorle et al., 2020). In this scheme, different inlet layouts affect the solid waste removal efficiencies. However, considering the current shortcomings of a rational-based design on inlet layout on the solid waste removal efficiency of octagonal RAS tanks, conventional systems in the aquaculture industry is largely relying on previous experience. Therefore, it is necessary to systematically optimize the inlet layout to form an appropriate aquaculture flow field environment while improving the removal efficiency.

Duarte et al. (2011) showed that the tank geometry significantly affects the overall flow pattern. Generally, aquaculture tanks are fabricated in five geometries, including rectangular, circular, octagonal, rectangular round chamfering, and runway. Among these geometries, octagonal tanks are easier to handle and construct than other tanks so that octagonal tanks have been more common in operational production (Zhao et al., 2022). Davidson and Summerfelt (2004) studied the effects of the inlet structure on the self-cleaning features of large circular aquaculture tanks and found that the appropriate direction of the inlet structure increases the rotation velocity in the tank. Moreover, Zhu et al. (2022) conducted experiments and studied the removal of solid wastes, and analyzed the flow field in a circular aquaculture tank with different inlet layouts. It was found that adjusting the inlet layout would affect the flow field characteristics and the solid waste removal efficiency. Venegaset et al. (2014) systematically evaluated the effect of different water injection devices on the tangential velocity of flow in octagonal RAS tank. Benoit (2007) showed that the structure of the water inlet and outlet systems significantly affects the hydraulic mixing performance and the flushing ability of precipitated particles in the tank. In addition to experiments, numerical techniques have been widely applied to analyze the flow field and improve solid waste removal efficiency (Xue et al., 2020; Ren et al., 2021). Gorle et al. (2018a) studied the use of wall drain to control flow patterns in the tank. It was found that flow features such as pressure, velocity, uniformity, and turbulence affect the flow pattern so these features should be further investigated. The octagonal RAS tank is a common culture tank with good space management, shared side walkways, and homogeneous fluid mixing, which is widely used in aquaculture farms. Considering the production and welfare of animals in intensive aquaculture, the design and application of octagonal tanks should be given more attention in future research (Xue et al., 2021; Zhao et al., 2022). However, there is no in-depth investigation of the effects of inlet layout on the performance of octagonal RAS tanks.

Based on the performed literature survey, the main objective of the present study is to investigate the influence of inlet layout on the solid waste removal efficiency of octagonal tanks and measure the flow field distribution to explore the hydrodynamic feature of the tank. In this respect, the effects of numerous parameters, including the inlet mode, inlet angle, and inlet position on the efficiency of solid waste removal are investigated comprehensively to maximize the water conservancy conditions. This article is organized in five sections. After introducing the problem and a review of the literature, materials and methods and the experimental setup are discussed in Section 2. The Influence of the inlet layout on the solid waste removal efficiency, hydrodynamic characteristics, and flow patterns are presented in Section 3. Then the obtained results are analyzed to achieve an insight into the mixing phenomenon and the discussions are presented in Section 4. Finally, the main conclusions are summarized in Section 5.

2 Material and methods

2.1 Tank configuration

In the present study, experiments were carried out using a RAS system consisting of an octagonal aquaculture tank model, a recirculating system, and a measurement system. During the experiments, solid waste removal (Figure 1A) and PIV flow field (Figure 1B) were studied. The tank model is made of transparent acrylic sheets and the dimensions of the test setup are presented in Figure 2. The tank model has a total side length of a = 100 cm and a height of 60 cm. Lekang (2013) demonstrated that optimal performance in an octagonal tank is achieved with a ratio of total side length to the corner side length of 5. Accordingly, four rectangular acrylic baffles with a height of 60 cm and a width of 28.28 cm were installed in four corners to form the octagonal aquaculture tank. The tank bottom was flat and a drain hole with a diameter of 4 cm was set in the tank center. The inlet pipe had a closed lower end and delivered water into the tank through 3 nozzles with a diameter of 2 cm. The diameter of nozzles were 0.6 cm and the distance of each nozzle from the end of the pipe was 2, 16.5, and 31 cm, respectively.

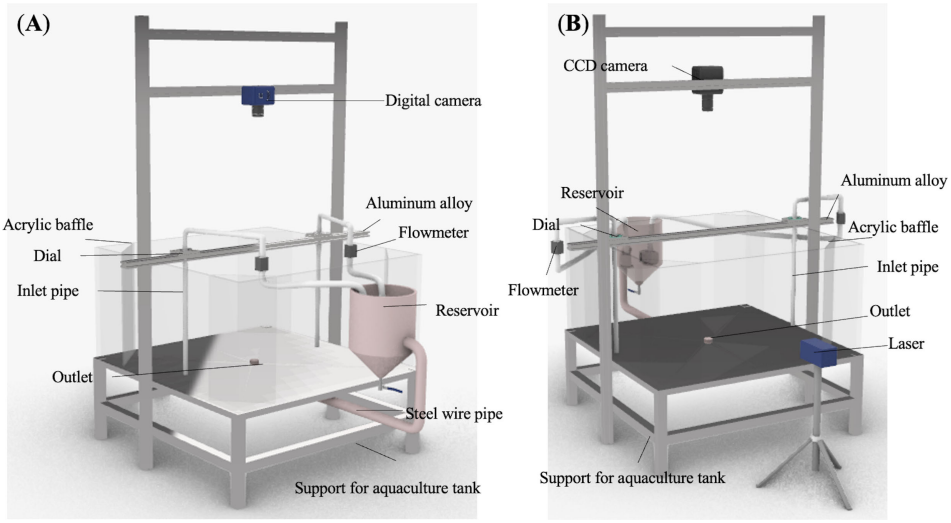

FIGURE 1
Configuration of the experiment setup: **(A)** Solid waste removal system; **(B)** PIV flow field measurement system.

Figure 3 shows that the recirculation system mainly consists of a reservoir (Figure 3A), pipes, and a 55 W water pump (Sensen HQB-2500, China) (Figure 3B). The tank water runs into the reservoir through the connecting tube and then returns to the tank using the water pump, creating a water recirculation system. The measurement system is schematically presented in Figure 3C. A flowmeter (Keyence FD-Q20C, Japan) and a valve are installed vertically on the water inlet pipe to monitor and adjust the real-time input flow rate (L/min) into the aquaculture tank to guarantee the hydraulic residence time (HRT) of 30 min approximately (the water exchange rate is 2 times/h). Note that the input flow rate was set constant during the experiments so as to isolate its coupled effects with jetting configuration. Thus, the effect of jetting configuration on solid waste removal can be comprehensively figured out. An inlet assembly (Figure 3D) was designed to adjust the inlet layout and the jetting angle was measured by a dial (Figure 3E). Moreover, a digital camera (Nikon P7100, Japan) was installed over the tank to capture the distribution of solid wastes in the tank bottom. To this end, the surface of the bottom layer was covered with a white architectural film to increase the contrast between solid wastes and the background layer and improve the accuracy of the

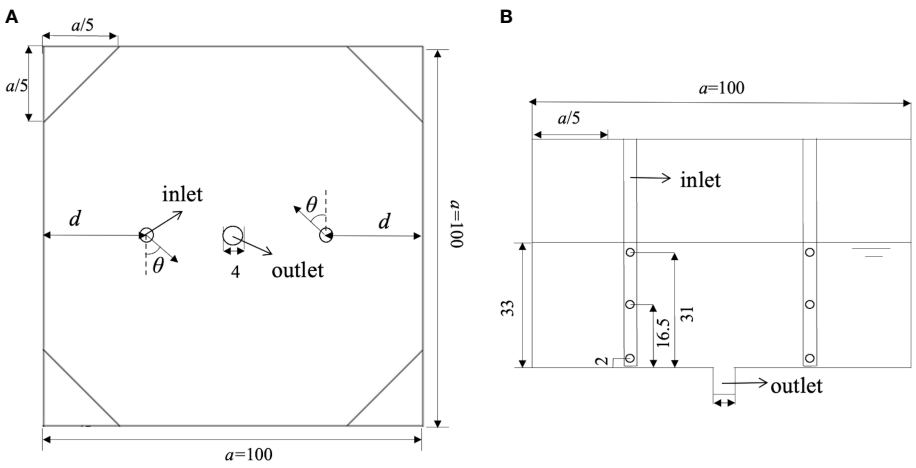

FIGURE 2
Configuration of the octagonal aquaculture tank: **(A)** Top view; **(B)** Front view (Unite: cm).

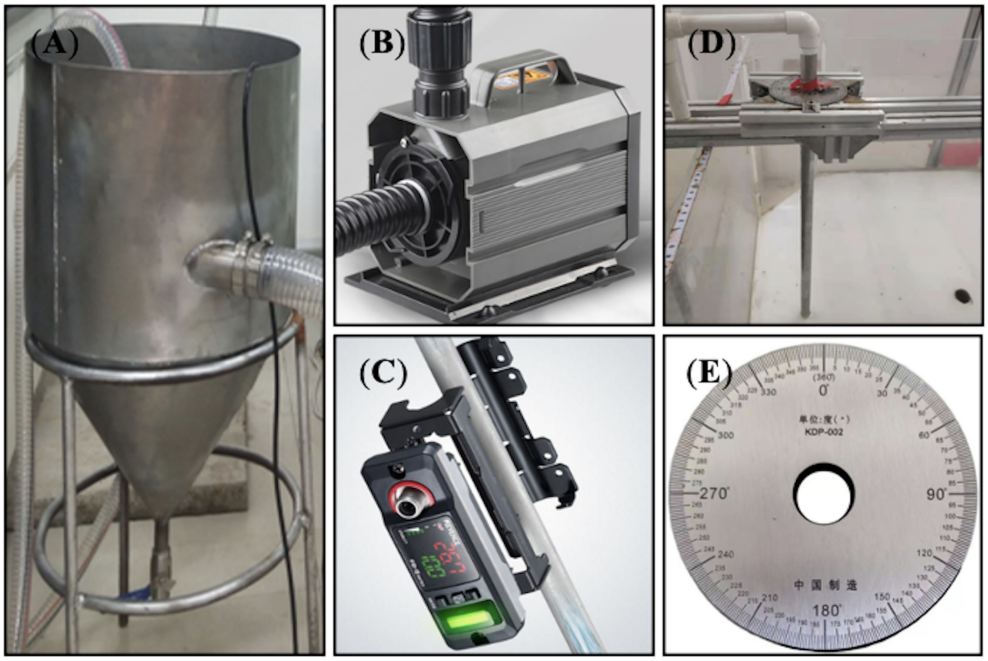

FIGURE 3
Main components of the experiment: **(A)** Reservoir; **(B)** Water pump; **(C)** Flowmeter; **(D)** Inlet assembly; **(E)** Dial.

analysis. Based on related previous studies (Patterson et al., 1999; Du et al., 2020; Davidson and Summerfelt, 2004; Sin et al., 2021; Xue et al., 2022), cylindrical-shaped feed with a diameter of 1.4 mm, a length of 2.0 to 2.5 mm and a density of 1.3 g/cm^3 were used to study the motions of settable solid waste such as uneaten feed and fish feces in the tank. The flow velocity was measured using the PIV system, which consists of a CCD camera, a laser device, and some particle tracers. In order to improve the quality of PIV images, black paint was sprayed on the bottom surface to eliminate undesired background light. In all experiments, tap water was used and the tank was filled to a depth of 33 cm to achieve a diameter-to-depth ratio of 1:3 and meet the design requirement for water depth (Lekang, 2013; Summerfelt et al., 2016).

In the present study, the influence of inlet mode, inlet jetting angle, and inlet jetting position on the octagonal aquaculture tank were analyzed comprehensively. It should be indicated that the inlet mode refers to the number of inlet pipes. In this regard, an inlet system with one pipe and two pipes is hereafter called single inlet mode and dual inlet mode, respectively. Moreover, the jetting angle refers to the acute angle between the jetting direction and the nearest tank wall. Therefore, the jetting angles of 0° and 90° are parallel and perpendicular to the nearest wall of the tank, respectively. Ten jetting angles of 0°, 10°, 20°, 30°, 40°, 45°, 50°, 60°, 70° and 80° were analyzed in the experiments. Particularly, the angle of 45° is also included for it is widely used in aquaculture practices (An et al,. 2018; Gorle et al., 2018b; Dauda et al., 2019). The jetting position refers to the position of the inlet pipe which is deployed in the tank. This parameter is reflected by d/a, where d is the distance from the pipe axis to the tank side. Based on the inlet pipe deployments that are commonly used in aquaculture practices, three jetting positions of d/a= 1/50, 1/8, and 1/4 were considered in the experiments. It should be indicated that when d/a= 1/50, the inlet pipe is just next to the tank wall. Further details of the experiment will be discussed in the following section.

2.2 Experimental procedure

Experiments were carried out in a laboratory-scale octagonal aquaculture tank in National Engineering Research Center for Marine Aquaculture, Zhoushan, China. The experimental procedures can be summarized as follows:

2.2.1 Solid waste removal experiment

The experimental cases can be categorized into single-inlet and dual-inlet cases. In each mode, three jetting positions (d/a) of 1/50, 1/8, and 1/4 and ten jetting angles of 0°, 10°, 20°, 30°, 40°, 45°, 50°, 60°, 70°, and 80° were considered. In total, 60 cases were analyzed in this section and each case was tested triple. A four-step framework was established to perform the experiments.

(1) Adjust the inlet layout of the jetting mode, jetting position, and jetting angle for each case. (2) Adjust the water

level in the tank and turn on the water pump to circulate water. After 30 minutes and achieving a steady-state condition, switched on the camera and settable feed (10 g) was evenly sprinkled into the tank as quickly as possible. Moreover, run the stopwatch to measure time. (3) Monitor the removal process of solid wastes by manual visual inspection. Based on previous studies (Summerfelt et al., 2016; Xue et al., 2022), the maximum monitoring time is set to 30 minutes. If the solid wastes are not drained completely after 30 minutes, the experimental system will be stopped and the residual solid waste will be collected by siphon, and the solid waste will be dried in the oven and weighted. On the other hand, if the solid waste removal process is completed in less than 30 minutes, the experiment will be stopped whenever the solid waste removal is completed. (4) Analyze the solid waste removal process using the captured images and compare the weight of the residual solid waste (Figure 4).

2.2.2 PIV flow field measurement experiment

In the experiment, the PIV technique was applied to measure the flow characteristics in the tank and investigate the solid waste removal mechanism under different working conditions. It is worth noting that the PIV technique gives quantitative information about the transient flow and is the most widely used flow velocity measurement technology in the field of experimental fluid mechanics (Robinson, 1991). Compared with single-point measuring instruments, the PIV technique can be applied to measure instantaneous flow fields without interference.

The measurements were carried out in a dark room in the Marine Measurement Laboratory of Qingdao Optical Flow Software Technology Co., Ltd, China. The main procedures of the PIV flow field experiment are consistent with those of the solid waste removal experiment (Figure 5). However, no solid waste was sprinkled into the aquaculture tank during the experiment due to the following facts: (1) Solid waste in the tank for a long time will affect the water clarity, thereby weakening the penetration degree of the laser and affecting the PIV results; (2) Solid waste has very little effect on the flow field. Since the removal of solid wastes is closely related to the bottom flow field, a CCD camera (5120 × 3800 pixels, 16 fps max) was deployed just above the tank to capture the tracer particles on the horizontal bottom layer. Accordingly, flow velocity contours and streamline patterns were obtained to analyze hydrodynamic parameters and flow field distributions. The captured images were preliminary processed using Flow pattern tracking master V50 software (Qingdao Optical Flow Software Technology Co., Ltd.) and then they were refined in the MATLAB (R2020b) platform to thoroughly analyze flow velocity and visualize the captured data. Figure 6 shows the obtained results in this respect.

2.3 Hydrodynamic analysis of a RAS aquaculture tank

A review of the literature indicates that different optimal velocities have been proposed to maximize the health and growth of fish in the aquaculture industry (Oca et al., 2007; Masaló et al., 2016; Wang, 2019). Generally, fish incline to swim in water with high dissolved oxygen. Accordingly, heterogeneous distribution of dissolved oxygen promotes fish aggregation due to higher spontaneous activity, which increased the risk of wound infection. Therefore, rapid solid waste flushing out of the culture tanks is an important prerequisite to increase fish welfare and aquaculture yield.

Average velocity (v_{avg}) and uniformity coefficient of velocity distribution (DU_{50}) were comprehensively analyzed to evaluate the solid waste removal efficiency. To this end, the effects of the inlet layout on the homogeneity of water velocity were determined using Eq. (1) (Masaló and Oca, 2007; Masaló and Oca, 2010; Masaló and Oca, 2014). In this equation, DU_{50} is a parameter to adjust the average velocity of a specific tank to meet the self-cleaning requirements and reach the desired distribution of the dissolved oxygen. The average velocity (v_{avg}) was measured using the PIV technique. It should be indicated that DU_{50} and v_{avg} can be mathematically expressed in the form below (Venegas et al., 2014):

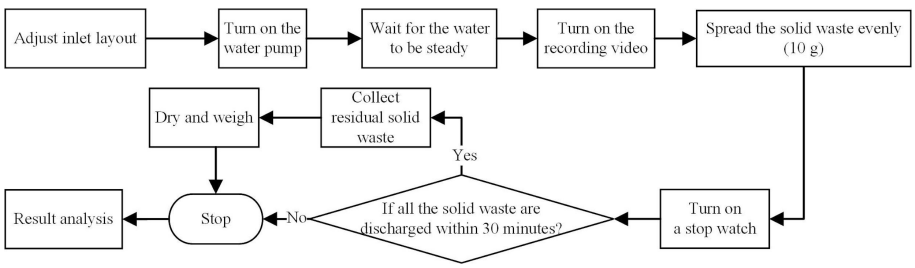

FIGURE 4
Flowchart of solid waste removal experiment.

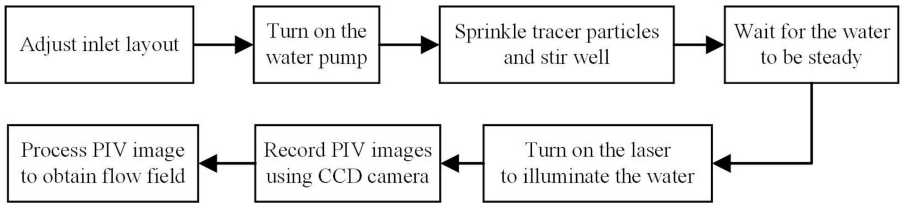

FIGURE 5
Flowchart of the flow field measurement experiment.

$$DU_{50} = \frac{v_{50}}{v_{\text{avg}}} \times 100 \quad (1)$$

$$v\text{avg} = \frac{\sum_{i=1}^{n} v_i r_i}{\sum_{i=1}^{n} r_i} \quad (2)$$

where v_{50} is the average velocity of the first 50% measured values at each point and v_{avg} is the average weighted velocity of 9240 points of a depth section, which can be measured by the PIV technique. Meanwhile, v_i is the velocity of the monitoring point, r_i denotes the distance from the monitoring point to the tank center, and i is the number of cross-sectional monitoring points at a certain depth.

3 Results

3.1 Influence of the inlet layout on the solid waste removal efficiency

Figure 7 shows that in some cases, the solid wastes can be discharged completely within 30 minutes, while the complete discharge does not occur in other cases. Obviously, the cases with complete discharge have higher performance in self-cleaning. In the present study, a systematic comparison was carried out between all the experimental cases, the incomplete removal cases were also analyzed based on the residual mass in the aquaculture tank.

Figure 8 shows the time taken for complete solid removal. It is reminded that complete removal of solid waste does not occur in all cases. The horizontal and vertical axis represent the jetting angle and the corresponding time for complete solid removal. This figure does not cover the cases in which the solid waste removal does not complete in 30 minutes. It is observed that in the tank with a single inlet and d/a of 1/50 and 1/8, the time taken for the complete removal of solid waste increases with an increase in the jetting angle. The minimum evacuation time occurs at the jetting angles of 10° and 40°. Figure 8A indicates that when d/a is set to 1/4 and θ increases from 10° to 45°, all solid wastes are discharged from the aquaculture tank, and the optimal solid waste removal efficiency occurs at the jetting angle of 10°. Figure 8B reveals that in a tank with dual inlets and d/a of 1/50, the lowest solid waste removal time can be achieved at a jetting angle of 10°. When d/a is set to 1/8, the time taken for complete solid waste removal increases monotonically from 10° to 60°. When the jetting angle exceeds 60°, solid waste could not be completely discharged from the aquaculture tank. When d/a is set to 1/4, the complete removal of solid waste can be achieved only for jetting angles less than 30°.

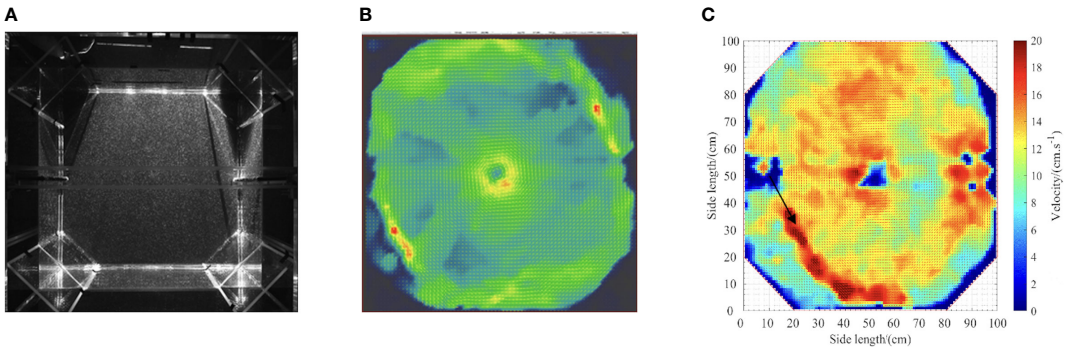

FIGURE 6
Image processing of PIV data: **(A)** Raw PIV image; **(B)** Preliminary treatment; **(C)** Refined treatment.

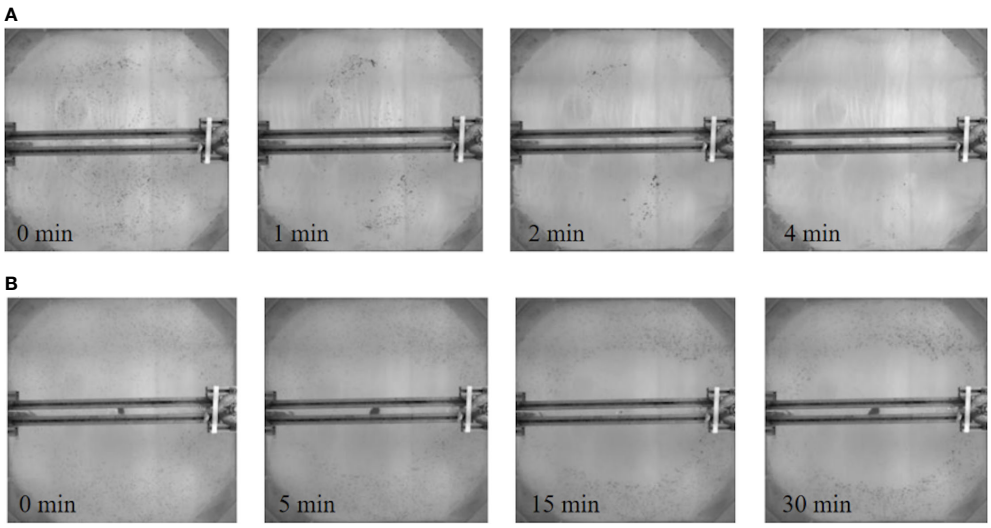

FIGURE 7
Samples of **(A)** complete and **(B)** incomplete solid waste removal processes within 30 minutes.

Figure 9 shows the residual mass of solid waste in cases where the solid waste removal does not complete in 30 minutes. It should be reminded that this figure does not cover the cases in which the complete removal time is larger than 30 minutes. Figure 9A presents the mass of the residual solid waste in a tank with a single inlet. It is observed that when θ is set to 80°, the aquaculture tank existed residual solid waste by different degrees in each working condition. When d/a=1/4 and θ=80°, the residual mass of solid waste was higher than that at θ=0°, 70°, and 60°. Figure 9B shows the distribution of the residual mass of solid waste in the tank with dual inlets and a jetting angle of 60° to 80°. It is found that this configuration has low performance in solid waste removal.

Compared with other working conditions, the tank with a single inlet and a d/a of 1/8 has a relatively low solid waste removal time regardless of the jetting angle. When d/a is set to 1/50, not all of the solid waste is discharged from the tank within 30 minutes, but the residual mass of solid waste is minimum at d/a=1/4. In this section, the tank performance with a dual inlet system and four different jetting angles were analyzed. It was found that the lowest time of complete solid removal can be achieved for d/a=1/8. When θ was increased from 60° to 80°, the solid waste could not be completely discharged regardless of the jetting position. At a given flow rate in a single-inlet aquaculture tank, a reasonable solid waste removal efficiency can be achieved when d/a is set to 1/8 and the jetting angle θ increases from 30° to 40°.

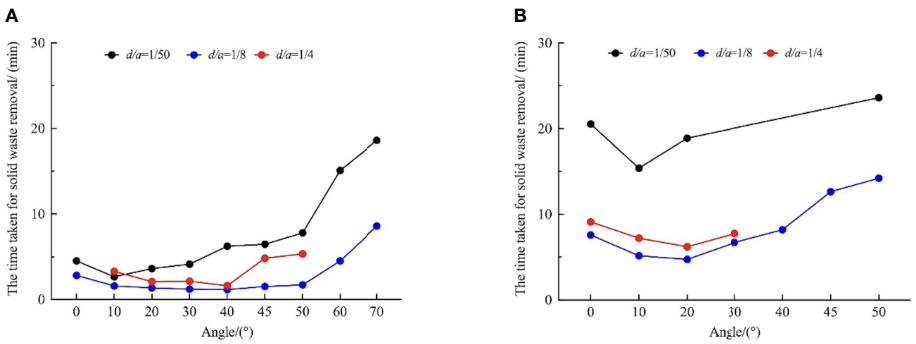

FIGURE 8
The time taken for solid waste removal under different conditions: **(A)** Single-inlet mode; **(B)** Dual-inlet mode.

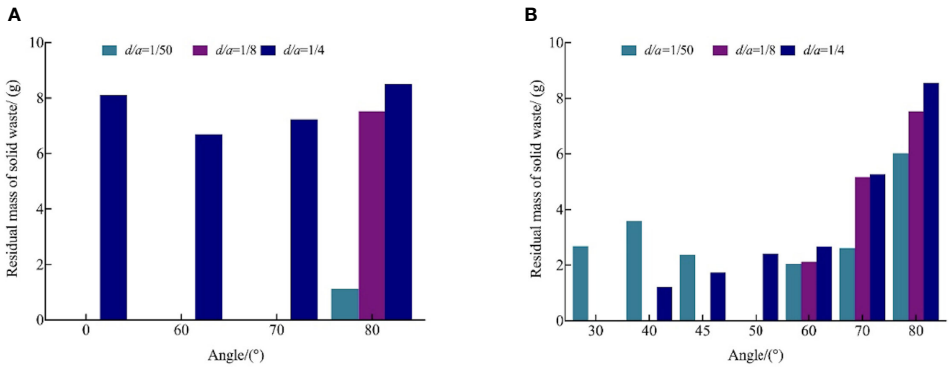

FIGURE 9
Residual mass of solid waste under different conditions: **(A)** Single-inlet mode; **(B)** Dual-inlet mode.

3.2 Influence of the inlet layout on the hydrodynamic characteristics of the tank

Masaló and Oca (2016) showed that the removal of solid waste is closely related to the flow field and hydrodynamic characteristics of the aquaculture tank. In this regard, parameter DU_{50} was introduced as a powerful tool to evaluate different configurations in a RAS tank.

The results of the average velocity and uniformity coefficient of velocity distribution under different conditions are shown in Figures 10 and 11, respectively. It is observed that in a single-inlet tank with a d/a of 1/50, as the jetting angle θ increases from 10° to 80°, the average velocity v_{avg} decreases, thereby decreasing DU_{50}. When d/a=1/8, the highest v_{avg}, and DU_{50} can be obtained at a jetting angle of 30° and 20°, respectively. When d/a=1/4, the highest v_{avg}, and DU_{50} occur at θ=20°. Figures 10B and 11B show that in a dual-inlet tank with a d/a of 1/50, as the jetting angle increases, v_{avg} decreases continuously, while DU_{50} decreases first and then increases. It is found that the maximum and minimum values of DU_{50} occur at jetting angles of 10° and 80°, respectively. When d/a=1/8, both v_{avg} and DU_{50} decrease with the increase in the jetting angle, and the maximum values of v_{avg} and DU_{50} occur at θ=20°. When d/a=1/4, the average velocity v_{avg} increases first and then decreases with the increase in the jetting angle, and the maximum value occurs at θ=40°.

3.3 Influence of the inlet layout on the flow field pattern

In a RAS tank, an effective solid waste collection strategy ensures clean and stable water quality. Meanwhile, the distribution of the flow velocity highly depends on solid waste removal efficiency. In this regard, the PIV technique was used and image processing was carried out on the MATLAB platform to visualize the measurements.

In the present study, sixty tests were carried out to analyze the flow field. Effects of the inlet layout in terms of the flow field on the

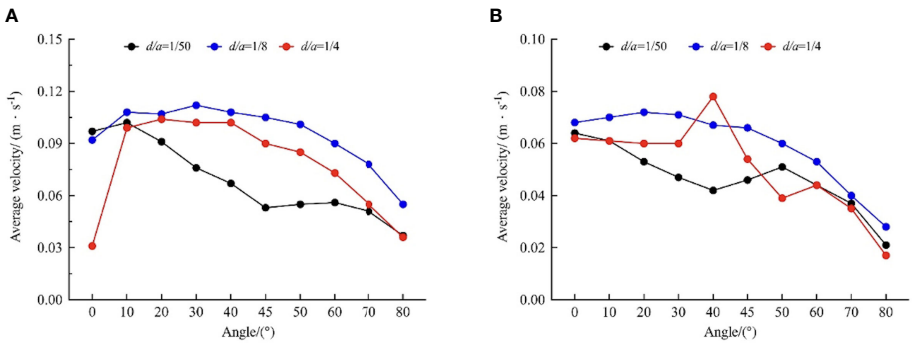

FIGURE 10
Distribution of the average velocity under different conditions: **(A)** Single-inlet mode; **(B)** Dual-inlet mode.

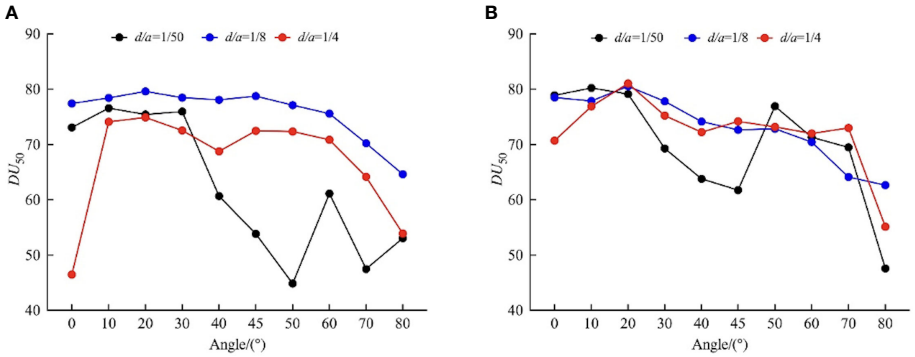

FIGURE 11
Distribution of the uniformity coefficient under different conditions: **(A)** Single-inlet mode; **(B)** Dual-inlet mode.

horizontal bottom plane were explained using velocity contours. In order to analyze the tank performance in removing solid wastes, the flow field characteristics are discussed in this section. Figures 12 and 13 show the flow fields of the best and worst cases in a single-inlet and a dual-inlet tank, respectively. The long black arrow represents the jetting angle of inlet, the color denotes the information of velocity magnitudes, the blue represents the lower velocity zone, and the red represents the higher velocity zone.

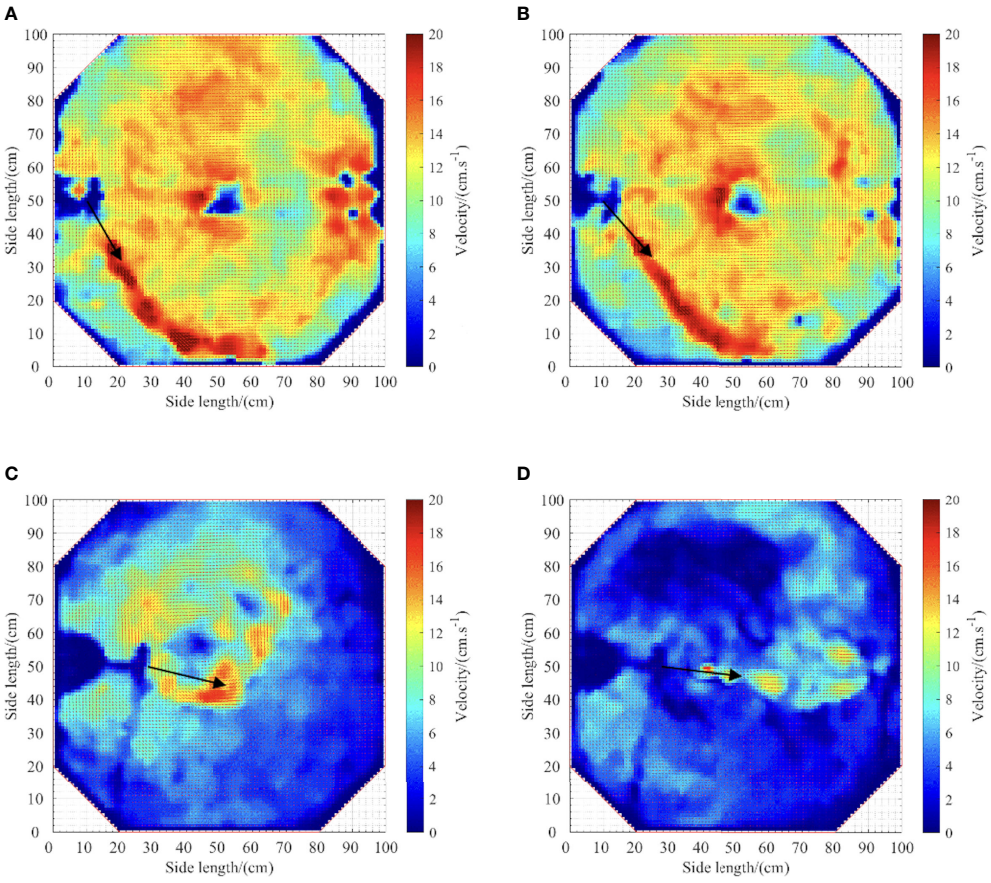

FIGURE 12
Flow field contours in a single-inlet aquaculture tank: **(A)** d/a=1/8; θ=30°; **(B)** d/a=1/8; θ=40°; **(C)** d/a=1/4; θ=70°; **(D)** d/a=1/4; θ=80°.

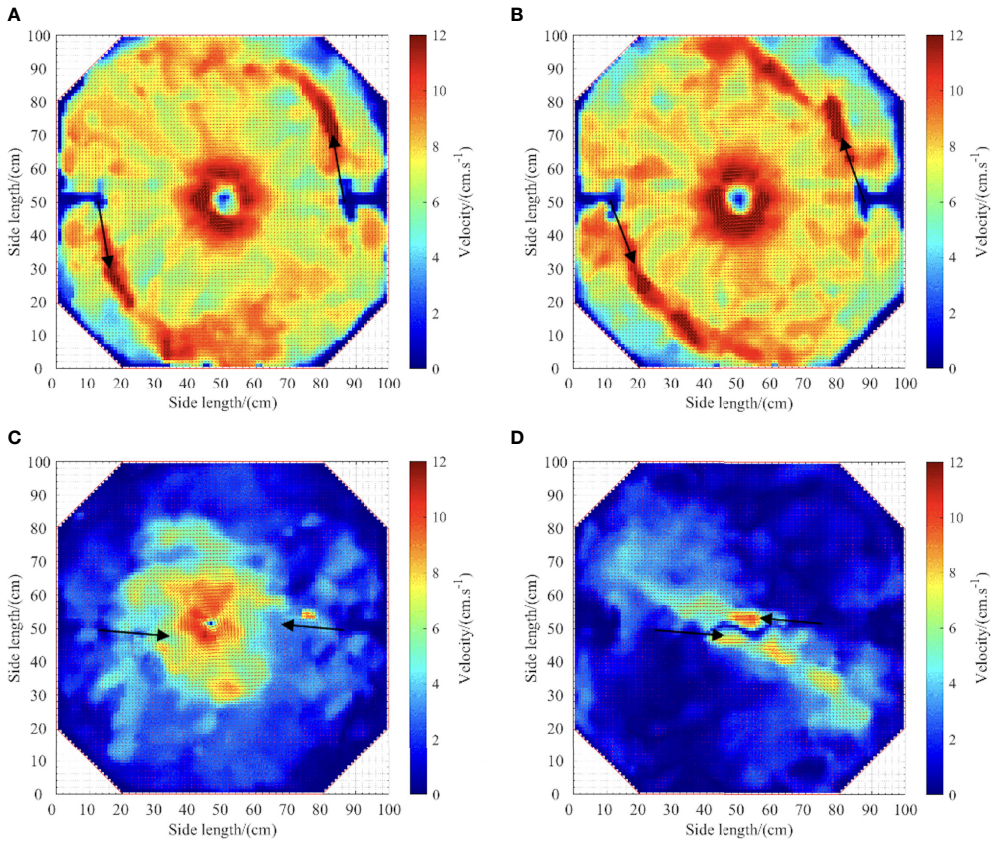

FIGURE 13
Flow field contours in a dual-inlet aquaculture tank: **(A)** d/a=1/8; θ=10°; **(B)** d/a=1/8; θ=20°; **(C)** d/a=1/8; θ=80°; **(D)** d/a=1/4; θ=80°.

Figures 12A, B show that a single-inlet tank with a d/a of 1/8 and a jetting angle of 30°-40° has a reasonable performance in removing solid wastes. It is observed that the solid waste removal efficiency with d/a=1/8 is higher than those with d/a=1/4 or 0. Accordingly, it is concluded that there is a high-intensity circulation near the outlet and only in a small zone of the low-velocity zone, which forms near the tank wall. Since high velocities in the central zone promote solid waste settling, this phenomenon has consequences on the self-cleaning features of the tank. When d/a =1/4, the solid waste removal efficiency is low for θ=70° and 80°. Figures 12C, D show that the jetting position and the center of the tank could be regarded as the radius of circular motion and there is a high-velocity region near the jetting where the water flow is driven by the vortex in the tank center. It is worth noting that the jetting position is a major contributor to the motion of the solid waste in the tank. The water flow makes a circular motion around the tank and the flow velocity gradually decreases from the tank center to the tank periphery. There is no circulation without a high-velocity zone around the tank.

Figures 13A, B show that in the dual-inlet tank with d/a=1/8, the highest solid waste removal efficiency, highest overall flow velocity, and good hydrodynamic characteristics can be achieved with jetting angles θ of 10° and 20°. The water flow rapidly contacts the tangent angle of the tank and brings sufficient orientation function, thereby forming a vortex in the center of the tank. Consequently, the energy loss caused by refraction and reflection reduces significantly. Obviously, the inlet angle is close to the center of the tank, and only a small circulation zone forms in the center of the tank, while Figures 13C, D reveal that there is a large zone of low-velocity flow around the tank wall at the jetting angle of 80°.

4 Discussion

Reaching a uniform flow distribution is a great challenge in the design and operation of culture tanks to improve feed efficiency, achieve good mixing, and improve water quality (Gorle et al., 2018a). The average velocity of the flow is proportional to the uniformity coefficient of the velocity distribution in experiments caused by the circulation vortex. The performed analyses demonstrate that when the flow velocity reaches a certain value, a vortex would appear. The variation of

vortex velocity is that the velocity diffuses and attenuates outward from the center, and the attenuation process is gradual, thus the evolution of the velocity in the tank is reflected in gradient descent. On the contrary, there is often no vortex and the kinetic energy tank is completely driven by the jetting port. Therefore, the energy attenuation is easier to occur and the velocity difference is more obvious. What's more, rapid removal of residual uneaten feed and fish feces in tanks is necessary for adequate fish welfare and performance. Xue et al. (2022) used the CFD-assisted design to investigate the hydrodynamics and self-cleaning property. The results showed that hydrodynamics is the direct-acting factor in the self-cleaning property of the aquaculture tank system and the existing culture tank could be improved by adjusting the inlet pipe layout position appropriately.

The configuration of experimental setups was consistent with those reported in (Oca and Masaló, 2007; Oca and Masaló, 2013), in which the effect of the straight cut angle on the inlet flow rate was studied in the rectangular aquaculture tank with a length/width (L/W) ratio of 0.95. When d/a=1/50, the straight cut angle brings the diversion effect sufficiently. Moreover, the energy loss greatly increases by the friction between the water flow and the tank wall. In this case, the solid waste around the tank hardly approaches the center. When d/a=1/8, a closed triangular zone does not form anymore so there is no backflip around the hypotenuse wall. These results are consistent with those reported by Wu and Gao (2005) . Xue et al. (2020) showed that small-scale turbulence forms between the inlet port and the tank wall, and the inlet structure promotes the creation of local jets and vortices behind them, which will adversely affect the solid waste removal efficiency. When d/a=1/4, more low-velocity zones appear at jetting angles of 70° and 80°, and the solid waste removal efficiency is lower than that of other cases (Gorle et al., 2020).

With a constant flow supplied in a confined domain, the velocity gradient mainly appears near the tank center, where the flow velocity is much higher than that of experiments with a dual-inlet tank. These results are consistent with those reported by Labatut et al. (2007). In a single-inlet tank, Zhang et al. (2022) showed that there is an optimal solid waste removal efficiency in a tank with a jetting angle of 15°. Compared with experimental results, the calculated results have small deviations, which may be attributed to the difference in hydraulic retention times. Gorle et al. (2019) revealed that radial orientation of lower inlet nozzles in a dual-inlet tank improves the overall hydrodynamic performance of the tank. However, these investigations were mainly focused on the effect of single factors on the tank performance and did not consider the possible effect of turbulence generated by the interaction between the jetting position and the jetting angle. Significantly, Zhao et al. (2022) pointed out that flow velocity in culture tanks can be adjusted to provide much higher swimming speeds and thus effectively exercise fish. Therefore, the design of the velocity must meet the self-cleaning ability and speed requirements of the fish growth jointly in actual aquaculture engineering.

5 Conclusion

In the present study, the effect of the inlet layout on the solid waste removal efficiency of the octagonal RAS tank is analyzed. To this end, the flow pattern in an octagonal RAS tank was investigated using the PIV technique. It was found that the inlet layout has a considerable impact on the solid waste removal efficiency of the aquaculture tank. The main conclusions can be summarized as follows:

1. A single-inlet tank with a d/a ratio of 1/8 has higher solid waste removal efficiency than a similar tank with a d/a ratio of 1/4 or 1/50. When the jetting angle θ varies in the range of 10 ~ 40°, the tank has reasonable self-cleaning features, and optimal solid waste removal efficiency can be achieved with d/a=1/8 and θ =30°.

2. A dual-inlet tank with a d/a ratio of 1/8 has higher solid waste removal efficiency than a similar tank with a d/a ratio of 1/4 or 1/50. When d/a=1/8, the optimal solid waste removal efficiency can be achieved for θ=10° or 20°.

3. For a given flow rate and a large jetting angle, the water flow in a dual-inlet tank is easily affected by resistance, and the energy consumption increases, which is not conducive to the removal of solid waste. Accordingly, the single-inlet tank outperforms the dual-inlet tank from the aspect of velocity performance.

Data availability statement

The original contributions presented in the study are included in the article/supplementary material. Further inquiries can be directed to the corresponding authors.

Ethics statement

The ethics committee approval from the authors' institution have been obtained for this study.

Author contributions

JH: Data curation, Formal analysis, Writing-original draft; DF: Conceptualization, Funding acquisition, Resources, Writing-review & editing; XQ: Conceptualization, Funding acquisition, Resources, Supervision; HZ: Methodology, Software; LW: Conceptualization, Supervision; XZ:

Investigation, Methodology; FG: Conceptualization, Funding acquisition, Resources. All authors contributed to the article and approved the submitted version.

Funding

This research was funded by the National Natural Science Foundation of China under grant number 31902425, the Natural Science Foundation of Zhejiang Province under grant number LGN21C190010, LGN19C190001 and the Bureau of Science and Technology of Zhoushan under grant number 2020C21003, 2021C31023.

Acknowledgments

The authors would like to thank all the reviewers who participated in the review, as well as MJEditor (https://www.mjeditor.com) for providing English editing services during the preparation of this manuscript.

Conflict of interest

The authors declare that the research was conducted in the absence of any commercial or financial relationships that could be construed as a potential conflict of interest.

Publisher's note

All claims expressed in this article are solely those of the authors and do not necessarily represent those of their affiliated organizations, or those of the publisher, the editors and the reviewers. Any product that may be evaluated in this article, or claim that may be made by its manufacturer, is not guaranteed or endorsed by the publisher.

References

An, C.-H., Sin, M.-G., Kim, M.-J., Jong, I.-B., Song, G.-J., and Choe, C. (2018). Effect of bottom drain positions on circular tank hydraulics: CFD simulations. *Aquac. Eng.* 83, 138–150. doi: 10.1016/j.aquaeng.2018.10.005

Benoit, D. (2007). Hydrodynamic chanracteristics of muti-drain circular tanks. [*dissertation/master's thesis*]. [Canada (NB)]: University of New Brunswick.

Dauda, A. B., Ajadi, A., Tola-Fabunmi, A. S., and Akinwole, A. O. (2019). Waste production in aquaculture: Sources, components and managements in different culture systems. *Aquac. Fish.* 4, 81–88. doi: 10.1016/j.aaf.2018.10.002

Davidson, J., and Summerfelt, S. T. (2004). Solids flushing, mixing, and water velocity profiles within large (10 and 150 m^3) circular' Cornell-type' dual-drain tanks. *Aquac. Eng.* 32 (1), 245–271. doi: 10.1016/j.aquaeng.2004.03.009

Duarte, S., Reig, L., Masalo, I., Blanco, M., and Oca, J. (2011). Influence of tank geometry and flow pattern in fish distribution. *Aquacult. Eng.* 44 (2), 48–54. doi: 10.1016/j.aquaeng.2010.12.002

Du, Y., Chen, F., Zhou, L., Qiu, T., and Sun, J. (2020). Effects of different layouts of fine-pore aeration tubes on sewage collection and aeration in rectangular water tanks. *Aquac. Eng.* 89, 102060. doi: 10.1016/j.aquaeng.2020.102060

Fisheries and Fishery Administration Bureau of the Ministry of Agriculture and Rural Zones. National Aquatic Technology Promotion Center, China Fisheries Association. China Fishery Statistical Yearbook. (Beijing: China Agriculture Press) (2022) pp. 17. *(China Fishery Statistical Yearbook)*

Gorle, J., Terjesen, B., and Summerfelt, S. (2020). Influence of inlet and outlet placement on the hydrodynamics of culture tanks for Atlantic salmon. *Int. J. Mech. Sci.* 188, 105944. doi: 10.1016/j.ijmecsci.2020.105944

Gorle, J. M. R., Terjesen, B. F., Mota, V. C., and Summerfelt, S. (2018b). Water velocity in commercial RAS culture tanks for Atlantic salmon smolt production. *Aquac. Eng.* 81, 89–100. doi: 10.1016/j.aquaeng.2018.03.001

Gorle, J. M. R., Terjesen, B. F., and Summerfelt, S. T. (2018a). Hydrodynamics of octagonal culture tanks with Cornell-type dual-drain system. *Comput. Electron. Agric.* 151, 354–364. doi: 10.1016/j.compag.2018.06.012

Gorle, J. M. R., Terjesen, B. F., and Summerfelt, S. T. (2019). Hydrodynamics of Atlantic salmon culture tank: Effect of inlet nozzle angle on the velocity field. *Comput. Electron. Agric.* 158, 79–91. doi: 10.1016/j.compag.2019.01.046

Labatut, R. A., Ebeling, J. M., Bhaskaran, R., and Timmons, M. B. (2007). Effects of inlet and outlet flow characteristics on mixed-cell raceway (MCR) hydrodynamics. *Aquac. Eng.* 37 (2), 158–170. doi: 10.1016/j.aquaeng.2007.04.002

Lekang, O. I. (2013). *Aquaculture engineering: Second edition* (Britain: Blackwell Pub Professional).

Masaló, I., and Oca, J. (2014). Hydrodynamics in a multivortex aquaculture tank: Effect of baffles and water inlet characteristics. *Aquac. Eng.* 58, 69–76. doi: 10.1016/j.aquaeng.2013.11.001

Masaló, I., and Oca, J. (2016). Influence of fish swimming on the flow pattern of circular tanks. *Aquac. Eng.* 74, 84–95. doi: 10.1016/j.aquaeng.2016.07.001

Masaló, I., and Oca, J. (2010). Distribution of velocities in aquaculture circular tanks with rotating flow and evaluation of uniformity. a: Aquaculture Europe 2010. seafarming tomorrow. *Eur. Aquaculture Soc.* 914–915.

Masaló, I., and Oca, J. (2007). Design criteria for rotating flow cells in rectangular aquaculture tanks. *Aquac. Eng.* 36 (1), 36–44. doi: 10.1016/j.aquaeng.2006.06.001

Masaló, I., and Oca, J. (2013). Flow pattern in aquaculture circular tanks: influence of flow rate, water depth, and water inlet and outlet features. *Aquac. Eng.* 52, 65–72. doi: 10.1016/j.aquaeng.2012.09.002

Patterson, R. N., Watts, K. C., and Timmons, M. B. (1999). The power law in particle size analysis for aquacultural facilities. *Aquac. Eng.* 19 (4), 259–273. doi: 10.1016/S0144-8609(98)00054-5

Ren, X. Z., Xue, B. R., Jiang, H. Z., Yu, L. P., Tiao., J., Ma., Z., et al. (2021). Numerical study on the influence of double-inlet pipes system for single-drain rectangular arc angle aquaculture tank on hydrodynamic characteristics. *Mar. Environ. Sci.* 40 (01), 50–56. doi: 10.13634/j.cnki.mes.2021.01.007

Robinson, S. K. (1991). Coherent motions in the turbulent boundary layer. *Annu. Rev. Fulid Mech.* 23, 601–639. doi: 10.1146/annurev.fl.23.010191.003125

Sin, M., An, C., Cha, S., Kim, M., and Kim, H. (2021). A method for minimizing the zone of low water flow velocity in a bottom center drain circular aquaculture tank. *J. World Aquac. Soc* 52. 1221–1233. doi: 10.1111/jwas.12792

Summerfelt, S. T., Mathisen, F., Holan, A. B., and Terjesen, B. F. (2016). Survey of large circular and octagonal tanks operated at Norwegian commercial smolt and post-smolt sites. *Aquac. Eng.* 74, 105–110. doi: 10.1016/j.aquaeng.2016.07.004

Timmons, M. B., Summerfelt, S. T., and Vinci, B. J. (1998). Review of circular tank technology and management. *Aquac. Eng.* 18, 51–69. doi: 10.1016/S0144-8609(98)00023-5

Venegaset, P. A., Narváez, A. L., Arriagada, A. E., and Llancaleo, K. A. (2014). Hydrodynamic effects of use of eductors (Jet-mixing eductor) for water inlet on circular tank fish culture. *Aquac. Eng.* 59, 13–22. doi: 10.1016/j.aquaeng.2013.12.001

Wang, Z. B. (2019). *Study on particle motion characteristics of liquid injected gas-solid fluidized bed based on PIV* (Changchun: Northeast Electric Power University).

Wu, G. L., and Gao, S. L. (2005). Flow characteristics and resistance of circum fluence in rectangle shrimp pond. *J. Zhanjiang Ocean Univ.* 1), 64–68.

Xue, B. R., Jiang, H. Z., Ren, X. Z., Yu, L. P., Zhang, Q., and Wang, G. F. (2020). Study on the influence of the relative inflow distance on the flow field characteristics in square arc angle aquaculture tank. *Fishery Modernization* 47 (04), 20–27. doi: 10.3969/j.issn.1007-9580.2020.04.004

Xue, B. R., Yu, L. P., Zhang, Q., Ren, X. Z., and Bi, C. W. (2021). A numerical study of relative inflow distance on the influence of hydrodynamic characteristics in the single-drain rectangular aquaculture tank with arc angles. *J. Fisheries China* 45 (3), 444–452. doi: 10.11964/jfc.20191112077

Xue, B. R., Zhao, Y. P., Bi, C. W., Cheng, Y., Ren, X. Z., and Liu, Y. (2022). Investigation of flow field and pollutant particle distribution in the aquaculture tank for fish farming based on computational fluid dynamics. *Comput. Electron. Agric.* 200, 107243. doi: 10.1016/j.compag.2022.107243

Zhang, X. S., Fu, L. L., and Lv, Z. M. (2017). Research development review of recirculation aquaculture mode in China and abroad. *Feed Industry* 38 (6), 61–64. doi: 10.13302/j.cnki.fi.2017.06.013.

Zhang, Q., Gui, J. S., Xue, B. R., Ren, X. Z., Xiong, Y. Y., and Wang, G. F. (2022). Study on the effect of dual-drain system on flow field characteristics in rectangular arc angle aquaculture tank. *Fishery Modernization* 47 (06), 19–25. doi: 10.3969/j.issn.1007-9580.2020.06.004

Zhao, Y. P., Xue, B. R., Bi, C. W., Ren, X. Z., and Liu, Y. (2022) Influence mechanisms of macro-infrastructure on micro-environments in the recirculating aquaculture system and biofloc technology system *Rev. Aquac.* 1–19 doi: 10.1111/raq.12713

Zhu, F., Hu, J. J., Gui, F. K., Kong, J. Q., Pan, X. R., Zhang, Z. K., et al. (2022). Influence of the inlet pipe setting angle on the self-cleaning performance of the circular recirculating aquaculture tank. *J. Fisheries China* 1–12. doi: 10.11964/jfc.20210612898

frontiers | Frontiers in Marine Science

TYPE Original Research
PUBLISHED 10 November 2022
DOI 10.3389/fmars.2022.1036289

OPEN ACCESS

EDITED BY
Amalia Pérez-Jiménez,
University of Granada, Spain

REVIEWED BY
Ishtiyaq Ahmad,
University of Kashmir, India
Cristina Trenzado,
University of Granada, Spain
Patricia Diaz-Rosales,
Centro de Investigación en Sanidad Animal, CISA (INIA-CSIC), Spain

*CORRESPONDENCE
Ce Shi
shice3210@126.com

SPECIALTY SECTION
This article was submitted to Marine Fisheries, Aquaculture and Living Resources, a section of the journal Frontiers in Marine Science

RECEIVED 04 September 2022
ACCEPTED 27 October 2022
PUBLISHED 10 November 2022

CITATION
Xu H, Shi C, Ye Y, Mu C and Wang C (2022) Effects of different photoperiods and feeding regimes on immune response, oxidative status, and tissue damage in juvenile rainbow trout (*Oncorhynchus mykiss*). *Front. Mar. Sci.* 9:1036289. doi: 10.3389/fmars.2022.1036289

Effects of different photoperiods and feeding regimes on immune response, oxidative status, and tissue damage in juvenile rainbow trout (*Oncorhynchus mykiss*)

Hanying Xu[1,2], Ce Shi[1,2,3]*, Yangfang Ye[1,3], Changkao Mu[1,3] and Chunlin Wang[1,3]

[1]Key Laboratory of Aquacultural Biotechnology Ministry of Education, School of Marine Sciences, Ningbo University, Ningbo, China, [2]Marine Economic Research Center, Dong Hai Strategic Research Institute, Ningbo University, Ningbo, China, [3]Collaborative Innovation Center for Zhejiang Marine High-efficiency and Healthy Aquaculture, School of Marine Science, Ningbo University, Ningbo, China

A three-month culture experiment was conducted to investigate the effects of the feeding regime on liver health, non-specific immunity, and apoptosis of juvenile rainbow trout under constant light conditions. A total of six experimental groups contained two photoperiods [LL (24L:0D) and LD (12L:12D)] and three feeding regimes [R (random feeding), D (mid-dark stage feeding), L (mid-light stage feeding)], defined as R-LL, D-LL, L-LL, R-LD, D-LD, L-LD. The experiment results revealed a significantly higher alanine aminotransferase (ALT) level in the nocturnal feeding group (D-LD) and significantly higher aspartate aminotransferase (AST) in the R-LL and D-LL groups, indicating possible liver damage in these groups. In addition, high serum levels of immunoglobulins M (IgM), complement 3 (C3), and complement 4 (C4) were observed in the LL (compared to LD), R (LL conditions), and D (LD conditions) groups, suggesting that stress may be present in these groups. Meanwhile, under LL, high cytokine genes (*tnf-α*, *il-1β*, *il-6*, and *il-8*) expression were observed in the liver and intestine of the L group, possibly reflecting a stronger immune response. In the liver, high malondialdehyde (MDA) content was observed in the LL (compared to LD), R (LD conditions), and D (LL conditions) groups, suggesting that these groups were subjected to oxidative damage. Further, higher apoptosis genes (*cytc* and *bcl-2*) expression in the liver was detected in the R and D-LD groups. The highest level of hepatic apoptotic cells was also observed in the D-LD group. Taken together, long-term exposure to LL, random feeding, and nocturnal feeding can cause oxidative damage to juvenile rainbow trout, leading to

hepatocyte apoptosis, while scheduled diurnal feeding can alleviate the oxidative damage caused by LL.

KEYWORDS

photoperiod, diurnal feeding, oxidative damage, apoptosis, rainbow trout

Introduction

Rainbow trout (*Oncorhynchus mykiss* Walbaum, 1792) is an economically important fish and occupies an essential position in global aquaculture. According to the latest Food and Agriculture Organization of the United Nations (FAO, 2022) statistics, global rainbow trout aquaculture production reached 959,600 tons in 2020 (including inland aquaculture of 739,500 tons, marine and coastal aquaculture of 220,100 tons). Rainbow trout has a wide consumer market in China as a high-grade aquatic product and has been farmed since the 1960s. However, as a cold-water fish, the suitable growth temperature for rainbow trout is 12-18°C. Due to the lack of cold-water resources, land-based rainbow trout culture development in China has reached a bottleneck (Huang et al., 2021). In recent years, some scholars tried to aquaculture rainbow trout in the cold-water masses of the Yellow Sea in China (Dong, 2019; Chu et al., 2020). Rainbow trout's seawater culture is viable and has faster growth rates and higher disease resistance than freshwater (Landless, 1976; Yada et al., 2001; Shepherd et al., 2005). Currently, farming rainbow trout in the cold-water masses of the Yellow Sea is still preliminary, and there are still many problems to be improved.

The first challenge of farming rainbow trout in the Yellow Sea cold-water mass is the water temperature fluctuation, especially in the summer high-temperature period. Currently, submerged offshore fish cages (such as "Shenlan 1") are used to escape the summer heat, and the fish cages are sunk to the suitable water temperature layer to meet the demand for cultured fish during the hot period (Dong, 2019; Chu et al., 2020). However, the photoperiod is deprived underwater and, as an important zeitgeber, is closely linked to immune function in fish (Esteban et al., 2006). Many studies have reported the impact on the immune system and health status of fish in the absence of photoperiodic environments, affecting the welfare of farmed fish. For example, in largemouth bass (*Micropterus salmoides*), continuous light (LL) was found to cause a significant increase in thiobarbituric acid reactive substances (TBARS) in the liver, brain, and gills compared to LD (12L:12D), indicating the presence of oxidative damage (Malinovskyi et al., 2022). In Atlantic salmon (*Salmo salar* L.), LL inhibits vertebral mineralization, leading to elevated deformities (Fjelldal et al., 2005; Wargelius et al., 2009; Fjelldal et al., 2012). Studies in rainbow trout have also found that LL has a stressful impact on the non-specific immune system (Valenzuela et al., 2022). The immune system responds rapidly to stress in fish, as reflected by a rapid increase in blood levels of IgM, C3, and C4 (Demers and Bayne, 2020; Abdollahpour et al., 2021). In European Sea Bass (*Dicentrachus labrax* L.), both LL and DD (continuous darkness) inhibited growth and caused oxidative stress (Li et al., 2021). In Nile tilapia (*Oreochromis niloticus*) and African catfish (*Clarias gariepinus*), both LL and DD were found to cause damage to both fish species, affecting swimming activity, behavior, coloration, and growth, which is a challenge to fish welfare (Mustapha et al., 2014). On the other hand, the liver is the central organ of metabolism, and metabolic disorders caused by the absence of photoperiod are often accompanied by liver damage. Under the healthy condition, there is abundant acid phosphatase (ACP), alkaline phosphatase (AKP), alanine aminotransferase (ALT), aspartate aminotransferase (AST), and lactate dehydrogenase (LDH) in the liver, and once the liver is injured, these enzymes will be released into the blood, so the activity of these enzymes in the serum are widely used as indicators of liver damage (Molayemraftar et al., 2022; Rahman et al., 2022).

Besides photoperiod, food is another important environmental cue able to synchronize organisms' circadian rhythms (Stephan, 2002; López-Olmeda, 2017). Immune function in many fish exhibits significant circadian rhythms. For example, in zebrafish (*Danio rerio*), the inflammatory response is regulated by the core biological clock genes *period1b* and *period 2* (Ren et al., 2018). In rainbow trout, significant circadian rhythms were also found for serum bactericidal activity and immune defense factors (Lazado et al., 2018) and in the number of leukocytes and myeloid cells (Montero et al., 2020). Further, the effect of feeding time on fish immune function was also reported in a zebrafish study where fish in the scheduled feeding group exhibited higher levels of *lysozyme*, *β-defensin*, and *hepcidin* transcripts (Lazado et al., 2019). Notably, some studies in mammals have shown that scheduled feeding alleviates biological clock dysregulation caused by photoperiod deficiency (Yamamuro et al., 2020) and prevents the development of metabolic diseases in models of biological clock deficiency (Chaix et al., 2019).

Thus, is it possible to mitigate the impact of photoperiod deficiency on fish immune function by scheduled feeding? This study aimed to investigate the effects of feeding regimes on oxidative stress, liver health, and non-specific immunity in juvenile rainbow trout (*Oncorhynchus mykiss*) in the absence of a photoperiod. It is expected to provide theoretical support for managing rainbow trout culture in offshore fish cages.

Materials and methods

Ethical issues

All experimental operations involving animals in this study were performed under the approval and supervision of the Animal Care and Use Committee of Ningbo University.

Experimental animals

The juvenile rainbow trout used in the experiments were purchased from a commercial nursery in Shandong province and delivered to the School of Marine Sciences, Ningbo University by live fish transporting vehicle. All juvenile fish were rapidly transferred to a recirculating aquaculture system (RAS, HISHING, Qingdao, China) for one month to acclimatize to the laboratory environment. During the acclimation period, commercial feed (crude protein ≥ 42.0% and crude lipid ≥ 10%, Tech-Bank, Ningbo, China) was randomly provided at about 2% of body weight per day; photoperiod was 12L:12D (lights-on at 6:00, the light intensity on the water surface is 100-200 lx); dissolved oxygen in the culture water was kept saturated; water temperature was at 16.5 ± 1°C; ammonia nitrogen was below 0.05 mg/L; the water circulation rate about 600L/h.

Experimental treatments

This study was a two-factor experiment including two independent variables of photoperiod: 24L:0D (LL) and 12L:12D (LD) and feeding regime: random feeding (R, The feeding schedule was provided by random number generator software [RAND function of Microsoft Excel) according to Nisembaum et al. (2012)], mid-dark stage feeding (D, feeding at 24:00 daily), and mid-light stage feeding (L, feeding at 12:00 daily), for a total of 6 experimental groups (R-LL, D-LL, L-LL, R-LD, D-LD, L-LD), each including 7 culture tanks. At the end of acclimation, a total of 840 juvenile rainbow trout of uniform size (18.98 ± 1.69 g/fish) were randomly placed in 42 culture tanks with 20 fish per tank. The formal culture experiment lasted 3 months, and the culture environment was consistent with the acclimation phase.

Sample collection and treatment

At the end of the culture experiment, fish in all treatment groups were deprived of food for 24 h. Subsequently, 12 fish were randomly retrieved from each tank (there was no fish mortality during the experiment, and a total of 20 fish remained in each tank), anesthetized with MS-222, and immediately weighed and measured body length (growth performance was placed in a separate unpublished manuscript). Afterward, about 2 ml of blood was drawn from the tail vein of each fish using a disposable syringe and stored in two 1.5 mL eppendorf (EP) tubes (4°C) of 1 mL each. One of the EP tubes contained EDTA-K_2 to prevent clotting and was used for total blood cell count. Another tube of blood was left overnight at 4°C and then centrifuged in a high-speed freezing centrifuge (3-18K, Sigma, Landkreis Osterode, Germany) at 2500 rpm for 10 min at 4°C. The supernatant (serum) was immediately stored at -80°C until analysis. The fish were dissected immediately after blood sampling, and the liver (one part was fixed directly in 10% neutral formalin), intestine, and dorsal muscle were isolated, quickly frozen in liquid nitrogen, and stored at -80°C until analysis.

The tissue homogenate was prepared according to the following steps: liver, intestine, and muscle tissues were homogenized using pre-cooled saline (4°C, 0.9% NaCl) at a ratio of 1:9 (V: W), and the homogenate was centrifuged at 2500 rpm for 10 min at 4°C in a high-speed freezing centrifuge (Fresco17, Thermo Scientific, Waltham, USA) to obtain the supernatant.

Serum immunological indicators

The serum acid phosphatase (ACP, A060-1-1), alkaline phosphatase (AKP, A059-1-1), alanine aminotransferase (ALT, C009-1-1), aspartate aminotransferase (AST, C010-1-1), albumin (ALB, A028-1-1), and lactate dehydrogenase (LDH, A020-1-2) were measured by commercial kits (Nanjing Jiancheng Bioengineering Institute, Nanjing, China) according to the instructions and the absorbance values were read at 532 nm (ACP, U/100 mL, 100 mL serum interacting with the substrate at 37°C for 15 minutes produced 1 mg of phenol is one unit; AKP, King unit/100 mL, 100 mL serum interacting with the substrate at 37°C for 15 minutes produced 1 mg of phenol is one King unit), 505 nm (ALT, U/L, the pyruvate produced within 1 min of 1 ml serum causes the oxidation of NADH to NAD+ and causes a decrease in absorbance of 0.001 is one unit; AST, U/L, same as ALT), 628 nm (ALB, g/L), and 440 nm (LDH, U/L, 1 L of serum interacting with the substrate at 37°C for 15 minutes produced 1 μmol of pyruvate is one unit) in a microplate reader (Multiskan Go, Thermo Scientific, Waltham, USA), respectively, and the

results were calculated according to the formula provided in the instructions.

The serum complement 3 (C3, μg/mL), complement 4 (C4, μg/mL), and immunoglobulins M (IgM, μg/mL) were measured using commercial enzyme-linked immunosorbent assay (ELISA) kits (Shanghai Qiaodu Biotechnology Co., Ltd., Shanghai, China) according to the instructions and the absorbance values were read at 450 nm in a microplate reader (Multiskan Go, Thermo Scientific, Waltham, USA), and the results were calculated according to the formula provided in the instructions.

Total blood cell counts

Total blood cell counts (TBC) were performed using a hemocytometer plate under a light microscope (DN-800M, NOVEL, Nanjing, China), according to Pan et al. (2010).

Antioxidant indicators

The serum, liver, intestine, and dorsal muscle malondialdehyde (MDA, A003-1-2), total antioxidant capacity (T-AOC, A015-1-2), total superoxide dismutase (SOD, A001-1-2), and catalase (CAT, A007-1-1) were measured by commercial kits (Nanjing Jiancheng Bioengineering Institute). Serum and tissue homogenates were analyzed according to the kit instructions, and the absorbance values were read at 532 nm (MDA, nmol/mL for serum; nmol/mgprot for tissue), 520 nm (T-AOC, U/mL for serum; U/mgprot for tissue, each 0.01 increase in absorbance value of the reaction system per minute per milliliter of serum (or per milligram of tissue protein) is one unit), 550 nm (SOD, U/mL for serum; U/mgprot for tissue, the amount of enzyme corresponding to 50% inhibition of SOD in this reaction system is one unit), and 405 nm (CAT, U/mL for serum; U/mgprot for tissue, decomposition of 1 μmol of H_2O_2 per second per milliliter of serum (or per milligram of tissue protein) is one unit) in a microplate reader (Multiskan Go, Thermo Scientific, Waltham, USA), respectively, and the results were calculated according to the formula provided in the instructions. Meanwhile, the total protein (TP, A045-2-2, g/L) content in the tissue homogenates was measured by the Coomassie brilliant blue method at 595 nm to normalize the antioxidant index in the tissues.

Non-specific immunity-related gene expression

The reagents and methods used to extract total RNA from the liver and intestine were consistent with Xu et al. (2022).

A real-time PCR system (QuantStudio™ 6 Flex, Life Technologies, Carlsbad, USA) was used to analyze the relative expression of non-specific immunity-related genes [Cytochrome c(*cytc*), Caspases 3 (*casp3*), Caspases 6 (*casp6*), Caspases 8 (*casp8*), Bcl2-associated X (*bax*), B-cell lymphoma-2 (*bcl-2*), Tumor suppressor p53 (*p53*), Interleukin-1β (*il-1β*), Interleukin-6 (*il-6*), Interleukin-8 (*il-8*), Tumor necrosis factor-α (*tnf-α*), Glutathione peroxidase (*gpx*), Cytosolic Cu/Zn superoxide dismutase (*sod1*), Mitochondrial Mn superoxide dismutase (*sod2*), Catalase (*cat*)] in the liver and intestine. The reaction system and program were consistent with Xu et al. (2022). The specific primers used in this study are shown in Table 1 and synthesized by a commercial company (Youkang Biological Technology Co., Ltd, Hangzhou, China). The relative expression level of target genes is normalized by elongation factor-1α (*ef1α*) and calculated by the comparative CT method ($2^{-\Delta\Delta CT}$ method) (Livak and Schmittgen, 2001).

Histology and apoptosis analysis

The fixed liver tissue (for 24 h) was flushed with running water overnight, followed by dehydration in gradient alcohol, transparency in alcohol, and xylene solution, and finally liver tissues were embedded in paraffin wax. The liver tissue was subsequently sectioned on a microtome (thickness 5 μm, HM325, Thermo Scientific, Waltham, USA). Liver sections were spread in warm water at 48°C and later dried at 45°C, followed by dewaxing and rehydration in xylene and gradient alcohol, and finally stained using a hematoxylin and eosin (H&E) staining kit (G1120, Solarbio, Beijing, China) following the steps of the instructions. Observations were performed under a light microscope (magnification 200×, CKX53, OLYMPUS, Tokyo, Japan).

The above obtained liver sections were stained with TUNEL using Colorimetric TUNEL Apoptosis Assay Kit (C1098, Beyotime, Shanghai, China) according to the steps of the instructions and then observed under a light microscope (magnification 200×, CKX53, OLYMPUS, Tokyo, Japan).

Statistical analysis

First, all data were checked for homogeneity and normal distribution through Levene's and Kolmogorov-Smirnov tests, respectively. Then a two-way ANOVA was performed with photoperiod and feeding regime. Meanwhile, t-tests were performed for photoperiod, and one-way ANOVA followed by Duncan's multiple range test was performed for the feeding regime. $P < 0.05$ and $P < 0.01$ were considered significant differences and extremely significant differences, respectively. All statistical analyses were performed on SPSS 22.0 and R 4.1.2 software. Data are presented as box plots (minimum, median, maximum, outliers) or heatmaps (mean).

TABLE 1 The specific primers used for real-time PCR in this study.

Gene	Sequence (5' to 3')	Reference or Access number
cytc	F: TGGGAAACCGATACCCTCAT	Zhou et al. (2019)
	R: GCTCGCCCTTCTTCTTGATG	
casp3	F: CTCCGTTGCTGATGACTC	Zeng et al. (2021)
	R: GCCTTTCTGGGTGTTCCT	
casp6	F: TGAGCCACGGAGAGAACGA	
	R: ACGGCACGCCTGTAGTATG	
casp8	F: GCAGCATAGAGAAGCAAGG	
	R: GTCTTACAGGATTGCGTCG	
bax	F: TTCGTGACGGTCATGGTTTA	Iturriaga et al. (2017)
	R: CCCGTTCCCAGAGAAATGTA	
bal-2	F: TGCATCCTGAAACTCTGTGTC	
	R: CCGAGTCCCCAGGTTGTG	
p53	F: GACAACCCTGGAGACCAAGA	Ferain et al. (2021)
	R: TCTCATCGTCACTCACAGCA	
il-1β	F: ACATTGCCAACCTCATCATCG	Ren et al. (2022)
	R: TTGAGCAGGTCCTTGTCCTTG	
il-6	F: CAGCTTCTTCTTCAGCACGTTAA	Zante et al. (2015)
	R: CGTAGACACCTCACCCAGAAC	
il-8	F: AGAATGTCAGCCAGCCTTGT	Ren et al. (2022)
	R: TCTCAGACTCATCCCCTCAGT	
tnf-α	F: CAAGAGTTTGAACCTCATTCAG	
	R: GCTGCTGCCGCACATAAAG	
gpx	F: AATGTGGCGTCACTCTGAGG	Fontagné-Dicharry et al. (2020)
	R: CAATTCTCCTGATGGCCAAA	
sod1	F: TGGTCCTGTGAAGCTGATTG	
	R: TTGTCAGCTCCTGCAGTCAC	
sod2	F: TCCCTGACCTGACCTACGAC	
	R: GGCCTCCTCCATTAAACCTC	
cat	F: TGATGTCACACAGGTGCGTA	
	R: GTGGGCTCAGTGTTGTTGAG	
ef1α	F: TCCTCTTGGTCGTTTCGCTG	Panserat et al. (2020)
	R: ACCCGAGGGACATCCTGTG	

cytc, Cytochrome c; *casp3*, Caspases 3; *casp6*, Caspases 6; *casp8*, Caspases 8; *bax*, Bcl2-associated X; *bcl-2*, B-cell lymphoma-2; *p53*, Tumor suppressor p53; *il-1β*, Interleukin-1β; *il-6*, Interleukin-6; *il-8*, Interleukin-8; *tnf-α*, Tumor necrosis factor-α; *gpx*, Glutathione peroxidase; *sod1*, Cytosolic Cu/Zn superoxide dismutase; *sod2*, Mitochondrial Mn superoxide dismutase; *cat*, Catalase; *ef1α*, Elongation factor-1α.

Results

Liver health indicators

Serum ACP, AKP, and LDH activities were not affected by experimental treatments. In group D, ALT activity was significantly higher in group LD than in group LL. AST activity was lower in group L than in groups R and D. The ALB was significantly lower in group R than in D and L groups (Figure 1).

Serum immunological indicators

The scheduled feeding group had higher TBC (Figure 2).

Under LL, the R group had higher C3 levels than the D group; under LD, the D group had higher C3 and IgM levels than R and L groups. In the R and L groups, the LL group had significantly higher C3, C4, and IgM (Figure 2).

Antioxidant indicators

Overall, MDA in the liver was significantly higher in the LL group than in the LD group, independent of the feeding regime (Table 2 and Figure 3). Specifically, under LL, the D group was significantly higher than the R group; under LD, the R group was significantly higher than the D and L groups. In group D, LL was significantly higher than that LD. In contrast, SOD activity was significantly lower in the D group than in the R group under LL; in the D group, the LD group was significantly higher than in the LL group; CAT activity was significantly higher in the LD group than in the LL group under all three feeding regimes.

Overall, the MDA in the intestine was significantly lower in the L group than R and D groups, independent of the photoperiod (Table 2 and Figure 4). In contrast, T-AOC was significantly higher in the L group than R and D groups.

The experimental treatments did not affect MDA levels in muscles (Figure 5).

In serum, MDA levels were significantly lower in the R group than in the D and L groups, independent of photoperiod (Table 2 and Figure 6). Similarly, T-AOC and SOD activities were significantly lower in the R group than in the D and L groups.

Liver and intestinal gene expression

Apoptosis, cytokine, and antioxidant gene expression in the liver and intestine were detected in this experiment (Figure 7 and Supplementary Figure 1).

In the liver, *cytc* gene expression was significantly higher in the R group under both photoperiods; in the D group, the LD was significantly higher than the LL. The *p53* gene was significantly lower in the R group under LL. In the R group, the LD was significantly higher than LL. The *bax* gene was significantly higher in the L group under LL. The *bcl-2* gene was significantly higher in the D group under LD; in the D group, the LD was significantly higher than the LL. The *tnf-α* gene was significantly lower in the R group under LL. In the D and L groups, the LL was significantly higher than LD. The *il-1β* gene was significantly higher in the L group under LL and significantly lower in the R group under LD. In the R and L

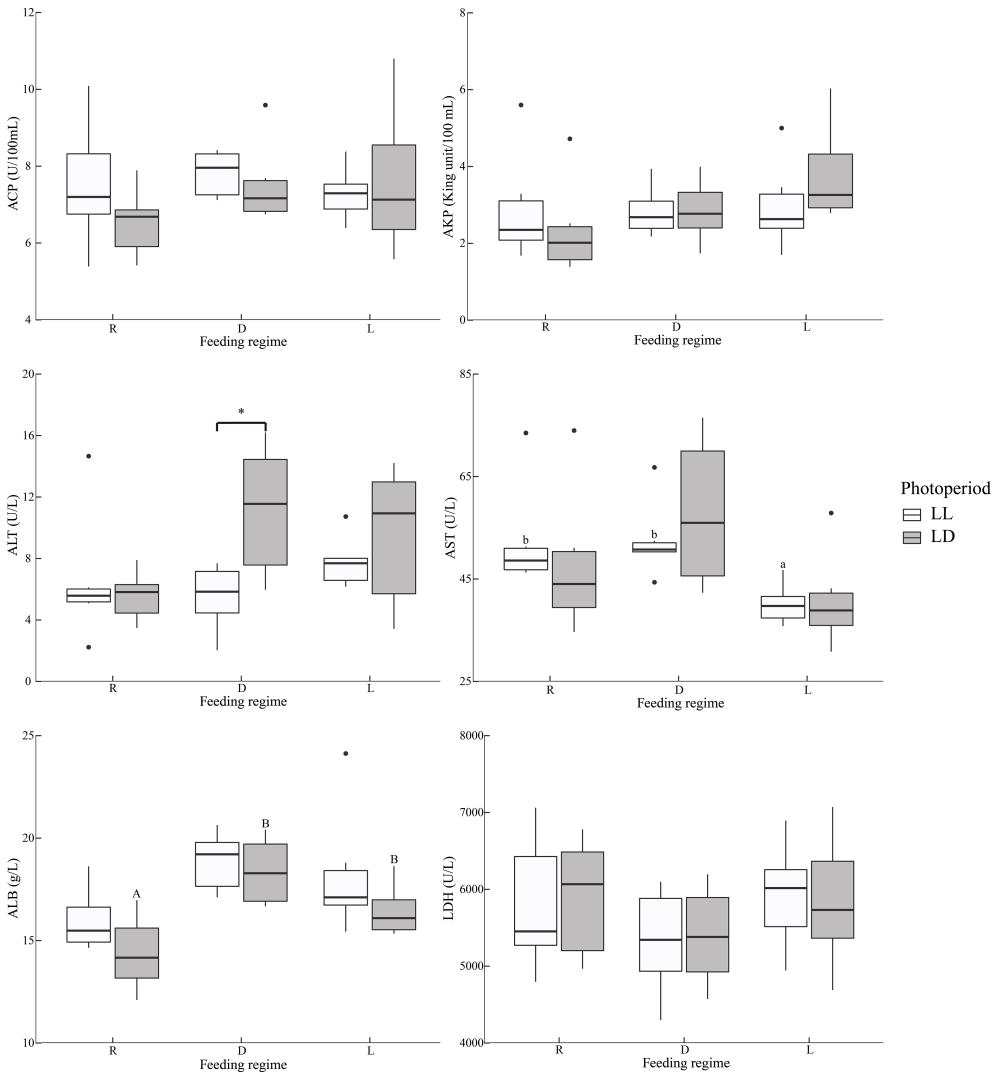

FIGURE 1
Liver health indicators of juvenile *Oncorhynchus mykiss* under different experimental treatments (n=6). ACP, Acid phosphatase; AKP, Alkaline phosphatase; ALT, Alanine aminotransferase; AST, Aspartate aminotransferase; ALB, Albumin; LDH, Lactate dehydrogenase; R, random feeding; D, mid-dark stage feeding; L, mid-light stage feeding; LL: 24L: 0D, LD: 12L: 12D. Different lowercase letters and capital letters indicate significant difference among different feeding regimes at the LL (24L: 0D) and LD (12L: 12D, lights-on at 6:00), respectively ($P < 0.05$). Asterisks denote significant differences between photoperiods at the same feeding regime (*$P < 0.05$). Points outside the box plot are outliers.

groups, LL was significantly higher than LD. in the D group, LD was significantly higher than LL. The *il-6* gene was significantly higher in group D under LL; the D group was significantly higher than the R and L groups under LD. The *gpx* gene was significantly higher in the L group under LL. The LL was significantly lower than LD in the R and D groups. The *sod1* and *sod2* genes were significantly lower in the R group under LL. In the R group, LL was significantly lower than LD. The *cat* genes were significantly lower in the R group under LL; under LD, the L group was significantly higher than the R and D groups. In the R group, LL was significantly lower than LD.

In the R group, the *cytc* gene in the intestine was significantly lower in LL than in LD. The *p53* and *bax* genes were significantly higher in the L group under LL and significantly lower in the L group under LD. In the R group, LL was significantly lower than LD; in the L group, LL was significantly higher than LD. The *casp6* and *casp8* genes were significantly higher in the R group under LD. The *tnf-α*, *il-1b*, *il-6*, and *il-8* genes exhibited significantly higher in the L group under LL. The L group was lower than the R and D groups under LD. In the R and D groups, LL was significantly lower than LD. The expression trends of antioxidant enzyme genes were also consistent, with the expression of *sod1*, *sod2*, and *cat* genes significantly higher in

10.3389/fmars.2022.1036289

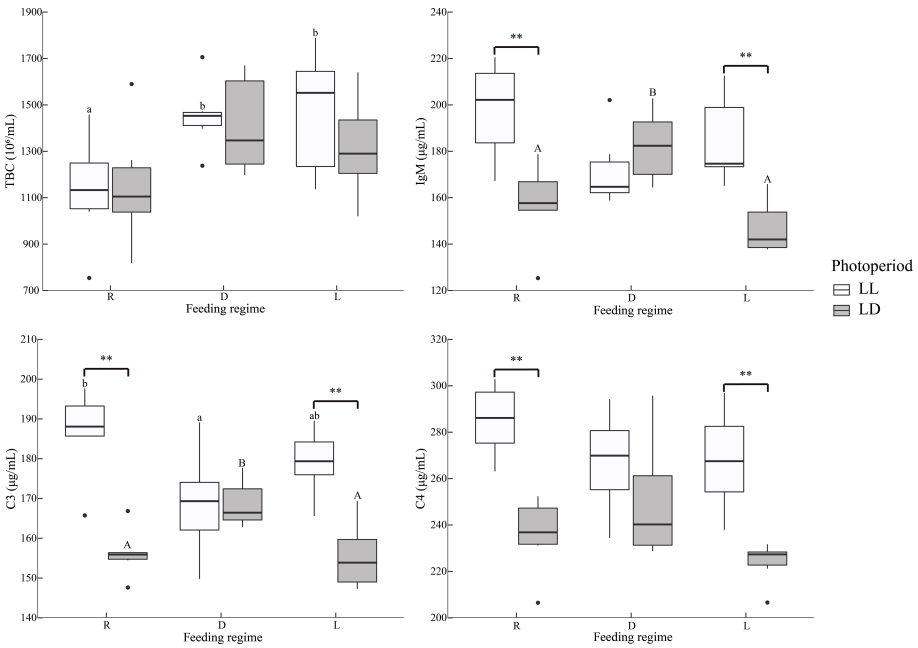

FIGURE 2
Serum immunological indicators of juvenile Oncorhynchus mykiss under different experimental treatments (n=6). TBC: Total blood cell counts, IgM: Immunoglobulins M, C3, Complement 3; C4, Complement 4; R, random feeding; D, mid-dark stage feeding; L, mid-light stage feeding; LL: 24L: 0D, LD: 12L: 12D. Different lowercase letters and capital letters indicate significant difference among different feeding regimes at the LL (24L: 0D) and LD (12L: 12D, lights-on at 6:00), respectively ($P < 0.05$). Asterisks denote significant differences between photoperiods at the same feeding regime (**$P < 0.01$). Points outside the box plot are outliers.

TABLE 2 Summary of two-way ANOVA: Immunity index and gene expression of juvenile *Oncorhynchus mykiss* under different experimental treatment.

Item	Photoperiod	Feeding regime	Photoperiod * Feeding regime
Serum			
TBC	NS	$P < 0.01$	NS
ACP	NS	NS	NS
AKP	NS	NS	NS
ALT	NS	NS	NS
AST	NS	$P < 0.01$	NS
C3	$P < 0.01$	NS	$P < 0.01$
C4	$P < 0.01$	NS	NS
IgM	$P < 0.01$	NS	$P < 0.01$
ALB	NS	$P < 0.01$	NS
LDH	NS	NS	NS
T-AOC	NS	$P < 0.01$	NS
SOD	NS	$P < 0.01$	NS
CAT	NS	NS	$P < 0.01$
MDA	NS	$P < 0.01$	NS
Liver			
T-AOC	NS	NS	NS
SOD	NS	NS	$P < 0.05$
CAT	$P < 0.01$	NS	NS

(Continued)

TABLE 2 Continued

Item			Photoperiod	Feeding regime	Photoperiod * Feeding regime
MDA			$P < 0.05$	NS	$P < 0.01$
Intestine					
T-AOC			NS	$P < 0.01$	NS
SOD			$P < 0.05$	NS	NS
CAT			NS	NS	$P < 0.01$
MDA			NS	$P < 0.01$	NS
Muscle					
T-AOC			$P < 0.05$	NS	$P < 0.01$
SOD			$P < 0.01$	$P < 0.01$	$P < 0.01$
CAT			NS	NS	NS
MDA			$P < 0.05$	NS	NS
Gene expression					
Liver	Apoptosis	*cytc*	NS	$P < 0.01$	NS
		casp3	NS	$P < 0.05$	NS
		casp6	$P < 0.05$	NS	NS
		casp8	NS	NS	$P < 0.05$
		bax	$P < 0.05$	NS	NS
		bcl-2	$P < 0.01$	$P < 0.01$	$P < 0.01$
		p53	$P < 0.05$	$P < 0.01$	NS
	Cytokines	*il-1β*	$P < 0.01$	$P < 0.01$	$P < 0.01$
		il-6	NS	$P < 0.01$	NS
		il-8	$P < 0.05$	NS	NS
		tnf-α	$P < 0.01$	$P < 0.01$	$P < 0.01$
	Antioxidase	*gpx*	$P < 0.01$	NS	NS
		sod1	NS	NS	$P < 0.05$
		sod2	NS	NS	$P < 0.05$
		cat	NS	$P < 0.01$	NS
Intestine	Apoptosis	*cytc*	$P < 0.05$	NS	NS
		casp3	$P < 0.05$	NS	NS
		casp6	$P < 0.05$	NS	$P < 0.05$
		casp8	NS	NS	$P < 0.01$
		bax	NS	NS	$P < 0.01$
		p53	NS	NS	$P < 0.01$
	Cytokines	*il-1β*	$P < 0.01$	$P < 0.01$	$P < 0.01$
		il-6	$P < 0.01$	$P < 0.01$	$P < 0.01$
		il-8	$P < 0.01$	NS	$P < 0.01$
		tnf-α	$P < 0.01$	$P < 0.01$	$P < 0.01$
	Antioxidase	*gpx*	NS	NS	NS
		sod1	$P < 0.05$	NS	$P < 0.01$
		sod2	$P < 0.01$	$P < 0.05$	NS
		cat	$P < 0.01$	$P < 0.01$	NS

TBC, Total blood cell counts; ACP, Acid phosphatase; AKP, Alkaline phosphatase; ALT, Alanine aminotransferase; AST, Aspartate aminotransferase; C3, Complement 3; C4, Complement 4; IgM, Immunoglobulins M; ALB, Albumin; LDH, Lactate dehydrogenase; T-AOC, Total antioxidant capacity; SOD, Superoxide dismutase; CAT, Catalase; MDA, Malondialdehyde; *cytc*, Cytochrome c; *casp3*, Caspase3; *casp6*, Caspase6; *casp8*, Caspase8; *bax*, Bcl-2 associated X; *bcl-2*, B-cell lymphoma-2; *p53*, tumor protein 53; *il-1β*, Interleukin-1β; *il-6*, Interleukin-6; *il-8*, Interleukin-8; *tnf-α*, Tumor necrosis factor-α; *gpx*, Glutathione peroxidase; *sod1*, Cytosolic Cu/Zn superoxide dismutase; *sod2*, Mitochondrial Mn superoxide dismutase. NS, non-significant differences.

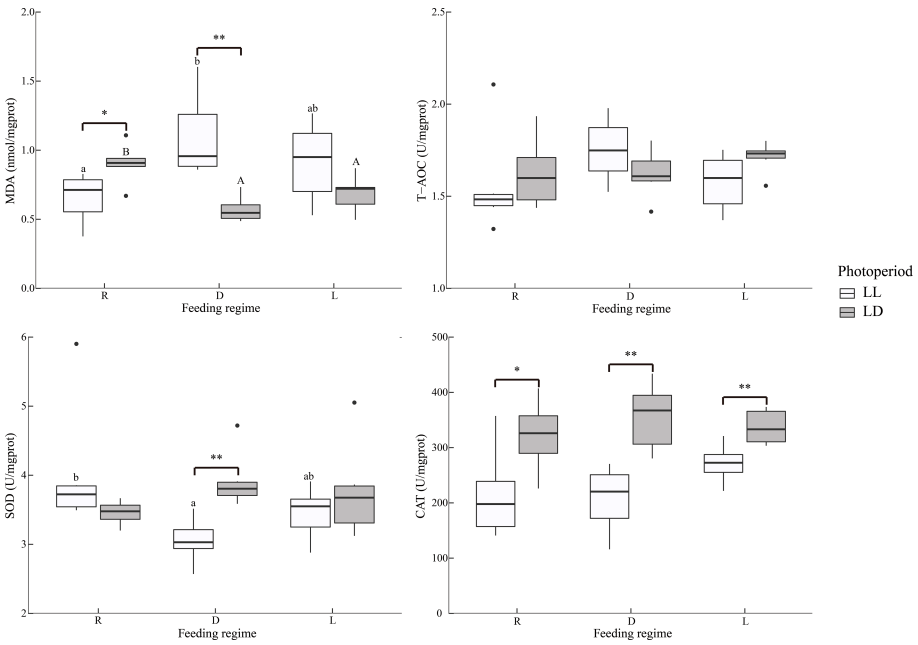

FIGURE 3
Liver antioxidant indicators of juvenile *Oncorhynchus mykiss* under different experimental treatments (n=6). MDA: Malondialdehyde, T-AOC: Total antioxidant capacity, SOD: Superoxide dismutase, CAT, Catalase; R, random feeding; D, mid-dark stage feeding; L, mid-light stage feeding; LL: 24L: 0D, LD: 12L: 12D. Different lowercase letters and capital letters indicate significant difference among different feeding regimes at the LL (24L: 0D) and LD (12L: 12D, lights-on at 6:00), respectively ($P < 0.05$). Asterisks denote significant differences between photoperiods at the same feeding regime (*$P < 0.05$; **$P < 0.01$). Points outside the box plot are outliers.

the R group under LD. The *sod1* and *sod2* genes were higher in LL than in LD under both D and L groups. The *cat* gene expression was highest in the R group under LL; in the R and L groups, LL was higher than LD.

Liver histology and apoptosis

The observation of liver paraffin sections with H&E staining revealed pathological changes between the six treatment groups (Figure 8). The liver parenchyma was looser in the R group, and some cellular vacuolation (black triangles) was present between the different treatment groups. The R and D groups observed significant capillary dilatation (black circles). Erythrocyte sludge in the blood sinusoids (black circles and green arrows) was observed in the R-LL, D-LL, R-LD, and D-LD groups.

TUNEL staining of liver tissue sections revealed that there were almost no apoptotic cells in the L group under both photoperiods, and apoptosis was most severe in the D-LD group (Figure 9).

Discussion

Blood indicators closely relate to fish's physiological, metabolic, and health status. When external environmental factors impact fish, they are usually reflected in blood indicators (Casanovas et al., 2021; Witeska et al., 2022). Some serum enzymes and metabolites are widely used as a reflection of liver functional statuses in fish, such as alkaline phosphatase (AKP, Casillas and Ames, 1985), acid phosphatase (ACP, Molayemraftar et al., 2022), alanine aminotransferase (ALT, Kim and Kang, 2016; Zhang et al., 2016), aspartate aminotransferase (AST, Kim and Kang, 2016; Zhang et al., 2016), lactate dehydrogenase (LDH, Rahman et al., 2022) and albumin (ALB, Mukherjee et al., 2022). In the present study, ALT was only significantly higher in the D-LD group than in the L-LD group. High levels of ALT in serum are considered a marker of fish liver damage (Hong et al., 2022). Therefore, this study showed that nocturnal feeding led to liver damage in juvenile rainbow trout under an LD environment. In addition, under LL, significantly low levels of AST were observed in the L group. Like ALT, high levels of AST in serum also reflect liver damage (Hong et al., 2022). This suggests that under LL conditions, scheduled diurnal feeding can alleviate liver damage in juvenile rainbow trout. In addition, significantly low ALB was detected in the random feeding group, suggesting that random feeding may cause stress to juvenile rainbow trout. Similarly, under chronic high salt stress, African catfish (*Clarias gariepinus*) serum levels of ALT and AST were increased, and ALB levels were decreased (Dawood et al., 2022).

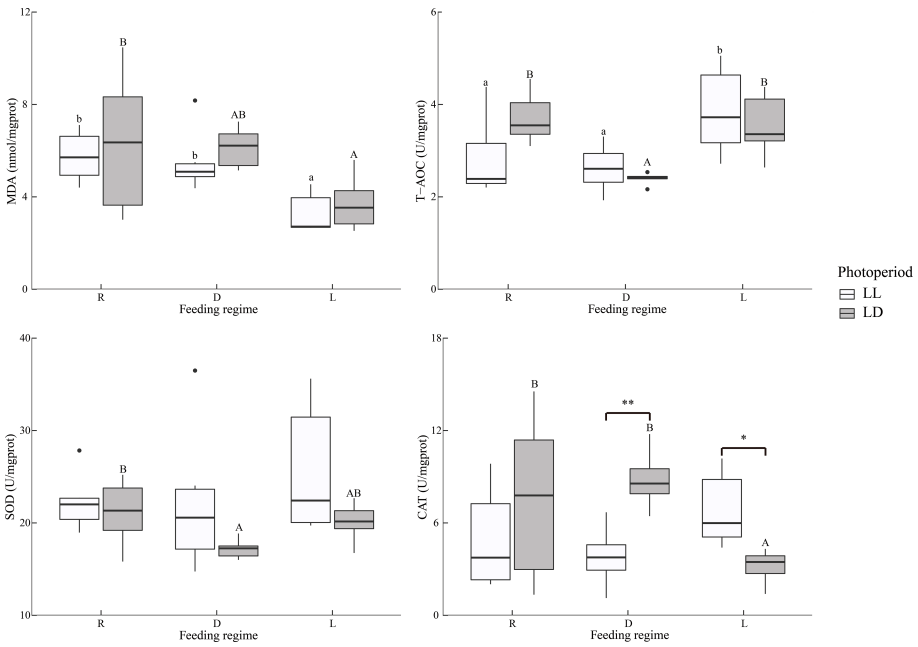

FIGURE 4
Intestine antioxidant indicators of juvenile *Oncorhynchus mykiss* under different experimental treatments (n=6). MDA: Malondialdehyde, T-AOC: Total antioxidant capacity, SOD: Superoxide dismutase, CAT, Catalase; R, random feeding; D, mid-dark stage feeding; L, mid-light stage feeding; LL: 24L: 0D, LD: 12L: 12D. Different lowercase letters and capital letters indicate significant difference among different feeding regimes at the LL (24L: 0D) and LD (12L: 12D, lights-on at 6:00), respectively ($P < 0.05$). Asterisks denote significant differences between photoperiods at the same feeding regime (*$P < 0.05$; **$P < 0.01$). Points outside the box plot are outliers.

Like mammals, fish's immune system includes both cellular and humoral immunity. A significantly higher total blood cell count (TBC) was observed in the scheduled feeding group, especially in the LL environment. Blood cells are an important component of the immune system in fish, and they play an irreplaceable role in innate and adaptive immunity (Kordon et al., 2018; Zhu and Su, 2022). High levels of TBC respond to a stronger immune function. Fish humoral immunity consists mainly of immunoglobulin and complements (Abdollahpour et al., 2021). Immunoglobulin M (IgM) is the dominant immunoglobulin in fish serum and is the first line of defense in the adaptive immune response (Xia et al., 2014; Mashoof and Criscitiello, 2016). The complement system is an important component of innate immunity in teleost and plays a role in adaptive immunity as a bridge between innate and adaptive immunity (Bavia et al., 2022). IgM triggers the classical pathway of complement activation, and the immune complex of antigen, IgM, and activated complement 3 (C3) significantly enhances the B-cell antibody response (Boes, 2000). In the complement system, C3 is the central component that plays an important role (Meng et al., 2019). Also, complement 4 (C4) plays an important role in complement activation and humoral defense (Holland and Lambris, 2002). Previous studies have shown a rapid increase in serum C3 in rainbow trout exposed to acute stress (Demers and Bayne, 2020). When grass carp (*Ctenopharyngodon idella*) are infested with *Aeromonas hydrophila*, the level of C3 increases to help repair damaged tissues (Meng et al., 2019). On the other hand, chronic stress also resulted in increased IgM and C3 levels in northern snakehead (*Channa argus*) serum (Li et al., 2019a; Li et al., 2019b) and common carp (*Cyprinus carpio*) liver (Qiu et al., 2018). Similarly, chronic high concentrations of thyroxine treatment induced stress in the sterlet sturgeon (*Acipenser ruthenus*) (significant high levels of serum cortisol, glucose, and lactate) while causing an increase in serum IgM, C3, and C4 levels (Abdollahpour et al., 2021). The present study observed high serum IgM, C3, and C4 levels in the LL, R, and D groups. The above results suggested that long-term exposure to LL and random/nocturnal feeding may be a stressor for juvenile rainbow trout and affect the immune system.

Cytokines are small molecular glycoproteins secreted by immune cells and play an important role in the innate immune response (Sakai et al., 2021). In northern snakehead (*Channa argus*), long-term exposure to selenium resulted in the upregulation of *il-1β*, *il-8*, and *tnf-α* genes expression (Li et al., 2019a; Li et al., 2019b). When pufferfish (*Takifugu rubripes*) were treated with lipopolysaccharide or polyinosinic-polycytidylic acid, the expression of *il-1β*, *il-6*, and *tnf-α* genes showed a significant increase (Sakai et al., 2021). Similarly, Chronic exposure to the ionic liquid [C_8mim] Br resulted in

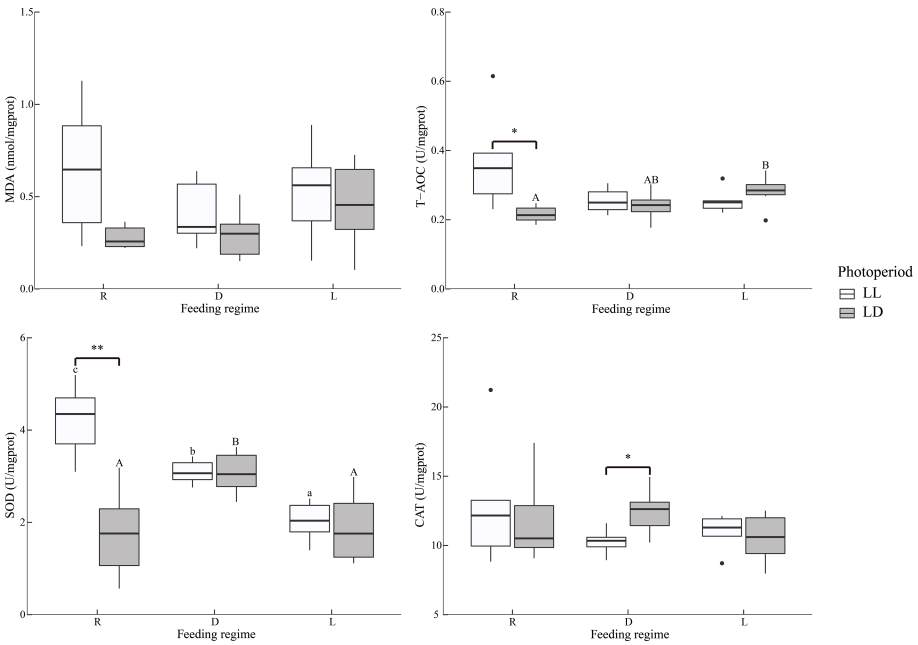

FIGURE 5
Dorsal muscle antioxidant indicators of juvenile *Oncorhynchus mykiss* under different experimental treatments (n=6). MDA, Malondialdehyde; T-AOC, Total antioxidant capacity; SOD, Superoxide dismutase; CAT, Catalase; R, random feeding; D, mid-dark stage feeding; L, mid-light stage feeding; LL: 24L: 0D, LD: 12L: 12D. Different lowercase letters and capital letters indicate significant difference among different feeding regimes at the LL (24L: 0D) and LD (12L: 12D, lights-on at 6:00), respectively ($P < 0.05$). Asterisks denote significant differences between photoperiods at the same feeding regime (*$P < 0.05$; **$P < 0.01$). Points outside the box plot are outliers.

increased levels of *il-1β*, *il-6*, and *tnf-α* in silver carp (*Hypophthalmichthys molitrix*) spleen (Ma et al., 2019). The above results suggest that the cytokine gene expression would be upregulated in some fish under stress. In this study, LL upregulated the expression of cytokine genes in the liver of juvenile rainbow trout. In addition, cytokine gene expression in the liver and intestine was significantly upregulated in the D-LD group. This result further indicated that LL and nocturnal feeding might cause stress to juvenile rainbow trout.

Photoperiodic changes are considered a chronic stressor in fish (Valenzuela et al., 2022). In the present study, the malondialdehyde (MDA) content in the liver of the LL group was significantly higher than that of the LD, while the catalase (CAT) activity was significantly lower than that of the LD. Similar results were reported for European Sea Bass (*Dicentrachus labrax* L.) (Li et al., 2021) and largemouth bass (*Micropterus salmoides*) (Malinovskyi et al., 2022). In addition, the feeding regime also affected the liver MDA content. Under LL, the D group obtained significantly higher MDA and lowest superoxide dismutase (SOD) activity, while under LD, the R group obtained significantly higher MDA. A significantly lower MDA was observed in the intestine under both photoperiods in the L group. Feeding that does not match its feeding rhythm has been found to negatively impact animal health and welfare (Oishi and Hashimoto, 2018), and rainbow trout are typically diurnal feeders (Iigo and Tabata, 1997; Bolliet et al., 2001). In addition, random feeding has been widely reported as a stressor in fish (Sánchez et al., 2009; Saiz et al., 2021). An unsuitable environment is a challenge and a stressor for fish. Anti-stress is a highly energy-consuming process (Chen et al., 2021), and fish need to satisfy additional energy requirements by increasing their energy metabolic rate (De Boeck et al., 2000; Lu et al., 2018). As a natural sub-product of cellular respiration, reactive oxygen species (ROS) production in mitochondria is also elevated under stress conditions (Luo et al., 2006; Mailloux, 2020). ROS is a highly reactive molecule; under normal conditions, organisms have a complete antioxidant system, including SOD and CAT, that can effectively scavenge ROS (Hoseinifar et al., 2020). MDA is a product of lipid peroxidation and is widely used to reflect the degree of oxidative damage in fish (Mendes et al., 2009; Sun et al., 2022). The above results suggest that long-term exposure to LL and random/nocturnal feeding can cause oxidative damage to juvenile rainbow trout.

However, the opposite result was observed in the serum, with significantly lower MDA levels in the random feeding group than in the scheduled feeding group (D and L). One possible reason relates to the unsaturation of fatty acids in the serum, with more unsaturated fatty acids being more susceptible

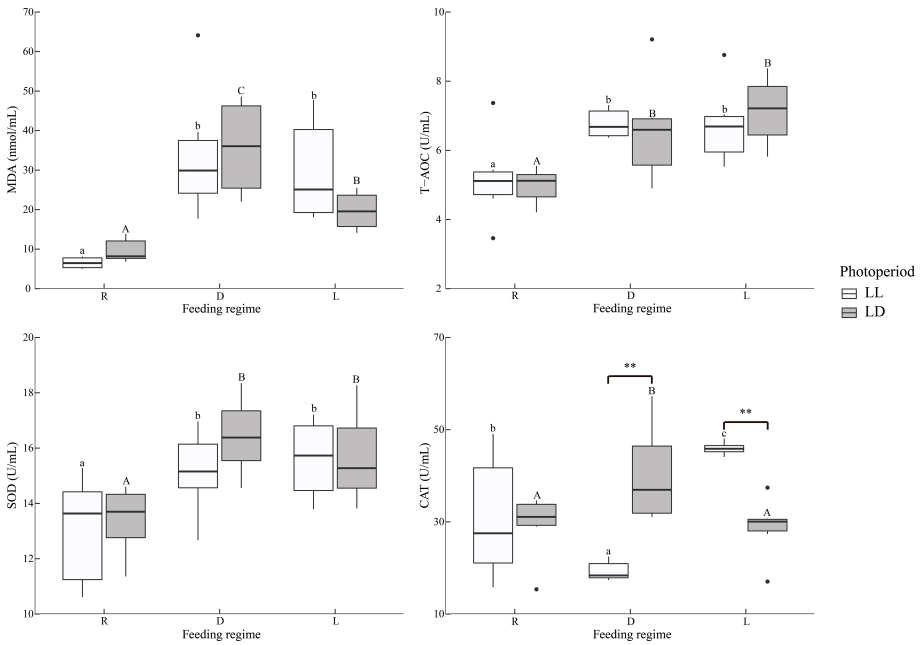

FIGURE 6
Serum antioxidant indicators of juvenile *Oncorhynchus mykiss* under different experimental treatments (n=6). MDA, Malondialdehyde; T-AOC, Total antioxidant capacity; SOD, Superoxide dismutase; CAT, Catalase; R, random feeding; D, mid-dark stage feeding; L, mid-light stage feeding; LL: 24L: 0D, LD: 12L: 12D. Different lowercase letters and capital letters indicate significant difference among different feeding regimes at the LL (24L: 0D) and LD (12L: 12D, lights-on at 6:00), respectively ($P < 0.05$). Asterisks denote significant differences between photoperiods at the same feeding regime (**$P < 0.01$). Points outside the box plot are outliers.

to oxidation (Lynn and Brown, 1959; Zhang et al., 2007), and we detected a higher ratio of monounsaturated and polyunsaturated fatty acids in the serum of the scheduled feeding group (data in a separate unpublished article). Additional evidence was found for significantly higher serum total antioxidant capacity (T-AOC) and SOD activities in the scheduled feeding group, suggesting that the antioxidant capacity was not limited in the scheduled feeding group.

Severe oxidative stress often causes cellular damage and apoptosis (Chandra et al., 2000). Two main pathways initiate apoptosis, the endogenous pathway (mitochondrial pathway) and the exogenous pathway (death receptor pathway). The endogenous apoptotic process begins with the release of cytochrome C (Cytc) from the mitochondria into the cytoplasm induced by cell death signals, which activates caspase and initiates the apoptotic program (Cheng et al., 2015). The exogenous pathway is activated by tumor necrosis factor (TNF) family receptors, which receive extracellular death signals and activate downstream caspase to initiate apoptosis (Gao et al., 2013). In addition, BCL-2 and BAX regulate apoptosis by affecting the release of mitochondrial Cytc during apoptosis (Cory and Adams, 2002). BAX is regulated by upstream p53 (Liu et al., 2005). p53 repairs cell DNA damage or induces cancer cell apoptosis (Polyak et al., 1997; Fridman and Lowe, 2003). In addition, p53 affects the transcription of *gpx* and *mnsod* genes in response to oxidative stress (Hussain et al., 2004). In this study, liver *cytc* gene expression was upregulated in the R group, and *bcl2* gene expression was upregulated in the D-LD group. Under LL, the expression of *p53* and *bax* genes was significantly higher in the L group than in the R group. This result indicated that the livers of the R and D-LD groups were subjected to oxidative stress and initiated the process of apoptosis. And the higher expression of the *p53* gene may reflect the repair of damaged cells. A similar expression trend to *p53* was also reflected in the expression of antioxidant enzyme genes *gpx*, *sod1*, *sod2*, and *cat*, which further supported that the scheduled feeding (especially the L group) mitigated oxidative damage by increasing the expression of antioxidant enzyme genes, thereby reducing apoptosis.

Under LL, *p53* and *bax* gene expression in the intestine was significantly higher in the L group than in the R group. However, the opposite phenomenon appeared under LD, with the lowest *p53* expression level in the L group. The antioxidant genes *sod1* and *sod2* showed a similar trend under LD. The lowest MDA levels were detected in the L-LD group, which indicated that the rainbow trout in this group were subjected to minimal oxidative

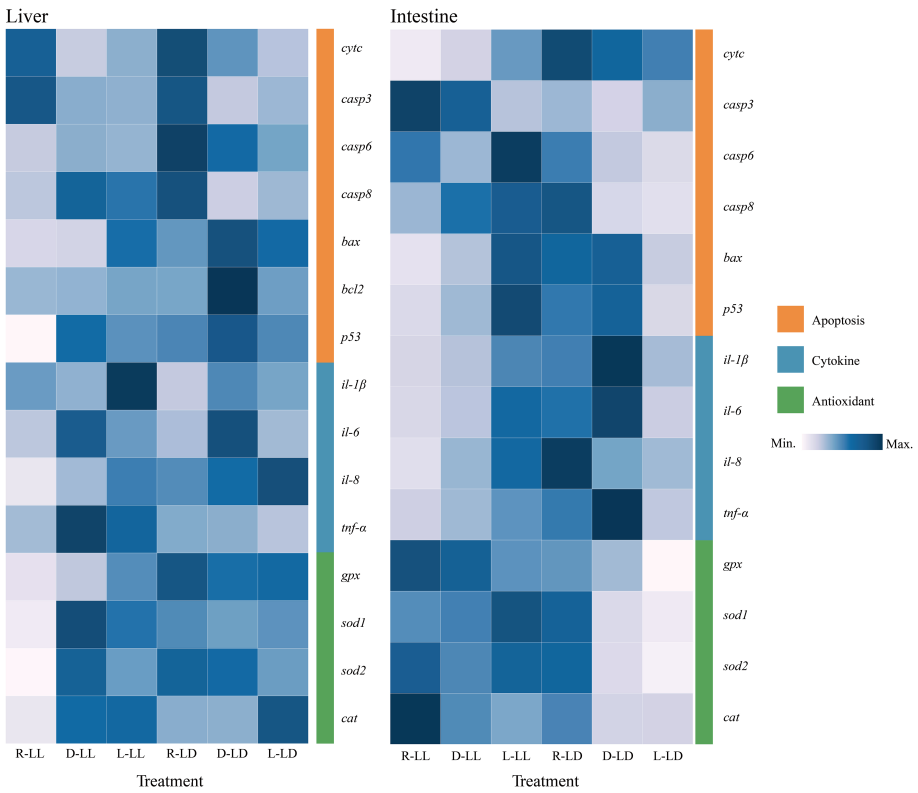

FIGURE 7
Liver and intestinal apoptosis, cytokine, and antioxidant-related gene expression of juvenile *Oncorhynchus mykiss* under different experimental treatments (n=6). R: random feeding, D: mid-dark stage feeding, L: mid-light stage feeding, LL: 24L: 0D, LD: 12L: 12D. *cytc*: Cytochrome c, *casp3*: Caspases 3, *casp6*: Caspases 6, *casp8*: Caspases 8, *bax*: Bcl2-associated X, *bcl-2*: B-cell lymphoma-2, *p53*: Tumor suppressor p53, *il-1β*: Interleukin-1β, *il-6*: Interleukin-6, *il-8*: Interleukin-8, *tnf-α*: Tumor necrosis factor-α, *gpx*: Glutathione peroxidase, *sod1*: Cytosolic Cu/Zn superoxide dismutase, *sod2*: Mitochondrial Mn superoxide dismutase, *cat*: Catalase.

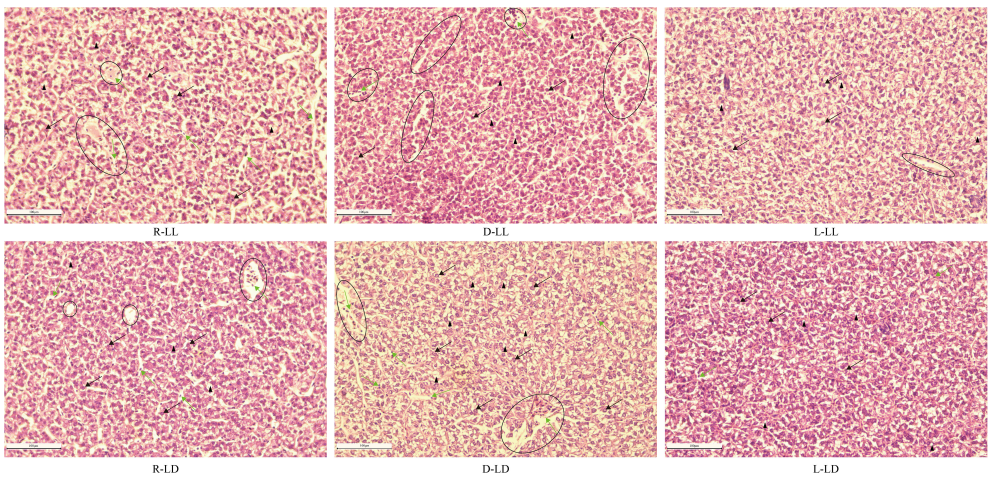

FIGURE 8
The histology of the liver in juvenile *Oncorhynchus mykiss* under different experimental treatments (200 × magnification, scale bars = 100 μm, slice thickness = 7 μm). R: random feeding, D: mid-dark stage feeding, L: mid-light stage feeding, LL: 24L: 0D, LD: 12L: 12D. The black arrow points to hepatocyte; the green arrow points to blood sinusoid including erythrocyte; the black triangle points to cavitation; the black circle points to vein including erythrocyte.

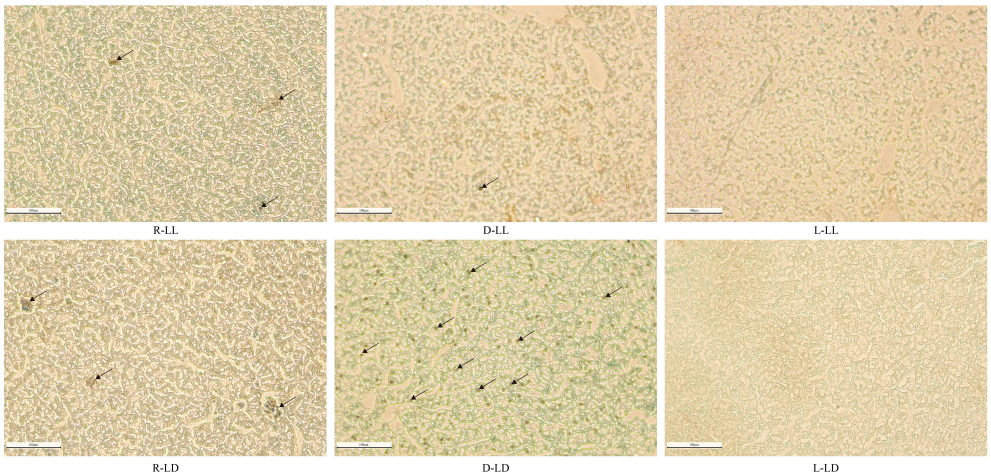

FIGURE 9
TUNEL staining analysis of liver in juvenile *Oncorhynchus mykiss* under different experimental treatments (200 × magnification, scale bars = 100 μm, slice thickness = 7 μm). R: random feeding, D: mid-dark stage feeding, L: mid-light stage feeding, LL: 24L: 0D, LD: 12L: 12D. The black arrows point to apoptotic cells.

stress and therefore, low levels of *p53*, *sod1*, and *sod2* gene expression also indicated that the fish were in a low-stress state. Similarly, the expression levels of *casp6* and *casp8* genes were significantly lower in the L-LD group.

Further H&E staining of liver paraffin sections revealed the presence of different degrees of pathological changes between the different groups. The R and D groups had significant capillary dilatation and erythrocyte sludge. This result suggested that random and nocturnal feeding could damage the liver of juvenile rainbow trout. On the other hand, TUNEL staining was used to detect apoptosis in liver cells (Liu et al., 2022), and it was found that a large number of apoptotic cells were observed in the D-LD group, and almost no apoptotic cells were observed in L-LL and L-LD. Overall, the histological observations of liver sections demonstrated that random and nocturnal feeding caused damage to the liver of rainbow trout, resulting in apoptosis. In contrast, there was no liver damage or apoptosis in the diurnal feeding group.

Conclusions

In this study, chronic exposure to LL caused oxidative stress in juvenile rainbow trout and affected liver health and immune system function. On the other hand, random and nocturnal feeding was also a stressor for juvenile rainbow trout, causing oxidative damage and apoptosis. The oxidative damage of LL was mitigated by scheduled diurnal feeding. Therefore, scheduled diurnal feeding could mitigate oxidative damage to rainbow trout from the lack of a photoperiodic environment. Further studies are needed to elucidate the biological clock mechanisms underlying the effects of photoperiod and feeding time on the health and welfare of juvenile rainbow trout.

Data availability statement

The raw data supporting the conclusions of this article will be made available by the authors, without undue reservation.

Ethics statement

The animal study was reviewed and approved by Animal Care and Use Committee of Ningbo University.

Author contributions

HX: methodology, data curation, visualization, and writing - original draft; CS: conceptualization and review and editing; YY, CW, CS, and CM: resources, review and editing, and supervision. All authors contributed to the article and approved the submitted version.

Funding

This study was supported by the National Key Research and Development Program of China (Project No. 2019YFD0901000), The Province Key Research and Development Program of

Zhejiang (Project No. 2021C02047), and K.C. Wong Magna Fund in Ningbo University.

Acknowledgments

The authors thank Professor Herve Migaud for his constructive comments on this research.

Conflict of interest

The authors declare that the research was conducted in the absence of any commercial or financial relationships that could be construed as a potential conflict of interest.

Publisher's note

All claims expressed in this article are solely those of the authors and do not necessarily represent those of their affiliated organizations, or those of the publisher, the editors and the reviewers. Any product that may be evaluated in this article, or claim that may be made by its manufacturer, is not guaranteed or endorsed by the publisher.

Supplementary material

The Supplementary Material for this article can be found online at: https://www.frontiersin.org/articles/10.3389/fmars.2022.1036289/full#supplementary-material

References

Abdollahpour, H., Falahatkar, B., and van der Kraak, G. (2021). The effects of long-term thyroxine administration on hematological, biochemical and immunological features in sterlet sturgeon (*Acipenser ruthenus*). *Aquaculture* 544, 737065. doi: 10.1016/j.aquaculture.2021.737065

Bavia, L., Santiesteban-Lores, L. E., Carneiro, M. C., and Prodocimo, M. M. (2022). Advances in the complement system of a teleost fish, *Oreochromis niloticus*. *Fish Shellfish Immunol.* 123, 61–74. doi: 10.1016/j.fsi.2022.02.013

Boes, M. (2000). Role of natural and immune IgM antibodies in immune responses. *Mol. Immunol.* 37 (18), 1141–1149. doi: 10.1016/S0161-5890(01)00025-6

Bolliet, V., Aranda, A., and Boujard, T. (2001). Demand-feeding rhythm in rainbow trout and European catfish-synchronisation by photoperiod and food availability. *Physiol. Behav.* 73 (4), 625–633. doi: 10.1016/S0031-9384(01)00505-4

Casanovas, P., Walker, S. P., Johnston, H., Johnston, C., and Symonds, J. E. (2021). Comparative assessment of blood biochemistry and haematology normal ranges between Chinook salmon (*Oncorhynchus tshawytscha*) from seawater and freshwater farms. *Aquaculture* 537, 736464. doi: 10.1016/j.aquaculture.2021.736464

Casillas, E., and Ames, W. (1985). Hepatotoxic effects of CCl4 on English sole (*Parophrys vetulus*): possible indicators of liver dysfunction. *Comp. Biochem. Physiol. C Comp. Pharmacol. Toxicol.* 84 (2), 397–400. doi: 10.1016/0742-8413(86)90112-X

Chaix, A., Lin, T., Le, H. D., Chang, M. W., and Panda, S. (2019). Time-restricted feeding prevents obesity and metabolic syndrome in mice lacking a circadian clock. *Cell Metab.* 29 (2), 303–319. doi: 10.1016/j.cmet.2018.08.004

Chandra, J., Samali, A., and Orrenius, S. (2000). Triggering and modulation of apoptosis by oxidative stress. *Free Radical Biol. Med.* 29 (3-4), 323–333. doi: 10.1016/S0891-5849(00)00302-6

Cheng, C. H., Yang, F. F., Liao, S. A., Miao, Y. T., Ye, C. X., Wang, A. L., et al. (2015). High temperature induces apoptosis and oxidative stress in pufferfish (*Takifugu obscurus*) blood cells. *J. Thermal Biol.* 53, 172–179. doi: 10.1016/j.jtherbio.2015.08.002

Chen, S. J., Migaud, H., Shi, C., Song, C. B., Wang, C. L., Ye, Y. F., et al. (2021). Light intensity impacts on growth, molting and oxidative stress of juvenile mud crab *Scylla paramamosain*. *Aquaculture* 545, 737159. doi: 10.1016/j.aquaculture.2021.737159

Chu, Y. I., Wang, C. M., Parka, J. C., and Lader, P. F. (2020). Review of cage and containment tank designs for offshore fish farming. *Aquaculture* 519, 734928. doi: 10.1016/j.aquaculture.2020.734928

Cory, S., and Adams, J. M. (2002). The BCL2 family: Regulators of the cellular life-or-death switch. *Nat. Rev. Cancer* 2 (9), 647–656. doi: 10.1038/nrc883

Dawood, M. A. O., Noreldin, A. E., and Sewilam, H. (2022). Blood biochemical variables, antioxidative status, and histological features of intestinal, gill, and liver tissues of African catfish (*Clarias gariepinus*) exposed to high salinity and high-temperature stress. *Environ. Sci. pollut. Res.* 29, 56357–56369. doi: 10.1007/s11356-022-19702-0

De Boeck, G., Vlaeminck, A., van der Linden, A., and Blust, R. (2000). The energy metabolism of common carp (*Cyprinus carpio*) when exposed to salt stress: An increase in energy expenditure or effects of starvation? *Physiol. Biochem. Zool.* 73 (1), 102–111. doi: 10.1086/316717

Demers, N., and Bayne, C. (2020). Immediate increase of plasma protein complement C3 in response to an acute stressor. *Fish Shellfish Immunol.* 107, 411–413. doi: 10.1016/j.fsi.2020.10.022

Dong, S. L. (2019). Researching progresses and prospects in large salmonidae farming in cold water mass of yellow Sea. *Periodical Ocean Univ. China* 49 (03), 1–6. doi: 10.16441/j.cnki.hdxb.20180303

Esteban, M. A., Cuesta, A., Rodriguez, A., and Meseguer, J. (2006). Effect of photoperiod on the fish innate immune system: a link between fish pineal gland and the immune system. *J. Pineal Res.* 41 (3), 261–266. doi: 10.1111/j.1600-079X.2006.00362.x

FAO (2022). *The state of world fisheries and aquaculture 2022. towards blue transformation* (Rome: FAO). doi: 10.4060/cc0461en

Ferain, A., Delbecque, E., Neefs, I., Dailly, H., De Saeyer, N., Van Larebeke, M., et al. (2021). Interplay between dietary lipids and cadmium exposure in rainbow trout liver: Influence on fatty acid metabolism, metal accumulation and stress response. *Aquat. Toxicol.* 231, 105676. doi: 10.1016/j.aquatox.2020.105676

Fjelldal, P. G., Hansen, T., Breck, O., Ørnsrud, R., Lock, E. J., Waagbø, R., et al. (2012). Vertebral deformities in farmed Atlantic salmon (*Salmo salar* l.) - etiology and pathology. *J. Appl. Ichthyol.* 28 (3), 433–440. doi: 10.1111/j.1439-0426.2012.01980.x

Fjelldal, P. G., Nordgarden, U., Berg, A., Grotmol, S., Totland, G. K., Wargelius, A., et al. (2005). Vertebrae of the trunk and tail display different growth rates in response to photoperiod in Atlantic salmon, *Salmo salar* l., post-smolts. *Aquaculture* 250 (1-2), 516–524. doi: 10.1016/j.aquaculture.2005.04.056

Fontagné-Dicharry, S., Véron, V., Larroquet, L., Godin, S., Wischhusen, P., Aguirre, P., et al. (2020). Effect of selenium sources in plant-based diets on antioxidant status and oxidative stress-related parameters in rainbow trout juveniles under chronic stress exposure. *Aquaculture* 529, 735684. doi: 10.1016/j.aquaculture.2020.735684

Fridman, J. S., and Lowe, S. W. (2003). Control of apoptosis by p53. *Oncogene* 22, 9030–9040. doi: 10.1038/sj.onc.1207116

Gao, D., Xu, Z. E., Zhang, X. Y., Zhu, C. C., Wang, Y. N., and Min, W. P. (2013). Cadmium triggers kidney cell apoptosis of purse red common carp (*Cyprinus carpio*) without caspase-8 activation. *Dev. Comp. Immunol.* 41 (4), 728–737. doi: 10.1016/j.dci.2013.08.004

Holland, M. C. H., and Lambris, J. D. (2002). The complement system in teleosts. *Fish Shellfish Immunol.* 12 (5), 399–420. doi: 10.1006/fsim.2001.0408

Hong, H. R., Liu, Z., Li, S. Q., Wu, D., Jiang, L. Q., Li, P. X., et al. (2022). Zinc oxide nanoparticles (ZnO-NPs) exhibit immune toxicity to crucian carp (*Carassius carassius*) by neutrophil extracellular traps (NETs) release and oxidative stress. *Fish shellfish Immunol.* 129, 22–29. doi: 10.1016/j.fsi.2022.07.025

Hoseinifar, S. H., Yousefi, S., Van Doan, H., Ashouri, G., Gioacchini, G., Maradonna, F., et al. (2020). Oxidative stress and antioxidant defense in fish: the

implications of probiotic, prebiotic, and synbiotics. *Rev. Fisheries Sci. Aquaculture* 29 (2), 198–217. doi: 10.1080/23308249.2020.1795616

Huang, M., Yang, X. G., Zhou, Y. G., Ge, J., Davis, D. A., Dong, Y. W., et al. (2021). Growth, serum biochemical parameters, salinity tolerance and antioxidant enzyme activity of rainbow trout (*Oncorhynchus mykiss*) in response to dietary taurine levels. *Mar. Life Sci. Technol.* 3 (4), 449–462. doi: 10.1007/s42995-020-00088-2

Hussain, S. P., Amstad, P., He, P. J., Robles, A., Lupold, S., Kaneko, I., et al. (2004). p53-induced up-regulation of MnSOD and GPx but not catalase increases oxidative stress and apoptosis. *Cancer Res.* 64 (7), 2350–2356. doi: 10.1158/0008-5472.CAN-2287-2

Iigo, M., and Tabata, M. (1997). Circadian rhythms of locomotor activity in the rainbow trout *Oncorhynchus mykiss*. *Fisheries Sci.* 63 (1), 77–80. doi: 10.2331/fishsci.63.77

Iturriaga, M., Espinoza, M. B., Poblete-Morales, M., Feijoo, C. G., Reyesa, A. E., Molina, A., et al. (2017). Cytotoxic activity of *Flavobacterium psychrophilum* in skeletal muscle cells of rainbow trout (*Oncorhynchus mykiss*). *Veterinary Microbiol.* 210, 101–106. doi: 10.1016/j.vetmic.2017.09.009

Kim, J. H., and Kang, J. C. (2016). Changes in hematological parameters, plasma cortisol, and acetylcholinesterase of juvenile rockfish, *Sebastes schlegelii* supplemented with the dietary ascorbic acid. *Aquac. Rep.* 4, 80–85. doi: 10.1016/j.aqrep.2016.07.001

Kordon, A. O., Karsi, A., and Pinchuk, L. (2018). Innate immune responses in fish: Antigen presenting cells and professional phagocytes. *Turkish J. Fisheries Aquat. Sci.* 18 (9), 1123–1139. doi: 10.4194/1303-2712-v18_9_11

Landless, P. J. (1976). Acclimation of rainbow trout to sea water. *Aquaculture* 7 (2), 173–179. doi: 10.1016/0044-8486(76)90006-5

Lazado, C. C., Gesto, M., Madsen, L., and Jokumsen, A. (2018). Interplay between daily rhythmic serum-mediated bacterial killing activity and immune defence factors in rainbow trout (*Oncorhynchus mykiss*). *Fish Shellfish Immunol.* 72, 418–425. doi: 10.1016/j.fsi.2017.11.025

Lazado, C. C., Nayak, S., Khozin-Goldberg, I., and Zilberg, D. (2019). The gut mucosal barrier of zebrafish (*Danio rerio*) responds to the time-restricted delivery of *Lobosphaera incisa*-enriched diets. *Fish Shellfish Immunol.* 89, 368–377. doi: 10.1016/j.fsi.2019.04.012

Li, M. Y., Guo, W. Q., Guo, G. L., Zhu, X. M., Niu, X. T., Shan, X. F., et al. (2019b). Effect of sub-chronic exposure to selenium and *Allium mongolicum regel* flavonoids on *Channa argus*: Bioaccumulation, oxidative stress, immune responses and immune-related signaling molecules. *Fish Shellfish Immunol.* 91, 122–129. doi: 10.1016/j.fsi.2019.05.002

Liu, Z. H., Lu, H. M., Shi, H. L., Du, Y. C., Yu, J., Gu, S., et al. (2005). PUMA overexpression induces reactive oxygen species generation and proteasome-mediated stathmin degradation in colorectal cancer cells. *Cancer Res.* 65, 1647–1654. doi: 10.1158/0008-5472.CAN-04-1754

Liu, E. G., Zhao, X. Q., Li, C. J., Wang, Y. F., Li, L. L., Zhu, H., et al. (2022). Effects of acute heat stress on liver damage, apoptosis and inflammation of pikeperch (*Sander lucioperca*). *J. Thermal Biol.* 106, 103251. doi: 10.1016/j.jtherbio.2022.103251

Livak, K. J., and Schmittgen, T. D. (2001). Analysis of relative gene expression data using real-time quantitative PCR and the $2^{-\triangle\triangle CT}$ method. *Methods* 25 (4), 402–408. doi: 10.1006/meth.2001.1262

Li, X., Wei, P. P., Liu, S. T., Tian, Y., Ma, H., and Liu, Y. (2021). Photoperiods affect growth, food intake and physiological metabolism of juvenile European Sea bass (*Dicentrachus labrax* l.). *Aquaculture Rep.* 20, 100656. doi: 10.1016/j.aqrep.2021.100656

Li, M. Y., Zhu, X. M., Tian, J. X., Liu, M., and Wang, G. Q. (2019a). Bioaccumulation, oxidative stress, immune responses and immune-related genes expression in northern snakehead fish, channa argus, exposure to waterborne selenium. *Mol. Biol. Rep.* 46 (1), 947–955. doi: 10.1007/s11033-018-4550-8

López-Olmeda, J. F. (2017). Nonphotic entrainment in fish. *Comp. Biochem. Physiol. Part A* 203, 133–143. doi: 10.1016/j.cbpa.2016.09.006

Lu, Y. L., Nie, M. M., Wang, L., Xiong, Y. H., Wang, F., Wang, L. J., et al. (2018). Energy response and modulation of AMPK pathway of the olive flounder *Paralichthys olivaceus* in low-temperature challenged. *Aquaculture* 484, 205–213. doi: 10.1016/j.aquaculture.2017.11.031

Luo, Y., Su, Y., Lin, R. Z., Shi, H. H., and Wang, X. R. (2006). 2-chlorophenol induced ROS generation in fish carassius auratus based on the EPR method. *Chemosphere* 65 (6), 1064–1073. doi: 10.1016/j.chemosphere.2006.02.054

Lynn, W. S., and Brown, R. H. (1959). Oxidation and activation of unsaturated fatty acids. *Arch. Biochem. Biophys.* 81 (2), 353–362. doi: 10.1016/0003-9861(59)90213-9

Ma, J. G., Chen, X., Xin, G. Y., and Li, X. Y. (2019). Chronic exposure to the ionic liquid [C_8 mim] br induces inflammation in silver carp spleen: Involvement of oxidative stress-mediated p38MAPK/NF-kappa b signalling and microRNAs. *Fish Shellfish Immunol.* 84, 627–638. doi: 10.1016/j.fsi.2018.09.052

Mailloux, R. J. (2020). An update on mitochondrial reactive oxygen species production. *Antioxidants* 9, 472. doi: 10.3390/antiox9060472

Malinovskyi, O., Rahimnejad, S., Stejskal, V., Boňko, D., Stará, A., Velišek, J., et al. (2022). Effects of different photoperiods on growth performance and health status of largemouth bass (*Micropterus salmoides*) juveniles. *Aquaculture* 548, 737631. doi: 10.1016/j.aquaculture.2021.737631

Mashoof, S., and Criscitiello, M. F. (2016). Fish immunoglobulins. *Biology* 5, 45. doi: 10.3390/biology5040045

Mendes, R., Cardoso, C., and Pestana, C. (2009). Measurement of malondialdehyde in fish: A comparison study between HPLC methods and the traditional spectrophotometric test. *Food Chem.* 112 (4), 1038–1045. doi: 10.1016/j.foodchem.2008.06.052

Meng, X. Z., Shen, Y. B., Wang, S. T., Xu, X. Y., Dang, Y. F., Zhang, M., et al. (2019). Complement component 3 (C3): An important role in grass carp (*Ctenopharyngodon idella*) experimentally exposed to *Aeromonas hydrophila*. *Fish Shellfish Immunol.* 88, 189–197. doi: 10.1016/j.fsi.2019.02.061

Molayemraftar, T., Peyghan, R., Jalali, M. R., and Shahriari, A. (2022). Single and combined effects of ammonia and nitrite on common carp, *Cyprinus carpio*: Toxicity, hematological parameters, antioxidant defenses, acetylcholinesterase, and acid phosphatase activities. *Aquaculture* 548, 737676. doi: 10.1016/j.aquaculture.2021.737676

Montero, R., Strzelczyk, J. E., Chan, J. T. H., Verleih, M., Rebl, A., Goldammer, T., et al. (2020). Dawn to dusk: Diurnal rhythm of the immune response in rainbow trout (*Oncorhynchus mykiss*). *Biology-Basel* 9 (1), 8. doi: 10.3390/biology9010008

Mukherjee, D., Saha, S., Chukwuka, A. V., Ghosh, B., Dhara, K., Saha, N. C., et al. (2022). Antioxidant enzyme activity and pathophysiological responses in the freshwater walking catfish, *Clarias batrachus* Linn under sub-chronic and chronic exposures to the neonicotinoid, thiamethoxam®. *Sci. Total Environ.* 836, 155716. doi: 10.1016/j.scitotenv.2022.155716

Mustapha, M. K., Oladokun, O. T., Salman, M. M., Adeniyi, I. A., and Ojo, D. (2014). Does light duration (photoperiod) have an effect on the mortality and welfare of cultured *Oreochromis niloticus* and *Clarias gariepinus*? *Turkish J. Zool.* 38 (4), 466–470. doi: 10.3906/zoo-1309-23

Nisembaum, L. G., Velarde, E., Tinoco, A. B., Azpeleta, C., de Pedro, N., Alonso-Gómez, A. L., et al. (2012). Light-dark cycle and feeding time differentially entrains the gut molecular clock of the goldfish (*Carassius auratus*). *Chronobiol. Int.* 29, 665–673. doi: 10.3109/07420528.2012.686947

Oishi, K., and Hashimoto, C. (2018). Short-term time-restricted feeding during the resting phase is sufficient to induce leptin resistance that contributes to development of obesity and metabolic disorders in mice. *Chronobiol. Int.* 35 (11), 1576–1594. doi: 10.1080/07420528.2018.1496927

Panserat, S., Plagnes-Juan, E., Gazzola, E., Palma, M., Magnoni, L. J., Marandel, L., et al. (2020). Hepatic glycerol metabolism-related genes in carnivorous rainbow trout (*Oncorhynchus mykiss*): insights into molecular characteristics, ontogenesis, and nutritional regulation. *Front. Physiol.* 11. doi: 10.3389/fphys.2020.00882

Pan, L. Q., Xie, P., and Hu, F. W. (2010). Responses of prophenoloxidase system and related defence parameters of *Litopenaeus vannamei* to low salinity. *J. Ocean Univ. China* 9 (3), 273–278. doi: 10.1007/s11802-010-1711-3

Polyak, K., Xia, Y., Zweier, J. L., Kinaler, K. W., and Vogelstein, B. (1997). A model for p53-induced apoptosis. *Nature* 389 (6648), 300–305. doi: 10.1038/38525

Qiu, W. H., Zhan, H. Y., Tian, Y. Q., Zhang, T., He, X., Luo, S. S., et al. (2018). The *in vivo* action of chronic bisphenol f showing potential immune disturbance in juvenile common carp (*Cyprinus carpio*). *Chemosphere* 205, 506–513. doi: 10.1016/j.chemosphere.2018.04.105

Rahman, A. N. A., Mohamed, A. A., Dahran, N., Farag, M. F. M., Alqahtani, L. S., Nassan, M. A., et al. (2022). Appraisal of sub-chronic exposure to lambda-cyhalothrin and/or methomyl on the behavior and hepato-renal functioning in *Oreochromis niloticus*: Supportive role of taurine-supplemented feed. *Aquat. Toxicol.* 250, 106257. doi: 10.1016/j.aquatox.2022.106257

Ren, Y. C., Men, X. H., Yu, Y., Li, B., Zhou, Y. G., and Zhao, C. Y. (2022). Effects of transportation stress on antioxidation, immunity capacity and hypoxia tolerance of rainbow trout (*Oncorhynchus mykiss*). *Aquaculture Rep.* 22, 100940. doi: 10.1016/j.aqrep.2021.100940

Ren, D. L., Zhang, J. L., Yang, L. Q., Wang, X. B., Wang, Z. Y., Huang, D. F., et al. (2018). Circadian genes period1b and period2 differentially regulate inflammatory responses in zebrafish. *Fish Shellfish Immunol.* 77, 139–146. doi: 10.1016/j.fsi.2018.03.048

Saiz, N., Gomez-Boronat, M., De Pedro, N., Delgado, M. J., and Isorna, E. (2021). The lack of light-dark and feeding-fasting cycles alters temporal events in the goldfish (*Carassius auratus*) stress axis. *Animals* 11 (3), 669. doi: 10.3390/ani11030669

Sakai, M., Hikima, J., and Kono, T. (2021). Fish cytokines: current research and applications. *Fisheries Sci.* 87 (1), 1–9. doi: 10.1007/s12562-020-01476-4

Sánchez, J. A., López-Olmeda, J. F., Blanco-Vives, B., and Sánchez-Vázquez, F. J. (2009). Effects of feeding schedule on locomotor activity rhythms and stress response in sea bream. *Physiol. Behav.* 98 (1-2), 125–129. doi: 10.1016/j.physbeh.2009.04.020

Shepherd, B. S., Drennon, K., Johnson, J., Nichols, J. W., Playle, R. C., Singer, T. D., et al. (2005). Salinity acclimation affects the somatotropic axis in rainbow trout. *Am. J. Physiol.-Regul. Integr. Comp. Physiol.* 288 (5), R1385–R1395. doi: 10.1152/ajpregu.00443.2004

Stephan, F. K. (2002). The "other" circadian system: food as zeitgeber. *J. Biol. Rhythms* 17 (4), 284–292. doi: 10.1177/074873002129002591

Sun, X. Q., Zhao, X., Li, L., Gao, Q. F., and Dong, S. L. (2022). Growth, oxidative stress and the non-specific immune response of *Oncorhynchus mykiss* exposed to different light spectra. *Aquaculture Res.* 53 (11), 4210–4216. doi: 10.1111/are.15915

Valenzuela, A., Rodríguez, I., Schulz, B., Cortés, R., Acosta, J., Campos, V., et al. (2022). Effects of continuous light (LD24:0) modulate the expression of lysozyme, mucin and peripheral blood cells in rainbow trout. *Fishes* 7 (1), 28. doi: 10.3390/fishes7010028

Wargelius, A., Fjelldal, P. G., Nordgarden, U., and Hansen, T. (2009). Continuous light affects mineralization and delays osteoid incorporation in vertebral bone of Atlantic salmon (*Salmo salar* l.). *J. Exp. Biol.* 212 (5), 656–661. doi: 10.1242/jeb.024000

Witeska, M., Kondera, E., Ługowska, K., and Bojarski, B. (2022). Hematological methods in fish - not only for beginners. *Aquaculture* 547, 737498. doi: 10.1016/j.aquaculture.2021.737498

Xia, H., Wu, K., Liu, W. J., Gul, Y., Wang, W. M., and Zhang, X. Z. (2014). Molecular cloning and expression analysis of immunoglobulin m heavy chain gene of blunt snout bream (*Megalobrama amblycephala*). *Fish Shellfish Immunol.* 40 (1), 129–135. doi: 10.1016/j.fsi.2014.06.026

Xu, H. Y., Dou, J., Wu, Q. Y., Ye, Y. F., Song, C. B., Mu, C. K., et al. (2022). Investigation of the light intensity effect on growth, molting, hemolymph lipid, and antioxidant capacity of juvenile swimming crab *Portunus trituberculatus*. *Front. Mar. Sci.* 9. doi: 10.3389/fmars.2022.922021

Yada, T., Azuma, T., and Takagi, Y. (2001). Stimulation of non-specific immune functions in seawater-acclimated rainbow trout, *Oncorhynchus mykiss*, with reference to the role of growth hormone. *Comp. Biochem. Physiol. Part B: Biochem. Mol. Biol.* 129, 695–701. doi: 10.1016/S1096-4959(01)00370-0

Yamamuro, D., Takahashi, M., Nagashima, S., Wakabayashi, T., Yamazaki, H., Takei, A., et al. (2020). Peripheral circadian rhythms in the liver and white adipose tissue of mice are attenuated by constant light and restored by time- restricted feeding. *PloS One* 15 (6), e0234439. doi: 10.1371/journal.pone.0234439

Zante, M. D., Borchel, A., Brunner, R. M., Goldammer, T., and Rebl, A. (2015). Cloning and characterization of the proximal promoter region of rainbow trout (*Oncorhynchus mykiss*) interleukin-6 gene. *Fish Shellfish Immunol.* 43 (1), 249–246. doi: 10.1016/j.fsi.2014.12.026

Zeng, C., Hou, Z. S., Zhao, H. K., Xin, Y. R., Liu, M. Q., Yang, X. D., et al. (2021). Identification and characterization of caspases genes in rainbow trout (*Oncorhynchus mykiss*) and their expression profiles after *Aeromonas salmonicida* and *Vibrio anguillarum* infection. *Dev. Comp. Immunol.* 118, 103987. doi: 10.1016/j.dci.2020.103987

Zhang, C. X., Huang, F., Li, J., Wang, L., Song, K., and Mai, K. S. (2016). Interactive effects of dietary magnesium and vitamin e on growth performance, body composition, blood parameters and antioxidant status in Japanese seabass (*Lateolabrax japonicus*) fed oxidized oil. *Aquac. Nutr.* 22, 708–722. doi: 10.1111/anu.12393

Zhang, W. H., Shi, B., and Shi, J. (2007). A theoretical study on autoxidation of unsaturated fatty acids and antioxidant activity of phenolic compounds. *J. Am. Leather Chem. Assoc.* 102 (3), 99–105.

Zhou, Z. Y., Zhou, B., Chen, H. M., Tang, X. X., and Wang, Y. (2019). Reactive oxygen species (ROS) and the calcium-(Ca^{2+}) mediated extrinsic and intrinsic pathways underlying BDE-47-induced apoptosis in rainbow trout (*Oncorhynchus mykiss*) gonadal cells. *Sci. Total Environ.* 656, 778–788. doi: 10.1016/j.scitotenv.2018.11.306

Zhu, W. T., and Su, J. G. (2022). Immune functions of phagocytic blood cells in teleost. *Rev. Aquaculture* 14 (2), 630–646. doi: 10.1111/raq.12616

frontiers | Frontiers in Marine Science

TYPE Original Research
PUBLISHED 24 November 2022
DOI 10.3389/fmars.2022.1021688

OPEN ACCESS

EDITED BY
Hüseyin Sevgili,
Hüseyin Sevgili, Turkey

REVIEWED BY
Lingling Wang,
Dalian Ocean University, China
Yiran Hou,
Freshwater Fisheries Research Center (CAFS), China

*CORRESPONDENCE
Zhangying Ye
yzyzju@zju.edu.cn
Jian Zhao
zhaojzju@zju.edu.cn

SPECIALTY SECTION
This article was submitted to Marine Fisheries, Aquaculture and Living Resources, a section of the journal Frontiers in Marine Science

RECEIVED 17 August 2022
ACCEPTED 09 November 2022
PUBLISHED 24 November 2022

CITATION
Wei D, Ji B, Li H, Zhu S, Ye Z and Zhao J (2022) Modified kinetic energy feature-based graph convolutional network for fish appetite grading using time-limited data in aquaculture. *Front. Mar. Sci.* 9:1021688. doi: 10.3389/fmars.2022.1021688

Modified kinetic energy feature-based graph convolutional network for fish appetite grading using time-limited data in aquaculture

Dan Wei[1], Baimin Ji[1], Haijun Li[1], Songming Zhu[1,2], Zhangying Ye[1,2]* and Jian Zhao[1]*

[1]College of Biosystems Engineering and Food Science, Zhejiang University, Hangzhou, China, [2]Ocean Academy, Zhejiang University, Zhoushan, China

Feed has the greatest impact on the carbon footprint of the aquaculture, and also determines the water quality in aquaculture to a great extent. Making appropriate feeding control strategies is one of the most effective ways to promote cleaner production as well as fish welfare in aquaculture. Reliable and accurate fish appetite grading especially based on time-limited data is a prerequisite for achieving high-precision and reasonable feeding control in practical production. To date, however, few efforts have been done on this challenge. For these, regarding *Micropterus salmoides* as the experimental fish, a novel and practical method, based on a modified kinetic energy feature-based graph convolutional network (GCN), was developed in this study. First, graphs were constructed based on the extracted modified kinetic energy features and their temporal correlation. Then, with the help of a series of the convolution and global pooling operations, a GCN model was customized based on the constructed graphs. Following this, the customized GCN model was enriched by the self-attention pooling mechanism and customized network structure. Results show that the proposed GCN-based approach outperforms other typical state-of-the-art methods in fish appetite grading, and the grading accuracy obtained here could be 98.60% using only the first 4.2 seconds as well as the first 8.3 seconds of input data, which is not much different from that (98.89%) using full-length (25 second-long) input data. What's more, compared to the recurrent neural network (RNN)-based method which performance is closest to our method, the space complexity of the proposed approach here can better satisfy the requirements of real aquaculture, in which the quantity of the trainable parameters here is only 6.4% ~ 31.8% of the RNN-based method. In summary, the proposed modified kinetic energy feature-based GCN approach is favorable for the appetite grading of fish like *Micropterus salmoides* with time-limited data, which is a

promising approach in dealing with feeding control tasks and alleviating the water environmental burden in aquaculture.

KEYWORDS

aquaculture, fish appetite grading, time-limited data, kinetic energy feature, customized graph convolutional network

Introduction

Aquaculture production has grown rapidly in the past few decades, thereinto, 52% consumption of the aquatic products worldwide in 2018 was provided by aquaculture (FAO, 2020). In the meantime, the concept of cleaner production and fish welfare is being emphasized due to its indispensable role in quality and yield of the aquatic products (Luna et al., 2019). Feeding is of great importance in managing aquaculture tasks, where the cost of feed is around 30%~70% of the total production costs (Føre et al., 2011; Atoum et al., 2015; Zhou et al., 2018). Underfeeding impedes fish growth, thus the strategy of overfeeding is commonly adopted in practical production to satisfy the nutritional needs of fish. However, overfeeding leads to left-over feed, which results in not only the extra cost, but also the poor water quality (Barraza-Guardado et al., 2014; Jescovitch et al., 2018; Zhao et al., 2019) and an extra load on water treatment equipment (Chang et al., 2005). Moreover, previous research has shown that feed has the greatest impact on the carbon footprint of the aquaculture (Luna et al., 2019). As a consequence, optimization of the feeding control is a prime consideration to realize cleaner production and promote fish welfare in aquaculture, especially in intensive modes.

Precise representation of fish appetite is the guarantee for the accurate feeding control. Relevant studies have shown that fish feeding behavior has significant advantages in fish appetite representation (Parra et al., 2018; Li et al., 2020; An et al., 2021), compared with many other mediums such as residual feed (Atoum et al., 2015; Wang et al., 2022) and water quality (Zhao et al., 2019; Zhao et al., 2020a). Until now, many works have been done to optimize the feeding based on fish school behavior. For example, the infrared photoelectric senor was used to capture the gathering behaviors of eels for the feeding control in indoor intensive aquaculture systems (Chang et al., 2005). Liu et al. (2014) proposed a computer vision-based feeding activity index for the automatic feeding of Atlantic salmon in recirculating aquaculture system (RAS) by analyzing differences in two consecutive frames. Ye et al. (2016) made use of the Lucas-Kanade optical flow and information entropy to assess and optimize the feeding of tilapia in RAS, and this method was then further improved by the quantification of fish spontaneous collective behaviors (Zhao et al., 2017). These methods, however, were based on human-made features (i.e., low-level features), which made them task-specific and weak in generalization capability. With the rapid development of deep learning, convolutional neural network (CNN) was gradually applied to fish appetite evaluation (Zhou et al., 2019). Profiting from the utilization of the high-level features of feeding behavior, fish appetite could be represented more precisely and robustly (Zhou et al., 2019; Ubina et al., 2021). From this, Wei et al. (2021) developed a method based on the modified kinetic energy model and customized recurrent neural network (RNN) to comprehensively utilize the spatial-temporal characteristics of fish feeding behavior, which therefore made fish appetite evaluation more accurate and practical. Similarly, by exploiting the spatial-temporal characteristics of fish feeding behavior, Feng et al. (2022) also realized the precise quantification of fish appetite resorted to a lightweight 3D ResNet-GloRe network, although a feeding strategy not commonly used in real production was adopted.

Methods mentioned above mainly rely on the characteristics of feeding behavior over time and have high requirement on the time-duration of data (i.e., data integrity). Generally speaking, the longer the time duration of data is, the better the data integrity and the better performance of the method would be. However, longer the time-duration of data normally means the more time taken in fish appetite assessment; what's more, the collection of data with long time-duration is a time-consuming process itself. In real production, in order to leave enough reaction time for the follow-up feeding control (including feeding strategy adjustment), the sooner of fish appetite assessment, the better. For this, increasing hardware investment seems to be a simplest and most direct solution, nevertheless, this will undoubtedly increase the production costs and affect the economic benefits (Feng et al., 2022). A promising alternative to the above solution is decreasing the time-duration of input data, namely, grading fish appetite using time-limited data particularly the beginning of time series data. But how to

construct an efficient fish appetite grading model with strong learning ability on this time-limited feeding behavior data is still a challenge. Few efforts on this challenge have been reported so far.

Given all that, regarding *Micropterus salmoides* as the experimental fish, a modified kinetic energy feature-based graph convolutional network (GCN), which could address the challenge mentioned above and grade fish appetite precisely with low space complexity, was developed in this study. In this network, each video frame was presented as a node. It's time information and the corresponding quantitative spatial information of fish feeding behavior were utilized as node features in the graph. In the meantime, the temporal connections between nodes were abstracted as edges in the graph. Benefiting by the specific graph constructed above and the customized network structure, the grading accuracy obtained by the proposed method here could be 98.60% using only the first 4.2 (one-sixth of the full-length data) seconds as well as the first 8.3 seconds (one-third of the full-length data) of input data, which is not much different from that on full-length (25 second-long) input data.

Materials and methods

Our experimental protocol was approved by the committee of the Care and Use of animals of the Zhejiang University. In addition, the experiments carried out on fish were conducted in strict accordance with the guidelines of the Association for the Study of Animal Behavior Use of Zhejiang University (ZJU20190074) in this study. Note that due to the indispensable role and rapid growth trend of industrial RAS in aquaculture, our experiment was conducted in RAS.

Fish

In this experiment, *Micropterus salmoides* were used. All experimental fish (quantity: 150) were first acclimated in the experimental RAS for one month. The average size of fish was 37.5 ± 5 g. During the entire experiment, the fish were placed under a 12h: 12h light-dark cycle (08:00-20:00 light, 20:00-08:00 dark) and fed 2 times a day (10:00 and 16:00) using commercial floating pellets. The feeding amount per day was set to 5% of the total mass of the fish.

Experimental system

The experimental aquaculture system (Figure 1) mainly consisted of a rearing tank (75 cm radius and 40 cm water depth), a feeding machine, and a computer vision system. During the entire acclimation and experiment, the following conditions were maintained: temperature at 26 ± 2°C, dissolved oxygen (DO) at (5.5 ± 0.5) mg/L, pH at 7.2 ± 0.5, nitrate ≤ 0.5 mg/L, and total ammonia nitrogen (TAN) ≤ 0.8 mg/L. The computer vision system possessed a Hikvision DS-2CD6233F-SDI camera, a Hikvision DS-7808NB-K2 Digital Video Recorder and a Server (GPU: NVIDIA 1080ti 11GB, CPU Intel Core i5-9400, 2.9 GHz, 8 GB memory). The camera was fixed 120 cm above the water surface of the rearing tank, with a 25fps frame rate and a 1080×1920 pixel.

To obtain sufficient fish feeding video data to verify the performance of the method proposed in this study, the overfed regime was adopted in this study. Food pellets were delivered with the same dose at intervals of ~25 s in each feeding event. Feeding wouldn't stop until fish showed no response to the delivered food. The residual pellets remaining on the water

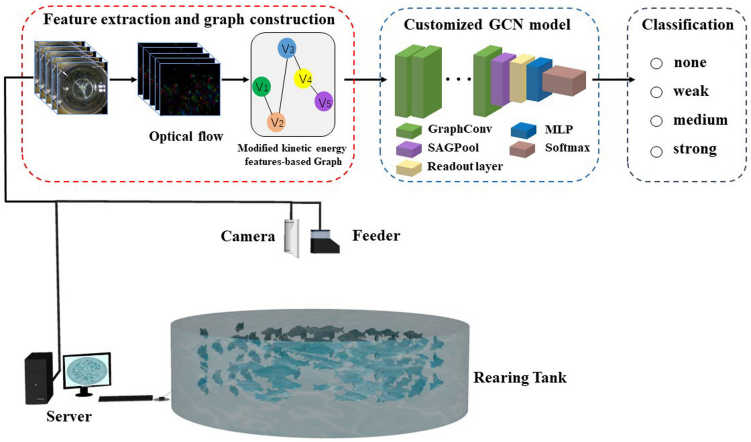

FIGURE 1
The overview of the fish appetite grading pipeline.

surface after feeding were then removed to prevent affecting the water quality.

Overview of the proposed approach

Accurate fish appetite grading is a prerequisite for intelligent feeding control and cleaner production in aquaculture. Therefore, we proposed a GCN-based fish appetite grading method, as shown in Figure 1. The method consists of two major steps: (1) feature extraction and graph construction: the improved kinetic energy model is used to extract the spatial characteristics of fish feeding behavior from feeding videos, and then a graph $G = (V, E)$ is constructed based on the modified kinetic energy features and their temporal correlation. (2) GCN-based classification model: the GCN-based model combines the graph structures and vertex features in the convolution, and propagated over the graph through multiple layers. Through the graph convolution layer by layer, the node features are extracted and updated. In addition, the GCN structure adopts the global graph pooling method based on self-attention mechanism, which fully considers the topology of nodes and graphs, and has significant advantages in graph classification tasks. In this study, the proposed method was developed using python3.7, and the customized neural networks grading model was trained on Pytorch1.10.0.

Feature extraction and graph construction

Graph, as a data structure that could simultaneously store target's feature information and its associated information, has been widely applied to efficient task classification (Lazer et al., 2009; Lee et al., 2019). This technique, however, is rarely used in aquaculture yet. For fish appetite grading, if it could be transformed into a simple graph classification task, the efficiency of this grading would be maximized. But how to extract efficient features as the graph features and construct the graph are the key to achieving this graph classification task. The spatial-temporal characteristics of fish feeding behavior shows great potential in fish appetite assessment (Wei et al., 2021; Feng et al., 2022), therefore, the feature extraction and graph construction in this study are carried out for the representation of these spatial-temporal characteristics.

First, the modified kinetic energy model (Eq. (1)) was used to extract spatial characteristics of fish behavior due to their strong motion feature extraction ability (Zhao et al., 2017).

$$E_K = C_E \times v_E^2 \tag{1}$$

Where C_E and v_E denote the disorder degree and velocity of the change in target areas, respectively.

The Gunner Farneback optical flow algorithm was used to calculate the v_E (Eq. (2)) of the changes in target areas in this study. Then, the scope of velocity was divided into a number of sections. As shown in Eq. (3), v_E was classified into the corresponding sections. In addition, to avoid the influence of the fish body length change on the motion feature extraction during the experiment, the v_E was calculated by the normalization method.

$$v_E = \frac{\sum_{x,y}|F_n(x,y)|}{N} \tag{2}$$

$$p(j) = \{(k(j)/N) \times 100\,\%,\ 1 \le j \le m\} \tag{3}$$

Where F_n is the normalized optical flow between two consecutive frames of images, (x, y) represents the coordinates of the reflective region in the current frame. m is the number of sections of v_E, N is the number of motion vectors in the current frame. k and p are the set of statistical numbers and statistical probability in each section, respectively. In this section, v_E was counted at intervals of 0.04 bl (bl is the average body length of *Micropterus salmoides*), and m was set to 25.

Then, C_E was calculated as:

$$C_E = -\sum_{j=1}^{m} p(j) log_2(p(j)) \tag{4}$$

Combined with Eq. (4), the normalized kinetic energy of the whole areas was defined as:

$$E_k = -\left(\sum_{j=1}^{m} p(j) log_2(p(j))\right) \times \left(\frac{\sum_{x,y}|F_n(x,y)|}{N}\right)^2 \tag{5}$$

Figure 2 shows the modified kinetic energy over time within a single round feeding event. As shown below, fish appetite, graded following the criterion of Øverli et al. (2006) and Eriksen et al. (2011), can be described well by the modified kinetic energy here.

Finally, graph G was constructed by the following two elements: (1) adjacency matrix A ($A \in R^{N\times N}$). This element is used to represent the connection between video frames (i.e., time correlation). The adjacency matrix contains only elements of 0 and 1. The element is 0 if there is no link between two video frames and 1 denotes there is a link. (2) feature matrix X. We regard the spatial-temporal characteristics of fish behavior (i.e., the normalized kinetic energy features and their temporal correlation) extracted from video frames as the attribute features of the node in the networks, expressed as $X \in R^{N\times P}$, where P represents the number of node attribute features.

To express the above algorithm more intuitively, the feature extraction and graph construction process are outlined in Algorithm 1.

Input: video frames; modified kinetic energy model (MKEM); normalization strategy N; adjacency matrix A ($A \in R^{N\times N}$); feature matrix X ($X \in R^{N\times P}$);

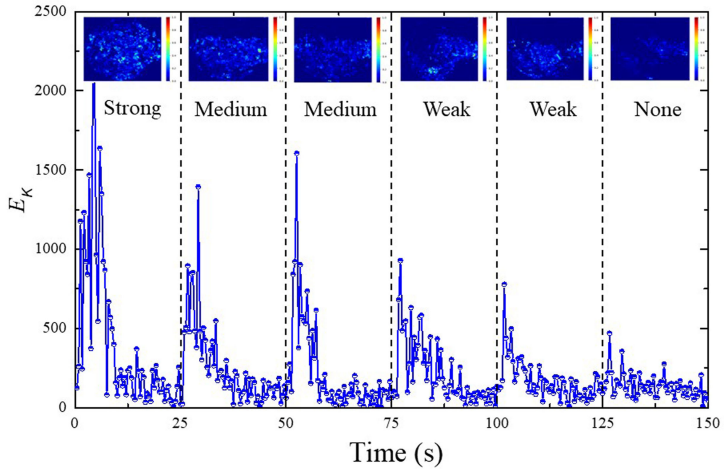

FIGURE 2
Diagram of the modified kinetic energy over time within a single round feeding event (None: fish do not respond to food; Weak: fish eat only pellets that fall directly in front of them but do not move to take food; Medium: fish move to take food, but return to their original positions; Strong: fish move freely between food items and consume all the available food. Noted that, the heat maps generated by the optical flow of the points with the maximum kinetic energy are used to better visualized fish appetite here).

Output: $G = (V, E)$
function feature extraction (video frames, MKEM, N)
$C_E \leftarrow$ video frames
$F_n(x,y) \leftarrow$ video frames & N
$v_E \leftarrow F_n(x, y)$
for x, y in video frames **do**
$E_K / C_E \times v_E^2$
return E_K
function graph construction (E_K, A, X)
$A \leftarrow$video frames
$X \leftarrow$ video frames & E_K
$G = (V, E) \leftarrow A$ & X
return G

ALGORITHM 1
Feature extraction and graph construction.

GCN-based fish appetite grading model

Advanced methods of applying deep learning to structured data such as graphs have been proposed in recent years. In particular, the method of generalizing the convolution operation to graphs has been proven to improve performance and has been widely used (Lee et al., 2019; Zhao et al., 2020b).

Given this, a customized GCN (Figure 3) following the constructed graph above was proposed in this study to achieve accurate fish appetite grading using time-limited data. This model consists of seven graph convolutional layers, and outputs of each layer are concatenated. Node and graph feature are updated and aggregated in the pooling layer with self-attention mechanism, and then transmitted to the MLP layer through the readout layer. Finally, the fish appetite level is determined with the help of softmax layer. The propagation rule of GCN can be summarized by the following expression:

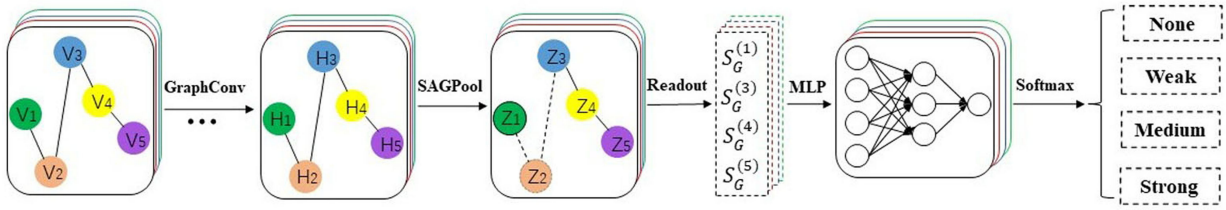

FIGURE 3
Schematic diagram of the proposed fish appetite grading model.

$$h^{(l+1)} = \sigma\left(\tilde{D}^{-\frac{1}{2}}\tilde{A}\tilde{D}^{-\frac{1}{2}}h^{(l)}\Theta\right) \quad (6)$$

Where $h^{(l)}$ represents the node representation of l-th layer and $\Theta \in \mathbb{R}^{F\times F'}$ represents the convolution weight with input feature dimension F and output feature dimension F', $\tilde{A} = A + I_N$ represents the matrix with added self-attentions, I_N represents the identity matrix, $\tilde{D} = \sum_i \tilde{A}_{ij}$, and σ is the activation function. The Rectified Linear Unit (Relu) function was used as an activation function in this study.

The attention mechanism has been widely used in recent deep learning studies (Cheng et al., 2016; Lee et al., 2019). Such a mechanism enables the model to focus more on important features and less on noncritical features (Lee et al., 2019), especially the self-attention mechanism. Thus, the self-attention pooling mechanism was used in this study. The self-attention score $Z \in \mathbb{R}^{N\times 1}$ was calculated as follow.

$$Z = \sigma\left(\tilde{D}^{-\frac{1}{2}}\tilde{A}\tilde{D}^{-\frac{1}{2}}X\Theta_{att}\right) \quad (7)$$

Where $X \in \mathbb{R}^{N\times F}$ is the input feature of the graph with N nodes and F-dimensional features, and $\Theta_{att} \in \mathbb{R}^{F\times 1}$ is the parameter of the self-attention pooling layer.

In the GCN-based classification model, the readout layer was used to aggregates node features to make a fixed size representation. The summarized output feature of the readout layer was as follows:

$$s = \frac{1}{N}\sum_{i=1}^{N} x_i \,\|\, \max_{i=1} x_i \quad (8)$$

Where N is the number of nodes, x_i is the feature vector i-th node, and || denotes concatenation.

Data collection and training set production

In this study, the video frames of fish school behavior under four feeding intensities were intercepted at equal intervals (12 frames per second). After data augmentation (referring to Wei et al., 2021), the total number of samples in the training set increased to 24300 (see https://github.com/Doubleblindpeerreview/fish-appetite-grading for details of dataset and codes). Of those data, 80% were used as the training set, 10% were used as the validation set, and 10% were used as the test set.

Setting appropriate parameters is the key step to training a robust model. In this study, Adam optimizer, early stopping criterion and hyperparameter selection strategy were used as the model architecture. If the validation loss did not improve for 60 epochs in an epoch termination condition with a maximum of 100k epochs, the training would be stopped. After many trials, the initial parameters and training strategies of the GCN-based method were set to the values shown in Table 1.

TABLE 1 The main parameters of GCN model.

Parameter	Value
Learning rate	5×10^{-4}
Batch size	128
Dropout rate	0.5
Pooling rate	0.8
Hidden size	256
Weight decay	1×10^{-4}

Performance evaluation

The results of testing for all approaches were arranged in confusion matrices, including true positive (*TP*), true negative (*TN*), false positive (*FP*), and false negative (*FN*). In this context, *TP* and *TN* respectively denote the numbers of the same samples with the current feeding appetite pertaining to the other fish appetite recognition results and actual results; *FP* and *FN* are the numbers of different videos with the current fish appetite pertaining to the other fish appetite recognition results and actual results, respectively.

To evaluate model performance, five widely used measures were calculated: accuracy, precision, recall, specificity and *F*1 score. Accuracy is the ratio of the number of correctly graded samples to the total number of samples; precision is the ratio of the number of samples for a specific level of fish appetite in the test set to the number of samples for that fish appetite in the recognition results, which shows the ability of the model to accurately grade the fish appetite; recall is the proportion of correctly classified items among all items to be classified; specificity is the ratio of the number of samples with wrong recognition to the number of samples with other fish appetite in the test set; *F*1 score is a harmonic means of the precision and recall (Jiang et al., 2020). All the above five measures are ranged from 0 to 1, high value means the good predictive ability of the model, their definitions are as follows:

$$accuracy = \frac{TP + TN}{FP + FN + TP + TN} \quad (9)$$

$$precision = \frac{TP}{TP + FP} \quad (10)$$

$$recall = \frac{TP}{TP + FN} \quad (11)$$

$$specificity = \frac{TN}{FP + FN} \quad (12)$$

$$F1 = 2 \times \frac{precision \times recall}{precision + recall} \quad (13)$$

TABLE 2 Grading results for each fish appetite level.

Fish appetite	Grading result				Precision (%)	Recall (%)	Specificity (%)	Accuracy (%)
	none	weak	medium	strong				
none	537	1	0	0	99.44	99.81	99.84	**98.89**
weak	3	669	0	0	98.82	99.55	99.54	
medium	0	7	611	3	97.92	98.39	92.28	
strong	0	0	13	586	99.49	97.83	99.84	

Results and discussion

Performance of the proposed method

As shown in Table 2, the average accuracy of the method under four fish appetite levels reached 98.89% (Precision: 98.92%, Recall: 98.90%, *F*1 score: 98.90%), which indicates the effectiveness of the proposed fish appetite grading method.

To verify the performance of the method, we compared it with the three most widely used GNNs including ChebNet, GraphSAGE, and GAT. In addition, to better reveal the performance of our method in fish appetite grading, the hierarchical pooling architecture and global pooling architecture were used in the same GNN-based method as a comparison. The hierarchical pooling architecture consists of three blocks, each consisting of a graph convolution layer and a graph pooling layer. The outputs of each block are summarized in the readout layer. The sum output of each readout layer is input to the linear layer for classification. For a fair comparison, we performed the same self-attention graph pooling strategy, training strategy, and hyperparameter optimization strategy for each method, and use the same dataset (full-length data).

Figure 4 and Figure 5 (see Table S1 in supplementary materials for details) show the grading results of fish feeding behavior datasets using different GNN-based models, where the suffix h indicates that the model adopts the hierarchical pooling mechanism, and g indicates that the model adopts the global pooling mechanism. Pleased node that based on the same global pooling or hierarchical pooling architecture, our GCN-based method dramatically outperforms other GNN-based methods. In addition, for the data structure used in this paper, the global pooling method is better than the hierarchical pooling method. The global pooling architecture minimizes the loss of information and outperforms hierarchical pooling on datasets with fewer nodes. Due to the limited number of nodes in the constructed graph dataset, the global pooling method shows better performance in this study.

Graph attention network (GAT), as a novel convolution-style neural networks that operate on graph-structured data, leveraging masked self-attentional layers. The network allows for assigning operations, and is parallelizable across all nodes within a neighborhood while dealing with different sized neighborhoods, and does not depend on knowing the entire graph structure upfront. As opposed to GCN, the GAT model

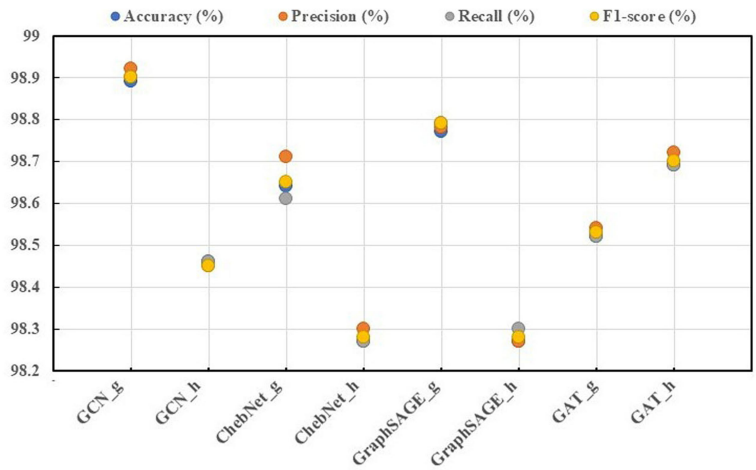

FIGURE 4
Fish appetite grading results of different GNN-based methods.

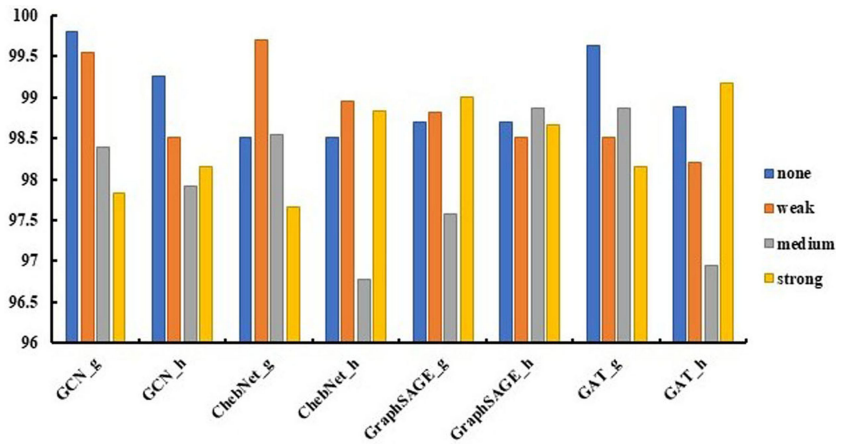

FIGURE 5
The accuracy of different GNN-based methods under different fish appetite levels.

can dynamically learn neighbor weights, but ignores the relationship between nodes (Xiang et al., 2021), which makes it not as effective as GCN under some conditions. As shown in Figure 4, although the accuracy of the GAT-based method under the two pooling mechanisms is similar, their accuracy is slightly lower than that of the GCN-based method. The GraphSAGE-based method uses an inductive method to calculate the node representation (Hamilton et al., 2017). Specifically, the method first extracts a fixed number of nodes from the adjacent nodes of each node, and then integrates the information of these neighbor nodes. This method has achieved good results in many large-scale inclusive learning problems. However, compared with the GraphSAGE-based method, the GCN-based method can capture the global information of the graph so as to better represent the characteristics of nodes, which is suitable for small-scale graphs. The dataset graph used in this study has a simple structure and few nodes. For this type of dataset, the GCN-based method has more advantages. The ChebNet-based method has strong expression ability. Its K-order convolution operator can cover the K-order neighbor nodes of nodes, but its complexity and parameter quantity are higher than GCN (Kipf and Welling, 2016). By stacking multiple GCN layers or expanding the empirical domain of graph convolution, the expressivity of the GCN- based method can be greatly improved. Therefore, under the dataset used in this study, the training accuracy of the ChebNet-based method is lower than that of the GCN-based method.

Feasibility demonstration

For the feeding control in real production, the most important is how to accurately assess fish appetite as soon as possible, and then leave enough reaction time for the next feeding operation. Therefore, it is crucial to evaluate the feasibility of the method proposed in this study whether the fish appetite can be accurately and effectively evaluated with time-limited data. In view of this, we divided the dataset into four subsets (as illustrated in Figure 6) to meet the needs of feasibility verification, which includes 1) the first 4.2 seconds of data (Dataset 1, one-sixth of the full-length data), 2) the first 8.3 seconds of data (Dataset 2, one-third of the full-length data), 3) the first 12.5 seconds of data (Dataset 3, one-half of the full-length data), and the first 25 seconds of data (Dataset 4, full-length data).

To verify the performance of the proposed method here, we compared it with two typical and state-of-the-art fish appetite grading methods, namely, the RNN-based method (Wei et al., 2021) and the CNN-based method (Zhou et al., 2019). Note that to make comparison more comprehensive, not only the RNN-based method but its normalized version (i.e., RNN'-based method) was used for the comparison here, allowing for the fact that the normalized motion features was adopted in our method. In particular, for the CNN-based method above, its image dataset in this study was obtained by extracting video frames owning the most obvious feeding behavior characteristic from the original video. Specifically, five consecutive frames of images with the strongest fish appetite were extracted from each feeding videos as the original image samples. And then, the original image samples were augmented to 24300 samples using rotation, flip, and translation image expansion techniques. Following this, the dataset was divided into a training set, a validation set, and a test set in a ratio of 8:1:1. It should be noted that, to obtain the optimal performance of the adopted methods above, the corresponding optimum hyperparameters were adopted here (details in Table S2 and Table S3 in the supplementary material).

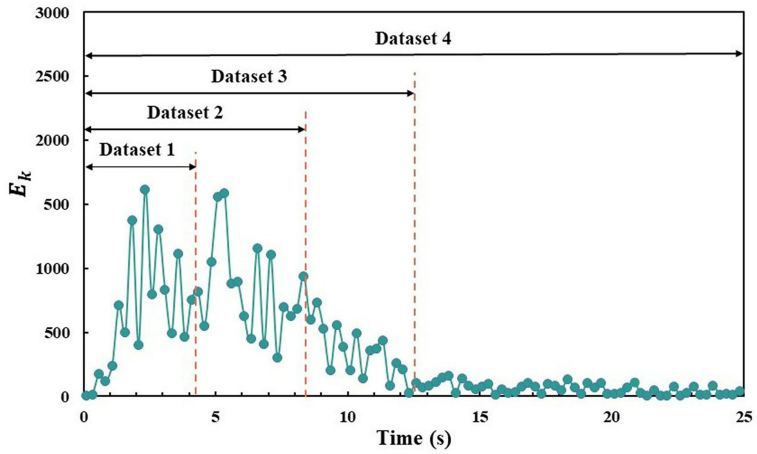

FIGURE 6
The illustration of dataset partition.

The grading accuracy of fish appetite based on our method (i.e., GCN-based method) and RNN-based method under different datasets were analyzed in this study, as well as the grading accuracy of CNN-based method (see Table S4 in supplementary materials for details). The average accuracy, precision, recall and *F*1-score of the CNN-based method were 83.54%, 83.90%, 84.15%, and 83.97%, respectively. Because the CNN-based method only uses the behavioral spatial characteristics of fish school to grade fish appetite, its performance is far from that of the other two fish feeding desire grading methods. Benefit from the spatial-temporal behavioral characteristics, the RNN-based method showed better performance than the CNN-based method. As shown in Figure 7 (since the results of the CNN-based fish appetite grading method are quite different from those of the GCN-based and RNN-based method, it is not shown in the figure to avoid affecting the expression), the RNN-based method achieved similar fish appetite grading results on normalized and non-normalized version. It should be noted that with the increase in the time duration of the dataset, the effect of the RNN-based fish appetite grading method shows an obvious upward trend. The RNN-based method achieved the best performance in Dataset 4, but the fish appetite grading accuracy is relatively low in time-limited datasets. Fish appetite representation is closely related to time (Wei et al., 2021). The RNN-based method is designed to counter the effect of diminishing gradients through layers and is suitable for time series data. However, the length of time series data also restricts the grading performance of RNN-based method on fish appetite. As presented in Figure 7, the GCN-based fish appetite grading method achieved the best performance in Dataset 4, but there was only a minor difference from the test results obtained from Dataset 1 and Dataset 2. Benefiting from the construction of the modified kinetic energy-based graph and the customization of GCN structure, our method indicated stronger learning ability than the state-of-the-art fish appetite assessing methods especially on time-limited feeding behavior data.

The t-SNE technique, which visualizes high-dimensional data by giving each datapoint a location in a two or three-dimensional map (Van Der Maaten and Hinton, 2008), is becoming more and more popular in data analysis. Thus, the t-SNE based two-dimensional analysis was used in this study to visualize the grading effect of the GCN-based, RNN-based, and CNN-based method on fish feeding desire. As illustrated in Figure 8, the CNN-based appetite grading method failed to divide fish appetite into four significant clusters (different colors represent different appetite levels), which also showed that the CNN-based method achieved poor fish feeding desire grading accuracy. On the contrary, both GCN-based and RNN-based grading methods can divide fish appetite into four significant clusters, so both methods have great appetite grading performance. However, compared with the RNN-based method, there are only a few data points with different colors mixed together in the GNN-based method (i.e., fewer data sample points prone to misclassification). To further analyze the causes of RNN-based method error identification, some false recognition examples are shown in Figure 9. It can be seen that there are a small number of "medium" or "weak" samples that were incorrectly recognized as "weak" or "strong" in all the four datasets. The main reason is that the modified kinetic energy has similar variation characteristics when the appetite level is "medium" or "weak" (as shown in Figure 2). Hence, the samples of these two are sometimes mis-recognized. In addition, Dataset 1 and Dataset 2 cannot reflect the whole process of fish feeding, which is also the key to limiting the accuracy of RNN-based method in fish appetite classification on

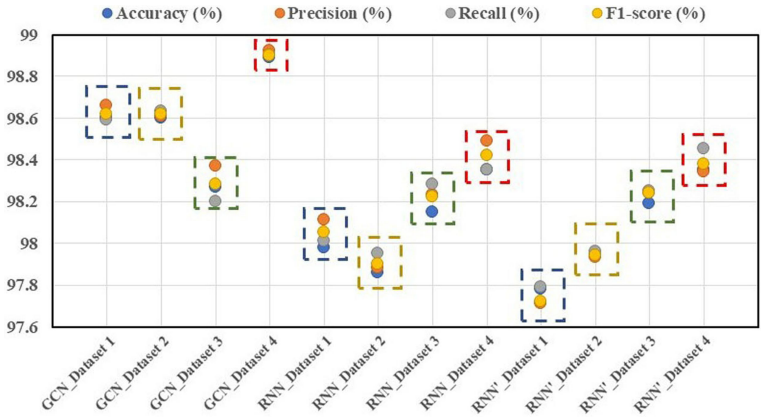

FIGURE 7
Fish appetite grading results under different datasets.

these two datasets. This reason also makes some "strong" samples incorrectly recognized as "medium".

In addition, Figure 10 shows the confusion matrixes of fish appetite grading results of the RNN-based and GCN-based methods on different datasets. It was obvious that in comparison with the RNN-based method, the classification accuracy of GCN-based method was equal or higher in each class to some extent, especially in Dataset 2 and Dataset 4. That means the proposed GCN-based approach learns new feature representation from the neighbor nodes through graph convolution, which improves the recognition ability under different datasets. Compared with the RNN-based method, the GCN-based method is more suitable to characterize the spatial and temporal topological information of fish feeding behavior. Therefore, the GCN-based method has achieved effective fish appetite grading results under different datasets, including the time-limit datasets.

It should be noted that, in order to achieve efficient grading of fish appetite in real production, the complexity especially the space complexity of the grading method itself is very important, as the valid training samples are limited in practical farming (Pan et al., 2019). We therefore calculated the quantity of the trainable parameters of RNN-based and GCN-based methods in this study, respectively (as illustrated in Figure 11). Combined with Figure 7 and Figure 9, the GCN-based method proposed in this study could not only obtain high accuracy in fish appetite grading, but take only 6.4% ~ 31.8% space complexity of that in RNN-based method, which can greatly improve the feasibility of fish appetite assessment in practical production.

The proposed modified kinetic energy feature-based GCN approach in this paper can effectively grade fish appetite with time-limited data, which is a promising approach in dealing with feeding control tasks and alleviating the water environment burden in aquaculture. Nonetheless, limitations still exist in

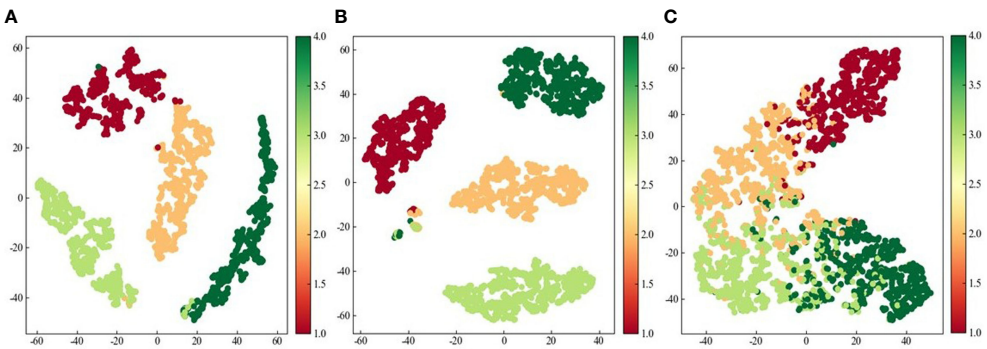

FIGURE 8
t-SNE based two-dimensional clustering analysis of different fish appetite grading methods (see Figure S1 in supplementary materials for more details). **(A)** GCN_Dataset 4. **(B)** RNN_Dataset 4. **(C)** CNN.

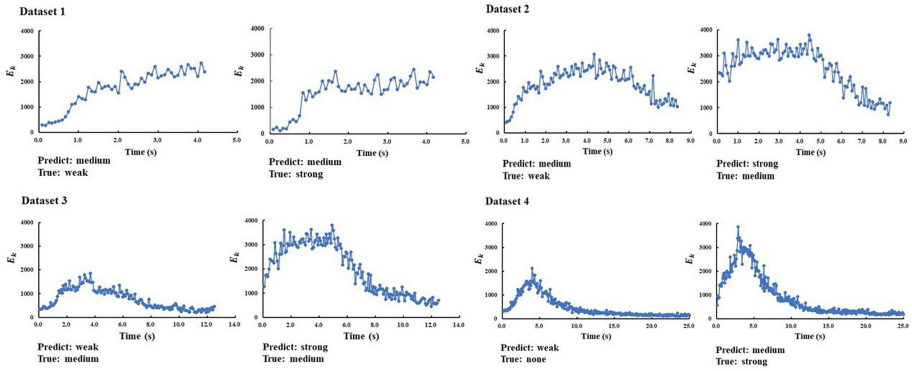

FIGURE 9
False recognition examples of the RNN-based method model in different datasets.

this method. First, our training on the model is based on experimental data under ideal conditions, which were derived from videos of specific growth periods of *Micropterus salmoides* in RAS, without monitoring the entire growth period of *Micropterus salmoides*. Therefore, when it comes to other scenarios, the practicability of our method may reduce. Besides, since the method proposed in this study is based on computer vision techniques, feed property also affects the performance of the model here to some extent, floating feed would be more beneficial to the performance maximization of the method here in contrast to sinking feed.

Conclusions

In order to leave enough reaction time for the follow-up feeding control and alleviate the water environment burden of the aquaculture, a novel, practical and promising fish appetite grading method with low space complexity was proposed in this study. Benefiting from the construction of the modified kinetic energy feature-based graph and the customization of GCN structure, our method indicated stronger learning ability than the typical state-of-the-art fish appetite assessing methods especially on time-limited feeding behavior data. And the grading accuracy of fish appetite obtained by the proposed method could reach 98.60% using only the first 4.2 (Precision: 98.66%, Recall: 98.59%, *F*1 score: 98.62%) as well as the first 8.3 seconds (Precision: 98.61%, Recall: 98.63%, *F*1 score: 98.62%) of input data, which is not much different from that (98.89%) on full-length (25 second-long) (Precision: 98.92%, Recall: 98.90%, *F*1 score: 98.90%) input data. Although limitations (such as feed property) still exist in this study, the findings here could not only provide references for the accurate control of fish feeding, but is of significance for the realization of cleaner production in practical aquaculture.

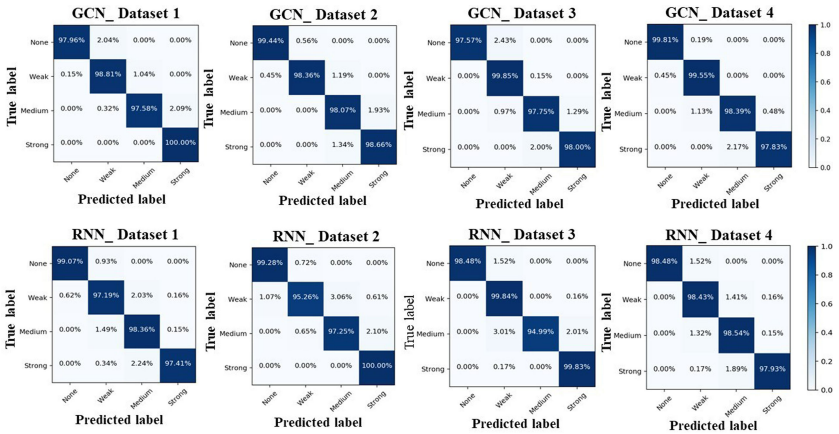

FIGURE 10
Confusion matrixes of fish appetite grading results of GNN-based and RNN-based methods on different datasets.

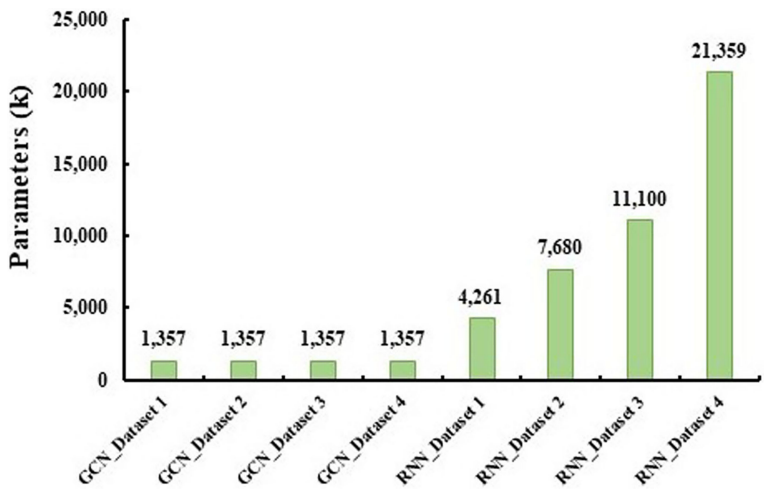

FIGURE 11
Space complexity of GCN-based and RNN-based methods on the different datasets.

Data availability statement

The datasets presented in this study can be found in online repositories. The names of the repository/repositories and accession number(s) can be found below: https://github.com/Doubleblindpeerreview/fish-appetite-grading.

Ethics statement

The animal study was reviewed and approved by the Association for the Study of Animal Behavior Use of Zhejiang University (ZJU20190074).

Author contributions

DW: Conceptualization, Methodology, Formal analysis, Writing-Original Draft, Visualization, Writing-Review & Editing. BJ: Formal analysis; Writing-Original Draft. HL: Methodology, Software; Writing-Original Draft. SZ: Supervision, Funding acquisition. ZY: Resources, Supervision, Funding acquisition. JZ: Conceptualization, Writing-Review & Editing, Project administration, Funding acquisition. All authors contributed to the article and approved the submitted version.

Funding

The authors acknowledge funding from the National Key R & D Program of China [grant number 2019YFD0900500], National Natural Science Foundation of China [grant number 31902359; 32173025], the Key Program of Science and Technology of Zhejiang Province [grant number 2021C02024] and Rural areas of Zhejiang Province [grand number 2020XTTGSC01].

Acknowledgments

The authors would like to thank Zequn Peng and Yanfeng Zhang for their aquaculture management and technology.

Conflict of interest

The authors declare that the research was conducted in the absence of any commercial or financial relationships that could be construed as a potential conflict of interest.

Publisher's note

Supplementary material

The Supplementary Material for this article can be found online at: https://www.frontiersin.org/articles/10.3389/fmars.2022.1021688/full#supplementary-material

References

Øverli, Ø., Sørensen, C., and Nilsson, G. E. (2006). Behavioral indicators of stress-coping style in rainbow trout: Do males and females react differently to novelty? *Physiol. Behav.* 87, 506–512. doi: 10.1016/j.physbeh.2005.11.012

An, D., Huang, J., and Wei, Y. (2021). A survey of fish behaviour quantification indexes and methods in aquaculture. *Rev. Aquac.* 13, 2169–2189. doi: 10.1111/raq.12564

Atoum, Y., Srivastava, S., and Liu, X. (2015). Automatic feeding control for dense aquaculture fish tanks. *IEEE Signal Process Lett.* 22, 1089–1093. doi: 10.1109/LSP.2014.2385794

Barraza-Guardado, R. H., Martínez-Córdova, L. R., Enríquez-Ocaña, L. F., Martínez-Porchas, M., Miranda-Baeza, A., and Porchas-Cornejo, M. A. (2014). Effect of shrimp farm effluent on water and sediment quality parameters off the coast of Sonora, Mexico. *Cienc. Mar.* 40, 221–235. doi: 10.7773/cm.v40i4.2424

Chang, C. M., Fang, W., Jao, R. C., Shyu, C. Z., and Liao, I. C. (2005). Development of an intelligent feeding controller for indoor intensive culturing of eel. *Aquac. Eng.* 32, 343–353. doi: 10.1016/j.aquaeng.2004.07.004

Cheng, J., Dong, L., and Lapata, M. (2016). "Long short-term memory-networks for machine reading," in *In Proceedings of the 2016 Conference on Empirical Methods in Natural Language Processing*. 551–561. (EMNLP Conference) doi: 10.18653/v1/d16-1053

Eriksen, M. S., Færevik, G., Kittilsen, S., McCormick, M. I., Damsgård, B., Braithwaite, V. A., et al. (2011). Stressed mothers-troubled offspring: a study of behavioural maternal effects in farmed salmo salar. *J. Fish Biol.* 79, 575–586. doi: 10.1111/j.1095-8649.2011.03036.x

Føre, M., Alfredsen, J. A., and Gronningsater, A. (2011). Development of two telemetry-based systems for monitoring the feeding behaviour of Atlantic salmon (Salmo salar l.) in aquaculture sea-cages. *Comput. Electron. Agric.* 76, 240–251. doi: 10.1016/j.compag.2011.02.003

FAO (2020). The state of world fisheries and aquaculture 2020. *Sustainability in action* (Rome: World series of the Food and Agriculture Organization of the United Nations).

Feng, S., Yang, X., Liu, Y., Zhao, Z., Liu, J., Yan, Y., et al. (2022). Fish feeding intensity quantification using machine vision and a lightweight 3D ResNet-GloRe network. *Aquac. Eng.* 98, 102244. doi: 10.1016/j.aquaeng.2022.102244

Hamilton, W. L., Ying, R., and Leskovec, J. (2017). Inductive representation learning on large graphs. *NIPS* 2017, 1025–1035. doi: 10.48550/arXiv.1706.02216

Jescovitch, L. N., Ullman, C., Rhodes, M., and Davis, D. A. (2018). Effects of different feed management treatments on water quality for pacific white shrimp litopenaeus vannamei. *Aquac. Res.* 49, 526–531. doi: 10.1111/are.13483

Jiang, H., Zhang, C., Qiao, Y., Zhang, Z., Zhang, W., and Song, C. (2020). CNN Feature based graph convolutional network for weed and crop recognition in smart farming. *Comput. Electron. Agric.* 174, 105450. doi: 10.1016/j.compag.2020.105450

Kipf, T. N., and Welling, M. (2016). Semi-supervised classification with graph convolutional networks. *ICLR* 2017, 1–14. doi: 10.48550/arXiv.1609.02907

Lazer, D. D., Pentland, A. A., Adamic, L. L., Aral, S. S., Barabasi, A. L. A. L., and Brewer, D. D. (2009). Life in the network: The coming age of computational social science. *Science* 323, 721–723. doi: 10.1126/science.1167742

Lee, J., Lee, I., and Kang, J. (2019). Self-attention graph pooling. *ICML* 2019, 6661–6670. doi: 10.48550/arXiv.1904.08082

Liu, Z., Li, X., Fan, L., Lu, H., Liu, L., and Liu, Y. (2014). Measuring feeding activity of fish in RAS using computer vision. *Aquac. Eng.* 60, 20–27. doi: 10.1016/j.aquaeng.2014.03.005

Li, D., Wang, Z., Wu, S., Miao, Z., Du, L., and Duan, Y. (2020). Automatic recognition methods of fish feeding behavior in aquaculture: A review. *Aquaculture* 528, 735508. doi: 10.1016/j.aquaculture.2020.735508

Luna, M., Llorente, I., and Cobo, Á. (2019). Integration of environmental sustainability and product quality criteria in the decision-making process for feeding strategies in seabream aquaculture companies. *J. Clean Prod.* 217, 691–701. doi: 10.1016/j.jclepro.2019.01.248

Pan, J.-S., Lee, C.-Y., Sghaier, A., Zeghid, M., and Xie, J. (2019). Novel systolization of subquadratic space complexity multipliers based on toeplitz matrix-vector product approach. *IEEE Trans. Very Large Scale Integr. (VLSI) Syst.* 27, 1614–1622. doi: 10.1109/TVLSI.2019.2903289

Parra, L., Sendra, S., García, L., and Lloret, J. (2018). Design and deployment of low-cost sensors for monitoring the water quality and fish behavior in aquaculture tanks during the feeding process. *Sensors (Basel Switzerland).* 18, 750. doi: 10.3390/s18030750

Ubina, N., Cheng, S. C., Chang, C., and C. Chen, H. Y. (2021). Evaluating fish feeding intensity in aquaculture with convolutional neural networks. *Aquac. Eng.* 94, 102178. doi: 10.1016/j.aquaeng.2021.102178

Van Der Maaten, L., and Hinton, G. (2008). Visualizing data using t-SNE. *J. Mach. Learn. Res.* 9, 2579–2625.

Wang, Y., Yu, X., Liu, J., An, D., and Wei, Y. (2022). Dynamic feeding method for aquaculture fish using multi-task neural network. *Aquaculture* 551, 737913. doi: 10.1016/j.aquaculture.2022.737913

Wei, D., Bao, E., Wen, Y., Zhu, S., Ye, Z., and Zhao, J. (2021). Behavioral spatial-temporal characteristics-based appetite assessment for fish school in recirculating aquaculture systems. *Aquaculture* 545, 737215. doi: 10.1016/j.aquaculture.2021.737215

Xiang, Z., Gong, W., Li, Z., Yang, X., Wang, J., and Wang, H. (2021). Predicting protein-protein interactions *via* gated graph attention signed network. *Biomolecules* 11, 799. doi: 10.3390/biom11060799

Ye, Z., Zhao, J., Han, Z., Zhu, S., Li, J., and Lu, H. (2016). Behavioral characteristics and statistics-based imaging techniques in the assessment and optimization of tilapia feeding in a recirculating aquaculture system. *Trans. ASABE* 59, 345–355. doi: 10.13031/trans.59.11406

Zhao, J., Bao, W. J., Zhang, F. D., Ye, Z. Y., Liu, Y., and Shen, M. W. (2017). Assessing appetite of the swimming fish based on spontaneous collective behaviors in a recirculating aquaculture system. *Aquac. Eng.* 78, 196–204. doi: 10.1016/j.aquaeng.2017.07.008

Zhao, S., Ding, W., Zhao, S., and Gu, J. (2019). Adaptive neural fuzzy inference system for feeding decision-making of grass carp *(Ctenopharyngodon idellus)* in outdoor intensive culturing ponds. *Aquaculture* 498, 28–36. doi: 10.1016/j.aquaculture.2018.07.068

Zhao, L., Song, Y., Zhang, C., Liu, Y., Wang, P., and Lin, T. (2020b). T-GCN: A temporal graph convolutional network for traffic prediction. *IEEE Trans. Intell. Transp. Syst.* 21, 3848–3858. doi: 10.1109/TITS.2019.2935152

Zhao, S., Zhu, M., Ding, W., Zhao, S., and Gu, J. (2020a). Feed requirement determination of grass carp *(Ctenopharyngodon idella)* using a hybrid method of bioenergetics factorial model and fuzzy logic control technology under outdoor pond culturing systems. *Aquaculture* 521, 734970. doi: 10.1016/j.aquaculture.2020.734970

Zhou, C., Xu, D., Chen, L., Zhang, S., Sun, C., and Yang, X. (2019). Evaluation of fish feeding intensity in aquaculture using a convolutional neural network and machine vision. *Aquaculture* 507, 457–465. doi: 10.1016/j.aquaculture.2019.04.056

Zhou, C., Xu, D., Lin, K., Sun, C., and Yang, X. (2018). Intelligent feeding control methods in aquaculture with an emphasis on fish: A review. *Rev. Aquac.* 10, 975–993. doi: 10.1111/raq.12218

frontiers | Frontiers in Marine Science

TYPE Original Research
PUBLISHED 08 December 2022
DOI 10.3389/fmars.2022.1037017

OPEN ACCESS

EDITED BY
Zhangying Ye,
Zhejiang University, China

REVIEWED BY
Saurav Kumar,
Central Institute of Fisheries Education (ICAR), India
Najiah Musa,
University of Malaysia Terengganu, Malaysia

*CORRESPONDENCE
Vasco C. Mota
vasco.mota@nofima.no

SPECIALTY SECTION
This article was submitted to Marine Fisheries, Aquaculture and Living Resources, a section of the journal Frontiers in Marine Science

RECEIVED 05 September 2022
ACCEPTED 23 November 2022
PUBLISHED 08 December 2022

CITATION
Mota VC, Brenne H, Kojen M, Marhaug KR and Jakobsen ME (2022) Evaluation of an ultrafiltration membrane for the removal of fish viruses and bacteria in aquaculture water.
Front. Mar. Sci. 9:1037017.
doi: 10.3389/fmars.2022.1037017

Evaluation of an ultrafiltration membrane for the removal of fish viruses and bacteria in aquaculture water

Vasco C. Mota[1]*, Hanne Brenne[1], Morten Kojen[2], Kine Rivers Marhaug[2] and Margit Ertresvåg Jakobsen[2]

[1]Nofima AS, The Norwegian Institute of Food, Fisheries and Aquaculture Research, Tromsø, Norway, [2]FiiZK AkvaFresh AS, Trondheim, Norway

Ultrafiltration (UF) membranes are used to successfully remove waterborne virus and bacteria from wastewater and drinking water. However, UF membrane application in aquaculture water treatment is limited. In this study we evaluate the performance of a capillary polyethersulfone UF membrane to remove two benchmark waterborne fish pathogens: i) the infectious pancreatic necrosis virus - IPNV, which is an unenveloped icosahedral virus, and ii) the bacterium *Aeromonas salmonicida*, which is a Gram-negative, facultative anaerobic bacilli. Moreover, the UF membrane bench-scale unit was tested at two temperatures according to salmonid aquaculture: low (4 - 7°C) and high (16 - 19°C). Sterilised natural seawater was spiked with laboratory cultured pathogens, the water was filtrated, and the membrane permeate collected. Both pathogen solution and permeate were evaluated using a cell culture method to estimate the colony-forming units (CFU/ml) for bacteria presence, a median tissue culture infectious dose ($TCID_{50}$/ml) assay for virus presence, and real-time quantitative polymerase chain reaction (RT-qPCR) for both bacteria and virus presence. The membrane permeate was negative for both virus and bacteria for all analysis and for both low and high temperatures. The results from this bench-scale study are encouraging for the application of UF membrane technology in aquaculture water treatment to prevent virus and bacteria outbreaks. Further studies should validate this UF membrane technology results in commercial aquaculture conditions.

KEYWORDS

***Aeromonas salmonicida*, infectious pancreatic necrosis virus - IPNV, Atlantic salmon pathogens, polyether sulfone membrane, ultrafiltration (UF), aquaculture water treatment**

Introduction

Membrane filtration is typically a pressure-driven process to force water particles through a membrane and retain them. The water that passes through the membrane is known as filtrate or permeate. Microfiltration, ultrafiltration, nanofiltration and reverse osmosis are the main membrane processes differentiated by the pore size. Ultrafiltration (UF) membrane is an emerging technology being applied in a wide range of industries from drinking water production to wastewater treatment to remove fine solids and microorganisms (Goswami and Pugazhenthi, 2020). However, UF membrane technology to treat aquaculture water is limited (Chiam and Sarbatly, 2011).

Currently UF membrane in aquaculture applications is used as support of ultraviolet (UV) irradiation and it was shown to eliminate waterborne microorganisms, small particles, and humic acids (M. Jakobsen personal communication, July 2022). A promising use of UF membrane technology in aquaculture is a stand-alone unit to treat production facilities intake water by removing waterborne viruses and bacteria. Despite the high biosecurity features in aquaculture facilities (Mota et al., 2022), pathogen outbreaks occurred account for several mass mortality events (Murray et al., 2014; Wiik-Nielsen et al., 2017). UF filters pore sizes range from 20 to 100 nm and are composed of non-cellulosic synthetics (such as polyvinylidene fluoride, polyacrylonitrile, or polyethersulfone) that are resistant to heat and chemical attacks, possess a low protein-binding characteristic, and are reusable (Winona et al., 2001; Olszewski et al., 2005). A recent review on membrane filtration usage to remove bacteria and virus from water showed the promising use of this technology for water purification (Goswami and Pugazhenthi, 2020). A particular UF membrane technology, a capillary fiber membrane made of polyethersulfone, was reported to be able to process large water volumes with extreme durability both in a drinking water treatment plant (Ming Chew et al., 2015) and in a textile wastewater treatment plant (Sahinkaya et al., 2019). The few applications of UF membrane technology in aquaculture are combined with ultraviolet (UV) irradiation. A stand-alone application of UF membrane technology can also be relevant for aquaculture operations. However, before an application of this disinfection barrier in aquaculture is suitable, it is necessary to evaluate its removal efficiency of relevant fish viruses and bacteria in aquaculture water quality.

In this study we evaluated the performance of a capillary polyethersulfone UF membrane to remove two benchmark waterborne salmonids pathogens: i) the infectious pancreatic necrosis virus (IPNV), which is an unenveloped icosahedral virus, and ii) the bacterium *Aeromonas salmonicida*, which is a Gram-negative, facultative anaerobic bacilli. Moreover, the removal efficiency was evaluated at low (4 - 7°C) and high (16 - 19°C) water temperatures for salmonids.

Material and methods

Experimental design

Two pathogens (IPNV and *A. salmonicida*) at two water temperatures (low: 4 - 7 °C and high: 16 - 19 °C) were used to test the removal performance of an UF membrane. Each condition was replicated three times in a total of 12 tests. Each test consisted in spiking sterile seawater (10 L) with a laboratory grown pathogen (virus or bacteria) and pumping the water through an UF membrane bench-scale unit. Water samples were collected from the seawater pathogen solution and from the membrane permeate to assess the presence and quantity of pathogens.

Water matrices and chemical analysis

The water used in this study was collected from surface seawater (0 – 1 m depth) at Håjafjorden 69°80'42.8áN 19° 01'58.8áE (Tromsø, Norway) during May and June 2022. After collection, the water was sterilised using a high-pressure steam steriliser (SX-700E, TOMY Digital Biology, Japan) and stored refrigerated until testing; at 4°C for low temperature test and 16° C for high temperature test. The sterilised seawater was analysed for the presence of IPNV and *A. salmonicida*, and it was negative for both microorganisms. Further, the water was characterised for salinity and pH (Tetra con 925 and Sentix 940 sensors, Multi 3630 IDS, WTW, Germany), turbidity (ORION AQ4500, Thermo Scientific®, Thermo Fisher Scientific, USA), and ultra-violet transmittance (UVT %), an indirect measure of turbidity (Table 1). The water absorbance at λ=254 nm (uniSPEC 2 Spectrophotometer, Lab logistics group, Germany) was measured and the UVT was calculated as follows:

$$\text{Equation 1: } UVT = 10^{-a} \times 100$$

where:
UVT = ultraviolet transmittance (%)
a = absorbance at 254 nm wavelength

Ultrafiltration membrane bench-scale unit

The UF membrane was installed as a bench-scale unit (FiiZK Aqua, Trondheim, Norway) and the experimental trials were carried out in two refrigerated rooms at Nofima research facilities (Tromsø, Norway). The UF membrane bench-scale unit is illustrated in Figure 1A. Briefly, it consisted of a cylindrical tank number 1 to add the pathogen solution, a magnet gear pump (MDG-M4S6B220, Iwaki CO, Japan), a water flow meter, a temperature sensor, a water pressure sensor, a UF membrane

TABLE 1 Water quality and operation conditions during ultrafiltration membrane test.

Parameters[1]	*A. salmonicida*	IPNV
Water quality		
Salinity (ppt)	34.0 ± 0.5	33.2 ± 2.0
pH	8.3 ± 0.0	8.7 ± 0.1
Turbidity (ntu)	2.1 ± 0.3	0.4 ± 0.1
UVT (%)	45 ± 5	95 ± 1
Operation conditions		
Pressure (bar)	0.36 ± 0.07	0.40 ± 0.10
Water flow (L/min.)	0.43 ± 0.02	0.41 ± 0.04
Contact time (min.)	24 ± 1	26 ± 3
Membrane flux (L/m^2/h)	51.5 ± 2.2	49.6 ± 5.2

[1]Values measured before ultrafiltration membrane and shown as mean ± standard deviation.

(Figure 1B), and a cylindrical tank number. 2 to collect the membrane permeate. The capillary membrane consisted of 63 fibres, each fibre had 7 capillaries with an inner diameter of 0.9 mm (dizzer® modules with Multibore® 0.9 membrane, inge GmbH, Germany) and was 50 cm in length measuring a total area of 0.5 m^2. The membrane material was polyethersulfone and the pore size was appr. 20 nm. The membrane was operated as inside-out filtration, i.e., pressured water and particles were forced into the membrane fibres capillaries where water and particles smaller than 20 nm escape forming the membrane permeate which flowed to a cylindrical tank number 2. Standard commercial operation settings were used in the tests (Table 1), such as pressure< 1 bar and flux ~50 L/h/m^2.

Disinfection of bench-scale unit

The bench-scale unit was disinfected between each test using a sodium hypochlorite solution. The disinfection protocol consisted in filtering 10 L of ultrapure water (18.2 MΩ/cm, PURELAB Chorus, ELGA Lab water, Veolia, USA) mixed with a sodium hypochlorite solution of 5% active chlorine (Thermo scientific, Belgium) at a concentration 5 ml/L (v/v), followed by rinsing the unit with 10 L of ultrapure water to remove any traces of the disinfection solution. The disinfection efficiency was assessed twice, one for IPNV and one for *A. salmonicida*, by collecting water samples for microorganism detection analysis and was negative both times. At the end of each test, the membrane permeate was treated with the above sodium hypochlorite solution at a concentration 20 ml/L (v/v) for 48h - 72h before the water was disposed into the domestic wastewater system.

Virus and bacterium preparation

IPN virus was isolated from the pylorus of an infected Atlantic salmon (*Salmo salar*) and preserved in a minimum

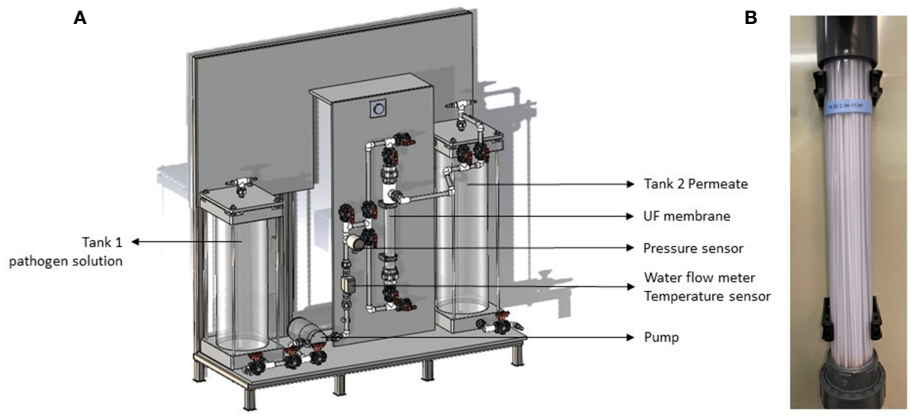

FIGURE 1
Sketch of the ultrafiltration membrane bench-scale unit **(A)** and picture of the membrane tested **(B)**.

essential media (MEM; Ref. 21090-022, Gibco, USA) with 2% fetal bovine serum (FBS, product number F7524, Sigma Aldrich) at -80 °C. The virus titration was estimated 1 x $10^{4.1}$ $TCID_{50}$/ml and 1 x $10^{7.8}$ $TCID_{50}$/ml. At the day of each trial IPNV serum was defrosted and 18.4 ml of virus stock solution was added to the 10 L refrigerated sterile seawater.

Aeromonas salmonicida subsp. salmonicida bacteria was isolated from the headkidney of Atlantic salmon and preserved in a glycerol and liquid heart infusion (BHI) solution at -80 °C. Prior to each test, bacteria isolates were defrosted and grown on blood agar standard Petri plates with 2% NaCl for 5 days. After, 1 colony forming unit (CFU) was transferred to 20 ml of BHI broth 4 days prior to testing for further bacteria growth. Two days before testing, 20 ml BHI culture was transferred to 400 ml of BHI liquid culture. This bacteria stock solution was 10^5 CFU/ml and 100 ml was added to the 10 L refrigerated sterile seawater.

Water sampling and filtration

IPNV water samples from both unit tanks were collected in triplicate (100 -200 ml) per test and filtered under vacuum through an electropositive charge filter disc (Zeta Plus 1MDS, Lenntech, The Netherlands) using a filtration pump (Milliflex Oasis, Millipore, Molsheim, France). The filter was stored in 100 µl nuclease-free water (Life technologies, USA) at -80 after filtration. For virus RNA extraction the whole filter was placed in a lysis buffer (RNAdvance Tissue kit, A32646, Beckman Coulter) and incubated for 30 min. at 37 °C. Thereafter, the solution (300 uL) was transferred to tubes for further extraction in a BiomekI5 automated workstation (Beckman Coulter). Extracted RNA (9 uL) was used to make cDNA, using High-Capacity RNA-to-cDNA™ Kit (4387406, Applied Biosystems).

A. salmonicida water samples from both tanks were collected in triplicate (100 ml) per test and filtered under vacuum through a cellulose ester MCE 0.45 µm sterilised filter (Millipore, Molsheim, France) using a filtration pump (Milliflex Oasis, Millipore, Molsheim, France). Filters were transferred to 2 ml tubes containing 200 µl of MilliQ water and heated for 10 min at 95°C to disrupt the bacteria cells. Bacteria lysate was used as a template in the real time quantitative polymerase chain reaction (RT-qPCR) assay.

Real-time quantitative polymerase chain reaction assay

QuantStudio™ Real-Time PCR System (Applied Biosystems, United States) was used to perform RT-qPCR. The RT-qPCR assays were performed in a final volume of 20 µl reaction mixture containing 2 µL of DNA template, 5.6 µL of nuclease-free water, 10 µl of 2X PowerUp™ SYBR® Green Master Mix (Thermo Fisher Scientific, USA) and 1.2 µl of primer. (Table 2). All samples were run in duplicate. The thermocycling parameters were as follows: 20 s of preincubation at 95°C, amplification with 40 cycles at 95°C for 1 s and 60°C for 20 s. A dissociation stage for 1 s followed at 95°C, 20 s at 60°C, and 1 s at 95°C. A five-step standard curve of 2-fold dilution series was prepared from pooled cDNA to determine the amplification efficiencies.

Median tissue culture infectious dose ($TCID_{50}$) assay

Prior to virus quantification, chinook salmon embryo cells (CHSE-214, LOT 00/F/031, ECACC, England) were grown in culture flasks with 9 mL of MEM and 8% FBS for one week at 20° C with 5% CO_2. Two days prior to virus quantification CHSE culture was moved to the 96-well microtiter plates (200 µL/well).

To quantify the virus, samples were added in 200 µl volumes to six wells per dilution (10-fold serial dilution, 2% FBS and MEM) of 96-well microtiter plates containing CHSE. The plates were incubated at 20°C with 5% CO_2 for 7 days. After the incubation period, the 96-well microtiter plates were examined for infection by visible cytopathic effect (CPE) using an inverted phase contrast microscope (TMS-F, Nikon, Japan). $TCID_{50}$ was calculated according to the method of Kärber (1931).

Bacteria plating and counting of colony-forming units

A. salmonicida water samples from both tanks were collected in duplicate (100 ml) per test and filtered under vacuum through a cellulose ester MCE filter as described above. Filters were immediately placed in blood agar 2% NaCl standard Petri plates and incubated at 12°C for 3-5 days. After the incubation period, bacteria colonies were counted, and the results calculated as

TABLE 2 List of primers used for the detection of the reference genes by RT-qPCR.

Gene	Orientation	Primer sequence (5'-3')	Amplicon size (bp)	Reference
AerSal	Forward Reverse	CGG AAC GTA ATC TGA ATT GTT CTT TTC ATT GCT TAT CGA GGC AGC CAA C	112	(Hiney et al., 1992; Balcazar et al., 2007)
IPNV specific	Forward Reverse	CCT GAC CTA CAA CAG CCT GAT GT TCG AAC CCT GTT GGT AGA TTC A	114	(Julin et al., 2009)

colony forming units per ml of sample (CFU/mL). Only plates with CFU between 25 and 250 were considered.

Results and discussion

Two benchmark waterborne salmonid pathogens were selected to represent a typical pathogen in these fish species' aquaculture operations. The infectious pancreatic necrosis virus (IPNV), which is an unenveloped icosahedral virus with an average size of around 55 – 70 nm is responsible for abnormal erratic corkscrew swimming and anorexia in fish (Dobos, 1995; Dopazo, 2020). The *A. salmonicida* is a Gram-negative bacterium with an average size 500 – 2000 nm, and is the causative agent of furunculosis, a bacterial septicaemia of salmonid fish (Pickup et al., 1996; Dallaire-Dufresne et al., 2014). The removal efficiency of water microorganisms was previously shown to be membrane and water quality specific (Goswami and Pugazhenthi, 2020). Microfiltration and ultrafiltration are the main membrane sizes used for water disinfection and their pore size range from 10 – 5000 nm (Jacangelo et al., 1997). For example, a suspension of poliovirus, one of the smallest known viruses that ranges between 28 - 30 nm, was found to pass through a microfiltration membrane but to be retained in a UF membrane (Madaeni et al., 1995). The UF membrane used in the current study has an approximate pore size of 20 nm (according to the manufacturer). The removal efficiency of IPNV and *A. salmonicida* by the UF membrane used in this study was 100%, i.e., the membrane permeate was found to be virus and bacteria free in all the replicated tests. Through consideration of the sizes of the target organisms and the membrane pore size, it was apparent that removal of these organisms was due to the membrane acting as a physical barrier that retained the microorganisms' particles.

UF membrane pore size was previously reported to be influenced by temperature (8.9 - 28.5 °C), where the pore size reduces at lower temperatures (Ma et al., 2017). In the current study, the UF performance was evaluated at a low (4 - 7°C) and high (16 - 19°C) temperature ranges for salmonid aquaculture, and both resulted in a 100% virus and bacteria removal. However, the pressure (bar) before the membrane was 11% higher at low temperature when compared to higher temperature, which may be a result on the effect of temperature on pore size as described by Ma et al. (2017).

Bacteria and virus removal were evaluated according to two different methods: $TCDI_{50}$/CFU platting and RT-qPCR. Table 3 shows RT-qPCR threshold cycle (Ct) values, estimated titres as $TCID_{50}$/ml and colony forming units as CFU/ml for both pathogen solution and membrane permeate. Virus titres and bacteria plating returned similar results as RT-qPCR. However, further membrane validation in commercial conditions should consider RT-qPCR method, as it generates faster results, and the primers can be designed specifically for the microorganism of interest.

Conclusion

The filtration of IPNV and *A. salmonicida* suspensions using a 20 nm capillary polyethersulfone membrane completely removed the microorganism. Water temperature did not affect membrane removal efficiency in the tested range (4 - 19 °C), though lower temperatures resulted in higher membrane water pressure. Moreover, both classical microorganism detection techniques, i.e., virus titres and bacteria plating, and the advanced detection technique RT-qPCR returned the same findings. Further studies should validate this UF membrane technology in commercial aquaculture conditions.

TABLE 3 Water temperature, RT-qPCR cycle threshold (Ct) values, estimated virus titres ($TCID_{50}$/ml) and bacteria colony forming units (CFU/ml).

Test	Temperature (°C)	RT-qPCR (Ct)		Virus titres ($TCID_{50}$/ml)		Bacteria counting (CFU/ml)	
		Pathogen Solution	Membrane permeate	Pathogen Solution	Membrane permeate	Pathogen solution	Membrane permeate
A. salmonicida							
Low temperature	6.5 ± 1.7	24.3 ± 0.8	N*	-	-	$2.5 \times 10^3 \pm 7.1 \times 10^2$	N
High temperature	18.7 ± 2.1	26.7 ± 0.9	N	-	-	$\leq 1 \times 10^{4\#}$	N
IPNV							
Low temperature	3.8 ± 0.2	24.7 ± 0.8	N	$1 \times 10^{3.7} \pm 1 \times 10^{1.4}$	N	–	-
High temperature	16.4 ± 0.4	31.5 ± 0.4	N	$1 \times 10^{4.8} \pm 1 \times 10^{0.5}$	N	-	-

*Negative (N) shows Ct values ≥ 35, no CFU plate growth or no infected cells observed.
#CFU counting< 25, only the counted dilution plated is shown.
Values are shown as mean ± standard deviation.

Data availability statement

The original contributions presented in the study are included in the article/Supplementary Material. Further inquiries can be directed to the corresponding author.

Author contributions

VM: Conceptualization, Project administration, Investigation, Formal analysis, Visualization, Writing – original draft, Writing – review & editing. HB: Conceptualization, Methodology, Formal analysis, Writing – review & editing. MK: Conceptualization Methodology, Resources. KM: Conceptualization. MJ: Conceptualization, Visualization, Writing – review & editing. All authors contributed to the article and approved the submitted version.

Funding

This project is part of CtrlAQUA SFI, Center for research-based innovation, and funded by the Research Council of Norway (grant number 237856/O30) and the partners of the center.

Acknowledgments

The authors are thankful for Are Nylund and Heidrun Nylund (University of Bergen, Norway) for kindly providing the electropositive charge filter discs and Lill-Heidi Johansen (Nofima, Norway) for helping with IPNV protocols. The authors would also like to acknowledge the dedication to construction of the UF unit by the technical staff in FiiZK AkvaFresh AS.

Conflict of interest

The authors VM and HB declare that they have no known competing financial interests or personal relationships that could have appeared to influence the work reported in this paper. The authors MK, KM and MJ declare the following financial interests or personal relationships which may be considered as potential competing interests: professional relationship with a commercial company selling the ultrafiltration membrane tested.

Publisher's note

All claims expressed in this article are solely those of the authors and do not necessarily represent those of their affiliated organizations, or those of the publisher, the editors and the reviewers. Any product that may be evaluated in this article, or claim that may be made by its manufacturer, is not guaranteed or endorsed by the publisher.

Supplementary material

The Supplementary material for this article can be found online at: https://www.frontiersin.org/articles/10.3389/fmars.2022.1037017/full#supplementary-material

References

Balcazar, J. L., Vendrell, D., De Blas, I., Ruiz-Zarzuela, I., Girones, O., and Muzquiz, J. L. (2007). Quantitative detection of *Aeromonas salmonicida* in fish tissue by real-time PCR using self-quenched, fluorogenic primers. *J. Med. Microbiol.* 56, 323–328. doi: 10.1099/jmm.0.46647-0

Chiam, C. K., and Sarbatly, R. (2011). Purification of aquacultural water: Conventional and new membrane-based techniques. *Separation Purification Rev.* 40, 126–160. doi: 10.1080/15422119.2010.549766

Dallaire-Dufresne, S., Tanaka, K. H., Trudel, M. V., Lafaille, A., and Charette, S. J. (2014). Virulence, genomic features, and plasticity of *Aeromonas salmonicida subsp. salmonicida*, the causative agent of fish furunculosis. *Veterinary Microbiol.* 169, 1–7. doi: 10.1016/j.vetmic.2013.06.025

Dobos, P. (1995). The molecular biology of infectious pancreatic necrosis virus (IPNV). *Annu. Rev. Fish. Dis.* 5, 25–54. doi: 10.1016/0959-8030(95)00003-8

Dopazo, C. P. (2020). The infectious pancreatic necrosis virus (IPNV) and its virulence determinants: What is known and what should be known. *Pathogens* 9, 94. doi: 10.3390/pathogens9020094

Goswami, K. P., and Pugazhenthi, G. (2020). Credibility of polymeric and ceramic membrane filtration in the removal of bacteria and virus from water: A review. *J. Environ. Manage.* 268, 110583. doi: 10.1016/j.jenvman.2020.110583

Hiney, M., Dawson, M., Heery, D., Smith, P., Gannon, F., and Powell, R. (1992). DNA Probe for *Aeromonas salmonicida*. *Appl. Environ. Microbiol.* 58, 1039–1042. doi: 10.1128/aem.58.3.1039-1042.19

Jacangelo, J. G., Trussell, R. R., and Watson, M. (1997). Role of membrane technology in drinking water treatment in the united states. *Desalination* 113, 119–127. doi: 10.1016/S0011-9164(97)00120-3

Julin, K., Johansen, L.-H., and Sommer, A.-I. (2009). Reference genes evaluated for use in infectious pancreatic necrosis virus real-time RT-qPCR assay applied during different stages of an infection. *J. Virol. Methods* 162, 30–39. doi: 10.1016/j.jviromet.2009.07.003

Kärber, G. (1931). Beitrag zur kollektiven behandlung pharmakologischer reihenversuche. *Naunyn-Schmiedebergs Archiv. Für. Experimentelle Pathol. Und Pharmakol.* 162, 480–483. doi: 10.1007/BF01863914

Madaeni, S., Fane, A., and Grohmann, G. (1995). Virus removal from water and wastewater using membranes. *J. Membrane Sci.* 102, 65–75. doi: 10.1016/0376-7388(94)00252-T

Ma, B., Wang, X., Liu, R., Qi, Z., Jefferson, W. A., Lan, H., et al. (2017). Enhanced antimony (V) removal using synergistic effects of fe hydrolytic flocs and ultrafiltration membrane with sludge discharge evaluation. *Water Res.* 121, 171–177. doi: 10.1016/j.watres.2017.05.025

Ming Chew, C., David Ng, K., Richard Ooi, H., and Ismail, W. (2015). Malaysia's largest river bank filtration and ultrafiltration systems for municipal drinking water production. *Water Pract. Technol.* 10, 59–65. doi: 10.2166/wpt.2015.008

Mota, V. C., Striberny, A., Verstege, G. C., Difford, G. F., and Lazado, C. C. (2022). Evaluation of a recirculating aquaculture system research facility designed to address current knowledge needs in Atlantic salmon production. *Front. Anim. Sci.* 26. doi: 10.3389/fanim.2022.876504

Murray, F., Bostock, J., and Fletcher, D. (2014). *Review of recirculation aquaculture system technologies and their commercial application* (Stirling, U.K: University of Stirling Aquaculture). H.a.I. Enterprise.

Olszewski, J., Winona, L., and Oshima, K. H. (2005). Comparison of 2 ultrafiltration systems for the concentration of seeded viruses from environmental waters. *Can. J. Microbiol.* 51, 295–303. doi: 10.1139/w05-011

Pickup, R., Rhodes, G., Cobban, R., and Clarke, K. (1996). The postponement of non-culturability in *Aeromonas salmonicida*. *J. Fish. Dis.* 19, 65–74. doi: 10.1111/j.1365-2761.1996.tb00121.x

Sahinkaya, E., Tuncman, S., Koc, I., Guner, A. R., Ciftci, S., Aygun, A., et al. (2019). Performance of a pilot-scale reverse osmosis process for water recovery from biologically-treated textile wastewater. *J. Environ. Manage.* 249, 109382. doi: 10.1016/j.jenvman.2019.109382

Wiik-Nielsen, J., Gjessing, M., Solheim, H., Litlab, A., Gjevre, A. G., Kristoffersen, A., et al. (2017). Ca. *Branchiomonas cysticola*, ca. *Piscichlamydia salmonis* and salmon gill pox virus transmit horizontally in Atlantic salmon held in fresh water. *J. Fish Dis.* 40, 1387–1394. doi: 10.1111/jfd.12613

Winona, L., Ommani, A., Olszewski, J., Nuzzo, J., and Oshima, K. (2001). Efficient and predictable recovery of viruses from water by small scale ultrafiltration systems. *Can. J. Microbiol.* 47, 1033–1041. doi: 10.1139/w01-111

frontiers | Frontiers in Marine Science

TYPE Original Research
PUBLISHED 19 January 2023
DOI 10.3389/fmars.2023.1116719

OPEN ACCESS

EDITED BY
Ce Shi,
Ningbo University, China

REVIEWED BY
Qian Ma,
Guangdong Ocean University, China
Baoliang Liu,
Yellow Sea Fisheries Research Institute (CAFS), China

*CORRESPONDENCE
Yangen Zhou
zhouyg@ouc.edu.cn
Shuanglin Dong
dongsl@ouc.edu.cn

SPECIALTY SECTION
This article was submitted to Marine Fisheries, Aquaculture and Living Resources, a section of the journal Frontiers in Marine Science

RECEIVED 05 December 2022
ACCEPTED 04 January 2023
PUBLISHED 19 January 2023

CITATION
Ma S, Li L, Chen X, Chen S, Dong Y, Gao Q, Zhou Y and Dong S (2023) Influence of daily rhythmic light spectra and intensity changes on the growth and physiological status of juvenile steelhead trout (*Oncorhynchus mykiss*). *Front. Mar. Sci.* 10:1116719. doi: 10.3389/fmars.2023.1116719

Influence of daily rhythmic light spectra and intensity changes on the growth and physiological status of juvenile steelhead trout (*Oncorhynchus mykiss*)

Shisheng Ma[1], Li Li[1], Xiaoqun Chen[1], Shujing Chen[1], Yunwei Dong[1,2], Qinfeng Gao[1,2], Yangen Zhou[1]* and Shuanglin Dong[1,2]*

[1]Key Laboratory of Mariculture, Ministry of Education, Ocean University of China, Qingdao, China, [2]Function Laboratory for Marine Fisheries Science and Food Production Processes, Qingdao National Laboratory for Marine Science and Technology, Qingdao, China

The objective of this study was to investigate the effects of different rhythmic light spectra and intensities on growth performance and physiological and biochemical parameters of juvenile steelhead trout (*Oncorhynchus mykiss*). Seven treatments were randomly assigned to 21 tanks using a single-flow system for 13 weeks (N = 3), namely blue–purple–red light (BPR), red–purple–blue light (RPB), blue light (VB), and red light (VR). These light treatments alternated at 300, 900, and 1,200 lx, as well as a constant 900 lx of blue light (CB), red light (CR), and white light (CW). Results showed that the highest feed intake (FI), final body weight (FBW), and specific growth rate (SGR) were observed in the BPR treatment, which were significantly higher than those in the CW, CR, CB, and VB treatments. BPR treatment resulted in higher levels of insulin-like growth factor 1 (IGF-1), free triiodothyronine (FT3) and thyroxine (FT4), superoxide dismutase (SOD), and catalase (CAT), and total antioxidant capacity (T-AOC) activities were found. Fish exposed to BPR showed significantly enhanced lipase (LPS) and trypsin (Trp) activity in the stomach and gut tissues which promoted digestion. Trout exposed to a constant light spectra and intensity environment showed decreased activities of antioxidant and gastrointestinal digestive enzymes. Our results indicate the positive influence of BPR light conditions on the growth, stress response, digestion, and metabolism of juvenile steelhead trout, which is likely related to its similarity to the light rhythm in natural water environments, and can be used to improve growth and physiological status in the aquaculture trout.

KEYWORDS

daily rhythmic light spectra, light intensity, growth, physiological status, steelhead trout

1 Introduction

Light including light spectra, intensity, and photoperiod, is one of the most important factors in aquaculture, as it affects endocrine organs, especially the hypothalamus and hypophysis, through visual and central nervous systems. It ultimately affects feeding, growth, development, physiological status, and behavior (Handeland et al., 2013; Gao et al., 2021; Zou et al., 2022). Fish have a specific preference for certain light conditions because of evolutionary adaptation to the changing light environment. Light spectra and intensity may have different effects on growth performance among fish species and across development stages with positive or negative influences (Wei et al., 2019; Honryo et al., 2020; Wang et al., 2020; Mandario et al., 2021; Zou et al., 2022).

Light spectra and intensity play fundamental roles in the feeding and growth of fish. Different species exhibit specific preferences for certain light environments (Villamizar et al., 2009; Handeland et al., 2013; Wei et al., 2019; Wang et al., 2020; Khanjani and Sharifinia, 2021; Wu et al., 2021; Zou et al., 2022). Self-feeding of rainbow trout (*Oncorhynchus mykiss*) can be affected by light intensity (Mizusawa et al., 2007). Increased light intensity improves feeding efficiency in juvenile Atlantic salmon (*Salmo salar*) (Fraser and Metcalfe, 1997). Under high light intensity conditions, the specific growth rate (SGR) and feed conversion ratio (FCR) of rainbow trout are higher than those under low light intensities (Taylor et al., 2006). Low intensity red light is beneficial for promoting growth of rainbow trout, whereas blue light induces stress and other negative effects on growth (Karakatsouli et al., 2007; Karakatsouli et al., 2008). Chen et al. (2022b) found that blue and red light combinations instead of constant light spectra enhanced growth of steelhead trout (*Oncorhynchus mykiss*). However, to date, many studies have focused on the constant light spectra and intensity conditions of trout growth. Meanwhile, the influence of daily rhythmic light spectra and intensity changes has been limited.

The impacts of light spectra and intensity on fish growth involves endocrine hormones, circulating biochemical processes, antioxidant defenses, and digestion. The pineal gland interprets light signals and rhythmically synthesizes melatonin (MT) to maintain the body's biological clock (Iigo et al., 2007). MT secretion is affected by light spectra, and simultaneous blue and green light exposure has shown a more pronounced inhibitory effect than red light in Atlantic salmon (Handeland et al., 2013). Growth hormone (GH), insulin-like growth factor 1 (IGF-1), and cortisol levels in olive flounder (*Paralichthys olivaceus*) were higher under green light than those under white light (Zou et al., 2022). Plasma free thyroxine (FT4) levels in Atlantic salmon significantly increased under high-intensity light (1000 lx) compared to those under low-intensity light (1 lx). Meanwhile, low-intensity light also led to abnormal development (Handeland et al., 2013). Various oxidative stress responses under different light spectrum and intensity have been highlighted in multiple fish species (Gao et al., 2016; Khanjani and Sharifinia, 2021; Wu et al., 2021; Chen et al., 2022b). Guller et al. (2020) found that blue light could enhance the antioxidant capacity and immune performance of rainbow trout. Digestive enzymes are crucial for nutrient absorption and synthesis, and are also significantly influenced by light spectra and intensity in steelhead trout (Chen et al., 2022a) and Nile tilapia (*Oreochromis niloticus*) (Khanjani and Sharifinia, 2021).

Light can be absorbed by water, and long-wavelength light spectra have a greater influence. As the height of the sun, namely the light incidence angle, changes regularly during the daytime, light spectra and intensity at a certain water depth simultaneously change rhythmically. Aquatic animals have evolved to adapt to these predictable changes and form rhythmic patterns of physiological and behavioral functions (Villamizar et al., 2011). In this study, we evaluated the growth, endocrine hormone levels, plasma biochemical parameters, antioxidant defense, and digestion of juvenile steelhead trout in response to different daily rhythmic light spectra and intensities. Our results provide more detailed insights into the influence of multi-level light conditions on fish growth and present novel evidence of optimal light conditions for trout aquaculture.

2 Materials and methods

2.1 Animal preparation

Steelhead trout eye eggs were purchased from Troutlodge Inc. (Washington, USA). Before the experiment commenced, the juvenile trout were acclimatized to fresh water for two weeks, when the fish were fed to apparent satiation twice a day at 08:00 and 16:00 with a commercial trout feed and maintained on a 24 h oxygen supply and 12 L:12D photoperiod.

2.2 Experimental design

Twenty-one fiberglass tanks (220 L volume, 0.60 m height × 0.84 m diameter) coated with white paint on the inner surface and blue paint on the outer surface were used during the experiment. Each tank was covered with shade cloth to avoid ambient light contamination. Customized LED lighting systems with the following spectra and intensities were used for seven treatments: red (λ = 660–670 nm, 0–100 W), blue (λ = 455–465 nm, 0–100 W), purple (λ = 400–435 nm, 0–100 W), and white (full spectrum, 0–100 W) (Wuxi Huazhaohong Optoelectronic Technology Co., Ltd., Wuxi, China). Light spectra and intensity were determined using a lighting analyzer (PLA-300; Everfine Inc., Hangzhou, China) and were adjusted every two days. The light intensity for different experimental requirements was determined by adjusting the power of the LED lamps and their height from the water surface. Each treatment had three replicates with 12 fish per tank.

The lighting conditions for the seven treatments were as follows: constant white (900 Lux, CW), constant red (900 Lux, CR), constant blue (900 Lux, CB), the same daily rhythmic change (600 + 900 + 1200 + 900 + 600 Lux) of red (VR) and blue (VB), daily rhythmic changes of red, purple, and blue (600 Lux red + 900 Lux purple + 1200 Lux blue + 900 Lux purple + 600 Lux red, RPB), and daily rhythmic changes in blue, purple, and red (600 Lux blue + 900 Lux purple + 1200 Lux red + 900 Lux purple + 600 Lux blue, BPR) (Figure 1). The tested light intensity in the present study are in order to confer to the reported light intensity from rainbow trout and Atlantic salmon (Mizusawa et al., 2007; Handeland et al., 2013), and our previous study on steelhead trout (unpublished data). The photoperiod for all treatments was set at 15 L: 9 D between 4:30 and 19:30. The light duration for rhythmic change groups was divided into five periods, each of which lasted three hours.

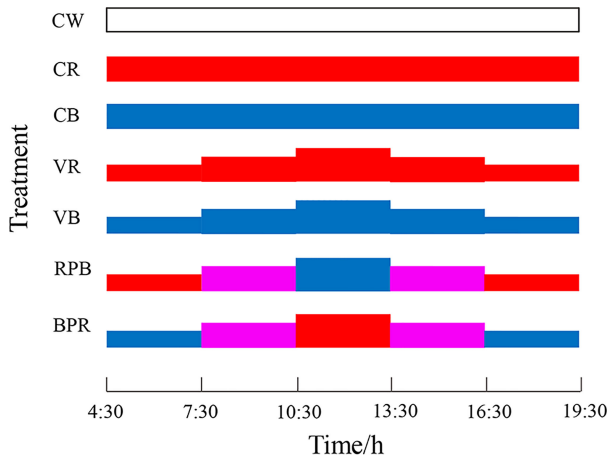

FIGURE 1
The lighting conditions for the seven treatments.

At the beginning and end of the experiment, the trout were starved for 24 h to ensure complete emptying of the digestive tract. Prior to commencing the experiment, the fish were anesthetized in a 30 mg/L tricaine methanesulfonate (MS-222; Sigma-Aldrich, USA) solution, after which they were gently dried and weighed. During the experiment, all the fish (initial weight, 30.01 ± 2.95 g) were fed twice daily (at 08:00 and 16:00) with commercial trout feed. Uneaten surplus feed was collected after feeding for 30 min. The feed intake was calculated by measuring the feed moisture content and correcting the actual daily intake. Water exchange capacity during the experiment was maintained at 70 L/h using a flowing water system. Water temperature, dissolved oxygen level, and pH were measured three times per day using a YSI professional water quality tester (YSI Inc., Ohio, USA). Water samples were collected every three days to determine phosphate, total ammonia nitrogen, nitrite, and nitrate nitrogen using an automatic chemical analyzer (Cleverchem 380 cadmium, DeChem-Tech, Germany). During the 13-week experimental period, constant water temperature, dissolved oxygen, and pH were obtained at 16 ± 0.2°C, > 6.5 mg/L, and 7.2 ± 0.2, respectively. Phosphate, total ammonia nitrogen, nitrite, and nitrate nitrogen were maintained at 0.065 ± 0.003 mg/L, 0.127 ± 0.003 mg/L, 0.09 ± 0.05 mg/L, and 3.43 ± 1.9 mg/L, respectively.

At the end of the experiment, 15 fish from each treatment with five fish per treatment, were randomly selected and immediately anesthetized using 100 mg/L MS-222 and were then placed in an ice tray. Liver, midgut, and stomach tissues were collected using sterilized scissors and forceps, placed in polyethylene tubes (5 mL; Beijing Labgic Technology Co., Ltd., Beijing, China), and immediately snap-frozen in liquid nitrogen. Blood samples were collected from the tail vein using a 2.5-mL syringe and stored in 1.5-mL polyethylene tubes, centrifuged at 875 rpm and 4°C for 10 min. The serum was separated from the red blood cells, transferred into polyethylene tubes, and immediately placed in liquid nitrogen. All the samples were stored at −80 °C until further analysis.

2.3 Growth parameters

To calculate and compare feeding and growth, fish biometry, including total number and weight, was measured at the beginning and end of the culture period. The number of fish at the beginning of the experiment and the number of fish remaining at the end of the experiment were recorded respectively to calculate the survival rate. Feeding, growth parameters, and nutrition indices included initial body weight (IBW), final body weight (FBW), specific growth rate (SGR), feed intake (FI), feed conversion ratio (FCR), and survival rate (SR). The SGR, FCR, and SR are calculated as follows:

$$Specific\ growth\ rate\ (SGR)\ (\%/day) = [100 \times (ln\ FBW - ln\ IBW)]/t\ (days)$$

$$Feed\ conversion\ ratio\ (FCR) = FI/(FBW - IBW)$$

$$Survival\ rate\ (SR)\ (\%/day) = 100 \times F_t/F_0$$

Where t is the number of experimental days, F_t is the number of fish at the end of the experiment, and F_0 is the number of fish at the beginning of the experiment.

2.4 Serum hormones and biochemical analyses

Melatonin (MT), growth hormone (GH), insulin-like growth factor 1 (IGF-1), free triiodothyronine (FT3), and free thyroxine (FT4) levels in serum were determined using enzyme-linked immunosorbent assay kits (Nanjing Jiancheng Bioengineering Institute, Nanjing, China). Serum triglyceride (TG), total cholesterol (TC), and glucose (GLU) levels were measured using a Cobas C-311 automatic biochemical analyzer (Roche, Basel, Switzerland). Activities of alanine transferase (ALT), alkaline phosphatase (ALP), and lactate dehydrogenase (LDH) were analyzed using kits (Roche, Inc., Basel, Switzerland).

2.5 Antioxidant capacity analyses

Superoxide dismutase (SOD), catalase (CAT), total antioxidant capacity (T-AOC) activity, and malondialdehyde (MDA) levels were analyzed using kits (Nanjing Jiancheng Bioengineering Institute, Nanjing, China).

2.6 Digestive enzyme activity analyses

Amylase (AMS), lipase (LPS), pepsin (Pep) and trypsin (Trp) were analyzed using assay kits (Nanjing Jiancheng Bioengineering Institute, Nanjing, China)

2.7 Statistical analysis

All parameters are expressed as mean ± standard deviation. SAS version 9.4 (SAS Institute Inc., Cary, North Carolina, USA) was used for the statistical analysis. Differences among treatments were analyzed using one-way analysis of variance (ANOVA), followed by

Tukey's multiple comparison tests. The significance level was set at $P = 0.05$.

3 Results

3.1 Growth parameters

The growth parameters for juvenile steelhead trout are presented in Table 1. Different daily rhythmic light spectra and intensity changes significantly affected trout growth ($P< 0.05$). The FBW and SGR in the BPR group were the highest and were significantly higher than those in the CW, CB, CR, and VB groups ($P< 0.05$). The highest FI levels were observed in the BPR and RPB groups. The FI in the CW, CR, CB and VB groups were significantly lower than those in the BPR and RPB groups ($P< 0.05$). There were no significant differences in FCR and SR among the groups ($P > 0.05$).

3.2 Serum hormones levels

The serum hormone levels in juvenile steelhead trout are presented in Figure 2. There was no significant difference in GH levels between groups ($P > 0.05$). However, IGF-1 levels were significantly higher in the BPR group than those in the other groups ($P< 0.05$). No significant difference was observed in MT levels among the groups ($P > 0.05$). FT3 levels were significantly higher in the BPR group than those in the other groups, and FT4 levels were significantly higher in the BPR group than those in the CW, VR, VB, and RPB groups ($P< 0.05$).

3.3 Serum biochemical parameters

Serum levels of TG, TC, and GLU and activities of ALT, ALP, and LDH are presented in Table 2. There were no statistically significant differences in serum TG, TC, and GLU levels ($P > 0.05$). ALT activity was significantly higher in the CW group than those in the CB, VR, RPB and BPR groups ($P< 0.05$). ALT activity was significantly lower in the VR and BPR groups than those in the CW, CR and VB groups ($P< 0.05$). ALP activity was significantly higher in the CW group than those in the CR, CB, VR, and VB groups ($P< 0.05$). Statistically higher LDH activity was observed in the CW group than those in the other groups ($P< 0.05$). The lowest LDH activity were observed in the BPR and RPB groups.

3.4 Antioxidant capacity

Antioxidant capacity was significantly affected by the daily rhythmic light spectra and intensity changes (Figure 3). CAT and T-AOC activities in the RPB and BPR groups were significantly higher than those in the other groups ($P< 0.05$). SOD activity in the BPR group was significantly higher than those in the CW, CR, CB, VR, and VB groups ($P< 0.05$), but not significantly higher than those in the RPB group ($P > 0.05$). The lowest SOD activity was observed in the CW and VR groups. T-AOC activity in the CW, CR and VR groups was significantly lower than those in the CB, VB, BPR and RPB groups ($P< 0.05$). MDA levels in the CR and VR groups were significantly higher than those in the CB, VB, RPB, and BPR groups ($P< 0.05$).

3.5 Digestive enzyme activity

Activities of AMS, LPS, Pep, and Trp in the midgut and stomach are shown in Figure 4. Midgut and gastric LPS activities were significantly higher in the BPR group than those in the other groups ($P< 0.05$). Statistically higher midgut Trp activity was observed in the BPR group than those in the other groups ($P< 0.05$). Trp activity in the CW and VB groups was significantly lower than those in the other groups ($P< 0.05$). No statistical differences were detected in AMS and gastric Pep among the groups ($P > 0.05$).

4 Discussion

In the natural aquatic environment, because of the strong absorption capacity of water for long-wavelength light and the regular height changes of the sun (light incidence angle) during the day, the light intensity and spectra change rhythmically at a certain

TABLE 1 The growth parameters of steelhead trout reared under different light conditions.

Parameters	CW	CR	CB	VR	VB	RPB	BPR	*P value*
Initial body weight (g)	30.05 ± 2.59	30.02 ± 2.04	30.01 ± 2.47	30.01 ± 2.68	30.02 ± 2.58	29.95 ± 2.66	30.01 ± 2.60	0.6220
Final body weight (g)	118.59 ± 14.25^{b}	125.35 ± 18.04^{b}	125.56 ± 17.82^{b}	134.77 ± 18.02^{ab}	125.80 ± 17.31^{b}	134.87 ± 19.96^{ab}	150.31 ± 19.80^{a}	0.0014
Specific growth rate(% day^{-1})	1.54 ± 0.01^{b}	1.56 ± 0.01^{b}	1.56 ± 0.03^{b}	1.58 ± 0.01^{ab}	1.56 ± 0.01^{b}	1.58 ± 0.01^{ab}	1.62 ± 0.01^{a}	0.0044
Feed intake (g)	109.93 ± 1.79^{d}	118.18 ± 2.45^{cd}	115.94 ± 9.44^{cd}	128.14 ± 5.52^{bc}	118.60 ± 1.86^{cd}	136.02 ± 5.86^{ab}	142.49 ± 5.31^{a}	0.0002
Feed conversion ratio	1.24 ± 0.01	1.24 ± 0.07	1.22 ± 0.11	1.22 ± 0.01	1.24 ± 0.07	1.30 ± 0.04	1.18 ± 0.02	0.6883
Survival rate (%)	100.00 ± 0.00	97.22 ± 3.93	97.22 ± 3.93	97.22 ± 3.93	97.22 ± 3.93	97.22 ± 3.93	100.00 ± 0.00	0.9081

Values (mean ± standard deviation) are the means of three replicates. Values on the same line with different superscript letters are significantly different (P< 0.05) based on one-way analysis of variance (ANOVA) with Tukey's test.

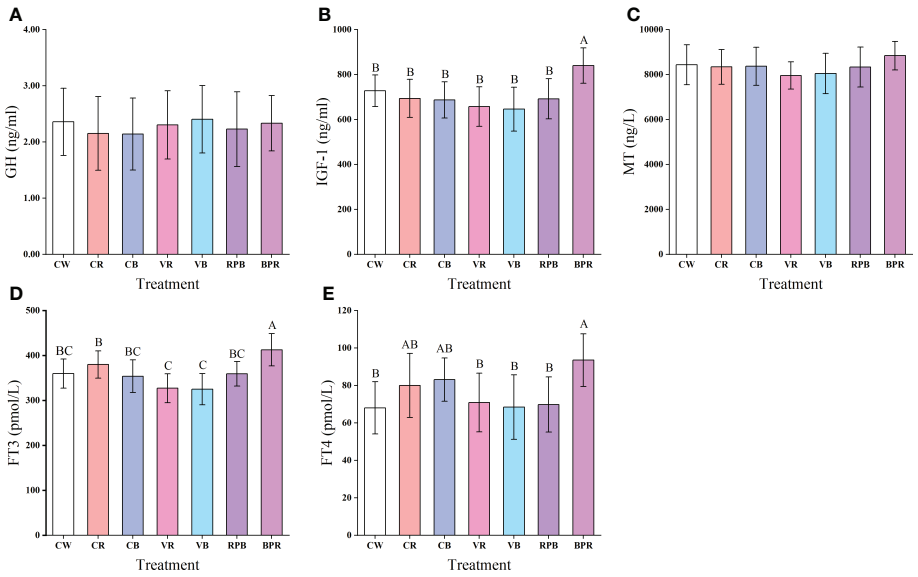

FIGURE 2
Serum hormones levels of GH **(A)**, IGF-1 **(B)**, MT **(C)**, FT3 **(D)** and FT4 **(E)** in juvenile steelhead trout reared under different light conditions. Different capital letters denote significant differences among the steelhead trout treatments. Results are expressed as mean ± standard deviation (n=15).

water depth (Sanchez-Vazquez et al., 2019; Ruchin, 2021). Teleost fish can experience reduced stress and maintain homeostasis because of evolutionary adaptation to their specific living light environment. This is conducive to growth, development, and reproduction (Kusmic and Gualtieri, 2000; Cheng and Flamarique, 2007; Villamizar et al., 2011; Grossman, 2014; Eilertsen et al., 2018). Different light conditions can affect fish feeding (Kraaij et al., 1998; Cobcroft et al., 2001; Kestemont and Baras, 2001; Marchand et al., 2002; Puvanendran and Brown, 2002). Feed intake by rainbow trout is positively correlated with light intensity within a tolerable range (Mizusawa et al., 2007). Karakatsouli et al. (2008) and Karakatsouli et al. (2007) showed that growth performance of rainbow trout exposed to a low intensity of red light was enhanced compared to blue light, and blue light induced an increased stress response.

In the present study, rhythmic rather than constant light intensity and spectra in the BPR group were more conducive to growth, feeding, and metabolism of juvenile steelhead trout (Table 1). Our results are consistent with those of Chen et al. (2022b). Chen et al. (2022b) reported that blue and red light combinations improved feeding conversion efficiency and enhanced growth of steelhead trout. Our data showed that the light variation pattern of the BPR group was closer to that of natural water than the constant light spectra and constant/rhythmic light intensity. Low light intensity in the morning and evening was akin to a small light incidence angle, long irradiation distance, and high proportion of short-wavelength light. Meanwhile, high light intensity and a large proportion of long-wavelength light were in line with the natural light conditions at noon. LED lights have been widely used in aquaculture as a controllable artificial light source (Song et al., 2018). Our results suggest that an LED lighting system closely simulating the light conditions of the natural habitat of steelhead trout, such as the daily rhythmic change in BPR lighting, can improve fish growth.

The pineal gland and retina of teleost fish are photoreceptors and the photosensitive rod photoreceptor and cone cells help them to identify specific wavelengths (Kraaij et al., 1998). Mediated by the hypothalamus-pituitary-growth hormone (HPGH) pathway, GH and IGF-1 have a significant influence on the growth of fish directly or indirectly (Bjornsson, 1997; Mommsen, 2001; Perez-Sanchez et al., 2002; Zou et al., 2022). However, fish metabolism and the external environment affect the levels of GH and IGF-1 (Bertucci et al., 2019;

TABLE 2 The serum biochemical parameters of steelhead trout reared under different light conditions.

Parameters	CW	CR	CB	VR	VB	RPB	BPR	*P value*
TG (mmol/L)	2.20 ± 0.39	1.91 ± 0.16	2.03 ± 0.31	1.97 ± 0.32	1.99 ± 0.36	2.09 ± 0.28	2.21 ± 0.37	0.0991
TC (mmol/L)	5.23 ± 0.59	5.03 ± 0.58	5.05 ± 0.55	4.90 ± 0.82	5.11 ± 0.69	5.29 ± 0.87	5.70 ± 0.79	0.0876
GLU (mmol/L)	0.86 ± 0.20	0.80 ± 0.18	0.77 ± 0.18	0.97 ± 0.17	0.86 ± 0.22	0.92 ± 0.22	0.86 ± 0.21	0.1429
ALT (U/L)	10.09 ± 1.22^{a}	9.55 ± 1.67^{ab}	8.54 ± 1.39^{bc}	7.87 ± 1.38^{c}	9.81 ± 1.39^{ab}	8.76 ± 0.86^{bc}	7.83 ± 1.23^{c}	<0.0001
ALP (U/L)	89.20 ± 15.86^{a}	70.40 ± 14.63^{b}	67.00 ± 11.55^{b}	73.13 ± 10.50^{b}	74.47 ± 14.52^{b}	79.53 ± 12.49^{ab}	79.27 ± 11.09^{ab}	0.0006
LDH (U/L)	725.00 ± 72.25^{a}	468.87 ± 54.74^{cd}	513.60 ± 64.02^{c}	473.13 ± 58.61^{cd}	569.40 ± 77.02^{b}	423.20 ± 66.18^{d}	438.07 ± 56.86^{d}	<0.0001

Values (mean ± standard deviation) are the means of three replicates. Values on the same line with different superscript letters are significantly different (P< 0.05) based on one-way analysis of variance (ANOVA) with Tukey's test.

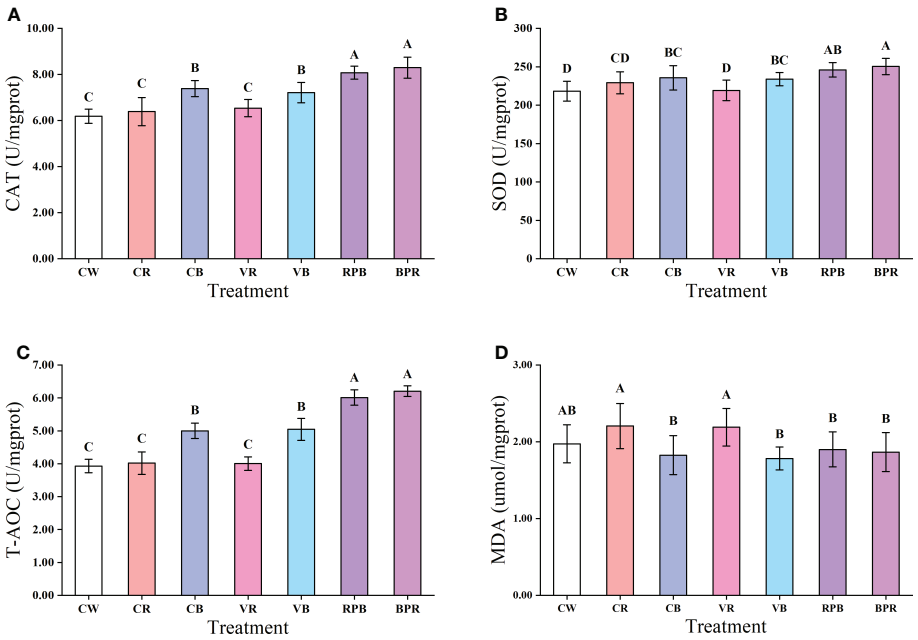

FIGURE 3
Antioxidant enzymes activities of the liver in juvenile steelhead trout reared under different light color conditions. **(A)** CAT activity; **(B)** SOD activity; **(C)** T-AOC activity; **(D)** MDA level. Different capital letters denote significant differences among the steelhead trout treatments. Results are expressed as mean ± standard deviation (n=15).

Triantaphyllopoulos et al., 2020). Some studies have shown that IGF-1 content is positively correlated with fish growth (Wang et al., 2020; Perello-Amoros et al., 2021; Chen et al., 2022b). Our findings show that daily rhythmic light spectra and intensity changes in the BPR group significantly increased IGF-1 concentrations through indirect stimulation of the visual system, which promoted the growth of steelhead trout (Figure 2). Our data showed that the serum GH content of steelhead trout was much lower than that of IGF, with no significant difference among the groups, which had no significant effect on the growth. A signal molecule that acts as a receptor of the external light environment, MT is predominantly involved in the circadian rhythm and gonad development of fish. It can also regulate

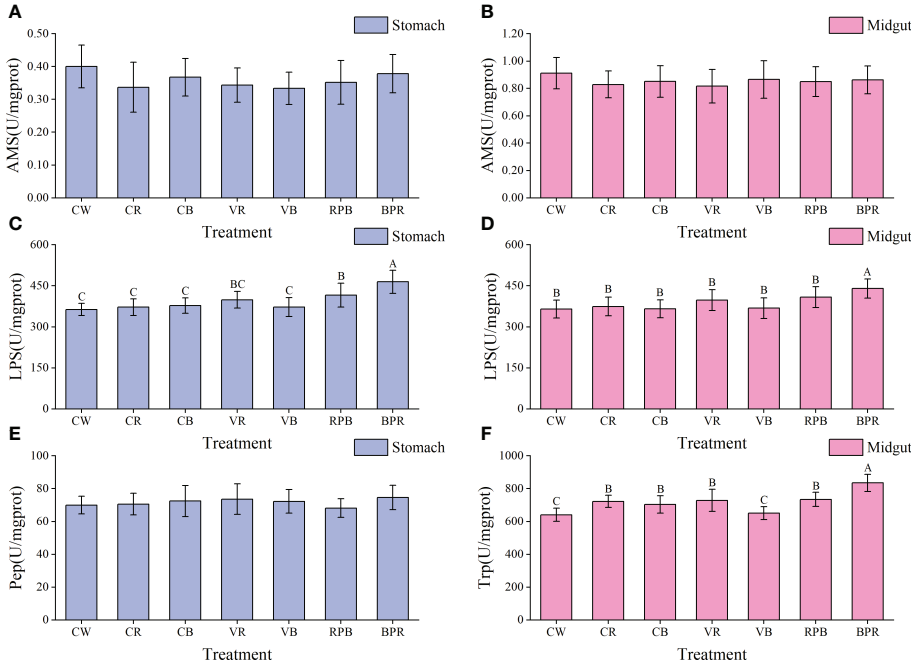

FIGURE 4
Digestive enzymes activities of the midgut and stomach in juvenile steelhead trout reared under different light color conditions. **(A)** AMS activity in the stomach; **(B)** AMS activity in the midgut; **(C)** LPS activity in the stomach; **(D)** LPS activity in the midgut; **(E)** Pep activity in the stomach; **(F)** Trp activity in the midgut. Different capital letters denote significant differences among the steelhead trout treatments. Results are expressed as mean ± standard deviation (n=15).

synthesis of related hormones (Bromage et al., 2001; Falcon et al., 2007; Zou et al., 2022). Thyroid hormones (THs) play an important role in regulating growth, development, reproduction, migration, metabolism, and osmotic pressure of fish. They mainly exist in the form of FT3 and FT4 in blood (Johnson and Lema, 2011; Peter, 2011; Mullur et al., 2014; Abdalla and Bianco, 2014). In this study, there was no significant difference in MT levels among groups. However, serum FT3 and FT4 levels in steelhead trout were significantly higher in the BPR group than in the other groups. Our results indicate that rhythmic BPR lighting exerted a positive effect on growth-related hormones in steelhead trout.

A uncomfortable light environment stimulates the visual system of fish and results in a stress response. This can subsequently disrupt the immune system and resulting in adverse outcomes (Song and Choi, 2019). Several biochemical parameters, including ALT, ALP, and LDH, reflect oxidative stress levels. In this study, liver and myocardium functions of juvenile steelhead trout were likely disrupted under constant 900 lx white light. This resulted in high levels of circulating ALT, ALP, and LDH, and consequently low growth rates. Our results indicate that conventional light sources that use constant white light in aquaculture are potentially harmful to trout.

The antioxidant defense system of fish can be disrupted by external environmental changes and produces reactive oxygen species (ROS).This can negatively impact fish health (Nyska and Kohen, 2002; Nishida, 2011). The appropriate light intensity and spectra can enhance the antioxidant enzymes activities of fish, including SOD, CAT, and T-AOC, comprising the antioxidant defense system and playing a crucial role in decreasing intracellular ROS, and reducing cell damage (Shin et al., 2011; Gao et al., 2016; Guller et al., 2020; Akhtar et al., 2022; Chen et al., 2022b). MDA can cause cell membrane damage and function loss, resulting in negative effects on other physiological functions. Therefore, it is used as an important index reflecting the oxidative damage level (Martinez-Alvarez et al., 2002). Long-wavelength red light emitted from LED lights can cause oxidative stress in fish. Meanwhile, short-wavelength light can effectively reduce oxidative stress and improve immunity. Our findings have shown that there has been an apparent decrease in the antioxidant capacity of juvenile steelhead trout exposed to red light. The MDA level in the constant and daily rhythmic change of red light groups was significantly higher than that in other groups, except for constant white light. Our results are in line with those of Guller et al. (2020), who reported that the activities of liver antioxidant enzymes in rainbow trout were higher when exposed to blue light than when exposed to red light. In this study, the CAT, SOD, and T-AOC activities of juvenile steelhead trout in the BPR and RPB groups exposed to daily rhythmic light spectra and intensity changes were significantly higher than those in the other groups. In a recent study on blue–red light combinations of juvenile steelhead trout, this combination improved antioxidant capacity by increasing activities of liver antioxidant enzymes, while constant red light increased MDA levels This led to intense stress and decreased immunity (Chen et al., 2022b). This phenomenon indicates that changes in light conditions induce a response in the antioxidant defense system *via* the visual system. This can contribute to preventing physiological damage to the changing environment.

Digestive enzyme activity is an important index for measuring fish digestion and metabolism ability (Perez-Sirkin et al., 2020; Yu et al., 2020a). This can be affected by feeding habits (Castro-Ruiz et al., 2019; Yu et al., 2020b) and light environment (Khanjani and Sharifinia, 2021; Chen et al., 2022a). In this study, activities of LPS and Trp in the stomach and midgut of juvenile steelhead trout were higher than those of AMS. This is consistent with the characteristics of steelhead trout as carnivorous fish. Our data showed no significant difference in FI between the BPR and RPB groups. However, LPS and Trp activities in the BPR group were significantly higher than those in the RPB group. FCR was also higher in the BPR group, suggesting improved digestion ability. Results of this study indicate that the positive influence of the BPR light environment improves feeding, IGF-1 level, antioxidant capacity, digestion and metabolism abilities of juvenile steelhead trout, which promote its growth. This may be explained by evolutionary adaptation of fish to their natural living light environment.

5 Conclusion

In this study, compared with other constant or rhythmic light treatments, the BPR light environment, which is akin to the light rhythm in natural waters, was beneficial to the feeding, growth, stress resistance, digestion, and metabolism of juvenile steelhead trout. These findings are worth considering in aquaculture lighting applications as an effective means of improving fish growth.

Data availability statement

The original contributions presented in the study are included in the article/Supplementary Material. Further inquiries can be directed to the corresponding authors.

Ethics statement

The animal study was reviewed and approved by Regulations of the Administration of Affairs Concerning Experimental Animals of China Regulations of the Administration of Affairs Concerning Experimental Animals of Shandong Province. Written informed consent was obtained from the owners for the participation of their animals in this study.

Author contributions

SM performed the trial and data analysis, wrote the original draft, and proposed the research methods and ideas. YZ and SD supervised research progress, proposed research methods and research ideas, and edited manuscript. XC and SC performed the trial. LL, YD, and QG reviewed and edited the original draft. All authors contributed to the article and approved the submitted version.

Funding

This publication was supported by the National Natural Science Foundation of China (NSFC) (Nos. U1906206 and 31872575), the National Key Research and Development Program of China (No. 2019YFD0901000), and the Scientific and Technological Demonstration for Offshore Facilities Fisheries of Shandong Province (2021SFGC0701).

Acknowledgments

The authors of this study would like to thank everyone who critically reviewed this manuscript and helped with the sample collection. This study was supported by the National Natural Science Foundation of China (NSFC) (Nos. U1906206 and 31872575), the National Key Research and Development Program of China (No. 2019YFD0901000), and the Scientific and Technological Demonstration for Offshore Facilities Fisheries of Shandong Province (2021SFGC0701), and the OUC-AUBURN Joint Research Center for Aquaculture and Environmental Sciences.

Conflict of interest

The authors declare that the research was conducted in the absence of any commercial or financial relationships that could be construed as a potential conflict of interest.

Publisher's note

References

Abdalla, S. M., and Bianco, A. C. (2014). Defending plasma T3 is a biological priority. *Clin. Endocrinol.* 81 (5), 633–641. doi: 10.1111/cen.12538

Akhtar, M. S., Tripathi, P. H., and Ciji, A. (2022). Light spectra influence the reproductive performance and expression of immune and anti-oxidative defense genes in endangered golden mahseer (*Tor putitora*) female brooders. *Aquaculture* 547, 737355. doi: 10.1016/j.aquaculture.2021.737355

Bertucci, J. I., Blanco, A. M., Sundarrajan, L., Rajeswari, J. J., Velasco, C., and Unniappan, S. (2019). Nutrient regulation of endocrine factors influencing feeding and growth in fish. *Front. Endocrinol.* 10. doi: 10.3389/fendo.2019.00083

Bjornsson, B. T. (1997). The biology of salmon growth hormone: from daylight to dominance. *Fish Physiol. Biochem.* 17 (1-6), 9–24. doi: 10.1023/a:1007712413908

Bromage, N., Porter, M., and Randall, C. (2001). The environmental regulation of maturation in farmed finfish with special reference to the role of photoperiod and melatonin. *Aquaculture* 197 (1-4), 63–98. doi: 10.1016/s0044-8486(01)00583-x

Castro-Ruiz, D., Mozanzadeh, M. T., Fernandez-Mendez, C., Andree, K. B., Garcia-Davila, C., Cahu, C., et al. (2019). Ontogeny of the digestive enzyme activity of the Amazonian pimelodid catfish *Pseudoplatystoma punctifer* (Castelna 1855). *Aquaculture* 504, 210–218. doi: 10.1016/j.aquaculture.2019.01.059

Cheng, C. L., and Flamarique, I. N. (2007). Chromatic organization of cone photoreceptors in the retina of rainbow trout: single cones irreversibly switch from UV (SWS1) to blue (SWS2) light sensitive opsin during natural development. *J. Exp. Biol.* 210 (23), 4123–4135. doi: 10.1242/jeb.009217

Chen, X., Zhou, Y., Huang, J., An, D., Li, L., Dong, Y., et al. (2022a). Blue and red light color combinations can enhance certain aspects of digestive and anabolic performance in juvenile steelhead trout *Oncorhynchus mykiss*. *Front. Mar. Sci.* 9. doi: 10.3389/fmars.2022.853327

Chen, X., Zhou, Y., Huang, J., An, D., Li, L., Dong, Y., et al. (2022b). The effects of blue and red light color combinations on the growth and immune performance of juvenile steelhead trout, *Oncorhynchus mykiss*. *Aquacul. Rep.* 24, 101156. doi: 10.1016/j.aqrep.2022.101156

Cobcroft, J. M., Pankhurst, P. M., Hart, P. R., and Battaglene, S. C. (2001). The effects of light intensity and algae-induced turbidity on feeding behaviour of larval striped trumpeter. *J. Fish Biol.* 59 (5), 1181–1197. doi: 10.1111/j.1095-8649.2001.tb00185.x

Eilertsen, M., Valen, R., Drivenes, O., Ebbesson, L. O. E., and Helvik, J. V. (2018). Transient photoreception in the hindbrain is permissive to the life history transition of hatching in Atlantic halibut. *Dev. Biol.* 444 (2), 129–138. doi: 10.1016/j.ydbio.2018.10.006

Falcon, J., Besseau, L., Sauzet, S., and Boeuf, G. (2007). Melatonin effects on the hypothalamo-pituitary axis in fish. *Trends Endocrinol. Metab.* 18 (2), 81–88. doi: 10.1016/j.tem.2007.01.002

Fraser, N. H. C., and Metcalfe, N. B. (1997). The costs of becoming nocturnal: Feeding efficiency in relation to light intensity in juvenile Atlantic salmon. *Funct. Ecol.* 11 (3), 385–391. doi: 10.1046/j.1365-2435.1997.00098.x

Gao, X. L., Li, X., Li, M. J., Song, C. B., and Liu, Y. (2016). Effects of light intensity on metabolism and antioxidant defense in *Haliotis discus hannai* ino. *Aquaculture* 465, 78–87. doi: 10.1016/j.aquaculture.2016.08.010

Gao, X. L., Pang, G., Luo, X., You, W., and Ke, C. (2021). Effects of light cycle on motion behaviour and melatonin secretion in *Haliotis discus hannai*. *Aquaculture* 532, 735981. doi: 10.1016/j.aquaculture.2020.735981

Grossman, G. D. (2014). Not all drift feeders are trout: a short review of fitness-based habitat selection models for fishes. *Environ. Biol. Fish.* 97 (5), 465–473. doi: 10.1007/s10641-013-0198-3

Guller, U., Onalan, S., Arabaci, M., Karatas, B., Yasar, M., and Kufrevioglu, O. I. (2020). Effects of different LED light spectra on rainbow trout (*Oncorhynchus mykiss*): *in vivo* evaluation of the antioxidant status. *Fish Physiol. Biochem.* 46 (6), 2169–2180. doi: 10.1007/s10695-020-00865-x

Handeland, S. O., Imsland, A. K., Ebbesson, L. O. E., Nilsen, T. O., Hosfeld, C. D., Baeverfjord, G., et al. (2013). Low light intensity can reduce Atlantic salmon smolt quality. *Aquaculture* 384-387, 19–24. doi: 10.1016/j.aquaculture.2012.12.016

Honryo, T., Okada, T., Kawahara, M., Sawada, Y., Kurata, M., and Ishibashi, Y. (2020). Effects of night-time light intensity and area of illumination in the sea cage culture of pacific bluefin tuna (*Thunnus orientalis*) juveniles. *Aquaculture* 521, 735046. doi: 10.1016/j.aquaculture.2020.735046

Iigo, M., Abe, T., Kambayashi, S., Oikawa, K., Masuda, T., Mizusawa, K., et al. (2007). Lack of circadian regulation of *in vitro* melatonin release from the pineal organ of salmonid teleosts. *Gen. Comp. Endocrinol.* 154 (1-3), 91–97. doi: 10.1016/j.ygcen.2007.06.013

Johnson, K. M., and Lema, S. C. (2011). Tissue-specific thyroid hormone regulation of gene transcripts encoding iodothyronine deiodinases and thyroid hormone receptors in striped parrotfish (*Scarus iseri*). *Gen. Comp. Endocrinol.* 172 (3), 505–517. doi: 10.1016/j.ygcen.2011.04.022

Karakatsouli, N., Papoutsoglou, S. E., Panopoulos, G., Papoutsoglou, E. S., Chadio, S., and Kalogiannis, D. (2008). Effects of light spectrum on growth and stress response of rainbow trout *Oncorhynchus mykiss* reared under recirculating system conditions. *Aquacul. Eng.* 38 (1), 36–42. doi: 10.1016/j.aquaeng.2007.10.006

Karakatsouli, N., Papoutsoglou, S. E., Pizzonia, G., Tsatsos, G., Tsopelakos, A., Chadio, S., et al. (2007). Effects of light spectrum on growth and physiological status of gilthead seabream *Sparus aurata* and rainbow trout *Oncorhynchus mykiss* reared under recirculating system conditions. *Aquacul. Eng.* 36 (3), 302–309. doi: 10.1016/j.aquaeng.2007.01.005

Kestemont, P., and Baras, E. (2001). Environmental factors and feed intake: Mechanisms and interactions. *Food Intake Fish* 6, 131–156. doi: 10.1002/9780470999516.ch6

Khanjani, M. H., and Sharifinia, M. (2021). Production of Nile tilapia *Oreochromis niloticus* reared in a limited water exchange system: The effect of different light levels. *Aquaculture* 542, 736912. doi: 10.1016/j.aquaculture.2021.736912

Kraaij, D. A., Kamermans, M., and Spekreijse, H. (1998). Spectral sensitivity of the feedback signal from horizontal cells to cones in goldfish retina. *Visual Neurosci.* 15 (5), 799–808. doi: 10.1017/s0952523898154184

Kusmic, C., and Gualtieri, P. (2000). Morphology and spectral sensitivities of retinal and extraretinal photoreceptors in freshwater teleosts. *Micron* 31 (2), 183–200. doi: 10.1016/s0968-4328(99)00081-5

Mandario, M. A. E., Castor, N. J. T., and Balinas, V. T. (2021). Interaction effect of light intensity and photoperiod on egg hatchability, survival and growth of polychaete *Marphysa iloiloensis* from larva to juvenile. *Aquaculture* 531, 735890. doi: 10.1016/j.aquaculture.2020.735890

Marchand, F., Magnan, P., and Boisclair, D. (2002). Water temperature, light intensity and zooplankton density and the feeding activity of juvenile brook charr (*Salvelinus fontinalis*). *Freshw. Biol.* 47 (11), 2153–2162. doi: 10.1046/j.1365-2427.2002.00961.x

Martinez-Alvarez, R. M., Hidalgo, M. C., Domezain, A., Morales, A. E., Garcia-Gallego, M., and Sanz, A. (2002). Physiological changes of sturgeon *Acipenser naccarii* caused by increasing environmental salinity. *J. Exp. Biol.* 205 (23), 3699–3706. doi: 10.1242/jeb.205.23.3699

Mizusawa, K., Noble, C., Suzuki, K., and Tabata, M. (2007). Effect of light intensity on self-feeding of rainbow trout *Oncorhynchus mykiss* reared individually. *Fish. Sci.* 73 (5), 1001–1006. doi: 10.1111/j.1444-2906.2007.01429.x

Mommsen, T. P. (2001). Paradigms of growth in fish. *Comp. Biochem. Physiol. B-Biochem0 Mol. Biol.* 129 (2-3), 207–219. doi: 10.1016/s1096-4959(01)00312-8

Mullur, R., Liu, Y. Y., and Brent, G. A. (2014). Thyroid hormone regulation of metabolism. *Physiol. Rev.* 94 (2), 355–382. doi: 10.1152/physrev.00030.2013

Nishida, Y. (2011). The chemical process of oxidative stress by copper(II) and iron(III) ions in several neurodegenerative disorders. *Monatshefte Fur Chemie* 142 (4), 375–384. doi: 10.1007/s00706-010-0444-8

Nyska, A., and Kohen, R. (2002). Oxidation of biological systems: Oxidative stress phenomena, antioxidants, redox reactions, and methods for their quantification. *Toxicol. Pathol.* 30 (6), 620–650. doi: 10.1080/01926230290166724

Perello-Amoros, M., Garcia-Perez, I., Sanchez-Moya, A., Innamorati, A., Velez, E. J., Achaerandio, I., et al. (2021). Diet and exercise modulate GH-IGFs axis, proteolytic markers and myogenic regulatory factors in juveniles of gilthead Sea bream (*Sparus aurata*). *Animals* 11 (8). doi: 10.3390/ani11082182

Perez-Sanchez, J., Calduch-Giner, J. A., Mingarro, M., de Celis, S. V. R., Gomez-Requeni, P., Saera-Vila, A., et al. (2002). Overview of fish growth hormone family. new insights in genomic organization and heterogeneity of growth hormone receptors. . *Fish Physiol. Biochem* 27 (3-4), 243–258. doi: 10.1023/B:FISH.0000032729.72746.c8

Perez-Sirkin, D. I., Solovyev, M., Delgadin, T. H., Herdman, J. E., Miranda, L. A., Somoza, G. M., et al. (2020). Digestive enzyme activities during pejerrey (*Odontesthes bonariensis*) ontogeny. *Aquaculture* 524, 735151. doi: 10.1016/j.aquaculture.2020.735151

Peter, M. C. S. (2011). The role of thyroid hormones in stress response of fish. *Gen. Comp. Endocrinol.* 172 (2), 198–210. doi: 10.1016/j.ygcen.2011.02.023

Puvanendran, V., and Brown, J. A. (2002). Foraging, growth and survival of Atlantic cod larvae reared in different light intensities and photoperiods. *Aquaculture* 214 (1-4), 131–151. doi: 10.1016/s0044-8486(02)00045-5

Ruchin, A. B. (2021). Effect of illumination on fish and amphibian: development, growth, physiological and biochemical processes. *Rev. Aquacul.* 13 (1), 567–600. doi: 10.1111/raq.12487

Sanchez-Vazquez, F. J., Lopez-Olmeda, J. F., Vera, L. M., Migaud, H., Lopez-Patino, M. A., and Miguez, J. M. (2019). Environmental cycles, melatonin, and circadian control of stress response in fish. *Front. Endocrinol.* 10. doi: 10.3389/fendo.2019.00279

Shin, H. S., Lee, J., and Choi, C. Y. (2011). Effects of LED light spectra on oxidative stress and the protective role of melatonin in relation to the daily rhythm of the yellowtail clownfish, *Amphiprion clarkii*. *Comp. Biochem. Physiol. A Mol. Integr. Physiol.* 160 (2), 221–228. doi: 10.1016/j.cbpa.2011.06.002

Song, J. A., and Choi, C. Y. (2019). Effects of blue light spectra on retinal stress and damage in goldfish (*Carassius auratus*). *Fish Physiol. Biochem.* 45 (1), 391–400. doi: 10.1007/s10695-018-0571-4

Song, C., Liu, L., Lu, P., Yang, H., Li, X., Gao, X., et al. (2018). Design of artificial LED lighting in aquaculture workshop. *J. Dalian Ocean Univ.* 33 (2), 145–150. doi: 10.16535/j.cnki.dlhyxb.2018.02.002

Taylor, J. F., North, B. P., Porter, M. J. R., Bromage, N. R., and Migaud, H. (2006). Photoperiod can be used to enhance growth and improve feeding efficiency in farmed rainbow trout, *Oncorhynchus mykiss*. *Aquaculture* 256 (1-4), 216–234. doi: 10.1016/j.aquaculture.2006.02.027

Triantaphyllopoulos, K. A., Cartas, D., and Miliou, H. (2020). Factors influencing GH and IGF-I gene expression on growth in teleost fish: how can aquaculture industry benefit? *Rev. Aquacul.* 12 (3), 1637–1662. doi: 10.1111/raq.12402

Villamizar, N., Blanco-Vives, B., Migaud, H., Davie, A., Carboni, S., and Sánchez-Vázquez, F. J. (2011). Effects of light during early larval development of some aquacultured teleosts: A review. *Aquaculture* 315 (1-2), 86–94. doi: 10.1016/j.aquaculture.2010.10.036

Villamizar, N., García-Alcazar, A., and Sánchez-Vázquez, F. J. (2009). Effect of light spectrum and photoperiod on the growth, development and survival of European sea bass (*Dicentrarchus labrax*) larvae. *Aquaculture* 292 (1-2), 80–86. doi: 10.1016/j.aquaculture.2009.03.045

Wang, K., Li, K., Liu, L., Tanase, C., Mols, R., and van der Meer, M. (2020). Effects of light intensity and photoperiod on the growth and stress response of juvenile Nile tilapia (*Oreochromis niloticus*) in a recirculating aquaculture system. *Aquacul. Fish* 8 (1), 85–90. doi: 10.1016/j.aaf.2020.03.001

Wang, T. T., Xu, M. M., Wang, J. T., Wan, W. J., Guan, D. Y., Han, H. J., et al. (2020). A combination of rapeseed, cottonseed and peanut meal as a substitute of soybean meal in diets of yellow river carp *Cyprinus carpio* var. *Aquacul. Nutr.* 26 (5), 1520–1532. doi: 10.1111/anu.13099

Wei, H., Li, H.-D., Xia, Y., Liu, H.-K., Han, D., Zhu, X.-M., et al. (2019). Effects of light intensity on phototaxis, growth, antioxidant and stress of juvenile gibel carp (*Carassius auratus gibelio*). *Aquaculture* 501, 39–47. doi: 10.1016/j.aquaculture.2018.10.055

Wu, L., Wang, Y., Li, J., Song, Z., Xu, S., Song, C., et al. (2021). Influence of light spectra on the performance of juvenile turbot (*Scophthalmus maximus*). *Aquaculture* 533, 736191. doi: 10.1016/j.aquaculture.2020.736191

Yu, Z., Li, L., Zhu, R., Li, M., Duan, J., Wang, J. Y., et al. (2020a). Monitoring of growth, digestive enzyme activity, immune response and water quality parameters of golden crucian carp (*Carassius auratus*) in zero-water exchange tanks of biofloc systems. *Aquacul. Rep.* 16. doi: 10.1016/j.aqrep.2020.100283

Yu, Z., Wu, X. Q., Zheng, L. J., Dai, Z. Y., and Wu, L. F. (2020b). Effect of acute exposure to ammonia and BFT alterations on *Rhynchocypris lagowski*: Digestive enzyme, inflammation response, oxidative stress and immunological parameters. *Environ. Toxicol. Pharmacol.* 78. doi: 10.1016/j.etap.2020.103380

Zou, Y., Peng, Z., Wang, W., Liang, S., Song, C., Wang, L., et al. (2022). The stimulation effects of green light on the growth, testicular development and stress of olive flounder *Paralichthys olivaceus*. *Aquaculture* 546, 737275. doi: 10.1016/j.aquaculture.2021.737275

frontiers | Frontiers in Marine Science

TYPE Original Research
PUBLISHED 23 January 2023
DOI 10.3389/fmars.2023.1114662

OPEN ACCESS

EDITED BY
Ce Shi,
Ningbo University, China

REVIEWED BY
Shijing Liu,
Fishery Machinery and Instrument Research Institute (CAFS), China
Jian Zhao,
Zhejiang University, China

*CORRESPONDENCE
Lei Gao
gaolei@dlou.edu.cn

SPECIALTY SECTION
This article was submitted to Marine Fisheries, Aquaculture and Living Resources, a section of the journal Frontiers in Marine Science

RECEIVED 02 December 2022
ACCEPTED 04 January 2023
PUBLISHED 23 January 2023

CITATION
Ma Z, Zhang J, Zhang X, Li H, Liu Y and Gao L (2023) Effects of temperature and photoperiod on growth, physiological, and behavioral performance in steelhead trout (*Oncorhynchus mykiss*) under indoor aquaculture condition.
Front. Mar. Sci. 10:1114662.
doi: 10.3389/fmars.2023.1114662

Effects of temperature and photoperiod on growth, physiological, and behavioral performance in steelhead trout (*Oncorhynchus mykiss*) under indoor aquaculture condition

Zhen Ma[1,2], Jia Zhang[1,2], Xu Zhang[1,3], Haixia Li[1,2], Ying Liu[1,2] and Lei Gao[1,3]*

[1]Key Laboratory of Environment Controlled Aquaculture, Ministry of Education, Dalian, China, [2]College of Marine Technology and Environment, Dalian Ocean University, Dalian, China, [3]College of Fisheries and Life Science, Dalian Ocean University, Dalian, China

Light and temperature are necessary conditions for migratory fish. The assessment of fish physiology and behavior is important for identifying fish welfare, but also for the assessment of the optimal setting of recirculating aquaculture systems (RASs). This study aimed to explore the interactive effect of photoperiod and temperature on steelhead trout culture. Four treatments were set up with specific settings were as follows: a LP-LT group treated with 16L:8D and 12°C, a LP-HT group treated with 16L:8D and 16°C, a SP-LT group treated with 12L:12D and 12°C, and a SP-HT group treated with 12L:12D and 16°C. Growth performance, behavioral and physiological parameters were measured. Two indexes, locomotor activity and social interaction were used for behavioral analysis, and the results were applied to interpret the behavioral responses to the photoperiod and temperature stimulation in juveniles. The growth performances were significantly lower in treatments LP-LT and SP-LT. The treatment LP-HT had significantly higher growth performance than the other treatments, but no significant differences were noted in survival rate and coefficient of variation. The results of fish behavior indicated that the movement of juveniles should be primarily monitored at high temperatures or long photoperiods, and the state parameters should be primarily monitored at low temperatures or short photoperiods. The results of the physiological parameters showed that the recovery time from stress varied among different treatments. After 60 days of the experiment, superoxide dismutase and alanine aminotransferase dropped back to their initial level. The results of Na+-K+-ATPase showed that although the combined effect of photoperiod and temperature could advance the time of smoltification, it may result in poorer salt tolerance. Our findings underscore the importance of the interaction of photoperiod and temperature on steelhead trout culture. The outcome could provide guidance for the development of effective aquaculture systems.

KEYWORDS

recirculating aquaculture system, steelhead trout, physiology, fish behavior, aquaculture facilities

Introduction

Rainbow trout (*Oncorhychus mykiss*) is a popular salmonidae for aquaculture, with a global production volume of more than 814,090 tons in 2016 (FAO, 2016; Pauly and Zeller, 2017; Yu et al., 2021; Liu et al., 2021). The two types of rainbow trout are non-migratory and migratory. The migratory type, known as steelhead trout in China, has a life cycle that includes freshwater and saltwater stages. With the development of aquaculture technology, the hatching and smolting processes of steelhead trout could be accomplished in land-based recirculating aquaculture systems (RASs). Under natural conditions, the length of the pre-smolt stage of juveniles depends on the latitude and longitude of their place of residence, i.e., the natural variation of light and temperature (Bowden et al., 2004; Rosengren et al., 2017; Archer et al., 2019). RAS is treated using artificial lighting and temperature control to promote fish growth and inhibit their gonadal development and maturation (Pauly and Zeller, 2017; Guraslan et al., 2017; Churova et al., 2020). Developing different light manipulation strategies (including constant light or darkness) to promote fish growth and counter-seasonal reproduction is common depending on the local environment at each site (Guraslan et al., 2017; Sievers et al., 2018).

The design and development of effective aquaculture systems are essential for successful aquaculture practice. The conditions of the freshwater stage could significantly affect the smolting processes and the viability in the seawater stage (del Villar-Guerra et al., 2019). Much research is devoted to reducing the duration of the freshwater stage of salmonids with low technology and low cost while ensuring high survival and growth rates in seawater (Rosengren et al., 2017; Sievers et al., 2018; Hines et al., 2019; Nemova et al., 2020; Suzuki et al., 2020). The culture of Salmonidae has considerably developed in terms of scale and distribution (Albert et al., 2019; Barrett et al., 2020; Hvas et al., 2021). Although the condition control of culture has been very mature in RAS and many studies about the environmental effects on fish performance have been conducted, only few studies have been reported on steelhead trout compared with other fish species (Ge et al., 2021; Salinas et al., 2022). The optimal environmental factor varies among species and developmental stages but is also related to requirements and mastery of farmers' skill degree. Thus, understanding how these key environmental factors affect fish's performance is important to reduce production costs (Pauly and Zeller, 2017; Hvas et al., 2021).

Migration time and success in Salmonidae are related to physiological basis, such as energy metabolic, osmolarity, and anti-oxidative stress (Höglund et al., 2008; Archer et al., 2019; Shry et al., 2019). However, a decrease or increase in physiological parameters as a response to increased stress makes it difficult to veridically predict the body state (Birnie-Gauvin et al., 2019). With the exception of morphology and physiology, the behavior of steelhead trout varies significantly during the transition from freshwater to saltwater. A search summarized 39 relevant studies on fish behavior applied to improve commercial aquaculture production processes or fish welfare between 1993 and 2020 (Macaulay et al., 2021). Understanding the features of fish behavior could help farmers clarify how they move, what diets they choose, how much they eat, and how they respond to potential stress (acute or chronic stress) (Huntingford et al., 2012; Damsgård et al., 2019). In this respect, fish behavior is used to provide necessary bioengineering information for feeding strategy (Conallin et al., 2016), system optimization (Dempster et al., 2019), and decreased labor consumption (Cogliati et al., 2019). However, the behavioral manifestations of successful migration and its underlying mechanisms remain poorly understood.

On the basis of the authors' previous work, the present study attempted to explore the interactive effect of photoperiod and temperature on steelhead trout culture from the aspects of growth, behavior and physiological performance, specifically whether the smoltification window could directly be judged by specific behavioral characteristics. In this study, the following questions were explored: 1) Is there an interaction between light and water temperature on growth performance of steelhead trout juveniles? 2) Could the environmental stimulation improve the regulation of osmolarity? 3) What are the key behavioral characteristics of steelhead trout during the smoltification window?

Materials and methods

Experimental animal and source

Steelhead trout juveniles were purchased from Wanzefeng Fishery Company (Rizhao, China). The experiment was conducted in 2021 at the Key Laboratory of Environment Controlled Aquaculture (AET), Dalian City, Liaoning Province, China. Juveniles with a mean initial body length of 3.32 ± 0.02 cm and a body weight of 4.40 ± 0.20 g were kept temporarily. The dissolved oxygen content was more than 7.0 mg/L, ammonia nitrogen was lower than 0.10 mg/L, and pH was adjusted at 7.50 ± 0.50; all were measured using a YSI 6920 multi-parameter water quality instrument (YSI Inc., Ohio, USA).

Experimental design

The experiment lasted for eight weeks. Based on the actual operations in aquaculture, the experimental conditions involved two photoperiods (L, 12L:12D and 16L:8D) and two temperatures (T, 12°C and 16°C), for a total of four treatments. Each treatment was represented by three replicates. The specific settings were as follows: long photoperiod, low water-temperature group treated with 16L:8D and 12°C (treatment LP-LT); long photoperiod, high water-temperature group treated with 16L:8D and 16°C (treatment LP-HT); short photoperiod, low water-temperature group treated with 12L:12D and 12°C (treatment SP-LT); and short photoperiod, high water-temperature group treated with 12L:12D and 16°C (treatment SP-HT).

A total of 12 randomly arranged plastic tanks were used, and the volume of freshwater was about 300 L (diameter of 0.8 m, water depth of 0.6 m) in each tank. All tanks were designed as a semi-closed recirculation system with a water outlet in the center. Dechlorinated freshwater temperature was controlled within ± 0.5°C with a customized temperature control system. The different treatments were insulated from one another by silver shading material. In total, 480 juveniles were used in this experiment and forty juveniles were used as biological replicates in each tank (n=40) and fed with commercial feed pellets (Qihao Aquatech Co., Ltd., China). All tanks

were thoroughly cleaned by scrubbing the walls and bottom after each weekly sampling to avoid unnecessary disturbances.

Behavior observations

Only 120 juveniles were tagged with visible implant elastomer (VIE) tags (Northwest Marine Technology, Shaw Island, WA, USA) allowing for individual identification throughout the experiment. The tagged fish were then randomly placed into each tank gently, that is, only 10 fish were tagged per tank to respect their welfare. The entire experiment area was surrounded by a black curtain to prevent external interferences and shadow rejection. The behavior of juveniles was recorded and tracked using an infrared camera mounted above the central arena during feeding. Each video lasted 10 minutes, and all the behavioral indicators were calculated using the Noldus EthoVision XT (version 12.0; Noldus Information Technology, Netherlands). Coordinates were set for each video to ensure that the observation area and fish movement exactly matched. The total observation area was divided into two subzones: the feeding zone and the remaining zone. The tracking data were additionally checked by all-occurrence recording method to ensure the accuracy of the results.

Sampling and analysis method

Growth performance

The number of dead fish was recorded and removed daily to calculate the survival rate (SR). Body length and body weight were measured every 10 days and nine fish were randomly selected from each treatment to determine growth parameters. The calculation formula for specific growth rate (SGR) and the coefficient of variation (CV) was as follows:

$$SGR = 100\,\% \times \frac{\ln W_2 - \ln W_1}{t_2 - t_1}$$

$$CV = 100\,\% \times \frac{SD}{M}$$

where W_1. the initial body weight, W_2. the final body weight, t_1. the initial sampling day, t_2. the sampling day, SD is the standard deviation of body weight, M is the average body weight.

Physiological parameters

After the end of the experiment, all tagged fish (a total of 120 juveniles) and random equal numbers of untagged fish were euthanized with an overdose of tricaine methanesulfonate (MS-222, Sigma), and tissues were sampled for physiological analysis. The liver, blood, and gill tissues were collected, immediately frozen in liquid nitrogen, and stored at −80°C. Superoxide dismutase (SOD) was detected by WST-1 method according to the SOD assay kit instructions. Alanine aminotransferase (ALT) was determined using a microplate reader using colorimetric detection at 570 nm as per kit instructions. Na^+-K^+-ATPase (NKA) was measured by Bonting method according to the NKA activity kit. The cortisol level wase determined using an ELISA kit. All measurements were performed at least three times and all assay kits were obtained from the Nanjing Jiancheng Bioengineering Institute, China.

Behavioral indicators

The assessment of fish behavior consisted of two aspects: locomotor activity and social interaction. Six behavioral indicators, including total distance moved (cm), maximum acceleration (cm/s^2), acceleration state (%), residence time in feeding zone (s), distance to central point (cm), and the distance between fish (cm), were measured and calculated every 10 days. The total distance moved was used to provide a general measure of activity, which was also used as the basis for calculating other parameters, such as acceleration. Moreover, acceleration was obtained by calculating the difference in velocity with the unit time and used to mark bursts of rapid movement. The activity state depends on the total pixel change within the analysis area per unit time of the fish. The residence time in feeding zone represented the discrete state of fish during feeding, which was a standard variable for the usage of space. Distance to central point indicated the radius of fish distribution during feeding (cluster radius). Distance between fish was used to characterize the distance between two individuals. The total distance moved, maximum acceleration, and acceleration state were used as indicators of movement quality. The other three behavioral indicators were used to evaluate the state of fish, such as area preference and social interaction.

Data analysis

In accordance with the study's purpose, different statistical methods were used. A completely randomized ANOVA was used to compare the differences in growth performance between groups. A generalized linear mixed model (GLMM) was constructed to assess the influence of the different experimental conditions on fish behavior, including a mixture of fixed and random effects. The individual ID of fish was included in the models as random effects. Statistical analysis was performed using *R* version 3.5.3. All statistical results were presented as the mean ± standard deviation (mean ± SD). The level of significance was set at $P< 0.05$. Multivariate statistical analysis, namely, principal component analysis (PCA), was used to obtain a low-dimensional representation of high-dimensional data to exact the key behavioral parameters in fish. The Kaiser-Mayer-Olkin (KMO) index and Bartlett's test of sphericity assessed the adaptive validity of PCA.

Results

Growth performance

Table 1 provides the growth performance of steelhead trout juveniles in different treatments. No deaths occurred during the entire experimental period. The results of ANOVA are presented in Table 1. The growth performance of juveniles was significantly influenced by photoperiod and temperature and their interaction

TABLE 1 Survival rate and growth performance of the different treatments at the end of the experiment.

Growth performance	Treatments			
	LP-LT	LP-HT	SP-LT	SP-HT
SR (%)	100%	100%	100%	100%
Final body Length (cm)	18.28 ± 0.78[a]	18.25 ± 0.94[a]	16.45 ± 0.34[b]	18.28 ± 0.68[a]
Final body Weight (g)	86.92 ± 1.40[a]	96.91 ± 1.66[b]	86.23 ± 1.37[a]	90.91 ± 1.52[c]
SGR (%/d)	2.40 ± 0.03[a]	2.58 ± 0.03[b]	2.38 ± 0.03[a]	2.47 ± 0.03[c]
CV (%)	1.61 ± 0.14[a]	1.71 ± 0.13[a]	1.59 ± 0.02[a]	1.67 ± 0.13[a]

The data were expressed in mean values and standard deviations (mean ± SD). Values with different superscript letters represent a significant difference, P < 0.05. LP-LT, abbreviation of long photoperiod, low water-temperature group treated with 16L:8D and 12 ℃; LP-HT, abbreviation of long photoperiod, high water-temperature group treated with 16L:8D and 16℃; SP-LT, abbreviation of short photoperiod, low water-temperature group treated with 12L:12D and 12℃; SP-HT, abbreviation of short photoperiod, high water-temperature group treated with 12L:12D and 16℃; SR, abbreviation of survival rate; SGR, abbreviation of specific growth rate; CV, abbreviation of coefficient of variation.

($P = 0.000 < 0.01$). No statistical differences ($P > 0.05$) were observed among treatments LP-LT, LP-HT, and SP-HT in terms of final body length, which was significantly higher than that in treatment SP-LT ($P < 0.05$). The final weight in treatment SP-HT was significantly lower than that in treatment LP-HT and significantly higher than that in treatments LP-LT and SP-LT ($P < 0.05$). The analysis results of SGR showed the same results as final weight. Regarding the consistency of fish growth rate, no significant differences were found in the CV level among the treatments ($P > 0.05$).

Post-hoc comparisons revealed significant differences in growth performance at different levels of conditions ($P = 0.000 < 0.01$) (Table 2). Photoperiod and temperature had no significant effect on CV values, but a significant effect was found in their interaction (Table 2). Simple effect analysis revealed no significant differences in final body length between the two photoperiod levels at 16°C ($P > 0.05$) and significant differences at 12°C ($P = 0.000 < 0.01$). For final body weight, the differences were significant between all levels, except for the 16°C groups (B and D) ($P = 0.000 < 0.01$). SGR also showed the same results as final body weight.

Physiological parameters

The changes in physiological parameters are presented in Figure 1. Photoperiod and water temperature could affect the level of antioxidant enzymes in steelhead trout. The SOD levels behaved a general trend of increasing first and then decreasing, but the maximum concentration of SOD in the different treatments appeared at different timepoints (Figure 1A). The highest SOD levels for treatments LP-LT and SP-HT were at approximately day 30, whereas treatments LP-HT and SP-LT reached the highest levels at approximately day 15. After 30 days, significantly higher and lower

TABLE 2 The Bonferroni post hoc test was used for multiple comparisons of growth performance among groups.

Parameters	Variable	F	Sig.	Post hoc comparisons		Simple effects tests	
				Photoperiod (*P*-value)	Temperature (*P*-value)	Photoperiod * Temperature (*P*-value)	Temperature * Photoperiod (*P*-value)
Final body length	(Intercept)	501425.76	0.00**	/	/	/	/
	Photoperiod	302.40	0.00**	0.00	/	/	0.00 (Low temperature)
							0.87 (High temperature)
	Temperature	327.97	0.00**	/	0.00	0 (Long photoperiod)	/
						0.89 (Short photoperiod)	
	Photoperiod * Temperature	35.09	0.00**	/	/	/	/
Final body weight	(Intercept)	307355.70	0.00**	/	/	/	/
	Photoperiod	105.60	0.00**	0.00	/	/	0.14 (Low temperature)
							0.00 (High temperature)
	Temperature	506.94	0.00**	/	0.00	0 (Long photoperiod)	/
						0 (Short photoperiod)	
	Photoperiod * Temperature	66.49	0.00**	/	/	/	/

(Continued)

10.3389/fmars.2023.1114662

TABLE 2 Continued

Parameters	Variable	F	Sig.	Post hoc comparisons		Simple effects tests	
				Photoperiod (*P*-value)	Temperature (*P*-value)	Photoperiod * Temperature (*P*-value)	Temperature * Photoperiod (*P*-value)
SGR	(Intercept)	671304.35	0.00**	/	/	/	/
	Photoperiod	99.78	0.00**	0.00	/	/	0.12 (Low temperature)
							0.00 (High temperature)
	Temperature	503.67	0.00**	/	0.00	0 (Long photoperiod)	/
						0 (Short photoperiod)	
	Photoperiod * Temperature	60.40	0.00**	/	/	/	/
CV	(Intercept)	2488.12	0.00**	/	/		
	Photoperiod	0.18	0.68	0.68	/	/	/
							0.80 (Low temperature)
	Temperature	1.80	0.22	/	0.22	0.35 (Long photoperiod)	0.74 (High temperature)
						0.39 (Short photoperiod)	
	Photoperiod * Temperature	0.00	0.95	/	/	/	/

*P<0.05, **P<0.01

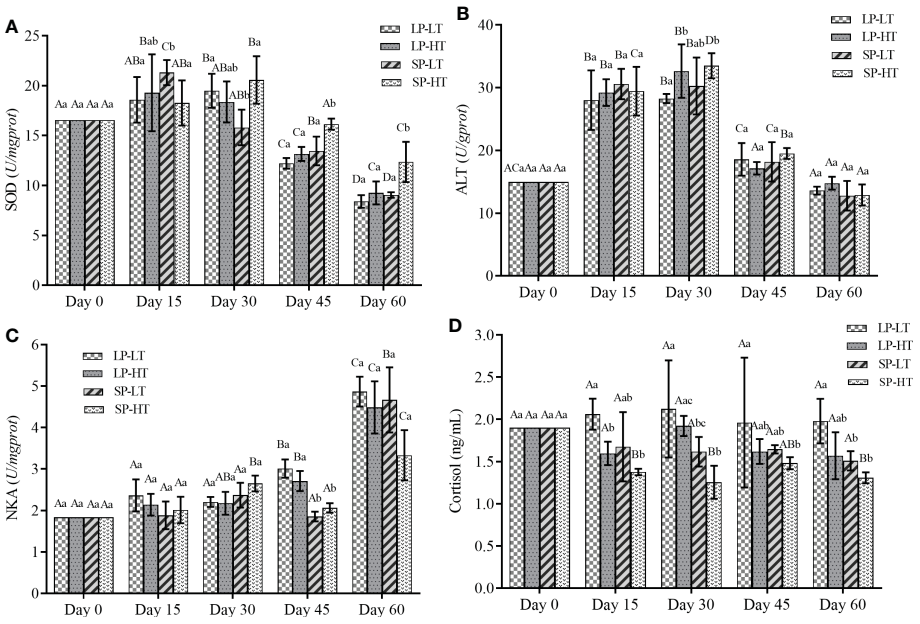

FIGURE 1
Effects of different treatments on different physiology parameters of steelhead trout juveniles. **(A)** SOD, **(B)** ALT, **(C)** NKA and **(D)** Cortisol content. The data were expressed in mean values and standard deviations (mean ± SD) (n=30 per treatment). Different capital letters represent significant differences between different treatments at the same time, different lowercase letters represent significant differences between different times of the same treatment ($P < 0.05$). LP-LT, abbreviation of long photoperiod, low water-temperature group treated with 16L:8D and 12 °C; LP-HT, abbreviation of long photoperiod, high water-temperature group treated with 16L:8D and 16°C; SP-LT, abbreviation of short photoperiod, low water-temperature group treated with 12L:12D and 12°C; SP-HT, abbreviation of short photoperiod, high water-temperature group treated with 12L:12D and 16°C. SOD, Superoxide dismutase; ALT, Alanine aminotransferase; NKA, Na+-K+-ATPase.

SOD contents were observed in treatments SP-HT ($P < 0.05$) and LP-LT ($P < 0.05$), respectively. Similar to SOD, ALT mainly revealed an upward trend in the first 30 days and a downward trend after 30 days (Figure 1B). The ALT content dropped back to the initial level in all other groups except for treatment LP-HT after 60 days of the experiment. For treatment LP-HT, no significant difference was observed in the ALT content compared with other timepoints after 45 days ($P > 0.05$).

In general, the NKA activity increased with time in all groups (Figure 1C). It significantly increased after 45 and 60 days in the treatments with long and short photoperiods' ($P < 0.05$), respectively. No statistical differences ($P > 0.05$) were observed in NKA among different treatments at different timepoints, and its activity was significantly higher than that in treatments SP-LT and SP-HT at 45 days ($P < 0.05$). The cortisol levels did not show clear trends compared with the other parameters. The cortisol levels in treatment SP-HT were significantly lower than those in other treatments throughout the experiment ($P < 0.05$), but no significant differences were observed among the three other treatments ($P > 0.05$).

Behavioral indicators

GLMM results are presented in Table 3. The fixed effects results revealed that both acceleration state and distance between fish were significantly affected by not only experimental condition but also the interaction of experimental condition and time. Experimental time had significant effects on the distance between fish. No significant main effects of body length and experimental time were found for all behavioral indicators except for the distance between fish. There was a significant effect of body weight on the total distance moved but not on the other behavioral indicators.

For the long photoperiod groups (treatments SP-LT and SP-HT), the mean total distance moved was significantly higher than the short photoperiod groups (treatments SP-LT and SP-HT) ($P < 0.05$) (Table 4). No significant difference was noted in the total distance moved at different temperatures for the same photoperiod ($P > 0.05$). For the low water-temperature groups (treatments LP-LT and SP-LT), the maximum acceleration was significantly higher than the high water-temperature groups (treatments LP-HT and SP-HT) ($P < 0.05$). When the water temperature was the same, there was no significant difference in the maximum acceleration between different photoperiod groups ($P > 0.05$). The acceleration state of treatment

TABLE 3 Repeated measures of behavioral indicators were analyzed using a generalized linear mixed model (GLMM) approach, considering treatment, time, body length, body weight, and treatment*time as fixed effects and individuals within the groups as random.

	Items	F	*P*-value
Total distance moved	Treatment	2.114	0.100
	Time	2.909	0.090
	Body length	1.426	0.234
	Body weight	4.475	0.036
	Treatment*Time	2.582	0.055
Acceleration	Treatment	1.372	0.253
	Time	0.000	0.984
	Body length	0.014	0.906
	Body weight	1.492	0.224
	Treatment*Time	0.068	0.977
Acceleration state	Treatment	12.387	0.000
	Time	0.793	0.374
	Body length	0.127	0.722
	Body weight	3.871	0.051
	Treatment*Time	7.086	0.000
Residence time in feeding zone	Treatment	0.365	0.778
	Time	0.576	0.449
	Body length	0.617	0.433
	Body weight	0.277	0.599
	Treatment*Time	0.549	0.650
Distance to central point	Treatment	1.855	0.139
	Time	3.037	0.083
	Body length	3.503	0.063
	Body weight	0.030	0.863
	Treatment*Time	0.859	0.464

(Continued)

TABLE 3 Continued

	Items	F	*P*-value
Distance between fish	Treatment	7.543	0.000
	Time	4.732	0.031
	Body length	4.000	0.047
	Body weight	0.309	0.579
	Treatment*Time	11.559	0.000

Significance level was P < 0.05.

TABLE 4 The significance differences with $P < 0.05$ (*P*-value) in the pair-wise comparisons of behavioral traits in all treatment groups.

	LP-LT vs. LP-HT	LP-LT vs. SP-LT	LP-LT vs. SP-HT	LP-HT vs. SP-LT	LP-LT vs. SP-HT	SP-LT vs. SP-HT
Total distance moved	0.819	0.031	0.002	0.002	0.019	0.421
Acceleration	0.014	0.997	0.000	0.045	0.064	0.034
Acceleration state	0.000	0.000	0.000	0.066	0.490	0.217
Residence time in feeding zone	0.257	0.456	0.164	0.565	0.953	0.490
Distance to central point	0.000	0.198	0.000	0.048	0.110	0.005
Distance between fish	0.001	0.984	0.595	0.000	0.000	0.525

LP-LT, abbreviation of long photoperiod, low water-temperature group treated with 16L:8D and 12℃; LP-HT, abbreviation of long photoperiod, high water-temperature group treated with 16L:8D and 16℃; SP-LT, abbreviation of short photoperiod, low water-temperature group treated with 12L:12D and 12℃; SP-HT, abbreviation of short photoperiod, high water-temperature group treated with 12L:12D and 16℃.

LP-LT was significantly higher than that of the other treatments ($P < 0.05$), but no difference was found between the other treatments ($P > 0.05$). Moreover, no significant differences were observed among all treatments in terms of residence time in the feeding zone ($P > 0.05$). The distance to central point was significantly lower in treatment LP-LT than in treatment SP-HT ($P < 0.05$). For the high-temperature groups, the distance to central point was significantly higher than the low-temperature group ($P < 0.05$). The distance between fish was significantly lower than that of the other treatments ($P < 0.05$), but no difference was found between the other treatments ($P > 0.05$).

The PCA in all groups extracted two principal components (PCs), which accounted for more than 70% of the total variance (Table 5). Between the two PCs obtained in treatment LP-LT, PC1 accounted for 46.41% of the total variance, and it had a strong positive loading on residence time in the feeding zone and distance between fish (> 0.85). PC2 accounted for 35.13% of the total variance, and it had a strong negative loading on distance to point. For treatment LP-HT, PC1 accounted for 46.41% of the total variance, with a strong positive loading on total distance moved and residence time in the feeding zone. PC2 accounted for 31.76% of the total variance, with a strong positive loading on acceleration state. For treatment SP-LT, PC1 accounted for 38.53% of the total variance, and it had a strong positive loading on residence time in the feeding zone. PC2 accounted for 33.39% of the total variance, and it had a strong positive loading on acceleration state. For treatment SP-HT, PC1 accounted for 53.71% of the total variance, with a strong positive loading on maximum acceleration and distance to point. PC2 accounted for 22.34% of the total variance, with a strong positive loading on acceleration state.

Discussion

Benefiting from the current application of technologies in RAS, growing Salmonidae (salmon and trout) under full light conditions (24:0 h photoperiod) for maximal growth performance is common (Hines et al., 2019; Churova et al., 2020). As shown in Table 1, a considerable variation could be found in the growth performance under different photoperiod conditions at the same temperature conditions. However, the 24:0 h photoperiod is not a natural photoperiod for most salmonids, and it may be stressful to fish. For example, continuous light exposure induces abnormal gonadal development or/and lack of synchronization of smoltification processes (Sievers et al., 2018; Churova et al., 2020). With the increasing attention on fish welfare, less extreme photoperiods, such as 12:12 or 16:8 h, are being used instead in aquaculture (Ge et al., 2021; Macaulay et al., 2021). However, systematic studies that determine the photoperiod conditions for optimal growth and minimal stimulation are still lacking (Hvas et al., 2021). One of the difficulties in undertaking such research is the limited knowledge on the synergistic and antagonistic effects between different environmental factors.

In general, increased temperature results in increased body weight (Nisembaum et al., 2020). Within the suitable temperature interval, high temperature could lead to early smoltification date and large fish size (Rosengren et al., 2017; Bernard et al., 2020). Therefore, temperature could be viewed as a regulatory factor, especially in controlling (accelerating or delaying) the growth rate. The results of the present study also confirmed this information. Photoperiod is an

TABLE 5 Loading of behavioral indicators on significant PCs for the four treatments.

Variables	PC1	PC2	Variables	PC1	PC2
LP-LT			**LP-HT**		
Total distance moved	0.77	0.52	**Total distance moved**	**0.94**	0.16
Maximum acceleration	0.56	0.70	**Maximum acceleration**	0.65	0.42
Acceleration state	0.37	0.81	**Acceleration state**	0.07	**0.89**
Residence time in feeding zone	**0.94**	0.01	**Residence time in feeding zone**	**0.94**	0.06
Distance between fish	0.17	**-0.88**	**Distance between fish**	0.70	0.50
Distance to central point	**0.91**	0.11	**Distance to central point**	0.31	0.81
KMO	**0.75**		**KMO**	**0.67**	
Cumulative % variance	46.40	**81.53**	**Cumulative % variance**	46.41	**78.17**
SP-LT			**SP-HT**		
Total distance moved	0.61	-0.21	**Total distance moved**	0.72	0.39
Maximum acceleration	0.45	0.74	**Maximum acceleration**	**0.90**	-0.30
Acceleration state	-0.12	**0.86**	**Acceleration state**	0.15	**0.96**
Residence time in feeding zone	**0.88**	0.42	**Residence time in feeding zone**	0.70	0.27
Distance between fish	0.82	0.31	**Distance between fish**	**0.87**	0.29
Distance to central point	0.59	0.65	**Distance to central point**	0.79	0.18
KMO	**0.73**		**KMO**	**0.63**	
Cumulative % variance	38.53	**71.92**	**Cumulative % variance**	53.71	**76.05**

LP-LT, abbreviation of 16L:8D and 12℃ treatment; LP-HT, abbreviation of 16L:8D and 16℃ treatment; SP-LT, abbreviation of 12L:12D and 12℃ treatment; SP-HT, abbreviation of 12L:12D and 16℃ treatment.

important environmental signal to initiate complex changes that coincide with marine migration for migratory fish (Nemova et al., 2020; van Rijn et al., 2020). Once the fish size reaches a critical number, photoperiod and temperature could play important roles in controlling the growth rate and the synchronization process of smoltification. The results also confirmed the first hypothesis that photoperiod and temperature have measurable interactions on growth performance in steelhead trout juvenile under indoor aquaculture condition. The results further showed that photoperiod promoted increased body length and temperature promoted a significant increase in the weight of fish. Several studies have noted an overall lack of synchrony in the absence of photoperiodic regulation, although smoltification characteristics still appear in trout (Nisembaum et al., 2020). No meaningful differences were observed among the groups in terms of CV values, suggesting that the two photoperiods in this experiment were appropriate for smoltification synchrony. However, as mentioned earlier, whether such conditions make the juvenile comfortable is unclear.

The response of fish to a stressor could be monitored by physiological changes, which are commonly used as markers of stress level and fish welfare (Vindas et al., 2018; Cogliati et al., 2019). Increasing evidence has suggested a direct link between oxidative stress and different ecological phenomena (Archer et al., 2019; Shry et al., 2019). A complete and balanced antioxidant system normally exists in fish. When the fish's body is in a state of stress, many oxygen-free radicals are produced in a short time, subsequently damaging the body's metabolic balance and self-repair functions. SOD is the predominant defensive enzyme in the antioxidant system of the body, and it could directly affect the antioxidant capacity (Liu et al., 2021; Yu et al., 2021). ALT is central in protein metabolism, and it could be measured to determine organ damage (Suzuki et al., 2020). Figure 1 shows that the SOD and ALT levels were significantly higher in treatment LP-LT at the beginning of the experiment, indicating that the juvenile fish had different degrees of stress response. Fish reduce their stress response to a stimulus through repeated exposure over time, a natural process often referred to as habituation (Bratland et al., 2010; Barrett et al., 2020). This phenomenon was manifested in the present study as the SOD and ALT levels showed a trend of descending sometime after the start of the experiment. However, differences in the time required for injury repair were found among the four treatments. The SOD and ALT levels in treatments LP-LT and SP-HT returned to initial level after 30 days, whereas it took only 15 days in treatments LP-HT and SP-LT. One possible reason is that lower temperatures lead to a slowing of immune mechanisms leading to increased disease susceptibility, which has been proven previously in other fish species (Martin et al., 2008; Valero et al., 2014). In addition, a shorter time required for injury repair was observed in treatment LP-HT, which is strong evidence that photoperiod and temperature could have significant interaction effects on physiological stress responses in steelhead trout juveniles.

Cortisol is considered a biomarker of stress (Birnie-Gauvin et al., 2019). The cortisol level is shown in Figure 1, and no significant

difference could be found among treatments in the whole experimental period. Cortisol may be influenced by many factors, including the state of fish at sampling and the high inter-dividual variability (Gaudio et al., 2018). The difference was not significant, probably due to the time of sampling interval being longer than that of cortisol clearance from the body. The "Smolt window" refers to a specific stage in which Salmonidae could significantly improve seawater tolerance and adapt to seawater environment due to the synergistic action of environmental factors. NKA plays an important role in the response to alterations in environmental salinity. The increased NKA in branchial chloride cells is beneficial to fish growth, swimming, and survival after smoltification (Bernard et al., 2020; Ge et al., 2021). All treatments showed an increase in the NKA level with increasing treatment time but to different degrees. Many studies have been conducted to identify the relationship between the success of migration and NKA concentration (Archer et al., 2019; Bernard et al., 2020; Ge et al., 2021). The higher the NKA concentrations were, the better the ability of migratory fish to adapt to seawater to a certain extent (Bernard et al., 2020). Moreover, increased cortisol level during smoltification was previously found coincident with increased gill NKA activity (Birnie-Gauvin et al., 2019; Shry et al., 2019). This finding was also demonstrated in the present study. Treatment LP-LT had higher cortisol and NKA level, indicating better readiness to enter seawater. A notable detail that relying solely on cortisol to determine the timing of migration is risky, as higher cortisol levels may also be due to individuals being under chronic stress and leaving to escape the stress (Damsgård et al., 2019). The role of temperature on smoltification has been controversial, with studies showing that elevated temperature alone could not play a driving role in smoltification (McCormick et al., 2000; Hines et al., 2019; Nisembaum et al., 2020). From the results presented in this paper, juveniles under long photoperiod treatments did have higher osmoregulatory capacity, but the difference was not significant. Furthermore, temperature had a regulatory role on smoltification, as the ability to regulate osmolality did not exhibit any significant differences among the groups under different photoperiods. These results showed that the combined effect of photoperiod and temperature could advance the time of smoltification, but may result in poorer salt tolerance.

The quantification analysis of fish behavior is extremely important for the design and operation of aquaculture system. Herbert et al. (2011) used light rings to induce optimal swimming motility in Atlantic salmon smolts and improve productivity. With the smoltification process, a series of behavior changes occurs in juvenile steelhead trout, in addition to changes in physiology (Macaulay et al., 2021). Table 3 shows that the total distance moved in treatments LP-LT and LP-HT was significantly lower than that in treatments SP-LT and SP-HT possibly because juvenile has higher willingness to search for food in the long photoperiod treatments (Stewart et al., 2012; Ye et al., 2016). In general, the higher the water temperature is, the greater the burst swimming speed (Ma et al., 2020). The results presented here showed that the acceleration status of treatment LP-LT was significantly higher than that of other treatments. This may be because the fish in this experiment were cold-water fish. The radius of treatments LP-HT and SP-HT was significantly larger than that of treatments LP-LT and SP-LT, indicating that lower temperature was more favorable for fish shoaling (Barrett et al., 2020; Bratland et al., 2010). The radius of fish distribution presented no significant difference between the treatments with same temperature, suggesting that temperature may be the main factor affecting fish feeding behavior compared with photoperiod. The organizational structure and individual interactions of fish are usually described by distance between them, which is influenced by photoperiod and temperature (Brakstad et al., 2018; Cogliati et al., 2019). In fact, the present and previous results showed that fish form a relatively stable structure regardless of the culture environmental condition. This structure is also significantly affected by the species type, population size, and individual interactions (Lei et al., 2020).

Fish are constantly moving and changing, and monitoring multiple fish behavior parameters simultaneously is difficult (Ye et al., 2016; Macaulay et al., 2021). The smaller the number of monitoring parameters, the higher the monitoring efficiency. Different management procedures may be necessary in fish that are under different culture conditions, such as more aggressive treatment in some cases. Therefore, feature extraction of fish behavior becomes crucial. Moreover, identifying the key behavioral indicators during smoltification process is a priority for future research (Dempster et al., 2019; Hvas et al., 2021). PCA is an effective tool to reduce the dimensionality of datasets in multivariate problems. It is capable of preserving the majority of its statistical information and identifying the most significant variations. The KMO values for all the four treatments were above 0.5, indicating that these treatments are suitable for PCA analysis. The PCA results showed that the main parameters (strong loadings) differed among the four treatments, proving the effectiveness and necessity of using PCA to identify key parameters in complex datasets. Except for treatment SP-HT, the residence time in the feeding zone was identified as the main component in all treatments. This finding is consistent with the findings of previous studies, as juvenile trout are stationary predators, whereas silvered trout are cruising predators (Folkedal et al., 2012b). The acceleration state was extracted as the main component, suggesting that the experimental conditions produced pressure on the movement smoothness of juvenile steelhead trout.

In summary, the fish status could be evaluated by continuously identifying and quantifying the key parameters of fish behavior. Although fish behavior is complex, it could be integrated into aquaculture management as an additional resource and pave the way for new approaches to fish farming. Future production of finfish continues to increase and optimizing production and improving fish welfare could become increasingly important. Indeed, incorporating fish behavior into production management still has a long way to go. However, with the increasing application of advanced technologies in aquaculture, such as computer vision and modern behavioral science, fish behavior × environment interactions could be widely used in aquaculture management in the near future (Barrett et al., 2020; Macaulay et al., 2021).

Data availability statement

The original contributions presented in the study are included in the article/supplementary material. Further inquiries can be directed to the corresponding author.

Ethics statement

The animal study was reviewed and approved by Dalian Ocean University (GBT 35892-2018).

Author contributions

ZM designed and performed the experiments, analyzed the data, and prepared the draft manuscript. LG provided suggestions in experiment design and manuscript preparation. All authors contributed to manuscript revision, read, and approved the submitted version.

Funding

This research was supported by Key Area Research Plan of Guangdong (2021B0202030001), the National Natural Science Foundation of China (32102753), the Fund of the Scientific and Technical Innovation of Dalian (2021JJ13SN73, 2021JJ13SN72), the Liaoning Applied Basic Research Program (2022JH2/101300140), Modern Agro-industry Technology Research System (CARS-49), Innovation Support Program for High-level Talents of Dalian City (2019RD12), and the Science & Technology Program of Liaoning Province (2021JH2/10200011).

Acknowledgments

We thank all laboratory members for their constructive suggestions and discussions. Special thanks are also given to the reviewers for their constructive comments regarding the manuscript.

Conflict of interest

The authors declare that the research was conducted in the absence of any commercial or financial relationships that could be construed as a potential conflict of interest.

Publisher's note

References

Albert, K. D., Frogg, N., Stefansson, S. O., and Reynolds, P. (2019). Improving sea lice grazing of lumpfish (*Cyclopterus lumpus* l.) by feeding live feeds prior to transfer to Atlantic salmon (*Salmo salar* l.) net-pens. *Aquaculture* 511, 734224. doi: 10.1016/j.aquaculture.2019.734224

Archer, L. C., Hutton, S. A., Harman, L., O'Grady, M. N., Kerry, J. P., Poole, W. R., et al. (2019). The interplay between extrinsic and intrinsic factors in determining migration decisions in brown trout (*Salmo trutta*): An experimental study. *Front. Ecol. Evol.* 7. doi: 10.3389/fevo.2019.00222

Barrett, L. T., Oppedal, F., Robinson, N., and Dempster, T. T. (2020). Prevention not cure: a review of methods to avoid sea lice infestations in salmon aquaculture. *Rev. Aquacult.*, 12 (4), 2527-2543. doi: 10.1111/raq.12456

Bernard, B., Leguen, I., Mandiki, S. N. M., Corne, V., Redivo, B., and Kestemon, P. (2020). Impact of temperature shift on gill physiology during smoltification of Atlantic salmon smolts (*Salmo salar* l.). *Com. Biochem. Phys. A* 244, 110685. doi: 10.1016/j.cbpa.2020.110685

Birnie-Gauvin, K., Flávio, H., Kristensen, M. L., Walton-Rabideau, S., Cooke, S. J., Willmore, W. G., et al. (2019). Cortisol predicts migration timing and success in both Atlantic salmon and sea trout kelts. *Sci. Rep.* 9 (1). doi: 10.1038/s41598-019-39153-x

Bowden, T. J., Butler, R., and Bricknell, I. R. (2004). Seasonal variation of serum lysozyme levels in Atlantic halibut (*Hippoglossus hippoglossus* l.). *Fish Shell. Immun.* 17 (2), 129–135. doi: 10.1016/j.fsi.2003.12.001

Brakstad, O. M., Hagspiel, V., Lavrutich, M. N., and Matanovic, D. (2018). Optimal investment decisions in lice-fighting technologies: A case study in Norway. *Aquaculture* 504, 300–313. doi: 10.1016/j.aquaculture.2019.01.040

Bratland, S., Stien, L. H., Braithwaite, V. A., Juell, J. E., Folkedal, O., Nilsson, J., et al. (2010). From fright to anticipation: Using aversive light stimuli to investigate reward conditioning in large groups of Atlantic salmon (*Salmo salar*). *Aquacult. Int.* 18, 991–1001. doi: 10.1007/s10499-009-9317-8

Churova, M. V., Shulgina, N., Kuritsyn, A., Krupnova, M. Y., and Nemova, N. N. (2020). Muscle-specific gene expression and metabolic enzyme activities in Atlantic salmon *Salmo salar* l. fry reared under different photoperiod regimes. *Com. Biochem. Phys. B* 239, 110330. doi: 10.1016/j.cbpb.2019.110330

Cogliati, K. M., Herron, C. L., Noakes, D. L. G., and Schreck, C. B. (2019). Reduced stress response in juvenile Chinook salmon reared with structure. *Aquaculture* 504, 96–101. doi: 10.1016/j.aquaculture.2019.01.056

Conallin, A. J., Smith, B. B., Thwaites, L. A., Walker, K. F., and Gillanders, B. M. (2016). Exploiting the innate behaviour of common carp, *Cyprinus carpio*, to limit invasion and spawning in wetlands of the river Murray, Australia. *Fish. Manage. Ecol.* 23, 431–449. doi: 10.1111/fme.12184

Damsgård, B., Evensen, T. H., Øverli, Ø., Gorissen, M., Ebbesson, L. O. E., Rey, S., et al. (2019). Proactive avoidance behaviour and pace-of-life syndrome in Atlantic salmon. *R. Soc Open Sci.* 6 (3), 181859. doi: 10.1098/rsos.181859

del Villar-Guerra, D., Larsen, M. H., Baktoft, H., Koed, A., and Aarestrup, K. (2019). The influence of initial developmental status on the life-history of sea trout (*Salmo trutta*). *Sci. Rep.* 9, 13468. doi: 10.1038/s41598-019-49175-0

Dempster, T., Bui, S., Overton, K., and Oppedal, F. (2019). Jumping to treat sea lice: harnessing salmon behaviour to enable surfacebased chemotherapeutant application. *Aquaculture* 512, 734318. doi: 10.1016/j.aquaculture.2019.734318

FAO (2016) Food outlook. In: *Biannual report on global food markets. food outlook* (Accessed October 2016).

Folkedal, O., Torgersen, T., Olsen, R. E., Fernö, A., Nilsson, J., Oppedal, F., et al. (2012b). Duration of effects of acute environmental changes on food anticipatory behaviour, feed intake, oxygen consumption, and cortisol release in Atlantic salmon parr. *Physiol. Behav.* 105, 283–291. doi: 10.1016/j.physbeh.2011.07.015

Gaudio, E., Bordin, S., Lora, I., Lora, M., Massignani, M., and De Benedictis, G. M. (2018). Leukocyte coping capacity chemiluminescence as an innovative tool for stress and pain assessment in calves undergoing ring castration. *J. Anim. Sci.* 96 (11), 4579–4589. doi: 10.1093/jas/sky342

Ge, J., Huang, M., Zhou, Y., Deng, Q., Liu, R., Gao, Q., et al. (2021). Effects of seawater acclimation at constant and diel cyclic temperatures on growth, osmoregulation and branchial phospholipid fatty acid composition in rainbow trout *Oncorhynchus mykiss*. *J. Comp. Physiol. B* 191 (2), 313–325. doi: 10.1007/s00360-020-01330-0

Guraslan, C., Fach, B. A., and Oguz, T. (2017). Understanding the impact of environmental variability on anchovy overwintering migration in the black sea and its implications for the fishing industry. *Front. Mar. Sci.* 4. doi: 10.3389/fmars.2017.00275

Herbert, N. A., Kadri, S., and Huntingford, F. A. (2011). A moving light stimulus elicits a sustained swimming response in farmed Atlantic salmon, *Salmo salar* l. *Fish Physiol. Biochem.* 37, 317–325. doi: 10.1007/s10695-011-9499-7

Hines, C. W., Fang, Y., Chan, V. K. S., Stiller, K. T., Brauner, C. J., and Richards, J. G. (2019). The effect of salinity and photoperiod on thermal tolerance of Atlantic and coho salmon reared from smolt to adult in recirculating aquaculture systems. *Com. Biochem. Phys. A* 230, 1–6. doi: 10.1016/j.cbpa.2018.12.008

Höglund, E., Gjøen, H. M., Pottinger, T. G., Pottinger, T. G., and Øverli, Ø. (2008). Parental stress-coping styles affect the behaviour of rainbow trout *Oncorhynchus mykiss* at early

developmental stages. *Comp. Biochem. Physiol. A* 73 (7), 1764–1769. doi: 10.1016/j.cbpa.2018.12.008

Huntingford, F., Jobling, M., and Kadri, S. (2012). Aquaculture and behavior. In Tools for Studying the Behaviour of Farmed Fish (eds M. L. Bégout, S. Kadri, F. Huntingford and B. Damsgård) Oxford, UK; Blackwell Publishing Ltd., pp. 65–67. doi: 10.1002/9781444354614

Hvas, M., Folkedal, O., and Oppedal, F. (2021). Fish welfare in offshore salmon aquaculture. *Rev. Aquacult.* 13 (2), 836–852. doi: 10.1111/raq.12501

Lei, L., Escobedo, R., Sire, C., and Theraulaz, G. (2020). Computational and robotic modeling reveal parsimonious combinations of interactions between individuals in schooling fish. *PloS Comput. Biol.* 16 (3), e1007194. doi: 10.1371/journal.pcbi.1007194

Liu, Z. L., Zhao, W., Hu, W. S., Zhu, B., Xie, J. J., Liu, Y. J., et al. (2021). Lipid metabolism, growth performance, antioxidant ability and intestinal morphology of rainbow trout (*Oncorhynchus mykiss*) under cage culture with flowing water were affected by dietary lipid levels. *Aquacult. Rep.* 19, 100593. doi: 10.1016/j.aqrep.2021.100593

Macaulay, G., Bui, S., Oppedal, F., and Dempster, T. (2021). Challenges and benefits of applying fish behaviour to improve production and welfare in industrial aquaculture. *Rev. Aquacult.* 13 (2), 934–948. doi: 10.1111/raq.12505

Ma, Z., Li, H. X., Hu, Y., Fan, J. Z., and Liu, Y. (2020). Growth performance, physiological, and feeding behavior effect of *Dicentrarchus labrax* under different culture scales. *Aquaculture* 534 (3), 736291. doi: 10.1016/j.aquaculture.2020.736291

Martin, L. B., Weil, Z. M., and Nelson, R. J. (2008). Seasonal changes in vertebrate immune activity: mediation by physiological trade-offs. *Phil. Trans. R. Soc B* 363 (1490), 321–339. doi: 10.1098/rstb.2007.2142

McCormick, S. D., Moriyama, S., and Björnsson, B. T. (2000). Low temperature limits photoperiod control of smolting in Atlantic salmon through endocrine mechanisms. *Am. J. Physiol.* 278, 1352–1361. doi: 10.1152/ajpregu.2000.278.5.R1352

Nemova, N. N., Nefedova, Z. A., Pekkoeva, S. N., Voronin, V. P., Shulgina, N. S., Churova, M. V., et al. (2020). The effect of the photoperiod on the fatty acid profile and weight in hatchery-reared underyearlings and yearlings of Atlantic salmon *Salmo salar l. Biomolecules* 10, 845. doi: 10.3390/biom10060845

Nisembaum, L. G., Martin, P., Fuentes, M., Besseau, L., Magnanou, E., McCormick, S. D., et al. (2020). Effects of a temperature rise on melatonin and thyroid hormones during smoltification of Atlantic salmon, *Salmo salar*. *J. Comp. Physiol. B* 190 (6), 731–748. doi: 10.1007/s00360-020-01304-2

Pauly, D., and Zeller, D. (2017). Comments on FAOs state of world fisheries and aquaculture (SOFIA 2016). *Mar. Policy* 77, 176–181. doi: 10.1016/j.marpol.2017.01.006

Rosengren, M., Thörnqvist, P. O., Johnsson, J. I., Sandblom, E., Winberg, S., and Sundell, K. (2017). High risk no gain-metabolic performance of hatchery reared Atlantic salmon smolts, effects of nest emergence time, hypoxia avoidance behaviour and size. *Physiol. Behav.* 175, 104–112. doi: 10.1016/j.physbeh.2017.03.028

Salinas, P., Molina, F., Hernández, N., and Sandoval, C. (2022). Phenotypic response of male and neomale of *O. mykiss* parr subjected to 8° and 16 °C water temperature during early life stage. *Aquacult. Rep.* 22, 100996. doi: 10.1016/j.aqrep.2021.100996

Shry, S. J., McCallum, E. S., Alanärä, A., Persson, L., and Hellström, G. (2019). Energetic status modulates facultative migration in brown trout (*Salmo trutta*) differentially by age and spatial scale. *Front. Ecol. Evol.* 7, 411. doi: 10.3389/fevo.2019.00411

Sievers, M., Korsøen, Ø., Dempster, T., Fjelldal, P. G., Kristiansen, T., Folkedal, O., et al. (2018). Growth and welfare of submerged Atlantic salmon under continuous lighting. *Aquacult. Env. Interac.* 10, 501–510. doi: 10.3354/aei00289

Stewart, A. M., Gaikwad, S., Kyzar, E., and Kalueff, A. V. (2012). Understanding spatio-temporal strategies of adult zebrafish exploration in the open field test. *Brain Res.* 1451, 44–52. doi: 10.1016/j.brainres.2012.02.064

Suzuki, S., Takahashi, E., Nilsen, T. O., Kaneko, N., Urabe, H., Ugachi, Y., et al. (2020). Physiological changes in off-season smolts induced by photoperiod manipulation in masu salmon (*Oncorhynchus masou*). *Aquaculture* 526, 735353. doi: 10.1016/j.aquaculture.2020.735353

Valero, Y., García-Alcázar, A., Esteban, M.Á., Cuesta, A., and Chaves-Pozo, E. (2014). Seasonal variations of the humoral immune parameters of European sea bass (*Dicentrarchus labrax l.*). *Fish Shell. Immun.* 39 (2), 185–187. doi: 10.1016/j.fsi.2014.05.011

van Rijn, C. A., Jones, P. L., Schultz, A. G., Evans, B. S., McCormick, S. D., and Afonso, L. O. B. (2020). Atlantic Salmon (*Salmo salar*) exposed to different preparatory photoperiods during smoltification show varying responses in gill Na^+/K^+-ATPase, salinity-specific mRNA transcription and ionocyte differentiation. *Aquaculture* 529, 735744. doi: 10.1016/j.aquaculture.2020.735744

Vindas, M. A., Fokos, S., Pavlidis, M., Höglund, E., Dionysopoulou, S., Ebbesson, L. O. E., et al. (2018). Early life stress induces long-term changes in limbic areas of a teleost fish: the role of catecholamine systems in stress coping. *Sci. Rep.* 8 (1), 5638. doi: 10.1038/s41598-018-23950-x

Ye, Z. Y., Zhao, J., He, Z. Y., Zhu, S. M., Li, J. P., and Lu, H. D. (2016). Behavioral characteristics and statistics-based imaging techniques in the assessment and optimization of tilapia feeding in a recirculating aquaculture system. *Trans. ASABE* 59 (1), 345–355. doi: 10.13031/trans.59.11406

Yu, H. R., Li, L. Y., Shan, L. L., Gao, J., Ma, C. Y., and Li, X. (2021). Effect of supplemental dietary zinc on the growth, body composition and anti-oxidant enzymes of coho salmon (*Oncorhynchus kisutch*) alevins. *Aquacult. Rep.* 20, 100744. doi: 10.1016/j.aqrep.2021.100744

frontiers | Frontiers in Marine Science

TYPE Original Research
PUBLISHED 26 January 2023
DOI 10.3389/fmars.2022.1119410

OPEN ACCESS

EDITED BY
Ce Shi,
Ningbo University, China

REVIEWED BY
Zhen Ma,
Dalian Ocean University, China
Zeng Yu,
China West Normal University, China

*CORRESPONDENCE
Ming Duan
duanming@ihb.ac.cn
Daxian Zhao
zhaodaxian@ncu.edu.cn

†These authors share first authorship

SPECIALTY SECTION
This article was submitted to Marine Fisheries, Aquaculture and Living Resources, a section of the journal Frontiers in Marine Science

RECEIVED 08 December 2022
ACCEPTED 28 December 2022
PUBLISHED 26 January 2023

CITATION
Mei F, Zhang C, Luo B, Zhang D, Hu S, Bao J, Lian Y, Zhao D and Duan M (2023) Effects of season and diel cycle on hydroacoustic estimates of density, Target Strength, and vertical distribution of fish in Yudong Reservoir, a plateau deep water reservoir in southwest China. *Front. Mar. Sci.* 9:1119410. doi: 10.3389/fmars.2022.1119410

Effects of season and diel cycle on hydroacoustic estimates of density, Target Strength, and vertical distribution of fish in Yudong Reservoir, a plateau deep water reservoir in southwest China

Feng Mei[1,2†], Chaoshuo Zhang[2,3†], Bin Luo[2,4], Dongxu Zhang[2,3], Shaoqiu Hu[2,5], Jianghui Bao[2], Yuxi Lian[6], Daxian Zhao[1,7*] and Ming Duan[2*]

[1]School of Life Sciences, Nanchang University, Nanchang, China, [2]State Key Laboratory of Freshwater Ecology and Biotechnology, Institute of Hydrobiology, Chinese Academy of Sciences, Wuhan, China, [3]College of Advanced Agricultural Sciences, University of Chinese Academy of Sciences, Beijing, China, [4]College of Animal Science, Guizhou University, Guiyang, China, [5]College of Fisheries, Huazhong Agricultural University, Wuhan, China, [6]College of Life Science, Anqing Normal University, Anqing, China, [7]Fisheries Laboratory, Chongqing Research Institute of Nanchang University, Chongqing, China

Hydroacoustics is a non-invasive fish stock assessment sampling technique that plays an important role in fishery science and management. However, non-standard hydroacoustic surveys could lead to biased results, and the factor of the sampling period (e.g., season and diel cycle) is extremely critical as it can greatly affect hydroacoustic results. Efforts to improve the accuracy and credibility of the hydroacoustic survey results are getting more and more attention. Thus, we conducted two diel hydroacoustic surveys *in situ* in summer and winter to detect whether there were diel and seasonal differences in density, Target Strength (*TS*) and vertical distribution of fish. The results indicated that nighttime had significantly higher fish mean density than daytime in summer and winter. No significant difference between summer and winter daytime, however, significant difference between summer and winter nighttime, but this bias could be accepted from the fisheries management perspective; The mean *TS* of the summer daytime was significantly higher than that of summer nighttime, winter daytime and winter nighttime, but there were no significant differences among summer nighttime, winter daytime, and winter nighttime, mainly due to mean *TS* may be overestimated from fish schooling behavior during summer daytime; The fish vertical distribution had significant seasonal correlations and was more dispersed in different water layers during the nighttime, proving that the assessment was better at nighttime than during the daytime. Consequently, the hydroacoustic surveys in Yudong Reservoir and other similar plateau deep water reservoirs should be performed at nighttime, which will yield relatively accurate density and *TS*, and dispersed vertical distribution of fish.

KEYWORDS

hydroacoustic, diel, seasonal, mean density, mean *TS*, vertical distribution

1 Introduction

The hydroacoustic technique has been developed for decades and is now considered a robust and reliable method (MacLennan and Simmonds, 2013). It has been widely used in assessing the density, biomass, body size, or spatial and temporal distribution of freshwater fish with the advantages of being efficient, rapid and not damaging biological resources compared to other fish stock assessment methods (e.g., gillnet and trawl) (Koslow, 2009). Therefore, hydroacoustics has become an excellent tool for research in the management of fish resources in reservoirs, the conservation of fish resources in rivers and lakes, and the monitoring of fish in dams and locks (Tan et al., 2011; Godlewska et al., 2016).

Like other sampling methods, hydroacoustics also has biases and limitations caused by fish species discrimination, acoustic dead zone (near the surface or bottom of reservoirs), and schooling due to fish rhythms Girard et al., (2020). It must be considered when choosing the suitable survey period, as species-specific behavior and spatial distribution add uncertainty to fish stock assessment (Ye et al., 2013; Lian et al., 2017). Therefore, selecting the sampling period (e.g., season and diel cycle) is essential for hydroacoustic surveys. Previous studies have demonstrated that the survey results of lakes and rivers in different periods were distinct. For example, Loures and Pompeu (2015) found that fish densities detected by hydroacoustics were significantly higher in the wet season than dry season in the Sao Francisco River. Lyons (1998) found that fish densities were 2.4-11.0 times higher during the nighttime than daytime in the River Trent; Girard et al., (2020) discussed that the hydroacoustic detection of fish density and biomass was higher during the nighttime than daytime in temperate lakes; Říha et al., (2015) concluded that hydroacoustic surveys of fish in Central European reservoirs should be performed at nighttime.

Reservoirs are artificially dammed bodies of water between lakes and rivers and are found worldwide, especially with scarce water resources (Straškraba et al., 1993). They have become the primary way to relieve water supply pressure and play an essential role in human development (Zhou et al., 2016). Certainly, they also have other important functions, such as power generation, flood control, agricultural irrigation and aquaculture (Fernando and Holčík, 1991). However, the operation of the reservoir has a significant impact on the waterbody. On the one hand, it changes the original runoff characteristics of the water and reduces the ability of the water to degrade pollutants. On the other hand, the nutrient level of the water will rise sharply due to the accumulation of nutrients in and around the inundated area, which will quickly cause the outbreak of harmful algal blooms and the deterioration of the water environment and threaten the safety of drinking water. Reducing the nutrient level of water can be achieved by controlling the number of algae in the water by releasing filter-feeding fish (Chen et al., 1991; Mei et al., 2016; Zhang et al., 2016). To achieve a scientific and reasonable fish release, the fish density of existing and the community structure in the reservoir needs to be clarified first.

Yudong Reservoir is located in the middle of the Yunnan-Kweichow Plateau. Like other plateau reservoirs, it is an artificial lake formed by building dams at the narrow mouth of the mountain. Influenced by anthropogenic activities, harmful algal bloom events often occur in Yudong Reservoir in recent years. The reasonable density of silver carp (*Hypophthalmichthys molitrix*) and bighead carp (*Hypophthalmichthys nobilis*) can control the harmful algae and purify the water. Thus, we need to assess accurately silver carp and bighead carp density and biomass to provide scientific recommendations for the reservoir management department. However, hydroacoustic surveys of plateau deep water reservoirs may differ from lakes, rivers and other types of reservoirs due to differences in fish behavior caused by environmental conditions and species-specific (Girard et al., 2020). The optimal period for hydroacoustic detection in plateau deep water reservoirs such as Yudong Reservoir has yet to be studied or reported. In this study, we chose three important indicators of the density, *TS* and vertical distribution of fish to indicate the effect of survey periods on survey results to identify the appropriate sampling period.

2 Materials and methods

2.1 Study area

Yudong Reservoir (27.359°N~ 27.479°N, 103.475°E~ 103.551°E) is located in Zhaotong City, Yunnan Province, China. Figure 1 illustrates the geographical location of Yudong Reservoir, whose mean elevation is 1985 m. The watershed area of Yudong Reservoir is approximately 709 km^2, and the water-spread area is approximately 16.3 km^2. In summer, Yudong Reservoir releases water for power generation and flood control, while it stores water for sufficient water supply in winter. The deepest point of Yudong Reservoir is 46.7 m, mean depth is approximately 22.0 m in summer. The deepest point is 57.4 m, and the mean depth is approximately 30.3 m in winter. It is the main water supply source for nearly three hundred thousand people in Zhaoyang District and Ludian County. In the present study, we divided Yudong Reservoir into nine areas based on mean depth (summer and winter) and distance: Dam (32.3 m), Huangnibao (44.6 m), Yanjiashan (16.1 m), Qimihei (15.1 m), Zhaojiayuan (27.8 m), Zujiaying (22.1 m), Yuba (16.3 m), Lan river (9.4 m) and Guazhai (14.2 m).

2.2 Hydroacoustic surveys

Two diel hydroacoustic surveys of fish resources were conducted in Yudong Reservoir in summer (August 10th - 11st, 2021) and winter (January 5th - 6th, 2022). Daytime surveys were conducted 1 hour after sunrise, and nighttime surveys were conducted 1 hour after sunset (Axenrot et al., 2016). The hydroacoustic survey equipment was BioSonics DT-X split-beam echo detector (BioSonics, Seattle, Washington, USA) (operating frequency 199 kHz, beam angle 6.8°×6.8°), latitude and longitude data were recorded and stored in real-time by Garmin GPS 17 X HVS (Garmin, Olathe, Kansas, USA), Acquisition 6.0 software (BioSonics, Seattle, Washington, USA) was used to collect hydroacoustic data, and calibrating the transducer by referring to the steps in the manual before detection. The transducer was fixed to the bow of speedboat using a homemade iron frame with a draft of 0.5 m, and the beam was emitted vertically downward. The

speedboat was driven forward at 10km/h on a "Z" course at a constant speed (Figure 1), While recording the transect and elevation with a handheld GPS (Magellan, San Dimas, California, USA). The four hydroacoustic survey transects were shown in Figure 1. The credibility of the hydroacoustic survey was judged by calculating the coverage ratio, which was defined as the ratio between the square root of the transect mileage (km) and the water-spread area of the reservoir (km^2) (Aglen, 1983). It was generally recommended that the coverage ratio was at least 3.0 and preferably higher than 6.0 (Emmrich et al., 2012), and all coverage ratios in our study were more significant than 8.0.

2.3 Hydroacoustic data analysis

The hydroacoustic data was analyzed by Visual Analyzer 4.3 software (BioSonics, Seattle, Washington, USA). The single echo detection method was used to analyze the target signals of fish in the water column, with the specific parameters shown in Table 1. To exclude external interference such as vessel engine noise and air bubbles, the hydroacoustic data were selected from 1 m below the transducer to 0.3 m above the reservoir bottom, and the aquatic plants, secondary bottom echoes, and non-fish echoes were manually removed. Finally, parameters such as real-time water depth, Fish Per Unit Area (FPUA, ind./m^2), Fish Per Cubic Meter (FPCM, ind./m^3), and *TS* were obtained. The real-time coordinates and density information (FPUA) returned from Visual Analyzer 4.3 (BioSonics, Seattle, Washington, USA) were imported into ArcGIS 10.7 software (ESRI, Redlands, California, USA), and the fish density distribution was mapped by Kriging spatial interpolation.

2.4 Relationship between *TS* and total length and biomass of fish

Target Strength in hydroacoustics is a physical quantity that responds to the size of fish. We use the term *TS* to refer to Target Strength throughout the paper, the unit is dB, and *TS* is proportional to the total length, the more significant the *TS*, the greater the total length of fish.

The equation (1) proposed by Foote (1987) for fish that have swim bladders was used to estimate the total length (*TL* in cm) of fish:

$$TS = 20 \lg TL - 71.9 \quad (1)$$

The equation (2) for the conversion between the *TL* and weight *W* (g) of bighead carp was proposed by Wanner and Klumb (2009).

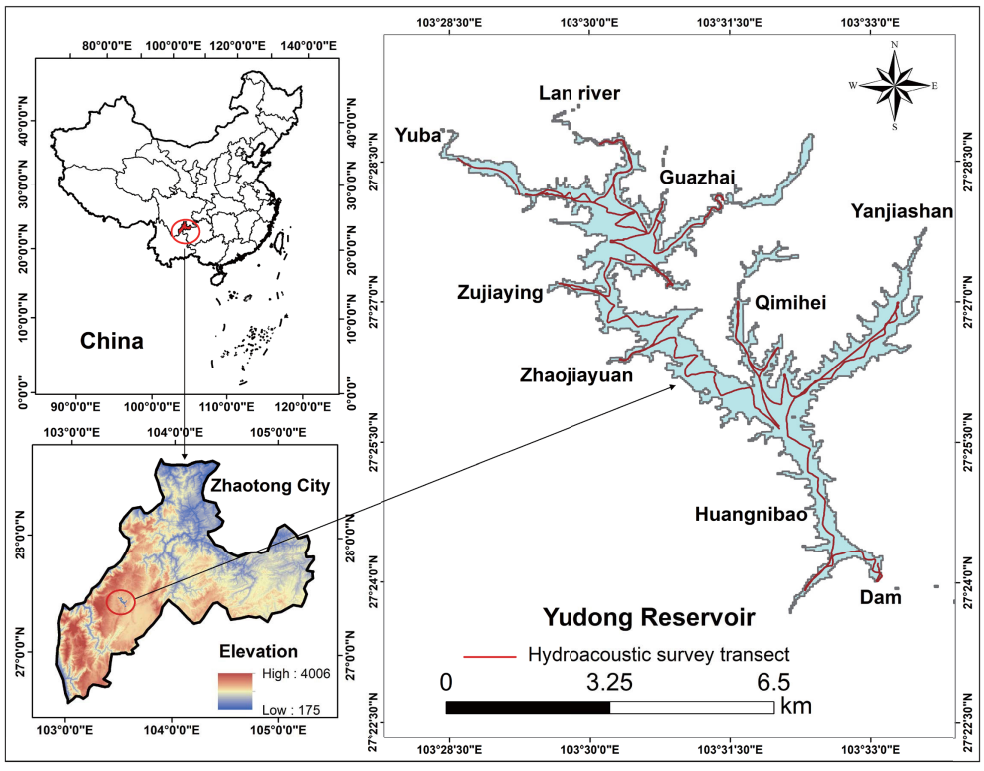

FIGURE 1
Map of the Yudong Reservoir showing its geographical location and hydroacoustic survey transect.

TABLE 1 Setting parameters for individual target analysis.

Echo Threshold	Correlation Factor	Min Pulse Width Factor	Max Pulse Width Factor	End Point Criteria	Time-Varied Gain
-70dB	0.9	0.75	3	-12dB	40lgR

$$W = 0.013TL^{2.96} \quad (2)$$

The mean biomass B (g/m) was calculated as the multiplication of fish mean density ρ (ind./m^2) estimated by hydroacoustics and the weight corresponding to mean TS , and equation (3) shows how it is calculated:

$$B = \rho W \quad (3)$$

2.5 Statistical analysis

We analyzed differences between density, TS, and vertical distribution of fish of each transect during the diel cycle in summer and winter. Hydroacoustic data used Student's t-test and nonparametric Wilcoxon test, when data homogeneity or normality was not achieved, a nonparametric test was used, otherwise, a Student's t-test was used. In addition, the standardized main axis (SMA) was performed (Warton et al., 2006). This test was previously used to compare hydroacoustic data from different scenarios (Mouget et al., 2019), and our study was mainly applied to the distribution of the density and TS of fish in nine areas. The method was suitable for extended and completed linear regression when the measurement error was unknown. The SMA evaluation compared whether the major-axis results followed the 1:1 line for different periods. All analyses were carried out using software R (version 4.1.2) (Team, 2013), and the Smatr package (version 3.4-8) for the SMA test (Warton et al., 2012).

3 Results

3.1 Seasonal and diel difference in fish density

The fish mean density was highest during the nighttime in winter (2.1 ind./m^2), followed by summer nighttime (1.7 ind./m^2), then summer daytime (0.9 ind./m^2), and finally winter daytime (0.7 ind./m^2) (Figure 2). Figure 3 shows the fish density distribution from four hydroacoustic surveys in Yudong Reservoir.

For diel differences, the mean density was significantly higher during the nighttime than daytime in summer (Wilcoxon test, $p < 0.05$) (Figure 2). The slope of the linear relationship was not significantly different from 1 (SMA r = 0.2576, $p > 0.05$) and the intercept was not significantly different from 0 (SMA t = -0.8299, $p > 0.05$) (Figure 4). Like summer, the mean density during the nighttime was significantly higher than daytime in winter (Wilcoxon test, $p < 0.05$). The intercept was not significantly different from 0 (SMA t = -1.758, $p > 0.05$), but the slope of the linear relationship was significantly different from 1 (SMA r = 0.8174, $p< 0.05$) (Figure 4).

For seasonal differences, the difference during the daytime was not significant (Wilcoxon test, $p > 0.05$) (Figure 2), and the linear relationship between slope and 1 was significant (SMA r = -0.7004, $p < 0.05$), but the intercept was not significantly different from 0 (SMA t = -1.471, $p > 0.05$) (Figure 4). The mean density of winter nighttime was slightly higher than summer nighttime and was significantly different (Wilcoxon test, $p < 0.05$) (Figure 2), the slope and intercept

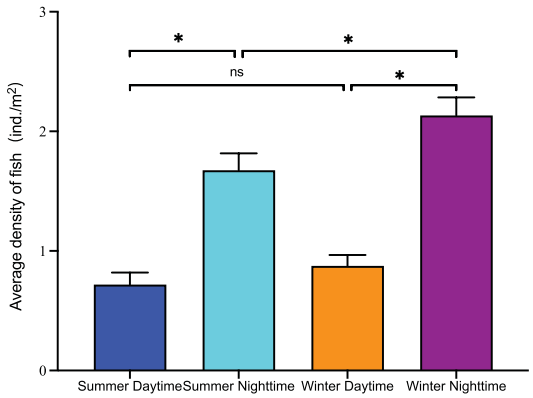

FIGURE 2
Mean density of four hydroacoustic surveys during different periods in Yudong Reservoir. Asterisks indicate significant correlations ($p < 0.05$), ns indicates no significant correlations ($p > 0.05$).

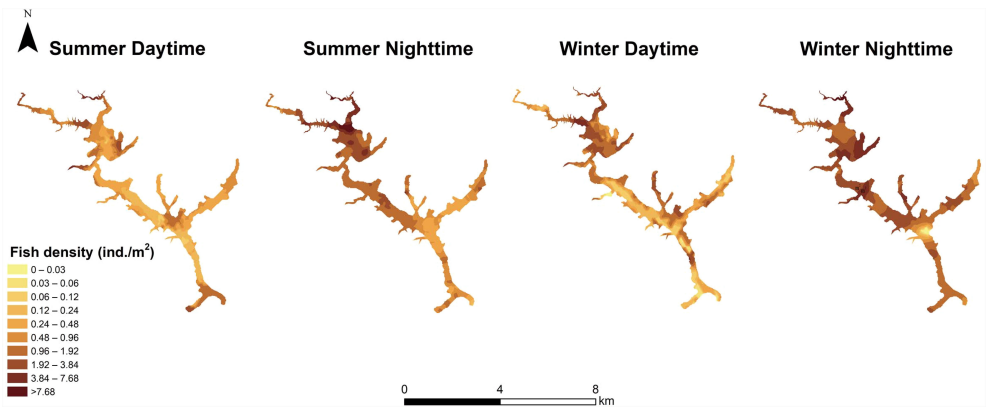

FIGURE 3
Fish density distribution from four hydroacoustic surveys in Yudong Reservoir.

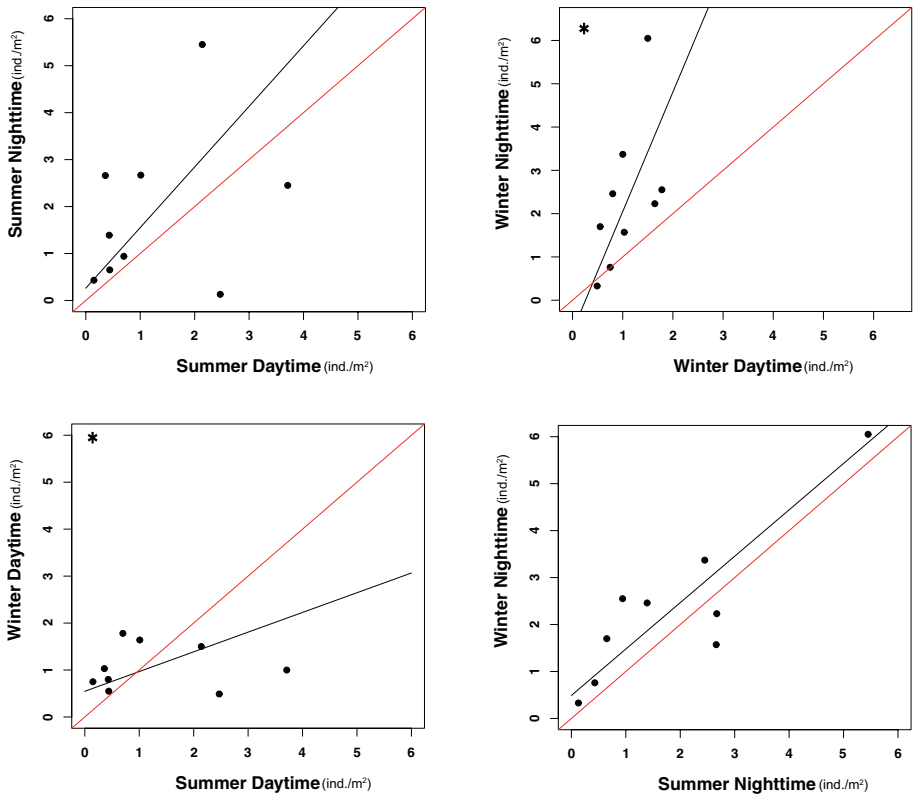

FIGURE 4
Linear relationship between seasonal and diel results for mean density in nine areas. Asterisks in the upper left corner indicates significant correlations ($p < 0.05$). The red line represents the 1:1 line, and the black line the relationship estimated by the SMA (N = 9).

were not significantly different from the expected value (SMA r = -0.01925, $p > 0.05$; SMA t = -0.9981, $p > 0.05$) (Figure 4).

3.2 Seasonal and diel difference in fish *TS*

The mean *TS* in summer daytime, summer nighttime, winter daytime, and winter nighttime were (-49.1 ± 3.7) dB, (-55.1 ± 4.3) dB, (-55.2 ± 4.4) dB, and (-55.7 ± 3.1) dB, respectively, and their corresponding total lengths of fish were 13.8 cm, 6.9 cm, 6.8 cm, and 6.5 cm according to equation (1). Their peaks were all focused around -58 dB. Figure 5 shows the *TS* distribution of fish from the four hydroacoustic surveys.

For diel differences, the mean was significantly higher during the daytime than nighttime in summer (Wilcoxon test, $p < 0.05$), but the slope and intercept of SMA were not significantly different from the

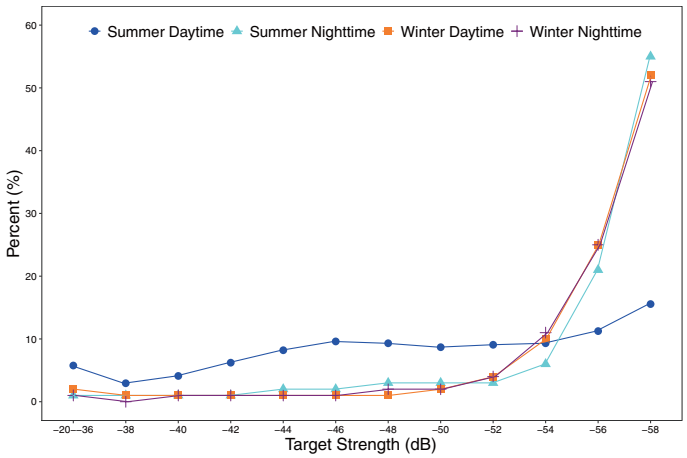

FIGURE 5
Fish *TS* distribution from four hydroacoustic surveys in Yudong Reservoir.

expected value (SMA r = 0.2432, $p > 0.05$; SMA t = 0.3098, $p > 0.05$). However, there was no significant correlation in the mean *TS* between daytime and nighttime in winter, but both the slope and intercept were significantly different from the expected values (SMA r = -0.6308, $p < 0.05$; SMA t = -3.147, $p < 0.05$) (Figure 6).

For seasonal differences, the daytime mean *TS* was significantly different (Wilcoxon test, $p < 0.05$), but the slope and intercept were not significantly different from the expected value (SMA t = 0.2663, $p > 0.05$; SMA r = 0.2856, $p > 0.05$). However, the nighttime mean *TS* was not significantly different (Wilcoxon test, $p > 0.05$), nor was the slope or intercept significantly different from the expected value (SMA t = -1.379, $p > 0.05$; SMA r = -0.3304, $p > 0.05$) (Figure 6).

3.3 Seasonal and diel difference in fish vertical distribution

According to the water depth of the Yudong Reservoir and the vertical distribution of fish in each water layer, the whole water column was divided into seven water layers, 0-5 m, 5-10 m, 10-15 m, 15-20 m, 20-25 m, 25-30 m and 30-60 m, and the percentage of fish density in each water layer in summer and winter seasons was calculated respectively (Figure 7).

For diel differences, there was significant difference in the vertical distribution in summer (Wilcoxon test, $p < 0.05$), but there was no significant difference in winter (Student's test, $p > 0.05$) (Figure 7).

For seasonal differences, there was significant difference in the vertical distribution during daytime and nighttime (Wilcoxon test, $p < 0.05$).

Summer and winter values showed different vertical distribution patterns. There were more than 90% of fish distributed in the water layer above 15m during both daytime and nighttime in summer, especially in the 0-5m water layer, which accounted about for 60%, but the number of fish active in the 5-10m water layer accounted for a higher percentage during the nighttime than daytime in the nighttime than at daytime, while the number of fish distributed in the 10-15m water layer during the daytime was higher than nighttime. Unlike summer, fish were mainly distributed between 5-30m water layer during the daytime and nighttime in winter. These results suggest that fish could migrate to the surface during the nighttime in summer but not in winter.

4 Discussion

4.1 Factors influencing changes in fish density

Regarding the density difference in diel cycle. (Figures 3, 4). The mean density detected during the nighttime was approximately twice as high as during the daytime in both winter and summer. Many studies also supported this result (Lyons, 1998; Ye et al., 2013; Lian

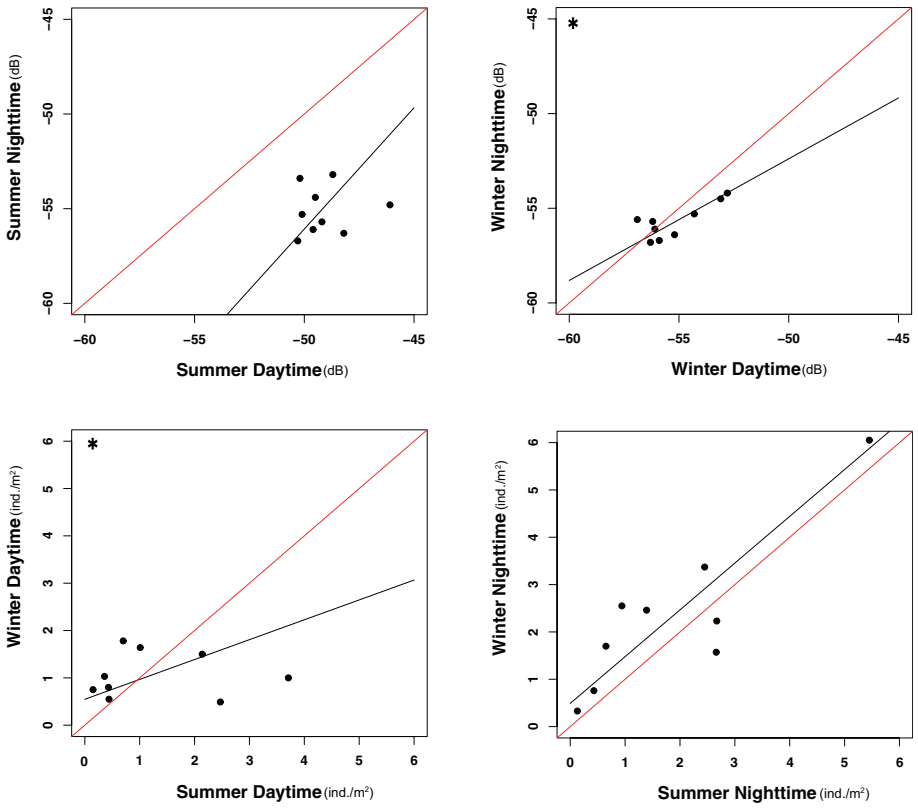

FIGURE 6
Linear relationship between diel and seasonal results for mean *TS* in nine areas. Asterisks in the upper left corner indicate significant correlations ($p < 0.05$). The red line represents the 1:1 line, and the black line the relationship estimated by the SMA (N = 9).

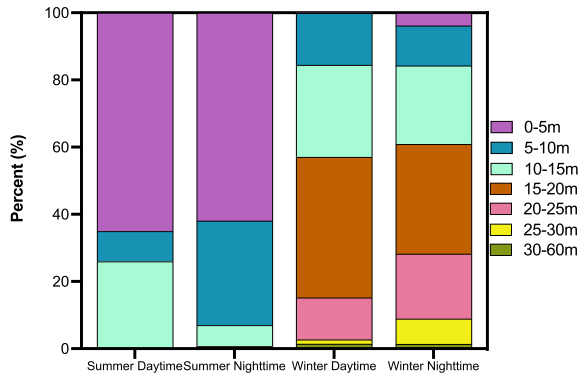

FIGURE 7
Fish density ratio of each water layer from four hydroacoustic surveys in Yudong Reservoir.

et al., 2017). Potential reasons may include the following, (i) Related to the diel rhythm of fish, the aggregation behavior of fish is more evident during the daytime than at nighttime (Appenzeller and Leggett, 1992). Hence, the beam from the hydroacoustic detector radiates on the acoustic scattering cross section of the upper fish, and it immediately reflects on the detector's receiving, resulting in the beam not penetrating the upper fish and detecting the lower fish (Orduna et al., 2021). (ii) Related to the anti-predatory behavior of fish, the light intensity during the daytime is favorable to the predatory activities of predators, and many fish migrate to shallow waters or hide under some shelters such as aquatic plants and rocks to avoid predators (Říha et al., 2015; Christensen and Persson, 1993; Wolter and Bischoff, 2001; Prchalová et al., 2008; Mehner, 2012), hydroacoustic surveys usually actively avoid these areas considering safety, but they return to deeper water during the nighttime, resulting in the detection of fish during the daytime density being higher than at nighttime. (iii) Fish are more active during the daytime than at nighttime and have a more extraordinary ability to avoid vessels and hydroacoustic detectors (DuFour et al., 2018).

Regarding the density difference in seasons, the mean density was significantly different during the nighttime but not daytime. This follows the result that the lower temperature, the higher density of fish detected during the nighttime (Winfield et al., 2007; Loures and Pompeu, 2015), however, this difference is acceptable from the fisheries management perspective. The SMA was significantly different during the daytime, which can only indicate greater seasonal variation in nine areas with more significant density (Figure 7), regardless of the overall density.

4.2 Factors influencing changes in fish *TS*

The SMA results showed that mean *TS* distribution has significant correlations in nine areas between daytime and nighttime in winter, indicating significant differences in the total length of fish detected in different areas. However, the mean *TS* during summer daytime was much higher than in the other three hydroacoustic surveys, and a similar result was also found by Girard et al., (2020). Some possible explanations for this might be that fish have an assertive aggregation behavior in late summer and early autumn, resulting in *TS* error assessment due to the thermal stratification effect of the waterbody. Secondly, there are high densities of juvenile fish in reservoirs, often in groups, migrating to shallower waters or under some shelter during the daytime to avoid predators and returning to deeper waters to feed during the nighttime (Appenzeller and Leggett, 1992; Wolter and Bischoff, 2001; Prchalová et al., 2008; Probst et al., 2009), resulting in a low density of fish detected during summer daytime. In addition, low water temperature affects the activity of fish digestive enzymes in winter (Russell et al., 1996; Person-Le Ruyet et al., 2004; Zhang et al., 2017), reducing the predation pressure on juvenile fish and increasing the probability of detection. Hence, the mean *TS* of fish detected in winter daytime and nighttime was smaller than that in summer daytime.

4.3 Factors influencing changes in fish vertical distribution

The vertical distribution of fish had significant seasonal characteristics. The fish were mainly distributed in the water layer above 15 m, and almost no fish activity in the water layer below 15 m in summer. The vertical distribution of fish showed diel differences in summer, indicating the existence of diel vertical migration of fish, which may be related to the vertical migration of plankton, which is influenced by light, nutrient salts and water disturbance (Ringelberg, 1995), etc., and will migrate down to the water surface in the dawn and up to the water surface in the evening (Han and Straskraba, 1998), and forced by feeding pressure, most fish will also migrate with the migration of plankton (Mehner, 2012). Secondly, it may be related to the dissolved oxygen content of the water column, the dissolution of oxygen in the air, and the photosynthesis of phytoplankton during the daytime, making the whole water column with sufficient dissolved oxygen. During the nighttime, photosynthesis is weakened, the respiration of organisms consumes a large amount of dissolved oxygen in the water column, and the lower water column is not replenished with oxygen (Bezerra-Neto and Pinto-Coelho, 2007; Du et al., 2019), forcing the middle and lower fish to move up to breathe oxygen, so the fish have a significant difference in summer diel cycle. In winter, plankton and dissolved oxygen are distributed in each water layer. They are less affected by diel and seasonal plankton (Magnesen, 1989; Zhang et al., 2022), so fish do not need to migrate vertically for oxygen and food. Therefore, there was no significant difference between daytime and nighttime in the vertical direction in winter.

5 Conclusions

The SMA test and vertical distribution of fish results indicate horizontal and vertical migratory behaviors of fish influenced by diel and seasonal rhythms, which could affect the hydroacoustic assessment of fish resources. The mean density was less influenced by season and more by diel cycle, and the nighttime estimates being

less influential than daytime. Nevertheless, there were no significant differences between mean *TS*, except for summer daytime, and this bias may be influenced by fish behavior. The density and *TS* are vital indicators for biomass, after calculation, the mean biomass in summer nighttime and winter nighttime were 6.63 (g/m) and 6.93 (g/m), and we believe this is well within experimental error, and thus such a difference is perfectly acceptable. Given the above considerations, hydroacoustic surveys could be conducted during the nighttime in Yudong Reservoir and other similar plateau deep water reservoirs. In addition, regardless of time and cost, hydroacoustic surveys during winter nighttime are recommended for more accurate assessments of fish populations density and biomass.

Data availability statement

The raw data supporting the conclusions of this article will be made available by the authors, without undue reservation.

Ethics statement

Ethical review and approval was not required for the animal study because the hydroacoustic experiment did not cause any harm to or involve direct intervention with the animals.

Author contributions

FM (co-first author): conceptualization, methodology, formal analysis, investigation, data curation, validation, writing–original draft. CZ (co-first author): conceptualization, methodology, investigation, data curation, validation, writing-review and editing. BL: investigation, data curation, writing-review and editing. DoZ: investigation, data curation, writing-review and editing. SH: investigation, data curation. JB: data curation, writing-review and editing. YL: writing-review and editing. DaZ (co-corresponding author): conceptualization, funding acquisition, writing-review and editing. MD (co-corresponding author): conceptualization, funding acquisition, writing-review and editing. All authors contributed to the article and approved the submitted version.

Funding

This work was financially supported by the Science and Technology Poverty Alleviation Program of the Chinese Academy of Sciences (KFJ-FP-201905), the National Natural Science Foundation of China (No. 32172955; No. 32202914), the National Key R and D Program of China (No. 2022YFB 3206903), the Scientific Instrument Developing Project of the Chinese Academy of Sciences (No. YJKYYQ 20190055), the Special Program for the Institute of National Parks of the Chinese Academy Sciences (No. KFJ-STS-ZDTP-2021-003), and Chongqing Scientific Research Institutions Performance Incentive R&D Investment Guidance Project (Tongnan District, tkx-2022-01).

Acknowledgments

We sincerely thank the staff of Yudong Reservoir for their help.

Conflict of interest

The authors declare that the research was conducted in the absence of any commercial or financial relationships that could be construed as a potential conflict of interest.

Publisher's note

References

Aglen, A. (1983). Random errors of acoustic fish abundance estimates in relation to the survey grid density applied. *FAO Fish. Rep.* 300, 293–298.

Appenzeller, A., and Leggett, W. (1992). Bias in hydroacoustic estimates of fish abundance due to acoustic shadowing: evidence from day–night surveys of vertically migrating fish. *Can. J. Fisheries Aquat. Sci.* 49, 2179–2189. doi: 10.1139/f92-240

Axenrot, T., Guillard, J., Riha, M., and Tuser, M. (2016). Applying the european hydroacoustic standard on fish abundance estimation (EN 15910).

Bezerra-Neto, J. F., and Pinto-Coelho, R. M. (2007). Diel vertical migration of the copepod thermocyclops inversus (kiefer 1936) in a tropical reservoir: The role of oxygen and the spatial overlap with chaoborus. *Aquat. Ecol.* 41, 535–545. doi: 10.1007/s10452-007-9119-x

Chen, S., Liu, X., and Hua, L. (1991). The role of silver carp and bighead in the cycling of nitrogen and phosphorus in the east lake ecosystem. *Acta Hydrobiol. Sin.* 15, 8–26.

Christensen, B., and Persson, L. (1993). Species-specific antipredatory behaviours: effects on prey choice in different habitats. *Behav. Ecol. Sociobiol.* 32, 1–9. doi: 10.1007/BF00172217

DuFour, M. R., Mayer, C. M., Qian, S. S., Vandergoot, C. S., Kraus, R. T., Kocovsky, P. M., et al. (2018). Inferred fish behavior its implications for hydroacoustic surveys in nearshore habitats. *Fisheries Res.* 199, 63–75. doi: 10.1016/j.fishres.2017.11.018

Du, Y., Peng, W., and Liu, C. (2019). A review of dissolved oxygen variation and distribution in the stratified lakes or reservoirs. *J. Hydraulic Eng.* 50, 990–998. doi: 10.13243/j.cnki.slxb.20190147

Emmrich, M., Winfield, I. J., Guillard, J., Rustadbakken, A., Verges, C., Volta, P., et al. (2012). Strong correspondence between gillnet catch per unit effort and hydroacoustically derived fish biomass in stratified lakes. *Freshw. Biol.* 57, 2436–2448. doi: 10.1111/fwb.12022

Fernando, C., and Holčík, J. (1991). Fish in reservoirs. *International Review of Hydrobiology* 76, 149–167. doi: 10.1002/iroh.19910760202

Foote, K. G. (1987). Fish target strengths for use in echo integrator surveys. *J. Acoustical Soc. Am.* 82, 981–987. doi: 10.1121/1.395298

Girard, M., Goulon, C., Tessier, A., Vonlanthen, P., and Guillard, J. (2020). Comparisons of day-time and night-time hydroacoustic surveys in temperate lakes. *Aquat. Living Resour.* 33, 9. doi: 10.1051/alr/2020011

Godlewska, M., Izydorczyk, K., Kaczkowski, Z., Jóźwik, A., Długoszewski, B., Ye, S., et al. (2016). Do fish and blue-green algae blooms coexist in space and time? *Fisheries Res.* 173, 93–100. doi: 10.1002/iroh.19910760202

Han, B.-P., and Straškraba, M. (1998). Modeling patterns of zooplankton diel vertical migration. *J. Plankton Res.* 20, 1463–1487. doi: 10.1093/plankt/20.8.1463

Koslow, J. A. (2009). The role of acoustics in ecosystem-based fishery management. *ICES J. Mar. Sci.* 66, 966–973. doi: 10.1093/icesjms/fsp082

Lian, Y., Ye, S., Godlewska, M., Huang, G., Wang, J., Chen, S., et al. (2017). Diurnal, seasonal and inter-annual variability of fish density and distribution in the three gorges reservoir (china) assessed with hydroacoustics. *Limnologica* 63, 97–106. doi: 10.1016/j.limno.2017.01.008

Loures, R. C., and Pompeu, P. (2015). Seasonal and diel changes in fish distribution in a tropical hydropower plant tailrace: evidence from hydroacoustic and gillnet sampling. *Fisheries Manage. Ecol.* 22, 185–196. doi: 10.1111/fme.12116

Lyons, J. (1998). A hydroacoustic assessment of fish stocks in the river trent, england. *Fisheries Res.* 35, 83–90. doi: 10.1016/S0165-7836(98)00062-9

MacLennan, D. N., and Simmonds, E. J. (2013). *Fisheries acoustics* Vol. 5 (Springer Science & Business Media).

Magnesen, T. (1989). Vertical distribution of size-fractions in the zooplankton community in lindåspollene, western norway. l. seasonal variations. *Sarsia* 74, 59–68. doi: 10.1080/00364827.1989.10413422

Mehner, T. (2012). Diel vertical migration of freshwater fishes–proximate triggers, ultimate causes and research perspectives. *Freshw. Biol.* 57, 1342–1359. doi: 10.1111/j.1365-2427.2012.02811.x

Mei, Y., Chang, C.-C., Dong, Z., and Wei, L. (2016). Stream, lake, and reservoir management. *Water Environ. Res.* 88, 1533–1563. doi: 10.2175/106143016X14696400495370

Mouget, A., Goulon, C., Axenrot, T., Balk, H., Lebourges-Dhaussy, A., Godlewska, M., et al. (2019). Including 38 khz in the standardization protocol for hydroacoustic fish surveys in temperate lakes. *Remote Sens. Ecol. Conserv.* 5, 332–345. doi: 10.1002/rse2.112

Orduna, C., Encina, L., Rodriguez-Ruiz, A., and Rodriguez-Sanchez, V. (2021). Testing of new sampling methods and estimation of size structure of sea bass (dicentrarchus labrax) in aquaculture farms using horizontal hydroacoustics. *Aquaculture* 545, 737242. doi: 10.1016/j.aquaculture.2021.737242

Person-Le Ruyet, J., Mahe, K., Le Bayon, N., and Le Delliou, H. (2004). Effects of temperature on growth and metabolism in a mediterranean population of european sea bass, dicentrarchus labrax. *Aquaculture* 237, 269–280. doi: 10.1016/j.aquaculture.2004.04.021

Prchalová, M., Kubečka, J., Vašek, M., Peterka, J., and Hohausová, E. (2008). Patterns of fish distribution in a canyon-shaped reservoir. *J. Fish Biol.* 73, 54–78. doi: 10.1111/j.1095-8649.2008.01906.x

Probst, W. N., Thomas, G., and Eckmann, R. (2009). Hydroacoustic observations of surface shoaling behaviour of young-of-the-year perch perca fluviatilis (linnaeus 1758) with a towed upward-facing transducer. *Fisheries Res.* 96, 133–138. doi: 10.1016/j.fishres.2008.10.009

Říha, M., Ricard, D., Vaek, M., Prchalová, M., Mrkvika, T., Jza, T., et al. (2015). Patterns in diel habitat use of fish covering the littoral and pelagic zones in a reservoir. *Hydrobiologia* 747, 111–113. doi: 10.1007/s10750-014-2124-x.

Ringelberg, J. (1995). Changes in light intensity and diel vertical migration: a comparison of marine and freshwater environments. *J. Mar. Biol. Assoc. U. K.* 75, 15. doi: 10.1017/S0025315400015162

Russell, N., Fish, J., and Wootton, R. (1996). Feeding and growth of juvenile sea bass: The effect of ration and temperature on growth rate and efficiency. *J. Fish Biol.* 49, 206–220. doi: 10.1111/j.1095-8649.1996.tb00017.x

Straškraba, M., Tundisi, J., and Duncan, A. (1993). "State-of-the-art of reservoir limnology and water quality management," in *Comparative reservoir limnology and water quality management* (Springer), 213–288.

Tan, X., Kang, M., Tao, J., Li, X., and Huang, D. (2011). Hydroacoustic survey of fish density, spatial distribution, and behavior upstream and downstream of the changzhou dam on the pearl river, China. *Fisheries Sci.* 77, 891–901. doi: 10.1007/s12562-011-0400-5

Team, R. C. (2013). *R: A language and environment for statistical computing* (vienna, austria: R. Foundation for statistical computing [Computer program]).

Wanner, G. A., and Klumb, R. A. (2009). Length-weight relationships for three asian carp species in the missouri river. *J. Freshw. Ecol.* 24, 489–495. doi: 10.1080/02705060.2009.9664322

Warton, D. I., Duursma, R. A., Falster, D. S., and Taskinen, S. (2012). smatr 3 -an r package for estimation and inference about allometric lines. *Methods Ecol Evol.* 3, 257–259. doi: 10.1111/j.2041-210X.2011.00153.x

Warton, D. I., Wright, I. J., Falster, D. S., and Westoby, M. (2006). Bivariate line-fitting methods for allometry. *Biol. Rev.* 81, 259–291. doi: 10.1017/S1464793106007007

Winfield, I., Fletcher, J., and James, J. (2007). Seasonal variability in the abundance of arctic charr (*salvelinus alpinus* (l.)) recorded using hydroacoustics in windermere, uk and its implications for survey design. *Ecol. Freshw. Fish* 16, 64–69. doi: 10.1111/j.1600-0633.2006.00170.x

Wolter, C., and Bischoff, A. (2001). Seasonal changes of fish diversity in the main channel of the large lowland river oder. *Regulated Rivers: Res. Manage.* 17, 595–608. doi: 10.1002/rrr.645

Ye, S., Lian, Y., Godlewska, M., Liu, J., and Li, Z. (2013). Day-night differences in hydroacoustic estimates of fish abundance and distribution in lake laojianghe, china. *J. Appl. Ichthyology* 29, 1423–1429. doi: 10.1111/jai.12367

Zhang, L., Zhao, Z., Fan, Q., Zhang, L., Zhao, Z., Fan, Q., et al (2017). Effects of water temperatureand initial weight on growth, digestion and energy budget of yellow catfish pelteobagrus fulvidraco (richardson, 1846). *J Appl Ichthyol.* 33, 6. doi: 10.1111/jai.13465

Zhang, W., Dunne, J. P., Wu, H., Zhou, F., and Huang, D. (2022). Using timescales of deficit and residence to evaluate near-bottom dissolved oxygen variation in coastal seas. *J. Geophysical Research: Biogeosciences* 127, e2021JG006408. doi: 10.1029/2021JG006408

Zhang, X., Liu, Z., Jeppesen, E., Taylor, W. D., and Rudstam, L. G. (2016). Effects of benthic-feeding common carp and filter-feeding silver carp on benthic-pelagic coupling: Implications for shallow lake management. *Ecol. Eng.* 88, 256–264. doi: 10.1016/j.ecoleng.2015.12.039

Zhou, T., Nijssen, B., Gao, H., and Lettenmaier, D. P. (2016). The contribution of reservoirs to global land surface water storage variations. *J. Hydrometeorol.* 17, 309–325. doi: 10.1175/JHM-D-15-0002.1

frontiers | Frontiers in Marine Science

TYPE Original Research
PUBLISHED 03 February 2023
DOI 10.3389/fmars.2023.1117043

OPEN ACCESS

EDITED BY
Zhangying Ye,
Zhejiang University, China

REVIEWED BY
Zengling Ma,
Wenzhou University, China
Tonmoy Ghosh,
Indian Institute of Technology Indore, India

*CORRESPONDENCE
Jilin Xu
xujilin@nbu.edu.cn

SPECIALTY SECTION
This article was submitted to Marine Fisheries, Aquaculture and Living Resources, a section of the journal Frontiers in Marine Science

RECEIVED 06 December 2022
ACCEPTED 27 January 2023
PUBLISHED 03 February 2023

CITATION
Zhang L, Han J, Ma S, Zhang Y, Wang Y and Xu J (2023) Comprehensive evaluation of growth characteristics, nitrogen removal capacity, and nutritional properties of three diet microalgae. *Front. Mar. Sci.* 10:1117043. doi: 10.3389/fmars.2023.1117043

Comprehensive evaluation of growth characteristics, nitrogen removal capacity, and nutritional properties of three diet microalgae

Lin Zhang[1], Jichang Han[2,3], Shuonan Ma[1], Yuanbo Zhang[1], Yumeng Wang[1] and Jilin Xu[1]*

[1]Key Laboratory of Marine Biotechnology of Zhejiang Province, School of Marine Sciences, Ningbo University, Ningbo, China, [2]Ningbo Institute of Oceanography, Ningbo, China, [3]College of Food and Pharmaceutical Sciences, Ningbo University, Ningbo, China

Nitrogen is one of the main pollution sources in aquaculture system. Microalgae are considered as one of the ideal bio-absorbents used in wastewater purification, due to their nitrogen removal capacity and more importantly nutritional value. *Nannochloropsis oceanica*, *Cyclotella atomus*, and *Conticribra weissflogii* are famous as diet microalgae. However, estimation of nitrogen removal capability and concomitant nutritional properties of the three species have been rarely reported, which was performed in this study. *N. oceanica*, *C. atomus*, and *C. weissflogii* were cultivated with two initial nitrate-N concentration, noted as NC (13.85 mg·L^{-1}) and NW (5 mg·L^{-1}) groups, respectively. All the three microalgal strains in NC group showed higher maximum cell density, specific growth rate, and biomass concentration, maximal quantum yield of PSII (Fv/Fm), total Chlorophyll and carotenoids contents than that in NW group. These results confirmed the importance of nitrogen for microalgal biomass generation and photosynthetic performance. From Fv/Fm, *N. oceanica* has better adaptability towards nitrogen depletion compared to other two selected strains. The three microalgae exhibited significantly stronger nitrate-N absorption efficiencies in NC group at the same timepoint, compared to NW. Analyzing the average amount of nitrate-N absorbed by each cell daily, *C. weissflogii* gained the largest value, followed successively by *C. atomus* and *N. oceanica*, likely due to species specificity. Moreover, three strains removed 90% of nitrate-N within five days and 99% of that within seven days, showing splendid nitrogen removal potentials. These results confirmed the feasibility of removing nitrogen from wastewater with the selected three microalgae. Nutritional properties of microalgal biomass were also investigated. For the three species, lower nitrate-N was beneficial for the production of soluble sugar, total lipid, and saturated fatty acid, while higher nitrate-N led to more soluble protein and polyunsaturated fatty acid. In summary, *N. oceanica*, *C. atomus*, and *C. weissflogii* all showed strong nitrogen removal capacity, whose

growth characteristics and nutritional properties varied with nitrogen concentration. In practical application for assimilating nitrogen, these findings could provide some references for the selection of suitable microalgae species in order to satisfy different nutritional requirements of various aquatic animals.

KEYWORDS

aquaculture, nitrate-N, microalgae, diet, growth, nitrogen removal capacity, nutritional property

Introduction

Recently, *Nature* published a review characterizing the rapid development in global aquaculture in the past two decades and highlighting the integration of aquaculture in the global food system (Naylor et al., 2021). It was expected that aquaculture would contribute 52% of the world total fishery production in 2025 (Ramli et al., 2020). Inevitably, the fast expansion of largescale intensive culture activities has brought about adverse effects, especially pollutions on the aquaculture ecosystem itself and the ambient environment (Liu and Su, 2017). According to statistics, aquaculture pollution represented above 20% of the total nutrient input into freshwater in some provinces of China (Naylor et al., 2021). It was reported by Ramli et al. (2020) that over 50% of feed nitrogen turned into waste in the aquaculture system, instead of being assimilated by cultured organisms (Ramli et al., 2020). And, the extensive use of antibiotics and chemicals further aggravated the excessive accumulation of nitrogenous waste in aquaculture ecosystems, which could not be ignored (Luo et al., 2018). It has been generally accepted that nitrogen is one of the main pollution sources (Yuan et al., 2021).

Improving the ecological status of aquaculture system has become a growing concern worldwide, in particular with reducing nitrogen in wastewater effluent to diminish the occurrence of eutrophication (Mohsenpour et al., 2021). To achieve the nitrogen concentration in wastewater effluent that is in compliance with the environmental quality standards for surface water of China (GB 3838-2002), various measures have been exerted in the intensive aquaculture practices. Among them, bioremediation is considered as an innovative and optimistic technology owing to its cost-effectiveness and environmental compatibility, with a diverse range of microorganisms, including fungi, bacteria, and microalgae (Bilal and Iqbal, 2020).

Unicellular microalgae, the microscopic eukaryotic organisms with short life cycles, are capable of generating biomasses *via* photosynthesis (Dai et al., 2022). For one thing, as a robust source of pigments, proteins, essential fatty acids, etc., microalgae have been regarded as a promising feed additive in aquaculture to boost the growth, immunity, and meat coloration/quality of aquatic animals (Ye et al., 2022). In many independent studies, certain microalgae belonging to genera *Nitzschia*, *Chaetoceros*, *Nannochloropsis*, *Pavlova*, *Chlorella*, *Isochrysis*, *Cyclotella*, *Thalassiosira*, *Porphyridium*, and *Phaeodactylum* are famous for great potentials for use in aquaculture (Pahl et al., 2010; Haas et al., 2016; Ding et al., 2021; Ye et al., 2022). For another thing, microalgae have received much interest in implementing them in wastewater treatment, profiting from their ability to utilize nutrition sources in wastewater (Saeed et al., 2022). Extensive studies have evaluated many microalgae species in treating a range wastewater types, including municipal, brewery, agricultural, and industrial effluents (Choi, 2016; Prandini et al., 2016). Thereof, *Scendesmus* sp., *Chlorella* sp., *Spirulina* sp., and *Chaetoceros muelleriare* were widely used in the treatment of aquaculture wastewater, with varying nitrogen absorption efficiencies (Godoy et al., 2012; Ansari et al., 2017; Ahmad et al., 2020). In brief, due to the potential for nitrogen uptake and more importantly the nutritional value of algal biomass generated, microalgae have been referred as one of the ideal bio-absorbents used in wastewater purification (Mohsenpour et al., 2021). However, most of these attempts were performed independent of one another under different conditions and did not focus on the nutritional properties of microalgae. Thus, to effectively couple nitrogen removal with nutritional value, selecting the proper microalgae species is the key in this field.

Nannochloropsis sp., *Cyclotella* sp., and *Conticribra weissflogii* (previously known as *Thalassiosira weissflogii*) are well-known as feed ingredients or live diets for aquaculture. It was reported that a 50 % fish oil replacement by *Nannochloropsis* sp. meal had positive effects on the growth performance and nutrient utilization of juvenile sea bass (Haas et al., 2016). Moreover, the disease resistance of gilthead seabream (*Sparus aurata*) was enhanced with *Nannochloropsis* sp. as functional ingredient in low fishmeal diets (Jorge et al., 2019). Several studies showed that *C. weissflogii* contributed to the improvement of the growth performance of shrimps (*Litopenaeus vannamei*), emphasizing the survival rate of juveniles (Godoy et al., 2012). Similar study was also conducted with *Cyclotella* sp. to investigate its nutritional value as an alternative feed for aquaculture (Pahl et al., 2010). Compared with their feed potential, there are very few reports on the assessment of nitrogen removal capacity for aquaculture wastewater treatment with these three algae, especially *Cyclotella* sp. and *C. weissflogii*. Only a few attempts have been made to improve the water quality of aquaculture system by aid of *Nannochloropsis* sp. (Ding et al., 2021), while ignoring analyses on their nutritional properties.

Over the years, our team has been committed to separation of various diet microalgae and exploration of their nutritional properties (Yang et al., 2015; Liao et al., 2017). In our previous work, *Nannochloropsis oceanica* and two diatom strains (*Cyclotella atomus* and *C. weissflogii*) were screened and characterized from

the rearing water of the shellfish hatchery (27°19′27″N, 120°13′0.16″ E) in Fuding city, Fujian province, China. Here, the comprehensive analyses on growth performances, absorption efficiencies of nitrate-N (NO_3^-), and nutritional properties were conducted in *N. oceanica*, *C. atomus*, and *C. weissflogii*.

Materials and methods

Microalgae strain and preculture condition

N. oceanica (NMBluh014), *C. atomus* (NMBguh026), and *C. weissflogii* (NMBguh021) were provided by the Microalgae Collection Center of Ningbo University (China) and maintained in the NMB3# medium (pH 7.9, salinity 24) (Cao et al., 2019). The microalgal cultures were cultivated at 25°C and under 60 μmol photons·m^{-2}·s^{-1}, following a light regime of 12 h/12 h light/darkness.

Experimental design

According to the environmental quality standards for surface water of China (GB 3838-2002), the limit of nitrogen concentration in the aquaculture area is 1 mg·L^{-1}. Based on the previous investigation on water quality in several intensive rearing ponds, the nitrogen concentration basically exceeds the limit and the main form of nitrogen is nitrate-N (Ding et al., 2021; Huang et al., 2022). In this context, this study aimed to evaluate the nitrogen absorption capacity and nutritional properties of *N. oceanica*, *C. atomus*, and *C. weissflogii* with nitrate-N as the only nitrogen source, with two initial concentrations. And, both of them were above the limit of 1 mg·L^{-1}.

Reaching the post-exponential phase, the three microalgal cells were respectively collected by centrifuging and then washed three times with sterilized seawater. Collected cells were divided into two parts. One part continued to be incubated in NMB3# medium with nitrate-N of 13.85 mg·L^{-1}, designated as NC group. The other part was incubated in the adjusted NMB3# medium with nitrate-N of 5 mg·L^{-1}, designated as NW group. And other components were consistent with NMB3#. The initial cell density of each group was adjusted to one third of that at post-exponential phase. Cultures were all filled with ultraviolet sterilized air with the flow rate of 0.5 L·min^{-1} and maintained at 25 °C and under 60 μmol photons·m^{-2}·s^{-1}. Growth performance, total Chlorophyll content, carotenoids (Car) content, maximal quantum yield of PSII (Fv/Fm), and nitrate-N concentration were monitored on a daily basis. Until day 8, microalgal cells were harvested and stored at -80 °C for analyses of dry biomass and nutritional properties (soluble sugar, soluble protein, total lipid, and fatty acid). The experiment was performed in three biological replicates and three technical replicates for each sample.

Microalgal growth performance

To plot the growth curve, cell density was monitored by cell counting with an optical microscope. At the end of cultivation, samples (30 mL each) were harvested and lyophilized to measure the dry biomass concentration. The specific growth rate (μ) was calculated as follows.

$$\mu = (lnN_t - lnN_1)/\Delta t$$

where N_t, and N_1 represented the maximum and initial density, respectively. Δt was the cultivation period (d).

Chlorophyll, carotenoids, and Fv/Fm

The contents of total Chlorophyll and Car were determined using a modified method described by Li et al. (2019). For spectrophotometric measurement of the above pigments, cells from 1.5 mL sample were centrifuged every day, resuspended in 80% acetone, and vortexed three times. The extract was recentrifuged at 14,000 *g* for 5 min and the supernatant was kept overnight in the dark. And then, the absorbance of the supernatant was respectively read at 450, 645, and 663 nm, in a 96-well plate reader. Total chlorophyll and Car contents were calculated using the equations of Li et al. (2019) and Singh et al. (2022). Fv/Fm was measured with a PSI fluorometer (AquaPen-C, Photon System Instruments, Czech Republic) as previous description of Li et al. (2019). All the samples were analyzed in triplicate.

Nitrate-N absorption efficiency and removal rate

To determine the nitrate-N concentration, 10 mL of algal culture was filtered with a polycarbonate membrane (0.22 μm pore-sized) every day. The filtered water was further analyzed using an automated spectrophotometer (Smart-Chem 450 Discrete Analyzer, Westco Scientific Instruments, Brookfield, USA). Referring to the description of Xu et al. (2012) and Ali et al. (2022), the nitrate-N absorption efficiency (pg·$cell^{-1}$·d^{-1}) was defined as the average amount (pg) of nitrate-N absorbed by each cell daily in this study. Nitrate-N removal rate was calculated with the equation given by Messer et al. (2022). The equations were listed as:

$$Nitrate-N\ \ absorption\ \ efficiency = (C_1 - C_t) * 10^9/Num/\Delta t$$

$$Nitrate-N\ \ \text{removal rate} = (C_1 - C_t)/C_1$$

where C_1 and C_t represented the nitrate-N concentration (mg·L^{-1}) at day 1 and day t, respectively; Num was the initial cell density (cells·mL^{-1}); Δt was the cultivation period (d). All the samples were analyzed in triplicate.

Soluble sugar, soluble protein, total lipid, and fatty acid

The content of soluble sugar was measured with anthracene ketone sulphuric acid colorimetric method (Tian et al., 2015). The soluble protein was quantified by Bradford Coomassie Brilliant Blue G-250 method (Bradford, 1976). The lyophilized algal powder of 10 mg was used to determine the total lipid content with the gravimetric method (Bligh and Dyer, 1959). And, chloroform and methanol were used as solvents for lipid extraction. Fatty acid extraction was

conducted with KOH-CH_3OH and HCl-CH_3OH, following the protocol reported by Zhang et al. (2021). Fatty acid was determined with gas chromatography–mass spectrometry (GC–MS) (7890B/7000C, Agilent Technologies, USA) and further identified based on the NIST14 commercial mass spectral database. The GC–MS analysis was performed with the method of Zhang et al. (2020). All the samples were analyzed in triplicate.

Statistical analysis

Statistical analysis was performed using one-way analysis of variance (ANOVA) with SPSS 20. The difference was analyzed with a Tukey's *post hoc* test and considered statistically significant when $P< 0.05$. All the data were displayed as mean ± SD (standard deviation) (n =3).

Results

Growth performances of three microalgae

The growth curves of *N. oceanica*, *C. atomus*, and *C. weissflogii* with different initial nitrate-N concentrations (NC and NW groups) were depicted in Figure 1. In the first five days, all three microalgae experienced a period of rapid proliferation, and then the trend tended to flatten out. Reasonably, the maximum cell density, specific growth rate, and biomass concentration in NC group were all significantly higher than that in NW group ($p< 0.05$), applicable for all three microalgae. At day 8, the biomass concentration of *N. oceanica*, *C. atomus*, and *C. weissflogii* in NC group was 1.59, 1.29, and 1.25 times that in NW group, respectively. These finding showed that the initial nitrate-N concentration had a substantial effect on microalgal growth performance.

Fv/Fm and pigment content

As a whole, the Fv/Fm values of *N. oceanica*, *C. atomus*, and *C. weissflogii* increased first and then decreased gradually with the process of culture (Table 1). Before day 3, there were almost no significant differences ($p > 0.05$) between two groups of all three microalgae. From day 4, higher values were observed in NC groups, compared to NW. At the end of cultivation, Fv/Fm values in NC groups were between 0.74 and 0.78, while that in NW groups were between 0.57 and 0.73.

Data on the total chlorophyll were shown in Table 1. Before day 5, total chlorophyll contents of *N. oceanica*, *C. atomus*, and *C. weissflogii*

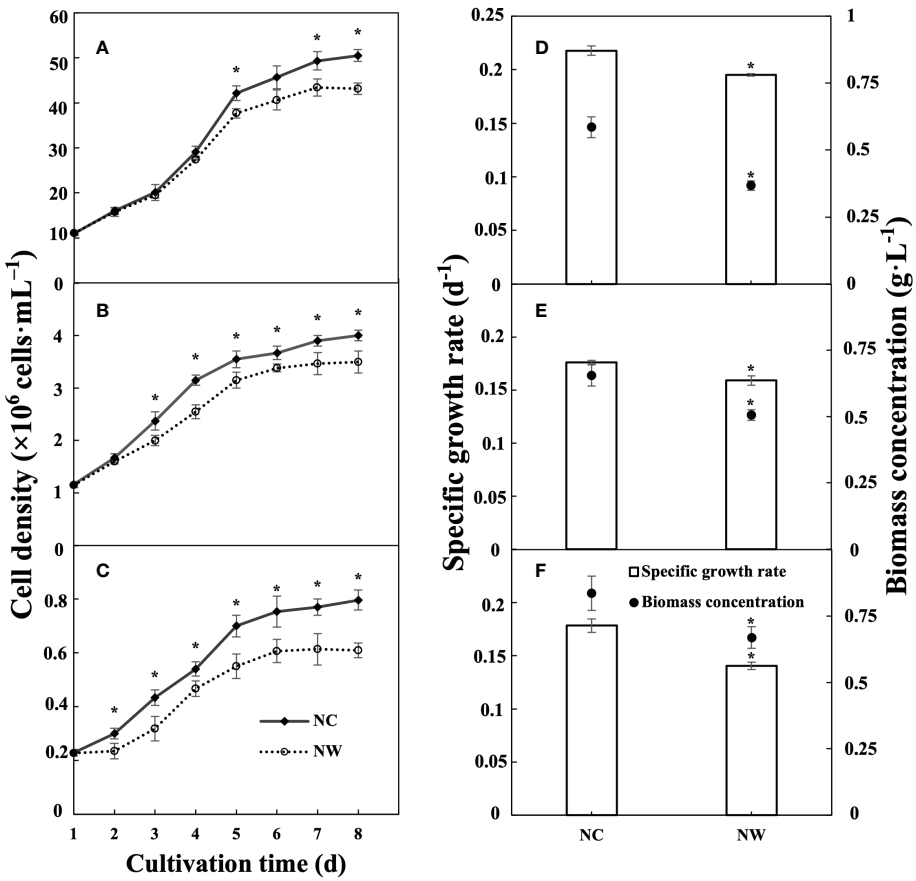

FIGURE 1
Growth performances of *N. oceanica* **(A, D)**, *C. atomus* **(B, E)**, and *C. weissflogii* **(C, F)**. NC, nitrate-N concentration of 13.85 mg·L^{-1}. NW, nitrate-N concentration of 5 mg·L^{-1}. The one-way ANOVA analysis and the Tukey's *post hoc* test were executed to estimate the differences. "*" indicates a significant difference ($P< 0.05$) between NC and NW at the same time point. Data are displayed as the mean ± SD (standard deviation) (n = 3).

10.3389/fmars.2023.1117043

steadily increased both in NC and NW groups, which slightly decreased from day 6 to day 8. What is more, for the three microalgae, the total chlorophyll content in NW group saw a significant decline compared to NC ($p< 0.05$). These results were aligned with the growth curves of three microalgae described above. As for Car content (Table 1), the general trend was similar to total chlorophyll for all the three microalgae. However, the Car peaks of NC and NW groups occurred at different timepoints. Specifically, the highest Car content occurred at day 7, 8, and 7 in NC group for *N. oceanica*, *C. atomus*, and *C. weissflogii*, respectively, whereas the highest values were observed at day 4 in NW groups for all of them.

Nitrate-N utilization by microalgae

In this study, nitrate-N was served as the only nitrogen source for *N. oceanica*, *C. atomus*, and *C. weissflogii*, with two initial concentrations. The concentration of residual nitrate-N in cultural water was monitored on a daily basis and hence the nitrate-N absorption efficiency and nitrate-N removal rate were calculated.

Overall, the absorption efficiencies of three microalgae decreased consistently over time in all groups (Figure 2). From Figure 2A, the highest absorption efficiencies by *N. oceanica* were observed at day 2,

TABLE 1 The maximal quantum yield of PSII (Fv/Fm) and contents of total Chlorophyll and carotenoids (Car) in *N. oceanica*, *C. atomus*, and *C. weissflogii* in two groups.

Cultivation time (d)	Fv/Fm		Total chlorophyll ($mg·L^{-1}$)		Car ($mg·L^{-1}$)	
	NC	NW	NC	NW	NC	NW
N. oceanica						
1	0.83±0.01a	0.83±0.01a	1.63±0.05a	1.63±0.05a	0.30±0.01a	0.30±0.01a
2	0.83±0.01a	0.82±0.01a	1.94±0.10a	1.81±0.10a	0.36±0.03a	0.34±0.01a
3	0.82±0.01a	0.82±0.01a	2.21±0.12a	2.02±0.09a	0.49±0.10a	0.46±0.03a
4	0.83±0.01a	0.81±0.00b	3.65±0.17a	2.82±0.11b	0.92±0.01a	0.54±0.01b
5	0.82±0.01a	0.80±0.01b	3.84±0.17a	3.17±0.10b	0.99±0.03a	0.51±0.01b
6	0.81±0.01a	0.78±0.01b	3.61±0.07a	2.82±0.11b	1.00±0.07a	0.50±0.02b
7	0.80±0.01a	0.77±0.01b	3.57±0.26a	2.73±0.07b	1.06±0.11a	0.45±0.05b
8	0.78±0.01a	0.73±0.02b	3.36±0.31a	2.66±0.13b	1.03±0.14a	0.42±0.01b
C. atomus						
1	0.80±0.01a	0.80±0.01a	1.34±0.05a	1.34±0.05a	0.23±0.01a	0.23±0.01a
2	0.83±0.01a	0.83±0.00a	1.81±0.05a	1.78±0.03a	0.42±0.02a	0.41±0.01a
3	0.83±0.01a	0.82±0.00b	2.80±0.10a	2.46±0.02b	0.78±0.03a	0.68±0.02b
4	0.82±0.00a	0.81±0.01b	3.37±0.12a	2.72±0.04b	1.02±0.02a	0.78±0.02b
5	0.81±0.01a	0.77±0.02b	3.83±0.16a	2.33±0.19b	0.96±0.03a	0.71±0.01b
6	0.80±0.01a	0.73±0.04b	3.55±0.09a	2.18±0.09b	1.01±0.12a	0.71±0.05b
7	0.79±0.02a	0.66±0.05b	3.13±0.20a	2.18±0.09b	1.16±0.06a	0.65±0.01b
8	0.75±0.02a	0.57±0.04b	2.83±0.05a	2.03±0.02b	1.26±0.03a	0.60±0.03b
C. weissflogii						
1	0.82±0.01a	0.82±0.01a	1.43±0.03a	1.43±0.03a	0.24±0.02a	0.24±0.02a
2	0.85±0.01a	0.85±0.01a	2.00±0.02a	1.81±0.01b	0.45±0.03a	0.41±0.02a
3	0.85±0.01a	0.85±0.01a	3.10±0.17a	2.44±0.08b	0.85±0.11a	0.67±0.02b
4	0.85±0.01a	0.81±0.01b	4.33±0.07a	3.16±0.14b	1.23±0.03a	0.88±0.01b
5	0.83±0.01a	0.78±0.01b	4.85±0.02a	3.53±0.05b	1.29±0.05a	0.87±0.06b
6	0.80±0.01a	0.75±0.01b	4.35±0.07a	3.35±0.18b	1.50±0.01a	0.87±0.01b
7	0.79±0.01a	0.74±0.01b	4.33±0.07a	3.26±0.17b	1.72±0.11a	0.82±0.05b
8	0.74±0.02a	0.68±0.01b	4.18±0.13a	3.24±0.12b	1.58±0.08a	0.76±0.02b

NC, nitrate-N concentration of 13.85 $mg·L^{-1}$. NW, nitrate-N concentration of 5 $mg·L^{-1}$. Different letters (a and b) indicate significant differences ($P< 0.05$) between NC and NW at the same timepoint. Data are displayed as the mean ± SD (standard deviation) (n = 3).

i.e., 0.40 (NC) and 0.36 pg·cell^{-1}·d^{-1} (NW). For *C. atomus*, the absorption efficiencies were between 4.61 and 1.91 pg·cell^{-1}·d^{-1} in NC group and between 4.23 and 0.98 pg·cell^{-1}·d^{-1} in NW group (Figure 2B). Compared to *N. oceanica* and *C. atomus*, the highest absorption efficiencies were obtained with *C. weissflogii* at day 2, reaching 19.02 (NC) and 16.28 pg·cell^{-1}·d^{-1} (NW), respectively (Figure 2C). The absorption efficiencies in NC groups by all the three microalgae were significantly higher than NW group ($p< 0.05$) at the same timepoint. These results revealed that the absorption efficiency was significantly affected by the initial N concentration.

By monitoring the residual nitrate-N in cultural water every day, it was found that nitrate-N was exhausted at day 8. As shown in Figure 2, the removal rates of *N. oceanica*, *C. atomus*, and *C. weissflogii* all exceeded 90% at day 4 and 99% at day 5 in NW group (Figure 2). Moreover, despite with higher initial N concentration in NC groups, they could also remove 90%/99% of

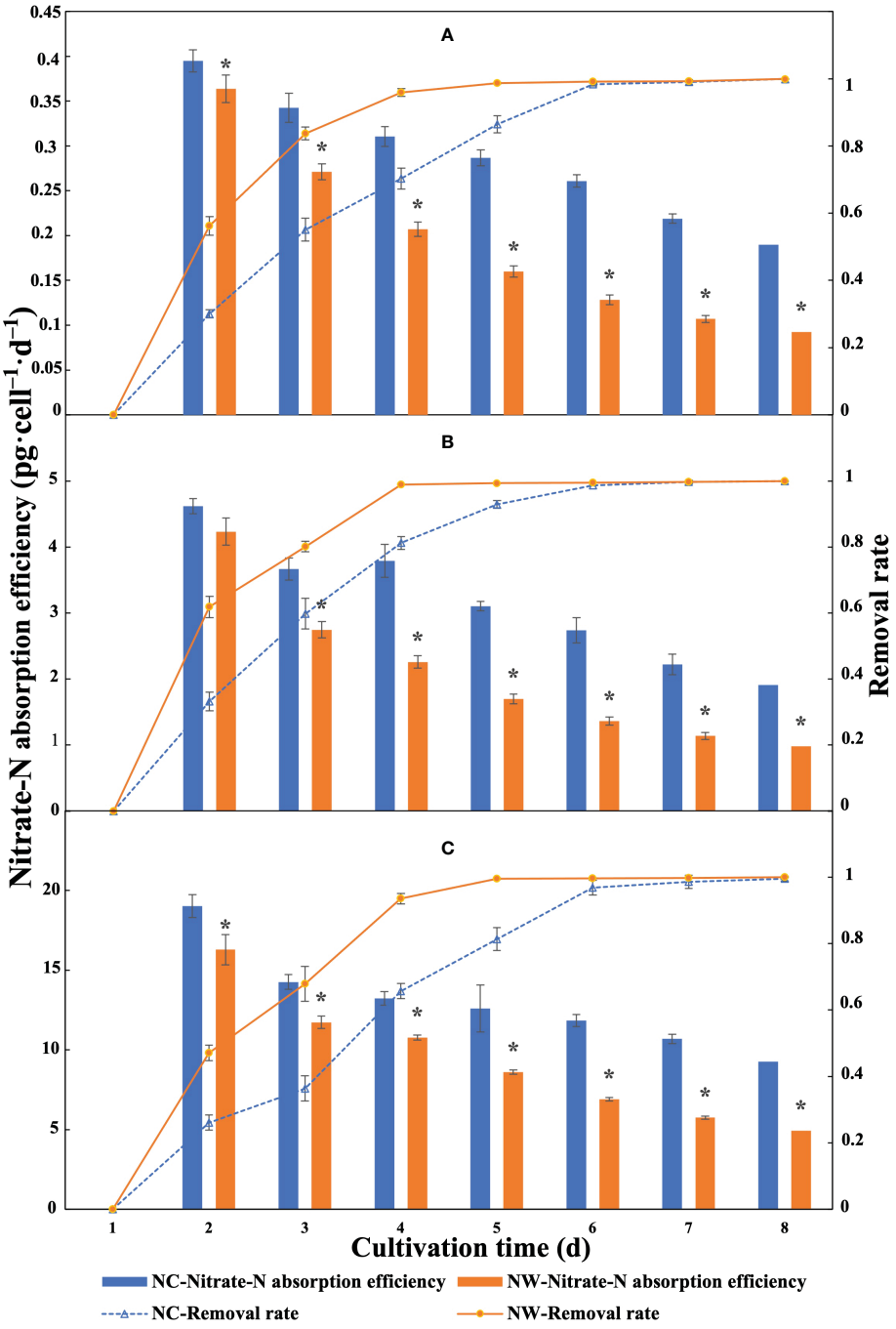

FIGURE 2
Nitrate-N absorption efficiency and nitrate-N removal rate of *N. oceanica* **(A)**, *C. atomus* **(B)**, and *C. weissflogii* **(C)**. NC, nitrate-N concentration of 13.85 mg·L^{-1}. NW, nitrate-N concentration of 5 mg·L^{-1}. The one-way ANOVA analysis and the Tukey's *post hoc* test were executed to estimate the differences. "*" above the column indicates a significant difference ($P< 0.05$) between NC and NW at the same timepoint. Data are displayed as the mean ± SD (standard deviation) (n = 3).

nitrate-N within five/seven days (Figure 2), showing excellent nitrate-N removal capacities.

Analyses on nutritional properties

At the end of cultivation, microalgal cells were respectively harvested for the assessment of nutritional composition. As displayed in Figure 3A, the soluble sugar and total lipid of *N. oceanica* in NW group were obviously higher (56.8% and 28.8%) than that in NC group ($p< 0.05$), while the soluble protein decreased by 37.3% ($p< 0.05$). Eleven fatty acids were identified in *N. oceanica* and listed in Table 2. C16:0, C16:1, C18:1 (trans-9), and C20:5 were the predominant types. C16:0 and C16:1 increased by 8.2% and 8.1% ($P< 0.05$) in NW group compared to NC, further leading to the significant increases in SFA and MUFA ($P< 0.05$). Conversely, C18:2, C20:4 (ARA), and C20:5 declined by 21.0%, 24.7%, and 30.6% ($P< 0.05$) in NW group compared to NC. As a result, PUFA decreased dramatically (27.4%, $P< 0.05$) in NW group.

As for *C. atomus* (Figure 3B), compared to NC, the soluble sugar and total lipid increased by 42.3% and 97.5%, while the soluble protein decreased by 36.9% ($p< 0.05$) in NW. Compared to *N. oceanica*, thirteen fatty acids were detected in *C. atomus* (Table 2). C14:0, C16:0, C16:1, and C20:5 were the predominant ones. SFA obviously increased in NW group compared to NC ($P< 0.05$), mainly attributing to the increasements of C14:0 (11.4%, $P< 0.05$) and C16:0 (6.1%, $P< 0.05$). Different from *N. oceanica* and *C. weissflogii*, no significant difference was observed in MUFA between NC and NW groups ($P > 0.05$). PUFA decreased significantly in NW group (13.7%, $P< 0.05$) by reason of the substantial reductions of C16:2 (29.1%, $P< 0.05$) and C16:3 (46.8%, $P< 0.05$).

Similar to *N. oceanica* and *C. atomus*, *C. weissflogii* accumulated more soluble sugar and total lipid but less soluble protein in NW group, in comparison to NC ($p< 0.05$) (Figure 3C). In particular, *C. weissflogii* seemed to produce more soluble sugars than *N. oceanica* and *C. atomus*, reaching 41.7% dry cell weight in NW group. Here, fourteen fatty acids were detected in *C. weissflogii* (Table 2). C14:0, C16:0, C16:1, and C20:5 accounted for the largest proportion, just like *C. atomus*. SFA (9.8%, $P< 0.05$) and MUFA (3.3%, $P< 0.05$) enjoyed the mark increases in NW groups compared to NC, caused by the increases of 16:0 (16.6%, $P< 0.05$) and C18:1 (trans-9) (33.9%, $P< 0.05$). What is more, higher PUFA was observed in NC group ($P< 0.05$).

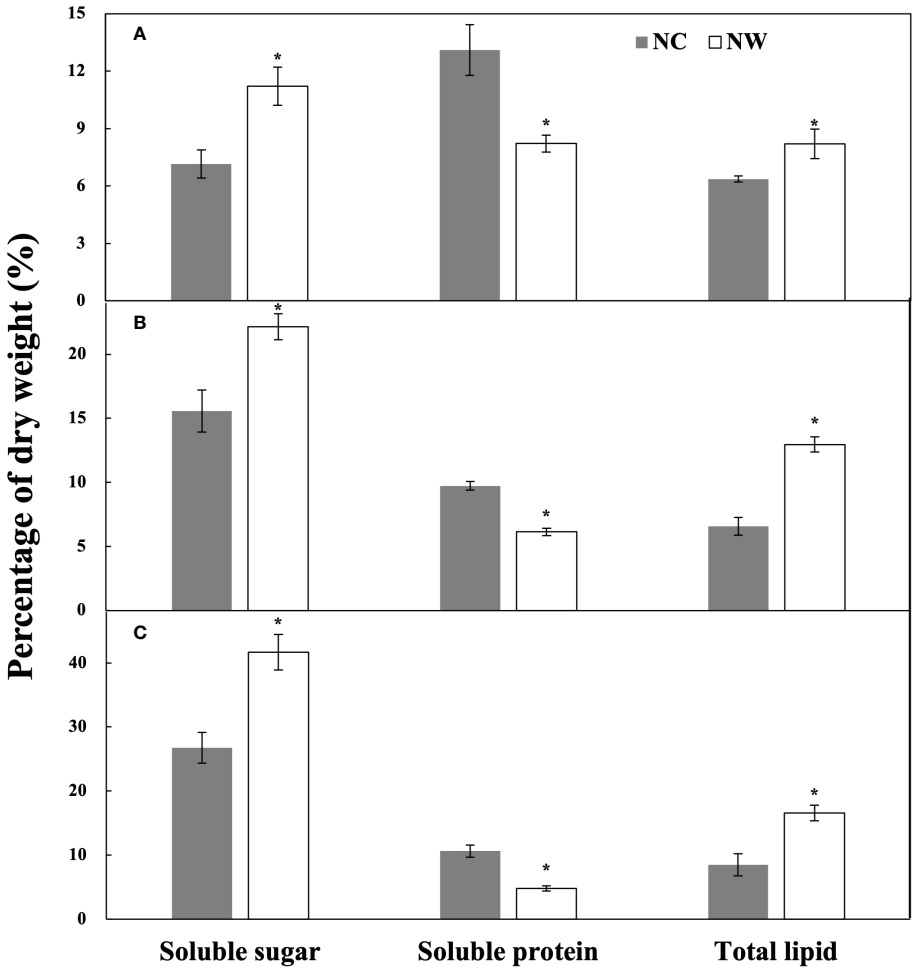

FIGURE 3
Contents of soluble sugar, soluble protein, and total lipid of *N. oceanica* **(A)**, *C. atomus* **(B)**, and *C. weissflogii* **(C)**. NC, nitrate-N concentration of 13.85 mg·L^{-1}. NW, nitrate-N concentration of 5 mg·L^{-1}. The one-way ANOVA analysis and the Tukey's *post hoc* test were executed to estimate the differences. "*" above the column indicates a significant difference ($P< 0.05$) between NC and NW. Data are displayed as the mean ± SD (standard deviation) (n = 3).

10.3389/fmars.2023.1117043

TABLE 2 The fatty acid composition (% of total fatty acids) of *N. oceanica*, *C. atomus*, and *C. weissflogii* under different nitrate-N concentrations.

	N. oceanica		*C. atomus*		*C. weissflogii*	
	NC	NW	NC	NW	NC	NW
C14:0	7.54±0.59a	7.18±0.53a	9.79±0.94a	10.91±0.31b	10.54±0.34a	10.33±0.51a
C15:0	0.83±0.05a	0.60±0.08b	1.76±0.21a	1.62±0.22a	3.09±0.02a	3.09±0.12a
C16:0	32.49±0.69a	35.16±0.77b	33.41±0.62a	35.45±0.53b	25.18±0.66a	29.36±0.17b
C18:0	3.65±0.10a	3.37±0.20a	1.06±0.12a	1.02±0.09a	1.11±0.04a	1.04±0.05a
SFA	44.51±0.14a	46.30±0.15b	46.02±1.06a	49.00±0.32b	39.92±0.92a	43.83±0.23b
C16:1	23.15±0.77a	25.02±0.65b	30.84±1.08a	31.50±0.98a	27.81±0.42a	28.27±0.44a
C18:1 trans-9	12.10±0.43a	12.88±0.61a	0.77±0.10a	0.55±0.07b	1.59±0.15a	2.13±0.15b
C18:1 cis-9	1.63±0.09a	2.28±0.05b	2.63±0.51a	1.92±0.44a	0.53±0.11a	0.52±0.08a
MUFA	36.88±0.44a	40.19±0.31b	34.24±0.70a	33.97±0.69a	29.93±0.36a	30.93±0.34b
C16:2			4.36±0.44a	3.09±0.12b	7.80±0.61a	5.80±0.27b
C16:3			2.22±0.31a	1.18±0.11b	4.07±0.18a	2.67±0.15b
C16:4			3.14±0.44a	3.19±0.25a		
C18:2	2.05±0.25a	1.62±0.15b			0.69±0.03a	0.41±0.03b
C18:3	0.44±0.05a	0.45±0.06a				
C18:4					2.40±0.15a	3.00±0.03b
C20:4 (ARA)	4.25±0.30a	3.20±0.11b				
C20:4 (ETA)					0.88±0.02a	0.67±0.06b
C20:5	11.87±0.24a	8.24±0.19b	8.65±0.15a	8.17±0.32a	12.28±0.36a	11.02±0.28b
C22:5			0.45±0.05a	0.48±0.06a		
C22:6			0.93±0.03a	0.91±0.11a	2.02±0.13a	1.68±0.05b
PUFA	18.61±0.57a	13.51±0.31b	19.74±1.38a	17.03±0.83b	30.15±1.24a	25.24±0.76b

NC, nitrate-N concentration of 13.85 mg·L^{-1}. NW, nitrate-N concentration of 5 mg·L^{-1}. SFA (saturated fatty acid) consisted of C14:0, C15:0, C16:0, and C18:0. MUFA (monounsaturated fatty acid) included C16:1, C18:1 (trans-9), and C18:1 (cis-9). PUFA (polyunsaturated fatty acid) comprised C16:2, C16:3, C16:4, C18:2, C18:3, C18:4, C20:4 (ARA), C20:4 (ETA), C20:5, C22:5, and C22:6. One-way ANOVA and Tukey's post hoc test were carried out to show the differences between NC and NW groups. Different letters (a and b) indicate significant differences ($P< 0.05$). Data are displayed as the mean ± SD (standard deviation) (n = 3).

Discussion

The demand for innovative wastewater treatment techniques has been growing in many nations, in particular with nitrogen removal. Microalgal cultivation using aquaculture wastewater is a promising technology for integrated nitrogen removal and subsequent biomass accumulation. Apart from improving water quality, microalgae have demonstrated to be an excellent living diet, which is the principal advantage of incorporating them into wastewater treatment (Mohsenpour et al., 2021). However, several practical challenges still hinder the industrial application of microalgae in this field, which need to be addressed (Mohsenpour et al., 2021). One such challenge is the availability of superior microalgal strains with optimal nitrogen removal capacity and nutritional properties. Many species of microalgae, e.g., *N. oceanica*, *C. atomus*, and *C. weissflogii*, have been applied in aquaculture as live diets. However, estimation of nitrogen removal capability and concomitant nutritional properties of the three species have been rarely reported. It is necessary to comprehensively analyze their growth performances, nitrogen removal capacities, and accumulations of sugar, protein, lipid, and fatty acid, which have been carried out in this study.

As referred above, nitrogen is one of the main pollution sources of aquaculture wastewater. The inorganic nitrogen forms in aquaculture wastewater comprise of nitrate, nitrite, nitric acid, ammonium, etc. (Wuang et al., 2016). Nitrate-N is the most oxidized and the most thermodynamically stable form. It is hence more common to find nitrate-N in aquaculture environments (Goncalves et al., 2017). Nitrate-N is also the main concern of this study and chosen as the nitrogen source with two concentrations, both of which exceeded the limit of the environmental quality standards for surface water of China (GB 3838-2002). For the selected three strains, there were significant differences observed in the maximum cell density, specific growth rate, biomass concentration, Fv/Fm, total chlorophyll and Car content between two groups. These results indicated nitrate-N concentration had a substantial effect on microalgal growth and photosynthetic performance. This has been a broad consensus proved in many microalgae (Ma et al., 2016). For instance, it was observed that *Chlorella zofingiensis* showed rapid growth with sufficient nitrogen, whereas growth inhibition under nitrogen limitation condition (Zhu et al., 2014). Additionally, the nitrogen removal rates were in line with the growth curves of the three microalgal strains in this study (Figures 1, 2), clearly reflecting the importance of nitrogen for

microalgal biomass generation and confirming the feasibility of removing nitrogen from wastewater with them.

Fv/Fm is a sensitive indicator of plant photosynthetic performance (Jägerbrand and Kudo, 2016). Generally, lower values of Fv/Fm may at least partly reflect stress, photoinhibition, or downregulation of photosynthesis (Jägerbrand and Kudo, 2016). Fv/Fm has been used as an indicator of environmental stress in algae, including nutrient depletion. For example, studies in *Scenedesmus obliquus*, *Chlorella sorokiniana*, and *Ankistrodesmus falcatus* demonstrated that Fv/Fm values obviously decreased with nutrient depletion (Ansari et al., 2017). Another study also indicated that the negative effect of ultraviolet radiation on *Isochrysis galbana* was partly supported by the decline of Fv/Fm (Cao et al., 2019). In the present study, photosynthetic efficiencies of the three strains were monitored in terms of Fv/Fm. The decline of Fv/Fm values was indicative of nitrogen consumption in both groups, which was further confirmed by analyses of nitrate-N utilization (Figure 2). It is worth mentioning that Fv/Fm of *N. oceanica* still maintained at a high level (0.78 and 0.73), even though there was almost no residual nitrate-N in cultural water at the end of culture process (Figure 2). However, Fv/Fm values of *C. atomus* and *C. weissflogii* decrease by a much wider margin, compared to that of the first day. It can be speculated that *N. oceanica* has better adaptability towards nitrogen depletion compared to other two selected strains.

In the current study, *N. oceanica*, *C. atomus*, and *C. weissflogii* removed 90% of nitrate-N within five days and 99% of that within seven days, showing splendid nitrogen removal potentials. Nevertheless, the nitrogen absorption efficiencies were quite different from one another. Analyzing the average amount of nitrate-N absorbed by each cell daily, *C. weissflogii* gained the largest value, followed successively by *C. atomus* and *N. oceanica*. This was likely due to species specificity. Similarly in a comparative study by Ansari et al. (2017), *A. falcatus* showed stronger nitrate-N absorption capacity than *S. obliquus* and *C. sorokiniana*. An additional aspect was that the absorption efficiency in NC group was significantly higher than that in NW group at the same timepoint, applicable for all three microalgae. We speculated that it was mainly caused by the discrepancy in nitrogen concentration. In two independent studies of Wang et al. (2010) and Cabanelas et al. (2013), *Chlorella* sp. both showed an improved nitrogen absorption efficiency when treating wastewater with higher nitrogen concentration, similar to the results observed in this study.

Indeed, apart from microalgal species and nitrogen concentration, there are many other factors influencing nitrogen absorption efficiency. One of them is the preference of nitrogen species. The assimilation of nitrate-N requires previous reduction into ammonium, in a two-step process catalyzed by nitrate reductase and nitrite reductase, while ammonium assimilation does not (Goncalves et al., 2017). Therefore, most algae prefer ammonium as the nitrogen source rather than nitrate-N, as less energy is needed (Ramli et al., 2020). *Nannochloropsis oculata*, *Stigeoclonium nanum*, and *Chlorella vulgaris* fall into this category (Ansari et al., 2017; Ramli et al., 2017). There are, of course, some exceptions. For example, diatoms prefer nitrate-N over ammonium (Ramli et al., 2020). Other factors, such as light intensity and temperature, are also deemed closely correlated with nitrogen uptake by microalgae (Goncalves et al., 2017). Considering that nitrate-N is the main nitrogen form in aquaculture wastewater, this study was conducted with nitrate-N as the only nitrogen source under the same light intensity and temperature. Further investigation is needed to ascertain the impacts of other factors.

Nitrogen, one of fundamental macronutrients, is required for the accumulation of nutritional components (Zarrinmehr et al., 2020). It was reported that many microalgal species could transform protein to lipid or sugar as energy reserve component when encountering nitrogen-depletion (Huo et al., 2011). For example, studies in *N. oceanica*, *I. galbana*, and *Scenedesmus* sp. have demonstrated that nitrogen depletion triggered more lipids (Pancha et al., 2014; Jia et al., 2015; Zarrinmehr et al., 2020). Nitrogen starvation was thus proposed to be an effective technique for lipid production in microalgae (Yaakob et al., 2021). On the other hand, limitation of nitrogen availability also seemed to be the most promising way of accumulating sugars in microalgae (Chen et al., 2013). Zarrinmehr et al. (2020) found that the sugar content in *I. galbana* was enhanced by 47% under nitrogen-deficient condition. Cultivating *Spirulina* sp. in nitrogen-reduction medium caused the dramatical elevation in sugars (Braga et al., 2018). Additionally, there are many reports showing that nitrogen bears directly on the fatty acid profile. The common view is that low nitrogen leads to more saturated fatty acid and monounsaturated fatty acid, while high nitrogen is more conducive to the synthesis of polyunsaturated fatty acid (Zhang et al., 2021). Our results further confirmed this view. Another notable aspect was C20:5, one famous polyunsaturated fatty acid (Zhang et al., 2021). The content of C20:5 changed drastically with nitrogen concentration, especially in *N. oceanica* and *C. weissflogii*.

Over the past decades, abundant studies have clearly shown that the nutritional requirements of aquatic animals depend on different species (fish, shrimp, shellfish, etc.) and different ages (e.g., larva or juvenile) (Ayisi et al., 2017; <xr rid="r106">Li et al., 2021</xr>). The appropriate supply of nutrition is beneficial for the growth, development, and production performance of aquatic animals. According to literatures, the concentration of nitrogen in aquaculture wastewater ranges from 2-110 $mg{\cdot}L^{-1}$ (Ansari et al., 2017). Since the nutritional properties of microalgae varies with nitrogen concentration, the selection of suitable microalgae species should be taken into consideration in practical application for assimilating nitrogen and simultaneously producing biomass as diet for various aquatic animals. Nitrogen concentration is one of key factors in the coupling system of wastewater treatment and biomass production of microalgae. The present study was designed to estimate the growth performances, absorption efficiencies of nitrate-N, and biochemical compositions of three diet microalgae with synthetic medium. However, Microalgal treatment of real wastewater exhibited many complexities, mainly resulting from the increased physiological stresses caused by variable nutrient levels as well as high concentrations of organics in real wastewater. In the follow-up studies, the effects of other nutrient (e.g., phosphorus) on the potentials of diet microalgae for wastewater treatment will be investigated. Furthermore, cultivation with real wastewater without any additional nutrients will be carried out.

Conclusion

In this study, *N. oceanica*, *C. atomus*, and *C. weissflogii* were cultivated with two initial nitrate-N concentration, designated as NC

(13.85 mg·L^{-1}) and NW (5 mg·L^{-1}) groups, respectively. Two nitrate-N concentrations both exceeded the limit of the environmental quality standards for surface water of China (GB 3838-2002). For the selected three strains, significant differences were observed in the maximum cell density, specific growth rate, biomass concentration, Fv/Fm, total chlorophyll and Car content between two groups. Judging from Fv/Fm, *N. oceanica* has better adaptability towards nitrogen depletion compared to other two selected strains. At the end of cultivation, the biomass concentration of *N. oceanica*, *C. atomus*, and *C. weissflogii* in NC group was 1.59, 1.29, and 1.25 times that in NW group, respectively. In addition, the three strains all showed excellent nitrogen removal potentials. The nitrate-N absorption efficiencies in NC group were all significantly higher than that in NW group at the same timepoint. From the average amount of nitrate-N absorbed by each cell daily, *C. weissflogii* gained the largest value, followed successively by *C. atomus* and *N. oceanica*. Further analyses on nutritional properties demonstrated lower nitrate-N was conductive to the synthesis of soluble sugar, total lipid, and saturated fatty acid, while higher nitrate-N resulted in more soluble protein and polyunsaturated fatty acid. To sum up, *N. oceanica*, *C. atomus*, and *C. weissflogii* all possessed strong nitrogen removal capacity. And their growth performance and nutritional properties were closely related with nitrogen concentration.

Data availability statement

The raw data supporting the conclusions of this article will be made available by the authors, without undue reservation.

Author contributions

LZ and JX designed the experiment. LZ analyzed the data and drafted the manuscript. JH and JX revised the paper. SM and YZ measured the microalgal growth and nitrogen removal capacity. YW contributed to the analyses of nutritional properties. All authors contributed to the article and approved the submitted version.

Funding

This work was supported by the Zhejiang Provincial Natural Science Foundation of China (grant number LY22C190001); the National Key Research and Development Program of China (grant number 2019YFD0900400); the Natural Science Foundation of Ningbo Government (grant number 2021J114); the Ningbo Science and Technology Research Projects, China (grant number 2019B10006); the Zhejiang Major Science Project, China (grant number 2019C02057); Ningbo Public Welfare Science and Technology Program (2022S161); the earmarked fund for CARS-49 and was partly sponsored by K. C. Wong Magna Fund in Ningbo University.

Conflict of interest

The authors declare that the research was conducted in the absence of any commercial or financial relationships that could be construed as a potential conflict of interest.

Publisher's note

References

Ahmad, M. T., Shariff, M., Yusoff, F. M., Goh, Y. M., and Banerjee, S. (2020). Applications of microalga *Chlorella vulgaris* in aquaculture. *Rev. Aquacult.* 12, 328–346. doi: 10.1111/raq.12320

Ali, M. A., Ghazy, A. I., Alotaibi, K. D., Ibrahim, O. M., and Al-Doss, A. A. (2022). Nitrogen efficiency indexes association with nitrogen recovery, utilization, and use efficiency in spring barley at various nitrogen application rates. *Agron. J.* 114, 2290–2309. doi: 10.1002/agj2.21128

Ansari, F. A., Singh, P., Guldhe, A., and Bux, F. (2017). Microalgal cultivation using aquaculture wastewater: Integrated biomass generation and nutrient remediation. *Algal. Res.* 21, 169–177. doi: 10.1016/j.algal.2016.11.015

Ayisi, C. L., Hua, X., Apraku, A., Afriyie, G., and Kyei, B. A. (2017). Recent studies toward the development of practical diets for shrimp and their nutritional requirements. *HAYATI J. Biosci.* 24, 109–117. doi: 10.1016/j.hjb.2017.09.004

Bilal, M., and Iqbal, H. M. (2020). Microbial bioremediation as a robust process to mitigate pollutants of environmental concern. *Case Stud. Chem. Environ. Eng.* 2, 100011. doi: 10.1016/j.cscee.2020.100011

Bligh, E. G., and Dyer, W. J. (1959). A rapid method of total lipid extraction and purification. *Can. J. Biochem. Physiol.* 37, 911–917. doi: 10.1139/o59-099

Bradford, M. M. (1976). A rapid and sensitive method for the quantitation of microgram quantities of protein utilizing the principle of protein-dye binding. *Anal. Biochem.* 72, 248–254. doi: 10.1006/abio.1976.9999

Braga, V., Mastrantonio, D.J.d. S., Costa, J. A. V., and de Morais, M. G. (2018). Cultivation strategy to stimulate high carbohydrate content in *Spirulina* biomass. *Bioresour. Technol.* 269, 221–226. doi: 10.1016/j.biortech.2018.08.105

Cabanelas, I. T. D., Ruiz, J., Arbib, Z., Chinalia, F. A., Garrido-Pérez, C., Rogalla, F., et al. (2013). Comparing the use of different domestic wastewaters for coupling microalgal production and nutrient removal. *Bioresour. Technol.* 131, 429–436. doi: 10.1016/j.biortech.2012.12.152

Cao, J., Kong, Z., Ye, M., Zhang, Y., Xu, J., Zhou, C., et al. (2019). Metabolomic and transcriptomic analyses reveal the effects of ultraviolet radiation deprivation on *Isochrysis galbana* at high temperature. *Algal. Res.* 38, 101424. doi: 10.1016/j.algal.2019.101424

Chen, C. Y., Zhao, X. Q., Yen, H. W., Ho, S. H., Cheng, C. L., Lee, D. J., et al. (2013). Microalgae-based carbohydrates for biofuel production. *Biochem. Eng. J.* 78, 1–10. doi: 10.1016/j.bej.2013.03.006

Choi, H. (2016). Parametric study of brewery wastewater effluent treatment using *Chlorella vulgaris* microalgae. *Environ. Eng. Res.* 21, 401–408. doi: 10.4491/eer.2016.024

Dai, N., Wang, Q., Xu, B., and Chen, H. (2022). Remarkable natural biological resource of algae for medical applications. *Front. Mar. Sci.* 9. doi: 10.3389/fmars.2022.912924

Ding, Y., Chen, N., Ke, J., Qi, Z., Chen, W., Sun, S., et al. (2021). Response of the rearing water bacterial community to the beneficial microalga *Nannochloropsis oculata* cocultured with pacific white shrimp (*Litopenaeus vannamei*). *Aquaculture* 542, 736895. doi: 10.1016/j.aquaculture.2021.736895

Godoy, L. C., Odebrecht, C., Ballester, E., Martins, T. G., and Wasielesky, W. (2012). Effect of diatom supplementation during the nursery rearing of *Litopenaeus vannamei* (Boone 1931) in a heterotrophic culture system. *Aquacult. Int.* 20, 559–569. doi: 10.1007/s10499-011-9485-1

Goncalves, A. L., Pires, J. C. M., and Simoes, M. (2017). A review on the use of microalgal consortia for wastewater treatment. *Algal. Res.* 24, 403–415. doi: 10.1016/j.algal.2016.11.008

Haas, S., Bauer, J. L., Adakli, A., Meyer, S., and Schulz, C. (2016). Marine microalgae *Pavlova viridis* and *Nannochloropsis* sp. as n-3 PUFA source in diets for juvenile European Sea bass (*Dicentrarchus labrax* l.). *J. Appl. Phycol.* 28, 1011–1021. doi: 10.1007/s10811-015-0622-5

Huang, C., Luo, Y., Zeng, G., Zhang, P., Peng, R., Jiang, X., et al. (2022). Effect of adding microalgae to whiteleg shrimp culture on water quality, shrimp development and yield. *Aquacult. Rep.* 22, 100916. doi: 10.1016/j.aqrep.2021.100916

Huo, Y. X., Cho, K. M., Rivera, J. G. L., Monte, E., Shen, C. R., Yan, Y. J., et al. (2011). Conversion of proteins into biofuels by engineering nitrogen flux. *Nat. Biotechnol.* 29, 346–351. doi: 10.1038/nbt.1789

Jägerbrand, A. K., and Kudo, G. (2016). Short-term responses in maximum quantum yield of PSII (Fv/Fm) to ex situ temperature treatment of populations of bryophytes originating from different sites in Hokkaido, northern Japan. *Plants (Basel)* 5, 22. doi: 10.3390/plants5020022

Jia, J., Han, D., Gerken, H. G., Li, Y., Sommerfeld, M., Hu, Q., et al. (2015). Molecular mechanisms for photosynthetic carbon partitioning into storage neutral lipids in *Nannochloropsis oceanica* under nitrogen-depletion conditions. *Algal. Res.* 7, 66–77. doi: 10.1016/j.algal.2014.11.005

Jorge, S. S., Enes, P., Serra, C. R., Castro, C., Iglesias, P., Teles, A. O., et al. (2019). Short-term supplementation of gilthead seabream (*Sparus aurata*) diets with *Nannochloropsis gaditana* modulates intestinal microbiota without affecting intestinal morphology and function. *Aquacult. Nutr.* 25, 1388–1398. doi: 10.1111/anu.12959

Liao, K., Chen, W., Zhang, R., Zhou, H., Xu, J., Zhou, C., et al. (2017). qPCR analysis of bivalve larvae feeding preferences when grazing on mixed microalgal diets. *PloS One* 12, e0180730. doi: 10.1371/journal.pone.0180730

Liu, H., and Su, J. (2017). Vulnerability of china's nearshore ecosystems under intensive mariculture development. *Environ. Sci. pollut. Res.* 24, 8957–8966. doi: 10.1007/s11356-015-5239-3

Li, Y., Zheng, M., Lin, J., Zhou, S., Sun, T., and Xu, N. (2019). Darkness and low nighttime temperature modulate the growth and photosynthetic performance of *Ulva prolifera* under lower salinity. *Mar. pollut. Bull.* 146, 85–91. doi: 10.1016/j.marpolbul.2019.05.058

Li, X., Zheng, S., and Wu, G. (2021). Nutrition and functions of amino acids in fish. *Adv. Exp. Med. Biol.* 1285, 133–168. doi: 10.1007/978-3-030-54462-1_8

Luo, Z., Hu, S., and Chen, D. (2018). The trends of aquacultural nitrogen budget and its environmental implications in China. *Sci. Rep.* 8, 10877. doi: 10.1038/s41598-018-29214-y

Ma, X., Liu, J., Liu, B., Chen, T., Yang, B., and Chen, F. (2016). Physiological and biochemical changes reveal stress-associated photosynthetic carbon partitioning into triacylglycerol in the oleaginous marine alga *Nannochloropsis oculata*. *Algal. Res.* 16, 28–35. doi: 10.1016/j.algal.2016.03.005

Messer, T. L., Miller, D. N., Little, H., and Oathout, K. (2022). Nitrate-n removal rate variabilities in floating treatment wetland mesocosms with diverse planting and carbon amendment designs. *Ecol. Eng.* 174, 106444. doi: 10.1016/j.ecoleng.2021.106444

Mohsenpour, S. F., Hennige, S., Willoughby, N., Adeloye, A., and Gutierrez, T. (2021). Integrating micro-algae into wastewater treatment: A review. *Sci. Total. Environ.* 752, 142168. doi: 10.1016/j.scitotenv.2020.142168

Naylor, R. L., Hardy, R. W., Buschmann, A. H., Bush, S. R., Cao, L., Klinger, D. H., et al. (2021). A 20-year retrospective review of global aquaculture. *Nature* 591, 551–563. doi: 10.1038/s41586-021-03308-6

Pahl, S. L., Lewis, D. M., Chen, F., and King, K. D. (2010). Growth dynamics and the proximate biochemical composition and fatty acid profile of the heterotrophically grown diatom. *Cyclotella Cryptica. J. Appl. Phycol.* 22, 165–171. doi: 10.1007/s10811-009-9436-7

Pancha, I., Chokshi, K., George, B., Ghosh, T., Paliwal, C., Maurya, R., et al. (2014). Nitrogen stress triggered biochemical and morphological changes in the microalgae scenedesmus sp. CCNM 1077. *Bioresour. Technol.* 156, 146–154. doi: 10.1016/j.biortech.2014.01.025

Prandini, J. M., da Silva, M. L. B., Mezzari, M. P., Pirolli, M., Michelon, W., and Soares, H. M. (2016). Enhancement of nutrient removal from swine wastewater digestate coupled to biogas purification by microalgae *Scenedesmus* spp. *Bioresour. Technol.* 202, 67–75. doi: 10.1016/j.biortech.2015.11.082

Ramli, N. M., Verdegem, M. C. J., Yusoff, F. M., Zulkifely, M. K., and Verreth, J. A. J. (2017). Removal of ammonium and nitrate in recirculating aquaculture systems by the epiphyte *Stigeoclonium nanum* immobilized in alginate beads. *Aquac. Environ. Interact.* 9, 213–222. doi: 10.3354/aei00225

Ramli, N. M., Verreth, J. A. J., Yusoff, F. M., Nurulhuda, K., Nagao, N., and Verdegem, M. C. J. (2020). Integration of algae to improve nitrogenous waste management in recirculating aquaculture systems: A review. *Front. Bioeng. Biotech.* 8, 1004. doi: 10.3389/fbioe.2020.01004

Saeed, M. U., Hussain, N., Sumrin, A., Shahbaz, A., Noor, S., Bilal, M., et al. (2022). Microbial bioremediation strategies with wastewater treatment potentialities - a review. *Sci. Total. Environ.* 818, 151754. doi: 10.1016/j.scitotenv.2021.151754

Singh, V., Mandhania, S., Pal, A., Kaur, T., Banakar, P., Sankaranarayanan, K., et al. (2022). Morpho-physiological and biochemical responses of cotton (*Gossypium hirsutum* l.) genotypes upon sucking insect-pest infestations. *Physiol. Mol. Biol. Plants* 28, 2023–2039. doi: 10.1007/s12298-022-01253-w

Tian, X., He, M., Wang, Z., Zhang, J., Song, Y., He, Z., et al. (2015). Application of nitric oxide and calcium nitrate enhances tolerance of wheat seedlings to salt stress. *Plant Growth Regul.* 77, 343–356. doi: 10.1007/s10725-015-0069-3

Wang, L., Min, M., Li, Y., Chen, P., Chen, Y., Liu, Y., et al. (2010). Cultivation of green algae chlorella sp. in different wastewaters from municipal wastewater treatment plant. *Appl. Biochem. Biotechnol.* 162, 1174–1186. doi: 10.1007/s12010-009-8866-7

Wuang, S. C., Khin, M. C., Chua, P. Q. D., and Luo, Y. D. (2016). Use of *Spirulina* biomass produced from treatment of aquaculture wastewater as agricultural fertilizers. *Algal. Res.* 15, 59–64. doi: 10.1016/j.algal.2016.02.009

Xu, G., Fan, X., and Miller, A. J. (2012). Plant nitrogen assimilation and use efficiency. *Annu. Rev. Plant Biol.* 63, 153–182. doi: 10.1146/annurev-arplant-042811-105532

Yaakob, M. A., Mohamed, R. M. S. R., Al-Gheethi, A., Aswathnarayana Gokare, R., and Ambati, R. R. (2021). Influence of nitrogen and phosphorus on microalgal growth, biomass, lipid, and fatty acid production: An overview. *Cells* 10, 393. doi: 10.3390/cells10020393

Yang, F., Chen, S., Miao, Z., Sheng, Z., Xu, J., Wan, J., et al. (2015). The effect of several microalgae isolated from East China Sea on growth and survival rate of postset juveniles of razor clam, *Sinonovacula constricta* (Lamarck 1818). *Aquacult. Nutr.* 22, 846–856. doi: 10.1111/anu.12310

Ye, B., Gu, Z., Zhang, X., Yang, Y., Wang, A., and Liu, C. (2022). Comparative effects of microalgal species on growth, feeding, and metabolism of pearl oysters, *Pinctada fucata martensii* and *Pinctada maxima*. *Front. Mar. Sci.* 9. doi: 10.3389/fmars.2022.895386

Yuan, B., Yue, F., Wang, X., and Xu, H. (2021). The impact of pollution on China marine fishery culture: An econometric analysis of heterogeneous growth. *Front. Mar. Sci.* 8. doi: 10.3389/fmars.2021.760539

Zarrinmehr, M. J., Farhadian, O., Heyrati, F. P., Keramat, J., Koutra, E., Kornaros, M., et al. (2020). Effect of nitrogen concentration on the growth rate and biochemical composition of the microalga, *Isochrysis galbana*. *Egypt. J. Aquat. Res.* 46, 153–158. doi: 10.1016/j.ejar.2019.11.003

Zhang, L., Yang, S., Xu, J., Liu, T., Yang, D., Wu, Z., et al. (2020). Application of exogenous salicylic acid on improving high temperature resistance of *Nannochloropsis oceanica*. *Aquacult. Int.* 28, 2235–2246. doi: 10.1007/s10499-020-00592-3

Zhang, L., Ye, S., Chen, W., Han, J., Tian, J., Zhang, Y., et al. (2021). Screening the rate-limiting genes in the ω6 polyunsaturated fatty acid biosynthesis pathway in *Nannochloropsis oceanica*. *Algal. Res.* 57, 102342. doi: 10.1016/j.algal.2021.102342

Zhu, S., Huang, W., Xu, J., Wang, Z., Xu, J., and Yuan, Z. (2014). Metabolic changes of starch and lipid triggered by nitrogen starvation in the microalga *Chlorella zofingiensis*. *Bioresour. Technol.* 152, 292–298. doi: 10.1016/j.biortech.2013.10.092

frontiers | Frontiers in Marine Science

TYPE Original Research
PUBLISHED 09 February 2023
DOI 10.3389/fmars.2023.1119411

OPEN ACCESS

EDITED BY
Ce Shi,
Ningbo University, China

REVIEWED BY
Zeng Yu,
China West Normal University, China
Gang Hou,
Guangdong Ocean University, China

*CORRESPONDENCE
Ming Duan
duanming@ihb.ac.cn

†These authors share first authorship

SPECIALTY SECTION
This article was submitted to Marine Fisheries, Aquaculture and Living Resources, a section of the journal Frontiers in Marine Science

RECEIVED 08 December 2022
ACCEPTED 23 January 2023
PUBLISHED 09 February 2023

CITATION
Luo B, Zhou X, Zhang C, Bao J, Mei F, Lian Y, Zhang D, Hu S, Guo L and Duan M (2023) Hydroacoustic survey on fish spatial distribution in the early impoundment stage of Yuwanghe Reservoir in southwest China. *Front. Mar. Sci.* 10:1119411. doi: 10.3389/fmars.2023.1119411

Hydroacoustic survey on fish spatial distribution in the early impoundment stage of Yuwanghe Reservoir in southwest China

Bin Luo[1,2†], Xianjun Zhou[1†], Chaoshuo Zhang[2,3], Jianghui Bao[2], Feng Mei[2,4], Yuxi Lian[5], Dongxu Zhang[2,3], Shaoqiu Hu[2,6], Longgen Guo[2] and Ming Duan[2*]

[1]College of Animal Science, Guizhou University, Guiyang, China, [2]State Key Laboratory of Freshwater Ecology and Biotechnology, Institute of Hydrobiology, Chinese Academy of Sciences, Wuhan, China, [3]College of Advanced Agricultural Sciences, University of Chinese Academy of Sciences, Beijing, China, [4]School of Life Sciences, Nanchang University, Nanchang, China, [5]College of Life Science, Anqing Normal University, Anqing, China, [6]College of Fisheries, Huazhong Agricultural University, Wuhan, China

Understanding the fish community structure and spatial distribution characteristics is essential for appropriate reservoir fishery management, especially in the early impoundment stage of the reservoir, which could help in obtaining basic data and performing artificial adjustments to biological communities. On the basis of this concept, we conducted a survey of the fish community and distribution at the newly constructed reservoir in southwest China by using a combination of methods, including hydroacoustic survey and fish sampling. Fish sampling showed a single fish community structure (six species belonging to four families) assembled in the reservoir, and the dominant species was *Pseudorasbora parva* which accounted for 98.79% of the fish population. In the hydroacoustic survey, the average fish density was 318.7 ± 256.1 individuals/1,000 m^2. Irregular distribution of the fish was observed in the horizontal direction. The fish densities in the head area, middle area, and tail area of the reservoir were 168.5 ± 60.1, 306.8 ± 124.7, and 696.4 ± 288.9 individuals/1,000 m^2, respectively, which showed a trend of increase in fish density with an increase in distance from the dam. More than 97.3% of the fish in the vertical direction were distributed in the water layer of depth 0 to 12 m. The average total length of fish was 75.4 mm, and the mean fish biomass in the reservoir was approximately 984.8 g/1,000 m^2. According to Pearson correlation analysis, the main factors affecting the spatial distribution of fish were water depth, water temperature, dissolved oxygen, total nitrogen, and plankton density. Our results suggested that the fish community structure should be adjusted by releasing native carnivorous fish to control the abundance of small fish. Moreover, filter-feeding fish such as silver carp and bighead carp should be released in the reservoir to control the plankton community; this will enable the maintenance of the reservoir ecosystem in a healthy state while increasing the economic benefits to the local area.

KEYWORDS

fish communication structure, spatial distribution, reservoir, early impoundment stage, hydroacoustic

1 Introduction

The increasing demand for water resources, combined with the nonuniform temporal and spatial distribution of precipitation, has resulted in severe water shortage in many parts of the world. Reservoirs, as important and effective means for ensuring adequate water resources, not only supply water for humans, enable the generation of hydroelectric energy, and prevent floods but also play an important role in fisheries and aquaculture (Prchalová et al., 2009; He, 2016). Among the different types of aquaculture, reservoir aquaculture is an important method of aquaculture in Guizhou Province, China. Based on the data from the China Fisheries Statistical Yearbook (Bureau of Fisheries, 2021), the reservoir aquaculture area in Guizhou Province accounted for 19.1% of the total aquaculture area in the province, while the output of aquaculture products in reservoirs constituted 23.1% of the total output in 2020. During the early operation period, the reservoir had a relatively homogeneous ecosystem and healthy quality of water (Han, 2010). However, because of dam construction, the velocity of the incoming water flow decreased, and the hydraulic retention time extended, which changed the original runoff characteristics of the water. Moreover, the industrial pollution sources around the reservoir area, domestic waste discharge, and other sources of pollution from the watershed enrichment increased the eutrophication in many reservoirs so that it further declined the quality of the water. It not only affected the production but also raised concerns regarding water safety for residents (Wu et al., 2012; Guo et al., 2018). To maintain the quality of large water bodies such as lakes and reservoirs, to reduce the loss of ecosystem energy, and to exploit the productive potential of water bodies, filter-feeding fish such as silver carp (*Hypophthalmichthys molitrix*) and bighead carp (*Aristichthys nobilis*) have been widely released into the water (Liu and Xie, 2003; Guo et al., 2015). It has therefore become crucial to conduct an assessment of fishery resources to determine appropriate methods to enhance the fish population and release them in a scientific and rational manner (Liu and Zhang, 2016).

There is a pressing need for knowledge of reservoir ecosystems in fishery management and monitoring water quality. Hydroacoustics is an effective tool to understand the dynamics of freshwater ecosystems, and many studies have applied hydroacoustics in their investigations. Hydroacoustics has been developed over several decades, and it is presently recognized as a robust and reliable method for fish assessment (Drastik et al., 2017; Anne et al., 2019). Traditional methods of fishery resource surveys, such as sampling fishes by gillnets, electricity, purse seine, or trawlnet, are based on rough estimates of the number and weight of catches, which are time-consuming and error-prone when implemented in deep reservoirs (Xie et al., 2003; Maclennan and Simmonds, 2005; Kubečka et al., 2009). Compared with the passive survey method, the hydroacoustic survey can provide long-term, continuous, and abundant fishery resource data; thus, this method has the advantages of highly efficient and nondestructive approach to the survey object and relatively low labor cost (Maclennan and Simmonds, 2005; Guillard et al., 2012; Winfield et al., 2013). Recent advances in hardware and software have enabled the more widespread use of hydroacoustic methods, which are more suitable for open water systems such as deep lakes and reservoirs (Godlewska et al., 2004; Anne et al., 2019). Hydroacoustic survey has been widely used in fishery resource assessment, fish behavior assessment, and aquatic plant and plankton research in large water bodies in China and abroad (Lian et al., 2015; Samedy et al., 2015; Anne et al., 2019).

Guizhou Province is located in the eastern part of the Yunnan-Kweichow Plateau, and 92.5% of its region is mountainous and hilly, which has a typical karst landform and constitutes a unique karst ecosystem in southwest China, resulting in poor soil quality and easy infiltration of surface water. Consequently, there are fewer natural lakes, thereby leading to a very severe water shortage, particularly in mountainous areas (Lv, 2019). To resolve this water shortage issue, the government has constructed several reservoirs. Reservoirs are an important water resource for ensuring an adequate water supply and the preservation of the natural environment in Guizhou (Ou, 2015; Lv, 2019). In the present study, we chose Yuwanghe Reservoir in southwest China as the study case. By using the hydroacoustic survey as the main tool, combined with the fish catch sampling method, we obtained the spatial distribution pattern and resources of fish at the early stage of the reservoir with an aim to provide a theoretical basis and technical support for reservoir management and development in the Yunnan–Guizhou region.

2 Materials and methods

2.1 Study area

Yuwanghe Reservoir is located in the northern part of Liupanshui, Guizhou Province; it belongs to Yuwanghe River, which is a first-class tributary of the Beipan River and is situated approximately 50 km from Shuicheng County (26°08′30–26°09′02N, 104°45′30—104°45′50E; Figure 1). The reservoir started to store water and began its operation in 2020 with a maximum depth of 42.3 m and an average depth of 18.8 m. The average capacity is 1.022×10^7 m^3. The main function of the reservoir is to provide water and irrigation facilities to the residents of the area. To analyze the horizontal distribution of fish assemblages, the reservoir was divided into three sections —namely, head area, middle area, and tail area —on the basis of its geographical features.

2.2 Hydroacoustic measurements

The hydroacoustic survey was conducted during daylight hours in May 2021. A DT-X split-beam echosounder (BioSonics, Seattle, WA, USA) operating at a frequency of 200 kHz was used, with a transducer beam angle of 6.8° × 6.8°. The transducer was mounted on the starboard side of the vessel at a distance from the bow equal to one-third of the hull length; thus, the transducer could reach a depth of 0.5 m below the water. The vertical geographic position and the hydroacoustic route of the beam were recorded in real-time by Garmin GPS 17×HVS. The echosounder was connected to a laptop to display and store the hydroacoustic data in real-time by using Acquisition 6.0 software. Water temperature and salinity data required for the data acquisition program were determined using the YSI6600V2 multiparameter water quality monitor. To reduce the impact of vessel noise on the survey, the hydroacoustic survey was

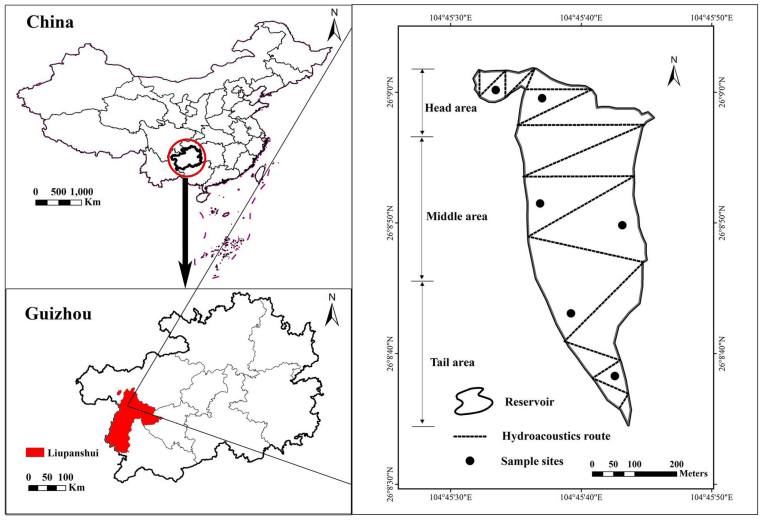

FIGURE 1
Map of Yuwanghe Reservoir in southwest China and the hydroacoustic sampling transects.

conducted along zigzag transects, with the vessel sailing at the speed of approximately 6–8 km·h^{-1} (Lian et al., 2018). The survey started from the head area of the reservoir and ended at the tail area (Figure 1). The route covered the entire reservoir. The investigation was repeated twice back and forth to ensure coverage of more than 6% (Matthias et al., 2012).

2.3 Fish sampling captures

Fish catch surveys were conducted to obtain the fish composition and community structure; the aim of these surveys was to determine the consistency between the hydroacoustic survey signals and the distribution of fish body length. Six fish sampling sites were selected, including two sites each at the head, middle, and tail areas (Figure 1). Composite gillnets of multiple meshes (50 m in length and 3 m in height; mesh size of 1.0, 1.6, 2.0, 2.5, 3.1, 4.0, 4.8, 6.0, 7.5, 8.5, 11.0, and 12.5 cm), trammel gillnets (200 m in length and 5 m in height; mesh size of 6.0, 8.0, 10.0, and 12.0 cm), and floor cage net (20 m in length, 0.4 m in width, 0.4 m in height, and mesh size of 5 mm) were used for the field sampling. The floor cage nets were installed in the coastal zone near each sample site at a position as distant as possible. The gillnets were installed at each sample site in the main area. The nets were set for 12 h from 17:00 to 5:00. Fish catches were identified, measured, and counted in fresh condition. Species identification was performed by referring to the guidelines of the Zoology of China (Chen, 1998; Yue, 2000). Spatial and trophic ecological niche classification was performed by referring to the Guizhou Fish Journal (Wu, 1989). Measurements were performed at the accuracy level of 1 mm in length and 0.01 g in weight.

2.4 Environmental variables

Quantitative samples of plankton and water were collected along with the catch collection. The plankton samples obtained from the mixtures of the bottom, middle, and surface water at each site were collected in 50- ml polyethylene bottles, and 1 ml of formaldehyde solution was added for preservation. The samples were then stored for laboratory tests (Zhang and Huang, 1991). Water samples were collected in 1, 000- ml black polyethylene bottles at a surface water depth of 0.5 m. The samples were brought to the laboratory under low temperature conditions to measure the content of total nitrogen, total phosphorus, ammonia nitrogen, and chlorophyll a. Water depth was measured based on acoustic signals. Water temperature, pH, dissolved oxygen, and conductivity were measured on site by using a YSI 6600V2 multiparameter water quality monitor (Zhang and He, 1991). A transparency disk was used to measure the water transparency.

2.5 Hydroacoustic data processing and analysis

The hydroacoustic data were converted and post-processed with Visual Analyzer version 4.3 software. Because the fish signals from the echosounder were scattered, the blind areas of detection and areas with high interference at 1 m below the level of the transducer and 0.5 m above the bottom of the probe were artificially eliminated; this step minimized the effect of noise (Li et al., 2022; Lian et al., 2022). The echograms of all survey sections were carefully examined and manually edited to regenerate the bottom surface if required. Background noise beyond the target signal, such as bubbles and noise interference from ships, was manually eliminated based on the characteristics of the echogram (Huang et al., 2019). To shield the echo signal from weak scatterers such as plankton, the minimum threshold in the target intensity echo image was set to –70 dB.

The total length of the fish was derived from the empirical formula (TS - TL) of target strength (TS) and total length (TL) of carp as proposed by Frouzova et al. (2005):

$$TS = 23.97lg\,TL - 103.9 \quad (1)$$

where TS is the target strength of the fish body, TL is the total length of the fish, and 103.9 is a constant value.

The conversion between the t otal length and the fish weight is based on the relational expression obtained by applying the power function $W = a^{*}TL^{b}$ (W is the fish weight and a and b are the parameters) to fit the total length and weight of the fish catch samples (Ricker, 1975; Ye et al., 2007).

The biomass for each transect was calculated by multiplying the average fish numerical density estimated acoustically with the weight corresponding to the average TS for this transect. The total biomass for the given area was calculated as a weighted mean.

2.6 Statistical analysis

The goodness of fit between fish catch samples and hydroacoustic data was analyzed by Mann–Whitney *U*-test. The differences between areas for mean fish density and fish biomass were analyzed with two-sample *t*-test. Pearson correlation coefficient was used to determine the correlation of fish spatial distribution and environmental factors. All analyses were completed with the OriginPro 2021 (OriginLab, 2021) and ArcGIS 10.2 software (Esri, 2013).

3 Result

3.1 Composition of fish catches

In the survey of fish catches, six species of fishes belonging to three orders and four families were found in Yuwanghe Reservoir, and a total of 1,892 fish were sampled. The status and the role of species in the community were classified according to their number and the weighted proportion of catches. Species with an index of relative importance (IRI) > 1,000 are defined as dominant, those with IRI between 100 to 1,000 are important species, those with IRI between 10 to 100 are common species, and those with IRI < 10 are occasional species (Jutagate and Sawusdee, 2022). On the basis of this criterion, topmouth gudgeon (*Pseudorasbora parva*) was the dominant species in the fish community, *Carassius auratus* and *Culter alburnus* were important species, and *Micropercops swinhonis* and *Paramisgurnus dabryanus* were common species (Table 1). The curve-fitting result between the total length and the weight of the fish catch samples (Figure 2) by using regression analysis showed that the relation formula was $W = 0.00295^{*}TL^{3.404}$ ($R^2 = 0.9755$), and the fitting degree was good.

3.2 Comparison between fish catches and hydroacoustic data

The total length range of the fish catches was 38 to 236 mm. Small fishes formed the main group, with more than 96% of the fish having a total length of <100 mm. The quantitative proportion of the fish in the catches decreased rapidly with the increase in the total length. The hydroacoustic survey showed that the target strength of fish was –62 to –48 dB, which showed a fluctuation in the value (Figure 3A). The target strength was concentrated in the range of –62 to –58 dB, with a peak strength appearing at around –58 dB. The total length of topmouth gudgeon, whose population accounted for 95.74% of the total population, ranged from 38 to 96 mm. Based on the empirical formula (Eq. 1), the target strength of –56 dB was converted into a length of approximately 100 mm. Thus, it can be inferred that the acoustic signal with the target strength of <–56 dB mainly originated from topmouth gudgeon. The results of the Mann–Whitney *U*-test indicated no significant difference ($P > 0.05$) in the total length between the fish catches and the hydroacoustic data; this finding indicated a good agreement between the results of the hydroacoustic survey and the field analysis (Figure 3B).

3.3 Horizontal distribution pattern of fish

The hydroacoustic survey showed an uneven horizontal distribution of fish in Yuwanghe Reservoir (Figure 4). Fish density

TABLE 1 Species composition and ecotypes of fish in Yuwanghe Reservoir.

Species	Vertical position	Feeding Type	TL/mm	Number percentage	Weight percentage	IRI
Cyprinidae						
Pseudorasbora parva	LL	O	58–96	95.74%	70.96	++++
Carassius auratus	LL	O	156–171	2.26%	12.59	+++
Culter alburnus	UL	C	38–228	1.01%	9.06	+++
Eleotridae						
Micropercops swinhonis	DL	O	46–52	0.36%	2.11	++
Cobitidae						
Paramisgurnus dabryanus	DL	O	87–191	0.53%	3.42	++
Synbranchidae						
Monopterus albus	DL	C	236	0.1%	1.86	++

LL, lower layer; UL, upper layer; DL, demersal layer; O, omnivorous; C, carnivorous.
++++, IRI >1,000; +++, 100 < IRI <1,000; ++, 10 < IRI <100.

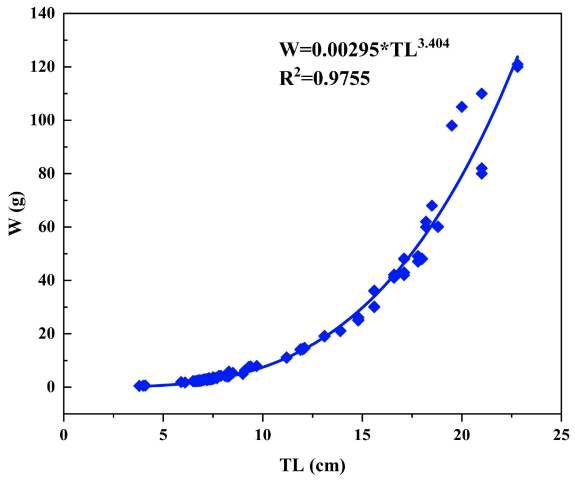

FIGURE 2
Relationship between total length and weight of the fish catches.

and fish biomass were significantly varied in the different areas of the reservoir ($P < 0.05$). The mean fish density of the entire reservoir was 318.7 ± 256.1 individuals/1,000 m^2, and the fish density tended to increase from the head area and the middle area to the tail area of the reservoir, with values of 168.5 ± 60.1 individuals/1,000 m^2, 306.8 ± 124.7 individuals/1,000 m^2, and 696.4 ± 288.9 individuals/1,000 m^2, respectively (Figure 5A). On the basis of the *W* - TL relation formula and the weighted average calculation, the mean fish biomass was 984.8 g/1,000 m^2, and the fish biomass from the head area and the middle area to the tail area of the reservoir was 532.5 ± 230.4 g/1,000 m^2, 1,264.2 ± 400.6 g/1,000, m^2 and 2,482.6 ± 600.8 g/1,000 m^2, respectively (Figure 5B). Based on fish density and biomass, the highest distribution of fish was in the tail area of the reservoir, and the lowest was in the head area (Figure 4).

3.4 Vertical distribution pattern of fish

Based on 3 m as the water layer according to the water depth of the reservoir, the proportion of fish density in different water layers in different areas of the reservoir to the sum of fish density in the entire water column was calculated as shown in Figure 5. The majority of the fish population was found in the water layer within the depth range of 0 to 12 m, where more than 97.3% of fish were distributed. In the water layer at depths of more than 12 m, the fish density tended to decrease gradually with the increase in water depth. However, differences were noted in the fish distribution pattern in the different areas of the reservoir along the vertical direction. Fish at the tail area preferred to move to the surface, and the proportion of fish in the depth range of 0 to 6 m was 81.5%; this proportion was higher than that at the head area (69.9%) and at the middle area (61.3%) (Figure 6). The reason for this difference may be the fact that the tail area of the reservoir has a shallow depth on average, and the fish were closer to the water surface. Consequently, the proportion of fish density in the surface waters was higher in the entire water column.

3.5 Relationship between fish distribution and environmental factors

According to Pearson correlation coefficient analysis, the main factors that influenced the fish distribution in Yuwanghe Reservoir were water depth (WD), water temperature (WT), dissolved oxygen (DO), total nitrogen (TN), and plankton (including zooplankton and phytoplankton) density (Figure 7). WT, DO, and plankton density were positively correlated with fish density, whereas WD was negatively correlated with fish density on the contrary. The pH, conductivity (Cond), total phosphorus (TP), ammonium nitrogen (NH_4^+–N), and chlorophyll a (Chl a) were not observed to have a significant connection with fish density.

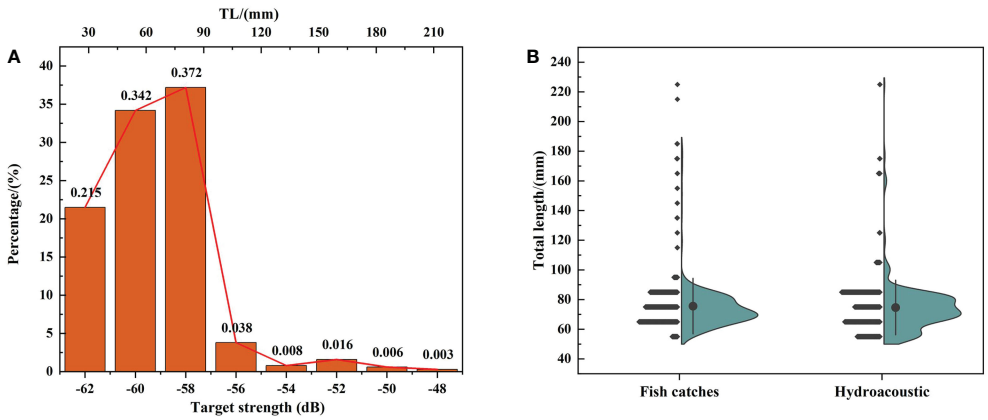

FIGURE 3
(A) Frequency distribution of fish target strength (TS). The bottom horizontal axis represents the intervals of TS (the width is 2 dB), the top horizontal axis represents the corresponding fish total length converted from fish target strength by empirical formula (1), and the vertical axis represents the percentage of individual fish corresponding to each interval of TS. **(B)** Comparison of fish catches and hydroacoustic data (fish target strength was converted to total length).

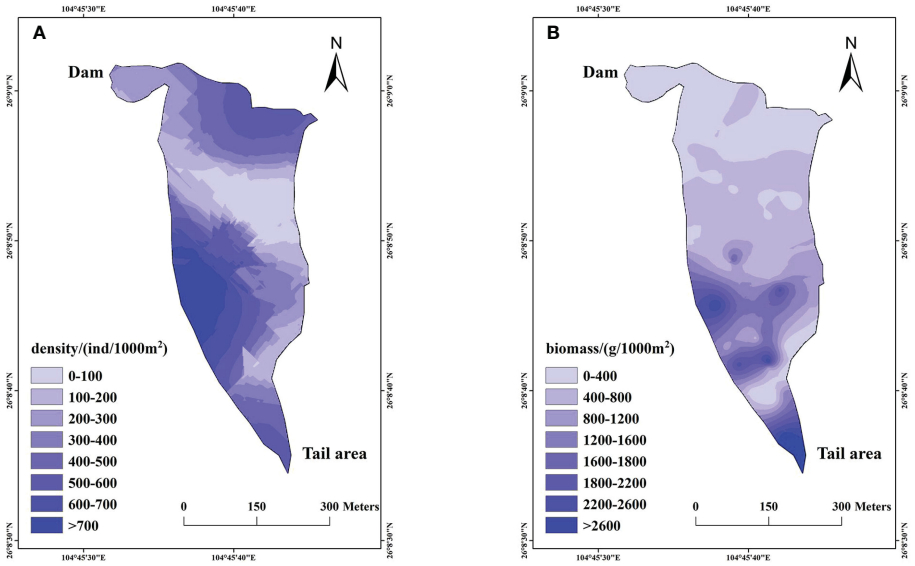

FIGURE 4
Horizontal distribution of fish in Yuwanghe Reservoir.

4 Discussion

4.1 Analysis of the fish community structure

From the survey data, only six species of fish were found in Yuwanghe Reservoir (Table 1). Regarding ecosystem stability, Yuwanghe Reservoir had fewer fish species, and the community structure was more based on a single species. Furthermore, the variety of trophic levels was poor, particularly for secondary consumers. A community with a very simple structure is extremely unstable and prone to retrograde succession under external interferences (Balazs et al., 2022; Wu et al., 2022). In terms of biological manipulation, the proportion of small fish in Yuwanghe Reservoir was too high. The hydroacoustic survey results showed the proportion of fish with a target strength of <–56 dB; accordingly, the proportion of fish with a total length of <100 mm was 92.9%. The proportion of fish with a total length of <100 mm in the collected fish catches was 96.3%, and the predominant species was topmouth gudgeon (*P. parva*). Zooplankton is an important prey population for small fish (Zhang, 2005; Liu et al., 2007; Lian et al., 2018). However, zooplankton feeds on phytoplankton, and the presence of a large number of small fish will result in a large decrease in zooplankton biomass in the water column, which is not favorable for controlling the phytoplankton biomass. Secondly, the absence of filter-feeding fish that feed on phytoplankton can easily lead to a massive growth of some algae under suitable conditions, which can trigger the occurrence of water blooms (Liu and Xie, 1999; Liu and Xie, 2003; Xie and Liu, 2001). Thirdly, because of the short generation cycle, early sexual maturity, and high reproductive capacity (Pollux and Korosi, 2006), topmouth gudgeon has been widely distributed in Central Asia, Europe, and North Africa in less than 50 years (Gozlan et al., 2010), and this fish species is listed as one of the most severe aquatic invasive species in Europe (Sala et al., 2000; Andreou et al., 2012) Following invasion into new areas, topmouth gudgeon poses a serious threat to the survival and reproduction of indigenous fish of the water bodies and can impair the stability of

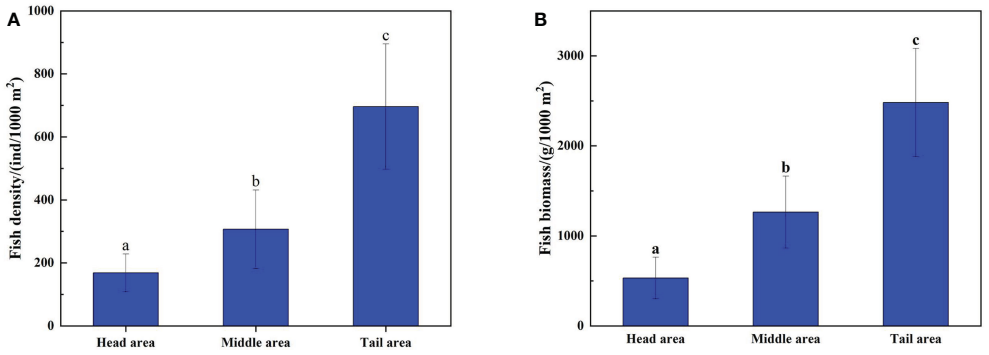

FIGURE 5
Horizontal distribution of the mean fish density [±SD, individuals/1,000 m^2 (**A**)] and biomass [±SD, g/1,000 m^2 (**B**)] in Yuwanghe Reservoir. Values with the same letters are not significantly different in different areas ($P > 0.05$); values with different letters are significantly different ($P < 0.05$).

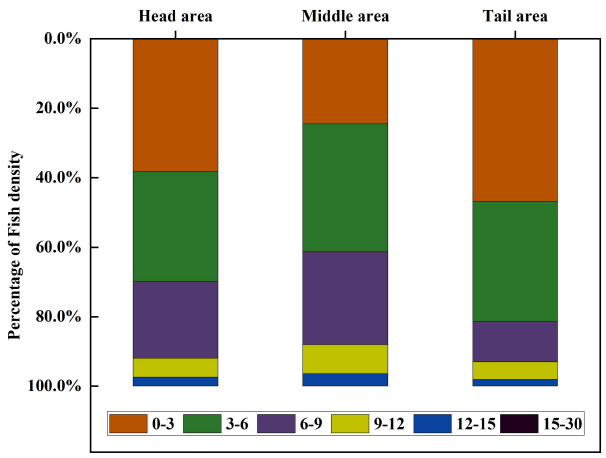

FIGURE 6
Vertical distributions of fish in Yuwanghe Reservoir.

aquatic ecosystems by competing for food and habitat, carrying new diseases, and changing the characteristics of the habitat (Fletcher et al., 2016)— for example, topmouth gudgeon invasion in the Yunnan Plateau lakes led to the reduction or even extinction of many native fish species and a series of knock-on ecological effects (Chen et al., 1998; Yan and Chen, 2009). In the British Lake District, the whelk has become the most abundant fish in the region after 4 years of invasion, thereby threatening the survival of other native fish species (Britton et al., 2007). Unfortunately, there were too few carnivorous fish in the reservoir, and topmouth culter (*Culter alburnus*) was the only carnivorous fish species; its proportion in the catches was also extremely low, with a population share of only 1.01%. Moreover, topmouth culter prefers to inhabit the upper layers of the water column, while topmouth gudgeon inhabits the lower layers; this makes the topmouth culter population insufficient in gaining effective control over topmouth gudgeon in terms of energy conversion efficiency and habits.

4.2 Analysis of the fish distribution and its influencing factors

In the horizontal direction of Yuwanghe Reservoir, the fish densities and biomass showed a trend of gradual increase from the head area to the tail area of the reservoir; this trend was related to WT, DO, TN, and plankton feed from the correlation analysis between fish density and environmental factors (Figure 7). Although there was no significant difference in water temperature between the different areas of Yuwanghe Reservoir, the overall trend of a gradual increase in temperature from the head area to the middle area to the tail area of the reservoir was observed. Fish do not like to move in areas with low water temperatures; hence, the fish density tends to increase as they move further away from the dam. A similar result was reported by Prchalova et al. in their study on Rimov Reservoir (Prchalová, 2009). The DO and TN levels were another major cause of differences in fish horizontal densities. The inflowing river is located at the tail area of the reservoir, and the highest DO levels are found at the tail area of the reservoir where the water flows in. The DO concentration slowly decreased as the exogenous nutrient salts diffused away from the inlet river. As the predominant species in Yuwanghe Reservoir, topmouth gudgeon prefers to inhabit shallow waters (Asaeda and Manatunge, 2005; Asaeda and Manatunge, 2007). The shallow water area of Yuwanghe Reservoir provides the necessary habitat for *P. parva*, and it also has little risk of fish predation because of the low percentage of carnivorous fish. Consequently, fish density is higher in shallow waters than in deep water. Furthermore, the sampling survey of plankton in Yuwanghe Reservoir revealed that the horizontal distribution of plankton in the reservoir area showed a gradual increase from the head area to the tail area of the reservoir; thus, the difference in bait organisms was also a primary factor that led to a difference in the horizontal distribution pattern of fish in Yuwanghe Reservoir in the present study.

Vertically, most of the fish in Yuwanghe Reservoir were distributed in the water layer within a depth of 0 to 12 m, and the fish density tended to decrease gradually with the increase in water depth. Some studies have been conducted on the distribution of fish density or biomass in different water layers. Mou et al. (2012) surveyed Hongfeng Lake, a large deep lake, by using the hydroacoustic method, and they found significant differences in fish density in different water layers, and the fish density gradually decreased with an increase in water depth. Lian et al. (2018) reported that more than 97.6% of fish were distributed in the water layer within the depth range of 0 to 10 m in a hydroacoustic study of deep-water reservoirs in Yunnan Plateau. Zhou et al. (2021) showed a negative correlation between fish density distribution and water depth in Hongchaojiang Reservoir. The results of the present study agreed with those of former studies. Fish lack the ability to regulate body temperature, and most warm-water fish prefer a suitable water temperature of 20 to 30°C; consequently, the either too high or too low water temperature will affect the growth and movement of fish (Yin, 1995). Hence, most fish tend to stay away from the water layer below the thermocline, while zooplanktons—which is the food of most fish —are mainly distributed in the water layer above the thermocline

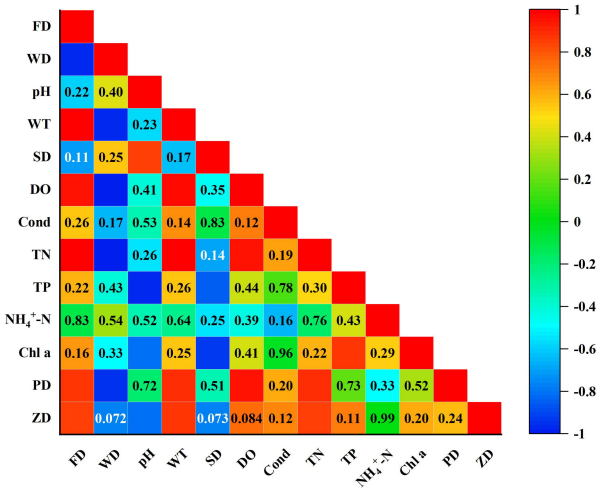

FIGURE 7
Pearson correlation between environmental factors and fish density. FD, fish density; WD, water depth; WT, water temperature; SD, Secchi disk depth; DO, dissolved oxygen; Cond, conductivity; TN, total nitrogen; TP, total phosphorus; NH_4^+–N, ammonia nitrogen; Chla, chlorophyll a; PD, phytoplankton density; ZD, zooplankton density. The different colors represent the size of the correlation coefficient; the number in the box is the *P*-value, and $P < 0.05$ is not displayed (significant level is 0.05).

(Lian et al., 2018). DO is also an important factor that affects the vertical distribution of fish. In general, DO concentration in the deep-water reservoir gradually decreases as the water depth increases; thus, fish will actively migrate to avoid low-oxygen or anoxic water (He and Cai, 1998; Lian et al., 2018). It was also the reason why most fish species were distributed in the upper water layer in the present study.

5 Conclusion

Yuwanghe Reservoir is a typical plateau deep-water reservoir in the early impoundment stage. Presently, although the quality of water is good and the phytoplankton biomass level is low, its biological community structure is relatively homogeneous, and topmouth gudgeon is the dominant species. There are serious concerns regarding the invasion of topmouth gudgeon into plateau lakes, which would severely affect the stability of water ecosystems (Chen et al., 1998). Typical examples include Tien Lake, Lake Erhai, and Fuxian lake in Yunnan, where the population of many indigenous fish species is declining or endangered because of the invasion of topmouth gudgeon (Yan and Chen, 2009; Li et al., 2017). In the absence of artificial control of the topmouth gudgeon population, the survival environment of indigenous fish in Yuwanghe Reservoir and the surrounding waters will be threatened, and a series of chain ecological effects will occur, which will be easily affected by human activities around the reservoir area, resulting in the occurrence of water deterioration events, such as eutrophication, in the future. We also found that the proportion of carnivorous fish was too low, which cannot control the population of topmouth gudgeon under natural conditions. Therefore, native carnivorous fish should be introduced to control the size of the small fish population to adjust the fish community structure; this can reduce the feeding pressure of small fish on zooplankton and thus control the phytoplankton population. Moreover, because of the current lack of filter-feeding fish, the reservoir should be appropriately increased, and silver and bighead carp should be released in the reservoir. This will strengthen the filter-feeding effect on plankton to prevent their proliferation and thus cause a competitive environment in the reservoir and also yield certain economically beneficial effects.

Data availability statement

The original contributions presented in the study are included in the article/supplementary material. Further inquiries can be directed to the corresponding author.

Ethics statement

This study was reviewed and approved by Research Ethics Committee of Institute of Hydrology, Chinese Academy of Sciences.

Author contributions

BL (co- first author): investigation, data curation, methodology, formal analysis, and writing—original draft. XZ (co- first author): data curation, methodology, writing—review and editing, and project administration. CZ: investigation, data curation, and writing—review and editing. JB: investigation, data curation, and writing—review and editing. FM: investigation, data curation, and writing—review and editing. YL: writing—review and editing. DZ: investigation and data curation. SH: investigation and data curation. LG: writing—review and editing. MD: conceptualization, writing—review and editing, and project administration. All authors contributed to the article and approved the submitted version.

Funding

This work was financially supported by the Guizhou Province Science and Technology Support Plan (numbers 2022129 and 2022165), the Science and Technology Poverty Alleviation Program of the Chinese Academy of Sciences (number KFJ-FP-202102), the National Natural Science Foundation of China (numbers 32202914 and 32172955), the National Key R and D Program of China (number 2022YFB 3206903), the Scientific Instrument Developing Project of the Chinese Academy of Sciences (number YJKYYQ 20190055), and the Special Program for the Institute of National Parks of the Chinese Academy Sciences (number KFJ-STS-ZDTP-2021-003).

Acknowledgments

The authors thank the vessel crew and staff at Guizhou Province Reservoir Operation and Management Corporation in Liupanshui for their collaboration.

Conflict of interest

The authors declare that the research was conducted in the absence of any commercial or financial relationships that could be construed as a potential conflict of interest.

Publisher's note

References

Andreou, D., Arkush, K. D., Guégan, J. F., and Gozlan, R. E. (2012). Introduced pathogens and native freshwater biodiversity: a case study of sphaerothecum destruens. *PloS One* 7, e36998. doi: 10.1371/journal.pone.0036998

Anne, M., Chloe, G., Thomas, A., Helge, B., Anne, L. D., Malgorzata, G., et al. (2019). Including 38 kHz in the standardization protocol for hydroacoustic fish surveys in temperate lakes. *Remote sens. Ecol. conserv.* 5, 332–345. doi: 10.1002/-rse2.112

Asaeda, T., and Manatunge, J. (2005). Foraging of a small planktivore (*Pseudoras-bora parva*: Cyprinidae) and its behavioral flexibility in an artificial stream. *Hydrobiol.* 549, 155–166. doi: 10.1007/s10750-005-5442-1

Asaeda, T., and Manatunge, J. (2007).). physiological responses of topmouth gudge-on, *Pseudorasbora parva*, to predator cuesand variation of current velocity. *Aquat. Ecol.* 2007, 41, 111–118. doi: 10.1007/s10452-006-9048-0

Balazs, K. R., Munson, S. M., and Butterfield, B. J. (2022). Functional composition of plant communities mediates biomass effects on ecosystem service recovery across an experimental dryland restoration network. *Funct. Ecol.* 36, 2317–2330. doi: 10.1111/1365-2435.14129

Britton, J. R., Davies, G. D., Brazier, M., and Pinder, A. C. (2007). A case study on the population ecology of a topmouth gudgeon (Pseudorasbora parva) population in the UK and the implications for native fish communities. *Aquat. Conserv. Mar. Freshw. Ecosyst.* 17, 749—759. doi: 10.1002/aqc.809

Bureau of Fisheries (2021). "Ministry of agriculture and rural affairs," in *China Fishery statistical yearbook* (Beijing: China: Agriculture Press).

Chen, Y. Y. (1998). *Fauna sinica, Osteichthyes, cypriniformes II* (Beijing: Science Press).

Chen, Y. R., Yang, J. X., and Li, Z. Y. (1998). The diversity and present status of fishes in yunnan province. *Chin. Biodiversity.* 6, 272–277.

Drastik, V. M., Godlewska, H., Balk, P., Clabburn, J., Kubecka, E., Morrissey,, et al. (2017). Fish hydroacoustic survey standardization: a step forward based on compareso-ns of methods and systems from vertical surveys of a large deeplake. *Limnol. Oceanogr. Methods* 15, 836–846. doi: 10.1002/lom3.10202

Esri (2013). *ArcGIS 10.2. a GIS software for discovering, consuming, creating, and sharing geographic data, maps, and apps designed to fulfill particular objectives* (California, USA). Available at: https://www.esri.com/en-us/home.

Fletcher, D. H., Gillingham, P. K., Britton, J. R., Blanchet, S., and Gozlan, R. E. (2016). Predicting global invasion risks: a management tool to prevent future introductions. *Sci. Rep.* 1, 26316. doi: 10.1038/srep26316

Frouzova, J., Kubecka, J., Balk, H., and Frouz, J. (2005). Target strength of some european fish species and its dependence on fish body parameters. *Fish. Res.* 75, 86–96. doi: 10.1016/j.fishres.2005.04.011

Godlewska, M., Świerzowski, A., and Winfield, I. J. (2004). Hydroacoustics as a tool for studies of fish and their habitat. *Ecohydrol. Hydrobiol.* 4, 417–427.

Gozlan, R. E., Britton, J. R., Cowx, I., and Copp, G. H. (2010). Current knowledge on non-native freshwater fish introductions. *J. Fish Biol.* 76, 751–786. doi: 10.1111/j.1095-8649.2010.02566.x

Guillard, J., Simier, M., Albaret, J. J., Raffay, J., Sow, I., and Tito, M. L. (2012). Fish biomass estimates along estuaries: A comparison of vertical acoustic sampling at fixed stations and purse seine catches. *Estuar. Coast. Shelf Sci.* 107, 105–111. doi: 10.1016/j.ecss.2012.05.022

Guo, A. H., Liu, J. D., Yuan, J. L., Hao, Y. B., Xin, J. M., and Gu, Z. M. (2018). Assessment of stock enhancement performance in reservoir using hydroacoustic method. *Fish. Sci.* 37, 201–207. doi: 10.16378/j.cnki.1003-1111.2018.02.009

Guo, L., Wang, Q., Xie, P., Tao, M., Zhang, J., Niu, Y., et al. (2015). A non-classical biomanipulation experiment in gonghu bay of lake taihu: Control of microcystis blooms using silver and bighead carps. *Aquacult. Res.* 46, 2211–2224. doi: 10.1111/are

Han, B. P. (2010). Reservoir ecology and limnology in China: a retrospective comment. *J. Lake Sci.* 22, 151–160.

He, L. (2016). *Investigation on present situation of fishery resources in tongwan reservoir* (Changsha: Hunan Agriculture University).

He, D. R., and Cai, H. C. (1998). *Fish behaviors* (Xiamen: Xiamen University Press).

Huang, G., Wang, Q. D., Chen, X. H., Godlewska, M., Lian, Y. X., Yuan, J., et al. (2019). Evaluating impacts of an extreme flood on a fish assemblage using hydroacoustics in a large reservoir of the Yangtze river basin, China. *Hydrobiologia.* 841, 31–43. doi: 10.1007/s10750-019-04003-4

Jutagate, T., and Sawusdee, A. (2022) Catch composition and risk assessment of two fishing gears used in small-scale fisheries of bandon bay, the gulf of Thailand. *Peer J.* doi: 10.10.7717/peerj.13878

Kubečka, J., Hohausova, E., Matena, J., Peterka, J., Amarasinghe, U. S., Bonar, S. A., et al. (2009). The true picture of a lake or reservoir fish stock: A review of needs and progress. *Fish. Res.* 96, 1–5. doi: 10.1016/j.fishres.2008.09.021

Li, H. J., Wang, Y. P., Leng, Q. L., Li, X. J., Li, X. F., Yu, T. L., et al. (2017). Study on the age and growth of *Pseudorasbora parva* from nanwan lake upstream the huaihe river. *Acta Hydrobiol. Sinca.* 41, 835–842. doi: 10.7541/2017.104

Li, H. F., Zhang, H., Yu, L. X., Cao, K., Wang, D. Q., Duan, X., et al. (2022). Managing water level for Large migratory fish at the poyang lake outlet: Implications based on habitat suitability and connectivity. *Water.* 14, 2076. doi: 10.3390/w14132076

Lian, Y. X., Huang, G., Godlewska, M., Li, C., Zhao, X., Ye, S. W., et al. (2015). Hydroacoustic assessment of spatio-temporal distribution and abundance of fish resource in the xiangxi river. *Acta Hydrobiol. Sinca.* 39, 920–929.

Lian, Y. X., Li, C., Ye, S. W., Li, W., Liu, J. ,. S., and Li, Z. ,. J. (2018). Fish spatial distribution patterns and controlling factors in yudong reservoir, yunnan plateau. *J. Lake Sci.* 30, 1755–1765. doi: 10.18307/2018.0626

Lian, Y. X., Ye, S. W., Godlewska, M., Huang, G., Wang, J. C., Liu, J. S., et al. (2022). Comparison of two types of survey designs for acoustic estimates of fish resources in the three gorges reservoir, China. *Water.* 14, 2745. doi: 10.3390/w14172745

Liu, E. S., Bao, C. H., Wu, L. K., and Cao, P. (2007). Comparison of food composition and analysis on mutual effects between *Neosal anx tangkah-keii taihuensis chen* and *Coilia ecten taihuensis yen et lin* in lake taihu. *J. Lake Sci.* 19, 103–110. doi: 10.18307/2007.0116

Liu, J. K., and Xie, P. (1999). Unraveling the enigma of the disappearance of water bloom from the East lake (Lake donghu) of wuhan. *Resour. Environ. Yangtze Basin.* 8, 312–319.

Liu, J. K., and Xie, P. (2003). Direct control of microcystis bloom through the use of planktivorous carp-closure experiments and lake fishery practice. *Ecol. Sci.* 22, 193–196.

Liu, Q. G., and Zhang, Z. (2016). Controlling the nuisance algae by silver and bighead carps in eutrophic lakes: disputes and consensus. *Lake Sci.* 28, 463–475. doi: 10.18307/2016.0301

Lv, H. (2019). *Study on sources and migration characteristics of heavy metals in water and suspended particulates of aha reservoir, guizhou province* (Tianjin: Tianjin University), 0043–0012. doi: 10.27356/d.cnki.gtjdu.2019

Maclennan, D. N., and Simmonds, E. J. (2005) *Fisheries acoustics: Theory and practice.* (Oxford: Blackwell Science). doi: 10.1002/9780470995303

Matthias, E., Ian, J. W., Winfield, J. G., Jean, G., Atle, R., Charlotte, V., et al. (2012). Strong correspondence between gillnet catch per unit effort and hydroacoustically derived fish biomass in stratified lakes. *Freshw. Biol.* 57, 2436–2448. doi: 10.1111/fwb.12022

Mou, H. M., Yao, J. J., Ni, C. H., Fang, G. Z., An, M., and Ma, S. (2012). Hydroacoustic survey of fish resource and spatial distribution in hongfeng lake. *S. China Fish. Sci.* 8, 62–69.

OriginLab (2021). *OriginPro: A software for data analysis and graphing* (Massachusetts, USA). Available at: https://www.originlab.com.

Ou, T. (2015). *Dynamic changes of phytoplankton community structure and its affecting factors in three reservoir of guizhou plateau* (Guiyang: Guizhou Normal University).

Pollux, B. J. A., and Korosi, A. (2006). On the occurrence of the Asiatic cyprinid *Pseudorasbora parva* in the Netherlands. *J. Fish Biol.* 69, 1575–1580. doi: 10.1111/j.1095-8649.2006.01218.x

Prchalová, M., Kubečka, J., Čech, M., Frouzová, J., Draštík, V., Hohausová, E., et al. (2009). The effect of depth, distance from dam and habitat on spatial distribution of fish in an artificial reservoir. *Ecol. Freshw. Fish.* 18, 247–260. doi: 10.1111/j.1600-0633.2008.00342.x

Ricker, W. E. (1975). Computation and interpretation of biological statistics of fish populations. *Bull. Fish. Res. Board Can.* 191, 1–382.

Sala, O. E., Chapin, F. S., Armesto, J. J., Berlow, E., Bloomfield, J., Dirzo, R., et al. (2000). Global biodiversity scenarios for the year 2100. *Sci.* 287, 1770–1774. doi: 10.1126/science.287.5459.1770

Samedy, V., Wach, M., Lobry, J., Selleslagh, J., Pierre, M., Josse, E., et al. (2015). Hydroacoustics as a relevant tool tomonitor fish dynamics in large estuaries. *Fish. Res.* 172, 225–223. doi: 10.1016/j.fishres.2015.07.025

Winfield, I. J., Bean, C. W., Gorst, J., Gowans, A. R. D., Robinson, M., and Thomas, R. (2013). Assessment and conservation of whitefish (*Coregonus lavaretus*) in the UK. *Adv. Limnol.* 64, 305–321. doi: 10.1127/1612-166X/2013/0064-0023

Wu, L. (1989). *Fishes of guizhou province* (Guiyang: Guizhou People's press).

Wu, W. J., Yang, K., Wang, Z. C., Li, G. B., and Liu, Y. D. (2012). Community structure and seasonal succession of phytoplankton in yudong reservoir of yungui plateau. *J. Hydroecol.* 33, 69–75. doi: 10.15928/j.1674-3075.2012.02.005

Wu, J. X., Yang, H. Q., Yu, W., Yin, C., He, Y., Zhang, Z., et al. (2022). Effect of ecosystem degradation on the source of particulate organic matter in a karst lake: A case study of the caohai lake, China. *Water.* 14, 1867. doi: 10.3390/w14121867

Xie, S. G., Cui, Y. B., and Li, Z. J. (2003). Studies on resource utility patterns of lake fish communities: progress and methods. *Acta Hydrobiol. Sinca.* 27, 78–84.

Xie, P., and Liu, J. K. (2001). Practical success of biomanipulation using filter-feeding fish to control cyanobacteria blooms: A synthesis of decades of research and application in a sub-tropical hypereutrophic lake. *Sci. World.* 1, 337–356. doi: 10.1100/tsw.2001.67

Yan, Y., and Chen, Y. (2009). Variations in reproductive strategies between one invasive population and two native populations of *Pseudorasbora parva*. *Curr. Zoology.* 55, 56–60. doi: 10.1093/czoolo/55.1.56

Ye, S. W., Li, Z. ,. J., Feng, G. P., and Cao, W. (2007). Length-weight relationships for thirty fish species in lake niushan, a shallow macrophytic Yangtze lake in China. *Asian Fish. Sci.* 20, 217–226. doi: 10.33997/j.afs.2007.20.2.007

Yin, M. C. (1995). *Fish ecology* (Beijing: Agriculture Press).

Yue, P. Q. (2000). *Fauna sinica, Osteichthyes, cypriniformes III* (Beijing: Science Press).

Zhang, T. L. (2005). *Life-history strategies, trophic patterns and community structure in the fishes of lake biandantang* (Wuhan: Institute of Hydrobiology, Chinese Academy of Sciences).

Zhang, J. M., and He, Z. H. (1991). *Inland waters fisheries natural resources survey manual*. (Beijing: China Agriculture Press).

Zhang, Z. S., and Huang, X. F. (1991). *Research methods of freshwater plankton* (Beijing: Science Press).

Zhou, L., Li, Y. S., Shi, J., Han, Y. Q., Kuang, T. X., Wu, W. J., et al. (2021). Spatial distribution of fish resources and its correlation with environmental factors in the hongchaojiang reservoir based on hydroacoustic detection. *Prog. Fish. Sci.* 42, 1–10.

frontiers | Frontiers in Marine Science

TYPE Original Research
PUBLISHED 30 March 2023
DOI 10.3389/fmars.2023.1120205

OPEN ACCESS

EDITED BY
Ce Shi,
Ningbo University, China

REVIEWED BY
Yong Cui,
Yellow Sea Fisheries Research Institute (CAFS), China
Ren Xiaozhong,
Dalian Ocean University, China

*CORRESPONDENCE
Xu Yang
2022188@zjou.edu.cn
Jiajun Hu
z20095136212@ziou.edu.cn

SPECIALTY SECTION
This article was submitted to Marine Fisheries, Aquaculture and Living Resources, a section of the journal Frontiers in Marine Science

RECEIVED 09 December 2022
ACCEPTED 04 January 2023
PUBLISHED 30 March 2023

CITATION
Zhang Y, Yang X, Hu J, Qu X, Feng D, Gui F and Zhu F (2023) Effect of inlet pipe design on self-cleaning ability of a circular tank in RAS.
Front. Mar. Sci. 10:1120205.
doi: 10.3389/fmars.2023.1120205

Effect of inlet pipe design on self-cleaning ability of a circular tank in RAS

Yuji Zhang[1], Xu Yang[1*], Jiajun Hu[1*], Xiaoyu Qu[2], Dejun Feng[1], Fukun Gui[1] and Fang Zhu[3]

[1]National Engineering Research Center for Marine Aquaculture, Zhejiang Ocean University, Zhoushan, China, [2]School of Fisheries, Zhejiang Ocean University, Zhoushan, China, [3]School of Naval Architecture and Maritime, Zhejiang Ocean University, Zhoushan, China

To improve the water reuse efficiency of circular recirculating aquaculture tanks in Recirculating Aquaculture Systems (RAS) this research investigated the effect of inlet pipe deployment distance *d* (the distance between the stream tube hole and the tank wall) and the inlet pipe deployment angle α (the acute angle between the inlet pipe jetting direction and the nearest tank wall) on the self-cleaning ability of the circular aquaculture tank under dual and single inlet pipe designs. First, waste collection experiments were conducted to figure out the preferable inlet pipe design based on the efficiency of waste collection. Then, flow field measurement experiments were carried out employing the Particle Image Velocimetry (PIV) technique to measure the flow field in the near bottom layer of the tank, and the essential mechanism of the inlet pipe deployment on the waste collection was explored by analyzing the flow field and the corresponding hydrodynamic characteristic indicators, such as the average flow velocity (v_{avg}), the uniformity coefficient of water flow (DU50), and the water resistance coefficient (Ct). The results indicate that the variations of waste movement, flow filed and hydrodynamic indicators are consistent in both designs of dual inlet and single inlet, and merely differ in the absolute value. Based on the comprehensive analysis, the optimal performance of self-cleaning can be obtained at α=0°~10°, 20°~30°, 40°~50° for d=1/2 *r*, 1/4 *r*, and 1/50 *r*, respectively. At the same flow rate condition, the jetting velocity of the inlet pipe in the single inlet pipe design is significantly greater than that in the dual inlet pipe design, and the hydrodynamic characteristics of the waste collection are better. Therefore, in circulating water aquaculture production, it is recommended to design the inlet pipe in a similar aquaculture tank to the single inlet pipe with d=1/4 *r*, α=20°~30°, thus improving the self-cleaning ability of the aquaculture tank. The study results also provide a reference for adjusting the inlet pipe in circular recirculating aquaculture tank.

KEYWORDS

recirculating water aquaculture, flow field distribution, waste collection, hydrodynamic characteristics, circular aquaculture tank

1 Introduction

China is the world's largest aquaculture country, with aquaculture production accounting for most of the world's total aquaculture production, but many problems need to be solved, such as low efficiency of the current production system, pollution of the aquaculture environment, and frequent occurrence of diseases. Under resource and environmental constraints, the Recirculating Aquaculture System (RAS) has been recognized as an effective solution for increased biosecurity and control of parasites and pathogens and gradually becomes one of the main directions for the future development of aquaculture in China. RAS is an advanced aquaculture method with a high level of aquaculture technology and a controllable aquaculture environment, which has the advantages of integrated use of space and water, intensive production, and fewer negative environmental impacts. Thus, it performs much better than traditional aquaculture methods, such as ponds and open-water aquaculture in the outdoor environment. Effective removal of offish wastes (uneaten feed and feces) is crucial for RAS since they can be decomposed into fine particles and release a series of harmful substances to cultured fishes. Overall, improving the self-cleaning ability to remove fish wastes from tank water is conducive to enhancing the water quality of the aquaculture system to maintain a good culture environment and achieve satisfactory production.

A good flow environment of aquaculture tanks contributes to the welfare and growth of cultured fish. The circular tank is widely used in RAS. However, there is few design criteria in particles to guide the inlet pipe design. Thus, it is of vital importance to figure out the effect of inlet pipe design on the flow environment to improve the self-cleaning ability of circular tanks. Many previous studies have focused on this problem and given many helpful results. Tvinnereim et al. (1989) and Skybakmoen et al. (1989) compared the effects of four inlet pipe designs of open-ended pipe point source, vertical inlet pipe with evenly spaced holes, lateral inlet pipe with evenly spaced holes, and a combination of horizontal and vertical inlet pipes. They recommended using the lateral inlet pipe to drive the water body in actual production, and the formula for calculating the average flow velocity in the culture tank was also given. Burrows et al. (1995) advanced the experimental method by injecting pigments into a model circular aquaculture tank to observe pigment distribution to visualize its hydrodynamic characteristics. Benoit et al. (2007) showed through an experiment that different inlet pipe angles significantly affect the flow field distribution in the aquaculture tank. Firstly, three-dimensional unsteady models were established by replacing a rectangular tank with a circular arc tank. Then, the hydrodynamics of recirculating aquaculture tanks were analyzed, including velocity distribution, vorticity strength, energy effective utilization coefficient, and the flow uniformity index. Furthermore, flow characteristics, including the evolution of turbulent structures and the relevant influence factors, were also analyzed. Finally, a comprehensive performance index was proposed to effectively evaluate the spatial utilization and hydrodynamic characteristics for different aquaculture tanks. In addition to experiments, numerical techniques have been widely applied to analyze the flow field and improve fish wastes removal efficiency (Ren et al., 2020; Xue et al., 2020). The study of Davidson et al. (2004) demonstrated that the deployment angle of the jetting pipe is an important parameter affecting the tangential and radial flow velocity in the aquaculture tank, while the average flow velocity (vavg) in the aquaculture tank is an important indicator of waste collection ability, and the larger the average flow velocity, the better the waste collection ability. Good water flow uniformity in the aquaculture tank can make the distribution of dissolved oxygen more uniform, which is beneficial to the growth of aquaculture objects. Oca and Masalo et al. (2013) used the velocity distribution uniformity coefficient (DU50) to measure velocity distribution uniformity. In addition, characteristic quantities such as torque, friction coefficient, wall shear stress, velocity gradient, and kinetic energy gradient affect the flow field distribution, the effect of waste collection and discharge, and the distribution pattern of dissolved oxygen in the tank. Venegas et al. (2014) conducted experiments on the effect of the injector on flow field characteristics in a circular aquaculture tank, where the inlet system was switched to an injector. Studies have indicated that injectors obtain better results than the conventional setup, e.g., producing significantly higher tangential velocity and uniformity of the flow field and lower mixing times and secondary flow patterns, thus ensuring self-cleaning of fish wastes. The hydrodynamic characteristics of the waste collection of the aquaculture tank have been studied by investigating the waste collection or discharge ability in the aquaculture tank. Optimizing the design of the tank shape and the internal structure parameters of the aquaculture tank system can improve the flow field conditions in the aquaculture tank, which is crucial to increasing energy utilization and improving the collection and discharge performance of the aquaculture tank system. investigated the effect of different water intake structures on the flow velocity and discharge in a circular aquaculture tank. They considered that the key to waste discharge was that the flow velocity at each point of the tank bottom was greater than the starting flow velocity of waste. Oca et al. (2007) carried out a comparative analysis of water flow patterns in rectangular aquaculture tanks with four different inlet and outlet modes, and they used Particle Tracking Velocimetry (PTV) to track the flow patterns in the tank. The study results indicated that the horizontal tangential inlet mode effectively reduces the low-flow velocity vortex zone, leading to higher and more uniform flow velocity in the tank and avoiding sludge settling. Currently, there are few studies on the self-cleaning ability of different inlet modes of circular aquaculture tanks, and the change in the parameters of the aquaculture tank system will directly affect the hydrodynamic characteristics of the aquaculture tank, which further affects the waste collection and discharge performance. Therefore, it is necessary to conduct in-depth systematic research on the self-cleaning ability of circular aquaculture tanks, optimize the flow field characteristics of the system, and enhance the self-cleaning ability of the aquaculture tank, thus ensuring the stable operation of the aquaculture tank system.

Currently, Hu et al. (2022) have explored the self-cleaning ability of octagonal aquaculture tanks and the results indicated that the inlet pipe design has considerable effects on the hydrodynamic characteristics and further the performance of fish wastes collection and discharge within the tank. However, similar studies on circular

aquaculture tanks are rare. To further investigate the self-cleaning ability of circular aquaculture tanks, this paper conducts an in-depth systematic study on the self-cleaning ability of circular aquaculture tanks based on the research of Hu et al. (2022). The study results can guide the design of the most common circular aquaculture tanks in actual production.

2 Material and methods

To elucidate the effect of inlet pipe design on the aquaculture tank's self-cleaning ability, waste collection and flow field experiments in the aquaculture tank were carried out. The details of the experiments are as follows.

2.1 Waste movement collection experiments in aquaculture tank

2.1.1 Setup of waste collection experiments

The experiment on the effect of the inlet pipe design on waste collection in the aquaculture tank was conducted at the National Engineering Research Center for Marine Aquaculture, Zhejiang Ocean University. The aquaculture tank is connected to the conical barrel through a wire pipe, and the water in the tank forms a circulation through the pump. As indicated in Figure 1, the blue arrow represents the direction of water flowing out of the aquaculture tank, and the red arrow represents the direction of water flowing into the aquaculture tank. The circular tank is made of transparent acrylic sheets, with a height of 50 cm, an internal diameter of 98 cm, a flat bottom, and a drainage opening right in the center with a diameter of 5 cm. The circular tank is placed on an operating table made of aluminum profiles. The inlet pipe is a rigid PVC pipe with an external diameter of 20 mm, which is set up on an aluminum operating table, and the distance of the inlet pipe is adjusted by changing the length of the horizontal PVC pipe above the aquaculture tank. A dial is placed at the connection of the inlet pipe and the bracket, a pointer is set on the inlet pipe in the same direction as the inlet, and the pointer is kept relatively stationary with the inlet pipe. When the inlet pipe turns, the pointer points out the corresponding angle on the dial, thus adjusting the angle of the inlet pipe. The flow meter measurement system consists of a valve and two flow meters (Keyence FD-Q20C) mounted on the inlet pipe. The valve regulates the volume of the water flow in the inlet pipe, and the flow meter monitors the flow rate (L/min) of the water input from the inlet pipe to the aquaculture tank in real time, thus achieving precise control of the inlet pipe flow. The inlet pipe has three uniform round holes of 5 mm at an interval of 3 cm from the bottom so that water enters the aquaculture tank evenly. The image acquisition system consists of a high-definition camera (VA-200PRO) placed directly above the tank and the corresponding control software, which mainly records the waste particle's movement process. Besides, a white film is laid on the bottom of the aquaculture tank to more clearly capture the waste distributed at the bottom of the tank.

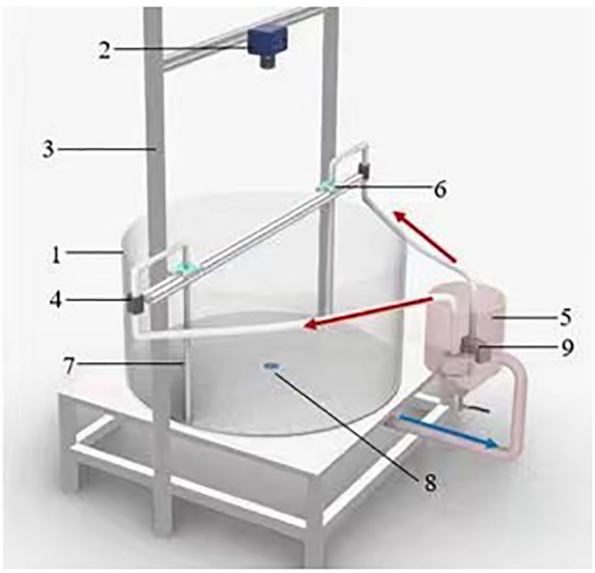

FIGURE 1
Diagram of experiment setup 1. Aquaculture tank; 2. Camera; 3. Aluminum bracket; 4. Flowmeter; 5. Cone-shaped bucket; 6. Angle adjusting device; 7. Inlet pipe; 8. Outlet hole; 9. Water pump.

2.1.2 Design of waste collection experiment

The effect of the deployment and the angle of the inlet pipe driven by the jet on the waste collection characteristics in the circular aquaculture tank is mainly studied in this research. The experimental design water depth for measuring the waste collection characteristics was 20 cm, the diameter-to-depth ratio (diameter/water depth) was about 5:1, the inlet flow rate was 5.2 L/min (the flow velocity at each inlet was about 0.51 m/s in the dual inlet experiment and about 1.02 m/s in the single inlet experiment, and the hydraulic retention time is about 30 minutes. Based on the previous studies Hu et al. (2021) and the inlet pipe design in aquaculture practices, we totally designed 54 inlet pipe design cases in this experiment, including two inlet pipe designs of a single inlet pipe and dual inlet pipes (Figure 2) three groups of inlet pipe layout distance of d=1/50 r, 1/4 r, and 1/2 r, and nine groups of inlet pipe design angles: α=0°, 10°, 20°, 30°, 40°, 45°, 50°, 60°, 70°. The angles above 70° are not considered in this paper since the self-cleaning ability is obviously poor in such conditions and 45° is included for its wide use in aquaculture practice Gorle et al. (2018). In which before the experiment was started, the angle and distance of the inlet pipe were first adjusted to the preset condition, the pump and the flow meter were turned on, and the valve regulated the flow of the inlet pipe. Then, the flow of water through the inlet pipe into the aquaculture tank was monitored in real-time (L/min) by the flow meter, and the flow was regulated to the required value of the experiment. After waiting about 30 min, the flow field in the tank tended to be stable (the pre-test results showed that the flow field in the aquaculture tank was almost unchanged when the system was operated for 30 minutes). At this time, the high-definition camera was turned on, and 10 g shrimp feed with a diameter of 1.6 mm and a length of 1.0-2.0 mm were sprayed quickly and evenly into the tank, and the waste collection situation and pattern in the tank were observed from this time (t=0 min at this point). Based on the previous studies Summerfelt et al. (2016), Xue et al. (2021), the maximum monitoring time was set to 30 min. That is to say, we

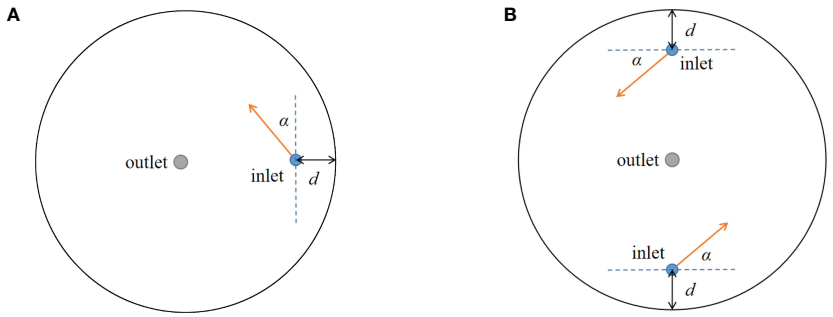

FIGURE 2
Top view **(A)** Single inlet deployment **(B)** Dual inlet deployment.

will turn off the recording camera and start the next cases even though not all the waste particles were completely discharged.

2.1.3 Data processing of waste collection experiment

In the experiment of waste collection under the dual inlet pipe design, it was found that the waste residuals could not completely discharge within 30 min. To quantitatively compare the self-cleaning ability, MATLAB R2020b software was used to process the raw image of the waste residuals in the tank. (1) After the raw image (Figure 3A) of the waste in the aquaculture tank was input into MATLAB software, the rgb2gray function was used to convert it into a grayscale image. (2) The grayscale image of the waste in the aquaculture tank was binarized, and the binarized image of the aquaculture tank was extracted by deploying the grayscale threshold after processing. In this study, the gray index value threshold was set to 200, i.e., when the gray value of a pixel point is greater than 200, the color of the pixel point is set to black; otherwise, it is set to white, and the black pixel point represents the waste residual in the aquaculture tank. (Figure 3B) (3) The calculation range in the binarized image was set, and all the black pixels outside the bottom of the aquaculture tank were removed to obtain the binarized bottom waste image. (Figure 3C) (4) After binarization, the number of black pixels in the bottom waste image of the aquaculture tank was calculated, and the self-cleaning ability of the aquaculture tank was quantified by comparing the number of pixels in the binarized image of the bottom waste residuals under different experimental working conditions.

2.2 Flow field measurement experiments

2.2.1 Setup of flow field measurement experiments

The flow field measurement experiment in the aquaculture tank was conducted in the marine measurement laboratory of QD GL Technology Co, Ltd. The flow field measurement setup (Figure 4) was similar to the waste collection experiments except for the flow field measurement system. In this test, the PIV technique was employed to measure the flow field distribution characteristics in the aquaculture tank. The circular aquaculture tank was embedded in a square acrylic tank to avoid refraction of the laser by the circular tank wall. The waste residuals have a small effect on the flow velocity in the aquaculture tank. The water clarity will be affected if the water is in the aquaculture tank for a long time, thus weakening the laser penetration and affecting the PIV experiment results. Considering this, no waste residuals were spread into the aquaculture tank in the flow field distribution characteristic measurement experiments.

The PIV system combines tracer particles, a laser transmitter, high-speed cameras, control systems, and data processing software. Measurements were conducted by scattering tracer particles in the aquaculture tank, and the velocity of the fluid in the flow field was represented with particle velocity. Meanwhile, a laser was applied to irradiate a test plane, and the position of particles exposed twice was recorded with an imaging method. An image analysis technique obtained the displacement of the particle swarm, and the flow velocity vector at each point was obtained by the time interval of displacement and exposure.

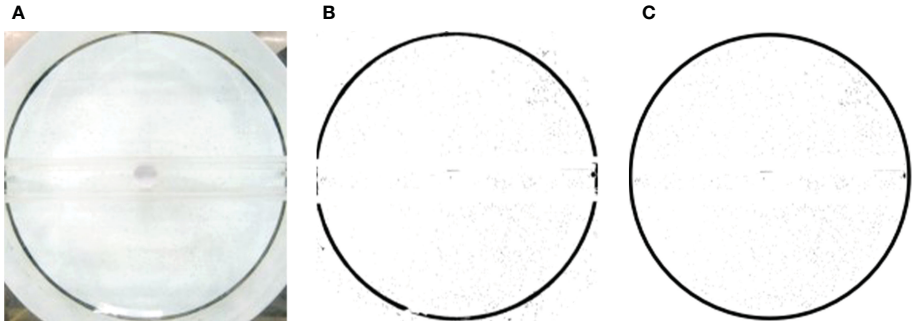

FIGURE 3
Image processing procedure **(A)** Raw image **(B)** Thresholding image **(C)** Diagram of waste residual pixel image.

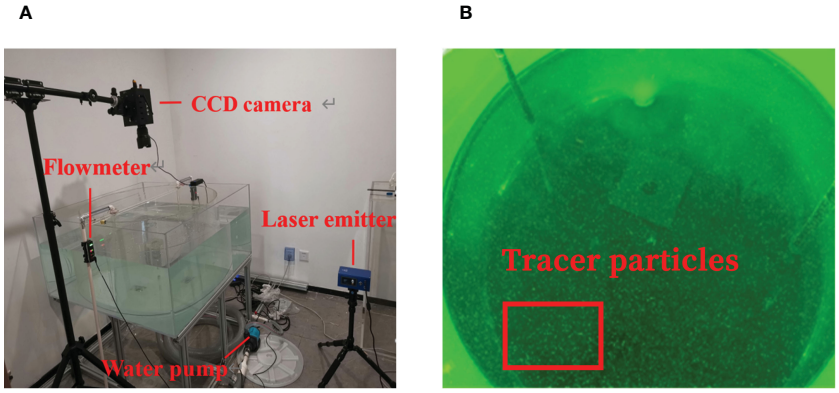

FIGURE 4
Photo of **(A)** PIV flow field measurement setup **(B)** PIV tracer particles.

50-μm polystyrene tracer particles were used in this experiment (the white particles in Figure 4B), with a density of 1.3 kg/m3 (close to the density of water) and good following and light diffusion characteristics. The laser is an ideal light source for the PIV system, which can ensure good collimation and uniformity of the slice beam. In the experiment, a continuous laser plane was generated by the GL-532-1045 model from QD GL Technology Co, Ltd. Besides, the GL-JR-20P high-speed camera was used, with a maximum frame rate of 16 fps and an image resolution of 5,120×3,800.

2.2.2 Data processing of flow field measurement experiments

The SVMC capture software of QD GL Technology Co, Ltd. was used for image acquisition of the flow field (Figure 5). The camera shooting frame rate was 16 fps, the image frequency was set to 8, and the number of images collected in the experiment was 96 (with every two images forming a group, there were 48 groups in total). The experimental acquisition duration was 6 s; dt is the acquisition time interval of two images in the same group, and the dt was set to 15000 μs. The high-speed camera automatically stopped shooting after 96 images were acquired, and the captured photos were stored automatically. The flow pattern tracking master V50 software performed preliminary flow field processing on the captured images and automatically saved the flow field image and flow velocity data.

The PIV images were analyzed by a direct cross-correlation method to obtain the flow field under different inlet pipe design cases. The removal efficiency of fish wastes is evaluated in a comprehensive analysis. For this purpose, the EQ method was deployed to determine the inlet setup considering the uniformity of water flow velocity (1) Masaló and Oca et al. (2016). To systematically compare the hydrodynamic characteristics in the aquaculture tank under different working conditions, the flow field was quantitatively analyzed based on the hydrodynamic characteristic quantities such as the average flow velocity (v_{avg}) in the aquaculture tank, the flow uniformity coefficient (DU_{50}), and the resistance coefficient (C_t) of the aquaculture tank. v_{avg} can be expressed mathematically in the following form Venegas, et al. (2014):

$$DU_{50} = \frac{v_{50}}{v} \times 100,$$

where,

$$v = \frac{\sum_{i=1}^{n} v_i r_i}{\sum_{i=1}^{n} r_i} \quad (1)$$

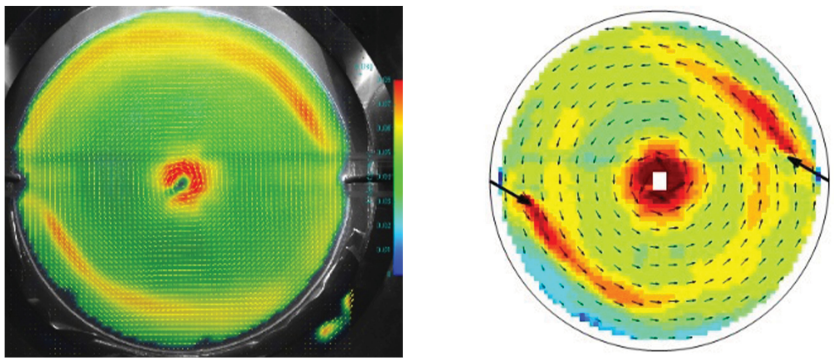

FIGURE 5
Diagram of **(A)** Flow pattern tracking master V50 treatment; **(B)** MATLAB treatment.

$$C_t = \frac{2Q(v_1 - v_{avg})}{(A \times v_{avg}^2)} \quad (2)$$

The average flow velocity (v_{avg}) is the average flow velocity of each monitoring point in the aquaculture tank. In formula (1), v is the average weighted velocity (m/s); v_i is the velocity of the monitoring point (m/s); r_i is the distance of the monitoring point from the center of the tank (m); DU_{50} is the uniformity coefficient of the water flow in the aquaculture tank; v_{50} is the average value of the first 50% of the velocity at each point of a depth section (m/s); DU_{50} is larger than 0 and smaller than 100, and the closer to 100 represents better velocity uniformity. In formula (1), the aquaculture tank resistance coefficient (C_t) refers to the quantified expression of the aquaculture tank on the energy obstruction of the water flow in the tank, and a larger aquaculture tank resistance coefficient represents more energy loss of the inlet pipe input to the aquaculture tank; Q is the inlet flow rate (m^3/s); v_1 is the inlet velocity (m/s).

3 Results

3.1 Effect of the inlet pipe design on the waste collection

3.1.1 Dual inlet pipe design

Figure 6 shows the waste residuals distribution driven by dual inlet pipe at t=30 min, and the inlet pipe design angles of 0°, 10°, 20°, 30°, 40°, 45°, 50°, 60°, and 70° and distance of 1/50 r, 1/4 r, and 1/2 r are represented in horizontal and vertical axis represents, respectively. Obviously, it can be observed that the angle and distance of the inlet pipe significantly affect the waste collecting process in the aquaculture tank.

When the distance of the inlet pipe is at d=1/50 r and the angle is at α=0°~70°, the waste collection ability of the aquaculture tank shows an overall trend of first strengthening and then weakening with the increase of the angle of the inlet pipe, and the highest ability was achieved when the angle of the inlet pipe was at α=50°; when the waste residual in the tank was distributed in a hollow oval shape, the overall waste collection ability was low. When the distance at d=1/4 r and the angle at α=0°~10°, some waste remained in the aquaculture tank, and the waste collection ability was low; when the angle of the inlet pipe was at α=20°~40°, the waste remained in the area near the outside of the aquaculture tank, and the outlet was reduced; meanwhile, most of the waste was gathered in the middle area of the aquaculture tank in a hollow elliptical distribution, and the waste collection ability was poor; when the angle of the inlet pipe was at α=50°~70°, a small amount of circular waste remained at the wall of the aquaculture tank, and the waste collection ability was low.

When the distance of the inlet pipe was at d=1/2 r, and the angle was at α=0°~20°, the waste in the aquaculture tank was basically discharged out of the tank, and the waste collection effect was the best; when the angle of the inlet pipe was at α=30°~70°, a small amount of circular waste remained at the wall of the aquaculture tank, and the waste collection effect was poor.

To further measure the effect of the distance and angle of the inlet pipe on the hydrodynamic characteristics of the waste collection of the aquaculture tank, the images in the aquaculture tank were quantitatively analyzed at t=30 min, and the results are illustrated in Figure 7. It can be observed from the figure that the overall amount of waste residual (pixel numbers) decreased with the increase in the distance of the inlet pipe, and the difference of waste residual between d=1/4 r and 1/2 r was significantly smaller than that at d=1/50 r. When the angle of the inlet pipe was at α=0°~20°, the amount of waste residual gradually decreased with the increase of d; when the angle of the inlet pipe was at α=30°~50°, the difference of waste residual between d=1/4 r and 1/2 r was small but significantly smaller than that of d=1/50 r. When the angle of the inlet pipe was at α=50°~70°, there was no obvious pattern change in the waste residual.

The above analysis indicates that the aquaculture tank achieves the best effect of collecting waste at distance of d=1/4 r, angle of α=20°~40° or at distance of d=1/2 r, angle of α=10° and its self-cleaning ability is the highest.

3.1.2 Single inlet pipe design

The single inlet pipe is to remove one inlet pipe in the dual inlet pipe experiment, and the rest of the device is the same as that of the dual inlet pipe experiment. The inlet pipe flow rate was set to 5.2 L/min in the single inlet pipe experiment to ensure the same hydraulic retention time. The single inlet pipe experiment design was identical to the dual inlet pipe experiment. However, during the experiment, it was found that due to the large flow rate of the single inlet pipe, the waste in the aquaculture tank could be completely discharged within the hydraulic retention time of 30 minutes except for three groups of special conditions. Thus, in the cases of single inlet, the time consumed for completing the discharge of waste residuals in the aquaculture tank was used as an index to quantify the waste collection ability of the aquaculture tank, and the shorter the waste collection time, the stronger the waste collection ability.

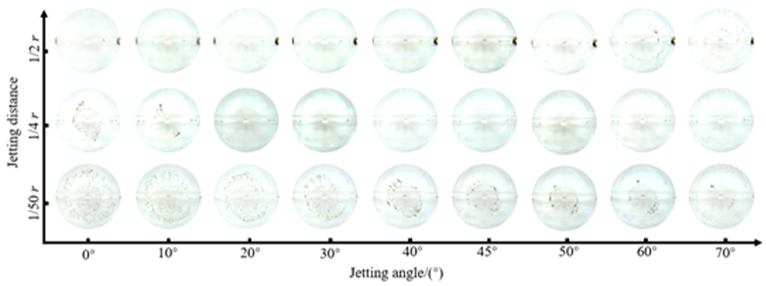

FIGURE 6
Photo of the waste collection under different conditions (Dual inlet deployment; t=30 min).

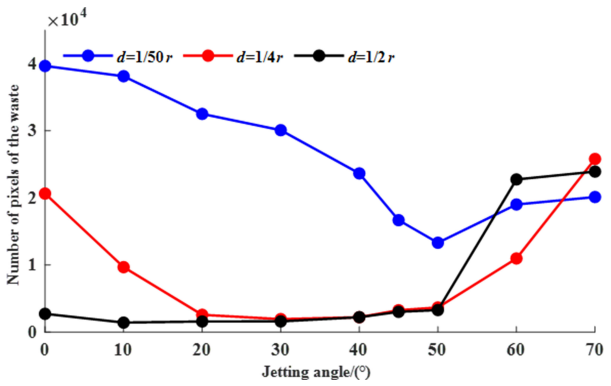

FIGURE 7
The number of pixels of the waste under different conditions (Dual inlet deployment; t=30 min).

The waste collection time under different inlet pipe design angles is indicated in Figure 8. Note that the data of waste collection time exceeding 30 min will not be displayed in the figure. In the case of d=1/50 r, the curve of waste collection time featured a parabolic shape, showing a bottom at the angle of α=45°. It decreased rapidly at α=0°~30°, slowing its reduction among angle of α=30°~45° and finally increased from 45°~70°. For the case the distance of d=1/4 r, the waste collection time was almost the same for the angles of α=0° ~45° and depicted an increasing trend from 45°~70°. The waste collection time increased gradually with the inlet pipe angle increment, achieving the best waste collecting performance for α=0° at the distance of d=1/2. The waste in the aquaculture tank cannot be completely discharged at the angle of α=60°~70°.

3.2 Effect of inlet pipe design on the flow field

The flow field in the near bottom (2 cm from the bottom) in the cases of dual inlet pipe design was indicated in Figure 9 with the variations of jetting angle and jetting distance in the horizontal and vertical axes, respectively. Two long black arrows (not so obvious) in each subpanel show the jetting angle and distance. Meanwhile, the small arrows and colormap indicated the velocity direction and magnitude, respectively. Not all the small arrows were displayed in the figure to enhance visibility.

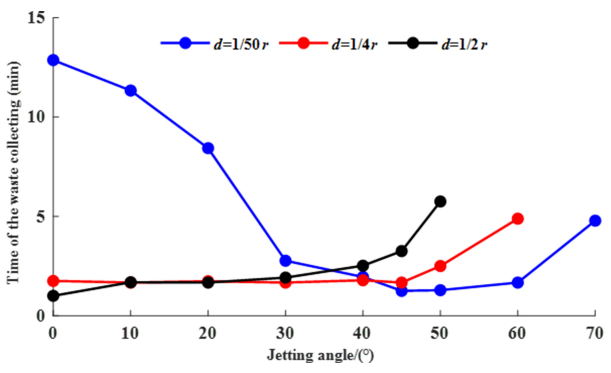

FIGURE 8
Time of the waste collecting under different conditions (Single inlet deployment).

3.2.1 Effect of inlet pipe design on the flow field

The flow field in the near bottom (2 cm from the bottom) in the cases of dual inlet pipe design was indicated in Figure 9 with the variations of jetting angle and jetting distance in the horizontal and vertical axes, respectively. Two long black arrows (not so obvious) in each subpanel show the jetting angle and distance. Meanwhile, the small arrows and colormap indicated the velocity direction and magnitude, respectively. Not all the small arrows were displayed in the figure to enhance visibility.

As depicted in Figure 9, two kinds of high-speed circulation flow were formed in the tank at all the cases, one is around the center of the tank caused by the narrow outlet and one is around the inlets due to the high jetting flow. However, the location and area of the high-speed circulation flow due to the jetting varied with the jetting angle. The flow evolution process with jetting angle is similar in general and still several little inconsistencies exist and the details are described in the following. For the case of d=1/50 r, with the increase of the jetting angle, the flow velocity close to the wall of the tank gradually decreases and the high-speed circulation flow moves away from the tank wall. In addition, the area of the high-speed flow increases from α=0° ~ 45° and decreases after α=45°, indicating a uniform good flow condition for aquaculture. The area increment arises from the less water flow collision between the jetting flow and the tank wall. On the contrary, the area decrement is caused by energy loss due to the discrepancy in the directions of the general flow in the tank and the jetting. The similar phenomenon (flow evolution) also can be found in the case of d=1/4 r but it differs in the velocity magnitude with obviously larger velocities than these in the case of d=1/50 r owing to the longer distance between the jetting and tank wall. Meanwhile, a gradual decrease in the area of high-speed flow with increasing jetting angle is observed in the case of d=1/2 r, revealing that the jetting distance is far enough to avoid the flow collision in this case. Figure 10 shows the flow field measured in the cases of single inlet pipe design. Although the inlet pipe design was adjusted to single pipe, the characteristics of flow field are basically the same with those in Figure 9. Notably, the maximum value of the colorbar in Figure 10 is twice that in Figure 9, thus the velocity magnitude in single inlet pipe design is generally larger. Assessing from the views of high-speed flow area and the flow uniformity, the optimum flow environment can be achieved at the angel of α=40° ~ 50°, 20° ~ 30° and 10° ~ 20° for d=1/50 r, 1/4 r and 1/2 r, respectively.

3.3 Effect of inlet pipe design on the hydrodynamic characteristics

The hydrodynamic characteristics in the case of dual inlet pipe design obtained from PIV measurements are displayed in Figure 11. Moreover, the average velocity, uniformity coefficient and resistance coefficient are presented in panels (A), (B) and (C). For the average velocity in Figure 11A, it shows a parabolic shape and reaches the peak around α=45° at d=1/50 r. A slow downward trend can be found at the cases of d=1/4 r and 1/2 r with the increasing jetting angle,

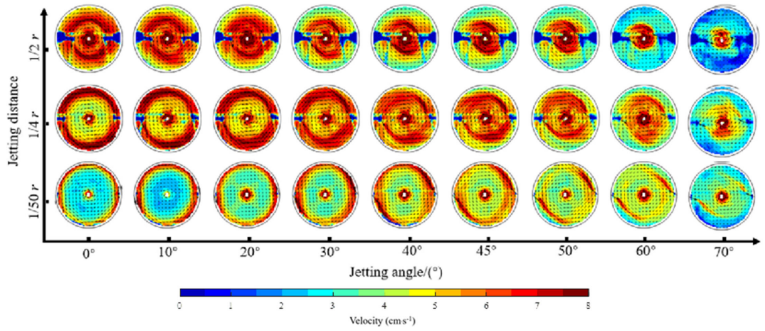

FIGURE 9
Distribution of flow field under different conditions (Dual inlet deployment).

resulting in the largest average velocity at α=20° ~ 30° and 10° ~ 20°, respectively. The uniformity coefficient can be regarded as an indicator for a better flow condition in the tank. However, it should be noted that the larger uniformity coefficient does not necessarily guarantee a better flow condition. For example, as shown in Figure 11B, it increases with the jetting angle for the case of d=1/50 r and achieved the maximum value at α=70°. However, the flow condition at d=1/50 r and α=70° is not good since its average velocity is so low. In short, the uniformity coefficient and average velocity should be considered comprehensively to evaluate the flow. For the case of d=1/4 r and 1/2 r, the variation in uniformity coefficient is consist with that in average velocity and achieves the maximum value at similar jetting angles. It can be observed in Figure 11C the variation in resistance coefficient of aquaculture tank is not obvious before α=50° and a significant increment is following after that. The lower resistance coefficient, the better the energy utilization of the aquaculture tank. Thus, the jetting angle is reasonably designed not larger than α=50°. The hydrodynamic characteristics in the tank equipped with single inlet pipe is exhibited in Figure 12. Obviously, it is very similar to those generated by dual inlet pipe design and only differs in the absolute value of each indicator.

4 Discussion

The core of RAS is to make the water in the system recyclable through efficient water treatment. The primary source of pollution in the water body of the system is the uneaten feed, feces and other waste produced by the culturing objects. The waste left in the tank for a long time will decompose, produce harmful substances such as ammonia and nitrogen, and consume dissolved oxygen, thus seriously affecting the safety of the culturing objects and greatly increasing the water treatment load. Therefore, how to quickly and efficiently discharge the waste from the aquaculture tank is the primary problem that needs to be solved for RAS. The optimal solution to this problem is to construct an aquaculture tank with excellent hydrodynamic characteristics of waste collection by appropriately designing the inlet structures.

The previous studies assessed the self-cleaning ability mainly from direct and indirect aspects by comparing the residual amount of waste. Scattering fish feed pellets (representing feces and uneaten feed) into the aquaculture tank and then observing and recording the process of waste movement is the most intuitive and effective way to study the hydrodynamic characteristics of the waste collection of the aquaculture tank. However, previous studies did not fully study the inlet pipe design. Venegas et al. (2014) scattered 10 feed pellets into the tank from a position 10 cm from the tank wall; Davidson et al. (2004) scattered 1 pellet feed particle into the tank from a position 0.6 m from the tank wall. This is not consistent with the actual culturing situation. The fish wastes are generated randomly distributed during the culturing process, and it is not concentrated at a fixed point. For this reason, in this study, the pellet feed was scattered evenly and densely into the aquaculture tank during the stable operation of the water circulation system to meet the actual culturing conditions.

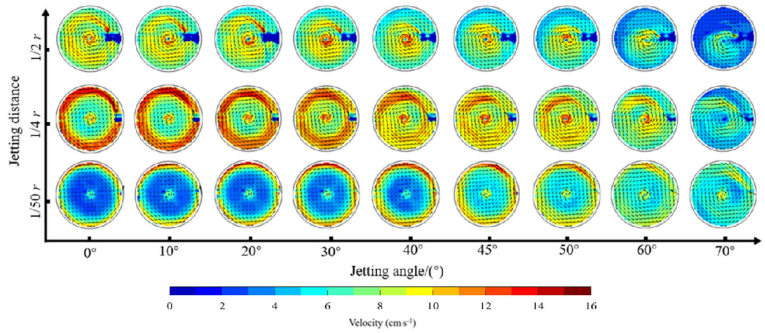

FIGURE 10
Distribution of flow field under different conditions (Single inlet deployment).

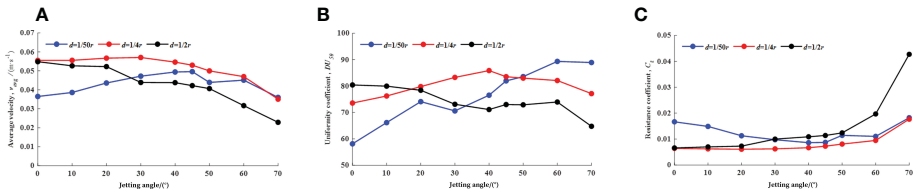

FIGURE 11
Hydrodynamic characteristics under different conditions ·**(A)** Distribution of average velocity under different conditions **(B)** Distribution of uniformity coefficient under different conditions **(C)** Distribution of resistance coefficient under different conditions (Dual inlet mode).

Therefore, it is necessary to integrate several hydrodynamic characteristics and the waste collection results to more reasonably analyze the aquaculture tank's advantages and disadvantages to better design the inlet pipe.

A comprehensive comparison of the two inlet designs revealed that high-speed flow from the inlet pipe collides with the tank wall, when the distance of the inlet pipe is set to d=1/50 r. In this case, a large amount of energy is lost, the overall flow velocity in the aquaculture tank is small, the high-speed circulation area is small, and the waste collection performance is not good. As the deployment distance increases to d=1/4 r, the collision between the high-speed flow from the inlet pipe and the tank wall is weakened, and the energy loss is apparently reduced. In this case, the overall flow velocity in the aquaculture tank is the highest, the high-speed circulation area is the largest, and the waste collection performance is satisfactory. Myong et al. (2021) found that in the case of a single inlet pipe, the self-cleaning ability of the tank is best at the golden split point, which is very close to the results in this paper. After further increasing the inlet pipe deployment distance to d=1/2 r, the high-speed flow was less affected by the tank wall due to the large deployment distance. Meanwhile, the overall flow velocity in the aquaculture tank is higher, the high-speed circulation area is larger, and the hydrodynamic characteristics of the waste collection are better. The numerical simulation results of Hu et al. (2022) indicated that the optimal waste collection efficiency was achieved when the inlet pipe was set at an angle of α=0° and 45° and at the distance of d=3/8 r and d=1/50 r, respectively, which basically agreed with the results of this paper and provided support for the experimental study of this paper.

The angle of the inlet pipe design is an essential factor affecting waste collection and flow field characteristics in the aquaculture tank. The loss of energy in the aquaculture tank is mainly due to the collision between the high-speed flow and the tank wall and the loss of the fusion of the high-speed flow and the overall circulation. The circular aquaculture tank studied in this paper exhibits good hydrodynamic characteristics of the waste collection when the distance and angle of the inlet pipe are set to d=1/4 r and α=20°~30° in the single inlet pipe design and d=1/2 r and α=0°~10° under the dual inlet pipe design. Ren et al. (2020) investigated the effect of angle on waste movement and collection in a square circular angle aquaculture tank with dual inlet pipe. The results show that when the angle is 40° and 50°, respectively, the performance of waste collection and hydrodynamic characteristics in the aquaculture tank are optimal, which is similar to the optimal single inlet pipe deployment angle when the distance is d=1/50 r in this paper. Since the difference between the optimal deployment angle and the data of the adjacent angle is small, for the convenience of the deployment operation in actual production, this study gives the reference range instead of a specific value of the deployment angle of the inlet pipe.

5 Conclusion

This paper investigated the effect of the inlet pipe design on the waste collection and hydrodynamic characteristics of the aquaculture tank under two types of inlet pipe design (dual and single inlet pipe designs) through physical model experiments, and the main findings are as follows:

1. The variations of waste movement, flow filed and hydrodynamic indicators are consistent in both designs of dual inlet and single inlet, and merely differ in the absolute value. Based on the comprehensive analysis, the optimal performance of self-cleaning can be obtained at α=0°~10°, 20°~30°, 40°~50° for d=1/2 r, 1/4 r, and 1/50 r, respectively.
2. By comparing the optimal results of each deployment distance in both inlet pipe designs, it is recommended to adopt the single inlet design with the setup of α=20°~30°, d=1/4 r on the condition of the same flow rate of these two inlet designs.

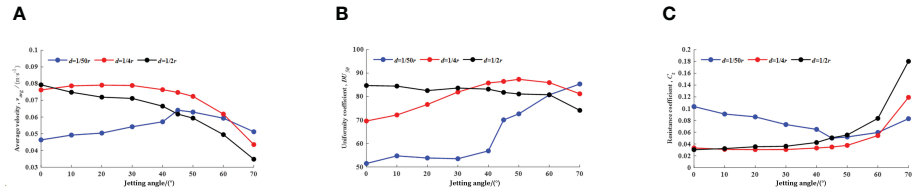

FIGURE 12
Hydrodynamic characteristics under different conditions **(A)** Distribution of average velocity under different conditions **(B)** Distribution of uniformity coefficient under different conditions **(C)** Distribution of resistance coefficient under different conditions (Single inlet mode).

Data availability statement

The original contributions presented in the study are included in the article/supplementary material. Further inquiries can be directed to the corresponding author.

Author contributions

YZ: Data curation, Formal analysis, Writing-original draft. XY: conceptualization; XQ: Conceptualization, Funding acquisition, Resources, Writing-review and editing. JH: Methodology, Software, Conceptualization, Supervision; FZ: Investigation, Methodology. FG: Conceptualization. DF: Funding acquisition, Resources. All authors contributed to the article and approved the submitted version.

Funding

This research was funded by the National Natural Science Foundation of China under grant number 31902425, the Natural Science Foundation of Zhejiang Province under grant number LGN21C190010, and the Bureau of Science and Technology of Zhoushan under grant number 2020C21003.

Acknowledgments

The authors would like to thank all the reviewers who participated in the review, as well as MJEditor (www.mjeditor.com) for providing English editing services during the preparation of this manuscript.

Conflict of interest

The authors declare that the research was conducted in the absence of any commercial or financial relationships that could be construed as a potential conflict of interest.

Publisher's note

References

Benoit, D. (2007). Hydrodynamic characteristics of muti-drain circular tanks. *Proc. Sixth. Int. Conf. Recirculating. Aquacult.*, 394–404.

Burrows, R. E., and Chenoweth, H. (1955). *Evaluation of three types of fish rearing tanks [M]* (US Government Printing Office).

Davidson, J., and Summerfelt, S. (2004). Solids flushing, mixing, and water velocity profiles within large (10 and 150 m3) circular 'Cornell-type' dual-drain tanks. *Aquacult. Eng.* 32 (1), 245–271. doi: 10.1016/j.aquaeng.2004.03.009

Gorle, J. M. R., Terjesen, B. F., Mota, V. C., and Summerfelt, S. (2018). Water velocity in commercial RAS culture tanks for Atlantic salmon smolt production. *Aquac. Eng.* 81, 89–100. doi: 10.1016/j.aquaeng.2018.03.001

Gorle, J. M. R., Terjesen, B. F., and Summerfelt, S. T. (2020). Influence of inlet and outlet placement on the hydrodynamics of culture tanks for Atlantic salmon. *Int. J. Mechanical. Sci.* 188. doi: 10.1016/j.ijmecsci.2020.105944

Hu, J., Zhang, H., Wu, L., Zhu, F., Zhang, X., Gui, F., et al. (2022). Investigation of the inlet layout effect on the solid waste removal in an octagonal aquaculture tank. *Front. Mar. Sci.* 9. doi: 10.3389/fmars.2022.1035794

Hu, J., Zhu, F., Yao, R., Gui, F., Liu, B., Zhang, Z., et al. (2021). Optimization of the inlet pipe layout of circular recirculating water aquaculture tank based on STAR-CCM+. doi: 10.11975/j.issn.1002-6819.2021.21.028

Masaló, I., and Oca, J. (2016). Influence of fish swimming on the flow pattern of circular tanks. *Aquac. Eng.* 74, 84–95. doi: 10.1016/j.aquaeng.2016.07.00

Oca, J., and Masalo, I. (2007). Design criteria for rotating flow cells in rectangular aquaculture tanks. *Aquacult. Eng.* 36), 36–44. doi: 10.1016/j.aquaeng.2006.06.001

Oca, J., and Masaló, I. (2013). Flow pattern in aquaculture circular tanks: Influence of flow rate, water depth, and water inlet & outlet features. *Aquacult. Eng.* 52 (52), 65–72. doi: 10.1016/j.aquaeng.2012.09.002

Oca, J., Masaló, I., and Reig, L. (2004). Comparative analysis of flow patterns in aquaculture rectangular tanks with different water inlet characteristics. *Aquacult. Eng.* 31 (3-4). doi: 10.1016/j.aquaeng.2004.04.002

Plew, D. R., Klebert, P., Rosten, T. W., et al. (2015). Changes to flow and turbulence caused by different concentrations of fish in a circular tank. *J. Hydraulic. Res.* 53), 364–383. doi: 10.1080/00221686.2015.1029016

Ren, X. Z., Wang, J. Z., and Zhang, Q. (2020). Influence of inlet structure on flow field in a rectangular arc angle tank in aquaculture. *Journal of Dalian Ocean University* 726–732. doi: 10.16535/j.cnki.dlhyxb.2020-097

Sin, M-G, An, C-H, Cha, S-J, Kim, M-J, and Kim, H-N (2021). A method for minimizing the zone of low water flow velocity in a bottom center drain circular aquaculture tank. doi: 10.1111/jwas.12792

Skybakmoen (1989). "Impact of water hydraulics on water quality in fish rearing units," in *Aqua Nor 89, Conference 3-water treatment and quality*. 17–21.

Summerfelt, S. T., Davidson, J., and Timmons, M. B. (2000). "Hydrodynamics in the 'cornell-type' dual-drain tank," in *The third international conference on recirculating aquaculture*. Eds. G. S. Libey and M. B. Timmons (Roanoke, VA, USA: Virginia Polytechnic Institute and State University), 160–166.

Summerfelt, S. T., Mathisen, F., Holan, A. B., and Terjesen, B. F. (2016). Survey of large circular and octagonal tanks operated at Norwegian commercial smolt and post-smolt sites. *Aquac. Eng.* 74, 105–110. doi: 10.1016/j.aquaeng.2016.07.00

Tvinnereim, K., and Skybakmoen, S. (1989). "Water exchange and self-cleaning in fish-rearing tanks," in *Aquaculture. a biotechnology in progress*. Eds. N. DePauw, E. Jaspers, H. Aokefors and N. Wiikens (Bredena, Belgium: European Aquaculture Society), 1041–1047.

Venegas, P. A., Narváez, A. L., Arriagada, A. E., and Llancaleo, K. A. (2014). Hydrodynamic effects of use of eductors (Jet-mixing eductor) for water inlet on circular tank fish culture. *Aquac. Eng.* 59, 13–22. doi: 10.1016/j.aquaeng.2013.12.00

Xue, B. R., Jiang, H.Z., and Ren, X. Z. (2020). Study on the influence of the relative inflow distance on the flow field characteristics in square arc angle aquaculture tank.. *Fishery Modernization*. doi: 10. 3969 /j. issn.1007-9580.2020.04.004

Xue, B. R., Yu, L. P., Zhang, Q., Ren, X. Z., and Bi, C. W. (2021). A numerical study of relative inflow distance on the influence of hydrodynamic characteristics in the single-drain rectangular aquaculture tank with arc angles. *J. Fisheries. China* 45 (3), –45.

frontiers | Frontiers in Marine Science

TYPE Original Research
PUBLISHED 15 May 2023
DOI 10.3389/fmars.2023.1094247

OPEN ACCESS

EDITED BY
Morten Omholt Alver,
Norwegian University of Science and Technology, Norway

REVIEWED BY
Bror Jonsson,
Norwegian Institute for Nature Research (NINA), Norway
Trygve Sigholt,
BioMar, Norway

*CORRESPONDENCE
Danielle P. Dempsey
ddempsey@perennia.ca

†PRESENT ADDRESS
Toby Balch,
Independent Researcher
Dartmouth, NS, Canada

RECEIVED 09 November 2022
ACCEPTED 20 April 2023
PUBLISHED 15 May 2023

CITATION
Dempsey DP, Reid GK, Lewis-McCrea L, Balch T, Cusack R, Dumas A and Rensel J (2023) Estimating stocking weights for Atlantic salmon to grow to market size at novel aquaculture sites with extreme temperatures. *Front. Mar. Sci.* 10:1094247. doi: 10.3389/fmars.2023.1094247

Estimating stocking weights for Atlantic salmon to grow to market size at novel aquaculture sites with extreme temperatures

Danielle P. Dempsey[1*], Gregor K. Reid[1], Leah Lewis-McCrea[1], Toby Balch[1†], Roland Cusack[2], André Dumas[3] and Jack Rensel[4]

[1]Centre for Marine Applied Research, Dartmouth, NS, Canada, [2]C&H Aquatic and Laboratory Veterinary Services Ltd, Halifax, NS, Canada, [3]Aquaculture Nutrition Services Inc., Souris, PEI, Canada, [4]System Science Applications Inc., Arlington, WA, United States

Land-based hatcheries are now capable of growing large Atlantic salmon (*Salmo salar*) post-smolts (approximately 150 – 1000 g), which means that marine net-pens can be stocked with substantially larger fish compared to traditional stocking sizes (< 150 g). This stocking strategy typically aims to reduce the time required for fish to grow to market size in the marine environment and limit risks (e.g., exposure to pathogens and diseases, opportunities for escapes). This study investigates another potential application of this strategy: the use of novel sites in areas previously considered unsuitable for aquaculture due to seasonally cold temperatures. The thermal-unit growth coefficient (TGC) model was applied to estimate the stocking weight needed to reach a harvest size of 5.5 kg, based on observed degree days for three sites. High resolution, depth-partitioned temperature time series from coastal locations in Atlantic Canada were used to represent a short, medium, and long growing season, as constrained by seasonal temperature extremes. Growing days for model inputs were defined as temperatures > 4 °C and trending up for stocking, < 18 °C to account for heat stress, and > -0.7 °C to avoid superchill conditions. Different TGC values were applied to simulate remedial, average, and elite growth performance. There was a range of model stocking weight estimates for each site (1.5 – 2.5 kg, 0.94 – 2.8 kg, and < 0.1 – 0.52 kg, for the short, medium, and long season sites, respectively). Results were sensitive to the number of degree days, heat stress threshold, and TGC value. At the two sites where season length was constrained by superchill, fish with a stocking weight of approximately 1.5 kg could grow to market size in shallow water depths (< 15 m), assuming elite growth performance. This investigation suggests that with appropriate growth performance assumptions and high-resolution temperature data, large post-smolt stocking strategies could enable the use of novel sites in coastal areas previously considered unsuitable for aquaculture.

KEYWORDS

degree days, growing days, heat stress, model, net-pen, Nova Scotia, post-smolt, thermal-unit growth coefficient

1 Introduction

In traditional Atlantic salmon (*Salmo salar*) aquaculture in temperate waters, fish typically spend 12 – 18 months in freshwater hatcheries prior to transfer to net-pens when they are smolts weighing 100 – 150 g (Gardner Pinfold Consultants Inc., 2019). These salmon are grown over the next 18 – 24 months and harvested when they reach market size at approximately 5.5 kg (Njåstad, 2020; MOWI, 2021). However, there has been recent industry interest in extending growth time in land-based facilities or semi-closed containment cages to stock large post-smolts between 500 – 1000 g or larger in marine net-pens (Calabrese, 2017; Grieg Seafood, 2020; Fish Farming Expert, 2021; Holland, 2021; Withers, 2021; Mayer, 2022). Growing such large post-smolts requires significant technological and infrastructure investment, but there can be substantial advantages to stocking these large fish (Calabrese, 2017; Gardner Pinfold Consultants Inc., 2019; EY, 2020; Grieg Seafood, 2020).

Post-smolt stocking strategies were initially developed to reduce the time required for marine grow-out (i.e., growth from stocking to market size) (Fish Farming Expert, 2019; Fish Farming Expert, 2021; MOWI, 2021). Less time in marine net-pens can reduce pathogen transfer (e.g., sea lice and diseases), exposure to harmful algal blooms, and opportunities for escapes (Calabrese, 2017; Gardner Pinfold Consultants Inc., 2019). Shorter grow-out times can enable more production cycles with a more flexible stocking schedule, which can increase site productivity and allow longer fallowing periods if necessary to reduce benthic impacts (Fish Farming Expert, 2019; Fish Farming Expert, 2020; Grieg Seafood, 2020). Finally, large post-smolts can be more robust than smolts, improving fish survival, health, and welfare (Grieg Seafood, 2020; Fish Farming Expert, 2021; Fisheries and Oceans Canada, 2022).

Another potential advantage of stocking large post-smolts appears to be unexplored in the scientific literature: this stocking strategy may enable use of novel sites in areas traditionally considered unsuitable for aquaculture due to seasonally cold temperatures. For example, decision-makers are unlikely to consider year-round culture in locations with historical superchill (i.e., when temperatures fall below the lethal limit for salmonids; Saunders et al., 1975). However, depending on the local temperatures and stocking weight, large post-smolts could potentially grow to market size at these locations in less than a year (Mayer, 2022), circumventing periods of lethally cold temperatures.

Temperature is a key consideration for salmon aquaculture site selection (Saunders, 1995; Feindel et al., 2013). Practically all fish (including salmon) are ectotherms, which means the environment regulates their body temperature and governs biological processes. If it is assumed that optimal nutritional needs are being met, which is a major objective for aquaculture, temperature is the primary growth driver until maturity (Reid et al., 2020). Fish can grow at a range of temperatures, but growth will slow if the water is too cold or too warm, particularly in the presence of other stressors such as low dissolved oxygen (Vikesa et al., 2017; Gamperl et al., 2020). Prolonged exposure to extreme temperatures can cause mortality (Elliott and Elliott, 2010; Pörtner and Peck, 2010). When given the option, fish tend to swim at their preferred temperature, which usually corresponds to the optimal temperature for growth (Jobling, 1981). These temperature ranges and thresholds depend on several factors, including species, life stage, body size, dissolved oxygen concentration, diet, food availability, and acclimation temperature (Jobling, 1981; Elliott and Hurley, 2000; Elliott and Elliott, 2010; Morita et al., 2010; Pörtner and Peck, 2010).

Atlantic salmon typically grow at temperatures between 4 – 18 °C, and heat stress begins to occur around 16 – 18 °C (Saunders, 1995; Johansson et al., 2009; Thyholdt, 2014; Gamperl et al., 2021; MOWI, 2021). Heat stress can cause salmon to stop eating, resulting in reduced growth, and warmer temperatures eventually become lethal (Thyholdt, 2014; Gamperl et al., 2020). Cold water (< 4 – 6 °C) also results in reduced growth rates, decreased response to stress, and eventually death (Saunders et al., 1975; Handeland et al., 2008). The superchill threshold (-0.7 °C) is a particular risk for salmon aquaculture in cold regions. At this temperature, ice crystals can form in salmon fluids and tissues, which can cause substantial mortalities at a site (Saunders et al., 1975; CBC, 2015).

The thermal-unit growth coefficient (TGC) model accounts for temperature effects on ectothermic growth (Iwama and Tautz, 1981), and is commonly used to project fish growth rates in aquaculture (Iwama and Tautz, 1981; Cho and Bureau, 1998; Dumas et al., 2007; Dumas et al., 2010; Chowdhury et al., 2013; Reid et al., 2017). There are more accurate fish growth models, although these have greater complexity and data needs (Aunsmo et al., 2014). For the purpose of assessing growth response under different temperature regimens, the TGC model was considered sufficient to meet conditions of good model parsimony. TGC models are also more simplistic than ecological fish growth models. There is no need to account for density dependent food availability and quality or partitioning of energetic flux because it is reasonably assumed that cultured fish consume energy-dense, high-quality feed to satiety. Consequently, the TGC model is a function of historical growth performance under a given temperature regimen, which is summarized by the degree days term (Equations 1A and 1B). Degree days are a useful metric for modelling the growth of ectotherms because it accounts for both calendar time and temperature. The TGC coefficient is calculated as shown in Equations 1A and 1B:

$$TGC = (\sqrt[3]{W_t} - \sqrt[3]{W_0}) * \frac{1000}{degree\ days} \quad (1A)$$

$$degree\ days = T_{Avg} * n_{days} \quad (1B)$$

where

TGC = thermal growth coefficient

W_t = final weight

W_0 = initial weight

T_{Avg} = average water temperature over a given number of days, n_{days}

n_{days} = number of growing days

degree days = time-integrated temperature

Note that the multiplier in Equation 1A is 1000 in some studies (e.g., Iwama and Tautz, 1981; Thorarensen and Farrell, 2011; Reid et al., 2020), and 100 in others (e.g., Cho and Bureau, 1998;

Chowdhury et al., 2013; Reid et al., 2013a). Additionally, the unit of weight used can differ (e.g., grams or kilograms), as long as the same units are used for W_t and W_0. Depending on these choices, the TGC value can be less than 1 or greater than 1. When applying TGC models from other studies the multiplier, units, and coefficient value should be reviewed and converted if necessary.

There are several TGC model assumptions for aquaculture application. Fish culture practices aim to harvest fish before sexual maturity, when less energy is directed into growth, to avoid reduced feed conversion efficiency (assuming oxic conditions). In this context, there is no need for TGC or other types of fish aquaculture models to consider reproductive growth. Salmonids may have different growth rates (i.e., stanzas) associated with different life stages, and therefore different TGCs may apply at the various stages (Dumas et al., 2007; Reid et al., 2017). However, the TGC value is typically averaged over the growth period of interest, which embodies this variation in the term. The major assumptions of the TGC model are discussed in detail in Jobling (2003). In summary, the model assumes that: 1) the growth rate increases with temperature, 2) weight is proportional to length cubed, and 3) length increases linearly over time.

Here we develop a method to explore the suitability of novel aquaculture sites using the TGC model and high-resolution coastal temperature profiles. The method is illustrated with three case study sites in Nova Scotia, Canada, which is located in a temperate region of the Northern hemisphere (Figure 1). Nova Scotia is a small Canadian province that supports a low-impact/high-value, sustainable aquaculture industry, despite relatively cool temperatures (Saunders, 1995). Multi-year, high-resolution temperature time series are available for discrete locations around the province, which show temperatures can dip below 4 °C as late as July, and winter temperatures can drop below the superchill threshold in some bays (Saunders, 1995; Centre for Marine Applied Research, 2022). Farm operators and fish health veterinarians have developed strategies to protect fish from extreme temperatures. For example, salmon smolts are stocked when the spring water temperature is not expected to fluctuate below 4 °C. Based on the authors' practical experience, this reduces occurrence of skin lesions and improves the recovery from transfer stress. The main strategy for avoiding superchill mortalities is to refrain from operating in areas where these lethal conditions have been observed. Large post-smolt stocking strategies could therefore enable novel culture sites in the province and afford additional opportunities for industry.

The objectives of this study are four-fold:

1. Select three different geographic coastal locations in Nova Scotia that reflect a range of seasonal temperatures as case studies.
2. Calculate degree days within operational temperature ranges to determine the maximum practical culture duration for each location and depth.
3. Apply the TGC model to determine stocking weight required to grow to market size, under the observed degree days at each location and depth.
4. Assess the sensitivity of model output to the heat stress threshold, TGC value, and depth strata.

2 Materials and methods

2.1 Stocking weight estimation

The TGC model was applied to calculate the initial weight (i.e., stocking weight) required for salmon to grow to market size (i.e.,

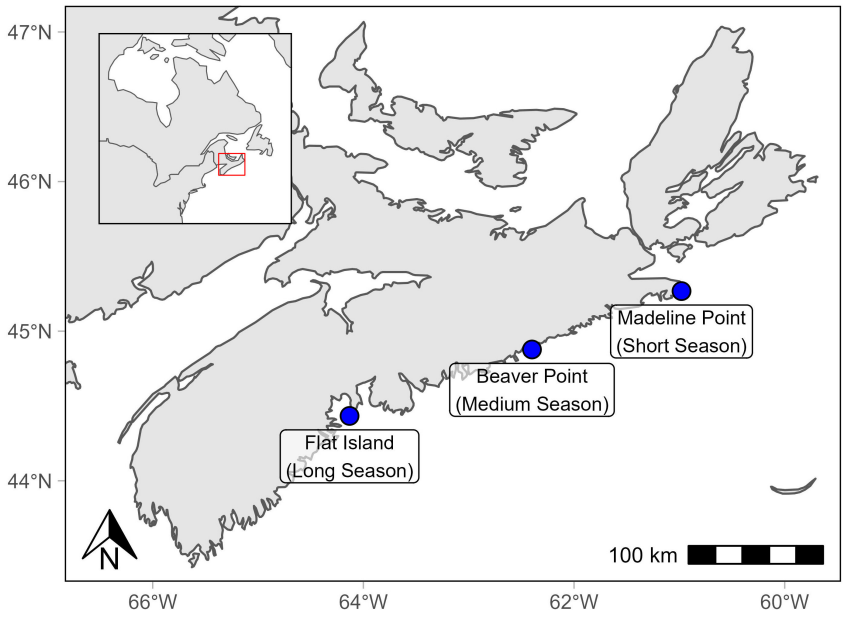

FIGURE 1
Stations selected to represent a short, medium, and long stocked season. Map made using the rnaturalearth and rnaturalearthhighres R packages (South, 2022a; South, 2022b).

harvest weight) given observed temperatures (Equation 2).

$$W_0 = (\sqrt[3]{W_t} - \frac{TGC}{1000} * degree\ days)^3 \quad (2)$$

Three different TGC values were applied to model a range of growth performance. Reid et al. (2013a) calculated a TGC value of 0.30 for commercial Atlantic salmon culture in Atlantic Canada. This value was calculated across the full grow-out season, and therefore embodies inherent differences in growth rates due to life stage and environment conditions. Here, a TGC value of 0.30 was assumed to represent average growth performance, 0.25 represented slower growing, "remedial" performance, and 0.35 represented faster growing, "elite" performance. A single TGC value was applied across the entire growth period because initial weights were calculated based on the final weight, as opposed to stepwise growth stanzas. The final weight (W_t) was set to 5.5 kg, because it is a typical target market size (Njåstad, 2020; MOWI, 2021).

To account for the effects of heat stress on growth rates, it was assumed that there was no growth for 24 hours after a temperature observation ≥ 18 °C. All such heat stress observations were filtered out of the data so that growing days were used to calculate the degree days (also called growing degree days; see Table 1 for terminology). Temperatures within the 24-hour window of heat stress were not included in T_{Avg}, and the corresponding number of days were not included in n_{days} (Equation 1). While it is known that salmon can migrate vertically in response to environmental cues including temperature (Johansson et al., 2006; Johansson et al., 2009; Oppedal et al., 2011), the model is constrained to one depth for the duration of the stocked season as a simplifying assumption. It is likely that fish would avoid depths with temperatures causing heat stress when possible. In consequence, the calculated stocking weights may be conservative.

Model sensitivity to the heat stress threshold was assessed using the average growth model (TGC value = 0.30). The results of the original model (heat stress threshold = 18 °C) were compared to results from a model with a lower heat stress threshold (16 °C) and a higher heat stress threshold (20 °C).

The model assumes that missing temperature values are the average of the growing day temperatures (T_{Avg}). To check this approximation, the average of the temperature for the 24 hours before and after any data gap was calculated (T_{Gap}) and compared to T_{Avg}. To assess the sensitivity of the results when T_{Gap} was close to the heat stress threshold (≥ 16 °C), the analysis was repeated assuming there was no growth during the period of missing data. If the data gap represented less than 5 % of the stocked season and T_{Gap} was not close to the heat stress threshold, it was assumed that the missing data had negligible impact on the results.

2.2 Case study

2.2.1 Data collection

The Centre for Marine Applied Research (CMAR) has coordinated an extensive Coastal Monitoring Program in Nova Scotia, Canada since 2017 (Centre for Marine Applied Research, 2022). Through this program, temperature and other essential ocean variables (Global Ocean Observing System, 2021) are measured at locations selected in collaboration with local stakeholders (Centre for Marine Applied Research, 2022). Temperature data is collected from sub-surface "sensor strings" (Figure 2). Each string is anchored to the seafloor and suspended under constant tension from a subsurface float. Autonomous sensors are attached at various depths, typically 2, 5, 10, 15 m below the surface (at low tide), or greater depending on total depth, and most strings include a sensor just above the seabed. Several types of temperature sensors are used, including HOBO Water Temp Pro v2 U22 series (Onset, 2012), aquaMeasure DOT (InnovaSea, 2021), and Vemco VR2AR (Vemco, 2016). A sensor string is generally deployed at a sampling station 200 m – 1000 m from shore in depths up to 75 m for 6 – 12 months. Sensors record data every 1 minute to 1 hour, depending on the deployment settings. At the time of analysis, CMAR had data from 84 stations around the coast of Nova Scotia, resulting in 338 time series at various depths. Time series range from 1 month to 4.6 years, although some stations have substantial data gaps caused by battery failure, accidental and intentional vandalism, or other disruptions. This data is publicly available to visualize and download from the CMAR website (https://cmar.ca/coastal-monitoring-program/), the Nova Scotia Open Data Portal (https://data.novascotia.ca/browse?tags=coastal+monitoring+program), and the Canadian Integrated Ocean Observing System (https://catalogue.cioosatlantic.ca/dataset?q=cmar) platforms.

TABLE 1 Definition of key terms.

Stocking date	First observation in the spring/summer when temperature exceeds 4 °C and does not return below this threshold.
Harvest date	Last observation before temperature decreases below the superchill threshold (-0.7 °C). If no superchill: 540 days after the stocking date.
Stocked days	Number of days the fish were stocked (from the stocking date to the harvest date).
Stocked season	Period the fish were stocked (from the stocking date to the harvest date).
Heat stress	Biological response to extreme warm temperature resulting in reduced or arrested growth rate. It was assumed that no growth occurred for 24 hours after a temperature observation ≥ the heat stress threshold (18 °C for the original model).
Growing days	Number of days with temperature amenable to growth (stocked days – number of days with heat stress).
Growing degree days	Degree days calculated from the growing days (Equation 1B).

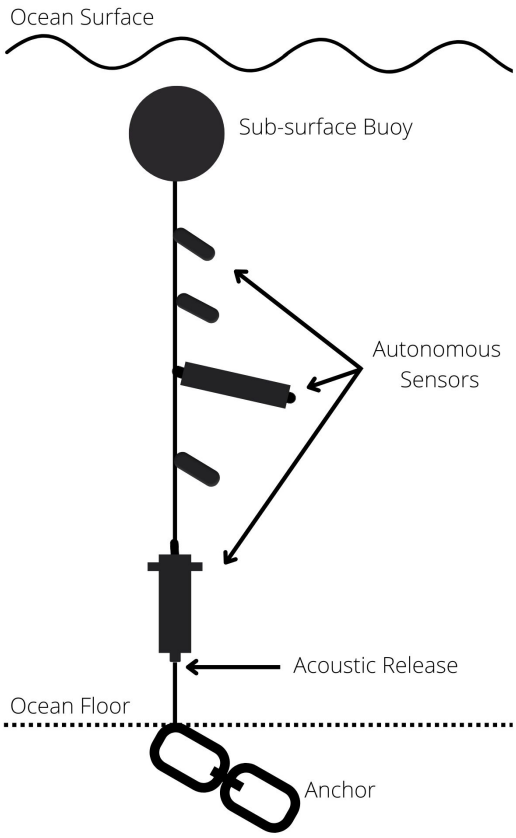

FIGURE 2
Example sensor string configuration (not to scale).

2.2.2 Site selection

The 338 time series of temperature at depth were carefully evaluated to select three case study stations that represent a short, medium, and long stocked season. First, stocked seasons were defined for each time series by identifying the optimal stocking and harvest dates (Table 1). The stocking date was defined as the first observation in the spring or summer when the temperature exceeded 4 °C and trended up (i.e., did not go below 4 °C), a threshold recommended by provincial fish health veterinarians in Nova Scotia to maximize fish heath and welfare. If superchill occurred the following winter, the harvest date was defined to end one minute before the first observation of superchill. If temperatures remained above this threshold, the harvest date was set at 540 days after the stocking date (i.e., a typical grow-out time). It was assumed that all fish were stocked on the stocking date and harvested on the harvest date, although in practice these events can take several weeks or months. Time series for which these dates could not be defined (e.g., data gaps) were excluded from the analysis, leaving 127 time series from 38 stations.

Next, any stocked season with more than 2 days of missing data was removed from the analysis, leaving 106 time series from 35 stations to evaluate. The durations of these remaining time series were used to inform season length categories, where "short" was less than 8.5 months; "medium" was 8.5 months to less than 17 months, and "long" was 17 months or more (i.e., seasons that did not experience superchill).

There were 12 stations with data for a short season, 10 stations with data for a medium season, and 14 stations with data for a long season. One station with data for at least 2, 5, 10 and 15 m was selected from each category to assess influence of depth on suitable temperatures. This left one station each in the short and medium season categories, and three in the long season category. Finally, the station to represent the long season was selected based on geography.

2.3 Software

All data analysis was done using R version 4.1.1. The R package tgc was developed by the authors to identify stocked seasons, filter out heat stress observations, apply the TGC model, and visualize results. The package can be installed from the GitHub repository at https://github.com/dempsey-CMAR/tgc. Data analysis code is available at https://github.com/dempsey-CMAR/TGC_Analysis.

3 Results

3.1 Stocking weight estimates

Stocking weight had an inverse relationship with growing degree days (Figure 3). For each TGC model, the stocking weight approached the harvest weight at lower degree days and approached 0 kg at very large degree days. For a given degree day, the elite growth model (TGC = 0.35) always resulted in the smallest stocking weight, and the remedial growth model (TGC = 0.25) resulted in the largest. The three models diverge the most at moderate degree days. For example, at a location with 2000-degree days, the stocking weight for the remedial model was 2.0 kg, while that of the elite model was only 1.2 kg. The modelled stocking weight decreased more rapidly for smaller number of degree days (Figure 3). For the average model, a 500-degree day increase from 1000 to 1500-degree days reduced the stocking weight by 0.88 kg (from 3.15 kg to 2.27 kg). In contrast, a 500-degree day increase from 3500 to 4000-degree days reduced the stocking weight by only 0.19 kg (from 0.37 kg to 0.18 kg).

3.2 Short season: Madeline Point

The station that met the criteria to represent a short season was Madeline Point, Guysborough County, located in the north-eastern part of mainland Nova Scotia (Figure 1). The station is approximately 500 m from shore and 22 m deep, with temperature sensors at 2, 5, 10, 15, and 22 m below the surface at low tide, and a tidal range of up to 2 m. The stocked season selected for analysis was approximately 8 months long (Table 2; Figure 4A), beginning on June 17 for the shallowest depths (2 m and 5 m), followed five days later by the mid-depths (10 m and 15 m), and one additional day later for the bottom (22 m). While 22 m is an impractical culture depth for this site, it is

included in this theoretical exercise for context and comparison with the other depths. The season ended in mid-February near the surface (2 m) and near the bottom (15 m and 22 m), followed a week later by the remaining strata.

There was an overall increasing temperature trend in the summer, with substantial diurnal variability (Figure 4A). Limited temperature stratification occurred between 2, 5, and 10 m (average July and August temperatures for these depths were 15.3 °C, 14.6 °C, and 13.5 °C, respectively), while the bottom temperature was typically cooler (average bottom temperature was 9.2 °C). There was a distinct decreasing temperature trend throughout the fall and winter months, with no appreciable diurnal variability or stratification (average temperature ranged from 6.2 °C at 22 m to 6.6 °C at 2 m).

Heat stress events were observed at all depths (Table 2; Figure 4A). The warmest temperatures typically occurred mid-August to early September, although surface depths (2 and 5 m) experienced earlier seasonal heat stress events. These shallow depths experienced the most heat stress, with no growth assumed for 31 days at 2 m depth and 27 days at 5 m depth (approximately 13 % and 11 % of the stocked days, respectively; Figure 5). In contrast, the bottom had only two short (< 2 days) heat stress events. As a result of heat stress and growing season length, the 2 m depth had the fewest growing days, and 22 m had the most (Table 2).

The top four depths had a very similar number of degree days (Figure 6A; Table 1). This translated to a negligible difference in the stocking weight required to grow salmon to market size at these depths (a difference of about 0.05 kg for each TGC value; Figure 6B). However, there was a substantial difference in the results between the remedial and elite models, with remedial growth requiring a stocking weight of approximately 2.3 kg and elite growth requiring a stocking weight of 1.5 kg. Near the bottom, the average temperature of the growing days was about 1 °C cooler, resulting in about 100 fewer degree-days, and a stocking weight about 0.1 kg higher than the other depths.

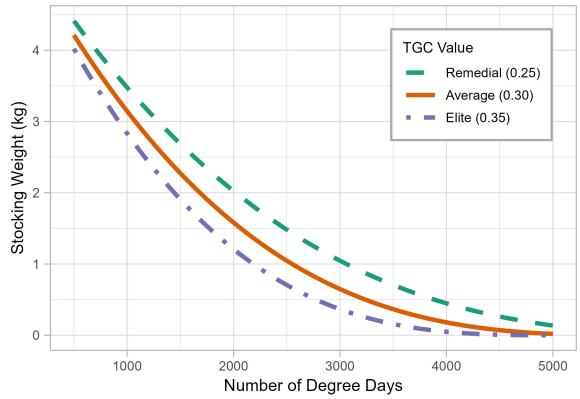

FIGURE 3
The thermal-unit growth coefficient model, showing the stocking weight required to grow a post-smolt salmon to market size (5.5 kg) for a given number of degree days, assuming remedial (TGC = 0.25), average (TGC = 0.30), and elite (TGC = 0.35) growth performance.

3.3 Medium season: Beaver Point

The station that met the criteria to represent a medium season was Beaver Point, located on the eastern shore of Halifax County (Figure 1). The station is approximately 300 m from shore and 15 m deep. Temperature was measured at 2, 5, 10, and 15 m below the surface at low tide, with a tidal range up to 2 m. The stocked season selected for analysis was approximately 9 months for the top three depths, beginning in late May and ending with the onset of superchill in late February (Table 2; Figure 4B). The bottom depth had a much shorter growing season of 6.4 months, because the temperature crossed the 4 °C and trending up threshold a month and a half later and experienced superchill about a month earlier than at the other depths (Table 2).

Temperature was stratified from June through to mid-August, with the average temperature at 2 m (9.8 °C) about 1 °C warmer than that at 5 m depth; in turn, the average temperature at 5 m was about 1 °C warmer than the temperatures at 10 and 15 m. Heat stress events occurred at all depths in late August, with the most prolonged at 2 m, where 26 days (9.4 % of stocked season) were assumed unsuitable for growth. In contrast, only 12 days and 5 days were considered unsuitable at 10 m and 15 m, respectively (Table 2; Figure 5). August through October was a period of rapid variability for the deeper waters. For example, in late August the temperature at 15 m dropped 13 °C over 6 days, and then rebounded 12 °C in the following 5 days. Temperature was less variable and more well-mixed in the winter months (Figure 4B), although temperature at the bottom was on average ~ 0.6 °C cooler than at the shallower depths.

The number of degree days ranged from 1450 degree days at the bottom (15 m) to 2247 degree days near the surface (2 m; Figure 6A), which translated to a difference in stocking weight of about 1 kg (Figure 6B). The smallest stocking weight occurred at 2 m, ranging from 1.7 kg for the remedial model to 0.93 kg for the elite model. The stocking weight at 5 m and 10 m had negligible differences at each TGC (~ 0.01 kg), owing to the similar number of degree days at these depths. The elite growth model at 2, 5, and 10 m required a smaller stocking weight than any of the depths for the remedial model (Figure 6B).

The 2 m temperature time series was missing 0.58 days of observations in mid-September. The average temperature for the 24 hours before and after the data gap was 17.8 °C, very close to the heat stress threshold. Assuming that there was no growth during the period of missing data (e.g., subtracting 0.58 days from n_{days}; Equation 1B) resulted in 5.2 fewer degree days (0.23 % fewer than the original model) and a stocking weight 0.006 kg larger (0.44 % larger for the average growth performance), which were considered negligible differences.

3.4 Long season: Flat Island

The three stations that met the criteria to represent a long season were Shad Bay, Flat Island, and Little Rafuse Island. These stations are within 35 km of each other, near the border of Halifax and Lunenburg Counties. The Flat Island station (Figure 1) was ultimately selected for analysis because it is geographically between

TABLE 2 Stocked season and degree day results for each station and depth.

Station	Depth (m)	Stocking Date (yyyy-mm-dd)	Harvest Date (yyyy-mm-dd)	Stocked Days	Filtered Days	Growing Days	Average Temperature (°C)	Degree Days
Madeline Point	2	2019-06-17	2020-02-15	243.02	30.98	212.04	8.26	1751
Madeline Point	5	2019-06-17	2020-02-22	249.60	27.12	222.49	7.98	1775
Madeline Point	10	2019-06-22	2020-02-22	244.45	21.14	223.31	7.92	1768
Madeline Point	15	2019-06-22	2020-02-15	237.59	15.54	222.05	7.84	1742
Madeline Point	22	2019-06-23	2020-02-15	236.42	3.46	232.96	7.05	1643
Beaver Point	2	2018-05-21	2019-02-22	276.30	26.14	250.16	8.98	2247
Beaver Point	5	2018-05-27	2019-02-22	271.16	21.93	249.23	7.15	1782
Beaver Point	10	2018-05-31	2019-02-22	267.48	12.14	255.34	7.03	1794
Beaver Point	15	2018-07-11	2019-01-20	193.08	5.04	188.04	7.71	1450
Flat Island	2	2019-05-01	2020-10-22	540.00	17.45	522.55	8.11	4240
Flat Island	5	2019-05-08	2020-10-29	540.00	9.67	530.32	9.05	4801
Flat Island	10	2019-05-19	2020-11-09	540.00	0.00	540.00	8.05	4350
Flat Island	15	2019-05-19	2020-11-09	539.99	0.00	539.99	7.14	3853
Flat Island	22	2019-06-19	2020-12-10	540.00	0.00	540.00	7.61	4107

the other two long season station candidates. The Flat Island station is approximately 22 m deep, with temperature sensors at 2, 5, 10, 15, and 22 m below the surface and a tidal range of up to 3 m. It is located approximately 5 km from shore, 2 km from Big Tancook Island, and 600 m from Flat Island.

The stocked season selected for analysis started in early May near the surface (2 and 5 m), later May at the middle depths (10 and 15 m), and mid-June at the bottom depth (22 m; Table 2). No superchill was observed in the following winter or spring, therefore the growing season lasted ~ 18 months (540 days) at each depth (Figure 4C). There was an overall increasing temperature trend at all depths in the spring and summer months, with notable stratification and diurnal variability. The temperature near the surface (2 m) was ~ 5 °C warmer than at the bottom (22 m) for the summer of 2019 and spring/summer of 2020. There was limited heat stress during this growing season, and when it occurred, it was confined to near the surface, with 17 days considered unsuitable for growth at 2 m and 9.7 days at 5 m (Table 2). Temperature was less stratified and less variable in the fall and winter months, with an overall decreasing temperature trend. Notably, there was a temperature inversion for most of mid-November through mid-March, with the coolest average temperature near the surface (3.8 °C) and the warmest average temperature near the bottom (7.6 °C; Figure 4C).

There was a range of nearly 1000-degree days for the different depths (Figure 6A). As a result of summer heat stress at the surface and the winter temperature inversion, the 5 m depth had the most degree days (4800-degree days), and the 15 m stratum had the least (3853 degree days; Table 2). The 2, 10, and 22 m depths all had relatively similar number of degree days, ranging from 4120 degree days to 4350 degree days. For the remedial growth model, this translated into modelled stocking weight ranging from 0.18 kg at 5 m to 0.52 kg at 15 m, while the results of the average model ranged from 0.034 kg to 0.23 kg. The elite model resulted in very small stocking weights, ranging from only 0.0006 kg to 0.072 kg (Figure 6B).

Delays in sensor redeployment resulted in two short gaps in the temperature data series: 1.5 days in early June 2019 (for all depths except for 22 m) and 0.2 days in November 2019. The temperature 24 hours before and after each gap is reasonably close to the average temperature (absolute difference from 0.26 °C to 2.1 °C), and the missing days represent only 0.30 % of the stocked season. The missing data was assumed to have negligible impact on the model results.

3.5 Sensitivity to heat stress threshold

3.5.1 Lower heat stress threshold (16 °C)

When the heat stress threshold was lowered to 16 °C there were ~ 20 (9 %) fewer growing days for most depths at Madeline Point and Beaver Point, which resulted in 227 (16 %) and 330 (19 %) fewer degree days, respectively. On average, this increased the stocking weight for each depth at Madeline Point by ~ 0.409 kg (22 %) and at Beaver Point by ~ 0.485 kg (26 %; Figure 7). The bottom temperature at Madeline Point rarely exceeded the 16 °C threshold, so there were only 5 fewer growing days at this depth, which required a 0.103 kg (5 %) larger post-smolt (Figure 7).

Flat Island had the largest reduction in number of growing days and degree days, particularly at the shallow depths. At 2 m, there were 88 (17 %) fewer growing days and 1184 (28 %) fewer degree days compared to the original heat stress threshold. At 5 m, there were 71 (13 %) fewer growing days and 1068 (22 %) fewer degree days. The increase in stocking weight was similar to the other

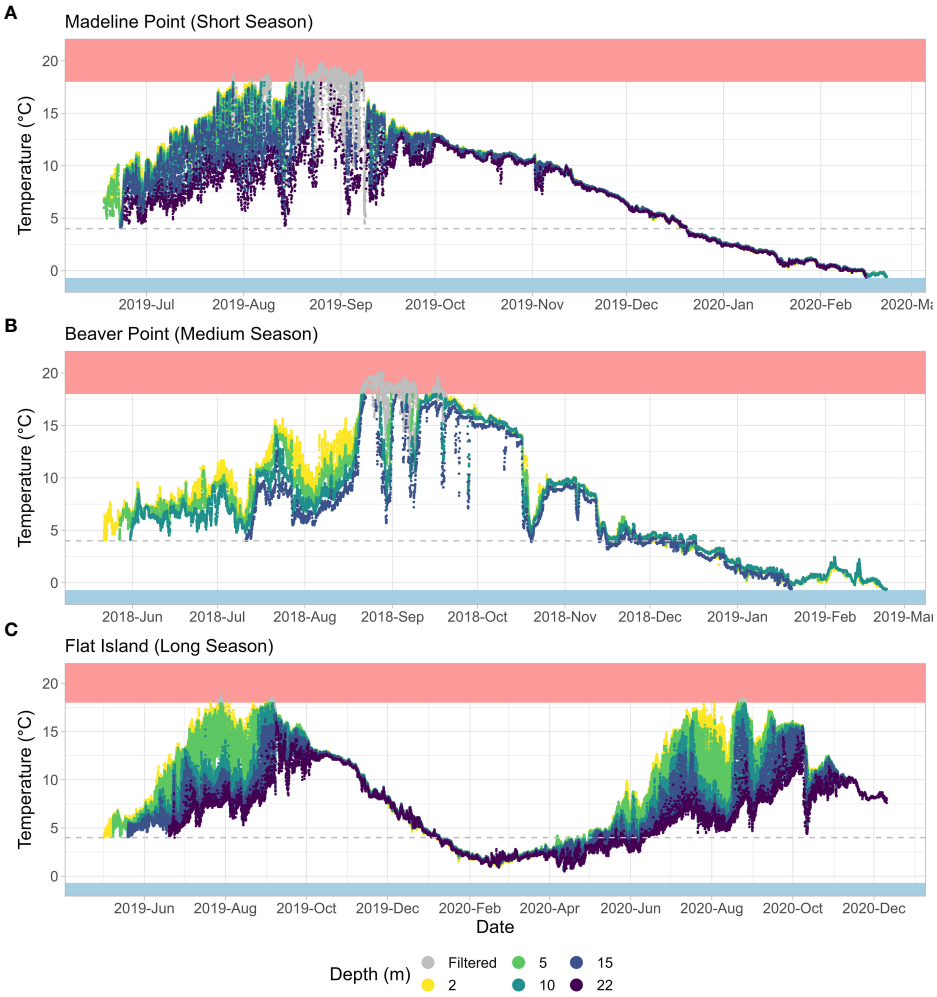

FIGURE 4
Temperature observations for **(A)** Madeline Point (short season), **(B)** Beaver Point (medium season), and **(C)** Flat Island (long season). The shaded blue area indicates the superchill threshold (-0.7 °C), the dashed grey line indicates the 4 °C threshold, and the shaded red area indicates the heat stress threshold (18 °C). Greyed observations were considered heat stress (within 24 hours of an observation ≥ 18 °C) and were filtered out of the analysis.

stations (0.491 kg at 2 m and 0.235 kg at 5 m; Figure 7). The difference at 10 m was also substantial, with 32 (6 %) fewer growing days and 464 (11 %) fewer degree days, which translated to an increase in stocking weight of 0.118 kg (121 %). The deeper strata rarely exceeded the 16 °C threshold and had small changes in stocking weight (< 0.030 kg; < 12 %).

3.5.2 Higher heat stress threshold (20 °C)

Increasing the heat stress threshold to 20 °C was nearly equivalent to not accounting for heat stress in the model. Few observations exceeded this threshold, with only 1 day considered unsuitable for growth at Madeline Point (2 m) and 2.3 days at Beaver Point (2 m). Consequently, there were additional growing days through the whole water column at these stations, most notably for the shallower depths. At 2 m and 5 m, there were over 25 (10 %) more growing days at Madeline Point, and over 20 (9 %) additional growing days at Beaver Point. At Madeline Point, this translated into an additional 540 (30 %) degree days at 2 m, and 478 (27 %) at 5 m. Similarly at Beaver Point, there were an additional 581 (26 %) degree days at 2 m and 396 (22 %) at 5 m. No heat stress events for Flat Island were observed in this simulation, which resulted in an increase of 241 (5.7 %) degree days at 2 m and 168 (3.5 %) degree days at 5 m. No heat stress events were observed in the original model at the other depths, and so those results did not change.

The largest absolute decrease in stocking weight was for the surface depths at Madeline Point, which were 0.653 kg (34 %) and 0.581 kg (31 %) smaller than in the original model for 2 m and 5 m. This was closely followed by Beaver Point, with a reduction of 0.528 kg (40 %) and 0.489 kg (26 %) at the same depths. There was a modest reduction of < 0.050 kg for the Flat Island example.

4 Discussion

4.1 Potential for seasonal site usage

The TGC model results showed that fish weighing 1.5 – 2.5 kg can theoretically grow to market size at seasonal sites. This suggests

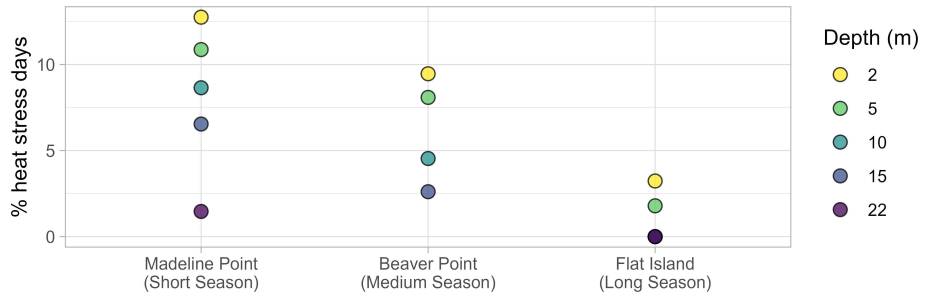

FIGURE 5
Percent of the stocked season at each station and depth with arrested growth caused by heat stress (≥ 18 °C). Note that there was no heat stress observed at Flat Island at 10, 15, and 22 m.

that post-smolt stocking strategies can potentially enable use of novel sites in areas previously considered unsuitable for aquaculture because of cold winter temperatures. The modelled stocking weight was substantially larger than typical target post-smolt weights (Fish Farming Expert, 2019; Gardner Pinfold Consultants Inc., 2019; Fish Farming Expert, 2021; MOWI, 2021); however, it is technically feasible to grow salmon to this size or larger on land (Atlantic Sapphire, 2020; Sustainable Blue, 2021). Several companies have successfully moved the entire Atlantic salmon production cycle to land-based Recirculating Aquaculture System (RAS) facilities (see Table 1 of Gardner Pinfold Consultants Inc., 2019). There are still substantial challenges in the grow-out phase at these facilities, including improving fish quality, maintaining fish health, preventing fish mortalities, and managing increased costs (Calabrese, 2017; Gardner Pinfold Consultants Inc., 2019; EY, 2020; Hoel and Howell, 2021). Transferring large post-smolts to marine net-pens may offset some of these challenges, and we recommend future research into the costs and benefits of growing large post-smolts on land to stock in novel sites.

4.2 Assessing site suitability

The approach discussed here highlights that the TGC model in conjunction with high-resolution, site-specific temperature data can be a useful tool for assessing the suitability of novel areas. This

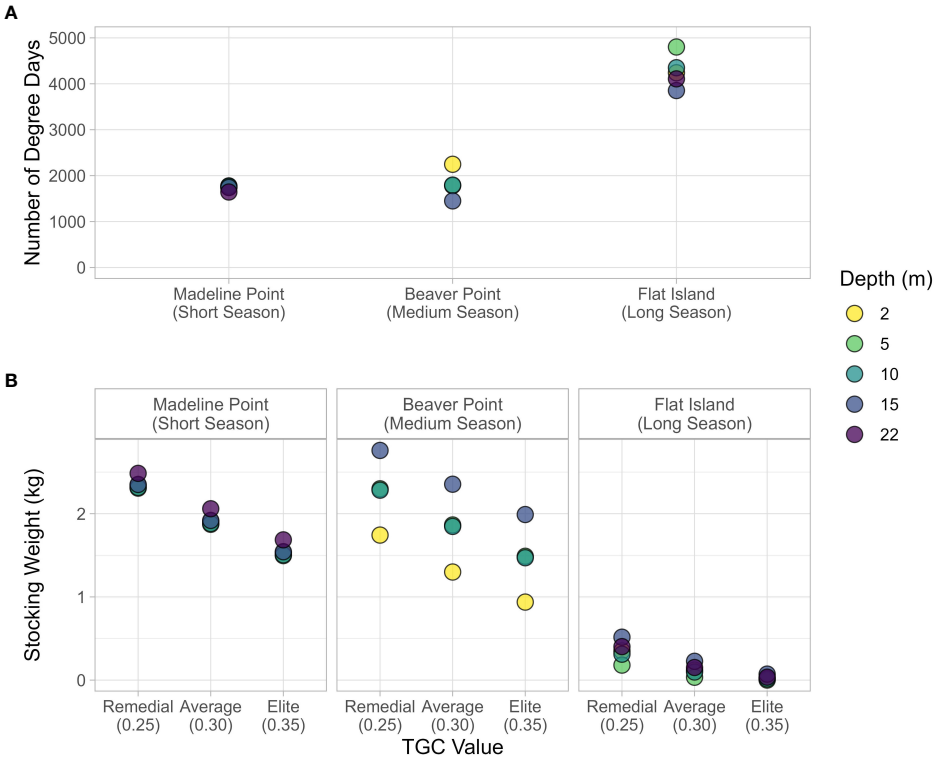

FIGURE 6
(A) The number of growing degree days observed at each station and depth, and **(B)** Stocking weight of post-smolts required to reach market size as a function of TGC value, location and depth (heat stress threshold ≥ 18 °C).

temperature data can provide insight on optimal stocking and harvest dates as well as anticipated heat stress. For example, local temperature profiles were key for informing the optimal stocking date, which was related to both latitude and depth. The season began in early May at Flat Island (the most southern station) and in mid-June at Madeline Point (the most northern station), illustrating the value of using local data to inform operational decisions. Despite being on the same coast, using Flat Island data to inform the timing of stocking at Madeline Point would subject the post-smolts to 6 weeks of sub-optimal temperatures. At each station, the season started progressively later with depth, with up to 7 weeks difference between the surface and the bottom at Beaver Point. This highlights the importance of incorporating the temperature profile throughout the water column, especially for the full cage depth, into stocking decisions. Using only the surface data to inform the timing of stocking could subject the fish to potentially harmfully cold temperatures. Inter-annual temperature variation was beyond the scope of this paper, but is known to vary substantially along the coast of Nova Scotia (Centre for Marine Applied Research, 2022), and would be an important site suitability consideration.

4.2.1 Superchill

Despite seasonal occurrence of superchill along some coastal regions, it is not always predictable and is therefore a major risk for the aquaculture industry. The ability to better predict the onset of superchill would be an asset to existing and new operations, especially for potential seasonal sites. Several days or weeks warning of impending superchill would provide time to implement risk management strategies, including preparing to harvest or ceasing feeding and other activities at the cage sites (LGL Limited, 2019; Sweeney International Marine Corp, 2019). Analyzing several years of historical high-resolution data at a given location could provide useful insight into inter-annual patterns, typical and extreme events, and early warning indicators. This information could eventually feed into model forecasts of superchill extent and timing (Payne et al., 2017). Our analysis suggests that the timing of superchill is not typically related to depth, due to minimal stratification in the winter/spring, when superchill occurs. The main exception was the bottom temperatures, where superchill was observed ~ 1 month earlier at Beaver Point and ~ 1 week earlier at Madeline Point than at other depths. The occurrence of superchill at the bottom could be an early warning indicator of superchill at shallower depths where cages are located. An extensive analysis of CMAR's Coastal Monitoring Program data to investigate whether this pattern is consistent spatially and inter-annually is recommended.

4.2.2 Heat stress

In contrast to superchill, the amount of heat stress was related to depth, with more days considered unsuitable for growth near the surface at each station (Figure 5). Surprisingly, the most heat stress was observed at Madeline Point (Table 2). This was the most northern site and had the earliest onset of superchill, and it was expected to be generally cooler than the other sites. Instead, over 8 % of the stocked days were unsuitable for growth as deep as 10 m (Figure 5). It may be worth investing in a deep net for this location so fish can avoid warm surface waters and continue to grow. In contrast, the only heat stress observed at Flat Island was near the surface, and so a typical net depth would be sufficient at this location. A major limiter of the industry in Nova Scotia is that sites are typically located in relatively shallow waters, so the net depth may be constrained by bathymetry. Site location in deeper water could

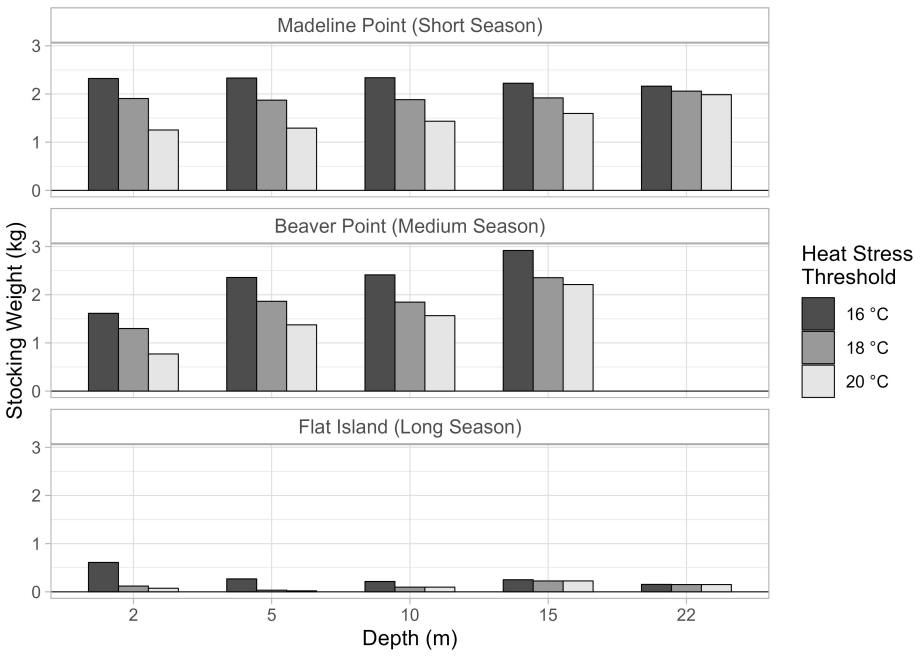

FIGURE 7
Stocking weight estimated from applying three different heat stress thresholds (16°C, 18°C, 20°C).

enable access to a wider range of stratified temperatures, although this could require management and infrastructure changes. Long-term, high-resolution data such as those provided by the CMAR Coastal Monitoring Program can assist to inform such cost-benefit analyses.

4.3 Heat stress threshold

It is critical to choose an appropriate heat stress threshold to account for reduced growth at high temperatures. The threshold value can substantially impact the results, and an erroneous value could lead to increased economic and ecologic risks. In the original model (heat stress threshold = 18 °C), heat stress was a major impediment to growth at all three locations, particularly at shallow depths (Figure 5). When the threshold was increased to 20 °C, few observations were considered heat stress. This resulted in more growing days and higher average temperatures, and therefore required smaller stocking weights (Figure 7). If this model was used to guide stocking weight decisions, the fish may not grow to market size in the allotted season. This would be of particular concern for the seasonal sites, which are constrained by superchill, making it challenging or impossible to extend the season. For example, smolts with a stocking weight estimated from this model for Madeline Point would only grow to 4.12 kg if the stock truly experiences heat stress at 18 °C.

Lowering the heat stress threshold to 16 °C reduced the number of growing days and associated average temperatures, resulting in higher stocking weights. This model provides a more conservative estimate of the stocking weight, i.e., these large post-smolts would likely grow to market size during the defined season. However, the fish would need to grow longer on land to reach this stocking weight, which has associated costs and risks (Gardner Pinfold Consultants Inc., 2019; Hoel and Howell, 2021). For example, fish transferred to Beaver Point would require an extra 4 to 6 weeks in the land-based facility to grow to the stocking weight estimated from this model.

4.4 Growth performance

Differences in temperature driven growth performance (Handeland et al., 2004) were reflected in the remedial, average, and elite models. As expected, the elite model resulted in the smallest stocking weights for each station (Figures 3, 6). The largest discrepancy between elite and remedial models occurred for the stations with moderate degree days, Madeline Point and Beaver Point (Figure 6). There was a much higher number of degree days at Flat Island (long season), which resulted in a relatively small absolute difference in stocking weight between TGC models (Figure 6). Using a smaller TGC value (i.e., assuming a slow growth) to calculate the stocking weight is more conservative for ensuring the smolts will grow to market size during a predefined season. However, an overly conservative estimate could result in unnecessary additional time in post-smolt facilities (Gardner Pinfold Consultants Inc., 2019; Hoel and Howell, 2021).

The TGC values applied here were based on estimates from the literature, which originated from 10 – 15-year-old data (Reid et al., 2013b). Ground truthing by Cooke Aquaculture Inc.'s average production model suggested these values were reasonable. This production model aims to stock 120 g – 150 g smolts, which grow out over 22 months to a market size of 5.5 – 6 kg (Jennifer Hewitt, Cooke Aquaculture Inc., personal communication October 2022). Using these initial and final weights and temperature data from the example stations, TGC values ranging from 0.234 – 0.263 were calculated (equation 1), which correspond with the remedial growth performance TGC. The elite growth performance value was derived based on the assumption that selective breeding suggests improved growth rate by about 10 % per generation (Gjøen and Bentsen, 1997; Gjedrem, 2000; Thorarensen and Farrell, 2011). This highlights the need for updated commercial TGC coefficients for Atlantic salmon grown in marine net-pens to improve confidence in the model results.

Determining whether elite performing stocks grow faster than the average and remedial performing salmon at high temperatures would be relevant for breeding programs. Tolerance to high temperature, often measured using the critical thermal maximum, varies between families (Anttila et al., 2013). Moreover, it has been shown that tolerance to heat stress, which is a heritable trait in salmon, and growth rate may be inversely correlated, suggesting that simultaneous selection for both traits is unattainable (Debes et al., 2021).

4.5 Degree days drivers and outcomes

Degree days are a key metric for modelling growth of ectotherms, accounting for both growing time and temperature. Our results reinforce that both degree day factors, n_{days} and T_{Avg}, are important drivers. For example, Flat Island and Madeline Point had similar average temperatures at 10 m; however, Flat Island had more than double the number of growing days (Table 2). The resulting stocking weights at Flat Island were 7 (remedial model) to 100 (elite model) times smaller than at Madeline Point (Figure 6). In this analysis, n_{days} was adjusted to account for reduced growth rates caused by heat stress. Other factors that affect growth rates (e.g., no-feed events, photoperiod influence) are assumed to be accounted for in the TGC value, which is derived from historical production data over the growth period. There is no historical production data for the novel locations assessed in this study, and so the application of remedial, average, and elite performing TGC values aimed to account for a range of potential influences to growth performance.

The Beaver Point and Madeline Point results illustrate the importance of temperature. At 5 m and 10 m, there were ~ 30 more growing days at Beaver Point (Table 2). A naïve prediction would be that smaller smolts could be stocked at Beaver Point because they have more time for grow-out. However, the average temperature of the growing days at Madeline Point was 0.8 °C warmer that that at Beaver Point, resulting in very similar stocking weights for both locations (Figure 6). It is therefore critical to have high-quality, ideally site-specific temperature data for useful estimates from the TGC model.

Under the TGC model, initial weight is related to the number of degree days through a non-linear (cubic) relationship (Equation 2), which can also lead to unintuitive results. For example, an absolute change in the degree days can result in a differential change in initial weight (Figure 3). A wide range in the number of degree days at Beaver Point results in a ~ 1 kg difference in stocking weight between the surface and the bottom depths. Flat Island had a similar range of degree days at depth, but a substantially smaller range of stocking weights, particularly for the elite model (Figure 6). This is because the range of degree days at Beaver Point (1450 – 2247 degree days) corresponds to a relatively steep part of the curve shown in Figure 3. In contrast, the number of degree days at Flat Island is substantially higher (3858 – 4801 degree days) and corresponds to a flat part of the curve, most notably for the elite model. These results illustrate that additional degree days at a location may not translate to appreciable differences in stocking weight. We recommend consulting a stocking weight-degree day curve (Figure 3) to inform cost-benefit of expanding to an additional depth or location with more degree days.

The Flat Island example also highlights that TGC results should be interpreted carefully and in context, especially at extreme degree day values. At high degree days the modelled stocking weight approaches zero and can even become negative (Figure 3). At Flat Island, the stocking weight of the elite growth model for all depths was less than 120 g, a typical size for smolt stocked in Nova Scotia (Jennifer Hewitt, Cooke Aquaculture, personal communication, October 2022). The stocking weight at 5 m was only 0.6 g, which is about the size of a fry and would not survive in the marine environment.

At very small degree days, the modelled stocking weight will approach market size (Figure 3). It may be impractical to transport such large fish to ocean net-pens for the remaining short grow-out period. Before modelling, it is important to identify operational thresholds including the minimum and maximum acceptable smolt size, and to inspect the results accordingly.

5 Conclusion

The method and results presented here suggest that further investigations into large post-smolt stocking to circumvent short periods of cold temperatures are warranted. The method is straightforward to apply to any potential site with observed temperature data. We recommend high-resolution, long-term, and site-specific temperature data for estimates of stocking and harvest dates and heat stress. This method could be easily adopted for other species with known TGC values and heat stress thresholds.

Data availability statement

Publicly available datasets were analyzed in this study. This data can be found here: Madeline Point: https://data.novascotia.ca/Nature-and-Environment/Guysborough-County-Water-Quality-Data/eb3n-uxcb Beaver Point: https://data.novascotia.ca/Nature-and-Environment/Halifax-County-Water-Quality-Data/x9dy-aai9 Flat Island: https://data.novascotia.ca/Nature-and-Environment/Lunenburg-County-Water-Quality-Data/eda5-aubu.

Author contributions

GR, DD, and LLM conceived of and designed the analysis. DD wrote the code, interpreted results, and drafted the manuscript. All authors contributed to the article and approved the submitted version.

Conflict of interest

Author RC is employed by C&H Aquatic and Laboratory Veterinary Services Ltd. Author AD is employed by Aquaculture Nutrition Services Inc. Author JR is employed by System Science Applications Inc.

The remaining authors declare that the research was conducted in the absence of any commercial or financial relationships that could be construed as a potential conflict of interest.

Publisher's note

References

Anttila, K., Dhillon, R. S., Boulding, E. G., Farrell, A. P., Glebe, B. D., Elliott, J. A., et al. (2013). Variation in temperature tolerance among families of Atlantic salmon (*Salmo salar*) is associated with hypoxia tolerance, ventricle size and myoglobin level. *J. Exp. Biol.* 216 (7), 1183–1190. doi: 10.1242/jeb.080556

Atlantic Sapphire (2020). *Annual report 2020*.

Aunsmo, A., Krontveit, R., Valle, P. S., and Bohlin, J. (2014). Field validation of growth models used in Atlantic salmon farming. *Aquaculture* 428–429 (0), 249–257. doi: 10.1016/j.aquaculture.2014.03.007

Calabrese, S. (2017). *Environmental and biological requirements of post-smolt Atlantic salmon (Salmo salar l.) in closed-containment aquaculture systems* (PhD, University of Bergen).

CBC (2015). *Nova Scotia Aquaculture fish killed by superchilled water* (Nova Scotia, Canada: Canadian Broadcasting Corporation (CBC). Available at: https://www.cbc.ca/news/canada/nova-scotia/nova-scotia-aquaculture-fish-killed-by-superchilled-water-1.2980172

Centre for Marine Applied Research (2022). *Coastal monitoring program* (Dartmouth, Nova Scotia: Centre for Marine Applied Research (CMAR). Available at: https://cmar.ca/coastal-monitoring-program/.

Cho, C. Y., and Bureau, D. P. (1998). Development of bioenergetic models and the fish-PrFEQ software to estimate production, feeding ration and waste output in aquaculture. *Aquat. Living Resour.* 11 (4), 199–210. doi: 10.1016/S0990-7440(98)89002-5

Chowdhury, M. A. K., Siddiqui, S., Hua, K., and Bureau, D. P. (2013). Bioenergetics-based factorial model to determine feed requirement and waste output of tilapia produced under commercial conditions. *Aquaculture* 410-411, 138–147. doi: 10.1016/j.aquaculture.2013.06.030

Debes, P. V., Solberg, M. F., Matre, I. H., Dyrhovden, L., and Glover, K. A. (2021). Genetic variation for upper thermal tolerance diminishes within and between populations with increasing acclimation temperature in Atlantic salmon. *Heredity* 127 (5), 455–466. doi: 10.1038/s41437-021-00469-y

Dumas, A., France, J., and Bureau, D. P. (2007). "Evidence of three growth stanzas in rainbow trout (Oncorhynchus mykiss) across life stages and adaptation of the thermal-unit growth coefficient," in *The XII international symposium on fish nutrition and feeding* (Elsevier).

Dumas, A., France, J., and Bureau, D. (2010). Modelling growth and body composition in fish nutrition: where have we been and where are we going? *Aquacult. Res.* 41 (2), 161–181. doi: 10.1111/j.1365-2109.2009.02323.x

Dunagan, C. (2021) *Taking the temperature of salmon*. Available at: https://www.eopugetsound.org/magazine/taking-temperature-salmon.

Elliott, J. M., and Elliott, J. A. (2010). Temperature requirements of Atlantic salmon *Salmo salar*, brown trout *Salmo trutta* and Arctic charr *Salvelinus alpinus*: predicting the effects of climate change. *J. Fish Biol.* 77, 1793–1817. doi: 10.1111/j.1095-8649.2010.02762.x

Elliott, J. M., and Hurley, M. A. (2000). Daily energy intake and growth of piscivorous brown trout, salmo trutta. *Freshw. Biol.* 44 (2), 237–245. doi: 10.1046/j.1365-2427.2000.00560.x

EY (2020). *The Norwegian aquaculture analysis 2020*.

Feindel, N., Cooper, L., Trippel, E., and Blair, T. (2013). "Climate change and marine aquaculture in Atlantic Canada and Quebec," in *Climate change impacts, vulnerabilities and opportunities analysis of the marine Atlantic basin. vol. 3012 of Canadian manuscript reports of fisheries and aquatic sciences*. Eds. N. L. Shackell, B. Greenan, P. Pepin, D. Chabot and A. Warburton (Nova Scotia: Fisheries and Oceans Canada (DFO), Ocean and Ecosystem Sciences Division, Bedford Institute of Oceanography), 195–255.

Fisheries and Oceans Canada (2022). *Fallowing as a tool for disease mitigation in marine finfish facilities in British Columbia* (Pacific Region: Canadian Science Advisory Secretariat Science Response 2022/023).

Fish Farming Expert (2019) *Huon bids to cut time at sea with 1kg nursery salmon*. Available at: https://www.fishfarmingexpert.com/article/huon-bids-to-cut-time-at-sea-with-1kg-plus-nursery-salmon/ (Accessed 2021).

Fish Farming Expert (2020) *Canadian Bigger smolts project given $1.8m funding*. Available at: https://www.fishfarmingexpert.com/article/canadian-bigger-smolts-project-given-18m-funding/ (Accessed 2021).

Fish Farming Expert (2021) *Half-kilo smolts will halve time at sea for Scottish salmon company fish*. Available at: https://www.fishfarmingexpert.com/article/half-kilo-smolts-will-halve-time-at-sea-for-scottish-salmon-co-fish/ (Accessed 2021).

Gamperl, A. K., Ajiboye, O. O., Zanuzzo, F. S., Sandrelli, R. M., Peroni, E., and Beemelmanns, A. (2020). The impacts of increasing temperature and moderate hypoxia on the production characteristics, cardiac morphology and haematology of Atlantic salmon (*Salmo salar*). *Aquaculture* 519, 734874. doi: 10.1016/j.aquaculture.2019.734874

Gamperl, A., Zrini, Z., and Sandrelli, R. (2021). Atlantic Salmon (Salmo salar) cage-site distribution, behavior, and physiology during a Newfoundland heat wave. *Front. Physiol.* 12. doi: 10.3389/fphys.2021.719594

Gardner Pinfold Consultants Inc. (2019). *State of salmon aquaculture technologies*.

Gjøen, H. M., and Bentsen, H. B. (1997). Past, present, and future of genetic improvement in salmon aquaculture. *ICES J. Mar. Sci.* 54 (6), 1009–1014. doi: 10.1016/s1054-3139(97)80005-7

Gjedrem, T. (2000). Genetic improvement of cold-water fish species. *Aquacult. Res.* 31 (1), 25–33. doi: 10.1046/j.1365-2109.2000.00389.x

Global Ocean Observing System (2021) *Essential ocean variables*. Available at: https://www.goosocean.org/index.php?option=com_content&view=article&id=14&Itemid=114 (Accessed June 1, 2021).

Grieg Seafood (2020) *Our impact: more sustainable farming with post smolt*. Available at: https://griegseafood.com/our-impact-post-smolt.

Handeland, S. O., Imsland, A. K., and Stefansson, S. O. (2008). The effect of temperature and fish size on growth, feed intake, food conversion efficiency and stomach evacuation rate of Atlantic salmon post-smolts. *Aquaculture* 283 (1), 36–42. doi: 10.1016/j.aquaculture.2008.06.042

Handeland, S. O., Wilkinson, E., Sveinsbø, B., McCormick, S. D., and Stefansson, S. O. (2004). Temperature influence on the development and loss of seawater tolerance in two fast-growing strains of Atlantic salmon. *Aquaculture* 233 (1), 513–529. doi: 10.1016/j.aquaculture.2003.08.028

Hoel, T., and Howell, D. (2021). Land-based salmon farming: key investment considerations. Available at: https://thefishsite.com/articles/land-based-salmon-farming-key-investment-considerations

Holland, J. (2021) *Mowi Scotland plans new post-smolt site*. Available at: https://www.seafoodsource.com/news/aquaculture/mowi-scotland-plans-new-post-smolt-site (Accessed April 26, 2022).

InnovaSea (2021). *Realtime monitoring product manual*.

Iwama, G. K., and Tautz, A. F. (1981). A simple growth model for salmonids in hatcheries. *Can. J. Fish. Aquat. Sci.* 38 (6), 649–656. doi: 10.1139/f81-087

Jobling, M. (1981). Temperature tolerance and the final preferendum–rapid methods for the assessment of optimum growth temperatures. *J. Fish Biol.* 19 (4), 439–455. doi: 10.1111/j.1095-8649.1981.tb05847.x

Jobling, M. (2003). The thermal growth coefficient (TGC) model of fish growth: a cautionary note. *Aquacult. Res.* 34 (7), 581–584. doi: 10.1046/j.1365-2109.2003.00859.x

Johansson, D., Ruohonen, K., Juell, J.-E., and Oppedal, F. (2009). Swimming depth and thermal history of individual Atlantic salmon (Salmo salar l.) in production cages under different ambient temperature conditions. *Aquaculture* 290 (3–4), 296–303. doi: 10.1016/j.aquaculture.2009.02.022

Johansson, D., Ruohonen, K., Kiessling, A., Oppedal, F., Stiansen, J.-E., Kelly, M., et al. (2006). Effect of environmental factors on swimming depth preferences of Atlantic salmon *(Salmo salar* l.) and temporal and spatial variations in oxygen levels in sea cages at a fjord site. *Aquaculture* 254 (1–4), 594–605. doi: 10.1016/j.aquaculture.2005.10.029

LGL Limited (2019). Placentia bay Atlantic salmon aquaculture project environmental effects monitoring plan: climate and weather. *LGL Rep. FA0159F. Rep*. by LGL Limited, St. John's, NL for Grieg NL, Marystown, NL. 11 p.

Mayer, L. (2022). Post-smolt initiatives are a' very safe bet,' will drive growth for farmers. *SalmonBusiness*. Available at: https://salmonbusiness.com/post-smolt-initiatives-are-a-very-safe-bet-will-drive-growth-for-farmers/?utm_source=SalmonBusiness+Subscribers&utm_campaign=21d11db504-RSS_EMAIL_CAMPAIGN_SalmonB&utm_medium=email&utm_term=0_dddf4df39a-21d11db504-101480067

Morita, K., Fukuwaka, M. A., Tanimata, N., and Yamamura, O. (2010). Size-dependent thermal preferences in a pelagic fish. *Oikos* 119 (8), 1265–1272. doi: 10.1111/j.1600-0706.2009.18125.x

MOWI (2021). *Salmon farming industry handbook*. Available at: https://www.intrafish.com/prices/farmed-salmon-prices-continue-freefall-were-losing-millions/2-1-829675

Njåstad, M. (2020). Farmed salmon prices continue freefall: 'We're losing millions'. *Intrafish*.

Onset (2012). *HOBO® water temp pro v2 (U22-001) manual*.

Oppedal, F., Dempster, T., and Stien, L. H. (2011). Environmental drivers of Atlantic salmon behaviour in sea-cages: a review. *Aquaculture* 311 (1–4), 1–18. doi: 10.1016/j.aquaculture.2010.11.020

Payne, M. R., Hobday, A. J., MacKenzie, B. R., Tommasi, D., Dempsey, D. P., Fässler, S. M. M., et al. (2017). Lessons from the first generation of marine ecological forecast products. *Front. Mar. Sci.* 4. doi: 10.3389/fmars.2017.00289

Pörtner, H.-O., and Peck, M. A. (2010). Climate change effects on fishes and fisheries: towards a cause-and-effect understanding. *J. Fish Biol.* 77 (8), 1745–1779. doi: 10.1111/j.1095-8649.2010.02783.x

Reid, G. K., Chopin, T., Robinson, S. M. C., Azevedo, P., Quinton, M., and Belyea, E. (2013a). Weight ratios of the kelps, *Alaria esculenta* and *Saccharina latissima*, required to sequester dissolved inorganic nutrients and supply oxygen for Atlantic salmon, *Salmo salar*, in integrated multi-trophic aquaculture systems. *Aquaculture* 408/409 (0), 34–46. doi: 10.1016/j.aquaculture.2013.05.004

Reid, G. K., Forster, I., Cross, S., Pace, S., Balfry, S., and Dumas, A. (2017). Growth and diet digestibility of cultured sablefish: implications for nutrient waste production and integrated multi-trophic aquaculture. *Aquaculture*. 470, 223–229. doi: 10.1016/j.aquaculture.2016.12.010

Reid, G. K., Lefebvre, S., Filgueira, R., Robinson, S. M. C., Broch, O. J., Dumas, A., et al. (2020). Performance measures and models for open-water integrated multi-trophic aquaculture. *Rev. Aquacult.* 12 (1), 47–75. doi: 10.1111/raq.12304

Reid, G. K., Robinson, S. M. C., Chopin, T., and MacDonald, B. A. (2013b). Dietary proportion of fish culture solids required by shellfish to reduce the net organic load in open-water integrated multi-trophic aquaculture: a scoping exercise with cocultured Atlantic salmon *(Salmo salar*) and blue mussel *(Mytilus edulis*). *J. Shellfish Res.* 32, 509–517. doi: 10.2983/035.032.0230

Saunders, R. L. (1995). "Salmon aquaculture: present status and prospects for the future," in *Cold-water aquaculture in Atlantic Canada, 2nd Edition*. Ed. A. D. Bogden (Moncton, N.B., Canada: Canadian Institute for Research on Regional Development).

Saunders, R. L., Muise, B. C., and Henderson, E. B. (1975). Mortality of salmonids cultured at low temperature in sea water. *Aquaculture* 5 (3), 243–252. doi: 10.1016/0044-8486(75)90002-2

South, A. (2022a). *"rnaturalearth: world map data from natural earth"*.

South, A. (2022b). *"rnaturalearthhires: high resolution world vector map data from natural earth used in rnaturalearth"*.

Sustainable Blue (2021) *Introducing RAS, our proprietary recirculating aquaculture system*. Available at: https://www.sustainableblue.com/innovation.

Sweeney International Marine Corp (2019). *"Liverpool bay development plans"*.

Thorarensen, H., and Farrell, A. P. (2011). The biological requirements for post-smolt Atlantic salmon in closed-containment systems. *Aquaculture* 312 (1), 1–14. doi: 10.1016/j.aquaculture.2010.11.043

Thyholdt, S. B. (2014). The importance of temperature in farmed salmon growth: regional growth functions for Norwegian farmed salmon. *Aquacult. Economics Manage.* 18, 189–204. doi: 10.1080/13657305.2014.903310

Vemco (2016). *"VR2AR user manual"*.

Vikesa, V., Nankervis, L., and Hevroy, E. M. (2017). Appetite, metabolism and growth regulation in Atlantic salmon (Salmo salar l.) exposed to hypoxia at elevated seawater temperature. *Aquacult. Res.* 48 (8), 4086–4101. doi: 10.1111/are.13229

Withers, P. (2021). Cooke Aquaculture proposes $58M salmon hatchery on digby neck. *CBC News*.

Frontiers in Marine Science

Explores ocean-based solutions for emerging global challenges

The third most-cited marine and freshwater biology journal, advancing our understanding of marine systems and addressing global challenges including overfishing, pollution, and climate change.

Discover the latest Research Topics

See more →

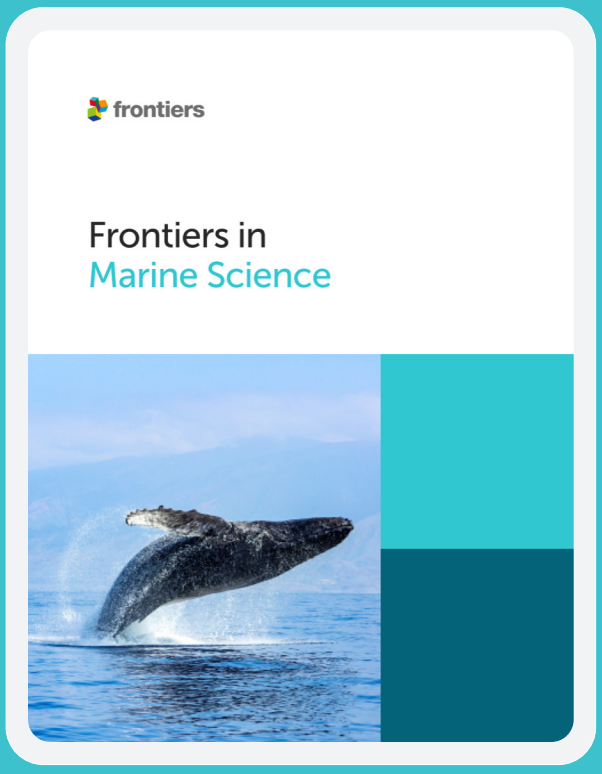

Frontiers

Avenue du Tribunal-Fédéral 34
1005 Lausanne, Switzerland
frontiersin.org

Contact us

+41 (0)21 510 17 00
frontiersin.org/about/contact